

Max-Planck-Institute
for Biophysical Chemistry
and Georg-August-University Göttingen

D O C T O R A L T H E S I S

**Ecdysone signaling and miRNA *let-7*
cooperate in regulating the
differentiation of the germline stem cell
progeny**

Dissertation for the award of the degree
"Doctor rerum naturalium"
of the Georg-August-University Göttingen
within the doctoral program "Genes and Development"
of the Georg-August-University School of Science (GAUSS)

submitted by
Annekatriin König
born in Jena, Germany

Göttingen 2014

Members of the thesis committee:

PD Dr. Halyna Shcherbata (1st reviewer, supervisor)	Max-Planck-Institute for Biophysical Chemistry Max Planck Research Group of Gene Expression and Signaling
--	---

Prof. Dr. Andreas Wodarz (2nd reviewer)	Georg-August-University Göttingen Department of Stem Cell Biology
--	--

Prof. Dr. Jörg Großhans	University-Medical-School Göttingen Department of Developmental Biochemistry
-------------------------	---

Further members of the examination board:

Prof. Dr. Sigrid Hoyer-Fender	Georg-August-University Göttingen Department of Developmental Biology
-------------------------------	--

Prof. Dr. Ernst Wimmer	Georg-August-University Göttingen Department of Developmental Biology
------------------------	--

PD Dr. Roland Dosch	University-Medical-School Göttingen Department of Developmental Biochemistry
---------------------	---

Date of the oral examination: 08.05.2014

Affidavit

I herewith declare, that I prepared the PhD thesis "Ecdysone signaling and miRNA *let-7* cooperate in regulating the differentiation of the germline stem cell progeny" on my own. All direct or indirect sources and aids are acknowledged as references.

Annekatriin König

Göttingen, March 21th, 2014

Contents

Affidavit	iii
Abstract	ix
Abbreviations	xi
List of Figures	xiii
1 Introduction	1
1.1 Stem cells can self-renew and generate differentiated cells	1
1.1.1 Pluripotent stem cells have a great potential in regenerative medicine	1
1.1.2 Direct lineage conversion illustrates cell plasticity	3
1.1.3 Adult stem cells are controlled by specialized compartments: niches	3
1.2 The <i>D. melanogaster</i> germarium – a model for GSC niche communication	5
1.2.1 The somatic niche cells signal to the GSCs	6
1.2.2 <i>bam</i> expression switches on a differentiation program in CBs	10
1.2.3 Adherens junctions between GSCs and CpCs are required for GSC maintenance	11
1.2.4 ECs are required for the differentiation of the GSC progeny	12
1.2.5 GSCs respond to environmental cues	16
1.2.6 CpCs constitute an important part of the GSC niche . . .	16
1.3 Ecdysteroids control various aspects of <i>D. melanogaster</i> development and adult life	17
1.3.1 Ecdysteroids regulate <i>D. melanogaster</i> development	17
1.3.2 The spatial and temporal specificity of ecdysone signaling is achieved via differential expression of transcriptional and translational coregulators	18
1.3.3 Ecdysone signaling fulfills various functions in the adult fly	19
1.3.4 <i>D. melanogaster</i> as a model to study the complexity of steroid hormone function	21
1.4 Small non-coding RNAs regulate a variety of processes	22
1.4.1 miRNAs regulate translation and degradation of target mRNAs	22
1.4.2 miRNAs are required for GSCs behavior	24
1.4.3 <i>let-7</i> is a highly conserved heterochronic miRNA	24

1.4.4	Expression of <i>let-7</i> is initiated by ecdysone signaling . . .	26
1.4.5	<i>let-7</i> is important for cell differentiation and cancer – also in mammals	27
1.5	The Wnt signaling pathway is a key determinant for development	28
1.5.1	The effects of the canonical Wnt signaling pathway are mediated by β -Catenin	29
1.5.2	β -Catenin has a dual role as a structural component of cell-adhesion complexes and as a major transmitter of Wnt signaling	29
1.5.3	Wnt signaling regulates many processes in <i>D. melanogaster</i>	30
1.6	Chromatin modifications present an additional level at which GSCs can be regulated	30
1.6.1	Chromatin modifications regulate GSC maintenance	30
1.6.2	Proper ubiquitination of histone H2B is required for GSC behavior	31
1.7	Maintaining sexual identity is required for germline differentiation	32
1.7.1	Sex is determined by a series of alternative splicing events in <i>D. melanogaster</i>	32
1.7.2	Germline tumor arise as a consequence of confused sexual identity	33
1.8	Research objectives	35
2	Results	37
2.1	Ecdysteroids affect <i>Drosophila</i> ovarian stem cell niche formation and early germline differentiation	37
2.2	The Histone H2B Monoubiquitination Regulatory Pathway is Required for Differentiation of Multipotent Stem Cells	52
2.3	Visualization of Adult Stem Cells Within Their Niches Using the <i>Drosophila</i> Germline as a Model System	62
2.4	A Genome-Wide Survey of Sexually Dimorphic Expression of <i>Drosophila</i> miRNAs Identifies the Steroid Hormone-Induced miRNA <i>let-7</i> as a Regulator of Sexual Identity	72
2.5	Soma influences GSC progeny differentiation via the cell adhesion-mediated steroid- <i>let-7</i> -Wingless signaling cascade that regulates chromatin dynamics	95
3	Discussion	113
3.1	Ecdysone signaling is non cell-autonomously acting on the germline	113
3.1.1	EC function is compromised upon loss of ecdysone signaling	113
3.1.2	ECs form a differentiation niche for the germline progeny .	114
3.2	Wg signaling – a connection between ECs and GSCs	118
3.2.1	Arm levels in the germline are cell non-autonomously affected by DE-Cad levels in the soma	118
3.2.2	Arm is at the intersection of Wnt signaling, cell adhesion and other pathways	119

3.3	Ecdysone signaling links germline differentiation to the overall body status	120
3.3.1	Ecdysone signaling mediates effects of stress and starvation	120
3.3.2	The tissue- and time-specific response to ecdysone signaling is controlled by a complex network of interacting partners	121
3.3.3	Maintaining the sexual identity requires intact ecdysone signaling	123
3.3.4	The ecdysone/ <i>let-7</i> /Ab signaling cascade modulates oogenesis in response to different conditions	124
3.4	The <i>D. melanogaster</i> germarium provides a model to decipher the more complex mechanisms of steroid hormone/ <i>let-7</i> action in vertebrates	124
3.4.1	Steroid action in <i>D. melanogaster</i> and humans show some parallels	125
3.4.2	Various aspects of <i>let-7</i> function are conserved in bilateria	125
3.4.3	<i>let-7</i> acts as a tumor suppressor in humans	127
References		I
Appendix		XIX
Ecdysteroids affect <i>Drosophila</i> ovarian stem cell niche formation and early germline differentiation: Supplementary Material		XIX
The Histone H2B Monoubiquitination Regulatory Pathway is Required for Differentiation of Multipotent Stem Cells: Supplementary Material		XXXI
A Genome-Wide Survey of Sexually Dimorphic Expression of <i>Drosophila</i> miRNAs Identifies the Steroid Hormone-Induced miRNA <i>let-7</i> as a Regulator of Sexual Identity: Supplementary Material		LXXI
Soma influences GSC progeny differentiation via the cell adhesion-mediated steroid- <i>let-7</i> -Wingless signaling cascade that regulates chromatin dynamics: Supplementary Material		CXII
Acknowledgments		CXXVIII
Curriculum vitae		CXXXI

Abstract

Adult stem cells are found in most adult tissues where they are responsible for replacing cells that are lost due to turnover or injury. They have the unique ability to give rise to differentiated progeny, while at the same time maintaining the stem cell population. In order to preserve tissue homeostasis, these two processes: maintenance *versus* differentiation have to be tightly regulated. It was shown that surrounding cells form a specific microenvironment, the stem cell niche, that controls the stem cell behavior. The results described in the present thesis show that stem cell progeny differentiation also requires specific interactions with the surrounding cells, the differentiation niche.

The *D. melanogaster* germarium provides an excellent model to study these interactions since adult stem cell maintenance and adult stem cell progeny differentiation can be analyzed in the same well characterized and easy to genetically manipulate organ.

We found that components of the ecdysteroid signaling pathway play a role in the germarium. It had been shown previously that ecdysteroids are required for later stages of oogenesis; the present thesis describes how ecdysteroids control the progression through the early stages of germline differentiation. Ecdysone signaling perturbations lead to a germline stem cell progeny differentiation delay. These delayed germline cells display a stem cell-like chromatin state; however, based on the analysis of specific markers, they are not stem cells. Differentiation markers also are not present, indicating that these germline cells are delayed at the pre-cystoblast to cystoblast transition.

Interestingly, we found that the ecdysone signaling pathway is acting on the germline cells in a cell non-autonomous way via the somatic germarial cells, a process that requires the spatially restricted cofactors Taiman and Aprupt, activator and inhibitor of ecdysone signaling. Deficit of ecdysone signaling during the development leads to enlarged functional niches, somatic cell differentiation defects and a confused sexual identity. The somatic escort cells fail to appropriately differentiate in the absence of functional ecdysone signaling: shape, division and cell adhesive characteristics are altered; cytoplasmic protrusions, required for interacting with the germline, are not formed and escort cells form a columnar-like epithelium. The cell adhesion proteins Armadillo and DE-Cadherin are found at higher levels in mutant escort cells; which subsequently affects the germline cells responsiveness to Wg signaling. Dampening of Wg signaling in the germline leads to a germline differentiation delay.

Furthermore, the miRNA *let-7* is modulating the tissue and time specific response to ecdysone via regulating the levels of Abrupt, that is both an inhibitor

of ecdysone signaling and a potent regulator of epithelial cell fate. miRNA *let-7* is induced by steroids, targets Ab and acts in a feedback loop to ensure the robustness of ecdysone signaling in escort cells in response to changing internal and external conditions such as aging, stress and nutrition.

Abbreviations

Ab	Abrupt
Arm	Armadillo
Bam	Bag of marbles
Bgcn	Benign gonial cell neoplasm
<i>C. elegans</i>	<i>Caenorhabditis elegans</i>
Br	Broad
Cad	Cadherin
CB	Cystoblast
CpC	Cap cell
<i>D. melanogaster</i>	<i>Drosophila melanogaster</i>
<i>D. rerio</i>	<i>Danio rerio</i>
DAF-12	Dauer formation 12
Dpp	Decapentaplegic
Dsx	Doublesex
EC	Escort cell
EcR	Ecdysone receptor
EGFR	Epidermal growth factor receptor
EMS	Ethyl methanesulfonate
FC	Follicle cell
FSC	Follicle stem cell
Gbb	Glas bottom boat
GSC	Germline stem cell
H2Bub1	Histone H2B ubiquitination
Hh	Hedgehog
ISWI	Imitation SWI
Med	Medea
miRNA	microRNA
Nanos	Nos
NURF	Nucleosome remodeling factor
Pan	Pangolin
piRNA	PIWI interacting RNA
pre-CB	pre-cystoblast
Pum	Pumilio
RISC	RNAi induced silencing complex
siRNA	small interfering RNA
SS	Spherical spectroosome
SSC	Single spectroosome cell
Stet	Stem cell tumor

Sxl	Sex lethal
Tai	Taiman
TF	Terminal filament cells
Tra	Transformer
Upd	Unpaired
Usp	Ultraspiracle
Wg	Wingless

List of Figures

1.1	<i>D. melanogaster</i> germarium is a model for research on adult stem cells	7
1.2	GSCs self renew and give rise to differentiating progeny	8
1.3	GSC maintenance and germline differentiation are regulated by various signaling pathways	15
3.1	Ecdysone signaling acts on germline differentiation in a cell non-autonomous way	117

1 Introduction

1.1 Stem cells can self-renew and generate differentiated cells

Stem cells have unique abilities: upon division, they give rise to both, a new stem cell and a cell that can differentiate into at least one specialized cell type. These two processes – maintenance of the stem cell population versus generation of differentiated cells – have to be very tightly balanced to preserve tissue homeostasis (maintenance of the proper cell number and type). Depending on source and potency, several types of stem cells can be distinguished: pluripotent embryonic stem cells are capable of generating all different cell types of the adult body, whereas tissue specific stem cells in the adult organism can give rise to only a subset of cell types. In general, stem cells have an enormous potential for regenerative medicine: however, each of the different stem cell types offers certain advantages and disadvantages with respect to availability, differentiation potential or probability of teratoma formation.

1.1.1 Pluripotent stem cells have a great potential in regenerative medicine

Embryonic stem cells are derived from the inner cell mass of pre-implantation blastocysts. Having the capability to produce all three germ layers, they are called pluripotent. In 1981 mouse embryonic stem cells were successfully generated (Evans and Kaufman, 1981; Martin, 1981) and 18 years later human embryonic stem cells were produced (Thomson et al., 1998). Using specific culture conditions, embryonic stem cells can be kept in culture (Smith et al., 1988) for a long time and it is possible to induce differentiation into different cell types including blood cells, pancreatic insulin-producing cells, neural cells, cardiomyocytes etc. (reviewed in Volarevic et al., 2011).

Despite of the great potential in medicine that embryonic stem cells have because of their regenerative capacity, there are a number of problems. First, undifferentiated pluripotent cells cannot be used for transplantation due to the risk of forming teratomas, tumors containing derivatives of several or all three germ layers. Only a few undifferentiated cells would be sufficient to form teratomas, which is one of the main reasons why the direct clinical use of pluripotent stem cells remains problematic. Instead, research is focused on the generation of homogeneous, completely differentiated cell populations (reviewed in Ho et al., 2012).

Second, generation of embryonic stem cells from *in vitro* fertilized eggs involves the destruction of human embryos, which is morally objectionable. *In vitro* fertilization involves the surgical retrieval of several mature eggs after an extensive treatment with "fertility drugs". In an attempt to maximize the chances of obtaining a viable blastocyst, typically a large number of donated eggs are fertilized. Since frequently not all fertilized eggs are implanted, this results in a number of "excess" blastocysts that are used for research. One way to circumvent these ethical problems is to directly reprogram somatic cells to a pluripotent status.

Somatic cells can be reprogrammed to a pluripotent state The reprogramming of fully differentiated somatic cells to a pluripotent stage is remarkable and can be achieved by transferring nuclear contents into oocytes, by cell fusion or by induction using transcription factors.

During the process called nuclear transfer, nuclei of differentiated cells are inserted into a donated egg cell that was denucleated before. This method was used successfully for the first time in 1962 by the laboratory of John Gurdon who generated tadpoles by inserting differentiated adult frog cells into unfertilized eggs (Gurdon, 1962). Somatic nuclear transfer was also adapted to mammals and resulted in the birth of live lambs from adult mammary gland tissue derived cells (Wilmut et al., 1997). The fusion of two cells can produce proliferating cells with fused nuclei (hybrids) or not-proliferating cells with several nuclei. Studies involving fused cells showed for the first time, that the differentiated state of a cell is not totally fixed, but rather the consequence of a complex regulation involving several factors. Differentiated somatic cell types can either be reprogrammed to produce genes typical for another differentiated cell type or pluripotent cells after fusion with embryonic stem cells (reviewed in Yamanaka and Blau, 2010). Induced pluripotent stem cells offer another option for generating cells that have similar characteristics as embryonic stem cells. It was shown by Takahashi and Yamanaka, 2006 and Takahashi et al., 2007 that, using a combination of four different factors, induced pluripotent stem cells can be generated from differentiated adult human fibroblasts. A number of laboratories work on the possible applications of induced pluripotent stem cells in modeling certain diseases, drug screening and regenerative therapy (reviewed in Yamanaka, 2009). Whether or not induced pluripotent stem cells and embryonic stem cells are remarkably different from each other is still controversial in the field, but certainly both cell types share a number of characteristics (reviewed in Blanpain et al., 2012).

Usage of induced pluripotent stem cells in clinical trials is problematic Generating pluripotent cells using a patients own somatic cells would allow the generation of tissue that is compatible to the donor, eliminating the risk of graft-versus-host-diseases. In addition, inducing pluripotency in differentiated cells does not require human blastocysts or oocytes, the generation of which involves extensive hormone treatment in order to stimulate the maturation of several oocytes per cycle for donation and subsequent destruction on human embryos. However, a number of problems remain to be solved before induced pluripotent stem cells can

be used for regenerative therapies. Introducing oncogenes like C-Myc to induce pluripotency into cells is of course highly problematic if the cells are supposed to be used for therapy. Furthermore, most studies on induced pluripotent stem cells have used viral methods to introduce genetic factors. Since this can lead to additional mutagenesis, it is not an acceptable method for clinical applications. Both the factors that are introduced for reprogramming and the method that is used to introduce these factors into the cell have to be carefully chosen and even though a lot of progress has been made in these fields, there are still relatively few clinical trials based on induced pluripotent stem cells (reviewed in Ho et al., 2012 and Daley, 2012).

1.1.2 Direct lineage conversion illustrates cell plasticity

Differentiation was classically viewed as irreversible with the undifferentiated cell on top of the hierarchy and as it moves towards terminal differentiation, the lineage potential becomes restricted and the cellular plasticity is reduced. Since Waddington and Kacser, 1957 illustrated this "epigenetic landscape" model in 1957, several findings necessitated an expansion of this classical model. First, as was discussed in the previous paragraph, the somatic epigenome can indeed be reprogrammed to a pluripotent state and interestingly, recent reports suggest that spontaneous dedifferentiation into stem-like stages can occur even in normal mammalian cells. Differentiation is thus not a unidirectional process but can be reverted. Second, terminally differentiated cells can be directly converted into another lineage, without going through a pluripotency state, a process that is also called transdifferentiation. Using specific transcription factors or miNRAs, cells can transdifferentiate into a cell type originating from the same or another germ layer (reviewed in Ladewig et al., 2013). Interestingly, some somatic cell types can be easily converted while others are more resistant (reviewed in Elshamy and Duhe, 2013). However, it is not clear, to which extent the converted cell can retain epigenetic marks from the donor cell. Altogether, a certain cell fate is not irrevocable and cells display a remarkable plasticity.

1.1.3 Adult stem cells are controlled by specialized compartments: niches

In contrast to the pluripotent embryonic stem cells that are capable to form all the different cell types that can be found in the adult organism, adult stem cells only have a limited differentiation potential and are multi-, oligo- or unipotent. They were found in virtually all human tissues and are required for growth, homeostasis and replacement of damaged cells after injury (regeneration) and under certain physiological and pathological conditions. A specific microenvironment, integrating local and systemic factors, that is also called the stem cell niche regulates the stem cells behavior. The stem cell niche hypothesis, according to which stem cells reside in these spatially restricted compartments of the tissue, was first developed from a study on hematopoietic stem cells by Schofield, 1978. The different cellular

and acellular components of the stem cell niche: secreted factors, cell adhesion, extracellular matrix, neural inputs, vascular network and mechanical cues regulate maintenance and self-renewal of the stem cells.

Model organisms are essential for studying stem cell-niche biology The identification of stem cell niches *in vivo* – especially in vertebrates – is rather difficult because stem cells are rare and specific stem cell markers are often not available or not reliable (reviewed in Morrison and Spradling, 2008). Well characterized mammalian adult stem cell niches include hematopoietic stem cells, neural stem cells, spermatogonial stem cells, satellite muscle cells, stem cells in intestinal epithelium, hair follicle bulge and interfollicular epidermis (reviewed in Walker et al., 2009 and Zapata et al., 2012). In contrast, model organisms such as *C. elegans* and especially *D. melanogaster* provide a variety of sophisticated genetic tools and thus studies in these animals first revealed several important features of stem cell-niche communication (reviewed in Jones and Wagers, 2008). The germline stem cell (GSCs) niche in the germarium of *D. melanogaster* is widely used and is today one of the best studied stem cell niches (see Section 1.2, page 5).

Maintenance and differentiation of adult stem cells have to be regulated by somatic niches Some stem cell niches have to balance maintenance and differentiation of the stem cell population throughout an individual's lifetime to continuously produce differentiated cell progeny without depleting the stem cell population – like stem cells in gut and epidermis. Other stem cells that give rise to long lived progeny like in skeletal muscle have to only differentiate if necessary because of injury or disease. Hematopoietic stem cells in turn have to fulfill both functions: continuous production of blood cells and responsiveness to external stimuli. In order to always provide the required amount of differentiated progeny, adult stem cells have to modulate their activity in response to the overall body status. That is, they have to respond to various stimuli like temperature, mechanical signals, nutrient situation, inflammatory and hormonal factors. Whereas in some cases, the stem cells are directly influenced by these signals, many external signals act on the niche cells and influence the stem cells in a cell non-autonomous fashion. Communication between the niche cells and between niche and stem cells is therefore essential in order to ensure that adult stem cells keep the correct balance between self renewal and differentiation. The niche controls its stem cell population via both signaling molecules and by physical attachment, mediated via cell adhesion molecules.

Adhesive contacts are major elements of stem cell-niche relations First evidence showing that adherens junctions – cell-cell contacts that are formed by homophilic interactions of Cadherin (Cad) proteins – came from studies in the *D. melanogaster* germarium. It was shown, that disrupting the function of *Cad* leads to a loss of stem cells (Song et al., 2002). Comparable analysis in mammalian models are, due to the complex architecture of tissue and stem cell niches,

rather difficult. However, it was suggested that N-Cad plays a role in adhering hematopoietic stem cells to their niche (reviewed in Xi, 2009). Integrins are transmembranous cell adhesion molecules that act as heterodimers to link the cell to the extracellular matrix. Again, first reports about integrins being required for adult stem cells came from studies in *D. melanogaster*: the follicle stem cells were shown not only to contact neighboring cells via DE-Cad, in addition they require integrin mediated contact to the basal lamina in order to maintain their position. Integrins also were shown to play a role in linking other stem cells including *D. melanogaster* intestinal stem cells, mouse epidermal, hair follicle and mammary stem cells to the basement membrane (reviewed in Xi, 2009). In addition to physically attaching stem cells to support cells or basal lamina, integrins and Cad also regulate the cell division plane in different stem cells including those in *D. melanogaster* neuroepithelium or mammalian skin (reviewed in Marthiens et al., 2010).

Establishment and turnover of niches affects stem cells Because of both, the complex interactions between niche and stem cells and the necessity to precisely regulate the stem cell behavior, it is clear that establishment and maintenance of the niche have to be tightly regulated as well. Stem cells and the niche can either co-develop or form independently from each other (reviewed in Jones and Wagers, 2008). Muscle satellite cells originate from the same precursors as their stem cells and it was suggested that epithelial stem cells are capable to generate their own niche (reviewed in Jones and Wagers, 2008). Other stem cells, like the hematopoietic and primordial stem cells, encounter different niches throughout the development. Hematopoietic stem cells are committed during development in a process that involves multiple hematopoietic sites including the yolk sac, the placenta, the fetal liver and the aorta-gonad-mesonephros region (reviewed in Christensen et al., 2004; Mikkola and Orkin, 2006). In the *D. melanogaster* ovary, niche and stem cells originate independently from each other and somatic gonadal cells are formed even in the absence of GSCs (Margolis and Spradling, 1995). Similar to that situation, fully competent Sertoli cells are also formed in aspermic gonads. Besides niche establishment, stem cell activity can also be controlled by the niche cell maintenance and turnover. The regenerative capacity of different tissues like skin, liver, blood and muscle decreases with age. Apart from cell-autonomous changes in the stem cells, stem cell niches also contribute to this decreasing ability to renew the tissue. Furthermore, it was shown in different systems that the age dependent changes in stem cell behavior can be reverted by restoring the niche function (reviewed in Voog and Jones, 2010).

1.2 The *D. melanogaster* germarium – a model for GSC niche communication

The first – and until now – best characterized stem cell niche is the one in the female *D. melanogaster* germarium (Xie and Spradling, 2000). The *D. melanogaster*

ovary is a paired organ that each consists of 13–16 ovarioles. Each ovariole contains the progressively developing egg chambers with two to three GSCs at the apical tip (see Figure 1.1, page 7). If a GSC divides, one GSC will remain as a stem cell and the other one – the pre-cystoblast (pre-CB) – will undergo differentiation to form the cystoblast (CB). After four rounds of division with incomplete cytokinesis the cysts will be enveloped by follicle cells (FCs), generated by follicle stem cells (FSC) and leave the germarium. The GSCs can be easily identified by their characteristic spherical cytoskeletal organelles – the spectrosomes. Upon CB/cyst division and differentiation the spectrosomes elongate and branch to form the fusome (Lin et al., 1994). Only GSCs and CBs therefore display a single spherical spectrosome (single spectrosome cells; SSCs), whereas cysts have branched fusomes. Since spectrosomes and fusomes can be visualized using specific antibodies, they are important markers for characterizing germline cell identity. Apart from the germline cells, the germarium houses several somatic cells. The terminal filament cells (TFs) at the apical end of the germarium hold the different ovarioles of an ovary whereas the cap cells (CpCs) – five to seven in each germarium – attach the GSCs. In addition, escort cells (ECs, also called inner germarial sheath cells in some publications) that form long cytoplasmic extensions with which they encase the developing germline cells, line the germarium.

The *D. melanogaster* germarium (see Figure 1.1, page 7) thus represents the key features of adult stem cell niches and contains a limited number of cells that can be easily identified and analyzed. GSCs are attached to the CpCs by cell-cell adhesions. In addition, signaling from the niche allows stem cell maintenance and represses differentiation, whereas cells that are even only one cell diameter further away from the niche cannot receive the niche signaling and lose stem cell characteristics. The germarium therefore provides an amazing and valuable model for analyzing key questions in stem cell biology: Which characteristics are necessary and sufficient to maintain the stem cell state? How does the surrounding somatic niche integrate systemic signals to control stem cells? How are niches and stem cells formed during development? Which factors are important for the first steps of germline differentiation? Since the germarium had been established as a model in the 1990s, our knowledge has expanded greatly, nevertheless a number of questions remain to be answered.

1.2.1 The somatic niche cells signal to the GSCs

The stem cell niche in the germarium is formed by CpCs, TFs and ECs, with the CpCs being particularly important to adhere the GSCs. Because of the close contact between GSCs and somatic cells, it is not feasible to ablate all CpCs, TFs or ECs from a germarium. Removing specific genes from all TFs and CpCs of single ovarioles, however, is not possible due to their polyclonal origin. Nevertheless, the sophisticated genetic tools that are available in *D. melanogaster* allowed the identification of several signaling pathways that are required for germline control (see Figure 1.3, page 15 for an overview).

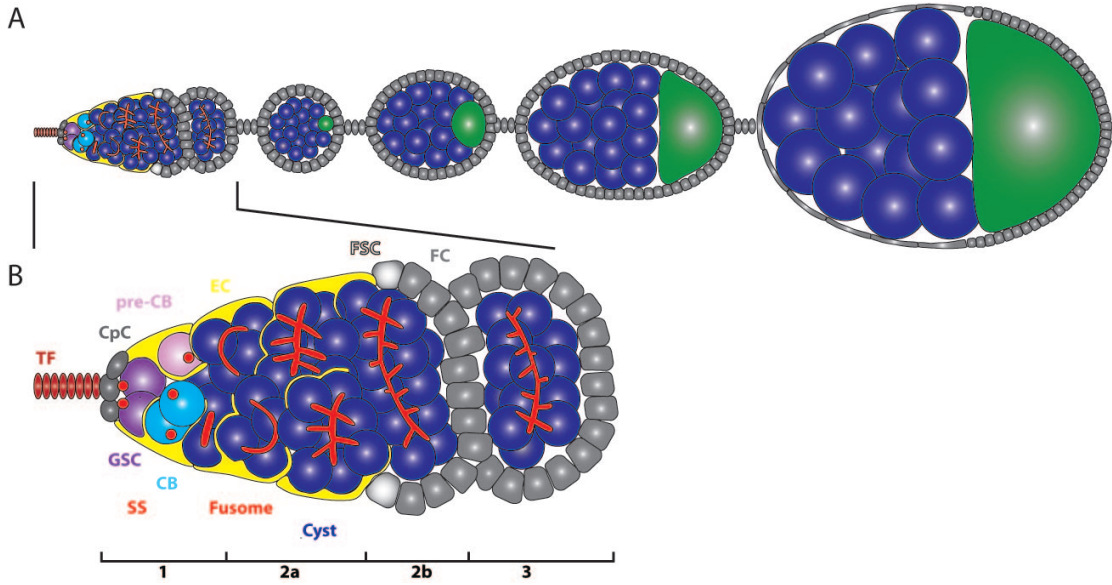


Figure 1.1: *D. melanogaster* gerarium is a model for research on adult stem cells (A) An ovariole with the progressively developing egg chambers and the gerarium at the anterior. Each egg chamber starts in the gerarium as a cyst containing 16 germ cells; one of them will become the oocyte (green) and the others will be nurse cells (dark blue). (B) The gerarium contains GSCs (purple) that are directly attached to the CpCs (dark gray). After the division, one stem cell daughter, the CB (turquoise) differentiates via the intermediate pre-CB (light purple) stage and undergoes four more rounds of division, forming the cyst (dark blue). GSCs and CBs contain spherical spectrosomes (SS, red) and are therefore called single spectrosome cells (SSCs), whereas cysts have branched fusomes (red). ECs (yellow) outline the gerarium and form long cytoplasmic protrusions that envelop the developing cysts. In region 2b, FCs (light gray), generated by FSCs (gray), surround the developing cysts, whereas the TFs (dark red) attach the individual ovarioles.

Bam is excluded from the GSCs by TGF- β signaling The master differentiation factor in the female germline is the protein Bag of marbles (Bam) that is excluded from the GSCs via TGF- β signaling. CpCs and TFs secrete the TGF- β ligands Gbb (Glass bottom boat) and Dpp (Decapentaplegic) (Song et al., 2004; Xie and Spradling, 1998). Upon receptor activation in GSCs, the transcription of the differentiation factor Bam is repressed: the *D. melanogaster* Smad Mad becomes phosphorylated upon TGF- β signaling, forms a complex with its partner Medea (Med), binds to the transcriptional silencer elements of the *bam* promoter and thereby inhibits its transcription (Chen and McKearin, 2003; Jiang et al., 2008; Song et al., 2004). After GSC division along the anterior-posterior axis of the germarium, only the anterior daughter cell that remains within the niche receives the signaling from the niche. In the other more proximal daughter cell, the differentiation factor Bam becomes expressed and the cell will differentiate.

GSCs differentiate via an intermediate pre-CB stage Few markers are available to follow the early steps of germline differentiation from GSC to CB in detail. GSCs, pre-CBs and CBs have single spherical spectrosomes; however, GSCs can be distinguished from CBs via two criteria: position (GSCs are directly attached to CpCs) and expression of *bam* which is present in CBs, but not in GSCs. Gilboa et al., 2003 and Ohlstein and McKearin, 1997 observed single cells away from the niche that lack Bam protein, suggesting that an intermediate pre-CB stage exists between GSCs and CBs. Thus, the germline differentiation process towards CB is gradual with low levels of pMad still found in pre-CBs/CBs and *bam* expression starting at the pre-CB/CB transition (Gilboa et al., 2003; Kai and Spradling, 2003a; Ohlstein and McKearin, 1997) (see Figure 1.2, page 8).

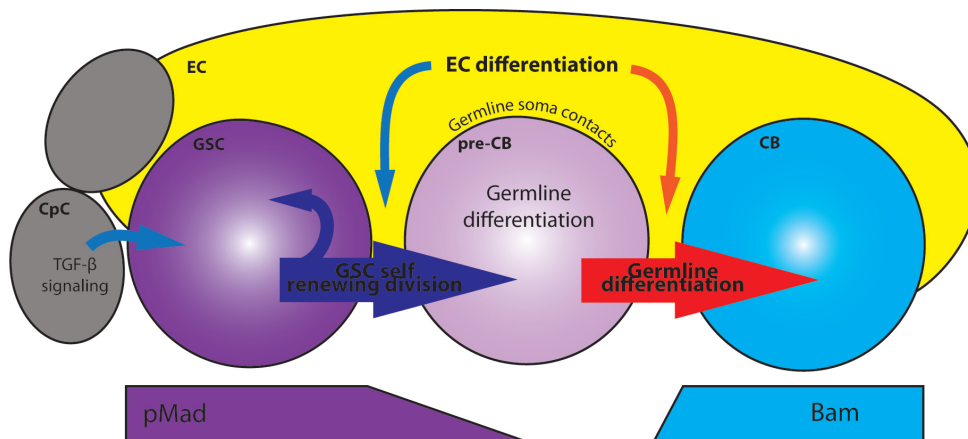


Figure 1.2: GSCs self renew and give rise to differentiating progeny CpCs (gray) provide "self renewal" signaling to the GSCs (purple) and thus are a major part of the GSC niche. Mad is phosphorylated in response to TGF- β signaling from the CpCs in the GSCs; at the pre-CB (light purple) to CB (turquoise) transition, *bam* is expressed. Via interacting with the germline, ECs (yellow) promote germline differentiation.

A functional niche is necessary and sufficient to maintain GSCs Different from other systems, GSC daughters are not thought to be inherently different. Instead, it seems that both cells compete for the available space in the niche, and the daughter cell outside the niche will not receive signaling from the niche and differentiate. In agreement with this, both GSC daughters can be recruited to become GSCs to replace lost ones (Xie and Spradling, 2000) and even four- or eight-cell cysts can break down, de-differentiate and repopulate the niche (Kai and Spradling, 2004). Which GSC daughter differentiates and which one will be maintained as the stem cell is therefore exclusively determined by interactions with the niche. The TGF- β signaling pathway that prevents *bam* to be expressed in the GSCs is particularly important for GSC maintenance: an overactivation of the TGF- β pathway via overexpressing the ligand *dpp* or a loss of the differentiation factor Bam have dramatic phenotypes and can block differentiation completely (McKearin and Ohlstein, 1995; McKearin and Spradling; Song et al., 2004; Xie and Spradling, 1998). Remarkably, the GSCs that respond to TGF- β signaling and the CBs that enter the differentiation program ruled by Bam are only one cell diameter apart from each other. This steep gradient of TGF- β reception in the germarium has to be tightly regulated: different mechanisms are in place to limit the range of Dpp production, stability and diffusion, to modulate the capacity of a cell to respond to TGF- β ligands and to cell-autonomously derepress *bam* expression in the CBs.

Dpp diffusion is limited to GSCs The type IV collagens Viking and Dcg1 can bind Dpp and Viking was shown to be present in the germarium between the somatic niche cells and between the GSC and niche cells. Dpp binding to type IV collagens thus seems to limit Dpp diffusion (Wang et al., 2008b). The heparin sulfate glycoprotein Dally is as well critical for GSC maintenance. It is highly expressed in CpCs and ectopic expression of Dally in somatic germarial cells leads to a higher number of GSC-like cells, suggesting that the presence of Dally contributes to limit the range of niche signaling (Guo and Wang, 2009; Hayashi et al., 2009).

JAK/STAT signaling controls Dpp signaling in the female germarium While the TGF- β signaling pathway is generally considered the most important one in the female germarium, the JAK/STAT signaling pathway is of similar importance for the male GSCs. Nevertheless, JAK/STAT signaling is also required in the female germarium. In *D. melanogaster* JAK/STAT signaling is activated if cytokines of the Unpaired (Upd) family are secreted and bind to the receptor Domeless which activates the Janus kinase, Hopscotch. Hopscotch then phosphorylates the transcription factor STAT92E, which translocates to the nucleus and activates the expression of target genes. The JAK/STAT signaling pathway is active in the somatic cells of the germarium: in TFs, CpCs and ECs (Decotto and Spradling, 2005; Lopez-Onieva et al., 2008). Loss of JAK/STAT activity leads to GSC loss, but interestingly it was shown that JAK/STAT is not required cell-autonomously in the GSCs. Instead it is required in the CpCs and ECs where it

positively regulates the expression of *dpp*. In agreement with this, ectopic over-expression of *Upd* in the somatic cells of the germarium leads to a higher number of SSCs (single spectrosome cells). Similar to GSCs, but unlike differentiating germline cells, these SSCs display pMad and Dad-lacZ, a reporter of TGF- β signaling pathway activity. This proposes a model in which JAK/STAT signaling in the niche is required to regulate the levels and range of Dpp signaling (Decotto and Spradling, 2005; Lopez-Onieva et al., 2008; Wang et al., 2008a).

CBs become insensitive to TGF- β signaling Cell-autonomous mechanisms are also required for transduction of the signal: the serine/threonine kinase Fused that acts in concert with the E3 ligase Smurf regulates the ubiquitination and degradation of the TGF- β receptor Thickveins in the CBs, which therefore quickly become insensitive to TGF- β signaling (Casanueva and Ferguson, 2004; Xia et al., 2010).

Several pathways regulate germline cells in the germarium Few other pathways with no known connection to TGF- β signaling are thought to be important for GSC maintenance. The first one that was suggested to control *D. melanogaster* GSCs is Hedgehog (Hh) signaling. Hh itself is present in TFs and CpCs but *hedgehog* mutant GSCs show only minor division defects (Forbes et al., 1996a,b). *fs(1)Yb* encodes a novel hydrophilic protein that is specifically expressed in the TFs and is required for the maintenance of GSCs. It controls Hh and Piwi levels by an unknown mechanism (King and Lin, 1999; King et al., 2001). In addition, the nuclear membrane protein Otefin was suggested to interact with Med, probably relocating the *bam* locus to the nuclear periphery, allowing for its silencing in the GSCs. In the absence of Otefin, GSCs cannot be maintained and are lost; however, a recent report suggested that GSCs are not lost by differentiation but due to cell death (Barton et al., 2013; Jiang et al., 2008). Altogether, a variety of signaling pathways act in concert to control germline differentiation, with or independently of TGF- β signaling.

1.2.2 *bam* expression switches on a differentiation program in CBs

Overexpressing *bam* is sufficient to induce GSCs differentiation and on the other hand, reduced Bam levels lead to the accumulation of GSC-like cells, illustrating the importance of *bam* as a master differentiation gene (McKearin and Ohlstein, 1995; McKearin and Spradling; Ohlstein and McKearin, 1997). In agreement with this, several mechanisms are in place to control *bam* expression (see Section 1.2.1, page 6). However, despite the importance of Bam, there is relatively little information about how it promotes differentiation.

Bam potentially acts via repressing Nos Bam forms a complex with its cofactor Benign gonial cell neoplasm (Bgen) that represses the expression of *nanos* (*nos*),

possibly via *nos* 3'UTR (Li et al., 2009). In agreement with this, it was found that *bam* expression is reciprocally to the one of *nos* (Li et al., 2009). Nos and its partner Pumilio (Pum) are components of a translational repressor complex (reviewed in Shen and Xie, 2010) and were shown to be critical for the maintenance of GSCs (Wang and Lin, 2004). The Nos-Pum complex supposedly acts via downregulating differentiation promoting mRNAs, most of which remain to be identified. However, one mRNA that is downregulated by the Nos-Pum complex is Brain tumor (Brat): Brat protein is limited to CBs and differentiating cysts. It promotes differentiation via forming a complex with Pum that inhibits translation of Mad and the growth regulator dMyc (Harris et al., 2011). Downregulating Mad in CBs limits the ability of the CBs to transduce the signal of Dpp or Gbb that may still be present in low levels and thereby contributes to limiting the range of Dpp signaling to the GSCs.

The strength of TGF- β signaling is carefully shaped In summary, several mechanisms are in place to assure that only GSCs receive niche signaling and to promote quick derepression of the respective factors in differentiating germline cells. However, it seems that the TGF- β signaling pathway is the most important one, with many other pathways influencing the strength and range of the signaling. This is further illustrated by the fact that overexpression of *dpp* in somatic cells leads to a differentiation block of germline cells, indicating that high Dpp levels can overrule antagonists (Song et al., 2004).

1.2.3 Adherens junctions between GSCs and CpCs are required for GSC maintenance

As mentioned before, adherens junctions between GSCs and CpCs are required to maintain GSCs in the niche. DE-Cad, a classical Cad (encoded by a gene called *shotgun*) is required for the formation of adherens junctions. Armadillo (Arm), the β -catenin homolog binds to the cytoplasmic domain of DE-Cad, linking adherens junctions to the cytoskeleton via α -catenin. Both DE-Cad and Arm were shown to be present at high levels between CpCs and GSCs and are crucial to recruit GSCs to the niche during development and to maintain them there (Song et al., 2002). In fact, the differentiation factor Bam itself was shown to reduce the levels of DE-Cad in complex with Bgen and the translation initiation factor eIF4A (Jin et al., 2008; Shen et al., 2009). The quick downregulation of DE-Cad in differentiating CBs further assures, that accidentally differentiating GSCs leave the niche and become replaced by functional GSCs. Interestingly, GSCs with even only slightly lower levels of DE-Cad are outcompeted by other GSCs and are lost from the niche (Jin et al., 2008). The strength of cell adhesion between CpCs and GSCs and the precise levels of DE-Cad in a given GSC therefore provide an additional level to control the behavior of GSCs: insulin signaling decrease for example leads to lower levels of DE-Cad and loss of GSCs (Hsu and Drummond-Barbosa, 2009).

1.2.4 ECs are required for the differentiation of the GSC progeny

ECs or – as they are sometimes called – inner germarial sheath cells line the germarium in regions 1 and 2a. They form long cytoplasmic extensions that envelope the developing CBs. It had been suggested, that ECs are maintained by a population of 4–6 escort stem cells and that their progeny moves along with the cysts through the germarium until they are lost by apoptosis (Decotto and Spradling, 2005). In contrast to this, it was recently shown that ECs show little movement and are stationary. Even though they are capable of dividing, they are mitotically quiescent most of the time, unless the ratio of ECs to germline cells increases. ECs do undergo some slow turnover, but the lost cells are replaced by dividing neighboring ECs and not by escort stem cells (Kirilly et al., 2011; Morris and Spradling, 2011).

Differentiating germline cells signal to the ECs ECs are of great importance for the differentiating germline cells: they form long cytoplasmic extensions that are believed to physically protect the differentiating CBs from the niche signaling. In addition, ECs and germline cells actively communicate, and perturbing these interactions leads to malformations and differentiation defects in both ECs and germline: Stem cell tumor (*Stet*), a Rhomboid homolog is an intramembrane protease that is required for the maturation of the epidermal growth factor receptor (EGFR) ligands Spitz, Gurken or Keren in the germline. Upon ligand secretion, the EGFR pathway is activated in the surrounding somatic ECs which leads to the activation of downstream signaling cascades including the mitogen-activated protein kinase (MAP kinase), the phosphatidylinositol 3-kinase and phospholipase C- γ pathways (Schulz et al., 2002; Yarden and Shilo, 2007). If *stet* function is removed from the germline, germaria with ectopic Dpp activity and a higher number of SSCs were observed, a phenotype that was accompanied by a disrupted formation of cytoplasmic extensions (Liu et al., 2010; Schulz et al., 2002). Interestingly, the EGFR signaling pathway in the somatic ECs is required to limit the expression of the glypican Dally, a Dpp stabilizing protein. Altogether, this proposes a model in which the activation of the EGFR pathway in the somatic ECs by ligands coming from the germline, is required to restrict the Dpp diffusion and thereby to enable CB differentiation. It was also shown that the differentiation status of the germline cells in the germarium is important for the maintenance of ECs extensions and ECs themselves. If GSCs are lost for example due to artificial *bam* overexpression, germaria also loose all ECs, indicating that the presence of GSCs is required for EC maintenance (Margolis and Spradling, 1995; Xie and Spradling, 2000). But then, germaria full of undifferentiated germline cells due to *bam* loss of function or overexpression of *dpp* also do not show cytoplasmic ECs protrusions (Kirilly et al., 2011). And last, ECs at different positions in the germarium show different morphologies, depending on the germline cells that they are associated with (Kirilly et al., 2011). These examples illustrate, that ECs

cannot properly form protrusions and even cannot be maintained in the absence of correctly differentiating germline cells.

ECs contribute to the GSC niche ECs are crucial for both the maintenance of GSCs and the differentiation of GSC progeny. They also express the TGF- β ligand Dpp which is mainly produced by CpCs and which is essential for GSC maintenance (Casanueva and Ferguson, 2004; Xie and Spradling, 2000; Zhu and Xie, 2003) and eliminating ECs from the germarium leads to GSC loss (Chen et al., 2011). Recently it was furthermore suggested, that ECs and CpCs cooperate via Hh signaling to regulate the levels of TGF- β signal that is transmitted to the GSCs. The CpCs are decorated with long filopodia or cytonemes via which the signal is transmitted to the ECs where it activates the transcription of *gbb* and *dpp* (Rojas-Rios et al., 2012). In summary, even though it seems to be clear, that CpCs are the main source for Dpp and Gbb, ECs also are an important part of the GSC niche in the *D. melanogaster* germarium.

Cytoplasmic EC protrusions are crucial for cyst differentiation Remarkably, besides its function for GSC maintenance, ECs are also required for cyst differentiation: as was mentioned before, it is thought that ECs send signals to the developing cysts and that EC protrusions also physically shield the germline from the niche signaling. Disturbing the formation of ECs extensions via downregulating the actin-regulator *cappuccino* leads to an increase of SSCs, which is a hallmark of delayed or blocked germline differentiation (Kirilly et al., 2011). Similarly, knocking down the GTPase Rho specifically in ECs disturbs the formation of ECs extensions, which cell non-autonomously affects the germline differentiation (Kirilly et al., 2011). The JAK/STAT signaling pathway is active in CpCs and ECs and perturbed JAK/STAT signaling leads to a disturbed EC morphology that results in a higher number of germline cells (Decotto and Spradling, 2005; Wang et al., 2008a). These results strongly suggest, that the proper formation of EC protrusions is required to create a microenvironment in which the germline cells receive differentiation promoting, but not TGF- β signaling from the CpCs and can differentiate. ECs therefore seem to have a dual role: they are required for both the maintenance of adult GSCs and for the differentiation of the GSC daughters. Also, it is becoming clear that germline progeny differentiation is not the default choice for germline cells that are not maintained as stem cells as the consequence of lacking signaling from the GSC niche. Instead, germline differentiation requires both appropriate physical interaction and communication with the surrounding somatic ECs. The nature of these interactions and the relevant signaling pathways remain poorly understood.

Systemic steroid hormone signaling is required for EC morphology In addition to the pathways already known to be required for EC morphology, we were recently able to show that ecdysone, the main steroid hormone in *D. melanogaster* is required for proper EC morphology. If ecdysone signaling is perturbed, ECs

lose their squamous shape and cytoplasmic protrusions and instead resemble a columnar-like epithelium. This affects the germline differentiation in a cell non-autonomous way, resulting in an increased number of cells at the GSC to CB transition, that are delayed in differentiation (König et al., 2011). This study is the first evidence for hormone signaling acting on the germline cells via ECs.

labeled by various signaling pathways The niche for the GSCs (purple) is formed by CpCs (gray), TFs (dark red), and ECs (yellow). The differentiating GSC daughter is the CB (turquoise) that is enveloped by cytoplasmic protrusions, sent from the ECs. Transcription of the master differentiation gene *bam* is inhibited by TGF- β signaling: Dpp and Gbb, sent from the niche lead to the phosphorylation of Mad in the GSCs. pMad partners with Med and translocates to the nucleus where it inhibits *bam* expression. CBs do not receive TGF- β signaling from the niche and *bam* therefore becomes expressed, leading to differentiation. Bam forms a complex with its partner Bgc and represses Nos, which – together with its partner Pum – is necessary for the maintenance of GSCs by repressing differentiation promoting mRNAs like Brat. Several other mechanisms contribute to the sharp gradient of TGF- β reception. The production of Dpp in the CpCs is regulated by *Lsd1* and the JAK/STAT signaling pathway, activated by the ligand Upd that is secreted from the TFs. Dpp diffusion is limited by type IY collagens whereas Dpp is stabilized by the glypican Dally that is itself downregulated in ECs by EGFR signaling. Several CB intrinsic pathways limit the responsiveness to TGF- β signaling and thereby assure that only one cell diameter away from the GSCs, differentiation can start. The translational repressor complex consists of Pum and Brat and downregulates the levels of Mad. The serine/threonine Fu together with the E3 ligase Smurf leads to the ubiquitination and subsequent degradation of the TGF- β receptor. The homophilic cell adhesion proteins DE-Cad and Arm are found at high levels between CpCs and GSCs, where they attach GSCs to the niche cells and at lower levels between ECs and CBs and cysts. See the main text for details.

1.2.5 GSCs respond to environmental cues

The division rate of GSCs has to be precisely regulated in response to the needs of the whole organism: dietary conditions, stress or aging regulate the GSCs via systemic signaling. Such general signals can either act on the GSCs directly or be integrated by the somatic niche. In older animals, the niche size and signaling are decreased, causing partial GSC loss which was suggested to be mainly the result of lower insulin levels in aging flies. Insulin signaling controls the niche size via Notch signaling and influences the GSC maintenance via acting on the adherens junctions between CpCs and GSCs (Hsu and Drummond-Barbosa, 2009; Pan et al., 2007). In addition, insulin signaling acts on the GSCs in a cell-autonomous fashion: insulin-like peptides promote GSC division and via phosphoinositide-3 kinase (PI3K) and dFOXO control the G2 phase of the GSC cell cycle (Hsu et al., 2008; LaFever and Drummond-Barbosa, 2005). The steroid hormone ecdysone in contrast acts in the somatic cells of the germarium, influencing the germline via altering cell adhesion.

1.2.6 CpCs constitute an important part of the GSC niche

Despite the importance of the GSC niche, relatively little is known about what constitutes a functional niche and how it is formed. CpCs are an important component of the GSC niche and it was shown that the number of CpCs and attached GSCs directly correlates (Ward et al., 2006; Xie and Spradling, 2000). CpCs in the adult animal are mitotically quiescent, establishing the niche with the correct number of CpCs is therefore essential to ensure the lifelong functionality of the GSC-niche unit.

The GSCs niche is formed during larval–pupal development Stacks of terminal filaments start to specify in third instar larvae and CpCs form at their base at the end of the third larval instar and until the first steps of pupation. Once the niches are established, the undifferentiated GSC precursors, the primordial germ cells are recruited to the niche to become GSCs (Song et al., 2002; Zhu and Xie, 2003). Several pathways were shown to be implicated in the formation and regulation of the GSC niche. Notch signaling is not only required for the switch from the mitotic cycle to the endocycle in FCs (Shcherbata et al., 2004), but also directly controls the size of the niche. The Notch ligands Delta and Serrate are present on the surface of GSCs and activate Notch signaling in the surrounding somatic cells that in turn control the GSC population. Expanded Notch activation leads to the formation of germaria with higher CpCs number and ectopic niches that are able to maintain fully functional GSCs (Ward et al., 2006). Furthermore, the histone methylase Lsd1 acts in ECs and is required to prevent the formation of ectopic niches and accordingly, its loss of function leads to the misplaced expression of CpC specific markers in ECs (Eliazer et al., 2011). Considering that CpCs are specified around pupation, when the ecdysone titer in the animal is high, it is not surprising that the ecdysone signaling pathway, that is discussed in more detail in

Section 1.3, page 17 was recently also shown to regulate the formation of the GSC niche. In early third instar larvae – before the ecdysone pulse that initiates pupation – the unliganded repressive ecdysone receptor complex is required to repress precocious differentiation of both niche and primordial germ cells. As ecdysone titers rise in mid and late third instar larvae, ecdysone signaling is necessary for the formation of the niche and the differentiation of the primordial germ cells (Gancz et al., 2011). In addition to the larval phenotypes that were described by Gancz et al., 2011, we could show that perturbing ecdysone signaling during larval and adult stages leads to a higher number of functional CpCs in the adult (König et al., 2011). However, many questions regarding niche formation remain and future analysis will help to reveal the exact origin of ECs and CpCs, the signals that lead to the CpC recruitment and the different signaling activities of the niche components.

1.3 Ecdysteroids control various aspects of *D. melanogaster* development and adult life

1.3.1 Ecdysteroids regulate *D. melanogaster* development

20-hydroxyecdysone, that is commonly called "ecdysone", is one of several steroid hormones that regulate the larval to adult metamorphosis in Arthropods as well as several other processes in the adult animal (reviewed in Thummel, 1996). It acts via activating a nuclear hormone receptor complex that consists of the Ecdysone receptor (EcR) and its dimerization partner Ultraspiracle (Usp), the *D. melanogaster* orthologs of the farnesoid X or liver X receptor and the retinoid X receptor (Oro et al., 1990; Thomas et al., 1993; Yao et al., 1993). The EcR belongs to the nuclear-receptor superfamily: an ancient protein family that can be found throughout the Metazoa and that contains well known vertebrate receptors like the estrogen, glucocorticoid, thyroid hormone and retinoic acid receptor. Nuclear receptors contain a DNA-binding domain and ligand-binding and dimerization domains (reviewed in King-Jones and Thummel, 2005). The EcR exists in three splicing variants in *D. melanogaster*, EcRA, EcRB1 and EcRB2 that share their DNA- and hormone binding domain, but differ in their N-terminal regions, whereas Usp exists only in one isoform (Talbot et al., 1993).

The unliganded EcR/Usp complex has a repressive function The EcR is constitutively present in the nucleus and the EcR/Usp complex binds to specific gene sequences called ecdysone responsive elements (Cherbas et al., 1991). The signaling cascade that is triggered by the activated EcR/Usp heterodimer is rather complex: many direct targets – or early response genes – of the EcR complex, including *Broad Complex* (Br), *E75A* and *E75B* activate themselves a variety of late response genes. Besides activating the transcription of target genes in the presence of ecdysone, the EcR/Usp complex is also thought to have a repressive function when unliganded (Cherbas et al., 1991; Dobens et al., 1991; Schubiger and

Truman, 2000). However, recently it was suggested that the EcR/Usp complex is not itself repressing: instead the early response gene *E75A*, a nuclear hormone receptor itself, is recruited to target genes and replaces the activating EcR/Usp complex if ecdysone titers are low (Johnston et al., 2011). Whether this mechanism also works for target genes, tissues and developmental stages that were not analyzed by Johnston et al., 2011 remains unclear.

1.3.2 The spatial and temporal specificity of ecdysone signaling is achieved via differential expression of transcriptional and translational coregulators

The ecdysone induced responses are remarkably diverse. Whereas solely larval tissues degenerate and lyse upon the ecdysone pulses during the larval to adult transition, the imaginal discs grow and give rise to the adult structures. This spatial and temporal specificity of ecdysone signaling is achieved via differential expression of the *EcR* itself, of several co-activators, co-repressors and translational regulators. In the last years several cofactors – repressing or activating – that are bound to the EcR/Usp complex were identified. Chromatin remodeler like the nucleosome remodeling factor (NURF) alter chromatin-DNA interaction and thereby affect transcription (Badenhorst et al., 2005). Another group of cofactors acts via influencing histones: SMRTER possibly mediates repression of ecdysone signaling by interacting with the repressor Sin3A and recruiting histone deacetylases (Tsai et al., 1999). The histone methyltransferase TRR and the acetyltransferase CBP in contrast are coactivators of ecdysone signaling (Kirilly et al., 2011; Sedkov et al., 2003). It is believed that histone chaperones like the *D. melanogaster* DEK that was identified as an EcR coactivator, are required for the assembly and disassembly of histones at transcribed loci, and thereby act as transcriptional cofactors (Sawatsubashi et al., 2010). In addition, several other cofactors including Alien, Bonus, Dor, Rigor mortis and Taiman (Tai) were characterized (Bai et al., 2000; Beckstead et al., 2001; Dressel et al., 1999; Francis et al., 2010; Gates et al., 2004; Jang et al., 2009).

Tai is an EcR-activator *tai* was initially characterized from a genetic screen for mutants that cause defects in border cell migration (Bai et al., 2000). The migration of *tai* mutant border cells was either completely inhibited or slowed down and *tai* loss of function was shown to cause an abnormal accumulation of DE-Cad, Arm and focal adhesion kinase. Based on *in vivo* colocalization of Tai and EcR, its ability to increase hormone induced transcription in cultured cells, and its direct EcR binding *in vitro*, Tai was shown to be a coactivator of the EcR in *D. melanogaster*. In accordance with these findings, Tai shows a high sequence similarity to members of the p160 class of steroid hormone coactivator proteins and is most closely related to AIB1, a steroid hormone coactivator protein that is amplified in breast and ovarian cancer (Bai et al., 2000; Chang and Wu, 2012). Like other steroid hormone receptor coactivators, Tai contains an

N-terminal bHLH and PAS domains, LXXLL motifs that are required for ligand dependent hormone receptor binding and polyglutamin transactivation domains. Interestingly, mutants of *tai* were identified in a candidate based screen in which clonal germaria of hsFlp;FRT40A lethals from the Drosophila Genetic Resource Center were analyzed, which was the first evidence for ecdysone signaling being important for the GSC-niche complex (see Weiss, 2009 Section 2, page 37).

Abrupt is a negative regulator of ecdysone signaling and a powerful transdetermination factor Another protein that was found in the above mentioned screen is Abrupt (Ab). Ab is a transcription factor that contains a **B**road, **T**ramtrack and **B**ric-a-Brac/**P**oxvirus and **Z**inc finger (BTB/POZ) domain (Hu et al., 1995). Ab is required for the formation of specific synaptic connections between a subset of motoneurons and a subset of muscles, cell-autonomously suppresses dendritic branching in a subset of neurons and is required for the morphogenesis of dendritic arborization neurons (Hu et al., 1995; Li et al., 2004; Sugimura et al., 2004). Furthermore, Ab was shown to be an inhibitor of the ecdysone signaling by interacting with the bHLH domain of Tai (Jang et al., 2009). It is interesting to note, that Ab was also shown to be a potent transdetermination factor, since overexpressing Ab in antennal imaginal discs leads to the transformation of arista into putative legs (Grieder et al., 2007). This is illustrating, that Ab is a powerful factor in development, whose levels and expression patterns have to be tightly regulated.

The expression of primary ecdysone response genes is regulated on the translational level In addition to the availability of nuclear receptor co-regulators or differential accessibility due to chromatin remodeling, translational control was recently shown to add another regulatory layer (Ihry et al., 2012). The DEAD box RNA helicase *belle/DDX3* controls the translation of the primary ecdysone signaling response gene *E74A*. In the absence of *belle*, genes downstream of *E74A* are not properly controlled and additionally, *E74A* mRNA is accumulating. *E74A* protein is necessary and sufficient to repress its own transcription. Translational control is therefore contributing to translating the global steroid hormone signal into a tissue specific response (Ihry et al., 2012).

1.3.3 Ecdysone signaling fulfills various functions in the adult fly

In larvae, ecdysteroids are produced in the prothoracic gland (a part of the ring gland) and are secreted into the hemolymph as inactive precursors that are further processed in peripheral tissues. Even though 20-hydroxyecdysone is generally considered the biologically active ecdysone form, it is also discussed, that other derivatives or precursors of 20-hydroxyecdysone are active signaling molecules (reviewed in Gilbert et al., 2002 and Gilbert and Warren, 2005). These issues are however also complicating attempts to measure ecdysone levels. Ecdysone

levels can be measured by radio- or enzyme-immunoassays, but both methods are not specific to 20-hydroxyecdysone, which makes precise measurements of the active hormone levels rather difficult (reviewed in Schwedes and Carney, 2012). Nevertheless, EcR and Usp are found in adult tissues and it is clear that ecdysone is present in the adult, albeit at lower levels than during the earlier steps of development (Bownes, 1984; Carney and Bender, 2000; Hagedorn, 1985; Schwedes et al., 2011; Schwedes and Carney, 2012). Even though the ovary seems to be the main ecdysone producing tissue in the adult, other tissues also may contribute to the overall ecdysone titer (Bownes, 1984).

Since ecdysone is absolutely essential during development, analyzing ecdysone function in adults is technically challenging

Whereas the roles of the ecdysone signaling pathway during development have been extensively studied, less attention has been put on its function in the adult animal. Severe perturbations of the ecdysone signaling pathway during development cause lethality, which complicates analysis of ecdysone function in the adult. To circumvent these problems, different strategies have been successfully applied: (1) using temperature sensitive mutations like *ecd1^{ts}* or *DTS3* that lead to reduced ecdysone levels when shifted to the appropriate temperature, (2) conditionally decreasing levels of functional EcR/Usp coactivators or increasing inhibitors of ecdysone signaling, (3) analyzing heterozygous mutants of ecdysone signaling pathway components, (4) generating homozygous loss of function clones of ecdysone signaling pathway components in a heterozygous background (Buszczak et al., 1999; Carney and Bender, 2000; König et al., 2011).

Oogenesis and oviposition are regulated by ecdysone signaling

It could be shown, that ecdysone signaling regulates various aspects in the adult like oogenesis, longevity, body size, sleep and long-term memory and the function in the ovary has been studied in more detail. Ovaries from *EcR* mutant animals show several defects, including FC differentiation defects, loss of stage 10–13, but increased numbers of stage 14 egg chambers, and many defective or degenerating egg chambers. Furthermore, at stage 8 of oogenesis, ecdysone controls, via Br, a point after which the egg chambers, depending on the environmental conditions, undergo apoptosis or develop further (Buszczak et al., 1999; Carney and Bender, 2000; Hackney et al., 2007; Kozlova and Thummel, 2000; Terashima and Bownes, 2005, 2006). In addition, ecdysone enhances the production of yolk proteins in fat body and FCs and is required to control the migration of a specialized set of FCs – the border cells (Bai et al., 2000; Hagedorn, 1985; Jang et al., 2009). Studies on the role of ecdysone signaling in the germarium have been published only throughout the last years: it was suggested, that the ecdysone signaling controls GSC self-renewal and proliferation in a cell-autonomous fashion via interacting with the intrinsic chromatin remodeling factors imitation SWI (ISWI) and NURF301 (Ables and Drummond-Barbosa, 2010). The present thesis describes how ecdysone signaling influences the germline cells in a non cell-autonomous fashion via the surrounding somatic cells, and is therefore partially conflicting to the model pre-

sented by Ables and Drummond-Barbosa, 2010. Altogether, this suggests that ecdysone signaling regulates multiple aspects of oogenesis.

Ecdysone signaling is required to adapt to changing environmental conditions

In addition to its role in certain organs, ecdysone signaling was shown to be critical for the overall body status: reduced ecdysone signaling activity results in an increased lifespan and a higher resistance to different stresses (Simon et al., 2003; Tricoire et al., 2009). Insulin signaling plays a central role in promoting animal growth and it was shown that it can be impeded by ecdysone signaling (Colombani et al., 2005). Applying ecdysone to adult *D. melanogaster* promotes sleep, whereas ecdysone signaling mutants sleep less (Ishimoto and Kitamoto, 2010). Finally, ecdysone is also required for longterm courtship memory (Ishimoto et al., 2009). Altogether, besides its function in the development of insects, ecdysone signaling is of great importance for various processes including reproduction, longevity, behavior, and stress response. If ecdysone signaling is required for responding to stressful stimuli, one would expect ecdysone levels to vary, depending on the environmental conditions. Indeed, ecdysone levels were shown to change if flies are exposed to unfavorable conditions like heat, food or sleep deprivation (Ishimoto and Kitamoto, 2010; Rauschenbach et al., 2000; Terashima and Bownes, 2005; Terashima et al., 2005). In the ovary for example, starvation induces apoptosis of nurse cells in stage 8 egg chambers, that are subsequently reabsorbed to provide energy. This apoptosis can also be observed upon injection of ecdysone, thus, it is believed that the ecdysone signaling pathway mediates the effects of starvation at the stage 8 checkpoint (Soller et al., 1999).

Altogether, it is becoming clear, that the adult functions of ecdysone are different from the ones in the developing animal. Especially, a potential role of ecdysone as a stress hormone – similar to cortisol in humans – is of interest.

1.3.4 *D. melanogaster* as a model to study the complexity of steroid hormone function

Humans contain several classes of steroid hormones including the sex steroids (estrogens, androgens, progestagens), glucocorticoids (cortisol), and mineralcorticoids that carry out diverse functions in metabolism, immune system, inflammation, reproduction, sexual differentiation and renal excretion (Litwack, 1994). But whereas hormone signaling pathways in humans are difficult to study due to their complexity, ecdysone and the juvenile hormone are the only known lipophilic hormones in *D. melanogaster*. Furthermore, similarities in several aspects of nuclear hormone receptor structure and signal transduction mechanisms suggests that the steroid receptors are highly conserved (Cherbas et al., 1991). This makes *D. melanogaster* an ideal model to study the complex networks regulating steroid receptors, and nuclear receptors in general.

1.4 Small non-coding RNAs regulate a variety of processes

Transposons are one of the best understood selfish genetic elements. They are able to multiply within the genome and to insert into new locations, possibly causing insertional mutagenesis and chromosomal recombination in the host genome. Eukaryotes, therefore, developed defense strategies to protect their genomes from transposon caused damage. Many of them involve small RNAs not encoding proteins that mediate silencing of mRNAs. Common to all small RNA pathways is the RNA induced silencing complex (RISC) that contains an Argonaute protein and a small bound RNA. Via complementary base pairing, the RISC binds to target mRNAs and mediates its translational silencing and/or degradation.

piRNAs protect germline cells from transposons PIWI proteins belong to the AGO family, and *D. melanogaster* contains the three PIWI proteins PIWI, Aubergine and Argonaute3 (reviewed in Samji, 2009). piRNAs (26–31 nucleotides) are produced from long single stranded RNA precursors that can be originating endogenously from transposons or viral transcripts or can be introduced exogenously. piRNAs and the interacting PIWI proteins are necessary to silence selfish genetic elements and thereby to protect the integrity of the GSC genome across generations (reviewed in Senti and Brennecke, 2010). Loss of PIWI protein or other components that interact with piRNA pathway and transposon control results in an altered GSC maintenance and loss of GSCs (Cox et al., 1998; King et al., 2001; Saito et al., 2010)

siRNAs are required for protection against viral nucleic acids In contrast to the piRNA pathway, that is mainly required for the defense against selfish genetic elements in the germline, miRNA and siRNA pathways play a major role in regulating gene expression. siRNA and miRNA pathways differ slightly in their molecular origin and binding complementarity to their target mRNAs, but nevertheless share a number of similarities. siRNAs mostly match perfectly with the target mRNA and usually lead to translational repression by degradation. siRNAs are produced from perfect double stranded precursors from exogenous or endogenous sources. One of the 21–25nt long strands is incorporated into the RISC and leads to the cleavage of the target mRNA. siRNAs are thought to mainly mediate a defense mechanism against foreign nucleic acids but also regulate the levels of target mRNA.

1.4.1 miRNAs regulate translation and degradation of target mRNAs

miRNAs are produced from certain precursors that are encoded in the genome, either with an independent promoter or embedded in the intron of another gene.

Polycistronic miRNAs – several miRNAs are encoded on one transcript – also occur. Pri-miRNAs are processed in the nucleus by the RNAase-III enzyme Drosha, producing ~70bp single stranded RNA precursors that form hair pins with mismatches and bulges (pre-miRNA). Exportin5 transports the pre-miRNAs into the cytoplasm, where they are further cleaved by the RNAase-III enzyme Dicer into small 21nt–25nt double strands with 3' and 5' overhang. Two different Dicer homologs were described in *D. melanogaster* (Dicer1 and Dicer2). In parallel, a number of Drosha- and Dicer-independent miRNA biogenesis pathways exist; misregulation of the "classical" biogenesis pathway, therefore, does not necessarily lead to a complete loss of miRNAs in a cell (reviewed in Yang and Lai, 2011). The mature miRNA is loaded onto the Argonaute containing RISC that targets mRNAs for repression. Most miRNAs bind to the 3'UTR of target mRNAs with incomplete complementarity and lead to the translational repression of target mRNAs (reviewed in He and Hannon, 2004). Interestingly, the first 2–7nt from the 5' end of the miRNA – called the seed sequence – often matches perfectly with the mRNA sequence.

miRNAs confer biological robustness Very often, loss or overexpression of a miRNA causes rather subtle phenotypes. It is, thus, believed that the main function of miRNAs is to fine tune protein levels: gene expression is subject to stochastic fluctuations and, in addition, endogenous and exogenous perturbations lead to variabilities. During development or upon environmental stress, this "transcriptional noise" has to be tightly controlled in order to ensure that biological processes are not disturbed (reviewed in Siciliano et al., 2013). Due to the imperfect complementarity, miRNAs can target a variety of mRNA targets at the same time; in addition, they provide a rapid way of regulating protein levels and are, thus, great candidates to confer cells robustness against endogenous or exogenous perturbations. miR-9a is, for example, required to ensure that "muscle specific" genes are not ectopically expressed in neurons (Kai and Spradling, 2003b).

The first miRNAs were found in *C. elegans* *Lin-4* is the first miRNA that was identified through a genetic screen as a heterochronic gene in *C. elegans*. Loss of *lin-4* leads to defects in the developmental timing: early larval fates are reiterated inappropriately at later stages. Opposite phenotypes – premature appearance of larval stage 2 patterns in larval stage 1 – are observed if the *lin-4* target *lin-14* is missing. *Lin-14* encodes a protein, the temporal regulation of which is required for correct sequence of cell lineages. The downregulation of *lin-14* via its 3'UTR is both necessary and sufficient to enable the posttranscriptional temporal regulation by *lin-4* (Lee et al., 1993; Wightman et al., 1993). Since the description of *lin-4*, the number of known miRNAs increased rapidly: miRbase 19.0 lists 2042 mature miRNAs in humans, 368 in *C. elegans*, and 426 in *D. melanogaster* (<http://www.mirbase.org/>). Even though the function of only a few miRNAs has been analyzed in more detail so far, it is becoming clear that miRNAs are capable to not only regulate various developmental processes, but also influence virtually all other cellular processes.

1.4.2 miRNAs are required for GSCs behavior

The miRNA pathway was shown to be of great importance for maintenance and division of GSCs, since mutating key components of the miRNA pathway like the double-stranded RNA-binding domain protein Loquacious, the double-stranded RNases-III-type Dicer-1 and Argonaute1 result in loss of GSCs (Forstemann et al., 2005; Hatfield et al., 2005; Jin and Xie, 2007; Park et al., 2007; Shcherbata et al., 2007; Yang et al., 2007; Yu et al., 2009). Interestingly, components of the miRNA pathway are differentially required in a stage-dependent manner (Shcherbata et al., 2007). In the *D. melanogaster* ovarian germline, miRNAs do not only control stem cell proliferation (Hatfield et al., 2005), but also define developmental, stage-specific requirements for stem cell maintenance and differentiation (Shcherbata et al., 2007) demonstrating that miRNAs are important components of the temporally and spatially coordinated gene regulation machinery.

Function of a few individual miRNAs in the germarium was studied One of the first miRNAs found in *D. melanogaster* is *bantam*. *Bantam* is expressed in GSCs and was shown to be a key miRNA that is required for GSC maintenance and division (Neumuller et al., 2008; Shcherbata et al., 2007). Mei-P26 is a TRIM-NHL protein that is required for proliferation control, differentiation of the GSC progeny and GSC maintenance. It is strongly induced in 16-cell cysts and *mei-P26* mutants display ovarian tumors. Mei-P26 functions by physically associating with Argonaute1 and, thereby, inhibiting the miRNA pathway (Li et al., 2012; Neumuller et al., 2008; Page et al., 2000). *miR-7* and *miR-278* act in concert to regulate the levels of Dacapo, a cyclin-dependent kinase inhibitor. Loss of *miR-7* or *miR-278* affects the proliferation of GSCs, in addition it was shown in male testes that *miR-7* can target the 3'UTR of the differentiation factor Bam and thereby possibly contribute to transcriptional downregulation of *bam* if dedifferentiation of cysts is needed (Pek et al., 2009; Yu et al., 2009). *miR-184*, in contrast, was shown to affect the range of Dpp signaling by targeting the Dpp receptor Saxophone, loss of *miR-184* therefore affects the differentiation of the GSC progeny (Iovino et al., 2009).

1.4.3 *let-7* is a highly conserved heterochronic miRNA

let-7* was identified as a heterochronic gene in *C. elegans The second small non-coding RNA that was identified in *C. elegans* is encoded by the heterochronic gene *let-7*. The *let-7* mutation was first identified through an EMS (ethyl methane-sulfonate) screen and was named after its late larval **lethal** phenotype in *C. elegans* (Meneely and Herman, 1979). Hypodermal blast cells are stem cells that normally divide at each larval transition; after the L4–adult transition, however, they exit the cell cycle, differentiate and form adult structures. In *let-7* mutant animals, the blast cell lineages undergo an additional round of division. Loss of *let-7*, therefore, leads to the reiteration of earlier larval cell division patterns and failure of stem cells to differentiate appropriately to generate adult structures. Overexpression of

let-7, in contrast, leads to precocious cell cycle exit (Reinhart et al., 2000; Slack et al., 2000). *Let-7* mutations can be rescued by mutations in the heterochronic *lin-41* gene; and *lin-41* mutations were shown to cause phenotypes that are opposite to the ones of *let-7*. Using reporter assays, deletion analysis and genetic interaction experiments it was proven that *lin-41* is posttranscriptionally regulated by *let-7*. Many other *let-7* targets, most of which are transcription factors or signaling molecules, were identified in *C. elegans* (Grosshans et al., 2005). In accordance with the time at which *let-7* mutant phenotypes become obvious, *let-7* is not detectable until the last larval stages, where it mediates the downregulation of *lin-41* gene activity (Reinhart et al., 2000; Slack et al., 2000). Thus, *lin-4* is required for proper timing during the first larval stages, whereas *let-7* is responsible for the transition from late larval to adult cell fates. In summary, *let-7* regulates the transition from proliferating stem cells to differentiated and mitotically quiescent cells in *C. elegans*.

***let-7* is highly conserved among bilateria** Interestingly, it was furthermore shown that *let-7* sequence is highly conserved: Northern blot analyzes showed identical 21nt *let-7* RNA in a variety of bilaterian clades including annelid, arthropod, mollusk, echinoderm, hemichordate and vertebrates but was absent from cnidaria, porifera, plants and fungi (Pasquinelli et al., 2000). Apart from its sequence, the temporal expression pattern of *let-7* also is highly conserved among species: similar to the situation in *C. elegans*, *D. melanogaster*, *let-7* cannot be detected until the late third instar. *D. melanogaster* and *C. elegans* both are ecdysozoans: that is, their development involves several molts, during which the animals shed their cuticle. In two mollusks and one annelid species, *let-7* was present only during adulthood and even in vertebrates *let-7* is temporally expressed (reviewed in Roush and Slack, 2008). In *D. melanogaster*, *let-7* is expressed from a common precursor and coordinately regulated with the *lin-4* homolog *miR-125* and *miR-100* (Bashirullah et al., 2003; Sempere et al., 2003). The expression of *miR-125* and *let-7* is first detected around day 9 of embryonic development and peaks at day 13. Interestingly, mouse *lin-41* – the homologs of which are regulated by *let-7* – shows an expression pattern reciprocally to the ones of *miR-125* and *let-7* (reviewed in Sokol, 2012). The high level of sequence and expression pattern conservation suggest that *let-7* may regulate developmental processes among bilateria.

Loss of *let-7* leads to heterochronic defects in *D. melanogaster* Since *let-7* sequence and temporal expression pattern are so highly conserved, it is possible that *let-7* function as a regulator of proliferation and differentiation is also conserved. Indeed, similar to the situation in the worm, loss of *let-7* leads to heterochronic defects in *D. melanogaster*. Dorsal internal oblique muscles are remnants of the larval body that normally disappear after eclosion, but persist in 90% of *let-7* mutants (Sokol et al., 2008). Furthermore, cells in the wing disc fail to exit the cell cycle short after puparium formation and instead continue dividing (Caygill and Johnston, 2008). The adult body wall muscles are smaller

than in control animals and the neuromuscular junctions are immature (Caygill and Johnston, 2008; Sokol et al., 2008). In summary, the absence of *let-7* results in both, the perdurance of larval and the presence of immature adult structures in *D. melanogaster*, which means that *let-7* has similar functions in the fly as in the worm, where it was initially identified as a heterochronic gene.

1.4.4 Expression of *let-7* is initiated by ecdysone signaling

As already mentioned, *let-7* expression follows a tight temporal regulation in several animals among bilateria (Pasquinelli et al., 2000). In *D. melanogaster*, *let-7* is first found in late third instar animals, coinciding with a pulse of ecdysone that initiates puparium formation, and peaks several hours afterwards (Bashirullah et al., 2003; Pasquinelli et al., 2000; Sempere et al., 2002). In addition, the known ecdysone response mRNA *E74A*, shows a similar expression pattern, altogether suggesting that *let-7* expression is regulated by ecdysone signaling (Bashirullah et al., 2003). Two different groups analyzed whether *let-7* expression is initiated by ecdysone signaling and reached contradictory conclusions (Bashirullah et al., 2003; Sempere et al., 2002). Incubating cultured *D. melanogaster* cells with ecdysone led to the induction of *let-7* expression and animals with the temperature sensitive *ecd1^{ts}* mutation, which leads to dramatically reduced ecdysone levels, almost completely lack *let-7* (Bashirullah et al., 2003; Sempere et al., 2002). In contrast, expression of *EcR*-RNAi caused no visible change in *let-7* levels, estimated by Northern blot (Bashirullah et al., 2003) and experiments, where third instar larval organs were cultured in media with or without ecdysone, produced different results (Bashirullah et al., 2003; Sempere et al., 2002). This discrepancy, however, was resolved by Garbuzov and Tatar, 2010, who, prior to the micromolar ecdysone treatment, incubated cells with nanomolar concentrations of ecdysone for a few hours, which resembles the *in vivo* situation much better. This pre-treatment with low concentrations of ecdysone primed cells to quickly respond to higher concentrations of ecdysone and induce *let-7* expression. In the light of these results, the conflicting data by Bashirullah et al., 2003 can be explained. In addition, it was shown that the *let-7 complex* promoter contains three ecdysone responsive elements via which the active EcR/Usp complex directly activate the transcription of the *let-7 complex*, containing the miRNAs *let-7*, *miR-100* and *miR-125* (Chawla and Sokol, 2012). In summary, several lines of evidence indicate that *let-7* expression is initiated by ecdysone pulse in the developing larvae.

The transcription factor Ab is negatively regulated by miRNA *let-7* miRNAs function by regulating the translation of target mRNAs, identifying the targets of a certain miRNA is, therefore, a key question to understand its role. Regulation of *ras* and *lin-41* by *let-7* is conserved in several organisms (reviewed in Boyerinas et al., 2010). In addition, the BTB/POZ protein Ab (see Section 1.3.2, page 19) that contains several *let-7* binding sites in its 3'UTR was shown *in vivo* to be a *let-7* target. Ab levels persist in *let-7* mutant cells and reducing Ab dose can partially rescue some of *let-7* mutant effects (Caygill and Johnston, 2008;

Kucherenko and Shcherbata, 2013; Sokol et al., 2008). Ab is a powerful trans-determination factor that was shown to be highly dosage dependent, suggesting that mechanisms are required to precisely regulate Ab levels in the cell – a task that may partially be fulfilled by the miRNA *let-7*. Keeping in mind that *ab* was identified in our screen to be important for the overall germarium architecture, it is interesting to consider that *let-7* may play a role in the germarium by modulating Ab levels. Co-immunoprecipitation analysis and genetic interaction analyses on border cells revealed that the transcription factor Ab functions by negatively regulating the EcR co-activator Tai (Bai et al., 2000). As we could show, the ecdysone signaling pathway is required for proper EC morphology and regulates germline differentiation cell non-autonomously via acting on cell-adhesion levels, which alters the responsiveness of germline cells to Wg signaling (König et al., 2011, Section 2.5, page 95). The spatially restricted cofactors that enhance (Tai) or inhibit (Ab) ecdysone signaling modulate the cell specific response to the systemic ecdysone signaling. Interestingly, *let-7* expression was shown to be initiated by ecdysone signaling (see Section 1.4.4, page 26), suggesting a model in which *let-7* and ecdysone signaling act in a double negative feedback loop to fine tune the strength of ecdysone signaling.

1.4.5 *let-7* is important for cell differentiation and cancer – also in mammals

***D. melanogaster* is the only model organism with only one *let-7* family member** Apart from the *let-7* sequence that is conserved among bilateria (*let-7a*), 9 other *let-7* family members were found in humans. Whereas *D. melanogaster* contains only one *let-7* gene that is encoded by one precursor, the human *let-7a* is generated by three different precursors (*let-7a* 1–3) (Roush and Slack, 2008). Similar numbers of *let-7* family members are found in zebrafish, chicken and mouse, which makes *D. melanogaster* an extremely valuable model for analyzing *let-7*.

***let-7* plays a role in neuronal development and cell differentiation** The early studies in *C. elegans* already revealed that *let-7* is critical for cell differentiation. Today, *let-7* is widely considered one of the key miRNAs in developmental regulation and cancer. Human and mouse embryonic stem cells lack *let-7*, while its levels increase during differentiation (reviewed in Boyerinas et al., 2010). The RNA binding protein LIN28 is one of four factors that is able to reprogram mouse fibroblasts to a stem cell state; repression of *let-7* is probably contributing to this reprogramming. LIN28 inhibits the processing of *let-7* miRNA and, thus, prevents cellular differentiation. When stem cells differentiate, *let-7* and *miR-125* promote their own expression by targeting their negative regulator LIN28 (reviewed in Mondol and Pasquinelli, 2012). In addition, *let-7* is highly expressed in neuronal tissues and regulates the remodeling of the neuromusculature, maturation of neuromuscular junctions, mushroom body morphology and several adult behaviors including learning in *D. melanogaster* (Caygill and Johnston, 2008; Kucherenko et al., 2012; Sempere et al., 2004; Sokol et al., 2008). An increase of *let-7* levels

is also observed during mammalian brain development and, in accordance with this, the mammalian *let-7* family was shown to promote neuronal differentiation programs (reviewed in Mondol and Pasquinelli, 2012). *C. elegans lin-41* is regulated by *let-7*, and *lin-41* orthologs were found in *D. melanogaster*, mouse and other animals (Grosshans et al., 2005; Slack et al., 2000). Remarkably, mouse and human *lin-41* contain putative *let-7* binding sites. The expression patterns of the two are reciprocal and it was suggested that its 3'UTR mediates its repression by *let-7* (Schulman et al., 2005). Not only is *let-7* sequence strictly conserved, but, in some cases, the *let-7* targets seem to be conserved among organisms. This opens intriguing prospects of this miRNA as an ancient regulator of cell differentiation, and future research in mammals will enable detailed comparisons of *let-7* function through evolution.

***let-7* is a tumor suppressor gene** Low levels of *let-7* family members in adult tissues are a hallmark of several cancer types and can indicate poor prognosis. Several cancer-relevant *let-7* targets have been identified: RAS, an oncogene and HMGA2, a chromatin-associated nonhistone protein that is misregulated in human cancers, are directly targeted by *let-7* (reviewed in Boyerinas et al., 2010). Many *let-7* family members are tumor suppressors, even though, in some cases *let-7* family members were found to be expressed at higher levels in cancer tissue. Analysis of *let-7* in vertebrates are, however, complicated by the relatively large number of *let-7* family members. Taking together, *let-7* plays a pivotal role in cell differentiation and temporal development across animal species and the importance of this miRNA is highlighted by its relevance in certain human diseases.

1.5 The Wnt signaling pathway is a key determinant for development

The Wnt signaling pathway presents a major molecular cascade that controls a variety of different processes including cell proliferation, differentiation, migration, and polarity. It is highly conserved in invertebrates and vertebrates and is activated by Wnt proteins, secreted glycoproteins that bind to transmembrane receptors, acting as short range signaling molecules or as long range morphogens. 19 Wnt family members were identified that have 7 homologs in *D. melanogaster* (reviewed in Saito-Diaz et al., 2013). The *D. melanogaster* ortholog Wingless (Wg) was first identified through its effect on wing development and is one of the best studied Wnt ligands. Signaling activated by Wnt proteins is traditionally divided in canonical and non-canonical pathways that differ regarding the involvement of β -Catenin (*D. melanogaster* homolog Arm). Depending on the cellular context, different Wnt ligands can activate either or both Wnt pathways (reviewed in MacDonald et al., 2009).

1.5.1 The effects of the canonical Wnt signaling pathway are mediated by β -Catenin

Canonical Wnt signaling leads to the stabilization of Arm and the subsequent activation of Arm target genes. If Wnt signaling is not active, Arm is phosphorylated, ubiquitinated and degraded by a complex containing Axin, shaggy/Zeste-white 3, and adenomatous polyposis coli. Upon binding of a Wnt ligand to the receptor Frizzled with its coreceptor LRP5/6 (*D. melanogaster* homolog Arrow), a protein called Dishevelled is activated and leads to the inactivation of the Arm degrading complex. Arm then accumulates, translocates to the nucleus and forms a complex with the Pangolin (Pan)/T-cell factor family of High mobility group transcription factors, activating the transcription of target genes (reviewed in Chien et al., 2009).

1.5.2 β -Catenin has a dual role as a structural component of cell-adhesion complexes and as a major transmitter of Wnt signaling

Besides its crucial role in Wnt signaling, Arm is a structural component of adherens junctions (see Section 1.2.3, page 11). Due to its different functions as signaling molecule and as structural component, β -Catenin was discovered independently twice. Arm can be found at different locations within the cell: bound to E-Cad at adherens junctions, as a transcription factor in the nucleus and in the cytoplasm – bound to the destruction complex or free. Arm contains armadillo repeats in its central region, flanked by C- and N-terminal domains. Each of the armadillo repeats forms three helices, composing a large super helix with a long positively charged groove. This groove serves as a platform for several Arm binding partners. As a consequence of this, the different partners with which Arm interacts in cell adhesion (DE-Cad), the destruction complex (APC) or in the nucleus cannot bind Arm simultaneously; the different pools of Arm in the cell, thus, influence each other (Kimelman and Xu, 2006; Wodarz et al., 2006). The binding preferences of β -catenin and the stability of the interactions can be influenced by several posttranslational modifications like phosphorylations, ubiquitinations, acetylations and glycosylations (reviewed in Valenta et al., 2012). If the Wnt signaling pathway is inactive, β -Catenin is mainly bound to E-Cad in cell-cell adhesions, whereas cytoplasmic β -Catenin is phosphorylated and marked for degradation by the destruction complex (reviewed in Kimelman and Xu, 2006). Activation of the pathway destabilizes the β -Catenin destruction complex, which leads to the accumulation of phosphorylated β -Catenin. Free β -Catenin then translocates to the nucleus, associates with transcription factors and activates or represses the transcription of target genes (reviewed in Chien et al., 2009).

1.5.3 Wnt signaling regulates many processes in *D. melanogaster*

D. melanogaster *wg* was first identified as a segmentation gene, the loss of which leads to the transformation of adult wings to thoracic notums; and it appeared that Wg and the vertebrate oncogene Int-1 are orthologs (Wg and int-1 were fused to Wnt; reviewed in Chien et al., 2009; Swarup and Verheyen, 2012). Misregulation of the Wnt signaling pathway plays a role in several human diseases (reviewed in MacDonald et al., 2009). The role of Wg signaling in the germarium however has not been studied extensively. Wg is expressed in CpCs and TFs and it was shown that *wg* loss of function affects GSC region and FCs in the germarium. Wg, produced from ECs, represents a key factor for controlling the FSC population (Forbes et al., 1996b; Nystul and Spradling, 2007; Sahai-Hernandez and Nystul, 2013; Song and Xie, 2003). Whereas the exact role of Wg in FSCs and FCs had been studied in more detail, the function of Wg signaling for GSCs and germline differentiation is rather unclear. Immunostaining reveals that the DE-Cad/Arm complex is found between GSCs and CpCs in large amounts and is essential for GSC maintenance (see Section 1.2.3, page 11). However, whether a perturbation of Wnt signaling due to altered cell adhesion also contributes to the observed phenotypes, has not been addressed.

1.6 Chromatin modifications present an additional level at which GSCs can be regulated

Apart from intrinsic and extrinsic signaling pathways that control stem cell fate, chromatin modifying factors have been shown to be indispensable for stem cell maintenance and differentiation (reviewed in Buszczak and Spradling, 2006). Histones can be post-transcriptionally modified in various ways, including methylation, acetylation and phosphorylation of single amino acids, which together establish histone codes of active or silent transcription.

1.6.1 Chromatin modifications regulate GSC maintenance

Which epigenetic features define the stem cell state and how do they change upon differentiation are key questions that need to be resolved in order to fully understand and to potentially manipulate stem cell maintenance and differentiation. The antagonizing Polycomb and Trithorax group proteins were discovered in *D. melanogaster* (reviewed in Ringrose and Paro, 2004), and the GSCs present an attractive model to study the complex interplay of chromatin modifications and adult stem cell fate. The histone methyl transferases Su(var)3-9 and Eggless, that is acting with its cofactor Windei, are required for the trimethylation of H3K9, which was shown to be required for normal oogenesis (Clough et al., 2007; Koch et al., 2009; Yoon et al., 2008). In addition, the H3K4 trimethylation, that is mediated by the E3 ubiquitin ligase dBre1 and the trimethylase dSet1, is

required for GSC maintenance and germline differentiation (Xuan et al., 2013). The ATP-dependent remodeling factor ISWI, a member of the SWI/SNF family of chromatin factors is required for GSC maintenance: *ISWI* mutant GSCs prematurely express the differentiation factor Bam and are lost quickly (Xi and Xie, 2005). In addition to ISWI, NURF301, another member of the NURF complex is also required for GSC proliferation and maintenance.

Chromatin modifications mediate ecdysone signaling Interestingly, Badenhorst et al., 2005 showed that NURF301 associates with the EcR in an ecdysone-dependent manner and cooperates with the EcR to mediate the effects of ecdysone signaling. Based on analysis of flies double heterozygous for components of ISWI or NURF301 and components of the ecdysone signaling pathway, it was suggested by Ables and Drummond-Barbosa, 2010 that the chromatin remodeling NURF complex functionally interacts with the ecdysone signaling pathway. These data show that the response to the ecdysone signaling can be transduced by chromatin modifications.

1.6.2 Proper ubiquitination of histone H2B is required for GSC behavior

The reversible addition of ubiquitin is another possible histone modification and histones that display ubiquitinated residues can serve as a platform for other modifications. The ubiquitination of histone H2B (H2Bub1) plays a role in various developmental processes in flies, plants and mice (reviewed in Wright et al., 2011). Recently, it was suggested that H2B monoubiquitination helps to mediate ecdysone induced gene transcription: the protease USP7 interacts with the biosynthetic enzyme GMP synthetase and removes the H2B ubiquitination mark. USP7/GMP synthetase associates with the *E74* and *E75* loci before these genes are induced by ecdysone signaling. In USP7 or GMP synthetase mutants, *E74* and *E75* are misregulated, and, furthermore, USP7/GMP synthetase physically and functionally interacts with the EcR (van der Knaap et al., 2010). Based on these findings, van der Knaap et al., 2010 suggest that USP7/GMP synthetase is a corepressor of ecdysone signaling. Scrawny, another H2Bub protease is required for the maintenance of GSCs, FSCs and intestinal stem cells (Buszczak et al., 2009). The histone demethylase Lsd1 is present in GSCs, FCs and ECs but it only seems to be required in ECs: reducing the Lsd1 levels leads to mutant germaria with a lot of undifferentiated GSC-like cells, which display high TGF- β signaling activities. Apparently, Lsd1 epigenetically reduces the levels of Dpp mRNA in ECs, contributing to the restriction of TGF- β signaling to CpCs (Eliazer et al., 2011).

In summary, there are accumulating reports about H2Bub1 functions in diverse processes. However, little is known about its role in stem cells. In cooperation with Prof. Johnsen we showed that H2Bub1 levels decrease upon differentiation of stem cells and, in particular, GSCs in *D. melanogaster* (Karpiuk et al., 2012).

1.7 Maintaining sexual identity is required for germline differentiation

Male and female GSCs are in principle controlled by similar mechanisms; however, there are sex specific differences with respect to how, when and to which extent certain signaling pathways are used (for review see Fuller and Spradling, 2007; Spradling et al., 2011). The *D. melanogaster* testis is a paired tubular organ; the GSCs reside at the apical tip and are attached to somatic hub cells. The cyst stem cells give rise to somatic cells that – similar to the ECs in the female ovaries – encapsulate the differentiating germline cells. The TGF- β ligands Dpp and Gbb are produced in the somatic hub and cyst cells and – like in the ovary – are required for GSC maintenance. Different from the situation in females, ectopic activation of the TGF- β pathway is not sufficient to induce self-renewal of germline cells (reviewed in Matunis et al., 2012). Bam is a differentiation factor in males as well, but acting at a different step than in the females: it is expressed in differentiating spermatocytes and is required to cease mitotic amplification divisions (reviewed in Spradling et al., 2011).

1.7.1 Sex is determined by a series of alternative splicing events in *D. melanogaster*

Different species use a variety of different mechanisms to establish and maintain the somatic sex. The X chromosome to autosome ratio determine the sexual identity: two X chromosomes (XX:AA) determines female, one X chromosome (X:AA) yields male identity. The Y chromosome has no influence on the sexual identity, but is required for spermatogenesis. Regulatory proteins lead to the activation of the gene encoding the RNA binding protein Sex lethal (Sxl) in XX:AA animals only. After the Sxl activity was set up early in embryogenesis, a positive feedback splicing mechanism is used, in which Sxl controls its own splicing. X:AA cells lack Sxl protein and all *Sxl* transcripts, therefore, contain an exon containing a translation termination codon. In XX:AA cells, however, Sxl protein affects splicing and thus, the male specific translation terminating codon is skipped and functional *Sxl* mRNA is generated. Sxl is both necessary and sufficient to pursue its own splicing loop and is on top of the cascade determining the female trait, directly or indirectly controlling all female specific programs (reviewed in Salz, 2011; Salz and Erickson, 2010). Sxl controls the splicing of *transformer* (*tra*). Tra – a female specific RNA binding protein as well – in turn, controls splicing of the transcription factors Doublesex (Dsx) and Fruitless. Dsx is the main factor controlling the sexual dimorphism of the somatic gonads. It is expressed in a subset of somatic cells and controls the sexually dimorphic development of the others via cell non-autonomous processes (reviewed in Murray et al. (2010)).

The germline sexual identity is determined in collaboration with the soma
Interestingly, the sexual identity of germline cells is determined differently from

the somatic cells in many species. In some, the somatic cells solely control the germline sexual fate. In others, such as fruit flies, mice or humans the sexual identity of the germ cells is important for the germ cells sex. *Tra* and *Dsx*, the main determinants of somatic sexual identity are not required in the germline for specifying the sexual identity. The role of *Sxl* in the germline is discussed controversial; while it was thought to act and be activated differently then in the soma (reviewed in Casper and Van Doren, 2009), it was recently shown that ectopic expression of *Sxl* is sufficient to induce female development in the pole cells (Hashiyama et al., 2011). Hence, *Sxl* is a key player in establishing sexual identity of both soma and germline, nevertheless a comprehensive analysis of downstream effectors is missing (reviewed in Murray et al., 2010; Salz and Erickson, 2010). The germline sexual identity is first detected after formation of the embryonic gonad and is mainly controlled by the soma at this point (Casper and Van Doren, 2009; Wei et al., 1994). As development goes on, the soma is not sufficient for keeping the germline sex; XX:AA or X:AA germ cells in the soma of the opposite sex do not follow the somatic sex. Transplant studies demonstrated, that XX:AA germ cells cannot form oocytes in the male soma and XY:AA germ cells do not give rise to spermatocytes when transferred into the female soma, but rather display a confused sexual identity (reviewed in Murray et al., 2010). It is therefore critical to understand, which pathways are used by the soma to control the germline sex. The JAK/STAT signaling pathway that is known to be one of the main mechanisms that control GSC maintenance in the testis also has a masculinizing effect on the germ cells (Wawersik et al., 2005). The mechanisms that are used by the female soma to control the germline sex remain undiscovered.

1.7.2 Germline tumor arise as a consequence of confused sexual identity

Mutations in *Sxl* lead to tumors in XX:AA germline cells that are blocked between GSC and CB stage. The tumorous cells not only express the differentiation factor *Bam*, but also the GSC specific marker *Nos* (Chau et al., 2009, 2012). Together with its partner *Pum*, *Nos* inhibits differentiation-promoting mRNAs, including *brat* and it is therefore critical to restrict *Nos* function to the GSC. It is known that *Bam* itself downregulates the levels of *Nos* (Li et al., 2009) and, in addition, Chau et al., 2009, 2012 showed that the translation of *nos* is directly repressed by *Sxl*. *Sxl*, thus, promotes differentiation of the GSC progeny; since *Sxl* is also present in the GSCs themselves, this raises the question how the *Nos* repression by *Sxl* is restricted to CBs. Based on epistasis experiments, Chau et al., 2009, 2012 suggest, that *Bam* itself is required for this germline cell specificity and that *nos* is ultimately repressed by *Bam* and *Sxl* functioning together. The misdirected expression of *nos*, however, is not sufficient to explain the described tumorous phenotypes (Chau et al., 2012; Li et al., 2009).

Mismatch of germline and somatic sexual identity leads to differentiation failure Interestingly, germline cells lacking *Sxl* or *bam* express a set of commonly

testis-specific markers, suggesting that their sexual identity is confused (Chau et al., 2009; Staab et al., 1996; Wei et al., 1994). Such "ovarian tumors", consisting of germline cells displaying both male and female characteristics are also observed when XX:AA germline cells are transplanted into a female soma (reviewed in Casper and Van Doren, 2006). Furthermore, mutations in *ovarian tumor* or *ovo*, which are thought to promote female identity, lead to germline overproliferation (King; Oliver et al., 1987). Altogether, there are many examples showing that the sexual identity of soma and germline have to match in order to allow for proper germline development. Considering that steroid hormones are key determinants for sexual development in mammals, these findings raise the question whether defects in maintaining the sexual identity contribute to the differentiation delay observed upon perturbed ecdysone signaling.

1.8 Research objectives

In a genetic pilot screen, clonal germaria of *hsFlp; FRT40A* lethals from the Drosophila Genomics Resource Center were analyzed in order to find novel genes that affect the GSC niche architecture. Out of 206 preselected genotypes, 53 were chosen for a secondary analysis (Weiss, 2009). Interestingly, components of a pathway, that had not been shown to play a role in GSC-niche communication at that point, were found. The gene *tai* codes for the *D. melanogaster* homolog of AIB1 (amplified in breast cancer) and its loss of function leads to severe defects in the germarium architecture. Tai is a co-activator of the nuclear hormone receptor for ecdysone, the hormone that triggers all developmental transitions in the fly (Bai et al., 2000). In addition to that, the transcription factor Ab that binds Tai and thereby is a repressor of ecdysone signaling, was also found to affect germarium architecture in the screen.

Whereas the developmental roles of ecdysone in the fly have been extensively studied, far less is known about the function of the only known steroid hormone in adult flies. Steroid hormones control various aspects of adult life in vertebrates, but since analysis of their function is technically challenging, good model systems are extremely valuable. We, therefore, decided to analyze the undescribed functions of the ecdysone signaling pathway in the adult germarium.

First analysis had revealed that germaria with *tai* mutant clonal cells were characterized by enlarged niches and disturbed differentiation of GSC progeny (Weiss, 2009). In addition, data gained by Weiss, 2009 pointed towards a somatic requirement of the ecdysone signaling pathway components. A first aim of the present thesis was, therefore, to confirm, that the ecdysone signaling acts on the germline in a cell non-autonomous fashion. For that purpose, the activity pattern of ecdysone signaling pathway in the germarium was analyzed and different mutations of ecdysone signaling pathway components – conditionally present in soma, germline or both – were compared. As is described in Section 1.2.4, page 12, ECs form long cytoplasmic protrusions and are essential to allow for germline differentiation. To reveal what happens in ECs upon perturbed ecdysone signaling, EC shape was analyzed using specific markers. Importantly, several pathways are known to be required for the communication between germline and soma in the germarium (see Section 1.2.1, page 6): does any of these contribute to transmitting the systemic ecdysone hormone signaling to the GSCs? Finally, specific germline markers and epistasis experiments were used to characterize the nature of the germline cells delayed in differentiation. In summary, the previously unknown role of ecdysone signaling, controlling the germline and especially germline differentiation was characterized.

2 Results

2.1 Ecdysteroids affect *Drosophila* ovarian stem cell niche formation and early germline differentiation

Annekatrin König, Andriy S Yatsenko, Miriam Weiss and Halyna R Shcherbata

Experiments	Done by
Analysis of <i>tai</i> transheterozygous mutants; in Figure 1, Supplementary table S1	Miriam Weiss
Analysis of <i>ecd1^{ts}</i> and dominant negative <i>EcR</i> mutants; in Figure 2, Supplementary table S2	Annekatrin König
Supply of 20E to ecdysone signaling mutants; in Figure 2, Supplementary table S3	Annekatrin König
Germline cell markers and dumbbell shaped fusomes; in Figure 3, Supplementary Figure 1	Annekatrin König
Analysis of pMad levels in <i>ecd1^{ts}</i> mutants; in Figure 3	Andriy S Yatsenko
Expression pattern of ecdysone signaling components; in Figure 4, Supplementary Figure 2	Annekatrin König
Analysis of mutants expressing <i>UAS ab</i> , <i>EcR RNAi</i> in the soma; in Figure 5, Supplementary table S5	Miriam Weiss and Annekatrin König
Analysis of <i>tai</i> clonal germlaria; in Figures 6+7, Supplementary Figure 3, Supplementary table S4	Miriam Weiss and Andriy Yatsenko
Analysis of mutants overexpressing <i>UAS ab</i> or <i>EcR RNAi</i> in the soma; in Figure 6	Miriam Weiss and Annekatrin König
Analysis of clonal overexpression of <i>ab</i> or <i>EcR RNAi</i> , <i>tai</i> mutant ECs; in Figure 7	Annekatrin König
Analysis of germlaria overexpressing <i>EcR</i> ; in Figure 7 and Supplementary table S6	Annekatrin König
Expression pattern of drivers; Supplementary Figure 4	Annekatrin König

Status of the manuscript: published (EMBO J. 2011 Apr 20;30(8))

Ecdysteroids affect *Drosophila* ovarian stem cell niche formation and early germline differentiation

This is an open-access article distributed under the terms of the Creative Commons Attribution Noncommercial No Derivative Works 3.0 Unported License, which permits distribution and reproduction in any medium, provided the original author and source are credited. This license does not permit commercial exploitation or the creation of derivative works without specific permission.

Annekatriin König, Andriy S Yatsenko,
Miriam Weiss and Halyna R Shcherbata*

Max Planck Research Group of Gene Expression and Signaling,
Max Planck Institute for Biophysical Chemistry, Göttingen, Germany

Previously, it has been shown that in *Drosophila* steroid hormones are required for progression of oogenesis during late stages of egg maturation. Here, we show that ecdysteroids regulate progression through the early steps of germ cell lineage. Upon ecdysone signalling deficit germline stem cell progeny delay to switch on a differentiation programme. This differentiation impediment is associated with reduced TGF- β signalling in the germline and increased levels of cell adhesion complexes and cytoskeletal proteins in somatic escort cells. A co-activator of the ecdysone receptor, Taiman is the spatially restricted regulator of the ecdysone signalling pathway in soma. Additionally, when ecdysone signalling is perturbed during the process of somatic stem cell niche establishment enlarged functional niches able to host additional stem cells are formed.

The EMBO Journal advance online publication, 18 March 2011; doi:10.1038/emboj.2011.73

Subject Categories: signal transduction; development

Keywords: *Drosophila*; ecdysone signalling; germline stem cell; stem cell niche

Introduction

One of the key characteristics of adult stem cells is their ability to divide for a long period of time in an environment where most other cells are quiescent. Typically, stem cells divide asymmetrically where a mother cell gives rise to two daughter cells with different fates, another stem cell and a differentiated progeny (Gonczy, 2008).

Adult stem cells also require niches. The niche itself is as significant as stem cell autonomous functions and its environment has the potential to reprogramme somatic cells and to transform them into stem cells (Brawley and Matunis, 2004; Kai and Spradling, 2004; Boulanger and Smith, 2009). The niche includes all cellular and non-cellular components that interact in order to control the adult stem cell. These interactions can be divided into one of two main mechanistic

types—physical contacts and diffusible factors. Diffusible factors travel over varying distances from a cell source to instruct the stem cell, often affecting transcription (Walker *et al*, 2009). Stem cells must be anchored to the niche through cell-to-cell interactions so they will stay both close to niche factors that specify self-renewal and far from differentiation stimuli. While multiple studies focused on the aspects of how the niche regulates stem cells, the question of how the niche is established itself has not been addressed in depth.

The *Drosophila* ovarian stem cell niche model is an exemplary system where two different stem cell types, germline stem cells (GSCs) and somatic escort stem cells (ESCs) share the same niche and coordinate their development. Niche cells contact GSCs via E-cadherin and Integrin-mediated cell adhesion complexes that bind to the extracellular matrix and connect to the cytoskeleton and this physical docking of stem cells to the niche is essential for GSC maintenance (Xie and Spradling, 2000; Tanentzapf *et al*, 2007). In addition, the stem cell niche sends short-range signals that specify and regulate stem cell fate by maintaining the undifferentiated state of GSCs next to the niche. Not only does the niche have an effect on stem cells, but also the stem cells communicate with the niche. A feedback loop exists between the stem cells and niche cells: Delta from the GSC can activate Notch in the somatic cells that maintains a functional niche and in turn controls GSC maintenance (Ward *et al*, 2006). While the management of GSCs within the niche is relatively well understood, the control of the other present stem cell type, ESCs is not clear. An ESC, like a GSC divides asymmetrically producing another ESC and a daughter, escort cell (EC) that will differentiate into a squamous cell that envelops the GSC progeny once disconnected from the niche. It is believed that developing cyst encapsulation by ECs protects from TGF- β signalling that maintains GSC identity (Decotto and Spradling, 2005). The ESC and GSC cycles have to be tightly coordinated, so a sufficient number of ECs will be produced in response to GSC division. However, the pathway used for GSC and ESC communication is unknown.

Adult stem cell division mostly is activated locally in response to tissue demands to replace lost cells. In addition, stem cells can be regulated via more general stimuli in response to systemic needs of the whole organism. Hormones are systemic regulators that regulate a variety of processes in different organs in response to the body's status. Even though the effects of hormonal signalling have been extensively studied, the specific roles for hormones in stem cell biology remain complex, poorly defined and difficult to study *in vivo*.

Drosophila is a great system to study the role of endocrine signalling as it contains only one major steroid hormone, ecdysone (20-hydroxyecdysone, 20E) that synchronises the

*Correspondence: Gene Expression and Signalling Group, Max Planck Institute for Biophysical Chemistry, Am Fassberg 11, Göttingen 37077, Germany. Tel.: +49 551 201 1656; Fax: +49 551 201 1755; E-mail: halyna.shcherbata@mpibpc.mpg.de

Received: 9 November 2010; accepted: 22 February 2011

behavioural, genetic and morphological changes associated with developmental transitions and the establishment of reproductive maturity (Shirras and Bownes, 1987; Riddiford, 1993; Buszczak *et al*, 1999; Kozlova and Thummel, 2003; Gaziova *et al*, 2004; Schubiger *et al*, 2005; Terashima and Bownes, 2005; McBrayer *et al*, 2007). Ecdysteroids act through the heterodimeric nuclear receptor complex consisting of the ecdysone receptor, EcR (Koelle *et al*, 1991) and its partner ultraspiracle (USP), the *Drosophila* retinoid X receptor homologue (Shea *et al*, 1990; Oro *et al*, 1992; Yao *et al*, 1992). The ecdysone/EcR/USP receptor/ligand complex binds to ecdysone response elements (EcREs) to coordinate gene expression in diverse tissues (Riddihough and Pelham, 1987; Cherbas *et al*, 1991; Dobens *et al*, 1991). Ecdysone signalling is patterned spatially as well as temporally; depending on the tissue type and the developmental stage, the EcR/USP complexes with different co-activators or co-repressors including Taiman, Alien, Rig, SMRTER, Bonus, Trithorax-related protein and DOR (Dressel *et al*, 1999; Tsai *et al*, 1999; Bai *et al*, 2000; Beckstead *et al*, 2001; Sedkov *et al*, 2003; Gates *et al*, 2004; Jang *et al*, 2009; Francis *et al*, 2010; Mauvezin *et al*, 2010). These co-factors can have other binding partners that are themselves regulated by different signalling pathways. For example, Abrupt controlled by JAK/STAT attenuates ecdysone signalling by binding to its co-activator Taiman (Jang *et al*, 2009). In addition, other signalling pathways (insulin, TGF- β) interact with ecdysone pathway components to further modulate cell type-specific responses (Zheng *et al*, 2003; Jang *et al*, 2009; Francis *et al*, 2010). This offers an additional level of combinatorial possibilities and suggests a model of gene expression regulation that is highly managed by this global endocrine signalling.

Data presented here show that ecdysone signalling is involved in control of early germline differentiation. When ecdysone signalling is perturbed, the strength of TGF- β signalling in GSCs and their progeny is modified resulting in a differentiation delay. Moreover, soma-specific disruption of ecdysone signalling affects germline differentiation cell non-autonomously. Ecdysteroids act in somatic ESCs and their daughters to regulate cell adhesion complexes and cytoskeletal proteins important for soma-germline communication. Misexpression of ecdysone signalling components during developmental stages leads to the formation of the enlarged GSC niche that can facilitate more stem cells.

Results

***Taiman*, a *Drosophila* homologue of a steroid receptor co-activator amplified in breast and ovarian cancer (AIB1) influences the size of the niche and GSC number**

The *Drosophila* ovary contains distinct populations of stem cells: GSCs, which give rise to the gametes, and two types of somatic stem cells: ESCs and follicle stem cells (FSCs) (Figure 1A). These stem cells reside in stereotyped positions inside the germarium, a specialised structure at the anterior end of the *Drosophila* ovary. Both GSCs and ESCs are adjacent to somatic signalling centres or niches consisting of the terminal filament (TF) and cap cells (CpCs), which promote stem cell identity. ESCs produce squamous daughters with long processes that encase developing cysts to protect them from niche signalling and allow differentiation. These different cell types have distinct morphologies and molecular markers (Figure 1C and E).

We performed a pilot genetic screen where clonal germaria of *hsFlp;FRT40A* lethals (DGRC) were analysed in order to find novel genes that affect stem cell niche architecture. One of the genes found in our screen encoding a *Drosophila* homologue of a human steroid receptor co-activator amplified in breast cancer *taiman* (*tai*) was of a particular interest. Downregulation of *Tai* using different combinations of *tai* amorphic and hypomorphic mutant alleles resulted in increased GSC number and an enlarged niche (Figure 1D and F). The GSC average number ranged from 3.2 to 5.1 depending on the genotype, which was significantly higher than in heterozygous control flies (2.1–2.4, Figure 1D, F and H; Supplementary Table S1). This increase in GSC number coincided with stem cell niche enlargement. While control germaria contained on average 6 niche cells, *tai* mutant niches consisted of 7–10 CpCs (Figure 1D, F and G; Supplementary Table S1). These observations imply that *Tai* participates in niche formation and/or GSC maintenance or differentiation.

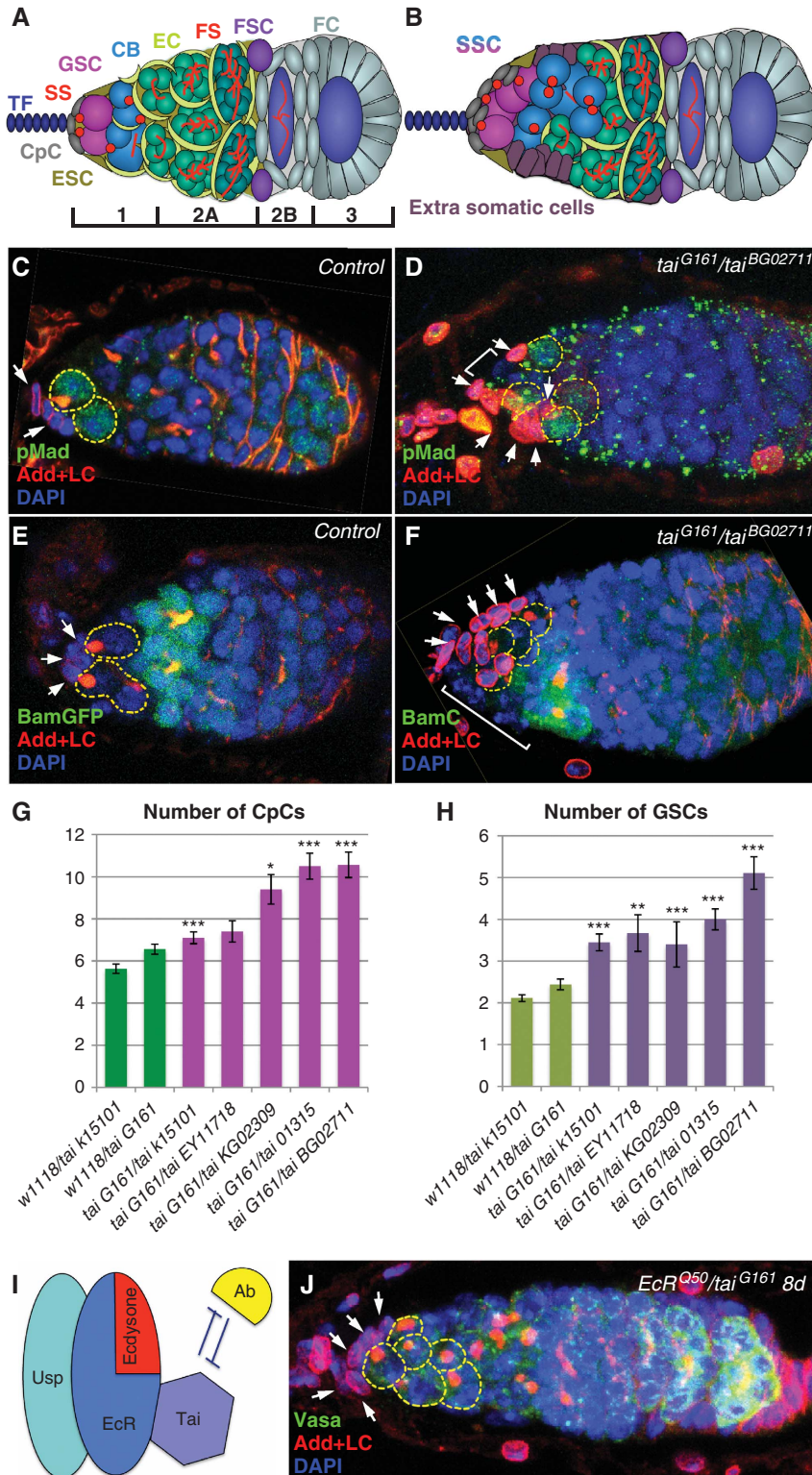
As it has been shown that in *Drosophila* Taiman is a co-activator of the ecdysone transcription-activating complex (Figure 1I; Bai *et al*, 2000), we tested if *tai* and ecdysone pathway components genetically interact in the process. Transheterozygous germaria (*tai*/EcR and *tai*/usp) also showed additional GSCs and enlarged niches (Figure 1J; Supplementary Table S1), suggesting that the ecdysone pathway regulates early germline progression and GSC niche assembly.

Figure 1 The ecdysone receptor co-activator Taiman controls the number of ovarian germline stem cell niche cells. (A) Schematic view of a wild-type germarium: germline stem cells (GSCs, pink) marked by anterior spectrosomes (SS, red dots) are located at the apex of the germarium next to the niche cap cells (CpCs, grey). Further noted are terminal filament (TF; dark blue), escort stem cells (ESCs, olive), differentiating cystoblasts (CBs, blue), escort cells (ECs, lime), 4, 8 (bright green) and 16 cell (green) cysts in region 2A, indicated by the presence of fusomes (FS, red branched structures), follicle stem cells (FSCs, violet) and follicle cells (FC, light grey) in regions 2B and 3. (B) Schematic view of a *tai* mutant germarium with an increased number of single spectrosome containing cells (SSCs, pink and blue), CpCs (grey) and additional somatic cells (plum). (C, E) In wild-type germaria, two GSCs marked by the presence of the stem cell marker pMad (C), spectrosomes (stained with Adducin) and the absence of the differentiation factor BamC (E) are directly attached to the niche (marked with LaminC, arrows). (D, F) In the *tai*^{61G1}/*tai*^{BG02711} transheterozygous mutant germarium, the enlarged niche is coupled with an increased number of GSCs that are pMad positive (D) and BamC negative (F). In addition, extra somatic cells are present at the anterior (marked with brackets). CpC (G) and GSC (H) numbers are increased in *tai* mutant germaria. (I) Scheme illustrating that *Tai* is a co-activator of the EcR/USP nuclear receptor complex that is activated upon binding of its ligand ecdysone; Ab negatively regulates the ecdysone signalling by direct binding to *Tai* (based on Bai *et al* (2000) and Jang *et al* (2009)). (J) EcR^{Q50st}/*tai*^{61G1} transheterozygous germaria also contain an increased number of GSCs and CpCs, indicating that *tai* genetically interacts with EcR (see Supplementary Table S1). (D–F, J) Projections of optical sections assembled through the germarial tissue; GSCs are outlined with yellow dashed lines, niche cells are marked with white arrows; Red, Adducin + LaminC; blue, DAPI; and green, pMad (C, D), BamGFP (E), BamC (F) and Vasa (J); Error bars represent s.e.m. **P* < 0.05, ***P* < 0.005, ****P* < 0.0005.

The steroid hormone ecdysone controls GSC progeny differentiation

To further test the role of the endocrine pathway in the germline, we used the *ecdysoneless1* temperature-sensitive mutation (*ecd1^{ts}*) that blocks biosynthesis of the mature ecdysteroid hormone, 20-hydroxyecdysone. *ecd1^{ts}* animals were allowed to develop normally at the permissive tempera-

ture and transferred to restrictive temperature conditions as 3-day-old adults. When ecdysone production was disrupted during adulthood, GSCs continued to divide increasing the germarium size, however, their progeny delayed progression through differentiation (Figure 2A and B). Similar phenotypes were obtained upon ecdysone signalling disruption using dominant-negative mutants for the



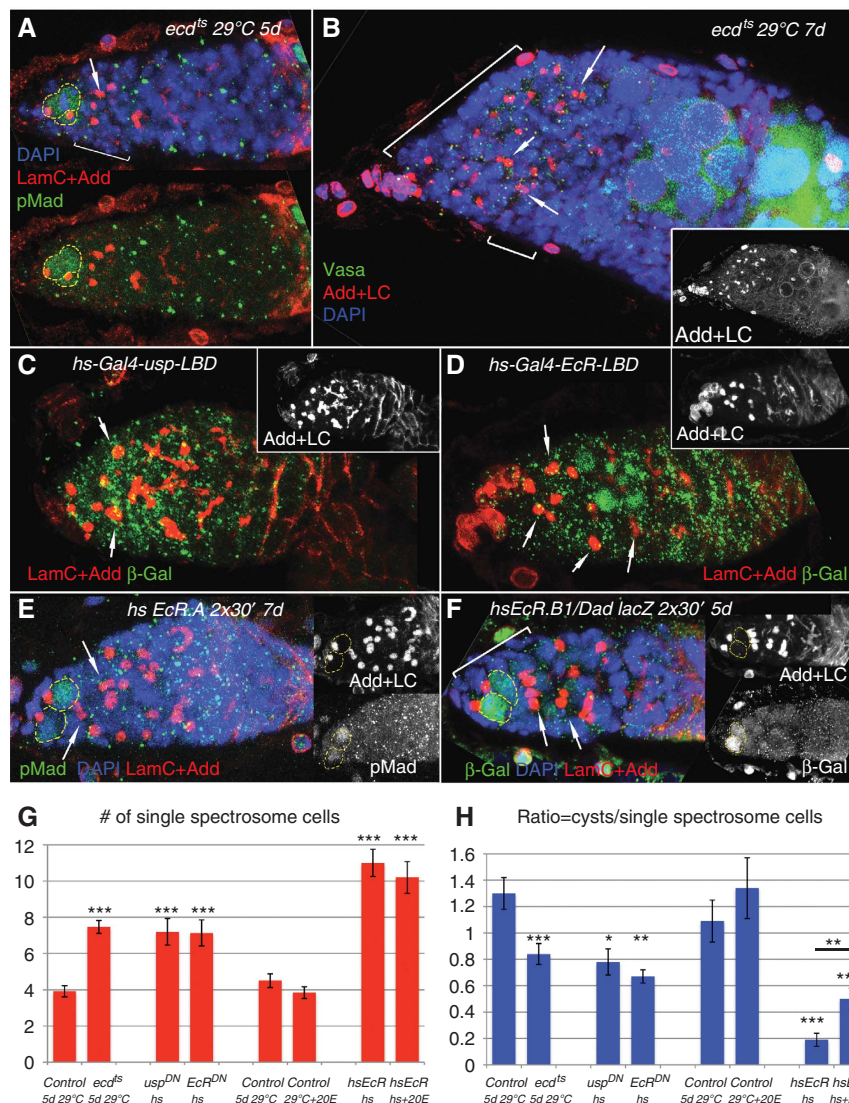


Figure 2 Disrupted ecdysone signalling during adulthood results in delayed germline differentiation. (A) At the restrictive temperature (29°C) *ecd1^{ts}* adult animals contain germaria filled with supernumerary SSCs. (B) Extended depletion of ecdysone furthermore increases the undifferentiated SSC number and causes somatic cell defects affecting cyst pinching off from the germarium. (C, D) Heat shock induced expression of USP and EcR dominant-negative forms (*usp^{DN}* (*hs-Gal4-usp-LBD*) and *EcR^{DN}* (*hs-Gal4-usp-LBD*)) also lead to the appearance of supernumerary SSCs. (E, F) Similarly to the effects that are caused by disturbing the ecdysone pathway via *ecd1^{ts}* or dominant-negative *EcR^{DN}* and *usp^{DN}* mutations, expression of the EcR isoforms *EcR.A* or *EcR.B1* induced by heat shock (twice per day for 30 min 4 days in a row) increases the number of SSCs, but not GSCs and influences CB differentiation. Note the presence of dumbbell-shaped fusomes in (A–F). (G) In control conditions around four SSCs per germarium are detected. Ecdysone withdrawal via *ecd1^{ts}* mutation as well as heat shock-induced expression of *usp^{DN}* or *EcR^{DN}* and overexpression of *EcR* led to a 2- or 2.5-fold increase in SSC number, whereas external supply of ecdysone does not change the amount of SSCs within the germarium. (H) The ratio of differentiating cysts to SSCs is about 1.5-fold decreased in *ecd1^{ts}*, *usp^{DN}* and *EcR^{DN}* mutant germaria. This decrease is even more pronounced (seven times) in *hsEcR* flies. Providing 20E externally can partially, but significantly alleviate this early germline differentiation delay. (A–F) Projections of optical sections assembled through the germarial tissue. GSCs are outlined with yellow dashed lines, dumbbell-shaped fusomes are marked with arrows and additional somatic cells are marked with brackets. Red, LaminC + Adducin; blue, DAPI; and green, pMad (A, E); Vasa (B) and β -galactosidase (C, D, F) Error bars represent s.e.m. * $P < 0.05$, ** $P < 0.005$, *** $P < 0.0005$.

ecdysone receptor, EcR and its dimerisation partner USP (*hs-Gal4-EcR-LBD* (*EcR^{DN}*) and *hs-Gal4-usp-LBD* (*usp^{DN}*); Kozlova and Thummel, 2002), (Figure 2C and D; Supplementary Table S2). Instead of progressively developed cysts, mutant germaria were filled with germline cells containing a single spectrosome (single spectrosome containing cells (SSCs)), on average seven SSCs per *ecd1^{ts}* or *EcR^{DN}* and *usp^{DN}* germarium were detected in comparison to four in control (Figure 2G; Supplementary Table S2). After longer ecdysone deprivation germaria look even more abnormal;

a slightly decreased GSC number and additional follicle cell defects along with abnormal cyst pinching off from the germarium, not shared by *tai* mutants, were observed (Figure 2B; Supplementary Table S2). The differentiation index or the ratio between developing fusome-containing cells and SSCs in the region 1–2A was decreased 1.5–2-fold in ecdysone mutant germaria (Figure 2H; Supplementary Table S2). Disruption of ecdysone signalling via overexpression of EcR (*hsEcR.A* and *hsEcR.B1*) also resulted in the appearance of germaria filled with supernumerary SSCs

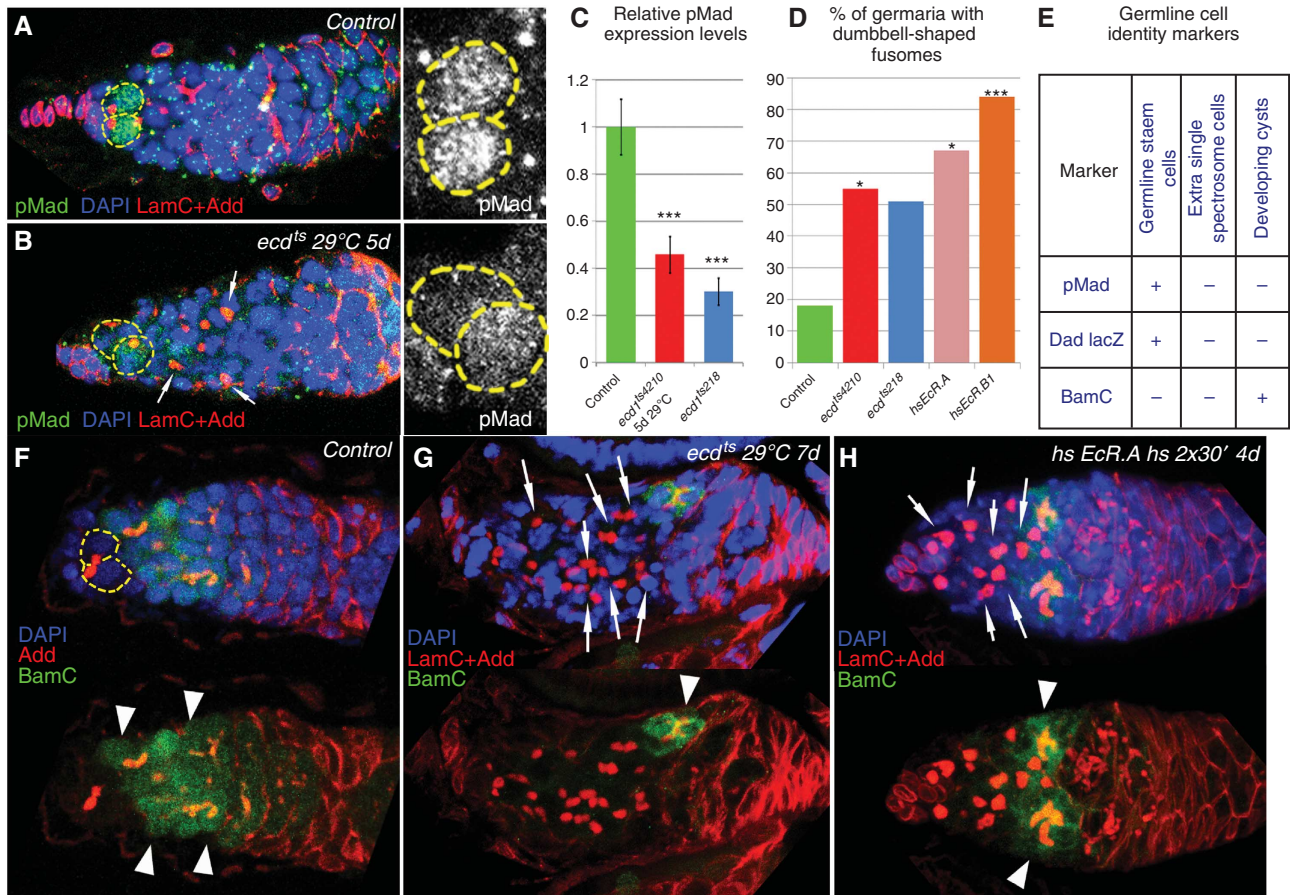


Figure 3 Ecdysone signalling affects the TGF- β pathway. (A) Wild-type germarium containing two GSCs, marked by pMad staining. (B) Upon blocked ecdysone production the relative pMad expression levels in GSCs are decreased (C, compare the pMad levels measured by grey value in A and B). (D) Disruption of ecdysone signalling results in the increase of dumbbell-shaped fusome quantity. In *ecd1^{ts4210}* mutant flies that were at the restrictive temperature for up to 7 days, 55% ($n = 33$) of the germaria have dumbbell-shaped fusomes (*ecd1^{ts218}* 51%, $n = 37$) whereas in equally treated *w¹¹¹⁸* germaria, only 18% ($n = 11$) of the germaria contain dumbbell-shaped fusomes. After overexpression of *EcR.A* or *EcR.B1* for 7 days 67% or 84% ($n = 15, 19$, respectively) of the analysed germaria contain dumbbell-shaped fusomes. (E) The characteristics of GSCs, SSCs and developing cysts are compared schematically. GSCs express the stem cell markers pMad and Dad lacZ and developing cysts the differentiation factor BamC, whereas additional SSCs in germaria deficient of ecdysone signalling are pMad, Dad lacZ and BamC negative, showing that they do not maintain stem cell identity and are delayed in development. (F) In wild-type germarium, BamC is present in developing CBs adjacent to GSCs, while in ecdysone pathway mutants, *ecd1^{ts}* (G) and *hsEcR* (H), the anterior part of the germarium is filled with cells that do not express the differentiation marker BamC and contain a single spectroscopic or a dumbbell-shaped fusome. (A, B, F–H) Projections of optical sections assembled through the germarial tissue. GSCs are outlined with yellow dashed lines, dumbbell-shaped fusomes are marked with arrows and BamC-positive differentiating cysts with arrowheads. Red, Adducin + LaminC; blue, DAPI; and green, pMad (A, B); BamC (F–H). Error bars represent s.e.m. Significance calculated using the *t*-test (C), χ^2 -test (D). * $P < 0.05$, *** $P < 0.0005$.

(on average 11 in comparison to 4 in control, Figure 2E–H; Supplementary Table S3).

The described phenotypes show that ecdysone signalling loss of function (by disruption of ecdysone biosynthesis or by expression of EcR and USP dominant-negative forms) and overexpression of the main receptor of the pathway, EcR cause similar abnormalities. Previously, it has been shown that the EcR can form homodimers in the absence of its binding partners *in vitro* (Elke *et al*, 1997), moreover the un-liganded receptor complex is repressive and this repression is relieved as the hormone titre increases (Schubiger and Truman, 2000; Schubiger *et al*, 2005).

To test if the latter can be the case in our system, we performed experiments where adult flies were fed with 20E. Feeding flies with ecdysone alone had no significant effect on the number of SSCs or germline differentiation measured by the ratio of differentiated cysts to SSCs within one germarium (Figure 2G and H; Supplementary Table S3). Interestingly,

feeding of ecdysone to the animals that overexpressed EcR moderately, but significantly rescued the cyst/SSC ratio (Figure 2H; Supplementary Table S3), indicating that EcR overexpression when the ecdysone receptor is abundant and the ligand is limited is unfavourable for germline differentiation.

Ecdysone signalling disturbance affects the intensity of TGF- β signalling

Next, we attempted to analyse the identity of supernumerary SSCs. If they are GSCs, they should express appropriate markers. However, we found that additional SSCs are negative for the stem cell markers, phosphorylated Mad and Dad (Figures 2A, E, F, 3B and E). We also noticed that levels of pMad in GSCs were significantly reduced upon ecdysone deficit (Figure 3A–C), suggesting that ecdysone signalling can modulate pMad levels.

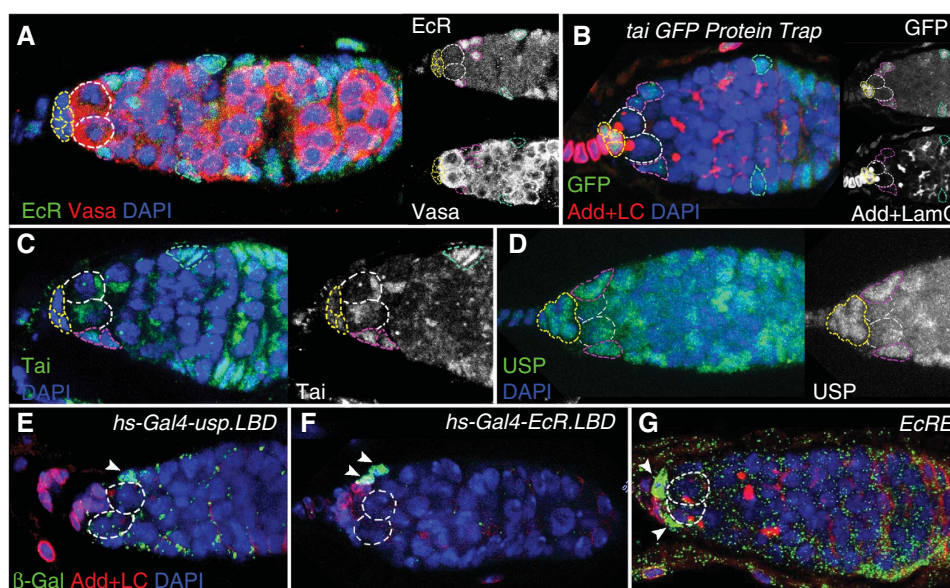


Figure 4 Expression pattern of the ecdysone pathway components in the *Drosophila* germarium. (A) The anti-EcR (common region) antibody detects high levels of EcR in ESCs and FCs. (B) In the *tai* G00308 protein trap line where GFP is expressed under the control of the endogenous *tai* promoter, high GFP levels were detected in CpCs, ESCs and FSCs. (C) Comparable expression pattern is observed with the anti-Tai antibody. (D) The nuclear receptor USP detected by the anti-USP antibody shows identical expression pattern to its binding partner EcR. (E, F) Spatial patterns of ecdysone signalling activation identified via β -Gal staining of heat-treated *hs-Gal4-usp.LBD/+; UAS-lacZ/+* (E) and *hs-Gal4-EcR.LBD/+; UAS-lacZ/+* (F) germaria prove ecdysone signalling being mainly active in the ESCs (marked with arrowheads). (G) The ecdysone signalling reporter *EcRE-lacZ* shows the presence of active ecdysone transcription complex in ESCs as well (marked with arrowheads). Different cell types are marked as follows: GSCs, white dashed lines; CpCs, yellow dashed lines; ESCs/ECs, red dashed lines; FCs, green dashed lines. Red, Vasa (A), Adducin + LaminC (B, E–G); blue, DAPI; and green, anti-EcR (common region) (A); GFP (B); anti-Tai (C), anti-USP (D) and β -galactosidase (E–G).

As supernumerary SSCs did not express the stem cell markers, we next analysed if the increased number of SSCs can be explained by abnormal organisation of fusomes, the structures that connect daughter cells within one cyst. Cysts are formed by a process of mitosis with incomplete cytokinesis, and all cells forming one cyst divide simultaneously (de Cuevas and Spradling, 1998). If ecdysone signalling affects fusome stability leading to the appearance of dot-like instead of branched fusomes, then SSCs are really cells within a differentiating cyst and should have synchronised divisions. However, staining with a mitotic marker phosphohistone H3 (PH3) showed that the cell cycle was not coordinated in SSCs, which shows that single spectrosomes are not the result of fusome breakage in pursuit of cyst de-differentiation into single stem cell-like cells (Supplementary Figure S1).

We also noticed that many fusomes had a dumbbell shape, which is a characteristic of perturbed Bam, a TGF- β signalling target (McKearin and Ohlstein, 1995) (Figures 2B–F, 3B, G and H). The amount of germaria with dumbbell-shaped fusomes increased from 18% in control to 51–84% in animals with exogenous EcR expression and ecdysone deficit (Figure 3D). Interestingly, SSCs in germaria mutant for ecdysone signalling, unlike wild-type differentiating cystoblasts do not express Bam, a factor essential for germline differentiation (Figure 3F–H). Taken together, these analyses show that additional SSCs resulting from ecdysone signalling disruption are ‘undecided’ cells that express neither stem cell nor differentiation markers (Figure 3E).

These data suggest that ecdysone signalling affects early germline differentiation possibly by modulation of the TGF- β signalling strength causing a developmental delay. Eventually

some germline differentiation takes place implying that ecdysone signalling is at least partially redundant with other pathways for germline progression.

Ecdysone signalling is predominantly active in ESCs and Taiman, an EcR/USP co-activator is spatially limited to the soma

Previous studies show that ecdysone signalling in *Drosophila* has a role in egg maturation and vitellogenesis (Shirras and Bownes, 1987; Riddiford, 1993; Buszczak *et al*, 1999; Kozlova and Thummel, 2003; Gaziova *et al*, 2004; Schubiger *et al*, 2005; Terashima and Bownes, 2005; McBrayer *et al*, 2007), now our data indicate that it is also required for differentiation of developing germline cysts. As germline differentiation can be regulated cell autonomously or cell non-autonomously, we decided to test what goes awry in the GSC niche community when the ecdysone pathway is perturbed. We began with analysing the expression pattern of ecdysone signalling pathway components to find out in which cell types ecdysone signalling is working. The EcR protein measured by a specific antibody was detected mostly in ESCs and ECs, thin cells which envelop the differentiating cystoblast to assist in differentiation by protecting it from the niche signals (Figure 4A). Next, we used a GFP protein trap line inserted in the *tai* gene and detected levels of GFP expression in CpCs that form the niche and also to a lesser amount in ESCs (Figure 4B). Similarly, staining with Tai and USP-specific antibodies (Figure 4C and D; Supplementary Figure S2) showed that these proteins are expressed predominantly in somatic cells, however, some low levels are also present in

the germline indicative of a possible dual role of this endocrine pathway in the germline and the soma.

After determining protein expression we wanted to confirm that the ecdysone signalling pathway was active. For this, we used reporters with a *Gal4* transcription factor fused to the ligand-binding domain of USP or EcR (*hs-Gal4-uspLBD*, *hs-Gal4-EcRLBD*; Kozlova and Thummel, 2002). The ecdysone pathway activity was detected mainly in ESCs and ECs analysed using a somatically expressed *UAS lacZ* transgene (Figure 4E and F). The *EcRE-lacZ* construct that senses the presence of the active ecdysone receptor transcription complex (Koelle *et al*, 1991) also validated the pathway activity in ESCs and random CpCs (Figure 4G).

Ecdysone signalling is required cell non-autonomously for progression through the early steps of germ cell lineage

Our expression data demonstrate that ecdysone signalling components are expressed in somatic cells within the GSC niche and the signalling is active predominantly in ESCs, leading to the hypothesis that ecdysone signalling controls germline cell differentiation extrinsically. This idea is further supported by the analysis of *tai* loss-of-function germline clones (Supplementary Figure S3) that show that *Tai* is not essential for germline progression: *tai* mutant GSCs were normally maintained (Supplementary Table S4; Supplementary Figure S3B) and in general germline differentiation was not affected (Supplementary Figure S3A). Together with spatially restricted somatic *Tai* expression this provides evidence that the ecdysone co-activator Taiman can act as a cell-specific co-activator of ecdysone signalling in niche and ECs.

To identify specific cellular processes regulated by the ecdysone pathway in somatic cells proximal to the ovarian stem cell niche, we downregulated ecdysone signalling using transgenic *UAS tai RNAi*, *UAS EcR RNAi* and *UAS ab* lines crossed to ovarian soma-specific drivers (*bab1Gal4* and *ptcGal4*, for expression patterns see Supplementary Figure S4) combined with the temperature-sensitive *Gal80* system to avoid the lethality caused by downregulation of ecdysone pathway components during developmental stages.

When the co-activator of ecdysone signalling *Tai* was downregulated or the co-repressor *Abrupt* overexpressed in soma, mutant germaria contained multiple SSCs (Figure 5A–C); this mutant phenotype became even more pronounced over time (Figure 5B and D) resembling older *ecd1^{ts}* (Figure 2B) as well as JAK/STAT mutant germaria (Decotto and Spradling, 2005). Similar phenotypes were observed when *EcR RNAi* flies were kept at the restrictive temperature; the development of germline cysts was retarded (Figure 5E–G), and the ratio of fusome-containing cysts to SSCs was reduced 2–3 times (Figure 5I; Supplementary Table S5). Downregulation of EcR for longer periods (15, 21 days) led to an increase in the number of SSCs (from 5 to 9–11 SSCs per germarium, Figure 5H; compare 5F and 5G). In addition, in proximity to undeveloped cysts mutant germaria contained extra somatic cells, most likely improperly differentiated ECs (Figure 5, brackets).

These data provide evidence that the soma-specific disruption of the ecdysone pathway is causing germline differentiation defects, indicating a cell non-autonomous role of this steroid hormone signalling.

Ecdysone signalling regulates turnover of cell adhesion proteins

In order to analyse how mutant somatic cells cause a block in germline cyst maturation, we used an FRT recombination system to compare ecdysone pathway deficient and wild-type somatic cells within one germarium. Detailed analysis of *tai* mutant ESCs and their progeny showed that they lose their squamous shape, and form a layer resembling columnar epithelium (Figure 6A). Interestingly, these mutant cells expressed higher levels of the cell adhesion molecules β -Catenin/Armadillo, DE-Cadherin and a cytoskeleton component Adducin (Figure 6A, C and D). DE-Cadherin was also upregulated in abnormal somatic cells resulting from somatic overexpression of *Abrupt* or downregulation of EcR (*UAS ab* or *UAS EcR RNAi* crossed to *ptcGal4/tubGal80^{ts}*; Figure 6E and F) pointing towards possible defects in cell–cell contacts, shape rearrangement and signalling transduction processes. These data imply that in our system the ecdysone pathway has a specific role in EC differentiation via regulation of cell adhesion complexes that are required for establishment of correct germline–soma communications. Perhaps, when connections between germline cysts and surrounding soma are perturbed, signalling cascades that initiate germline differentiation are also perturbed causing a developmental delay.

Ecdysone signalling controls the stem cell niche formation

Another process in the germarium that should require a very accurate regulation of cell adhesion is the niche establishment. If ecdysone signalling is essential to control this process as well, we would expect to see abnormalities in niche formation in ecdysone pathway mutants. Recall that mutant *tai* animals indeed had enlarged niches and extra GSCs (Figure 1C and D), a phenotype not seen in other cases analysed here. This discrepancy can be explained by the time during the animal's development when the mutation was introduced. In the *tai* experiment, animals were *tai* deficient during all developmental stages, including the period of niche establishment. In other cases in this study the ecdysone pathway was misregulated during adulthood after the niche was already formed and CpCs had stopped division. Also, in *tai* heterozygotes both the soma and the germline were mutant and the germline can affect via Notch signalling the size of the niche (Ward *et al*, 2006). To prove that the niche expansion is a soma-originated phenotype, we knocked down *tai* in somatic pre-adult cells that contribute to niches using the *FRT/bab1Gal4/UASFlp* system that allows to induce mutant CpC clones during niche formation. As expected, germaria with *tai* clonal CpCs had substantially enlarged niches (Figure 7A and B), which provides evidence that the ecdysone pathway co-activator *Tai* is required during developmental stages specifically in the pre-niche cells to control the GSC niche assembly. Possibly in *tai* mutant somatic cells within the larval ovary, like in ECs in adults, increased levels of cell adhesion molecules allow them to adhere better to germline cells and receive more signalling (Notch for example) which makes them adopt the niche cell fate.

To confirm that the niche enlargement is an ecdysone signalling-reliant phenotype and is not associated with *Tai*-independent function, we introduced other ecdysone pathway component mutations during the period of niche

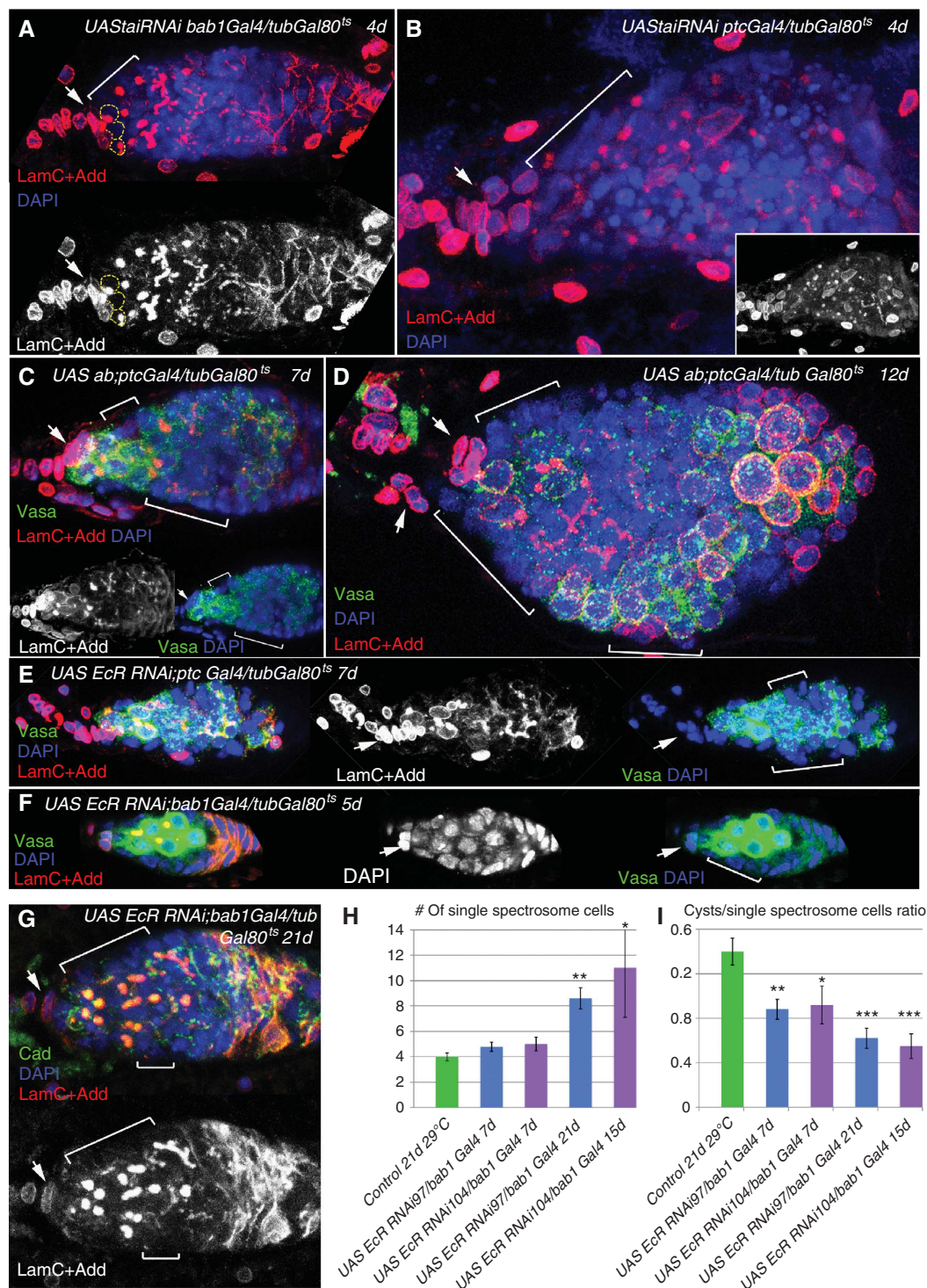


Figure 5 Ecdysteroids act from the soma to regulate the progression of germline development in the germarium. (A, B) The EcR co-activator Tai is downregulated specifically in the somatic cells of the germarium using *ptcGal4* and *bab1Gal4* in combination with *tubGal80^{ts}* system to avoid lethality. Upon downregulation of *tai* in the soma, the number of developmentally delayed SSCs increases dramatically. (C, D) Overexpression of the Tai repressor, Abrupt using *UAS ab* with the same drivers causes similar phenotypes as seen with downregulation of *tai*. (B, D) The *tai* and *ab* mutant germaria are filled with undifferentiated SSCs, cysts are not pinching off and additional somatic cells (brackets) are in the vicinity. Note the similarity of phenotypes caused by ecdysteroid deficit (*ecd1^{ts}*, Figure 2B) and disruption of ecdysone signalling pathway components just in germarial soma. (E–G) The downregulation of the EcR in the somatic cells of the germarium via expression of *UAS EcR RNAi⁹⁷* under control of *ptcGal4* (E) and *bab1Gal4* (F, G) leads to an increase of SSCs at the expense of developing cysts. Note the presence of dumbbell-shaped spectroscopic cells and additional somatic cells. (H) Bar graph showing extra quantities of SSCs upon EcR downregulation via expression of *UAS EcR RNAi⁹⁷* or *UAS EcR RNAi¹⁰⁴* with the somatic drivers *ptcGal4* or *bab1Gal4*. This phenotype gets more pronounced with longer duration of EcR abolition. (I) The ratio of differentiating cysts to SSCs is also decreased correspondingly to the increase in the SSC number. (A–G) Projections of optical sections assembled through the germarial tissue are shown. CpCs are marked with arrows, additional somatic cells with brackets. Red, Adducin + LaminC (A–G); blue, DAPI; and green, Vasa (C–F), Cadherin (G). Error bars represent s.e.m. **P* < 0.05, ***P* < 0.005, ****P* < 0.0005.

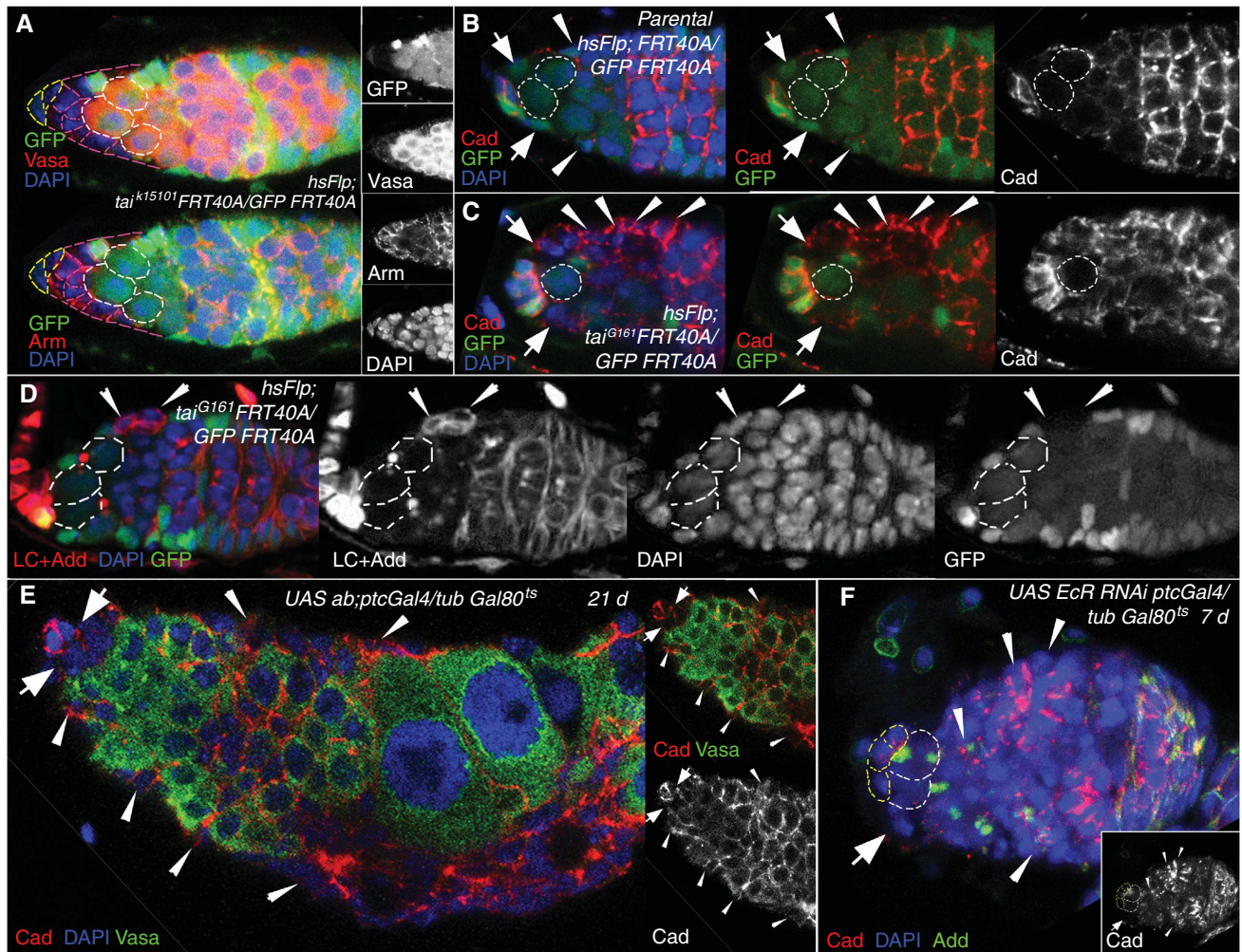
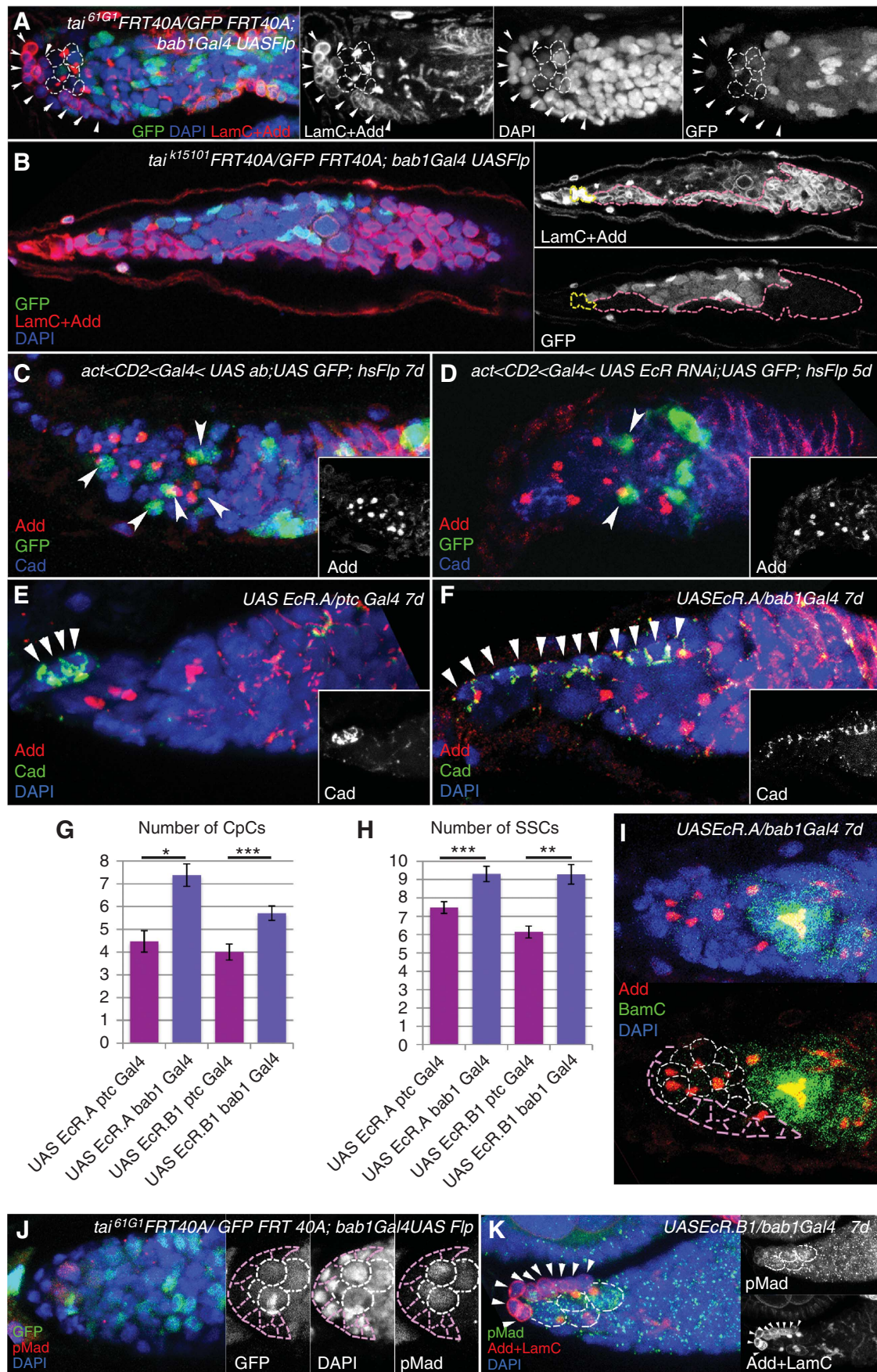


Figure 6 Cell adhesion and cytoskeleton proteins are misregulated in escort cells mutant for ecdysone signalling pathway components. (A) The progeny of *tai*^{k15101} deficient ESCs marked by the absence of GFP (*hsFlp; tai*^{k15101}*FRT40A/UbiGFP FRT40A*) formed a columnar epithelium-like somatic tissue adjacent to the stem cell niche. These cells also express higher levels of β -catenin/Armadillo than normal. (B) In the control germarium (*hsFlp; FRT40A/UbiGFP FRT40A*) ESCs (marked by arrows) and EC (marked by arrowheads) show moderate levels of DE-Cadherin, while niche-GSC cell contacts have higher DE-Cadherin levels. (C) *tai*^{G161} deficiency (*hsFlp; tai*^{G161}*FRT40A/UbiGFP FRT40A*) led to the upregulation of the cell adhesion protein DE-Cadherin in ECs (arrowheads) and ESCs (arrows). Note also that the number of abnormally shaped *tai* mutant escort cells is increased in (A, C). (D) *tai* mutant escort cells (arrowheads, *hsFlp; tai*^{G161}*FRT40A/UbiGFP FRT40A*) do not properly change their morphology and show higher levels of the cytoskeletal protein Adducin and nuclear envelope marker LaminC. (E) The overexpression of the ecdysone signalling inhibitor Abrupt leads to a strongly mutant germarial structure. Somatic cells (marked by the absence of the germline marker Vasa) are forming layers all along the germarium and show high DE-Cadherin levels. (F) Somatic abolition of EcR (*UAS EcR RNAi; ptcGal4/tub Gal80^{ts}*) also increases levels of cell adhesion and cytoskeleton proteins, DE-Cadherin and Adducin. Wide arrows, ESCs; arrowheads, ECs; Red, Vasa, Armadillo (A), Cadherin (B, C, E, F), Adducin + LaminC (D); blue, DAPI; and green, GFP (A–E).

development. As most of the tested mutant combinations affected viability, we could disrupt ecdysone signalling during development only via induction of single cell clones using the *act<CD2<Gal4, hsFlp* system and via *EcR* overexpression. Mutant single somatic clonal cells expressing *UAS ab* or *UAS EcR RNAi* resembled niche cells by their shape and ability to hold SSCs (Figure 7C and D). On average, mutant germaria contained 7.5–8.5 germline SSCs oriented either towards *ab* or *EcR* mutant or niche cells. *UAS EcR.A* and *UAS EcR.B1* expressed by the niche cell-specific driver *bab1Gal4* also caused formation of an enlarged niche (on average 10 CpCs in comparison to 6 in control, Figure 7F, G and K; Supplementary Table S6) and appearance of supernumerary SSCs (Figure 7H and I; Supplementary Table S6). To test if these excessive niches were able to host extra stem cells, we analysed the number of GSCs per germarium by staining

mutant germaria with specific markers. We observed that in *tai* and *EcR* mutants additional SSCs that are touching expanded niches are positive for the stem cell marker pMad and do not stain positively for the differentiation factor Bam (Figure 7H–K). The number of pMad-positive GSCs per germarium significantly increased in clonal *tai* mutants (4.47 ± 0.26 ($P = 4.29 \times 10^{-7}$, $n = 15$) in *tai*^{G161}*FRT40A/UbiGFP FRT40A; bab1Gal4Flp* in comparison to 2.18 ± 0.26 ($n = 12$) in control) and ecdysone mutants (3.50 ± 0.43 ($P = 0.02$, $n = 6$) in *UAS EcR.A bab1Gal4* and 3.33 ± 0.29 ($P = 0.01$, $n = 9$) in *UAS EcR.B1 bab1Gal4* in comparison to 2.36 ± 0.20 ($n = 11$) in *UASlacZ, bab1Gal4* control). These observations infer that additional cells in enlarged niches are functional and can facilitate extra GSCs. We assume that during development the ecdysone signalling pathway has a role in the establishment of the stem cell niche.



Discussion

Here, we show for the first time that in *Drosophila* ecdysone signalling regulates differentiation of a GSC daughter and modulates ovarian stem cell niche size (Figure 8). The delay in GSC progeny differentiation correlates with reduced expression levels of TGF- β pathway components. Based on expression patterns it appears that germarial somatic cells, niche and ECs are the critical sites of ecdysteroid action and a co-activator of ecdysone receptor, Taiman is the spatially restricted regulator of ecdysone signalling in soma. During adulthood the ecdysone pathway has a specific role in EC differentiation and soma-germline cell contact establishment. In addition, during development the ecdysone signalling pathway has a role in somatic niche formation (Figure 8).

Ecdysteroids in general control major developmental transformations such as metamorphosis and morphogenesis in *Drosophila*. Different tissues and even different cell types within the same tissue respond to this broad signalling in a specific fashion and in a timely manner. In the developing *Drosophila* ovary steroid hormone receptors are expressed in

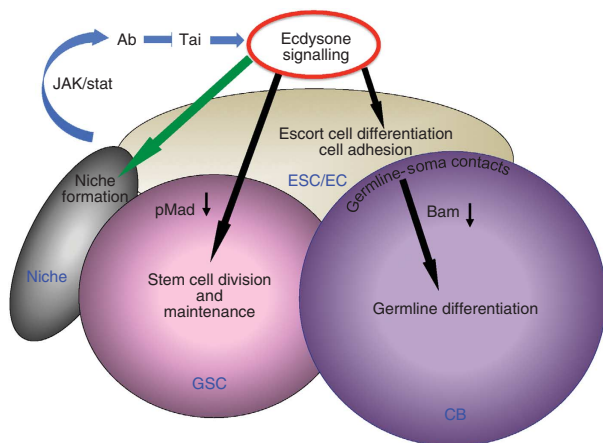


Figure 8 Model showing the role of the ecdysone signalling in *Drosophila* ovarian stem cell niche. During development (green arrow) ecdysone signalling participates in defining the stem cell niche size. During adulthood (black arrows) this hormonal pathway has a dual role in regulation of early germline differentiation: regulation of cell contacts and cell shape rearrangements via adjustment of adhesion complexes and cytoskeletal proteins in ESCs and their progeny and control of the potency of TGF- β signalling.

a well-timed mode, high levels coinciding with proliferative and immature stages and low levels preceding reduced DNA replication and differentiation (Hodin and Riddiford, 1998). Mutations in ecdysone pathway components affect ovarian morphogenesis, including heterochronic delay or acceleration in the onset of TF differentiation. During the niche establishment the levels of both ecdysone receptors, EcR and USP are greatly downregulated in anterior somatic cells that will contribute to the niche *per se* (Hodin and Riddiford, 1998). Now, we show that perturbation of ecdysone signalling in pre-adult ovarian soma leads to the formation of enlarged niches. The specific response to systemic hormonal signalling in niche precursors is achieved by a specific function of the ecdysone receptor co-activator Taiman. When timely regulation of ecdysone signalling does not occur, more cells are recruited to become niche cells resulting in enlarged niches that are capable to host more stem cells. These data first show that ecdysone steroid hormonal signalling regulates the formation of the adult stem cell niche and suggest that a developmental tuning of ecdysone signalling controls the number of anterior somatic cells that will differentiate into CpCs.

It is logical that stem cell division and germline differentiation are regulated by some systemic signalling depending on the general state of the organism, which depends on age, nutrition, environmental conditions and so on. Hormones are great candidates for this type of regulation as they act in a paracrine fashion and their levels are changing in response to ever-changing external and internal conditions. Steroid binding to nuclear receptors in vertebrates triggers a conformational switch accompanied by increased histone acetylation that permits transcriptional co-activators binding and the transcription initiation complex assembly (Collingwood *et al*, 1999; Privalsky, 2004). In *Drosophila*, the trithorax-related protein, a histone H3 methyltransferase that like Taiman belongs to the p160 class of co-activators, and an ISWI-containing ATP-dependent chromatin remodelling complex (NURF), that regulates transcription by catalysing nucleosome sliding, both bind EcR in an ecdysone-dependent manner (Sedkov *et al*, 2003; Badenhorst *et al*, 2005), showing that chromatin modifications can mediate response to this general signalling. Transcriptional regulation has a key role in GSC maintenance and differentiation, for example, the TGF- β ligand dpp secreted by niche cells induces phosphorylation of the transcription factor Mad in GSCs that in turn suppresses transcription of the differentiation factor Bam (McKearin and Ohlstein, 1995; Xie and Spradling, 1998; Chen and

Figure 7 Ecdysone signalling is required for niche formation. (A) Downregulation of *tai*^{G1G1} before the niche is established (*tai*^{G1G1}FRT40A/UbiGFP FRT40A; *bab1Gal4* UASFlp) causes significant niche enlargement (CpCs marked with arrowheads) that allows to anchor more GSC-like cells (marked with white dashed lines). (B) In some extreme cases *tai*^{K15101} mutant somatic cells (marked with pink dashed lines) encapsulate the whole germlarium that is filled with SSCs. CpCs are marked with yellow dashed lines. (C) Clonal overexpression of the Tai repressor Ab (UAS<CD2<Gal4 UAS ab; UAS GFP; *hsFlp*) in somatic cells results in the appearance of supernumerary SSCs that are anchored to UAS ab cells marked by GFP. (D) The same can be observed in somatic clonal EcR mutant cells (UAS<CD2<Gal4 UAS EcR RNAi; UAS GFP; *hsFlp*). (E, F) The pre-adult expression of exogenous EcR only in the niche progenitor cells (*bab1Gal4*, F), but not in other somatic cells (*ptcGal4*, E) results in the appearance of enlarged niches marked by DE-Cadherin (arrowheads). The average numbers of CpCs (G) and SSCs (H) are significantly increased when UAS EcR.A or UAS EcR.B1 are overexpressed during the niche establishment in most anterior pre-niche somatic cells (*bab1Gal4*), but not in other intermingled somatic cells (*ptcGal4*) within the larval ovary. (I) The niche expansion increases the number of SSCs that are also negative for the differentiation marker BamC. Niche is outlined with pink and GSCs with white dashed lines. (J, K) The enlarged *tai* clonal niches (*tai*^{G1G1}FRT 40A/Ubi GFP FRT 40A; *bab1 Gal4 Flp*) and niches overexpressing EcR bear a higher number of GSCs whose identity is confirmed by the stem cell marker pMad. Niche is outlined with pink dashed lines in (J) and arrowheads in (K), GSCs are marked with white dashed lines. (A–F, I–K) Projections of optical sections assembled through the germarial tissue are shown. Red, Adducin + LaminC (A, B, K), Adducin (C–F, I), pMad (J); blue, DAPI; and green, GFP (A–D, J), Cadherin (E, F), BamC (I), pMad (K). Error bars represent s.e.m. **P* < 0.05, ***P* < 0.005, ****P* < 0.0005.

McKearin, 2003; Song *et al*, 2004). In addition, it has been shown recently that in *Drosophila* adult GSC ecdysone modulates the strength of TGF- β signalling through a functional interaction with the chromatin remodelling factors ISWI and Nurf301, a subunit of the ISWI-containing NURF chromatin remodelling complex (Ables and Drummond-Barbosa, 2010). Therefore, it is plausible that ecdysone regulates Mad expression cell autonomously via chromatin modifications. As pMad directly suppresses a differentiation factor Bam, it is expected that Bam would be expressed in pMad-negative cells. Interestingly, our findings show that ecdysone deficit decreases amounts of phosphorylated Mad in GSCs and also cell non-autonomously suppresses Bam in SSCs. As SSCs that express neither pMad nor Bam are accumulated when the ecdysone pathway is perturbed it suggests that there should be an alternative mechanism of Bam regulation. Even though eventually this still can be done on the level of chromatin modification, our data suggest that the origin of this soma-generated signal may be associated with cell adhesion protein levels. Further understanding of the nature of this signalling is of a great interest.

The progression of oogenesis within the gerarium requires cooperation between two stem cell types, germline and somatic (escort) stem cells. In *Drosophila*, reciprocal signals between germline and escort (in female) or somatic cyst (in male) cells can inhibit reversion to the stem cell state (Brawley and Matunis, 2004; Kai and Spradling, 2004) and restrict germ cell proliferation and cyst growth (Matunis *et al*, 1997). Therefore, the non-autonomous ecdysone effect can be explained by the necessity of two stem cell types that share the same niche (GSC and ESC) to coordinate their division and progeny differentiation. This coordination is most likely achieved via adhesive cues, as disruption of ecdysone signalling affects turnover of adhesion complexes and cytoskeletal proteins in somatic ECs: mutant cells exhibited abnormal accumulation of DE-Cadherin, β -catenin/Armadillo and Adducin.

Cell adhesion has a crucial role in *Drosophila* stem cells; GSCs are recruited to and maintained in their niches via cell adhesion (Song *et al*, 2002). Two major components of this adhesion process, DE-Cadherin and Armadillo/ β -catenin, accumulate at high levels in the junctions between GSCs and niche cells, while in the developing CB and ECs levels of these proteins are strongly reduced. Levels of DE-Cadherin in GSCs are regulated by various signals, for example, nutrition activation of insulin signalling or chemokine activation of STAT (Hsu and Drummond-Barbosa, 2009; Leatherman and Dinardo, 2010), and here we show that in ESCs it is regulated by steroid hormone signalling. Possibly, these two stem cell types respond to different signals but then differentiation of their progeny is synchronised via cell contacts. While hormones, growth factors and cytokines certainly manage stem cell maintenance and differentiation, our evidence also reveals that the responses to hormonal stimuli are strongly modified by adhesive cues.

Specificity to endocrine signalling can be achieved via availability of co-factors in the targeted tissue. Tai is a spatially restricted co-factor that cooperates with the EcR/USP nuclear receptor complex to define appropriate responses to globally available hormonal signals. Tai-positive regulation of ecdysone signalling can be alleviated by Abrupt via direct binding of these two proteins that prevents Tai

association with EcR/USP (Jang *et al*, 2009). Abrupt has been shown to be downregulated by JAK/STAT signalling (Jang *et al*, 2009). Interestingly, JAK/STAT signalling also has a critical role in ovarian niche function and controls the morphology and proliferation of ESCs as well as GSCs (Decotto and Spradling, 2005). JAK/STAT signalling may interact with ecdysone pathway components in ECs to further modulate cell type-specific responses to global endocrine signalling. A combination of regulated by different signalling pathway factors that are also spatially and timely restricted builds a network that ensures the specificity of systemic signalling.

Knowledge of how steroids regulate stem cells and their niche has a great potential for stem cell and regenerative medicine. Our findings open the way for a detailed analysis of a role for steroid hormones in niche development and regulation of germline differentiation via adjacent soma.

Materials and methods

Fly stocks

Drosophila melanogaster stocks were raised on standard cornmeal-yeast-agar-medium at 25°C unless otherwise stated. Clones were induced using the *hsFlp/FRT* system for mitotic recombination. The following stocks were used: $y^{d2}w^{1118};tai^{k15101}FRT40A/CyO$ (DGRC Kyoto), $dp^{ov}tai^{61G1}FRT40A/CyO$, $tai^{01351}cn^1/CyO;ry^{506},w^{1118};tai^{BG02711},tai^{KG02309}/CyO$, $w^{1118};y^{1w^{67c23}};tai^{EY11718}/CyO$, $w^{1118};pUAS\ tai, EcR^{M554fs}/SM6b$, $EcR^{Q50st}/SM6b$, $w^{1118};hs-GAL4-EcR.LBD$, $w^{1118};hs-GAL4-usp.LBD$, $w^{1118};EcRE.lacZ$, $w^{1118};hs-EcR.B1$, $w^{1118};hs-EcR.A$, $w^{1118};UAS-EcR-RNAi^{97}$, $w^{1118};UAS-EcR-RNAi^{104}$, $usp^4/FM7a$, usp^{EP1193} , $w^{1118};UAS-EcR.A$, $w[*];UAS-EcR.B1$, $w^{1118};UAS-ab.B$, $UAS-lacZ$, $ecd1^{218}$, ecd^{4210} (Bloomington Stock Centre), $tai\ G00308/CyO$ (Carnegie GFP trap line), $tai\ RNAi$ (w^{1118} ; P{GD4265}, VDRC), *BamGFP* (Dennis McKearin), w^{1118} was used for wild-type analysis.

Transheterozygous interaction

We used the amorph and hypomorph *tai* alleles and ecdysone pathway mutants $EcR^{Q50st}/SM6b$ or $usp^4/FM7a$, usp^{EP1193} . Both the number of GSCs (single spectroscopy cells that are touching the CpCs) and the number of CpCs itself were counted. As a control, $dp^{ov}tai^{61G1}FRT40A/CyO$ and $y^{d2}w^{1118};tai^{k15101}FRT40A/CyO$ were crossed to w^{1118} flies.

Disruption of EcR in soma

To specifically disrupt the ecdysone signalling in the somatic cells of the gerarium, $w^{1118};UAS\ EcR\ RNAi^{97}$, $w^{1118};UAS\ EcR\ RNAi^{104}$, $w^{1118};UAS\ ab.B$ or $tai\ RNAi$ (w^{1118} ; P{GD4265}), females were crossed to *ptcGal4*; *tubGal80^{ts}* or *tubGal80^{ds}*; *bab1Gal4/TM6* males at 18°C. The hatched flies were then transferred to 29°C and aged for 7, 14 and 21 days. Controls were treated the same.

Clonal analysis

Germline and somatic cell clones were done as described previously (Shcherbata *et al*, 2004, 2007) using *hsFlp/FRT* system for mitotic recombination. Early formation of clones in CpCs and ESCs were obtained via crossing $y^{d2}w^{1118};tai^{k15101}FRT40A/CyO$ and $dp^{ov}tai^{61G1}FRT40A/CyO$ to *Ubi-GFP FRT40A/CyO*; *bab1Gal4:UAS-Flp/TM2* flies (gift from A González-Reyes). Mutant clones were identified by the absence of GFP.

To induce adult clones $y^{d2}w^{1118};tai^{k15101}FRT40A/CyO$ and $dp^{ov}tai^{61G1}FRT40A/CyO$ males were crossed to *hsFlp; FRT40A GFP/CyO* females. 2–4-day-old adult F1 females were heat shocked in empty vials for 60 min 2 days in a row in a 37°C water bath and analysed 5, 7, and 12, 14 days after heat shock. CpC and ESC clones were identified by the absence of GFP.

For generation of somatic ovarian clones we crossed *hsFlp;; UAS GFPact > FRT-CD2-FRT > Gal4/TM3* males to $w^{1118};UAS\ ab.B$ or $w^{1118};UAS\ EcR\ RNAi$ females. Third instar larvae were heat shocked 2 days in a row for 2 h. Clonal cells expressing *ab.B* or *EcR RNAi* were identified by GFP expression.

Overexpression analysis

For overexpression of EcR isoforms in adult flies, *w¹¹¹⁸;hsEcR.A* flies were crossed to *w¹¹¹⁸* flies. The offspring with one copy of the transgene were heat shocked (37°C) twice per day for 30 min 4 or 7 days in a row. Controls were heat shocked as well. Furthermore, flies with a copy of the *hsEcR.A* transgene were kept at 25°C without heat treatment.

To overexpress the different EcR isoforms specifically in the soma *w¹¹¹⁸;UAS EcR.A* and *w¹¹¹⁸;UAS EcR.B1* (Bloomington Stock Center) were crossed to *bab1Gal4/TM6* or *ptcGal4*.

Alteration of ecdysone signalling

To supply more ecdysone hormone, 20-Hydroxyecdysone (20E, Sigma-Aldrich) was diluted in 5% ethanol to a 1 µM concentration and mixed with dry yeast to reach a dough-like consistency. The mixture was then placed on top of agar juice plates to culture flies. In all, 5% ethanol was used for controls.

The *ecd1^{ts}* temperature-sensitive mutation is known to reduce ecdysone levels at the non-permissive temperature. Fly stocks were kept at the permissive temperature (18°C) and adult flies were shifted to the restrictive temperature (29°C) in order to block ecdysone synthesis. As a control, wild-type flies were kept at 29°C for the same time and *ecd1^{ts}* flies that had not been shifted to 29°C were analysed.

w¹¹¹⁸;hs-GAL4-EcR.LBD and *w¹¹¹⁸;hs-GAL4-usp.LBD* (Kozlova and Thummel, 2002) animals were heat shocked 30 min/day, 1–3 days in a row.

Ecdysone signalling pattern

To analyse the ecdysone signalling in the germarium, *w¹¹¹⁸;hs-GAL4-EcR.LBD* and *w¹¹¹⁸;hs-GAL4-usp.LBD* (Kozlova and Thummel, 2002) females were crossed to *UAS-lacZ* males. Flies were heat shocked for 60 min in a water bath before they were fixed and stained. *EcRE-lacZ*, a homozygous viable stock with seven EcREs inserted into a *lacZ* promoter was used to determine the pattern of ecdysone signalling (Koelle *et al*, 1991). Adult flies were stained for β-galactosidase. Taiman expression was identified with the *tai G00308/CyO* enhancer-trap line (Morin *et al*, 2001).

Immunofluorescence and antibodies

Ovaries were fixed in 5% formaldehyde (Polysciences, Inc.) for 10 min and the staining procedure was performed as described (Shcherbata *et al*, 2004). We used the following mouse monoclonal antibodies: anti-Armadillo (1:40); anti-Adducin (1:50), anti-LaminC (1:50), anti-EcR Ag10.2 (1:20, EcR common region) (Developmental Studies Hybridoma Bank), anti-usp (1:50, RB Olano, F Kafatos), rat anti-DE-Cadherin (1:50, DSHB), anti-BamC (1:1000, D McKearin) and rat anti-Vasa (1:1000, P Lasko), rabbit anti-pMad (1:5000, D Vasiliauskas, S Morton, T Jessell and E Laufer), anti-β-Gal (1:1000), rabbit anti-tai (1:1000, D Montell), rabbit anti-PH3 (1:3000, Upstate

Biotechnology) and anti-GFP-directly conjugated with AF488 (1:3000, Invitrogen), Alexa 488, 568 or 633 goat anti-mouse, anti-rabbit (1:500, Molecular Probes), goat anti-rat Cy5 (1:250, Jackson Immunoresearch). Images were obtained with a confocal laser-scanning microscope (Leica SPE5) and processed with Adobe Photoshop.

Analysis and statistics

To determine the number of CpCs, LaminC-positive cells on the tip of the germarium were counted. Single spectroscopic cells that were touching the niche cells were counted as GSCs. Single spectroscopic cells that were not touching the niche were counted separately. In addition, the number of fusomes (indicating the number of cysts) until region 2B, where follicle cells start cyst encapsulation, was counted. To describe the differentiation in a given germarium the number of cysts was divided by the number of SSCs (ratio = cysts/SSCs). The percentage of germaria-containing dumbbell-shaped fusomes (McKearin and Ohlstein, 1995) was counted. The intensity of the pMad-positive area was determined via measuring the grey value in at least 10 GSCs with Leica LAS AF Lite software, the background levels were measured by the intensity of the pMad-negative area in the germarium. Background levels were subtracted to normalise the levels of antibody staining in different germaria. Intensity levels relative to control were calculated. GSC maintenance was determined by comparison of the percentage of germaria with clonal GSCs between two different time points after clonal induction.

χ²-test was used to determine if the percentage of dumbbell-shaped fusomes was significantly increased. For all other statistical analyses, the two-tailed Student's *t*-test was performed.

Supplementary data

Supplementary data are available at *The EMBO Journal* Online (<http://www.embojournal.org>).

Acknowledgements

We thank Hannele Ruohola-Baker, Acaimo González-Reyes, Dennis McKearin, Ed Laufer, Denise Montell, Rosa Barrio Olano and Fotis Kafatos for flies and reagents, Department of Stefan Hell for use of confocal microscope, April Marrone and Mariya Kucherenko for comments on the manuscript and Department of Herbert Jäckle for discussion. The Max Planck Society supported this work.

Conflict of interest

The authors declare that they have no conflict of interest.

References

- Ables ET, Drummond-Barbosa D (2010) The steroid hormone ecdysone functions with intrinsic chromatin remodeling factors to control female germline stem cells in *Drosophila*. *Cell Stem Cell* **7**: 581–592
- Badenhorst P, Xiao H, Cherbas L, Kwon SY, Voas M, Rebay I, Cherbas P, Wu C (2005) The *Drosophila* nucleosome remodeling factor NURF is required for ecdysteroid signaling and metamorphosis. *Genes Dev* **19**: 2540–2545
- Bai J, Uehara Y, Montell DJ (2000) Regulation of invasive cell behavior by taiman, a *Drosophila* protein related to AIB1, a steroid receptor coactivator amplified in breast cancer. *Cell* **103**: 1047–1058
- Beckstead R, Ortiz JA, Sanchez C, Prokopenko SN, Chambon P, Losson R, Bellen HJ (2001) Bonus, a *Drosophila* homolog of TIF1 proteins, interacts with nuclear receptors and can inhibit betaFTZ-F1-dependent transcription. *Mol Cell* **7**: 753–765
- Boulanger CA, Smith GH (2009) Reprogramming cell fates in the mammary microenvironment. *Cell Cycle* **8**: 1127–1132
- Brawley K, Matunis E (2004) Regeneration of male germline stem cells by spermatogonial dedifferentiation *in vivo*. *Science* **304**: 1331–1334
- Buszczak M, Freeman MR, Carlson JR, Bender M, Cooley L, Segreaves WA (1999) Ecdysone response genes govern egg chamber development during mid-oogenesis in *Drosophila*. *Development* **126**: 4581–4589
- Chen D, McKearin DM (2003) A discrete transcriptional silencer in the bam gene determines asymmetric division of the *Drosophila* germline stem cell. *Development* **130**: 1159–1170
- Cherbas L, Lee K, Cherbas P (1991) Identification of ecdysone response elements by analysis of the *Drosophila* Eip28/29 gene. *Genes Dev* **5**: 120–131
- Collingwood TN, Urnov FD, Wolffe AP (1999) Nuclear receptors: coactivators, corepressors and chromatin remodeling in the control of transcription. *J Mol Endocrinol* **23**: 255–275
- de Cuevas M, Spradling AC (1998) Morphogenesis of the *Drosophila* fusome and its implications for oocyte specification. *Development* **125**: 2781–2789
- Decotto E, Spradling AC (2005) The *Drosophila* ovarian and testis stem cell niches: similar somatic stem cells and signals. *Dev Cell* **9**: 501–510
- Dobens L, Rudolph K, Berger EM (1991) Ecdysterone regulatory elements function as both transcriptional activators and repressors. *Mol Cell Biol* **11**: 1846–1853
- Dressel U, Thormeyer D, Altincicek B, Paululat A, Eggert M, Schneider S, Tenbaum SP, Renkawitz R, Baniahmad A (1999)

- Alien, a highly conserved protein with characteristics of a corepressor for members of the nuclear hormone receptor superfamily. *Mol Cell Biol* **19**: 3383–3394
- Elke C, Vogtli M, Rauch P, Spindler-Barth M, Lezzi M (1997) Expression of EcR and USP in *Escherichia coli*: purification and functional studies. *Arch Insect Biochem Physiol* **35**: 59–69
- Francis VA, Zorzano A, Teleman AA (2010) dDOR is an EcR coactivator that forms a feed-forward loop connecting insulin and ecdysone signaling. *Curr Biol* **20**: 1799–1808
- Gates J, Lam G, Ortiz JA, Losson R, Thummel CS (2004) Rigor mortis encodes a novel nuclear receptor interacting protein required for ecdysone signaling during *Drosophila* larval development. *Development* **131**: 25–36
- Gazdova I, Bonnette PC, Henrich VC, Jindra M (2004) Cell-autonomous roles of the ecdysoneless gene in *Drosophila* development and oogenesis. *Development* **131**: 2715–2725
- Gonczy P (2008) Mechanisms of asymmetric cell division: flies and worms pave the way. *Nat Rev Mol Cell Biol* **9**: 355–366
- Hodin J, Riddiford LM (1998) The ecdysone receptor and ultraspiracle regulate the timing and progression of ovarian morphogenesis during *Drosophila* metamorphosis. *Dev Genes Evol* **208**: 304–317
- Hsu HJ, Drummond-Barbosa D (2009) Insulin levels control female germline stem cell maintenance via the niche in *Drosophila*. *Proc Natl Acad Sci USA* **106**: 1117–1121
- Jang AC, Chang YC, Bai J, Montell D (2009) Border-cell migration requires integration of spatial and temporal signals by the BTB protein Abrupt. *Nat Cell Biol* **11**: 569–579
- Kai T, Spradling A (2004) Differentiating germ cells can revert into functional stem cells in *Drosophila melanogaster* ovaries. *Nature* **428**: 564–569
- Koelle MR, Talbot WS, Segraves WA, Bender MT, Cherbas P, Hogness DS (1991) The *Drosophila* EcR gene encodes an ecdysone receptor, a new member of the steroid receptor superfamily. *Cell* **67**: 59–77
- Kozlova T, Thummel CS (2002) Spatial patterns of ecdysteroid receptor activation during the onset of *Drosophila* metamorphosis. *Development* **129**: 1739–1750
- Kozlova T, Thummel CS (2003) Essential roles for ecdysone signaling during *Drosophila* mid-embryonic development. *Science* **301**: 1911–1914
- Leatherman JL, Dinardo S (2010) Germline self-renewal requires cyst stem cells and stat regulates niche adhesion in *Drosophila* testes. *Nat Cell Biol* **12**: 806–811
- Matunis E, Tran J, Gonczy P, Caldwell K, DiNardo S (1997) punt and schnurri regulate a somatically derived signal that restricts proliferation of committed progenitors in the germline. *Development* **124**: 4383–4391
- Mauvezin C, Orpinell M, Francis VA, Mansilla F, Duran J, Ribas V, Palacin M, Boya P, Teleman AA, Zorzano A (2010) The nuclear cofactor DOR regulates autophagy in mammalian and *Drosophila* cells. *EMBO Rep* **11**: 37–44
- McBrayer Z, Ono H, Shimell M, Parvy JP, Beckstead RB, Warren JT, Thummel CS, Dauphin-Villemand C, Gilbert LI, O'Connor MB (2007) Prothoracicotropic hormone regulates developmental timing and body size in *Drosophila*. *Dev Cell* **13**: 857–871
- McKearin D, Ohlstein B (1995) A role for the *Drosophila* bag-of-marbles protein in the differentiation of cystoblasts from germline stem cells. *Development* **121**: 2937–2947
- Morin X, Daneman R, Zavortink M, Chia W (2001) A protein trap strategy to detect GFP-tagged proteins expressed from their endogenous loci in *Drosophila*. *Proc Natl Acad Sci USA* **98**: 15050–15055
- Oro AE, McKeown M, Evans RM (1992) The *Drosophila* retinoid X receptor homolog ultraspiracle functions in both female reproduction and eye morphogenesis. *Development* **115**: 449–462
- Privalsky ML (2004) The role of corepressors in transcriptional regulation by nuclear hormone receptors. *Annu Rev Physiol* **66**: 315–360
- Riddiford LM (1993) Hormone receptors and the regulation of insect metamorphosis. *Receptor* **3**: 203–209
- Riddihough G, Pelham HR (1987) An ecdysone response element in the *Drosophila* hsp27 promoter. *EMBO J* **6**: 3729–3734
- Schubiger M, Carre C, Antoniewski C, Truman JW (2005) Ligand-dependent de-repression via EcR/USP acts as a gate to coordinate the differentiation of sensory neurons in the *Drosophila* wing. *Development* **132**: 5239–5248
- Schubiger M, Truman JW (2000) The RXR ortholog USP suppresses early metamorphic processes in *Drosophila* in the absence of ecdysteroids. *Development* **127**: 1151–1159
- Sedkov Y, Cho E, Petruk S, Cherbas L, Smith ST, Jones RS, Cherbas P, Canaani E, Jaynes JB, Mazo A (2003) Methylation at lysine 4 of histone H3 in ecdysone-dependent development of *Drosophila*. *Nature* **426**: 78–83
- Shcherbata HR, Althausen C, Findley SD, Ruohola-Baker H (2004) The mitotic-to-endocycle switch in *Drosophila* follicle cells is executed by Notch-dependent regulation of G1/S, G2/M and M/G1 cell-cycle transitions. *Development* **131**: 3169–3181
- Shcherbata HR, Ward EJ, Fischer KA, Yu JY, Reynolds SH, Chen CH, Xu P, Hay BA, Ruohola-Baker H (2007) Stage-specific differences in the requirements for germline stem cell maintenance in the *Drosophila* ovary. *Cell Stem Cell* **1**: 698–709
- Shea MJ, King DL, Conboy MJ, Mariani BD, Kafatos FC (1990) Proteins that bind to *Drosophila* chorion cis-regulatory elements: a new C2H2 zinc finger protein and a C2C2 steroid receptor-like component. *Genes Dev* **4**: 1128–1140
- Shirras AD, Bownes M (1987) Separate DNA sequences are required for normal female and ecdysone-induced male expression of *Drosophila melanogaster* yolk protein 1. *Mol Gen Genet* **210**: 153–155
- Song X, Wong MD, Kawase E, Xi R, Ding BC, McCarthy JJ, Xie T (2004) Bmp signals from niche cells directly repress transcription of a differentiation-promoting gene, bag of marbles, in germline stem cells in the *Drosophila* ovary. *Development* **131**: 1353–1364
- Song X, Zhu CH, Doan C, Xie T (2002) Germline stem cells anchored by adherens junctions in the *Drosophila* ovary niches. *Science* **296**: 1855–1857
- Tanentzapf G, Devenport D, Godt D, Brown NH (2007) Integrin-dependent anchoring of a stem-cell niche. *Nat Cell Biol* **9**: 1413–1418
- Terashima J, Bownes M (2005) A microarray analysis of genes involved in relating egg production to nutritional intake in *Drosophila melanogaster*. *Cell Death Differ* **12**: 429–440
- Tsai CC, Kao HY, Yao TP, McKeown M, Evans RM (1999) SMRTER, a *Drosophila* nuclear receptor coregulator, reveals that EcR-mediated repression is critical for development. *Mol Cell* **4**: 175–186
- Walker MR, Patel KK, Stappenbeck TS (2009) The stem cell niche. *J Pathol* **217**: 169–180
- Ward EJ, Shcherbata HR, Reynolds SH, Fischer KA, Hatfield SD, Ruohola-Baker H (2006) Stem cells signal to the niche through the Notch pathway in the *Drosophila* ovary. *Curr Biol* **16**: 2352–2358
- Xie T, Spradling AC (1998) Decapentaplegic is essential for the maintenance and division of germline stem cells in the *Drosophila* ovary. *Cell* **94**: 251–260
- Xie T, Spradling AC (2000) A niche maintaining germ line stem cells in the *Drosophila* ovary. *Science* **290**: 328–330
- Yao TP, Segraves WA, Oro AE, McKeown M, Evans RM (1992) *Drosophila* ultraspiracle modulates ecdysone receptor function via heterodimer formation. *Cell* **71**: 63–72
- Zheng X, Wang J, Haerry TE, Wu AY, Martin J, O'Connor MB, Lee CH, Lee T (2003) TGF-beta signaling activates steroid hormone receptor expression during neuronal remodeling in the *Drosophila* brain. *Cell* **112**: 303–315



The EMBO Journal is published by Nature Publishing Group on behalf of European Molecular Biology Organization. This work is licensed under a Creative Commons Attribution-NonCommercial-No Derivative Works 3.0 Unported License. [<http://creativecommons.org/licenses/by-nc-nd/3.0>]

2.2 The Histone H2B Monoubiquitination Regulatory Pathway is Required for Differentiation of Multipotent Stem Cells

Oleksandra Karpiuk, Zeynab Najafova, Frank Kramer, Magali Hennion, Christina Galonska, **Annekattrin König**, Nicolas Snaidero, Tanja Vogel, Andrei Shchebet, Yvonne Begus-Nahrman, Moustapha Kassem, Mikael Simons, Halyna Shcherbata, Tim Beissbarth and Steven A. Johnsen

Experiment	done by
analysis of H2Bub1 expression in germlaria; in Figure 1	Annekattrin König
All other experiment were performed by the other authors.	

Status of the manuscript: published (Mol Cell. 2012 Jun 8;46(5):705-13)

The Histone H2B Monoubiquitination Regulatory Pathway Is Required for Differentiation of Multipotent Stem Cells

Oleksandra Karpiuk,¹ Zeynab Najafova,^{1,4} Frank Kramer,² Magali Hennion,¹ Christina Galonska,¹ Annekatrin König,⁵ Nicolas Snaidero,⁶ Tanja Vogel,⁷ Andrei Shchebet,¹ Yvonne Begus-Nahrmann,¹ Moustapha Kassem,^{8,9} Mikael Simons,^{3,6} Halyna Shcherbata,⁵ Tim Beissbarth,² and Steven A. Johnsen^{1,4,*}

¹Department of Molecular Oncology, Göttingen Center for Molecular Biosciences

²Department of Medical Statistics

³Department of Neurology

University Medical Center Göttingen, Göttingen 37077, Germany

⁴Department of Tumor Biology, University Medical Center Hamburg-Eppendorf, Hamburg 20246, Germany

⁵Gene Expression and Signaling Group, Max-Planck-Institute for Biophysical Chemistry, Göttingen 37077, Germany

⁶Max-Planck-Institute for Experimental Medicine, Göttingen 37075, Germany

⁷Department of Molecular Embryology, Institute for Anatomy and Cell Biology, University of Freiburg, Freiburg 79104, Germany

⁸Molecular Endocrinology and Stem Cell Research Unit (KMEB), University Hospital of Odense and University of Southern Denmark, Odense 5000, Denmark

⁹Stem Cell Unit, Department of Anatomy, College of Medicine, Riyadh 11451, Kingdom of Saudi Arabia

*Correspondence: sjohnsen@alumni.mayo.edu

DOI 10.1016/j.molcel.2012.05.022

SUMMARY

Extensive changes in posttranslational histone modifications accompany the rewiring of the transcriptional program during stem cell differentiation. However, the mechanisms controlling the changes in specific chromatin modifications and their function during differentiation remain only poorly understood. We show that histone H2B monoubiquitination (H2Bub1) significantly increases during differentiation of human mesenchymal stem cells (hMSCs) and various lineage-committed precursor cells and in diverse organisms. Furthermore, the H2B ubiquitin ligase RNF40 is required for the induction of differentiation markers and transcriptional reprogramming of hMSCs. This function is dependent upon CDK9 and the WAC adaptor protein, which are required for H2B monoubiquitination. Finally, we show that RNF40 is required for the resolution of the H3K4me3/H3K27me3 bivalent poised state on lineage-specific genes during the transition from an inactive to an active chromatin conformation. Thus, these data indicate that H2Bub1 is required for maintaining multipotency of hMSCs and plays a central role in controlling stem cell differentiation.

INTRODUCTION

Both embryonic development and tissue homeostasis require the expansion and differentiation of multipotent self-renewing stem cells. Stem cells can differentiate into a variety of cell types depending upon the stimulus provided. A deeper understanding

of the molecular mechanisms determining cell-type-specific differentiation may provide therapeutic opportunities for treating a variety of pathological conditions.

Stem cells exhibit specific gene expression signatures which dictate cell fate during differentiation (Fisher and Fisher, 2011). A unique pattern of posttranslational histone modifications in stem cells governs gene expression patterns and differentiation potential (Fisher and Fisher, 2011; Meissner, 2010). Genome-wide studies have revealed that many developmental genes exhibit “bivalent” chromatin domains displaying both “active” (H3K4me3) and “repressive” (H3K27me3) histone modifications (Azuara et al., 2006; Bernstein et al., 2006). This “poised” state is proposed to allow for correct temporal gene expression.

The transcriptional apparatus and chromatin modifications exhibit a high degree of crosstalk. For example, phosphorylation of Ser2 (P-Ser2) within the heptapeptide repeat of the RNA polymerase II (RNAPII) C-terminal domain (CTD) provides a platform for recruiting the WW domain containing adaptor protein with coiled coil (WAC) (Zhang and Yu, 2011). In turn, WAC recruits the RNF20/RNF40 ubiquitin ligase complex which monoubiquitinates H2B (Kim et al., 2009; Zhu et al., 2005). Knockdown of either CDK9 (Pirngruber et al., 2009b) or WAC (Zhang and Yu, 2011) elicits an effect on H2Bub1 similar to that of RNF20 or RNF40 depletion.

Consistent with its dependence upon the elongating form of RNAPII, H2Bub1 is primarily associated with the transcribed regions of active genes (Minsky et al., 2008) where it facilitates transcriptional elongation (Pavri et al., 2006; Prenzel et al., 2011). However, despite its association with active genes, H2Bub1 is only required for the transcription of a subset of inducible genes (Prenzel et al., 2011; Shema et al., 2008). Consistent with a specific regulation of tumor-relevant transcriptional pathways, H2Bub1 is a proposed tumor suppressor whose levels decrease during tumor progression (Johnsen, 2012; Prenzel

et al., 2011; Shema et al., 2008). The inverse relationship between differentiation status and malignancy may indicate that decreased H2Bub1 in advanced tumors leads to a less differentiated phenotype. However, the role of H2Bub1, its modifying enzymes, and upstream regulators in controlling cell-fate determination in mammalian systems remains unexplored.

Here we demonstrate that H2Bub1 levels increase in diverse cell differentiation systems. Perturbation of H2B monoubiquitination via depletion of its ubiquitin ligases RNF40 and RNF20, or upstream regulators CDK9 and WAC impairs stem cell differentiation. RNF40 depletion affects multipotency by preventing the resolution of bivalent histone marks on lineage-specific genes. These results uncover a previously unknown function of H2Bub1 and its upstream regulatory pathway in stem cell differentiation and shed light into the mechanism by which its loss may increase malignant potential.

RESULTS

H2Bub1 Increases during Cellular Differentiation

We previously reported decreased H2Bub1 levels during malignant progression (Prenzel et al., 2011). Given the inverse correlation between tumor differentiation status and malignancy, we hypothesized that H2Bub1 may increase during normal cellular differentiation. We therefore examined H2Bub1 levels in various differentiation systems including telomerase-immortalized human mesenchymal stem cells (hMSCs) (Simonsen et al., 2002) differentiated to either the osteoblast (Figure 1A) or adipocyte lineages (Figure 1B), human fetal osteoblast (hFOB) cells (Figure 1C), mouse neurospheres (Figure 1D, see Figure S1A available online), and oligodendrocytes (Figure 1E). In each of the investigated mammalian model systems, H2Bub1 levels increased concomitantly with the induction of lineage specification which was accompanied by increased RNF40 protein levels in hMSC (Figure S1B). In contrast, the levels of H2A monoubiquitination remained constant during hMSC differentiation (Figure S1C).

In order to determine whether the increase in H2Bub1 levels during cellular differentiation is conserved across species, we performed immunofluorescence analyses of H2Bub1 in the *Drosophila melanogaster* ovary. As observed in undifferentiated mammalian cells, H2Bub1 was undetectable in *Drosophila* germline stem cells (characterized by the presence of phospho-Mad; Figure 1F). In contrast, differentiated cystoblasts displayed readily detectable H2Bub1 levels. Thus, increased H2Bub1 levels during cellular differentiation are common to multiple differentiation programs and across species.

RNF40 Knockdown Impairs hMSC Differentiation

To test whether H2Bub1 is required for differentiation, we examined the effects of RNF40 depletion on hMSC differentiation. As assessed by staining for differentiated osteoblasts (alkaline phosphatase) or adipocytes (oil red O), we observed a clear decrease in both differentiation models following RNF40 knockdown with independent RNF40 siRNAs (Figures 2A and 2B; Figures S2A–S2F). Consistently, no lipid droplet formation was observed by electron microscopy in RNF40-depleted cells grown under adipocyte differentiating conditions (Figure S2G).

RNF40 Knockdown Impairs Differentiation-Regulated Transcription

In order to determine the extent of the effects elicited by RNF40 knockdown on hMSC differentiation, we performed siRNA knockdown and transcriptome-wide gene expression microarray analyses of undifferentiated hMSCs and cells differentiated to the adipocyte or osteoblast lineages for 2 or 5 days. RNF40 knockdown had little or no effect on gene expression in undifferentiated hMSCs (Figure S2J). Strikingly, the differentiation-induced gene expression changes were significantly impaired following RNF40 knockdown (Figures 2C and 2D) without affecting the expression of the osteoblast and adipocyte-regulatory factors *RUNX2*, *CEBPA*, and *CEBPG* (Figures S2H and S2I). The effects of RNF40 knockdown were evident for common (Figure S2K) as well as lineage-specific (Figures S2L and S2M) transcriptional programs. Pathways significantly enriched in gene sets differentially regulated in each differentiation program and by RNF40 depletion (Table S1) include focal adhesion (Figures S2N–S2Q), cell cycle (Figures S2R–S2U), adipocytokine signaling (Figures S2V and S2W), and pathways in cancer (Figures S2X–S2AA). Microarray data were verified on a number of osteoblast (*BGLAP*, *ALPL*, and *G6PD*)- and adipocyte (*PPARG*, and *RASD1*)-specific genes (Figures 2E and 2F, respectively). Consistent with the obligate heterodimeric function of RNF20 and RNF40, RNF20 knockdown also decreased H2Bub1 levels and impaired the induction of osteoblast- and adipocyte-specific gene expression (Figures S2AB–S2AE). Importantly, RNF40 depletion did not affect mRNA levels of other pathway components (CDK9, WAC, RNF20; Figures S2AF and S2AG).

CDK9 Controls hMSC Differentiation

Since CDK9 controls the global and gene-specific levels of H2Bub1 (Pirngruber et al., 2009b; Shchebet et al., 2012), we hypothesized that CDK9 may also be required for hMSC differentiation by directing RNF40-dependent H2B monoubiquitination through P-Ser2 RNAPII CTD. Consistent with this notion, the levels of P-Ser2 increased during hMSC differentiation (Figure S3A).

We next examined the effects of CDK9 knockdown on hMSC differentiation. Similar to the effects of RNF40 knockdown, adipocyte differentiation and gene expression (Figures 3C and 3D, Figure S3F) were impaired following CDK9 knockdown, as was the expression of the osteoblast marker genes *BGLAP* and *G6PD* (Figure 3B) and global H2Bub1 levels (Figures S3B and S3C). Surprisingly, the induction of alkaline phosphatase activity (Figure 3A, Figure S3E) and *ALPL* gene expression (Figure 3B) was increased following CDK9 knockdown. Since alkaline phosphatase is also a marker of pluripotency, these results may indicate a reversion to an earlier stem cell phenotype. These effects were not due to impaired expression of H2Bub1 pathway regulators (Figures S3G and S3H). Thus, we conclude that CDK9 knockdown prevents hMSC differentiation irrespective of cell lineage.

WAC Knockdown Phenocopies RNF40 Depletion

WAC functionally links CDK9 and H2Bub1 during transcription by recruiting the RNF20/RNF40 complex to P-Ser2 RNAPII

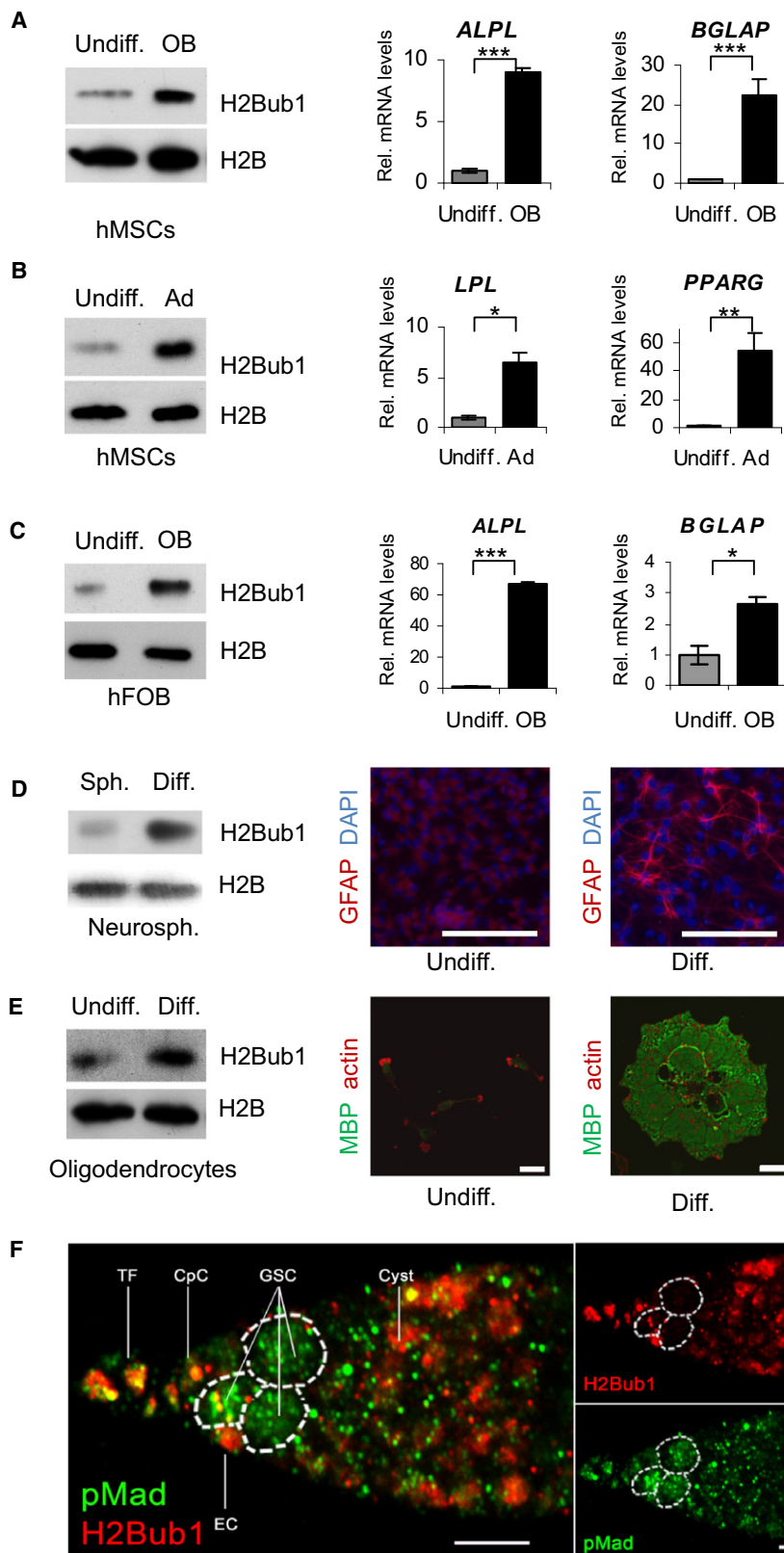


Figure 1. H2Bub1 Levels Increase upon Differentiation

(A and B) Immortalized human mesenchymal stem cells (hMSCs) were induced to differentiate into the osteoblast (A) or adipocyte (B) lineages for 5 days. Protein extracts were analyzed by western blot using antibodies against H2Bub1 or H2B (left panel). The expression of the osteoblast (*ALPL*, *BGLAP*; A) or adipocyte (*LPL*, *PPARG*; B) marker genes was verified by qRT-PCR. Gene expression was normalized to a control gene (*HNRNPK*) and the undifferentiated condition and expressed as "relative mRNA levels." Mean \pm SD, $n = 3$. Statistical analysis, * $p < 0.05$; ** $p < 0.01$; *** $p < 0.001$.

(C) Human fetal osteoblasts (hFOB) were differentiated and analyzed by western blot for H2Bub1 and H2B as in (A). Induction of osteoblast marker genes (*ALPL*, *BGLAP*) was verified as in (A). Mean \pm SD, $n = 3$.

(D) Mouse neurospheres were induced to differentiate and analyzed by western blot as in (A). Differentiation to glial cells was examined by immunofluorescence staining of GFAP (red). Nuclei were costained with DAPI (blue).

(E) Mouse oligodendrocytes were differentiated for 5 days and analyzed for H2Bub1 and H2B levels by western blot. Differentiation was verified by immunofluorescence staining against myelin basic protein (MBP, green) and actin (red).

(F) Immunofluorescence analysis of *Drosophila melanogaster* ovary stained for H2Bub1 and phosphorylated Mad (pMad; marker of proliferating stem cells). TF, terminal filament cells; CpC, cap cells; GSC, germline stem cells; Cyst, cystoblast; EC, escort cells.

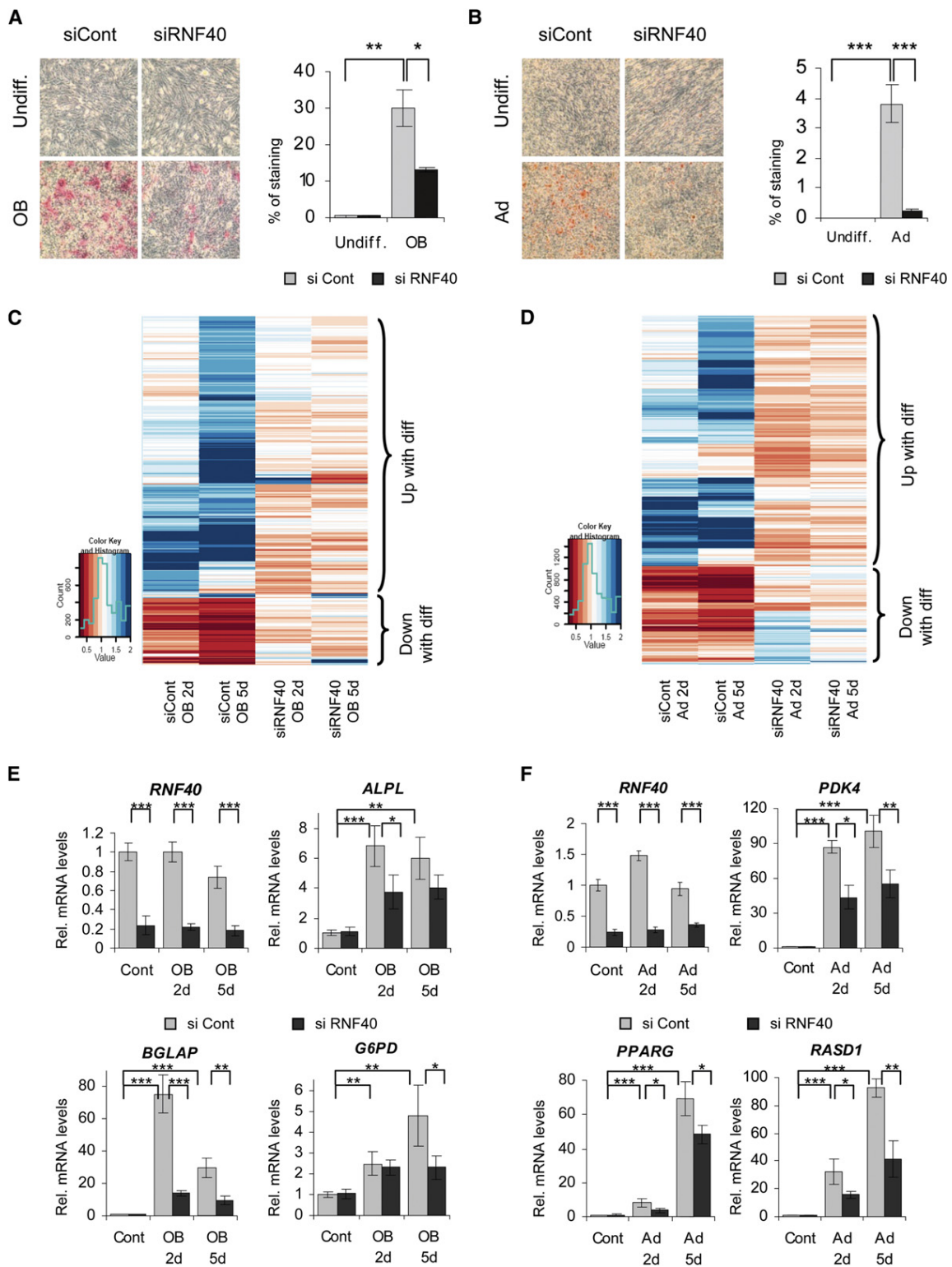


Figure 2. RNF 40 Is Required for hMSC Differentiation

(A and B) hMSCs were transfected with control and RNF40 siRNAs and induced to differentiate into osteoblasts (A) or adipocytes (B) for 5 days. Differentiation was verified by alkaline phosphatase (A) or oil red O (B) staining (left). The stained area was quantified using ImageJ software and displayed as percentage of area (right). Mean \pm SD, $n = 3$.

CTD (Zhang and Yu, 2011). Consistent with this report, WAC was required for the stability of the RNF20/40 complex (Figures S3I and S3J) and maintaining H2Bub1 levels (Figures S3K–S3N). Importantly, WAC knockdown impaired osteoblast (Figure 3E and Figure S3O) and adipocyte (Figure 3G and Figure S3P) differentiation and the induction of marker gene expression (Figures 3F and 3H). While RNF20, RNF40, and WAC protein levels were dependent upon one another (Figures S3I and S3J), their mRNA levels were unaffected by WAC knockdown (Figures S3Q and S3R). These results provide a mechanistic explanation for how CDK9 directs H2Bub1 during differentiation through RNAPII CTD phosphorylation and recruitment of the WAC/RNF20/RNF40 ubiquitin ligase complex. Perturbation of any component similarly impairs stem cell differentiation.

RNF40 Is Required for Resolution of Bivalency

In order to test whether the effects of RNF40, RNF20, CDK9, and WAC depletion on hMSC differentiation may be a direct effect of H2Bub1, we performed chromatin immunoprecipitation analyses on the adipocyte-specific genes *PDK4*, *PPARG*, and *RASD1* as well as positive (*GAPDH*) and negative (*TFF1*) control genes. Indeed, all three lineage-specific genes showed increased levels of H2Bub1 during differentiation (Figure 4A). Importantly, the levels of H2Bub1 were constantly present on the *GAPDH* gene and decreased following RNF40 knockdown but were constitutively absent from the silenced *TFF1* gene.

Embryonic stem cells and some lineage-committed stem cells display a unique combination of both activating (H3K4me3) and repressing (H3K27me3) histone modifications on many lineage-specific genes (Collas, 2010; Fisher and Fisher, 2011). During differentiation, bivalency on adipocyte-specific genes is resolved in favor of an active state in which H3K4me3 is retained while H3K27me3 is lost (Collas, 2010; Noer et al., 2009). Perturbations in the resolution of bivalency impair the inducibility of lineage-specific genes during differentiation. The analysis of genome-wide chromatin immunoprecipitation-sequencing data (ChIP-Seq) from human embryonic stem cells (hESCs) and normal adipose nuclei confirmed that the investigated adipocyte-specific genes (*PDK4*, *PPARG*, *RASD1*) are all bivalent in hESC and lose their bivalency in favor of H3K4me3 during terminal adipocyte differentiation (Figure 4B).

Given the established dependence of H3K4me3 on H2Bub1 in some systems (Kim et al., 2009; Pirngruber et al., 2009a; Zhu et al., 2005), we hypothesized that the impaired differentiation observed following RNF40 knockdown (with no major effects on the global gene expression profile) may be due to changes in the bivalency status of differentiation-induced genes. Surprisingly, while adipocyte-specific genes (*PDK4*, *PPARG*, *RASD1*) exhibit significant levels of both H3K4me3 and H3K27me3 in the undifferentiated state (Figures 4C and 4D), neither the global (Figure S4) nor the gene-associated levels of H3K4me3 were reduced following RNF40 knockdown (Figure 4C). This supports

the findings that H3K4me3 may be independent of H2Bub1 in some systems (Shema et al., 2008; Vethantham et al., 2012). As previously reported (Noer et al., 2009), bivalency was resolved in favor of H3K4me3 on adipocyte-specific genes during differentiation (Figure 4D). In contrast, H3K27me3 was retained on bivalent adipocyte-specific genes following RNF40 knockdown. Thus RNF40-dependent H2B monoubiquitination appears to be dispensable for H3K4me3 but essential for the resolution of bivalency on lineage-specific genes.

DISCUSSION

In order to obtain a clearer understanding of the roles of specific chromatin modifications in the transition from stem cells into a differentiated phenotype, we investigated the effects of perturbing H2Bub1 levels during cellular differentiation. We show that both global and lineage-specific gene-associated H2Bub1 levels increase during hMSC differentiation. Although a recent study reported a decrease in H2Bub1 during myoblast differentiation (Vethantham et al., 2012), our data suggest that H2Bub1 levels increase in multiple diverse differentiation systems. Furthermore, this process is evolutionarily conserved. Notably, in addition to the investigated mouse and human cell culture differentiation models, we demonstrate that H2Bub1 is suppressed in stem cells in vivo. Although a suppression of H2Bub1 was previously suggested to be essential for stem cell maintenance in *Drosophila* (Buszczak et al., 2009), we now show that H2Bub1 levels indeed increase during differentiation and that its modifying enzymes and upstream regulators are essential for the differentiation process.

We have demonstrated that CDK9 activity is essential for the induction of lineage-specific gene expression. Data in *Drosophila* and *C. elegans* support this observation, since a suppression of CDK9 activity is required for stem cell maintenance (Batchelder et al., 1999; Hanyu-Nakamura et al., 2008; Zhang et al., 2003). Furthermore, it has been shown that CDK9 activity is required for differentiation in several mammalian cell systems, including adipocyte (Iankova et al., 2006), myoblast (Simone et al., 2002), monocyte (Yu et al., 2006), and cardiomyocyte differentiation (Kaichi et al., 2011). Given that a large fraction of unexpressed genes in ESCs exhibit paused RNAPII lacking P-Ser2 (Guenther et al., 2007), suppression of CDK9 activity may be a general mechanism employed for maintaining a stem cell state. Like bivalent chromatin domains, the presence of a paused RNAPII is expected to allow the timely induction of differentiation-related genes.

Specific chromatin states play an essential role in controlling pluripotency, and dynamic changes in these states are required for proper lineage-specific differentiation (Fisher and Fisher, 2011; Meissner, 2010). We have confirmed that adipocyte-specific genes exist in a bivalent chromatin state in multipotent hMSCs. In parallel with the global increase in H2Bub1 levels,

(C and D) Transcriptome-wide gene expression microarray analysis of hMSC induced to differentiate into the osteoblast (C) or adipocyte (D) lineages for 2 or 5 days after RNF40 knockdown. The heatmaps indicate the fold changes in mRNA levels in the various conditions relative to the undifferentiated control transfected cells. Color code indicates downregulated genes in red and upregulated genes in blue. Mean values, $n = 3$.

(E and F) qRT-PCR analyses verify the knockdown of RNF40 in the RNA samples utilized for microarray analyses in (C and D) as well as the changes in gene expression of selected osteoblast (*ALPL*, *BGLAP*, *G6PD*; E) and adipocyte (*PDK4*, *PPARG*, *RASD1*; F) marker genes. Mean \pm SD, $n = 3$.

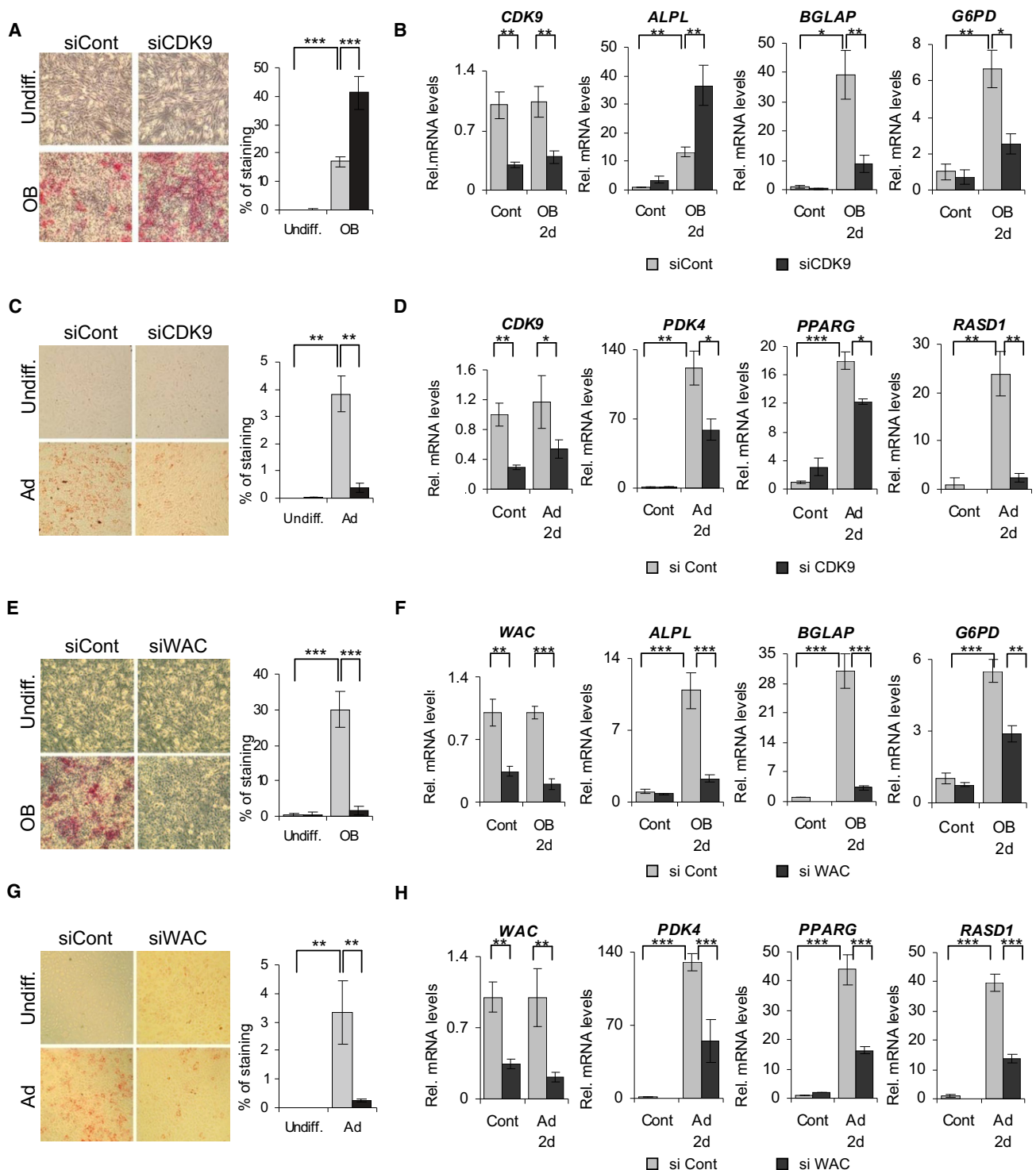
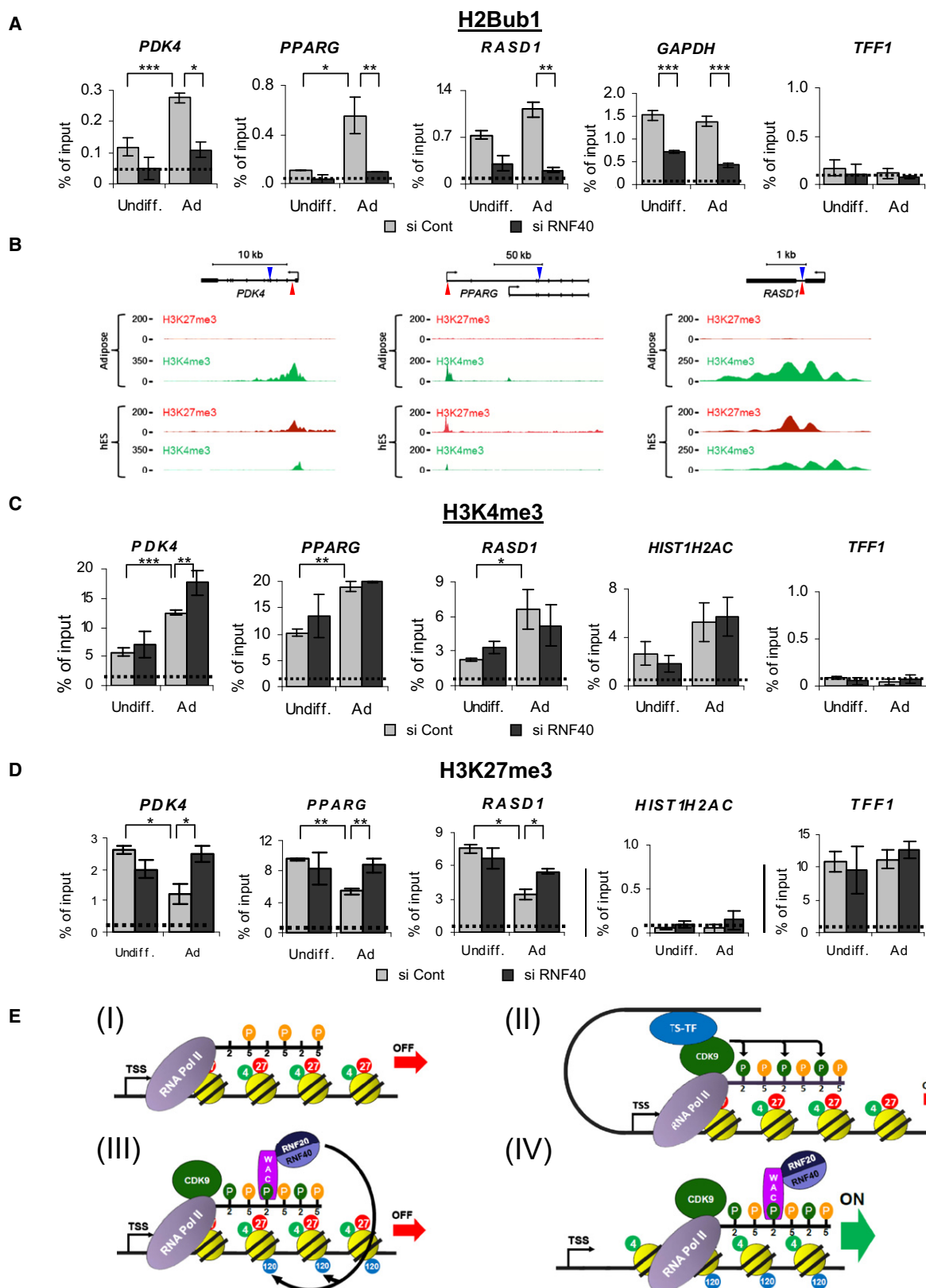


Figure 3. CDK9 and WAC Direct H2Bub1 during Differentiation

(A–H) hMSCs transfected with siRNAs against CDK9 (A–D) or WAC (E–H) were induced to differentiate into the osteoblast (A and B, E and F) or adipocyte (C and D, G and H) lineages. Cells were stained for alkaline phosphatase activity (A and E) or oil red O (C and G) for osteoblast and adipocyte lineages, respectively. Staining was quantified as in Figures 2A and 2B. Mean \pm SD, $n = 3$. (B, D, F, and H) The knockdown efficiency and the effects on osteoblast- (*ALPL*, *BGLAP*, *G6PD*; B and F) and adipocyte-specific (*PDK4*, *PPARG*, *RASD1*; D and H) gene expression were verified by qRT-PCR and analyzed as in Figures 2E and 2F following 2 days of differentiation. Mean \pm SD, $n = 3$.



this bivalency is resolved, and these genes become fully active and exhibit a decrease in H3K27me3 while retaining H3K4me3. In our model, tissue-specific transcription factors promote differentiation in a CDK9-dependent manner by directing H2Bub1 (Figure 4E). In turn, H2Bub1 (or possibly RNF40 directly) likely directs dynamic changes in chromatin structure which facilitate the demethylation of H3K27me3 during the transition from a repressive to an active chromatin state. Consistently, we and others have shown that RNF20 and RNF40 cooperate with the FACT histone chaperone complex to stimulate histone exchange and facilitate transcriptional elongation (Pavri et al., 2006; Prenzel et al., 2011). Consistent with a CDK9→WAC→RNF20/RNF40→H2Bub1→FACT regulatory circuit, the presence of both H2Bub1 and FACT on target genes depends upon CDK9 activity rather than transcriptional activity per se (Gomes et al., 2006; Pirngruber et al., 2009b). Interestingly, the chromatin remodeling factor CHD1 is required for pluripotency (Gaspar-Maia et al., 2009) and was independently identified in complexes containing CDK9 (Park et al., 2010) and FACT (Kelley et al., 1999). Furthermore, a recent study identified a functional interaction between H2Bub1 and Chd1 in yeast (Lee et al., 2012). Moreover, mammalian CHD1 interacts directly with H3K4me3 through its chromodomain (Sims et al., 2007) but is excluded from bivalent domains (Gaspar-Maia et al., 2009). Thus, the maintenance of H3K27me3 at bivalent genes following RNF40 knockdown may function in part by preventing CHD1 recruitment.

In conclusion, our data establish a role for CDK9, WAC, and RNF40 in directing H2B monoubiquitination and transcriptional reprogramming during stem cell differentiation. This effect appears to be due to dynamic changes in chromatin structure during differentiation, which facilitate a transition from an inactive to an active chromatin state. In keeping with this, we observed maintenance of H3K27me3 levels on bivalent adipocyte-specific genes following RNF40 depletion. Thus these data place H2Bub1 and its regulatory pathway as central players in cell-fate determination and underscore the importance of dynamic changes in chromatin structure during cellular differentiation.

EXPERIMENTAL PROCEDURES

Cell Culture, Differentiation, and Knockdowns

hMSC and hFOB1.17 cells were cultured and differentiated as previously done (Simonsen et al., 2002; Harris et al., 1995) and are described together with staining procedures and the generation, culture, and differentiation of neurospheres and oligodendrocytes in the Supplemental Experimental Procedures. Knockdown procedures and siRNAs utilized are listed in the Supplemental Information.

Western Blot Analysis, RNA Isolation, qRT-PCR, ChIP

Western blot analysis was performed with antibodies and dilutions listed in the Supplemental Information. RNA isolation, reverse transcription, ChIP, and quantitative RT-PCR were performed as described (Prenzel et al., 2011) with the modifications listed in the Supplemental Experimental Procedures. ChIP-Seq results were obtained from the NIH Roadmap Epigenomics Project (Bernstein et al., 2010), visualized using the UCSC Genome Browser, and used under permission from the NIH Epigenome Mapping Center at Broad Institute.

Microscopy

For analyzing H2Bub1 levels in vivo, ovaries from OregonR *Drosophila* were fixed and stained as described in the Supplemental Experimental Procedures.

Microarray Studies

Whole-genome gene expression analysis was performed by the Vancouver Prostate Centre Laboratory for Advanced Genome Analysis (Vancouver, Canada) using the Illumina human HT-12 v4 beadchip. Gene expression data were analyzed as previously described (Prenzel et al., 2011). Gene set pathway analyses were performed as described in the Supplemental Experimental Procedures. All gene expression data will be made publicly available through the GEO repository.

ACCESSION NUMBERS

The Gene Expression Omnibus (GEO) accession numbers for the ES and adipose nuclei ChIP-Seq reported in this paper are GSM669889, GSM669897, GSM669925, and GSM669930. The GEO accession number for the gene expression microarray analyses reported in this paper is GSE38173.

SUPPLEMENTAL INFORMATION

Supplemental Information includes four figures, one table, Supplemental Experimental Procedures, and Supplemental References and can be found with this article online at doi:10.1016/j.molcel.2012.05.022.

ACKNOWLEDGMENTS

The authors would like to thank S. Le Bihan and A. Haegert for performing microarray experiments, and the NIH Epigenome Mapping Center at Broad Institute for allowing the use of the unpublished ChIP-Seq data. O.K. and Z.N. were supported by fellowships from the Dorothea-Schlözer Program of the University of Göttingen and the German Academic Exchange Service (DAAD), respectively. This work was funded by an ERC Starting Grant to M.S.; the German Research Foundation (DFG) Research Group 942 to T.B.; and the State of Lower Saxony, Hannover, Germany (VWZN2562) and the DFG (JO 815/1) to S.A.J.

Received: October 24, 2011

Revised: February 28, 2012

Accepted: May 17, 2012

Published online: June 7, 2012

Figure 4. RNF40 Expression Is Required for the Resolution of Bivalent Chromatin Marks

(A) ChIP analysis of H2Bub1 on adipocyte-regulated genes (*PDK4*, *PPARG*, and *RASD1*) upon RNF40 knockdown. hMSCs were differentiated to adipocytes for 2 days following RNF40 depletion for 24 hr. *GAPDH* serves as a positive control for an active gene displaying H2Bub1, and *TFF1* serves as a control for an inactive gene with no detectable H2Bub1. Background (IgG) levels are indicated as dotted lines. Mean ± SD, n = 3.

(B) Human ESCs demonstrate bivalent domains containing both H3K4me3 and H3K27me3 on the adipocyte-regulated genes *PDK4*, *PPARG*, and *RASD1* while this bivalency is resolved in favor of H3K4me3 in adipose nuclei. Red triangles indicate amplicons used for detection of bivalent domains; blue triangles indicate amplicons used for detection of H2Bub1 within the transcribed region.

(C and D) H3K4me3 (C) and H3K27me3 (D) occupancy on adipocyte-regulated genes as well as one active gene (*HIST1H2AC*) and one repressed (*TFF1*) control gene. ChIP analysis was performed in hMSCs as in (A) following RNF40 depletion. Mean ± SD, n = 3.

(E) Model of the role of H2Bub1 in differentiation. “4” in green circles, H3K4me3; “27” in red circles, H3K27me3; “120” in blue circles, H2Bub1; “P” in orange circles, Ser5 phosphorylation of CTD; “P” in green circles, Ser2 phosphorylation of CTD; TSS, transcription start site.

REFERENCES

- Azuara, V., Perry, P., Sauer, S., Spivakov, M., Jorgensen, H.F., John, R.M., Gouti, M., Casanova, M., Warnes, G., Merkenschlager, M., and Fisher, A.G. (2006). Chromatin signatures of pluripotent cell lines. *Nat. Cell Biol.* 8, 532–538.
- Batchelder, C., Dunn, M.A., Choy, B., Suh, Y., Cassie, C., Shim, E.Y., Shin, T.H., Mello, C., Seydoux, G., and Blackwell, T.K. (1999). Transcriptional repression by the *Caenorhabditis elegans* germ-line protein PIE-1. *Genes Dev.* 13, 202–212.
- Bernstein, B.E., Mikkelsen, T.S., Xie, X., Kamal, M., Huebert, D.J., Cuff, J., Fry, B., Meissner, A., Wernig, M., Plath, K., et al. (2006). A bivalent chromatin structure marks key developmental genes in embryonic stem cells. *Cell* 125, 315–326.
- Bernstein, B.E., Stamatoyannopoulos, J.A., Costello, J.F., Ren, B., Milosavljevic, A., Meissner, A., Kellis, M., Marra, M.A., Beaudet, A.L., Ecker, J.R., et al. (2010). The NIH Roadmap Epigenomics Mapping Consortium. *Nat. Biotechnol.* 28, 1045–1048.
- Buszczak, M., Paterno, S., and Spradling, A.C. (2009). *Drosophila* stem cells share a common requirement for the histone H2B ubiquitin protease scrawny. *Science* 323, 248–251.
- Collas, P. (2010). Programming differentiation potential in mesenchymal stem cells. *Epigenetics* 5, 476–482.
- Fisher, C.L., and Fisher, A.G. (2011). Chromatin states in pluripotent, differentiated, and reprogrammed cells. *Curr. Opin. Genet. Dev.* 21, 140–146.
- Gaspar-Maia, A., Alajem, A., Polesso, F., Sridharan, R., Mason, M.J., Heidersbach, A., Ramalho-Santos, J., McManus, M.T., Plath, K., Meshorer, E., and Ramalho-Santos, M. (2009). Chd1 regulates open chromatin and pluripotency of embryonic stem cells. *Nature* 460, 863–868.
- Gomes, N.P., Bjerke, G., Llorente, B., Szostek, S.A., Emerson, B.M., and Espinosa, J.M. (2006). Gene-specific requirement for P-TEFb activity and RNA polymerase II phosphorylation within the p53 transcriptional program. *Genes Dev.* 20, 601–612.
- Guenther, M.G., Levine, S.S., Boyer, L.A., Jaenisch, R., and Young, R.A. (2007). A chromatin landmark and transcription initiation at most promoters in human cells. *Cell* 130, 77–88.
- Hanyu-Nakamura, K., Sonobe-Nojima, H., Tanigawa, A., Lasko, P., and Nakamura, A. (2008). *Drosophila* Pgc protein inhibits P-TEFb recruitment to chromatin in primordial germ cells. *Nature* 451, 730–733.
- Harris, S.A., Enger, R.J., Riggs, B.L., and Spelsberg, T.C. (1995). Development and characterization of a conditionally immortalized human fetal osteoblastic cell line. *J. Bone Miner. Res.* 10, 178–186.
- Iankova, I., Petersen, R.K., Annicotte, J.S., Chavey, C., Hansen, J.B., Kratchmarova, I., Sarraf, D., Benkirane, M., Kristiansen, K., and Fajas, L. (2006). Peroxisome proliferator-activated receptor gamma recruits the positive transcription elongation factor b complex to activate transcription and promote adipogenesis. *Mol. Endocrinol.* 20, 1494–1505.
- Johnsen, S.A. (2012). The enigmatic role of H2Bub1 in cancer. *FEBS Lett.* 586, 1592–1601.
- Kaichi, S., Takaya, T., Morimoto, T., Sunagawa, Y., Kawamura, T., Ono, K., Shimatsu, A., Baba, S., Heike, T., Nakahata, T., and Hasegawa, K. (2011). Cyclin-dependent kinase 9 forms a complex with GATA4 and is involved in the differentiation of mouse ES cells into cardiomyocytes. *J. Cell. Physiol.* 226, 248–254.
- Kelley, D.E., Stokes, D.G., and Perry, R.P. (1999). CHD1 interacts with SSRP1 and depends on both its chromodomain and its ATPase/helicase-like domain for proper association with chromatin. *Chromosoma* 108, 10–25.
- Kim, J., Guermah, M., McGinty, R.K., Lee, J.S., Tang, Z., Milne, T.A., Shilatifard, A., Muir, T.W., and Roeder, R.G. (2009). RAD6-mediated transcription-coupled H2B ubiquitylation directly stimulates H3K4 methylation in human cells. *Cell* 137, 459–471.
- Lee, J.S., Garrett, A.S., Yen, K., Takahashi, Y.H., Hu, D., Jackson, J., Seidel, C., Pugh, B.F., and Shilatifard, A. (2012). Codependency of H2B monoubiquitination and nucleosome reassembly on Chd1. *Genes Dev.* 26, 914–919.
- Meissner, A. (2010). Epigenetic modifications in pluripotent and differentiated cells. *Nat. Biotechnol.* 28, 1079–1088.
- Minsky, N., Shema, E., Field, Y., Schuster, M., Segal, E., and Oren, M. (2008). Monoubiquitinated H2B is associated with the transcribed region of highly expressed genes in human cells. *Nat. Cell Biol.* 10, 483–488.
- Noer, A., Lindeman, L.C., and Collas, P. (2009). Histone H3 modifications associated with differentiation and long-term culture of mesenchymal adipose stem cells. *Stem Cells Dev.* 18, 725–736.
- Park, G., Gong, Z., Chen, J., and Kim, J.E. (2010). Characterization of the DOT1L network: implications of diverse roles for DOT1L. *Protein J.* 29, 213–223.
- Pavri, R., Zhu, B., Li, G., Trojer, P., Mandal, S., Shilatifard, A., and Reinberg, D. (2006). Histone H2B monoubiquitination functions cooperatively with FACT to regulate elongation by RNA polymerase II. *Cell* 125, 703–717.
- Pirngruber, J., Shchebet, A., and Johnsen, S.A. (2009a). Insights into the function of the human P-TEFb component CDK9 in the regulation of chromatin modifications and co-transcriptional mRNA processing. *Cell Cycle* 8, 3636–3642.
- Pirngruber, J., Shchebet, A., Schreiber, L., Shema, E., Minsky, N., Chapman, R.D., Eick, D., Aylon, Y., Oren, M., and Johnsen, S.A. (2009b). CDK9 directs H2B monoubiquitination and controls replication-dependent histone mRNA 3' end processing. *EMBO Rep.* 10, 894–900.
- Prenzel, T., Begus-Nahrmann, Y., Kramer, F., Hennion, M., Hsu, C., Gorsler, T., Hintermair, C., Eick, D., Kremmer, E., Simons, M., et al. (2011). Estrogen-dependent gene transcription in human breast cancer cells relies upon proteasome-dependent monoubiquitination of histone H2B. *Cancer Res.* 71, 5739–5753.
- Shchebet, A., Karpiuk, O., Kremmer, E., Eick, D., and Johnsen, S.A. (2012). Phosphorylation of cyclin-dependent kinase-9 controls ubiquitin-conjugating enzyme-2A function. *Cell Cycle* 11, 1–6.
- Shema, E., Tirosh, I., Aylon, Y., Huang, J., Ye, C., Moskovits, N., Raver-Shapira, N., Minsky, N., Pirngruber, J., Tarcic, G., et al. (2008). The histone H2B-specific ubiquitin ligase RNF20/hBRE1 acts as a putative tumor suppressor through selective regulation of gene expression. *Genes Dev.* 22, 2664–2676.
- Simone, C., Stiegler, P., Bagella, L., Pucci, B., Bellan, C., De Falco, G., De Luca, A., Guanti, G., Puri, P.L., and Giordano, A. (2002). Activation of MyoD-dependent transcription by cdk9/cyclin T2. *Oncogene* 21, 4137–4148.
- Simonsen, J.L., Rosada, C., Serakinci, N., Justesen, J., Stenderup, K., Rattan, S.I., Jensen, T.G., and Kassem, M. (2002). Telomerase expression extends the proliferative life-span and maintains the osteogenic potential of human bone marrow stromal cells. *Nat. Biotechnol.* 20, 592–596.
- Sims, R.J., III, Millhouse, S., Chen, C.F., Lewis, B.A., Erdjument-Bromage, H., Tempst, P., Manley, J.L., and Reinberg, D. (2007). Recognition of trimethylated histone H3 lysine 4 facilitates the recruitment of transcription postinitiation factors and pre-mRNA splicing. *Mol. Cell* 28, 665–676.
- Vethantham, V., Yang, Y., Bowman, C., Asp, P., Lee, J.H., Skalniak, D.G., and Dynlacht, B.D. (2012). Dynamic loss of H2B ubiquitylation without corresponding changes in H3K4 tri-methylation during myogenic differentiation. *Mol. Cell Biol.* 32, 1044–1055.
- Yu, W., Wang, Y., Shaw, C.A., Qin, X.F., and Rice, A.P. (2006). Induction of the HIV-1 Tat co-factor cyclin T1 during monocyte differentiation is required for the regulated expression of a large portion of cellular mRNAs. *Retrovirology* 3, 32. 10.1186/1742-4690-3-32.
- Zhang, F., and Yu, X. (2011). WAC, a functional partner of RNF20/40, regulates histone H2B ubiquitination and gene transcription. *Mol. Cell* 41, 384–397.
- Zhang, F., Barboric, M., Blackwell, T.K., and Peterlin, B.M. (2003). A model of repression: CTD analogs and PIE-1 inhibit transcriptional elongation by P-TEFb. *Genes Dev.* 17, 748–758.
- Zhu, B., Zheng, Y., Pham, A.D., Mandal, S.S., Erdjument-Bromage, H., Tempst, P., and Reinberg, D. (2005). Monoubiquitination of human histone H2B: the factors involved and their roles in HOX gene regulation. *Mol. Cell* 20, 601–611.

2.3 Visualization of Adult Stem Cells Within Their Niches Using the *Drosophila* Germline as a Model System

Annekatrin König and Halyna R. Shcherbata

All experiments were done by Annkatrin König.

Status of the manuscript: published (Methods Mol Biol. 2013;1035:25-33)

Visualization of Adult Stem Cells Within Their Niches Using the *Drosophila* Germline as a Model System

Annekatrin König and Halyna R. Shcherbata

Abstract

The germaria of the fruit fly *Drosophila melanogaster* present an excellent model to study germline stem cell–niche interactions. Two to three adult stem cells are surrounded by a number of somatic cells that form the niche. Here we describe how *Drosophilae* germaria can be dissected and specifically immunostained to allow for identification and analysis of both the adult stem cells and their somatic niche cells.

Key words *Drosophila*, Germarium, Ovary, Adult stem cells, Stem cell niche, Germline, Ovarian soma, Immunostaining

1 Introduction

Adult stem cells usually reside in the stem cell niche, a unique physiological microenvironment that helps stem cells to carry on self-renewing divisions throughout the lifetime of an organism. The niche includes cellular and noncellular elements that can be divided into one of the two main mechanistic types—physical contacts and diffusible factors [1]. Close contacts include tight junctions, adherens junctions, gap junctions, the Notch signaling pathway, the basement membrane, and extracellular matrix proteins. Diffusible factors, which are secreted by niche cells and travel over varying distances to keep stem cell identity, often affect transcription. Stem cells must be anchored to the niche through cell–cell interactions so that they will stay both close to niche factors that specify self-renewal and far from differentiation stimuli.

Presently the existence of a stem cell niche has been demonstrated for mammalian adult stem cells in the hematopoietic, epidermal, neural, and intestinal systems. However, the stem cell niches involved in maintenance of adult mammalian tissues and particularly their role in cancer development remain complex, poorly defined, and difficult to study in vivo [2].

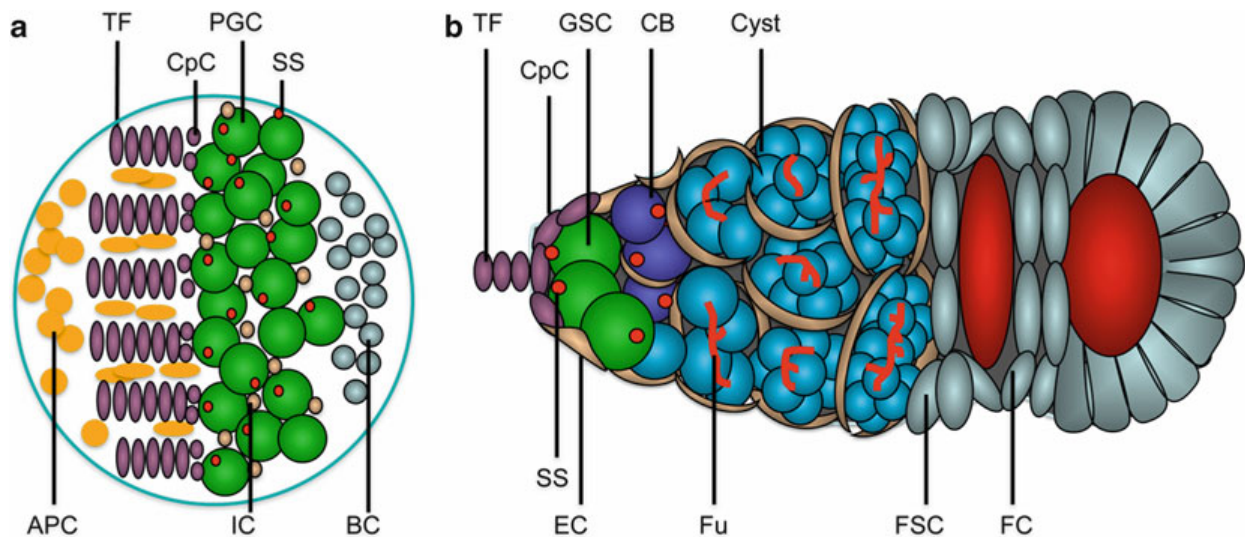


Fig. 1 Scheme of larval ovary and adult germarium. **(a)** The primordial germ cells (PGC) that can be identified by their characteristic spherical spectrosomes (SS spherical skeletal organelles) are intermingled with somatic cells (IC, intermingled cells). Stacks of the terminal filament (TF) cells have already formed in late L3 larvae. Cap cells (CpCs) are forming in late L3 larvae through the early pupal stages at the base of TFs. Two populations of somatic cells (APC, apical cells, BC, basal cells) are also found in the larval ovary. **(b)** In the adult ovaries, the individual ovarioles with the germaria are separated by peritoneal sheath. The germline stem cells (GSCs) are positioned at the anterior of the germarium and directly attached to cap cells. Upon asymmetric division, the stem cells give rise to another stem cell and a differentiating daughter, the cystoblast (CB). The cystoblast divides four more times with incomplete cytokinesis, forming the cyst. During that process, the spherical spectrosomes of the GSCs elongate and branch to form the fusome (Fu). The terminal filament cells are in close proximity to the cap cells, but have a more *oval shape*. The GSCs are furthermore in contact with another type of somatic cells that presents an important component of the niche: the escort cells (EC). Follicle cells (FC) that are produced by follicle stem cells (FSC) encapsulate the developing egg. Anterior is to the *left*

The *Drosophila* ovarian stem cell niche is very well characterized and has been used for many years to unravel the complex stem cell–niche interactions. The insights gained from these studies led to a better understanding of how stem cells work: in addition to cell–cell interactions [3] between stem and niche cells, a variety of signaling pathways involved in stem cell control were described [4–13].

The easily identifiable and analyzable cells in the *Drosophila* germline niches and the sophisticated genetic tools that are available in *Drosophila* make it an ideal system for studying stem cell–niche interactions [14]. The paired ovaries of the adult female fly each consist of 16–20 ovarioles that contain developing egg chambers. Located at the anterior of every ovariole is the germarium, where two to three stem cells are held by 5–7 cap cells and are in contact with other somatic cells (*see* Fig. 1b). By asymmetric division, the adult stem cells give rise to both new stem cells and differentiated cells that will become the egg. The differentiated germline cells are surrounded by somatic escort cells that are another important component of the stem cell niche [4, 15]. More posteriorly, follicle cells that are generated by specific stem cells encapsulate the differentiating germline [16]. The individual ovarioles are held together by the

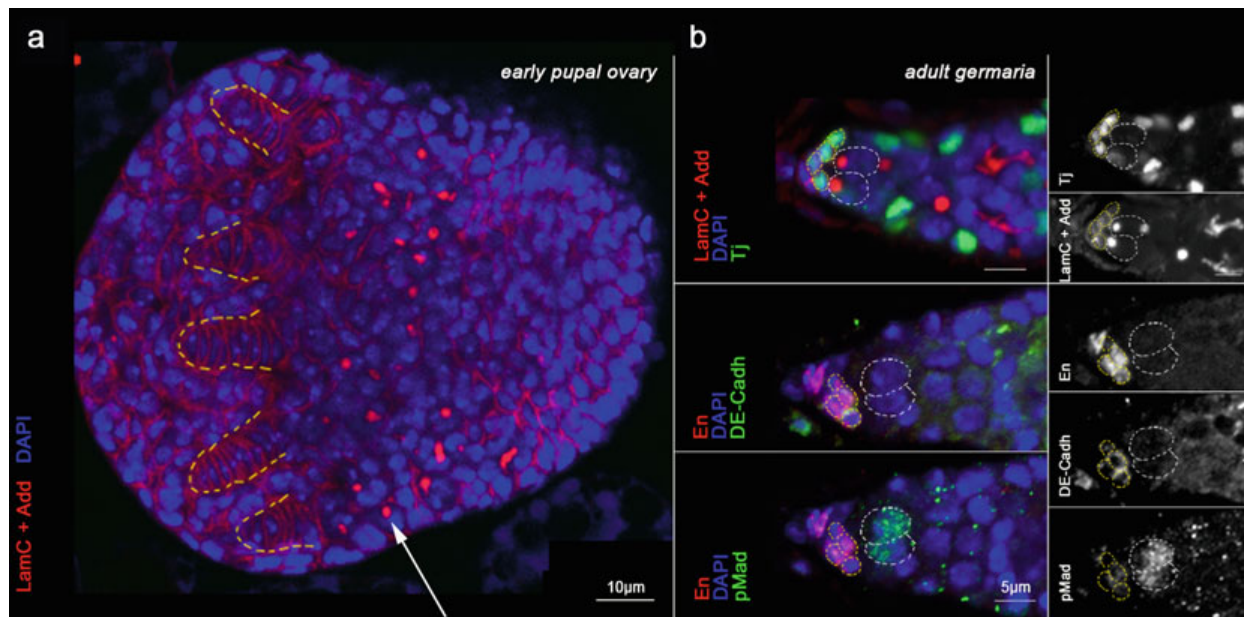


Fig. 2 Pre-adult ovary and adult germaria. **(a)** In the late larval and early pupal ovaries, terminal filament stacks become visible (outlined in *yellow*). The PGCs (*arrow*), that can be identified by their spherical SSs, are not separated yet into individual ovarioles and intermingled with somatic cells. **(b)** Adult ovaries consist of several germaria, each containing 2–3 GSCs, that can be not only identified by their characteristic Adducin-marked SSs but also stained with the stem cell marker pMad. Directly attached to the stem cells are several somatic cells that are forming the stem cell niche: the CpCs can be marked using LaminC or Engrailed. DE-Cadherin staining shows the adhesion contacts between the GSCs and CpCs. Furthermore, ECs and CpCs are marked here with Traffic jam

terminal filaments. A variety of different markers makes it possible to nicely immunostain and analyze number, localization, shape, and interactions of the individual cells (*see* Fig. 2b). In addition, the development of the stem cell niche itself can be directly observed in developing larvae and early pupae where the cap cells divide and terminally differentiate (*see* Figs. 1a and 2b) [17].

In this chapter we show how to visualize adult stem cells in their niches in adult female *Drosophila*.

2 Materials

2.1 Fly Husbandry

1. Standard cornmeal agar food (recipes can be found at <http://fly.bio.indiana.edu/>).
2. Yeast paste: Dry yeast should be mixed in 5 % propionic acid (*see* **Note 1**).

2.2 Ovary Dissection

1. Ice block for immobilization of the flies.
2. Sharp tweezers.
3. Small Petri dish for dissections.
4. Stereomicroscope for dissection.
5. Pasteur pipettes.

2.3 Fixation and Washing

1. Fixing solution: 4 % formaldehyde in phosphate-buffered saline (PBS) (*see Note 2*).
2. Nutator.
3. PBT: 0.2 % Triton X in PBS.

2.4 Antibodies

1. Blocking solution: 0.2 % bovine serum albumin, 5 % normal goat serum in PBT (*see Note 3*).
2. Primary antibodies: Many antibodies are available to study germline–niche interactions; some of these are listed in Table 1. Dilute primary antibodies in blocking solution and store at 4 °C (*see Notes 4–8*).

Table 1
A subset of antibodies that are useful to study germline stem cell niche interactions is shown

Protein recognized	Name of the antibody	Raised in	Antibody source	Used to mark in the germarium	Dilution
Armadillo	N2 7A1	Mouse, IgG2a	DSHB Iowa	Cell-Cell adhesion between cap cells and between stem cells and cap cells	1:50
Bag of marbles (BAM)	BamC (cytoplasmic)	Mouse, Rat	D. McKearin	Differentiating germline cysts, not in germline stem cells	1:1,000
E-Cadherin, extracellular domain	5D3	Mouse, IgG2b	DSHB Iowa	Cell-Cell adhesion between cap cells and between stem cells and cap cells	1:50
Engrailed	4D9	Mouse, IgG1	DSHB Iowa	Cap cells	1:50
Held out wings (HOW)	HOW	Rabbit, Rat	T. Volk	Germline stem cells, cystoblasts	1:1,000
Hts/Adducin-like	1B1	Mouse, IgG1	DSHB Iowa	Spectrosomes and fusomes	1:50
Lamin C	LC28.26	Mouse, IgG1	DSHB Iowa	Cap cells	1:50
Phosphorylated Mothers against Dpp (pMAD)	pMad	Rabbit	E. Laufer	Germline stem cells	1:5,000
Traffic jam	TJ	Guinea pig	D. Godt	Escort cells, cap cells	1:3,000
Vasa		Rat	P. Lasko	Germline cells	1:1,000

Scientists who generated a particular antibody are named as source. Their addresses are available from flybase (<http://flybase.org/>). DSHB Developmental Studies Hybridoma Bank at the University of Iowa

3. Secondary antibodies: Conjugated Alexa fluor goat anti-mouse, goat anti-rabbit, or goat anti-rat from Molecular Probes, diluted 1:500 in blocking solution (Molecular Probes); store at 4 °C (*see* **Notes 8** and **9**). The secondary antibodies have to be chosen with respect to the laser lines of the available microscope.

2.5 DNA Staining and Mounting

1. DAPI solution: Make a 100× DAPI solution (1 mg/ml) and store aliquots at −20 °C. For staining, dilute in PBS (*see* **Note 10**).
2. Glycerol: 70 % Glycerol, 3 % n-propyl gallate (NPG) (*see* **Note 11**).
3. Tungsten needles.

2.6 Analysis

Laser scanning confocal microscope is used for analysis.

3 Methods

3.1 Dissection

All steps are carried out at room temperature unless otherwise stated. During all incubations and washes, the Eppendorf tubes are placed on a nutator.

3.1.1 Adult Ovaries

1. Immobilize 5–10 female flies by putting them on an ice block.
2. The ovaries are positioned in the abdomen of the fly and are simple to find in well-fed individuals (*see* **Note 12**). Dissect the flies in 1× PBS using a stereomicroscope, and hold the fly with one pair of tweezers at the thorax. Carefully open the cuticle at the posterior end of the animal with another pair of tweezers. If necessary, gently push the abdomen to squeeze out the paired ovaries. Remove all remnants of guts and cuticle and place the ovaries in an Eppendorf tube using Pasteur pipettes (*see* **Note 13**).

3.1.2 Larval Ovaries

1. Pick up late third instar larvae from the wall of the food vial or bottle.
2. Select a female larva and hold with a pair of tweezers at the anterior end.
3. The larval ovaries are located in the fat body. Cut off the larval head and hold the posterior end of the remaining larval body with one pair of tweezers. Carefully now invert the larvae by pulling it over the tweezers with another pair of tweezers. Remove cuticle and guts and transfer the fat body into an Eppendorf tube or a 24-well plate (*see* **Note 14**).

3.1.3 Fixation

1. Add fixing solution and incubate for 10 min. Remove the fixing solution carefully and wear protective gloves when handling the fixative.
2. Wash the ovaries three times for 15 min each with PBT (*see* **Notes 15** and **16**).

3.2 Antibody Staining

1. Add blocking solution and incubate for 1 h.
2. Remove the blocking solution and add primary antibody solution. Incubate overnight at 4 °C.
3. Remove the antibody solution (*see* **Note 5**) and wash the ovaries three times for 15 min each with PBT.
4. Block again in blocking solution for 1 h.
5. Incubate the ovaries in secondary antibody solution overnight at 4 °C or for 3 h at room temperature.
6. Remove the secondary antibody solution and wash with PBT twice for 15 min. Add DAPI solution and incubate for 10 min.
7. Remove the DAPI solution and wash three times for 15 min with PBT.
8. Remove as much PBT as possible and add a few drops of glycerol to the ovaries.
 - (a) Adult ovaries: Place the ovaries on a slide and use tweezers and tungsten needles to separate the individual ovaries and to remove the mature eggs.
 - (b) Larval ovaries: Place the fat bodies on a slide and locate the larval ovaries. Carefully remove remnants of the fat body.
9. Place a coverslip on top of the samples and analyze using a confocal microscope.

4 Notes

1. The yeast paste should have a “peanut butter-like” texture. The propionic acid helps to avoid fungal or bacterial contamination.
2. Prepare the solution fresh from a 16 % stock solution at room temperature.
3. Goat serum is used in the blocking solution if the secondary antibody was produced in goat. If you have to use secondary antibodies that were generated in another animal, use other serums from the appropriate animal.
4. Primary antibodies: Apart from several monoclonal antibodies, that are available from the Developmental Studies Hybridoma Bank, a variety of different polyclonal rabbit, goat, sheep, and

guinea pig antibodies have been made by different labs (*see* Table 1). However, make sure not to use goat serum in the blocking solution if the primary antibody is goat derived.

5. When analyzing GFP-marked clonal cells, you may use an anti-GFP antibody to better visualize the GFP.
6. Stability of primary antibodies: Some primary antibodies can be reused a couple of times, whereas others can be used only once. Dilution and stability of every antibody or antibody batch have to be tested separately.
7. If the antibody staining shows a high level of nonspecific background, it may be pre-absorbed with fixed embryos: incubate fixed embryos overnight with the antibody solution. Use this antibody solution and use it for staining your sample.
8. To avoid bacterial contamination and to extend stability of the antibody solution 0.05 % of sodium azide can be added.
9. Choose an antibody that targets the animal in which the primary antibody was produced. Conjugated Alexa fluor antibodies that were raised to target different animals and that have sufficiently different emission spectra can be combined to immunostain different antigens at a time. Additionally, if the primary antibodies are from different antibody subclasses (IgM or IgG subclasses) secondary antibodies specific to the antibody subclass can be used to discriminate the patterns. Sensitivity and/or cross-reactivity can vary. We have had good experiences with Alexa 568 goat anti-mouse (emits red light), combined with for example Alexa 488 goat anti-rabbit/rat (emits green light) and Alexa 633 goat anti-rat/rabbit (emits far-red light).
10. If the available confocal microscope does not have a UV laser illumination system that is necessary to detect DAPI-stained DNA, you may use propidium iodide to stain the nuclei instead. Propidium iodide staining: Incubate the ovaries for 15 min in PBS containing 2 µg/ml propidium iodide. Staining with DAPI allows you to use three other secondary antibodies emitting green, red, and far-red light in parallel with DNA staining, whereas propidium iodide emits red light itself.
11. Add NPG to the glycerol and vortex. If the NPG will not dissolve, heat the solution at 37 °C overnight.
12. Oogenesis is highly dependent on the individual's environment. Therefore, the flies should be "fattened" on wet yeast prior to dissection for at least 2 days and should also be kept in a community with males. However, when analyzing ovarian phenotypes it is recommended to collect and stain wild-type and mutant females at different timepoints and in several independent experiments.

13. Depending on the antibody used, the immunostaining protocol can vary. If the used antibody is also staining the peritoneal muscle sheath, it is necessary to destroy the sheath around the ovarioles by sucking them up and down several times in a Pasteur pipette.
14. The larval fat body that contains the ovaries will not sink to the ground, but floats in the solution. It is therefore recommended to check under the stereomicroscope that the fat bodies are not washed away when adding or removing liquids from the sample.
15. The ovaries should be fixed as fast as possible after dissection to preserve the cellular structures. It is important not to exceed or shorten the fixation time to avoid poor immunostaining.
16. Upon all incubation and washing steps make sure to add an amount of liquid that is sufficient to allow the ovaries to float in the tube or the plate upon gentle rocking. Furthermore, when removing solutions from the tube do not pull up the ovaries into the pipette and do not damage the ovaries. The ovaries should stay intact until the very end of the procedure since the individual germaria are otherwise very easily lost.

References

1. Walker MR, Patel KK, Stappenbeck TS (2009) The stem cell niche. *J Pathol* 217(2):169–180. doi:[10.1002/path.2474](https://doi.org/10.1002/path.2474)
2. Scadden DT (2006) The stem-cell niche as an entity of action. *Nature* 441(7097):1075–1079. doi:[10.1038/nature04957](https://doi.org/10.1038/nature04957)
3. Song X, Zhu CH, Doan C, Xie T (2002) Germline stem cells anchored by adherens junctions in the *Drosophila* ovary niches. *Science* 296(5574):1855–1857. doi:[10.1126/science.1069871](https://doi.org/10.1126/science.1069871)
4. Decotto E, Spradling AC (2005) The *Drosophila* ovarian and testis stem cell niches: similar somatic stem cells and signals. *Dev Cell* 9(4):501–510. doi:[10.1016/j.devcel.2005.08.012](https://doi.org/10.1016/j.devcel.2005.08.012)
5. Xie T, Spradling AC (1998) Decapentaplegic is essential for the maintenance and division of germline stem cells in the *Drosophila* ovary. *Cell* 94(2):251–260
6. Yu JY, Reynolds SH, Hatfield SD, Shcherbata HR, Fischer KA, Ward EJ, Long D, Ding Y, Ruohola-Baker H (2009) Dicer-1-dependent Dacapo suppression acts downstream of Insulin receptor in regulating cell division of *Drosophila* germline stem cells. 2009 136(9):1497–507. doi:[10.1242/dev.025999](https://doi.org/10.1242/dev.025999)
7. McKearin D, Ohlstein B (1995) A role for the *Drosophila* bag-of-marbles protein in the differentiation of cystoblasts from germline stem cells. *Development* 121(9):2937–2947
8. Song X, Wong MD, Kawase E, Xi R, Ding BC, McCarthy JJ, Xie T (2004) Bmp signals from niche cells directly repress transcription of a differentiation-promoting gene, bag of marbles, in germline stem cells in the *Drosophila* ovary. *Development* 131(6):1353–1364. doi:[10.1242/dev.01026](https://doi.org/10.1242/dev.01026)
9. König A, Yatsenko AS, Weiss M, Shcherbata HR (2011) Ecdysteroids affect *Drosophila* ovarian stem cell niche formation and early germline differentiation. *EMBO J* 30(8):1549–1562. doi:[10.1038/emboj.2011.73](https://doi.org/10.1038/emboj.2011.73)
10. Shcherbata HR, Ward EJ, Fischer KA, Yu JY, Reynolds SH, Chen CH, Xu P, Hay BA, Ruohola-Baker H (2007) Stage-specific differences in the requirements for germline stem cell maintenance in the *Drosophila* ovary. *Cell Stem Cell* 1(6):698–709. doi:[10.1016/j.stem.2007.11.007](https://doi.org/10.1016/j.stem.2007.11.007)
11. Hatfield SD, Shcherbata HR, Fischer KA, Nakahara K, Carthew RW, Ruohola-Baker H (2005) Stem cell division is regulated by the

- microRNA pathway. *Nature* 435(7044): 974–978. doi:[10.1038/nature03816](https://doi.org/10.1038/nature03816)
12. Ward EJ, Shcherbata HR, Reynolds SH, Fischer KA, Hatfield SD, Ruohola-Baker H (2006) Stem cells signal to the niche through the Notch pathway in the *Drosophila* ovary. *Curr Biol* 16(23):2352–2358. doi:[10.1016/j.cub.2006.10.022](https://doi.org/10.1016/j.cub.2006.10.022)
 13. Wang L, Li Z, Cai Y (2008) The JAK/STAT pathway positively regulates DPP signaling in the *Drosophila* germline stem cell niche. *J Cell Biol* 180(4):721–728. doi:[10.1083/jcb.200711022](https://doi.org/10.1083/jcb.200711022)
 14. Losick VP, Morris LX, Fox DT, Spradling A (2011) *Drosophila* stem cell niches: a decade of discovery suggests a unified view of stem cell regulation. *Dev Cell* 21(1):159–171. doi:[10.1016/j.devcel.2011.06.018](https://doi.org/10.1016/j.devcel.2011.06.018)
 15. Kirilly D, Wang S, Xie T (2011) Self-maintained escort cells form a germline stem cell differentiation niche. *Development* 138(23):5087–5097. doi:[10.1242/dev.067850](https://doi.org/10.1242/dev.067850)
 16. Margolis J, Spradling A (1995) Identification and behavior of epithelial stem cells in the *Drosophila* ovary. *Development* 121(11): 3797–3807
 17. Gilboa L, Lehmann R (2006) Soma-germline interactions coordinate homeostasis and growth in the *Drosophila* gonad. *Nature* 443(7107): 97–100. doi:[10.1038/nature05068](https://doi.org/10.1038/nature05068)

2.4 A Genome-Wide Survey of Sexually Dimorphic Expression of *Drosophila* miRNAs Identifies the Steroid Hormone-Induced miRNA let-7 as a Regulator of Sexual Identity

Delphine Fagegaltier, **Annekatriin König**, Assaf Gordon, Eric C. Lai, Thomas R. Gingeras, Gregory J Hannon, Halyna R. Shcherbata

Experiments presented in Figure 1–3 were performed by Delphine Fagegaltier; experiments shown in Figures 4, 5 and 6 were done by Annkatrin König.
Status of the manuscript: published (Genetics. 2014 Oct;198(2):647-68)

A Genome-Wide Survey of Sexually Dimorphic Expression of *Drosophila* miRNAs Identifies the Steroid Hormone-Induced miRNA let-7 as a Regulator of Sexual Identity

Delphine Fagegaltier,^{*,†,1} Annekatrin König,[‡] Assaf Gordon,^{*} Eric C. Lai,[§] Thomas R. Gingeras,[†]

Gregory J. Hannon,^{*,†} and Halyna R. Shcherbata^{*,1}

^{*}Howard Hughes Medical Institute, Watson School of Biological Sciences, Cold Spring Harbor Laboratory, Cold Spring Harbor, New York 11724, [‡]Max Planck Research Group of Gene Expression and Signaling, Max Planck Institute for Biophysical Chemistry, Göttingen 37077, Germany, [§]Department of Developmental Biology, Sloan-Kettering Institute, New York, New York 10065, and

[†]Watson School of Biological Sciences, Cold Spring Harbor Laboratory, Cold Spring Harbor, New York 11724

ABSTRACT MiRNAs bear an increasing number of functions throughout development and in the aging adult. Here we address their role in establishing sexually dimorphic traits and sexual identity in male and female *Drosophila*. Our survey of miRNA populations in each sex identifies sets of miRNAs differentially expressed in male and female tissues across various stages of development. The pervasive sex-biased expression of miRNAs generally increases with the complexity and sexual dimorphism of tissues, gonads revealing the most striking biases. We find that the male-specific regulation of the X chromosome is relevant to miRNA expression on two levels. First, in the male gonad, testis-biased miRNAs tend to reside on the X chromosome. Second, in the soma, X-linked miRNAs do not systematically rely on dosage compensation. We set out to address the importance of a sex-biased expression of miRNAs in establishing sexually dimorphic traits. Our study of the conserved let-7-C miRNA cluster controlled by the sex-biased hormone ecdysone places let-7 as a primary modulator of the sex-determination hierarchy. Flies with modified let-7 levels present doublesex-related phenotypes and express sex-determination genes normally restricted to the opposite sex. In testes and ovaries, alterations of the ecdysone-induced let-7 result in aberrant gonadal somatic cell behavior and non-cell-autonomous defects in early germline differentiation. Gonadal defects as well as aberrant expression of sex-determination genes persist in aging adults under hormonal control. Together, our findings place ecdysone and let-7 as modulators of a somatic systemic signal that helps establish and sustain sexual identity in males and females and differentiation in gonads. This work establishes the foundation for a role of miRNAs in sexual dimorphism and demonstrates that similar to vertebrate hormonal control of cellular sexual identity exists in *Drosophila*.

SEXUAL dimorphism is pervasive throughout the animal kingdom. From insects, fishes, reptiles, and birds to mammals, hormones and genes shape the morphological, be-

havioral, and reproductive potential of each sex throughout development and adult life. *Drosophila* is no exception, with males and females differing in many ways: anatomical differences include the number of abdominal segments and their pigmentation, the proboscis, labial parts, dimorphic reproductive organs, the formation of sex combs exclusively in males, and 25% larger size in females. Differences that affect male and female behavior exist also in the nervous system and the brain. Y chromosome aside, male and female cells possess a strictly identical genomic content. Most of the differences between the sexes arise and persist via the regulation of sets of genes in a sex-specific manner.

The question of how hundreds if not thousands of genes are differentially expressed in males and females to produce

Copyright © 2014 by the Genetics Society of America

doi: 10.1534/genetics.114.169268

Manuscript received May 20, 2014; accepted for publication July 14, 2014; published Early Online July 31, 2014.

Supporting information is available online at <http://www.genetics.org/lookup/suppl/doi:10.1534/genetics.114.169268/-/DC1>.

Available freely online through the author-supported open access option.

miRNA libraries from male and female tissues have been submitted to the GEO database at NCBI as series GSE57029.

¹Corresponding authors: Cold Spring Harbor Laboratory, McClintock Bldg., 1 Bungtown Road, Cold Spring Harbor, NY 11724. E-mail: fagegalt@cshl.edu; Max Planck Institute for Biophysical Chemistry, Am Fassberg 11, Göttingen 37077, Germany. E-mail: halyna.shcherbata@mpibpc.mpg.de

sexually dimorphic individuals is extensively studied. Refined genomic and genetic studies have converged toward a model of differential expression that requires that both spatial and temporal programs be established throughout development (Arbeitman *et al.* 2002; Parisi *et al.* 2004; Lebo *et al.* 2009; Chatterjee *et al.* 2011). Probably the most important of these programs in flies is the sex-determination hierarchy (Baker *et al.* 1989; Christiansen *et al.* 2002; Camara *et al.* 2008; Clough and Oliver 2012). The primary determinant of *Drosophila* sex is the X chromosome to autosome (X:A) ratio (Bridges 1921), which determines the production of alternative splice variants of Sex lethal (*Sxl*) to generate an active SXL protein in females and a nonfunctional truncation in males (Cline 1978). *Sxl* activity is sufficient to direct the entire developmental programs of both somatic and germline sex determination (Christiansen *et al.* 2002; Robinett *et al.* 2010; Salz 2011; Whitworth *et al.* 2012). *Sxl* serves two essential functions: it restricts dosage compensation to males and controls the sex-determination hierarchy in each sex.

Dosage compensation is the process by which males double the transcription of genes on their single X chromosome to match the levels found in diplo-X females. This process requires a ribonucleoprotein complex, the compensasome, composed of two noncoding RNAs (*roX1* and *roX2*) and six proteins (male-specific lethals MSL-1, -2, -3, the helicase/ATPase MLE, histone acetyltransferase MOF, and histone kinase JIL1). In females, SXL represses the production of MSL-2 at both the transcriptional and translational level, therefore preventing dosage compensation. In males, lack of SXL function allows the male-specific expression of MSL-2 and its assembly into compensasomes to initiate dosage compensation (Bashaw and Baker 1997; see Duncan *et al.* 2006 for review).

At the top of the sex-determination hierarchy, SXL controls which sex-specific isoform is being processed from the doublesex (*dsx*) transcripts (reviewed in Christiansen *et al.* 2002). If the X:A ratio is 1, *Sxl* produces a female-specific splicing factor that causes female-specific splicing of the transformer (*tra*) transcript. TRA interacts with the transformer-2 (TRA2) splicing factor to produce a female-specific splice variant of *dsx* (Belote *et al.* 1989; Sosnowski *et al.* 1989; Ryner and Baker 1991). The female-specific DSX^F protein then activates female and inhibits male development. Because males lack SXL and subsequently TRA, a “default” male-specific splicing of *dsx* transcript generates the DSX^M protein, which inhibits female and promotes male traits. Loss-of-function mutations in *Sxl*, *tra*, and *tra2* transform XX individuals into males, but have no effect in XY males. In contrast, the *dsx* gene is important for the sexual differentiation of both sexes—in the absence of *dsx*, both XX and XY flies are anatomically and behaviorally intersex (Baker and Ridge 1980; Belote *et al.* 1985).

Only a few transcriptional targets through which DSX ultimately functions are known (Luo *et al.* 2011). DSX regulates sex-specific pigmentation patterns with abdominal-B (*Abd-B*) and bric-a-brac1 (*bab1*), resulting in males’ darker

abdomen (Williams *et al.* 2008). DSX^M controls the development of male-specific bristles or sex combs on the forelegs with sex-comb reduced (*Scr*) (Tanaka *et al.* 2011). In each sex, DSX orchestrates the differentiation of larval genital discs into mature dimorphic reproductive organs, external genitalia, and analia (Hildreth 1965; Chatterjee *et al.* 2011). DSX^F directly upregulates the expression of yolk proteins (*Yp1*, *Yp2*) (Burtis *et al.* 1991), and DSX^M downregulates their transcription.

The thorough dissection of *dsx* expression reveals that DSX presents two main characteristics (Lee *et al.* 2002; Hempel and Oliver 2007; Rideout *et al.* 2010; Robinett *et al.* 2010). First, the levels of DSX protein vary greatly throughout development within cells and tissues, implying a tight regulation of its steady states. Second, DSX is not present in all cells in a given tissue, so only some cells know their sex while others remain asexual.

MicroRNAs (miRNAs) appear as critical regulators of development and are themselves highly regulated (Ambros and Chen 2007; Bartel 2009; Smibert and Lai 2010; Dai *et al.* 2012). The interaction of microRNAs with the 3′-UTRs of transcribed mRNAs affects both a transcript’s stability and its translation. Each miRNA can target several different mRNAs and each mRNA can be targeted by multiple miRNAs, generating an intricate network of gene expression regulation. As miRNAs could provide a rapid and tissue-specific means to alter gene expression, they represent ideal candidates for the regulation of spatial and temporal expression patterns of sex-determination genes, their cofactors, and downstream targets. Ultimately, the sex-biased expression of miRNAs could control directly the differential expression of many genes contributing to sexually dimorphic traits at a given time and place during development.

Sexually dimorphic miRNA profiles have been reported in mouse and chicken gonads, and in whole adult *Caenorhabditis elegans* (Mishima *et al.* 2008; Kato *et al.* 2009; Baley and Li 2012). In *Drosophila*, probing miRNA populations in whole animals during development has revealed widespread developmental regulation (Aravin *et al.* 2003; Ruby *et al.* 2007). However, the small RNA libraries generated in these studies came from either mixed-sex samples or single-sex but non-homogenous tissues, which may mask important sex- and tissue-specific variability in miRNA expression and function. To date, *Drosophila* lacks a critical examination of miRNA expression in two important contexts: sex-biased expression that may lead to sexually dimorphic function or spatial and temporal heterogeneity in expression that may drive tissue-specific functions. Both are critical to understanding the role of miRNAs across development.

To investigate these issues, we first established the profiles of miRNAs in several male and female adult parts and organs, larval dissected tissues, and embryonic cells. Their comparison reveals, in each tissue, sets of male- and female-biased miRNAs, increasing in number and extent with the complexity and sexual dimorphism of each tissue. We further address two aspects of miRNA functions in the

context of sexual identity: first, we test whether X-linked miRNAs are regulated by dosage compensation in males and, second, we explore the role of the steroid-induced miRNA *let-7* in regulating sexually dimorphic traits and how its male-biased expression in the gonads affects germline differentiation programs.

Materials and Methods

Fly strains and genetics

Oregon-R flies were used for miRNA profiling. *Msl3^P*, *mle¹*, and *pr mle^{12.17}* mutants are described in Fagegaltier and Baker (2004). All chromosomes but the mutant-bearing allele were exchanged to create isogenized lines by back crossing to a *w¹¹¹⁸*; *MKRS/TM6B* stock for >10 generations. Wandering non-*Tb*-mutant male and female larvae were identified by their gonads. Overexpression of miRNAs was performed using a *dsx-GAL4* driver (Robinett *et al.* 2010). *UAS-NLS-GFP* flies are from Bloomington (BL4776); *UAS-let-7*, *UAS-mir-100*, *UAS-mir-125*, and *UAS-let-7-C* constructs are described in Bejarano *et al.* (2012). In *let-7-C* and *ecd* mutant studies, flies were raised on standard cornmeal–yeast–agar–medium at 25° and fattened on wet yeast paste 1 day before dissection unless otherwise stated. The two knockout alleles *let-7-C^{GK1}* and *let-7-C^{KO1}* lack the whole *let-7-C* cluster; *let-7-C^{GK1}* contains the transcriptional activator GAL4 under the control of the *let-7-C* promoter; *let-7-C^{GK1}/let-7-C^{KO1}* are referred to as *Δlet-7-C* (Sokol *et al.* 2008). Flies with a transgene rescuing the *let-7-C* cluster (*P{W8, let-7-C}*; *let-7-C^{GK1}/let-7-C^{KO1}*) are referred to as *let-7-C Rescue*. The *P{W8, let-7-C Δlet-7}* construct restores all *let-7-C* miRNA members except for *let-7*. For miRNA loss of function, *let-7-C^{GK1}/let-7-C^{KO1}*; *P{W8, let-7-C Δlet-7}/+* flies referred to as *Δlet-7* were used. The following additional fly stocks were used: *FRT40A let-7 mir-125/CyO* and *UAS-let-7-C*; *Sco/CyO* (Caygill and Johnston 2008), *UAS-let-7/TM6* (Sokol *et al.* 2008), *Ubi-GFP FRT40A/CyO*; *bab1-Gal4:UAS-Flp/TM2* (a gift from A. González-Reyes), *UAS-CD8GFP:UAS-nuc lacZ* (a gift from F. Hirth), *Oregon-R, w¹¹¹⁸*, and *ecd^{1ts}* (BL4210).

Sample collections for miRNA-Seq and validation

To ensure that miRNA-Seq samples are not contaminated by other tissues, ~120 Oregon-R heads were individually separated with a scalpel from the rest of the body of ~24-hr-old males and females, collected on ice and quickly frozen. Salivary glands were dissected from ~130 wandering late L3 larvae of each sex identified by their gonads. For qPCR validations of miRNA-Seq data sets, at least two additional independent collections were performed as above. We also collected ovaries and testes from 0- to 2- and 2- to 4-day-old Oregon-R individuals, S2 (Invitrogen), and Kc-167 cells (DGRC) washed in 1× PBS. All dissected tissues and cells were quickly snap frozen in liquid nitrogen and RNA preparations enriched for small RNAs using an adapted Trizol protocol.

miRNA-Seq

30–100 μg of total RNAs were subject to 2S rRNA depletion and DNase treated. Size selected 18–29nt sRNAs were cloned according to (Malone *et al.* 2012). Libraries were clustered and sequenced on the Illumina GAIIx platform.

Cuticle preparations

Three- to 4-day-old flies were placed in ethanol and incubated in 10% NaOH for 1 hr at 70°. Adult abdominal cuticles were mounted and flattened in 30% glycerol. Pictures were taken at the same magnification using a Nikon SMZ150 microscope and Nikon DS-Ri1 camera.

Perturbation of ecdysone levels

The *ecd^{1ts}* temperature-sensitive mutation is known to reduce ecdysone levels at the nonpermissive temperature (Garen *et al.* 1977). Oregon-R and *ecd^{1ts}* flies were kept at the permissive temperature (18°) and 2- to 4-day-old adults were shifted to the restrictive temperature (29°) for 5–11 days to block ecdysone synthesis. Control Oregon-R and *ecd^{1ts}* flies were kept at 18° for the same time.

Clonal analysis

Somatic cell clones in CpCs and ECs were induced using mitotic recombination as described previously (König *et al.* 2011). *FRT40A let-7 mir-125/CyO*; *P{W8, let-7-C Δlet-7}* flies were crossed to *Ubi-GFP FRT40A/CyO*; *bab1-Gal4:UAS-Flp/TM2*. Third-instar larvae were heat shocked for 2 hr on 2 consecutive days in a 37° water bath and returned to 25°. Mutant clones were identified by the absence of GFP in 5-day-old adult ovaries.

Immunofluorescence and antibodies

Ovaries and testes were fixed in 5% formaldehyde (Polysciences, Inc.) for 10 min and stained as described in König and Shcherbata (2013). We used the following mouse monoclonal antibodies: anti-adducin (1:50), anti-lamin C (1:50), anti-arm (1:50), anti-FasIII (1:50), rat monoclonal antibody anti-DE-cadherin (Developmental Studies Hybridoma Bank), guinea pig anti-Tj (1:3000, D. Godt), rabbit anti-vasa (1:5000, gift from R. Pflanz), anti-β-Gal (1:3000, Cappel), and anti-GFP-directly conjugated with AF488 (1:3000, Invitrogen), Alexa 488, 568, or 633 goat anti-mouse, anti-rabbit (1:500, Molecular Probes), goat anti-rat Cy5 (1:250, Jackson ImmunoResearch). Images were obtained with a confocal laser-scanning microscope (Zeiss LSM700) and processed with Adobe Photoshop.

Testis analysis and statistics

To determine the frequency of somatic cell differentiation defects in testis, the percentage of testis with somatic cell clusters (<5, ≥5, and >10) and epithelium appearance at the apex or at the lateral side of the anterior region of testicular tube were quantified. Statistics were calculated using two-way tables and chi-square test.

Determination of *let-7* expression

To analyze the expression pattern of *let-7-C*, *let-7-C^{GK1}/CyO* flies were crossed to *UAS-mCD8-GFP:UAS-nuc-lacZ*. To analyze *let-7-C* levels upon stress, 3- to 5-day-old *let-7-C^{GK1}/UAS-mCD8GFP:UAS-nuc-lacZ* flies were heat shocked for 1 hr at 37° and their gonads were dissected and assayed for immunohistological analysis.

Quantitative PCR Assays (RT-qPCR)

For qPCR validation of the miRNA-Seq data sets and X-linked miRNA expression studies, 100 ng/μl RNA samples were spiked after DNase digestion with a synthetic primer at 6.10e9 copies/μl, polyadenylated and reverse transcribed according to the miScript reverse transcriptase kit instructions (Qiagen). Each miRNA was quantified with a specific primer (Supporting Information, Table S1) following the miScript SYBR green PCR kit instructions. All miRNAs were tested in triplicates on two independent biological replicates with the appropriate controls. Ct values were normalized to *U6* snRNA levels in miRNA-Seq validation experiments using the $\Delta\Delta C_T$ method and $2^{-\Delta\Delta C_T}$ values calculations and to *Dspt4* mRNA levels in the dosage compensation mutant studies (see Table S11, Table S12, Table S13, Table S14, Table S15, and Table 16).

For *let-7* quantification, reverse transcription and qPCR were performed following the manufacturers' protocol using TaqMan MicroRNA assay, with 2S rRNA as an endogenous control. *Let-7* levels were determined in gonads and carcasses from Oregon-R males and females. To eliminate effects that could possibly arise because ovaries contain different amounts of eggs and late egg chambers, late-stage egg chambers and eggs were removed from the dissected ovaries, leaving only the anterior part of the ovary containing the germaria. To measure *let-7* levels upon perturbation of ecdysone, ovaries and testes of Oregon-R and *ecd^{1ts}* mutants raised at 18° and shifted to 29° for 5 or 11 days (or kept at 18° for control for the same amount of time) were dissected. RNA was extracted in Trizol according to the manufacturer's instructions before proceeding with RT-qPCR.

Sex-specific mRNA transcript levels were assessed in 5- to 7-day-old Δ *let-7* and *let-7-C* Rescue control whole flies that were raised at 25° and shifted to 33° for 4 days or in Oregon-R and *ecd^{1ts}* mutants raised at 18° and shifted 1–3 days after hatching to 29° (or kept at 18° for control) for 5 or 11 days. cDNA was generated using the cDNA reverse transcription kit (Applied Biosystems) according to the manufacturer's instructions and qPCR performed using the fast SYBR Green Master Mix (Applied Biosystems). A Step One Plus 96 well system (Applied Biosystems) was used for all analyses. All reactions were run in triplicates with appropriate blanks. The reactions were incubated at 95° for 10 min followed by 40 cycles at 95° for 15 sec and 60° for 60 sec (TaqMan MicroRNA). The ΔC_T value was determined by subtracting the C_T value of the endogenous control from the experimental C_T value. $\Delta\Delta C_T$ was calculated by subtracting the ΔC_T of the control sample from the suspect ΔC_T value. The relative

RNA levels were calculated using $2^{-\Delta\Delta C_T}$. Primers are described in Table S1.

Bioinformatics

The libraries produced in this study (NCBI GEO series record GSE57029) were complemented with existing libraries from lymphoid cells (GSM272653, Kc cells; GSM272652, S2 cells) (Chung *et al.* 2008) and from 2- to 4-day-old Oregon-R adult testis (GSM280085) and ovary (GSM280082) (Czech *et al.* 2008). Reads were clipped of the adapter sequences, filtered for sequences mapping to viruses and simple repeats, and aligned to the *Drosophila melanogaster* genome (BDGP R5/dm3) with no mismatches using NexAlign (program available from the OSC: Data & Resource website). Uniquely mapped reads were annotated using a priority pipeline as in (Czech *et al.* 2008) and FlyBase r5.26, miRbase r.15 and in-house miRNA annotations. Reads corresponding to 184 annotated miRNAs were extracted and counts reported to estimate expression levels (Table S9). For each library, miRNA reads are normalized using the trimmed median ratio used to calculate a correction factor applied to all miRNA counts in a given library. Normalized counts (Table S10) were then input to calculate the relative expression and fold change in expression in pairwise comparisons between male and female samples. The contribution of each miRNA to a library was calculated as the normalized read counts over the total number of miRNA reads in the library (Table S22). The relative abundance of a miRNA across tissues was calculated by dividing the normalized count by the total of normalized counts across all libraries. Heatmaps were generated in R using the *hclust()* function to perform hierarchical cluster analysis.

Results and Discussion

MiRNA profiling in male and female tissues

We adopted a genomic approach and surveyed the populations of miRNAs in several *Drosophila* male and female tissues selected at various stages of development. Sexed miRNA-Seq data sets include late-embryo-derived lymphoid cells, larval salivary glands, and ~1-day-old adult head and body, as well as germline-enriched tissues (ovary and testis) from mature adults (2- to 4-day-old).

Libraries prepared in different ways have been shown to result in variable sequencing efficiencies for individual miRNAs, so that differences in miRNA read counts between libraries may be caused by differential cloning efficiencies rather than reflect differences in their expression. To assess potential biases between sexes as accurately as possible, we prepared libraries and integrated carefully selected existing data sets (see *Materials and Methods*). All provide sufficient depth and breadth and were prepared with the Rnl2 truncated ligase, identical 5' and 3' cloning adaptors, and PCR conditions.

Several methods are available to analyze high-throughput miRNA profiling; however, none has reached a consensus.

The choice of a processing and normalization method can affect greatly the estimates of differentially expressed miRNAs between tissues, especially when comparing tissues that differ substantially in their miRNA content (Dillies *et al.* 2013). We find the trimmed median method most suitable to normalize our data sets, which cover a wide range of tissues (see *Materials and Methods*). Normalized counts were then input to get empirical estimates of the relative abundance of a given miRNA in a library, in pairwise comparisons between male and female tissues, and across all samples. To assess the accuracy of our analyses, we assayed the expression of miRNAs across these samples using an independent method (qPCR; Figure S1). Of the 22 miRNAs tested for validation, 16 miRNAs show similar trends by qPCR and deep sequencing consistently across all samples. For five additional miRNAs, the enrichment trend and/or sex biases could not be confirmed in one or more tissues, while consistent in others. One miRNA showed systematically different profiles by qPCR and deep sequencing due to the presence of miRNAs with very close sequences that qPCR could not distinguish. Although cloning artifacts that may alter miRNA expression profiles in some libraries cannot be excluded, the highly overlapping trends of our qPCR validation set with those of normalized miRNA-Seq data suggest that our analysis reflects miRNA populations in each tissue and supports our main conclusions.

Samples included in our data set were selected to allow a detailed examination of the biases in miRNA content between male and female in tissues of increasing complexity with regard to the nature and number of different cells they contain and in tissues ranging from poorly to highly sexually dimorphic. We assess sex biases of miRNAs at the level of single cells in culture (lymphoid cells), in a very simple tissue with functions in both sexes (salivary glands), and in several fly parts of variable complexity and sexual dimorphism (head, body, ovary, and testis).

Each tissue is enriched for specific miRNAs, highlighted in clusters in Figure 1A, many of which are enriched in both sexes. Ubiquitous and evolutionary conserved miRNAs (*mir-14*, *bantam*, *mir-8*, *mir-1*) are highly expressed in most tissues (Table 1). However, even for such prevalent miRNAs, their relative abundance varies greatly depending on the tissue and stage studied (Table 1 and Figure 1A), denoting a high degree of variation in miRNA populations between tissues and the compartmentalization of their functions in a dynamic fashion.

In addition to a temporal and spatial regulation of miRNAs during development (Ruby *et al.* 2007), a novel layer of complexity arises as we compare miRNA populations between males and females. Regardless of its heterogeneity, each tissue examined reveals miRNAs differentially or even exclusively expressed in one sex (Figure 1, B–H). The example of *mir-8* illustrates how a miRNA classically regarded as abundant presents unexpected differences at the cellular level: *mir-8* ranks within the top two most abundant miRNAs in heads and salivary glands (10–15% of reads), but fourth in lymphoid Kc cells (4%), and only

17th in S2 cells (<1%; Table 1). Following from this example, we systematically analyzed the miRNAs families present in each tissue and estimate their sex-biased expression.

MiRNAs in lymphoid embryonic-derived cells

We examined miRNAs populations in two embryonic hemocyte-derived cell lines commonly considered as male (S2) and female (Kc-167) based on the status of dosage compensation (Alekseyenko *et al.* 2012). In S2 cells, the X chromosome is upregulated by compensasomes recruited along the X chromosome at sites identical to those seen in embryos, male salivary glands, and whole larvae (Alekseyenko *et al.* 2006; Legube *et al.* 2006; Straub *et al.* 2008). In Kc cells, dosage compensation does not occur.

In our assays, most miRNAs are common to both Kc and S2 cell lines (Figure 1B). Overall, *mir-14*, *mir-184*, and *bantam* are most abundant and account for about half of all miRNA reads (Table 1) in both cell lines. Our miRNA profiles agree with the medium levels of *mir-2* (*mir-2a/-2b* mainly) and high levels of *mir-34* described in S2 cells (Sempere *et al.* 2003). High expression of *mir-14* in these immortalized cell lines is consistent with its role as a cell-death suppressor (Xu *et al.* 2003). In addition, we do not detect miRNAs from the *let-7-C* cluster (*let-7*, *mir-100*, *mir-125*) in either cell type. This is consistent with previous reports in which the *let-7-C* miRNAs are detected only upon addition of the steroid hormone ecdysone, which has the opposite repressive effect on *mir-34* (Sempere *et al.* 2003; Chawla and Sokol 2012).

For sexually dimorphic expression, we identify sex biases for several miRNAs: *mir-12*, *mir-304*, *mir-92a*, and *mir-278* are more abundant in female Kc cells, whereas *mir-252*, *mir-307*, *mir-282*, and *mir-980* are more prominent in male S2 cells (full lists in Table S2). Simple male and female embryonic cell lines express comparable miRNAs, yet differ in the level at which they express them.

MiRNAs in larval salivary glands

We examined miRNAs in larval salivary glands, organs that secrete the “glue” allowing the larva to attach to a substrate before pupariation. Salivary glands consist of two simple cell types (Kerman *et al.* 2006): secretory cells and duct cells that connect them to the larval mouth. Each type originates from ~100 cells in the embryonic ectoderm. The secretory cells initiate multiple rounds of DNA replication and differentiate without subsequent division (endoreplication) to create the giant polytene chromosomes needed to meet the increased metabolic requirements of these cells to produce secretory proteins.

Among all samples, miRNAs with a strong preference for expression in salivary glands are, in descending expression levels, *mir-263a*, *mir-375*, *mir-304*, *mir-275*, *mir-283*, *mir-308*, *mir-286*, *mir-5*, and *mir-307-as* (Figure 1A). Many of these highly expressed miRNAs (e.g., *mir-8*, *mir-263a*, *mir-275*, *mir-12*, and *mir-304*) match those whose expression peaks during the larval stages (Ruby *et al.* 2007). In contrast, others (*bantam*, *mir-13b*, *mir-11* or *mir-14*, *mir-2b*) are expressed more ubiquitously during development.

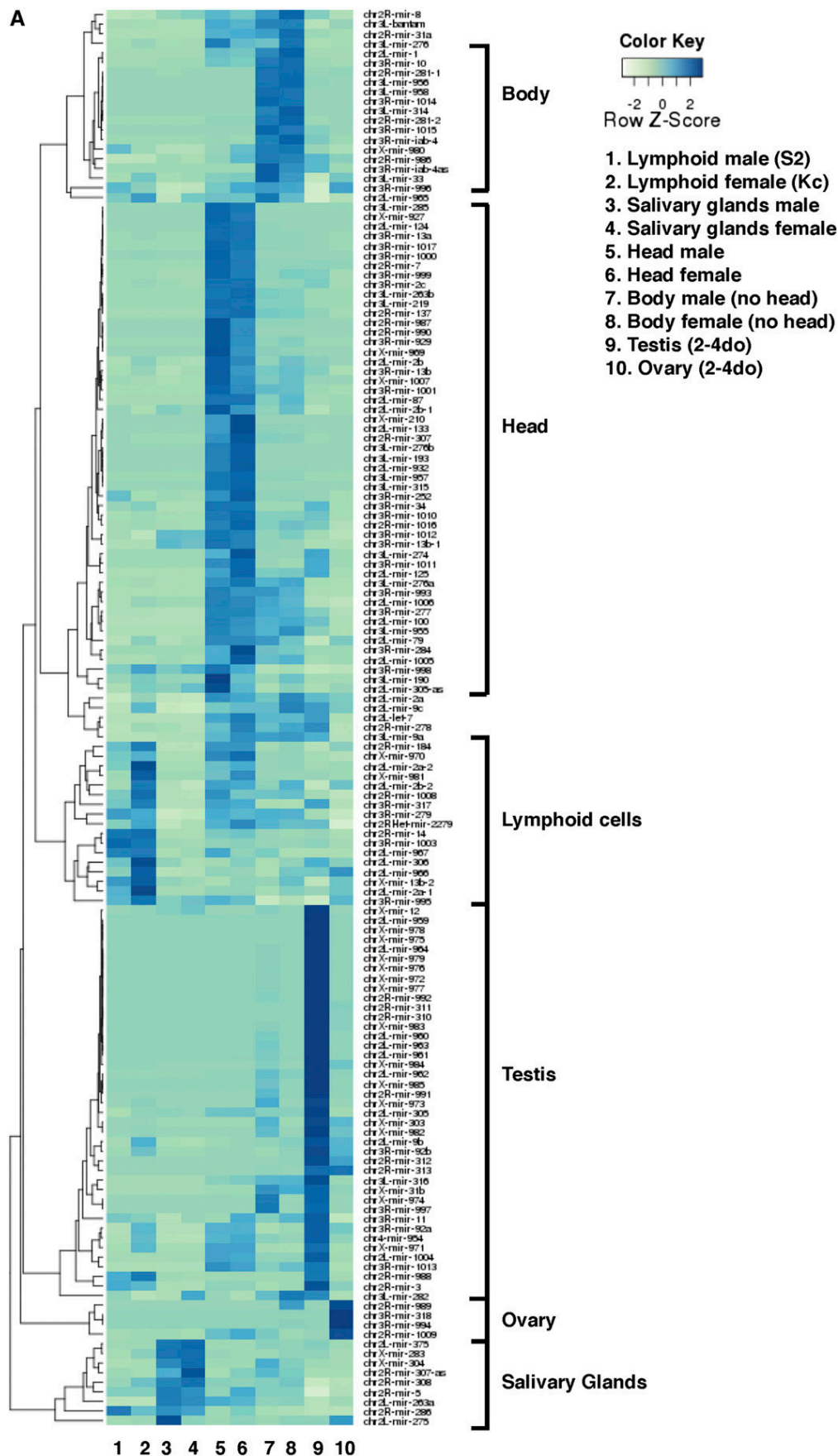


Figure 1 Expression of miRNAs in various male and female tissues. (A) Expression of miRNAs across 10 sexed libraries. Blue color intensity ranging from light to dark indicates an increasing abundance of normalized counts estimates for a given miRNA relative to all miRNAs in that library and to all libraries. Clusters of miRNAs enriched in a given tissue are highlighted. The 147 miRNAs with >30 normalized reads across all libraries were retained. 2–4 do: 2- to 4-day-old flies. The biased expression of miRNAs and their expression levels are shown in pairwise comparisons in each tissue in (B) embryonic hemocyte-derived S2 (male) and Kc-167 (female) cells. (C) Late larvae L3 Salivary Glands. (D) Adult Head. (E) Adult body (head removed). (F) Testis compared to male Body. (G) Ovary compared to female Body. (H) Testis compared to ovary. For each miRNA, the ratio of normalized reads (M/M+F or F/M+M+F) (x-axis) is plotted against its normalized expression level (% , log scale). Each dot represents a miRNA; miRNA's present in one sexed tissue have a ratio of 0 or 1. Pearson correlations between male and female samples: 0.95 in lymphoid cells; 0.98 in salivary glands; 0.96 in heads; 0.99 in body; 0.25 in testis/ovary. M, Male; F, Female.

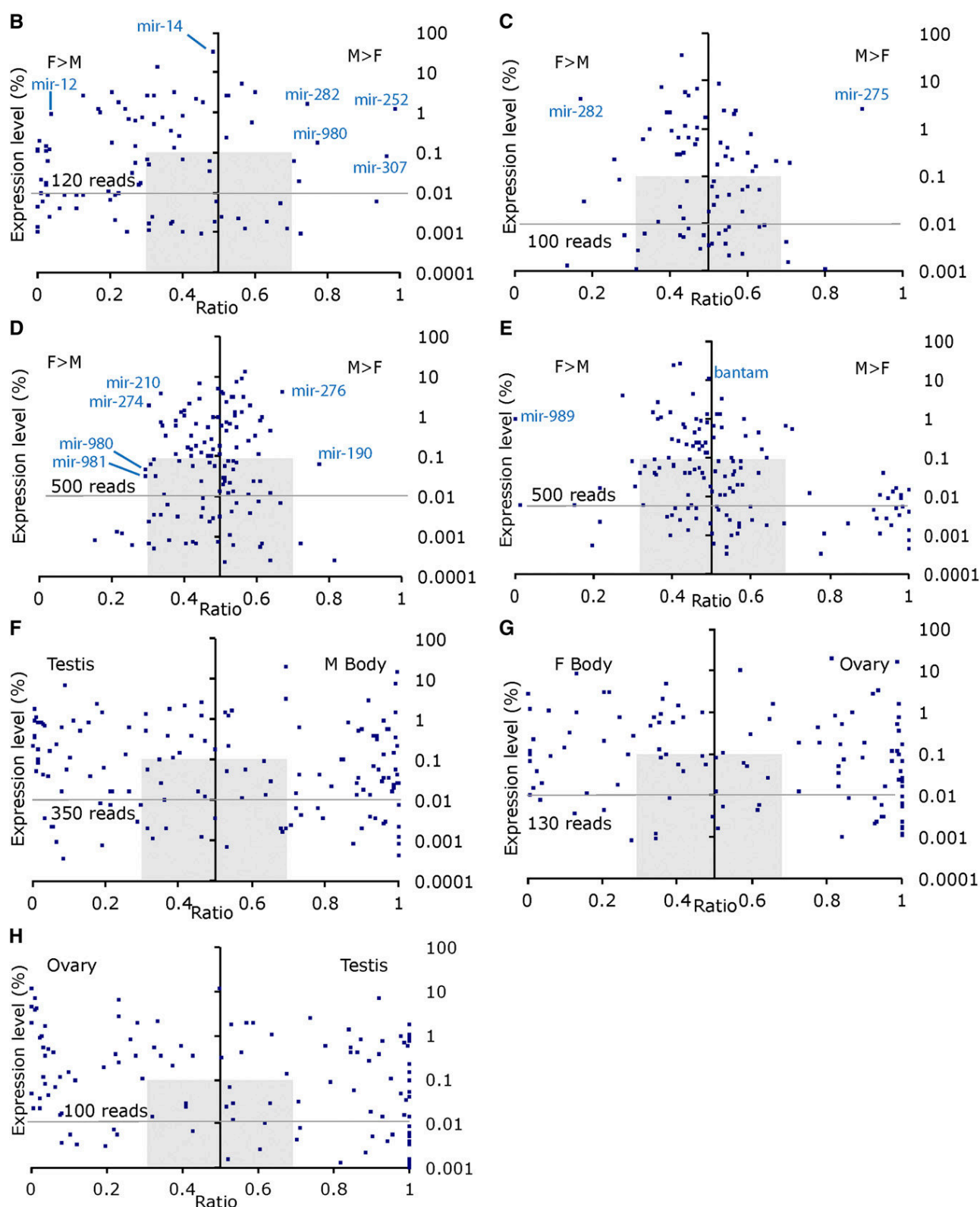


Figure 1 (Continued)

As expected from a tissue of low complexity with functions essential to both sexes, miRNAs are found in most instances at levels comparable in male and female

salivary glands (Figure 1C). This overwhelming similarity is not without exceptions. Salivary glands present a limited number of miRNAs whose expression is biased toward

Table 1 Twenty-five most abundant miRNAs in male and female libraries from embryonic lymphoid cells (S2, male; Kc, female), third-instar larval salivary glands, 1-day-old adult head and body, and 2- to 4-day-old adult gonads

Embryonic lymphoid cells			Larval salivary glands			Adult heads			Adult body			Adult gonads							
S2	%	Kc	%	Male	%	Female	%	Male	%	Female	%	Male	%	Female	%	Testis	%	Ovary	%
mir-14	38.35	mir-14	29.10	mir-8	32.42	mir-8	35.67	mir-8	14.57	mir-8	11.44	mir-1	25.56	mir-1	26.75	mir-12	16.87	mir-989	18.37
mir-184	11.35	mir-184	16.38	mir-263a	10.45	mir-12	8.49	mir-1	10.00	mir-1	8.18	mir-8	23.01	mir-8	25.64	mir-8	15.35	bantam	11.43
bantam	7.44	mir-2a	4.44	mir-375	7.15	mir-263a	7.75	bantam	8.19	mir-276a	7.63	bantam	12.56	bantam	9.79	mir-305	5.04	mir-8	9.30
mir-996	4.85	mir-8	4.15	mir-12	6.25	mir-375	6.72	mir-276a	5.81	bantam	7.14	mir-276a	4.66	mir-276	5.02	mir-959	4.68	mir-2a	7.73
mir-279	3.47	bantam	4.08	mir-304	5.73	mir-282	6.30	mir-276	5.39	mir-210	5.00	mir-277	3.91	mir-276a	4.27	mir-2a	3.85	mir-318	7.25
mir-11	3.29	mir-34	3.40	mir-275	5.19	mir-304	6.01	mir-277	4.66	mir-277	4.90	mir-276	2.47	mir-2a	2.93	let-7	3.13	mir-184	6.40
mir-34	2.93	mir-988	3.37	bantam	4.71	bantam	4.82	mir-184	4.06	mir-184	4.17	mir-2a	2.20	mir-277	2.68	mir-34	3.11	mir-996	5.92
mir-988	2.90	mir-317	3.15	mir-2a	3.04	mir-11	2.46	mir-34	3.58	mir-34	3.61	mir-996	1.54	mir-989	1.76	mir-282	3.00	mir-2b	3.30
mir-282	2.84	mir-2b	3.11	mir-305	2.73	mir-13b	2.45	mir-2b	3.42	mir-14	3.20	let-7	1.49	mir-282	1.68	mir-964	2.74	mir-994	3.01
mir-252	2.79	mir-276	2.30	mir-2b	2.43	mir-305	1.93	mir-2a	3.23	mir-285	2.95	mir-9a	1.48	mir-31a	1.48	mir-277	2.59	mir-275	2.62
mir-13b	2.43	mir-996	2.30	mir-13b	1.99	mir-2a	1.91	mir-285	3.22	mir-2a	2.92	mir-14	1.34	mir-2b	1.21	mir-11	2.51	mir-13b	2.20
mir-2b	2.09	mir-279	2.26	mir-11	1.91	mir-2b	1.55	mir-14	2.46	mir-2b	2.73	mir-31a	1.28	mir-9a	1.18	mir-978	2.29	mir-9b	2.20
mir-317	1.92	mir-13b	2.20	mir-283	1.79	mir-283	1.54	mir-210	2.44	mir-276	2.72	mir-282	1.20	mir-996	1.08	mir-977	2.20	mir-263a	1.46
mir-276a	1.92	mir-11	2.09	mir-282	1.58	mir-996	1.20	mir-124	2.35	mir-274	2.60	mir-12	1.10	let-7	1.08	mir-274	2.15	mir-79	1.40
mir-2a	1.65	mir-9b	1.77	mir-996	1.14	mir-276	1.15	mir-13b	2.20	let-7	2.39	mir-13b	1.08	mir-184	1.06	mir-976	2.04	mir-282	1.38
mir-276	0.95	mir-276a	1.62	mir-308	1.06	mir-308	1.00	let-7	1.62	mir-124	2.28	mir-10	0.98	mir-13b	0.96	mir-9a	1.86	mir-11	1.34
mir-8	0.84	mir-12	1.58	mir-14	0.99	mir-998	0.99	mir-1000	1.47	mir-252	1.76	mir-2b	0.94	mir-10	0.84	mir-983	1.83	mir-34	1.32
mir-995	0.79	mir-305	1.54	mir-998	0.81	mir-276a	0.74	mir-263a	1.37	mir-13b	1.63	mir-281-1	0.91	mir-11	0.75	mir-9b	1.82	mir-305	1.08
mir-277	0.78	mir-2a-2	1.45	mir-276	0.74	mir-79	0.69	mir-987	1.16	mir-9a	1.53	mir-304	0.88	mir-14	0.74	mir-14	1.82	mir-9c	0.94
mir-305	0.70	mir-306	0.91	mir-34	0.63	mir-995	0.64	mir-252	1.14	mir-996	1.28	mir-184	0.79	mir-281-1	0.72	mir-988	1.79	mir-12	0.92
mir-998	0.65	mir-998	0.89	mir-995	0.62	mir-34	0.59	mir-274	1.09	mir-263a	1.21	mir-279	0.75	mir-314	0.60	mir-2b	1.64	mir-33	0.84
mir-306	0.52	mir-9c	0.84	mir-79	0.61	mir-14	0.52	mir-7	1.09	mir-1000	1.20	mir-11	0.74	mir-279	0.56	mir-960	1.47	mir-995	0.76
mir-9b	0.52	mir-995	0.84	mir-9a	0.59	mir-275	0.51	mir-9a	0.95	mir-31a	1.03	mir-305	0.72	mir-263a	0.52	mir-13b	1.41	mir-14	0.63
mir-79	0.43	mir-79	0.81	mir-9b	0.48	mir-33	0.45	mir-929	0.95	mir-11	1.00	mir-79	0.62	mir-305	0.50	mir-317	1.22	mir-1	0.62
mir-2a-2	0.42	mir-282	0.69	mir-33	0.47	mir-9a	0.43	mir-31a	0.91	mir-7	0.97	mir-263a	0.61	mir-34	0.44	mir-316	1.20	mir-312	0.58

miRNAs are ranked in decreasing order and their contribution to the library given as a percentage of all miRNA reads in the library. The full list and percentages are provided in Table S22.

male (*mir-275*) and female cells (*miR-279*, *mir-282*) (Table S3).

For several miRNAs, including *mir-304*, *mir-12*, *mir-283*, *mir-314*, and *mir-981*, the relative abundance in male and female salivary glands is matched in whole larvae, suggesting widespread or general functions (D. Fagegaltier, data not shown). Others vary, suggesting more discrete roles—these include *miR-210*, *mir-13b*, *mir-100*, *mir-1013*, and *miR-979* (note that the latter has low reproducibility in salivary glands in our assay). Supporting this view, we detect by qPCR higher amounts of *mir-979*, *mir-210*, and *mir-314* in whole larvae compared to salivary glands, and *mir-979* and *mir-314* are expressed in mixed L1-L3 larval imaginal discs (Ruby *et al.* 2007).

Surprisingly, although *let-7* is undetectable by Northern blot on unsexed whole L3 larvae (Sempere *et al.* 2002), we find *let-7* in salivary glands of both males (48 normalized reads) and females (219 reads) (Table S3). The function of *let-7* in salivary glands is unknown, but sex-biased expression could reveal interesting differences and asynchrony in tissue homeostasis during male and female transition from larval to pupal stages.

MiRNAs in adult heads

In adult heads from 1-day-old flies, the most prominent miRNAs are *mir-8*, *mir-1*, *mir-276a*, and *bantam* (Table 1). All were shown to act on neural target genes, genes controlling circadian rhythms, eye development, and growth (see Smibert and Lai 2010 for review; Marrone *et al.* 2012; Li *et al.* 2013). Interestingly, whole heads do not differ dramatically in their miRNA profiles between males and females (Figure 1, A–D). *Mir-2a*, *mir-2b*, *mir-277*, *mir-278*, and, importantly, *let-7*, *mir-34*, and *mir-124* are expressed at comparable levels in both sexes, in agreement with their general role in specifying neuronal cell fate, plasticity, and neurodegeneration (Kucherenko *et al.* 2012; Liu *et al.* 2012; Weng and Cohen 2012; Wu *et al.* 2012). Conversely, head expression of *mir-276* and *mir-190* is enriched in males, and *mir-210*, *mir-274*, *mir-980*, and *mir-981* in females (Table S4). This finding hints toward sexually dimorphic functions of these miRNAs in neuronal tissues.

Finally, *miR-252* and *miR-980* were previously detected by qPCR in adult male and female heads 2–4 days after eclosion, while no *miR-984* could be detected (Marrone *et al.* 2012). The present analysis provides evidence that all three miRNAs are expressed in the head and establishes the expression of both *mir-252* and *miR-984* as slightly more prominent in female heads compared to males. The functional significance of such biases is yet to be determined.

MiRNAs in the adult body, testis, and ovary

Almost all known miRNAs (155 miRNAs) are detected in the body, the most complex sample in our data set that covers all body parts of the adult fly with the exception of the head. We find primarily *mir-1*, *mir-8*, *bantam*, *mir-276a*, *mir-277*, *mir-276*, *mir-2a*, *mir-996*, and *let-7* in the fly body (Table 1). The adult fly presents striking biases for miRNAs in males and females (Figure 1E and Table S5). *Mir-989* represents

the strongest female-biased miRNA in the body. Among a larger set of highly male-biased miRNAs, few are detected in females. Of the 22 most strongly male-biased miRNAs in the body (above fivefold), 17 miRNAs appear exclusively in males and the remaining miRNAs (*mir-960*, *mir-961*, *mir-963*, *mir-983*, and *mir-984*) yield at best a few tens of reads in females. Valuable insights into the origin of these discrepancies come from the following comparisons.

We compared the populations of miRNAs in testes and ovaries. We have seen so far that from single lymphoid cells to more complex and dimorphic heads and bodies, the most abundant miRNAs remain overall conserved between males and females with a few exceptions such as *mir-8*. This is strikingly not the case in testes and ovaries in which the most abundant miRNAs differ. In 2- to 4-day-old flies, about half of the miRNAs cloned from ovaries correspond to *mir-989*, *bantam*, *mir-8*, *mir-2a*, and *mir-318* (Table 1). In testes, this set only partially overlaps with that of ovaries and includes *mir-12*, *mir-8*, *mir-305*, *mir-959*, *mir-2a*, *let-7*, and *mir-34*. Younger males exhibit the same set of abundant miRNAs in testes (D. Fagegaltier, data not shown) indicating that their high expression persists in testes at least over the early adult stages.

Each tissue in our data set presents a set of miRNAs underrepresented in the other tissues examined; although their relative abundance varies between male and female, these tissue-enriched miRNAs are usually overrepresented in both sexes (Figure 1).

Ovaries and testes are enriched for certain miRNAs, but very few are enriched in both tissues. Instead, two distinct sets of miRNAs emerge: a large cluster of testis-enriched miRNAs and a smaller set of ovary-enriched miRNAs (Figure 1A). The miRNA populations of these highly sexually dimorphic tissues are highly skewed and sexually dimorphic (Figure 1H). 47 miRNAs show higher levels of expression in testes compared to ovaries (above fivefold), whereas 29 are preferentially expressed in the ovary (Table S6). Fourteen strongly testis-biased miRNAs are not detected in ovaries and may carry important and specialized functions.

During maturation, oocytes express several classes of miRNAs whose levels vary upon fertilization and later during the initiation of zygotic transcription. Maternal deposition of miRNAs has been reported in *Drosophila* to serve a variety of functions, including the destabilization of a large number of maternal mRNAs in early embryos via the SMAUG protein (Giraldez *et al.* 2006; Bushati *et al.* 2008; Soni *et al.* 2013).

In whole ovaries from 2- to 4-day-old females, we identify all but one of the reported maternally deposited miRNAs previously described in oocytes, including miRNA populations denoted as unstable (class I, restricted to stage 14 oocytes), and stable (class II, including maternally deposited and zygotically expressed miRNAs). Specifically, we identified *mir-318*, *mir-276a*, *mir-34*, *mir-317*, *mir-284*, *let-7* (class I); *mir-13b*, *mir-2a*, *mir-306*, *mir-184*, *mir-312*, and *mir-310* (class II). Zygote-specific miRNAs of class III were not detected, namely the *miR-309* cluster zygotically expressed ~2- to 4-hr-post-fertilization (*miR-309*, *miR-3*, *miR-286*, *miR-4*,

miR-5, miR-6-1, miR-6-2, and miR-6-3). We note, however, that the expression of miR-3 and miR-5 for class III could start earlier than previously described: six to eight reads match miR-3 and miR-5. Supporting this view, low counts for miR-3 and miR-5 in 2- to 4-day-old female ovaries increase in *loqs* mutants in Czech *et al.* (2008). A low expression of these two miRNAs in the ovary therefore remains a possibility.

In summary, in addition to expressing highly divergent sets of miRNAs, both testes and ovaries express very different sets of miRNAs compared to other tissues (Figure 1A): their respective miRNA profiles appear as the most divergent of our data set.

To gain insight into the sexually dimorphic functions of miRNAs in somatic tissues, we compared the miRNA populations in testes and male body or ovaries and female body, respectively. We reasoned that a miRNA present in the male body sample (that includes testes) but not enriched in testes is likely to have at least a somatic function outside the testes. Thirty such miRNAs are enriched at least fivefold in the male body (Figure 1F and Table S7), suggesting that they carry distinct functions in the soma.

In a similar comparison between female body and ovaries, we identify 45 miRNAs enriched in female somatic tissues, 28 of which are almost exclusively detected in the female body (Figure 1G and Table S8).

Finally, the tallies of miRNAs enriched in ovaries and testes compared to the body samples establish that most of the differences in miRNA expression between male and female body come primarily from these highly dimorphic internal reproductive tissues.

Male- and female-biased somatic miRNAs

We next looked specifically for miRNAs presenting a consistent bias toward males or toward females in all somatic tissues studied. We considered miRNAs presenting at least a twofold enrichment in one sex in lymphoid cells, salivary glands, head, and/or body. Interestingly, not a single miRNA presented male biases in all four or even three tissues, suggesting that there is no ubiquitous male-biased somatic miRNA. However, a total of 23 miRNAs are male biased in two tissues, generally salivary glands and S2 cells, or head and body (Figure S2A). Of these 23 somatic male miRNAs, 10 are also enriched in testes (compared to the male body) and might therefore repress sex-specific targets in the male soma and gonads. The remaining 13 miRNAs are not enriched in testes and represent somatic male-biased miRNAs.

For females, 32 miRNAs are consistently female biased in the soma (more than twofold; Figure S2B). Interestingly, miR-318 is enriched in females in all four somatic tissues and several other miRNAs in three tissues. Eight of these female-biased miRNAs are also enriched in ovaries. The remaining 24 miRNAs represent somatic female-biased miRNAs.

Ovary and testis miRNAs

We next searched for miRNAs prevalent in ovaries, testes, or both to identify those with possible functions in gameto-

genesis or the organization of the adult gonads. Compared to same-sex somatic tissue, 32 miRNAs are enriched in the ovary and 51 in testis. Of these, 18 are enriched in both testis and ovary, likely underscoring important processes common to gonads of both sexes. Conversely, 8 miRNAs enriched in ovaries but not in testes and 30 miRNAs enriched in testes but not in ovaries could control sex-specific aspects of gonad development (Figure S2C).

The 30 testis-enriched miRNAs reflect a remarkable genomic homogeneity: 11 of these miRNAs are located on the X chromosome (Figure S2C). This fraction is much higher than expected ($P = 0.0018$, hypergeometric distribution) and significantly greater than the proportion of X-linked miRNAs found in other tissues (male soma, $P = 0.0747$; ovaries, $P = 0.2115$). This enrichment of miRNAs originating from the X chromosome is therefore a phenomenon specific to testes. The prevalence of X-linked miRNAs expression in testes has been reported in mouse and was explained by X-linked gene dosage (Ro *et al.* 2007; Mishima *et al.* 2008). It is tempting to speculate that such a mechanism may hold true in *Drosophila* testes as well. To date, the mechanisms regulating X-linked genes expression in testes such as meiotic sex-chromosome inactivation and dosage compensation remain unclear (Vibrantovski *et al.* 2009; Deng *et al.* 2011; Meiklejohn *et al.* 2011; Vibrantovski *et al.* 2012).

Are X-linked miRNAs transcriptionally regulated by dosage compensation?

We next asked whether the transcriptional regulation of X-linked miRNAs depends on dosage compensation in male somatic tissues. At the genomic level, miRNAs are evenly distributed across the *Drosophila* genome with no obvious pattern on the X chromosomes. The X chromosome represents ~20% of the *Drosophila* genome and bears an even share of miRNAs. The 149 genomic miRNA loci queried in this study are distributed evenly across all chromosomes with 34, 33, 22, 29, and 27 miRNAs on chromosomes 2L and 2R, 3L and 3R, and the X chromosome. Together, the fourth chromosome and heterochromatin of chromosome 3 (3h) account for 4 additional miRNAs. To date, no miRNA has been reported on the Y chromosome.

Two classes of miRNAs are present as typical genic miRNAs and mirtrons. A total of 37 mirtrons (24.8%) reside within introns in the genome. Compared to miRNAs regulated by their own promoter, mirtrons are slightly enriched on chromosome 2L (32.4% of chromosome 2L miRNAs) and underrepresented on chromosome 3L (13.6%); on the X chromosome, 22.2% are encoded as mirtrons.

To address whether dosage compensation controls miRNA expression directly on the X chromosome, we first examined whether X-linked miRNAs reside in regions bound by MSL-1 in ChIP-Chip experiments reported by Straub *et al.* (2008) in S2 cells and embryos. We note that X-linked miRNAs reside outside the primary “high affinity sites” defined in these studies and are therefore not primary strong binding sites for

compensosomes. MSL-1 levels were further divided into high, medium, low, or MSL-1 absent subtypes (Figure 2A). With the exception of two miRNA loci residing in regions not addressed in this study, 67% of X-linked miRNA loci reside in regions bound by compensosomes, indicating that some miRNAs could be dosage compensated.

For those X-linked miRNAs residing in regions bound by MSL1, dosage compensation could provide a direct means to equalize their expression in both sexes. To test this possibility, we assayed by quantitative PCR the levels of X-linked miRNAs expressed in salivary glands, a tissue in which dosage compensation has been extensively studied, and compared miRNA levels in wild-type animals and mutants for compensosomes function (*msl-3* and *mle*; Figure 2, B and C). In mutant males, X-linked *mir-304*, *mir-13b*, and *mir-12* levels are reduced approximately twofold, as expected for genes whose expression depends on compensosomes; autosomal controls *mir-100* (2L), *mir-981*, and *mir-1013* (3R) were unaffected. However, levels of two miRNAs *mir-979* and *mir-210* did not change significantly in mutants, implying that some X-linked miRNAs escape dosage compensation—these join the short list of X-linked protein coding genes (*Lsp1-α*, *dpr8*, *CG9650*) that similarly avoid compensation. Interestingly, *mir-12* and *mir-304* belong to the same cluster as *mir-283* but behave differently in mutants. The milder reduction of *mir-283* levels in mutant animals supports previous observations that *mir-12* and *mir-304* expression patterns show little correlation with that of *mir-283*. Although they share a common Pol II promoter, post-transcriptional processing could account for these differences (Ryazansky *et al.* 2011).

In summary, only a few X-linked miRNAs are influenced to some extent by dosage compensation. Two X-chromosome miRNAs clearly escape dosage compensation (*mir-979*, *mir-210*). One major difference between miRNA and protein-coding genes escaping dosage compensation is that the latter tend to reside outside MSL-bound domains. Overall, it is tempting to speculate that dosage compensation presents only limited advantages for short, rapidly regulated miRNA genes.

A role for the *let-7-C* locus in sexual dimorphism

We investigated the functional relevance of sex-biased expression of miRNAs using the example of *let-7*. Two miRNAs in the *let-7-C* cluster, *mir-125* and *let-7*, are highly expressed in the fly head, body, and testis and poorly in the ovary (Figure 4A). *Mir-100* levels are consistently lower in all tissues expressing *let-7* and *mir-125*. From worms to flies and humans, the *let-7-C* locus has an important role throughout development (Pasquinelli *et al.* 2000). In flies, *let-7-C* is under the control of ecdysone and mimics the hormone peaks required for each of the developmental transitions that turn an embryo into an adult (reviewed in Ambros 2011). We set out to investigate the functional implications of the male-biased expression of the *let-7-C* miRNAs in the gonads and more generally its function in adult males and females.

Sex-biased *let-7* miRNA expression in gonadal somatic cells sustains germline differentiation

We analyzed *let-7-C* expression pattern in the adult *Drosophila* gonads using *Gal4* under the control of the intrinsic *let-7-C* promoter. In the germarium, *let-7-C* is expressed in some of the somatic escort (ECs) and cap cells (CpCs; Figure 3, A, B, and D). The number of *let-7-C*-expressing cells and the activity of the *let-7-C* promoter *per se* fluctuate in CpCs and ECs in different germaria and within the same germarium (compare Figure 3, D and D'), demonstrating that the expression pattern of *let-7-C* is highly dynamic.

In testes, somatic cells, namely cyst stem cells (CySC's), and their lineage express *let-7-C* (Figure 3, E–E'). We find consistently higher levels of *let-7-C* per cell and higher numbers of *let-7-C*-positive cells per testicular apex compared to positive cells in the germarium (compare Figure 3, D–D' and E, green).

We confirmed by RT-qPCR the male-biased expression of *let-7* in the gonads. *Let-7* levels are about eight times higher in testes compared to those in ovaries (Figure 3C). In addition, *let-7* is enriched in the gonads of both sexes compared to carcasses. Together, these findings support the biased expression of *let-7-C* and *let-7* reported here by miRNA profiling. Further, they establish a stronger transcriptional activity of the *let-7-C* promoter in the testicular soma compared to the activity in the ovarian soma.

In addition, *let-7* has been detected in the hub cells of old male testes, demonstrating its responsiveness to aging in males (Toledano *et al.* 2012). The dynamic expression of *let-7* and its responsiveness to external and internal conditions (temperature—see below, aging) in both sexes prompted us to ask whether *let-7* regulates gonadal somatic cell behavior.

We analyzed the tissue architecture of the germaria and testes upon *let-7* depletion. In the ovary, *Δlet-7* clones induced specifically in somatic ECs result in a peculiar germarium architecture where both the germline and soma are abnormal (Figure 3G). Mutant germaria contain supernumerary single spectrosome germline cells (arrows) and oddly shaped somatic ECs expressing higher amounts of cell adhesion molecules (Figure 3G). *Let-7* deficiency results in excessive single spectrosome germline cells (GSCs, CBs) and reduced numbers of differentiating cysts (compare Figure 3, F and G), reflective of a delayed early germline differentiation. Altered ECs lacking *let-7* likely fail to protect the differentiating germline cysts from the niche signaling. The phenotypes observed imply that *let-7* controls somatic ECs behavior, which in turn non-cell-autonomously modulates the efficiency of early ovarian germline differentiation.

In the testes too, *let-7* deficiency affects somatic cell behavior. Normally, two squamous cells encapsulate one goniblast, such that only small clusters of somatic cells (fewer than five cells) marked by a nuclear marker can be detected (Figure 3, H and I). Instead, CySC lineage cells lacking *let-7* form large aggregates of >10 cells (Figure 3, I, J, and J'). Interestingly, these clustered cells accumulate the cell adhesion molecule FasIII, indicative of a columnar epithelium that resembles the

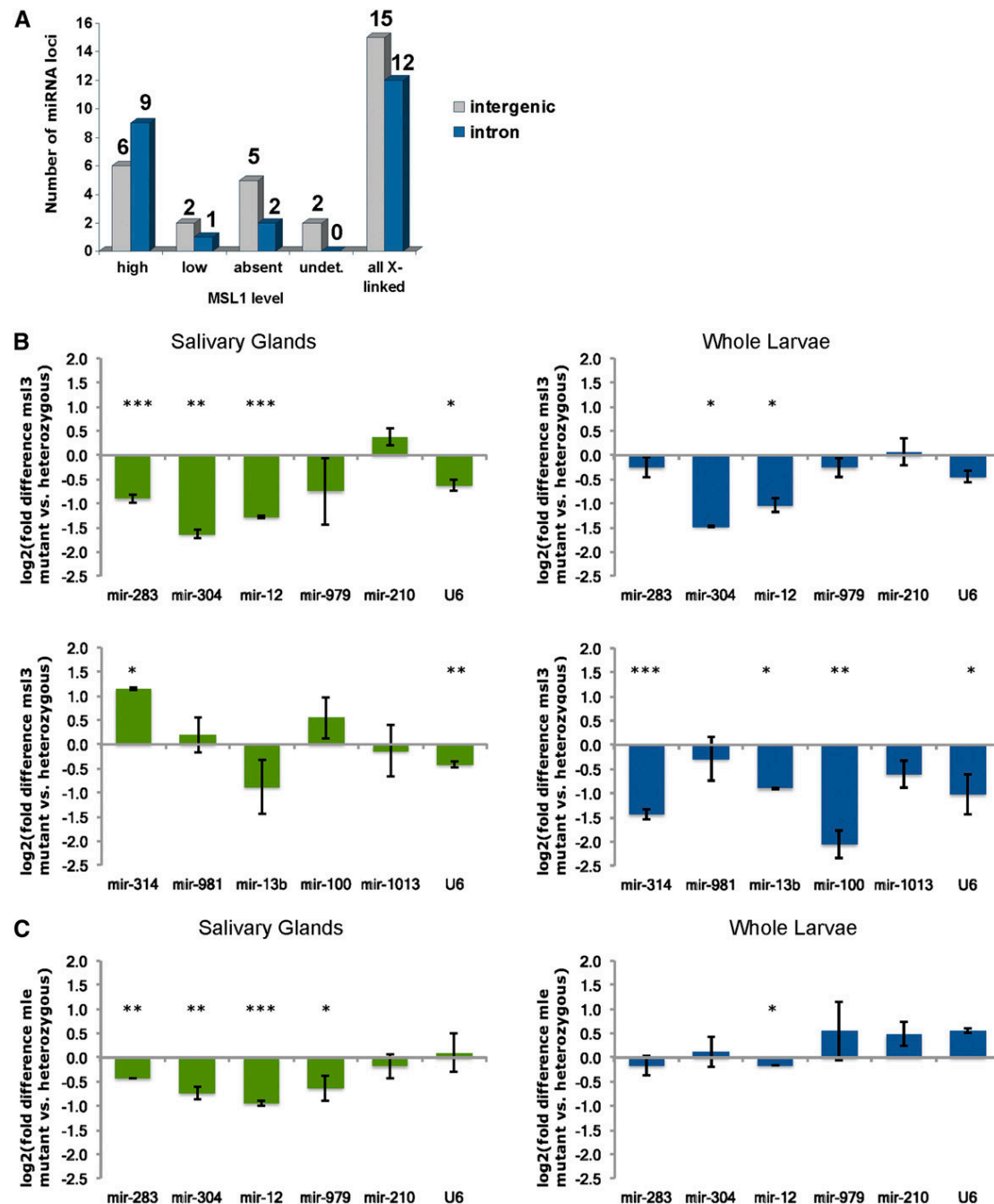


Figure 2 Effects of dosage compensation on X-linked miRNAs expression. (A) Compensasome association at the 27 X-linked miRNA loci vary, with 15 miRNAs located in regions highly populated by compensasomes (high), three miRNAs with low MSL coverage and seven miRNAs residing in regions deprived of compensasomes. Two miRNAs loci in regions not covered by the arrays (undet.) could not be assessed. We observe no difference in MSL occupancy for miRNAs residing in intronic or intergenic regions. The level of expression of miRNAs in the absence of a functional dosage-compensation complex was examined in male salivary glands (green charts) and whole larvae (blue charts) mutant for *msl3* (B) or *mle* (C). Of the six X-linked miRNAs expressed in these tissues, mir-304, mir-12, and mir-13b show the expected twofold decrease in all mutant samples compared to controls. MiRNA levels remain unchanged, however, for X-linked mir-979, mir-210, or mir-283. Autosomal mir-981, mir-100, or mir-1013 levels did not change. Mir-314 levels increase in *msl3* mutant salivary glands and decrease in whole larvae. All miRNAs were tested in triplicates on two independent biological replicates. Values were normalized to the autosomal gene standard, *Dspt4*, whose levels remain unchanged between males, females, or compensasome mutants (Chiang and Kurnit 2003). We observe similar trends between male and female salivary glands miRNAs in wild-type Oregon-R and *msl3* heterozygous mutant controls for all 10 miRNAs tested (mir-100, mir-979, mir-12, mir-314, mir-981, mir-210, mir-1013, mir-283, mir-13b, mir-304). Error bars represent standard deviations. *P*-values: (*) *P* < 0.05; (**) *P* < 0.005; (***) *P* < 0.0005. Calculations are provided in Table S11, Table S12, Table S13, Table S14, Table S15, and Table S16.

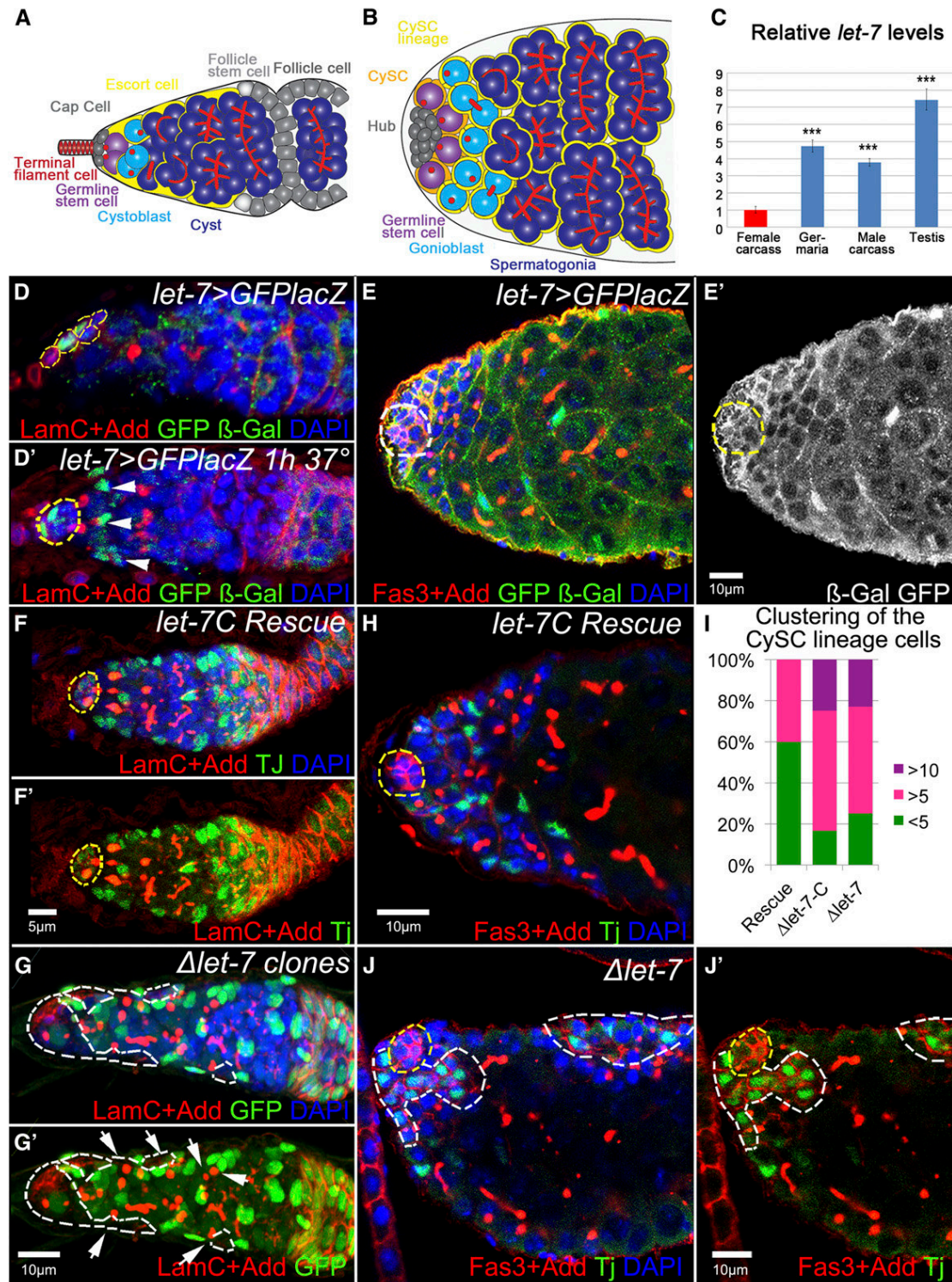


Figure 3 *let-7* deficiency affects somatic cells behavior in ovaries and testes, which cell-non-autonomously influences early germline differentiation. *Drosophila* ovaries and testes present commonalities in their general organization and the type of cells they comprise (Fuller and Spradling 2007). The ovary is a paired organ consisting of 16–20 ovarioles, each representing a string of progressively developing egg chambers. (A) At the apex of an ovariole, the germarium comprises somatic cells (terminal filament, TF; cap cells, CpC's; escort cells, ECs; follicle stem cells, FSCs; follicle cells, FCs) and germline cells (germline stem cells, GSCs; cystoblast, CB; differentiating cyst, Cyst). GSCs are physically attached to the somatic cluster of cap cells that, with the terminal filament cells, represent the GSC niche. GSCs divide into a differentiating cystoblast, which then divides four times with incomplete cytokinesis, producing a 16-cell cyst in which 1 cell becomes the oocyte while the others develop as nurse cells. These different germline cell populations can be easily identified by their location and specific markers in the germarium. For example, *Drosophila* adducin homolog antibody marks an actin-rich cellular organelle represented as a dot-like structure in single

ovarian follicular epithelium. Such aggregates do not develop in *let-7-C* rescue flies (Figure 3, H and I).

Let-7 levels are important to specify male and female sexual identity

Let-7 levels fluctuate at each developmental transition of the fly, including a major pulse in late pupae. During development, *let-7* miRNA first appears in L3 larvae and has been detected in genital discs of L3 male and female larvae (Sokol *et al.* 2008). *Dsx* levels vary as well during development and are especially important from the L3 larval to the late pupal stages to transform genital discs into adult genital and anal structures. To ask whether *let-7* influences the transformation of these structures, we expressed *UAS-let-7-C* in patterns that mimic pulses of the major controller of the sex-determination hierarchy DSX using the *dsx-Gal4* driver. Animals overexpressing *let-7-C* in *dsx*-expressing cells develop severe phenotypes: males and females fail to develop segments A8–A10 and lack a terminalia (analia and genitalia) (Figure 4B). Overexpressing individual miRNAs from the cluster alters the same segments (Figure 4, B and C): females overexpressing *mir-125* form additional vaginal teeth, up to a full second row of teeth, and a vulva overgrowth. Additional vaginal teeth appear toward the posterior part of the vulva in females overexpressing *let-7*. Males overexpressing *let-7* show an overgrowth of the genital ring/arch. In males overexpressing *mir-125*, this structure proliferates yet collapses into a more compact bulged ring (Figure 4, B and C). In addition, overexpressing *let-7* or *mir-125* in *dsx*-expressing cells results in the overall reduction of the male external genital structures. Importantly, the external terminalia of males and females lacking *let-7* present similar defects (Figure 4C).

Finally, in animals overexpressing *mir-125*, the typical female abdominal pigmentation darkens in the posterior stripes of segments A3–A5 and in the terminal A6 and A7 segments where it widens (Figure 4B). Females overexpressing the whole *let-7-C* cluster show a similar increase in pigment, but not those overexpressing *let-7* alone, pointing at *mir-125* as the miRNA responsible for the pigment defects. Controls expressing *UAS-NLS-GFP* or *UAS-mir-100* constructs do not present such phenotypes. Together, these results suggest that the ectopic expression of *let-7-C*, *let-7*, or *mir-125* in *dsx*-expressing cells represses gene(s) necessary for pigmentation in most abdominal segments and importantly, gene(s) critical for the formation of the highly dimorphic segments A8–A10 in both sexes. The transformation of the genital disc into a male or female adult terminalia and the sexually dimorphic pigmentation pathway are both orchestrated by DSX during the pupal stages. It is likely that the respective timing and levels of expression of *let-7-C* miRNAs and *dsx* at this stage are important. None of the miRNAs in the *let-7-C* cluster, however, are predicted to target the *dsx* transcripts, suggesting that the phenotypes reflecting alterations of the levels of DSX or of the genes it acts with are generated upstream or in parallel to DSX action rather than from a direct interaction.

To test whether sex determination is affected by *let-7*, we quantified in animals lacking *let-7* the male- (*dsx^M*) and female-specific transcripts (*Sxl*, *tra*) of the sex-determination hierarchy and DSX downstream target *Yp1* (Figure 5, A and B). In *let-7* mutant females, the levels of *Sxl* and *tra* remain unchanged but *Yp1* mRNA levels are significantly lower. The background levels of *dsx^M* remain stable in females lacking *let-7*, implying that the levels of the direct activator of *Yp1*,

cells (GSCs and CBs) and as a branched fusome in the developing cysts. There is another class of somatic cells at the anterior of the germarium, called the escort cells. These squamous cells are mitotically quiescent and envelop differentiating cysts to protect them from niche signaling, an important role for germline differentiation (Chen *et al.* 2011). ECs guide differentiating cysts to the posterior end of the germarium, where the germline becomes encapsulated by the follicular epithelium and pinched off from the germarium. (B) The *Drosophila* testes are a paired tubular organ that consists of somatic and germline cells. Scheme depicting the testis apex somatic cells (hub cells, Hub; cyst stem cells, CySC's; cyst stem cells lineage, CySC lineage) and germline cells (germline stem cells, GSCs; gonoblast, GB; differentiating spermatocysts and spermatogonia). Attached to the stem cell niche, termed the hub, reside two types of stem cells: GSCs and CySC's. While the hub is made by a cluster of postmitotic somatic cells, both stem cell types divide in synchrony to produce differentiating germline cysts, each of which is encapsulated by two somatic CySC's lineage cells. This encapsulation is critical for proper germline differentiation (Leatherman and Dinardo 2010). Similar to the ovarian GSC progeny, the germline gonoblast undergoes four rounds of incomplete cytokinesis to produce 16 primary spermatocytes in a cyst, eventually generating 64 sperm cells. (C) The relative expression levels of miRNA *let-7* in female and male carcasses, ovaries, and testes show that *let-7* miRNA is sex biased and expressed at the higher levels in testes (see also Table S17). (D, D', E, E') Localization of *let-7-C* miRNAs in the ovaries and testes, detected via membrane *GFP* and nuclear *lacZ* expressed under the control of the *let-7-C* promoter (*let-7-C^{GK1}-Gal4/UAS-CD8-GFP::nuc-lacZ*). In the ovary, *let-7-C* is expressed in the somatic cells of the germarium, CpCs and ECs (D). (D') More ECs express *let-7-C*, shown by the presence of *lacZ* (β -Gal, green) when adult flies were subject to a heat shock for 1 hr prior to dissection. (E and E') In the testis, *let-7-C* is broadly expressed in all somatic cells, CySC's and their lineage and the hub cells (*let-7-C^{GK1}-Gal4/UAS-CD8-GFP::nuc-lacZ*). (F and F') Control *let-7-C* rescue germaria (*P{W8, let-7-C}/+*; *let-7-C^{GK1/KO1}*) show typical numbers of germline SSCs and developing cysts (marked by the spectrosome and fusome marker Adducin, Add, red) as well as somatic ECs (marked by Traffic jam, Tj, green). The GSC niche (marked by Lamin C, LamC, red) is outlined by yellow dashed lines. (G and G') Somatic cell Δ *let-7* clones (*Ubi-GFP, FRT40A/FRT40A, let-7 mir-125; bab1-Gal4, UAS-Flp/P{W8, let-7-C^{\Delta}let-7}*) are marked by the absence of GFP and outlined by white dashed lines. Upon *let-7* depletion in the soma of the germarium, the number of somatic ECs and germline SSCs increases, while the number of fusome-containing cysts decreases. The magnification is the same in F and G. (H) The testicular apex of a control *let-7-C* rescue (*P{W8, let-7-C}; let-7-C^{GK1/KO1}*) displays typical numbers of germline CBs and cysts (marked by spectrosome and fusome marker Add, red) and the CySC lineage cells (marked by Tj, green); yellow dashed lines outline the hub (marked by Fasciclin III, Fas3, red). (I) In Δ *let-7* mutant testis (*let-7-C^{GK1/KO1}; P{W8, let-7-C^{\Delta}let-7}/+*) the CySC lineage cells cluster in larger groups and express the ovarian follicular epithelium marker, Fas3. These clusters (outlined by white dashed lines) can be found at the apex or the side of the testicular tube. (J) Percentages of mutant testes containing large ≥ 5 or > 10 somatic cell clusters in comparison to control *let-7-C* Rescue. Ten to 20 testes were analyzed for each genotype. Red: LamC + Add in D, D', F, F', G, G'; Fas3 + Add in E, H, J, J'. Green: GFP + β -Gal in D and E; GFP in G, G'; Tj in F, F', H, J, J'. White: GFP + β -Gal in E'. Blue: DAPI in D–H, G–J'. D, E + E', H, J + J' are single confocal sections while D', F + F', and G + G' are projections of several z-stacks.

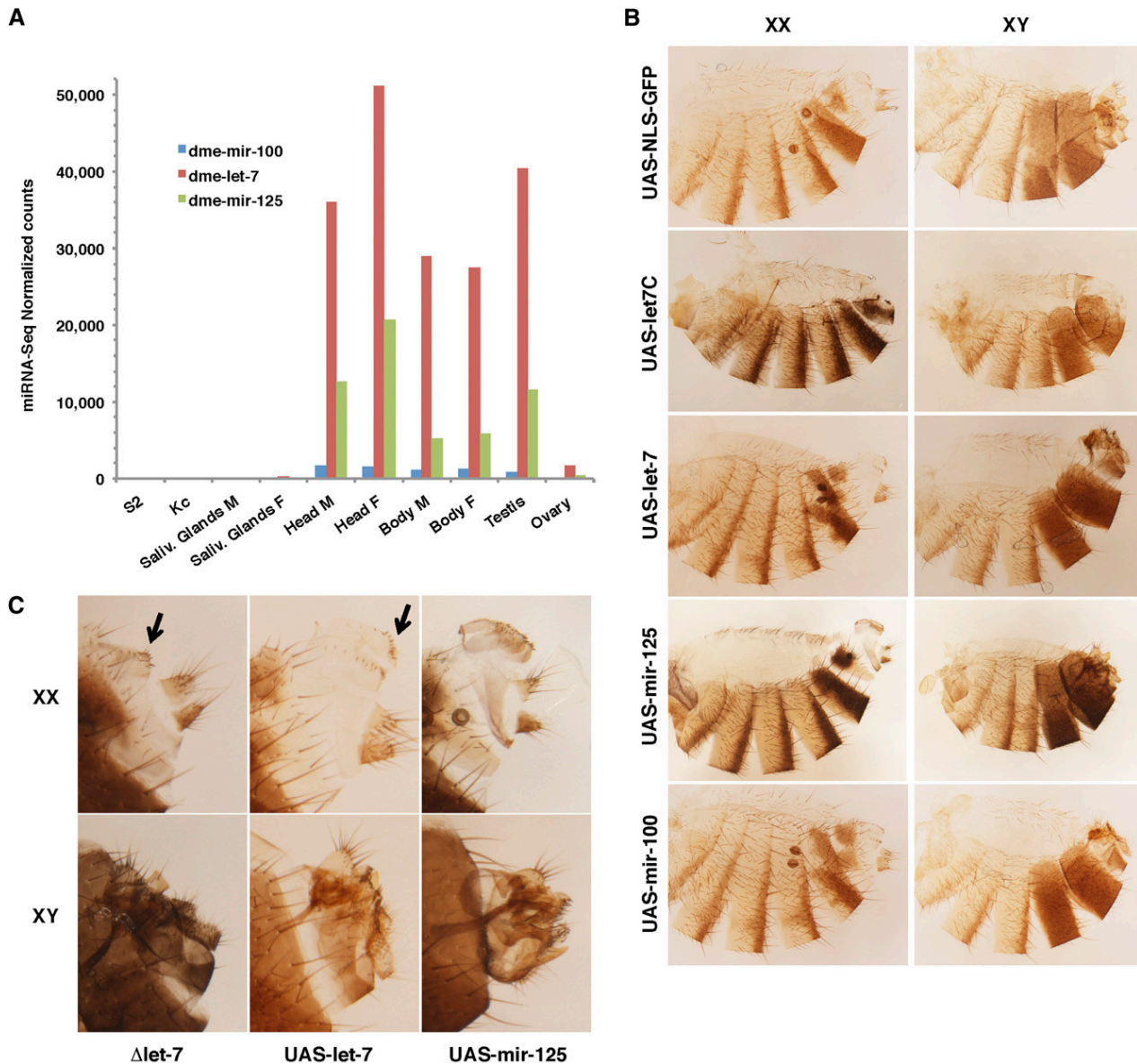


Figure 4 Let-7-C miRNAs abundance across tissues and overexpression. (A) The three miRNAs of the let-7-C locus are almost undetectable in salivary glands and lymphoid cells and highly expressed in male and female heads and body. All let-7-C miRNAs are highly expressed in testes compared to ovaries. Let-7 is consistently more abundant than mir-125 in all tissues expressing let-7-C, while mir-100 remain comparably low. (B) Cuticle preparations of *dsx-Gal4* > *UAS-let-7-C* males (XY) and females (XX): both fail to transform A8–A10 segments into a proper genitalia and analia. Increased abdominal pigmentation in let-7-C and mir-125 overexpressing flies (compare *UAS-let-7-C* or *UAS-mir-125* to *UAS-NLS-GFP*). (B and C) Terminalia phenotypes of flies overexpressing single miRNAs of the locus: additional vaginal teeth toward the posterior section of the vulva in *dsx-Gal4* > *UAS-let-7* females, similar to Δ let7 flies (arrows in closeups in C); additional row of vaginal teeth and overgrowth of the anterior vulva in *dsx-Gal4* > *UAS-mir-125* females; overgrowth of the genital ring/arch *dsx-Gal4* > *UAS-let-7* male genitalia; *dsx-Gal4* > *UAS-mir-125* male genital ring collapses into a more compact bulged ring (lateral view in C). Note the reduced size of male external genital and anal structures in *UAS-let-7*, *UAS-mir-125*, and Δ let7 males. *Dsx-Gal4* > *UAS-NLS-GFP*, and *dsx-Gal4* > *UAS-mir-100* males and females appear normal.

DSX^F, but not its repressor DSX^M, are compromised. A general depletion of *let-7* during development generates more dramatic effects in males. Specifically, males deficient for *let-7* present a spurious expression of two genes normally restricted to females, *Sxl* and *Yp1*. Altogether these results point at a role of *let-7* in modulating the sex-determination cascade during development, at least during the late-larval to late-pupal stages.

Ecdysone signaling via *let-7* maintains sexual identity during adulthood

We attempted to determine what signaling pathway acts upstream of *let-7* in the process of sexual identity establishment but also its maintenance. Hormonal signaling is a strong candidate for this type of regulation, since it may coordinate the sex-specific differentiation of different tissues in the whole organism. The ecdysteroid signaling cascade governs various

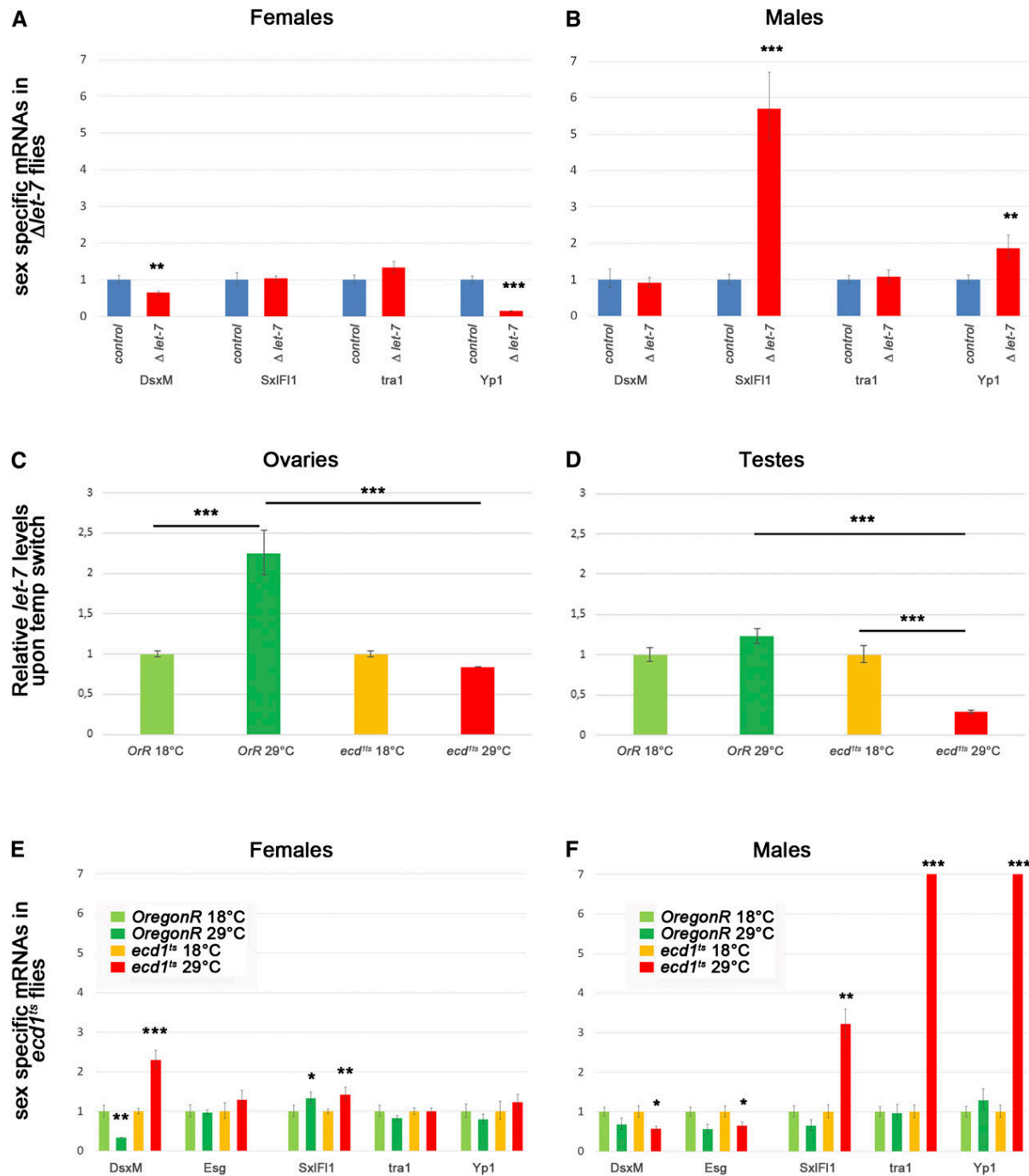


Figure 5 Levels of sex-specific mRNAs are altered due to loss of function of steroid-dependent miRNA let-7 and ecdysone deficiency. (A and B) Relative levels of sex-specific mRNAs in $\Delta let-7$ mutant (*let-7-C^{GK1/KO1}*; *P{W8, let-7-C^{Δlet-7}}/+*) and control rescue (*P{W8, let-7-C}/+*; *let-7-C^{GK1/KO1}*) females (A) and males (B). (C and D) Relative levels of let-7 miRNA expression in wild-type (Oregon-R) and *ecd^{1ts}* mutants kept at permissive (18°) and restrictive (29°) temperatures measured in the anterior parts of ovaries (C) and testes (D). (E and F) Relative levels of sex-specific mRNAs in wild-type (Oregon-R) and *ecd^{1ts}* females (E) and males (F) kept at permissive (18°) and restrictive (29°) temperatures. Samples at restrictive temperature were compared to the respective genotype and sex at permissive temperature. Error bars represent the range of mRNA levels; *P*-values are calculated by Student *t*-test: (*) *P* < 0.05, (**) *P* < 0.005, (***) *P* < 0.0005. See also Table S18, Table S19, and Table S20.

biological responses during *Drosophila* lifetime. Its specificity depends on the differential spatiotemporal expression of downstream components specific to various cell types and developmental stages. Steroid-coupled regulation of *let-7* expression

takes place during the developmental transition from larval-to-reproductive animals (Sempere *et al.* 2002, 2003; Garbuzov and Tatar 2010; Chawla and Sokol 2012; Kucherenko *et al.* 2012). During this period, DSX most actively controls the

transformation of the A8–A10 genital primordia into dimorphic male and female terminal structures. In addition, we and others have reported that a deficit in ecdysone signaling generates non-cell-autonomous defects in early female germline differentiation (König *et al.* 2011; Morris and Spradling 2012). These defects resemble the *let-7* loss-of-function defects described here in ovaries. Moreover, we report similar germline differentiation defects in *let-7* mutant testes. Together, the steroid-dependent onset of *let-7* expression during development and the similarity of the germline phenotypes observed in adult males and females lacking *let-7* converge toward a model in which ecdysone signaling acts upstream of the *let-7* miRNA to modulate (i) sex determination in tissues and (ii) germ-cell differentiation via the gonadal soma.

Whether *let-7* also depends on ecdysone signaling in adults has not been addressed previously. To address this, we took advantage of a temperature-sensitive *ecdysoneless* mutation, *ecd^{1ts}*, that blocks the production of ecdysone at restrictive temperature (29°) (Garen *et al.* 1977). After impairing ecdysone signaling specifically in adults, we analyzed *let-7* levels in germaria and testes of Oregon-R and *ecd^{1ts}* flies. Shifting Oregon-R male and female adults to 29° results in increased *let-7* levels, showing that *let-7* expression is dependent on temperature (Figure 5, C and D). Enhanced activity of the *let-7*-C promoter is also visible at the cellular level in the ovarian CpC's and ECs upon heat shock (Figure 3D'). Contrary to wild-type flies, *let-7* levels drop at the restrictive temperature in *ecd^{1ts}* mutant female and more significantly in male gonads, demonstrating that *let-7* expression depends on ecdysone signaling in the adult germaria and testes (Figure 5, C and D).

While the signaling cascade that establishes sexual identity has been studied extensively, the question of whether certain cues are needed to actively maintain sexual identity throughout the adult life has not been addressed. We quantified the expression of female- and male-specific components of the sex-determination hierarchy 3 days after inducing an ecdysone deficit in mature adults. Females lacking ecdysone begin to express the male-specific isoform of *dsx*, *dsx^M* (Figure 5E). In males lacking ecdysone, conversely, male-specific mRNA levels of *dsx^M* and *escargot* (*esg*) fall significantly while the female *Sxl*, *tra*, and *Yp1* transcripts undergo a dramatic burst in expression (Figure 5F). Because *Sxl* and *tra* become aberrantly produced in males, and both are required to produce the female-specific isoform of *dsx*, it is likely that *Yp1* hyperactivation in males is a consequence of the production of DSX^F when ecdysone signaling is disrupted.

Together, our data support the hypothesis that ecdysone is required to maintain the sexual fate of adult cells. Interestingly, ecdysone effect on sex-specific mRNAs expression is significantly stronger than that of *let-7* alone (compare Figure 5, A, B, E, and F), indicating that this systemic hormonal signaling regulates in addition to *let-7* other key players in the maintenance of sexual identity during adulthood. Critically, these data suggest that ecdysone signaling plays an essential role in the maintenance of sexual identity in the adult *Drosophila*, primarily in males,

and that this function is mediated at least in part by *let-7* miRNA.

Ecdysone signaling via *let-7* maintains male cell fate of the testicular soma during adulthood

Ecdysone-deficient (*ecd^{1ts}*) males have reduced fertility and most become completely sterile after 3 days at restrictive temperature (Garen *et al.* 1977). At the tissue level, ecdysone signaling appears important to maintaining the proper behavior and function of the somatic CySC's lineage in the adult testis (Figure 6, A–C). In adult males subject to ecdysone deficiency, the CySC's lineage overproliferates, expresses epithelial markers, and non-cell-autonomously affects germline differentiation. Massive clusters of somatic cells appear at the testis apex, forming occasionally epithelial-like sheaths surrounding the testicular tube (Figure 6, B and C). The appearance of aggregates coincides with defects in germline differentiation at two levels. First, somatic cells clustering at the apex displace germline stem cells from the hub, forcing their premature differentiation (Figure 6B'). Second, somatic cells accumulating in lateral sheaths further disrupt their progression through germline differentiation programs (Figure 6C'). Flies deprived of ecdysone for a longer period show more severe phenotypes (Figure 6, D and E). Still, these alterations remain partial sex transformations. We never observed a full transformation resulting in the production of sperm or egg in mutants of the opposite sex. These findings suggest that sustained steroid activity is required to maintain *let-7* levels within testicular somatic cells.

Taken together, our analyses show that steroid signaling is involved in the maintenance of sexual identity in adult flies and in the maintenance of germline differentiation programs in the gonads. This hormonal signal engages miRNAs to execute this regulation in a gender-specific manner. Therefore the maintenance of sexual identity in the adult life requires a systemic signaling that strongly depends on the general state of the organism and external conditions. This type of regulation is common in higher vertebrates including humans, implying that the analysis of sex-biased miRNAs and their targets will be of great importance to better understanding of sexual identity safeguarding throughout life at the cellular level in different organisms.

Evidence supporting the existence of a long-range gonadal axis in flies has emerged recently. Ecdysone is metabolized in the fat body in both sexes and is also present exclusively in the female germline late follicles. As a result, ecdysone titers are higher in females (Bownes *et al.* 1983; Parisi *et al.* 2010). Germline ablation largely decreases ecdysone titers and affects sex-biased somatic genes, including ecdysone biosynthesis genes exclusively in females (Parisi *et al.* 2004, 2010). In fact, half of the sex-biased genes in the female soma are estimated to be germline-dependent genes that respond to ecdysone, the other half comprising germline-independent sex-biased genes regulated by the sex-determination hierarchy. The absence of germline, however, does not affect somatic expression of the canonical

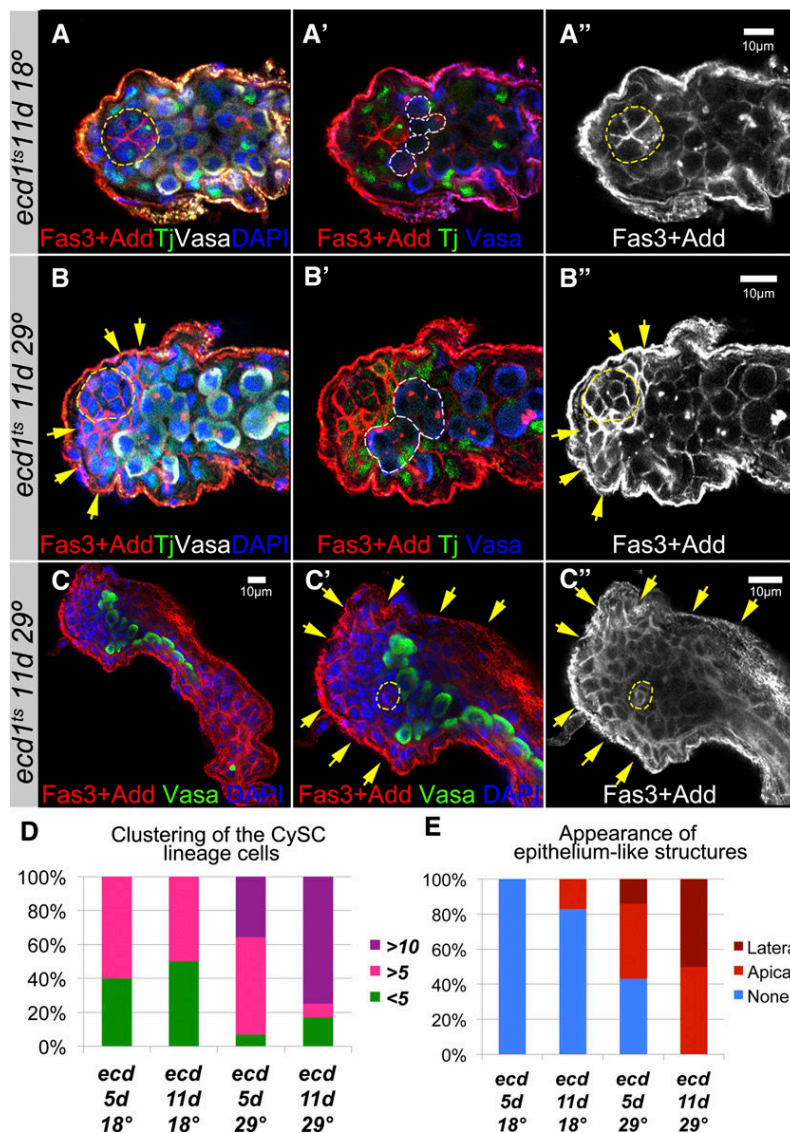


Figure 6 Ecdysone signaling controls testicular soma behavior and function. (A) In control (*ecd^{1ts}*, 11 days at 18°), the hub (outlined in yellow, A, A'') is surrounded by proportional numbers of CySC's and GSCs (outlined in white, A'). (B and C) In mutants (*ecd^{1ts}*, 11 days at 29°), somatic cells aggregate in large epithelium-like clusters next to the hub (yellow arrows, B, B''). In contrast, GSCs that would be seen as germline cells with a single spectrosome are no longer attached to the hub, indicating that they were pushed away from the niche and their differentiation was induced. Differentiating cysts are outlined in white, B'. Sometimes these abnormal epithelial-like sheets are found around the whole testicular tube (yellow arrows, C', C''), affecting germline differentiation: differentiating cysts that would be marked by branched fusomes are not seen. Note that the aberrant somatic cells express the Fas3 marker of hub cells and ovarian follicular epithelium. (D and E) The frequency of testes displaying clustering of the CySC lineage cells (D) and the appearance of epithelium sheets (E) increase with the time flies were deprived of ecdysone (5 or 11 days). See also Table S21. Red: Fas3 + Add in A, A', B, B', C, C'. White: Vasa in A, B; Fas3 + Add in A'', B'', C''. Green: Tj in A, A', B, B'; Vasa in C, C'. Blue: DAPI in A, B, C; Vasa in A', B', C'. All pictures are single confocal sections.

sex-determination genes in either sex. Our study shows that sex-determination gene expression depends largely on ecdysone-mediated let-7 signaling in the soma, primarily in males. The pronounced effects on *dsx* and *Sxl* in males suggest that ecdysone and let-7 constitute the system that supports the expression of somatic sex-biased genes in males.

The effects of let-7 depletion on *Yp1* and, importantly, the influence of ecdysone signaling on the sex-determination hierarchy in males raise the possibility that, although more weakly, all sex-biased genes eventually depend on hormones in females as well. If true, their sex-biased expression would result from two pathways regulated by ecdysone: a germline-dependent influence of ecdysone known as the gonadal sex hormone axis and a second pathway regulated by the sex-determination hierarchy that is germline independent but, as shown here, influenced mildly by hormones and let-7. Supporting this view, females require ecdysone receptor (*EcR*) expression in FRU expressing neurons to

modulate precopulatory behavior just like males (see below), and ecdysone deficient females present male behaviors (Dalton *et al.* 2009; Ganter *et al.* 2012).

Intrinsic sex-specific factors and the proper sexual identity of the fat body are important for courtship behavior orchestrated by DSX and FRU in the brain, suggesting a fine interplay between signaling from the fat body and the sex-specific regulation of the nervous system (Lazareva *et al.* 2007; Camara *et al.* 2008). In particular, the EcR-A isoform that may interact with let-7 signaling is required in the FRU^M neural circuit for male courtship behavior (Sanders and Arbeitman 2008; Dalton *et al.* 2009).

FRU^M and DSX establish neural circuits differentially in each sex at mid-metamorphosis, a time at which they show strongest expression. Let-7 pulses could affect the FRU and DSX branches of the sex-determination hierarchy in the neural circuitry during this period. Let-7 may well contribute to a feedback loop in the nervous system since FRU targets include a preponderance of genes regulated by the steroid

hormone ecdysone (Dalton *et al.* 2009, 2013; Neville *et al.* 2014). However, the reported FRU^M and DSX binding sites in Luo *et al.* (2011) do not include the *let-7-C* locus, suggesting an indirect interaction.

In addition to ecdysone titers, *let-7* levels and its mode of action are particularly important to understanding the impact of hormones in each sex and how they may regulate sex determination. *Let-7* expression is dependent on ecdysteroids in both male and female adult gonads; however, ecdysone signaling facilitates cell gender maintenance in the organism via *let-7* primarily in males, suggesting that *let-7* response to ecdysone signaling and/or its effectors differ between the sexes. During metamorphosis, *let-7* is induced by ecdysone signaling to control the timing of neuronal differentiation by way of BTB transcription factors. Two of them, *Abrupt* and *Chinmo*, act as negative regulators of ecdysone signaling, therefore creating a feedback loop (Zhu *et al.* 2006; Wu *et al.* 2012). By targeting repressors, *let-7* finely modulates and reinforces steroid hormone signaling pulses in the brain. Interestingly, *Abrupt* modulates ecdysone signaling in the ovary as well (Jang *et al.* 2009). Increasing ecdysone titers established during oocyte development coincide with the gradual decrease of *Abrupt* concentration in the ovary. When ecdysone signaling is very high, *Abrupt* fails to bind the EcR coactivator *Taiman*, resulting in ecdysone signaling block. Whether *let-7* controls *Abrupt* in the gonads and contributes to reinforcing ecdysone signaling via a feedback loop has not been studied. Nonetheless, naturally low levels of *let-7* in the ovary where ecdysone levels are plenty, contrary to testes, allows *let-7* to generate in the germarium soma a sharper threshold response to the systemic signaling only when ecdysone titers are high (A. König and H. Shcherbata, unpublished results). In turn, because ecdysone and *let-7*-deficient phenotypes are just as strong in male and female gonads, higher levels of *let-7* seem required to respond to lower ecdysone titers in males.

The two *bona fide* targets of *let-7* in the brain present intriguing parallels in the gonads. Under the control of ecdysone, *Chinmo* and *Abrupt* control the differentiation of the gonadal soma specifically in one sex: *Abrupt* acts in the germarium and *Chinmo* in testis (Jang *et al.* 2009; Flaherty *et al.* 2010). Both are effectors of the JAK/STAT pathway, known to act differently in male and female gonads (Decotto and Spradling 2005). As exemplified by the JAK/STAT pathway in the gonads, sex-specific transcription factors controlled by differential levels of *let-7* may respond differently to ecdysone signaling and lead to sex-specific functions. This may hold true in the brain where *Chinmo* is a direct target of Fru^M in males (Neville *et al.* 2014).

Another important aspect of our findings is the temporal character of ecdysone-*let-7* involvement in the gonadal soma. It has been shown previously that there are differential requirements for the miRNA pathway in preadult and adult stages for the maintenance of germline stem cells (Shcherbata *et al.* 2007). In addition, augmentation of JAK/STAT signaling via *let-7* miRNA in the testicular stem cell niche is essential for

male germline stem cell preservation in aging flies (Toledano *et al.* 2012).

The temporal ecdysteroid-*let-7* signaling cascade also cooperates with the JAK/STAT cytokine pathway in neuronal cell fate determination (Kucherenko and Shcherbata 2013). One possibility is that the ecdysteroid-*let-7* effect on somatic gender identity also has a temporal character and incorporates JAK/STAT cytokine signaling to control sex determination in the somatic cells.

Interestingly, one of the JAK/STAT pathway ligands, Unpaired (*Upd*), is an X-linked signal element gene that affects *Sxl* expression (Sefton *et al.* 2000). *Upd* is a genuine target of *miR-279* that regulates circadian rhythms (Luo and Sehgal 2012). Knockdown of *Upd* rescues the behavioral phenotype of *miR-279* mutants. Further studies of the ecdysone-miRNA-JAK/STAT signaling cascade will determine upstream and downstream components sustaining cellular sexual identity during the postembryonic stages, adulthood, and aging.

Finally, the significant upregulation of *Sxl* in both wild-type and *ecd^{1ts}* females upon temperature shift (Figure 5E) indicates that *Sxl* expression is temperature dependent in flies and also modulated by ecdysteroid hormones. This provides a direct role for hormones in regulating sex determination in females. Clearly our understanding of this unprecedented complexity of sex determination requires both temporal and cell-specific examinations of the interplay between miRNAs, steroid hormones, and sex determination.

These results comprehensively demonstrate an important role for miRNAs as regulators of sexual dimorphism and identify several sets of candidate miRNAs to achieve differential functions in each sex. The function of *let-7* provides a proof of concept of the importance of sex-biased miRNA expression in the developing and aging adult gonad and reproductive apparatus. In mammals, sex hormones produced in the gonads coordinate gene expression in distant tissues and organs. The existence of a similar hormonal axis in *Drosophila* has remained elusive. We show here for the first time that ecdysone signaling controls sex-determination genes in flies, via the miRNA *let-7*. Misregulation of *let-7* in mammals has been shown to impair differentiation and leads to the development of diseases including cancer. *Let-7* appears as a master regulator of the cell-proliferation pathways altered in lung, breast, colon, and prostate cancer (Takamizawa 2004; Johnson *et al.* 2007; Trang *et al.* 2009; reviewed in Lo *et al.* 2013). Notably, such cancer cells present unusually low levels of *let-7*. In addition, connections between *let-7* and hormone signaling have been established in mammals. *Let-7c* plays an important role in the regulation of androgen signaling in castration-resistant prostate cancers, acting by downregulation of the androgen receptor. In turn, androgen signaling further increases cellular levels of *miR-125b* (Shi *et al.* 2007), suggesting that both *miR-125* and *let-7* respond to hormonal imbalances. Whether sex determination is affected in these contexts will require future studies.

We provide an extensive repertoire of sex-biased and gender neutral miRNAs that will help address the varied

functions of miRNA activity across development and aging, as well as in the context of human diseases.

Acknowledgments

We thank Laura Johnston, Nicholas Sokol, Frank Hirth, Ralf Pflanz, Bruce Baker, Carmen Robinett, Acaimo Gonzalez-Reyes, the Bloomington Stock Center for providing flies and reagents, and Mark Siegal for advice on cuticle preparations. We thank all members of the Hannon lab, Ilaria Falcioni, the Department of Herbert Jäckle and the Shcherbata Lab for helpful discussions, the two reviewers and Alexander Vaughan for providing constructive comments that helped improve this manuscript. This work was supported by grants from the National Institutes of Health, a kind gift from Kathryn W. Davis to G.J.H., and by the Max Planck Society to A.K. and H.R.S.

Literature Cited

- Alekseyenko, A. A., E. Larschan, W. R. Lai, P. J. Park, and M. I. Kuroda, 2006 High-resolution ChIP-chip analysis reveals that the *Drosophila* MSL complex selectively identifies active genes on the male X chromosome. *Genes Dev.* 20: 848–857.
- Alekseyenko, A. A., J. W. K. Ho, S. Peng, M. Gelbart, M. Y. Tolstorukov *et al.*, 2012 Sequence-specific targeting of dosage compensation in *Drosophila* favors an active chromatin context. *PLoS Genet.* 8: e1002646.
- Ambros, V., 2011 MicroRNAs and developmental timing. *Curr. Opin. Genet. Dev.* 21: 511–517.
- Ambros, V., and X. Chen, 2007 The regulation of genes and genomes by small RNAs. *Development* 134: 1635–1641.
- Aravin, A. A., M. Lagos-Quintana, A. Yalcin, M. Zavolan, D. Marks *et al.*, 2003 The small RNA profile during *Drosophila melanogaster* development. *Dev. Cell* 5: 337–350.
- Arbeitman, M. N., E. E. M. Furlong, F. Imam, E. Johnson, B. H. Null *et al.*, 2002 Gene expression during the life cycle of *Drosophila melanogaster*. *Science* 297: 2270–2275.
- Baker, B. S., and K. A. Ridge, 1980 Sex and the single cell. I. On the action of major loci affecting sex determination in *Drosophila melanogaster*. *Genetics* 94: 383–423.
- Baker, B. S., K. Burtis, T. Goralski, W. Mattox, and R. Nagoshi, 1989 Molecular genetic aspects of sex determination in *Drosophila melanogaster*. *Genome* 31: 638–645.
- Baley, J., and J. Li, 2012 MicroRNAs and ovarian function. *J. Ovarian Res.*
- Bartel, D. P., 2009 MicroRNAs: target recognition and regulatory functions. *Cell* 136: 215–233.
- Bashaw, G. J., and B. S. Baker, 1997 The regulation of the *Drosophila* msl-2 gene reveals a function for Sex-lethal in translational control. *Cell* 89: 789–798.
- Bejarano, F., D. Bortolamiol-Becet, Q. Dai, K. Sun, A. Saj *et al.*, 2012 A genome-wide transgenic resource for conditional expression of *Drosophila* microRNAs. *Development* 139: 2821–2831.
- Belote, J. M., M. B. McKeown, D. J. Andrew, T. N. Scott, M. F. Wolfner *et al.*, 2002 Control of sexual differentiation in *Drosophila melanogaster*. *Cold Spring Harb. Symp. Quant. Biol.* 50: 605–614.
- Belote, J. M., M. McKeown, R. T. Boggs, R. Ohkawa, and B. A. Sosnowski, 1989 Molecular genetics of transformer, a genetic switch controlling sexual differentiation in *Drosophila*. *Dev. Genet.* 10: 143–154.
- Bownes, M., M. Blair, R. Kozma, and M. Dempster, 1983 20-Hydroxyecdysone stimulates tissue-specific yolk-protein gene transcription in both male and female *Drosophila*. *J. Embryol. Exp. Morphol.* 78: 249–268.
- Bridges, C. B., 1921 Triploid intersexes in *Drosophila melanogaster*. *Science* 54: 252–254.
- Burtis, K. C., K. T. Coschigano, B. S. Baker, and P. C. Wensink, 1991 The doublesex proteins of *Drosophila melanogaster* bind directly to a sex-specific yolk protein gene enhancer. *EMBO J.* 10: 2577–2582.
- Bushati, N., A. Stark, J. Brennecke, and S. M. Cohen, 2008 Temporal reciprocity of miRNAs and their targets during the maternal-to-zygotic transition in *Drosophila*. *Curr. Biol.* 18: 501–506.
- Camara, N., C. Whitworth, and M. Van Doren, 2008 The creation of sexual dimorphism in the *Drosophila* soma. *Curr. Top. Dev. Biol.* 83: 65–107.
- Caygill, E. E., and L. A. Johnston, 2008 Temporal regulation of metamorphic processes in *Drosophila* by the let-7 and miR-125 heterochronic microRNAs. *Curr. Biol.* 18: 943–950.
- Chatterjee, S. S., L. D. Uppendahl, M. A. Chowdhury, P.-L. Ip, and M. L. Siegal, 2011 The female-specific doublesex isoform regulates pleiotropic transcription factors to pattern genital development in *Drosophila*. *Development* 138: 1099–1109.
- Chawla, G., and N. S. Sokol, 2012 Hormonal activation of let-7-C microRNAs via EcR is required for adult *Drosophila melanogaster* morphology and function. *Development* 139: 1788–1797.
- Chen, S., S. Wang, and T. Xie, 2011 Restricting self-renewal signals within the stem cell niche: multiple levels of control. *Curr. Opin. Genet. Dev.* 21: 684–689.
- Chiang, P.-W., and D. M. Kurnit, 2003 Study of dosage compensation in *Drosophila*. *Genetics* 165: 1167–1181.
- Christiansen, A. E., E. L. Keisman, S. M. Ahmad, and B. S. Baker, 2002 Sex comes in from the cold: the integration of sex and pattern. *Trends Genet.* 18: 510–516.
- Chung, W.-J., K. Okamura, R. Martin, and E. C. Lai, 2008 Endogenous RNA interference provides a somatic defense against *Drosophila* transposons. *Curr. Biol.* 18: 795–802.
- Cline, T. W., 1978 Two closely linked mutations in *Drosophila melanogaster* that are lethal to opposite sexes and interact with daughterless. *Genetics* 90: 683–698.
- Clough, E., and B. Oliver, 2012 Genomics of sex determination in *Drosophila*. *Brief Funct. Genomics* 11: 387–394.
- Czech, B., C. D. Malone, R. Zhou, A. Stark, C. Schlingehayde *et al.*, 2008 An endogenous small interfering RNA pathway in *Drosophila*. *Nature* 453: 798–802.
- Dai, Q., P. Smibert, and E. C. Lai, 2012 Exploiting *Drosophila* genetics to understand microRNA function and regulation. *Curr. Top. Dev. Biol.* 99: 201–235.
- Dalton, J. E., M. S. Lebo, L. E. Sanders, F. Sun, and M. N. Arbeitman, 2009 Ecdysone receptor acts in fruitless: expressing neurons to mediate *Drosophila* courtship behaviors. *Curr. Biol.* 19: 1447–1452.
- Dalton, J. E., J. M. Fear, S. Knott, B. S. Baker, L. M. McIntyre *et al.*, 2013 Male-specific Fruitless isoforms have different regulatory roles conferred by distinct zinc finger DNA binding domains. *BMC Genomics* 14: 659.
- Decotto, E., and A. C. Spradling, 2005 The *Drosophila* ovarian and testis stem cell niches: similar somatic stem cells and signals. *Dev. Cell* 9: 501–510.
- Deng, X., J. B. Hiatt, D. K. Nguyen, S. Ercan, D. Sturgill *et al.*, 2011 Evidence for compensatory upregulation of expressed X-linked genes in mammals, *Caenorhabditis elegans* and *Drosophila melanogaster*. *Nat. Genet.* 43: 1179–1185.
- Dillies, M.-A., A. Rau, J. Aubert, C. Hennequet-Antier, M. Jeanmougin *et al.*, 2013 A comprehensive evaluation of normalization methods for Illumina high-throughput RNA sequencing data analysis. *Brief. Bioinform.* 14: 671–683.

- Duncan, K., M. Grskovic, C. Strein, K. Beckmann, R. Niggeweg *et al.*, 2006 Sex-lethal imparts a sex-specific function to UNR by recruiting it to the msl-2 mRNA 3' UTR: translational repression for dosage compensation. *Genes Dev.* 20: 368–379.
- Fagegaltier, D., and B. S. Baker, 2004 X chromosome sites autonomously recruit the dosage compensation complex in *Drosophila* males. *PLoS Biol.* 2: e341.
- Flaherty, M. S., P. Salis, C. J. Evans, L. A. Ekas, A. Marouf *et al.*, 2010 chinmo is a functional effector of the JAK/STAT pathway that regulates eye development, tumor formation, and stem cell self-renewal in *Drosophila*. *Dev. Cell* 18: 556–568.
- Fuller, M. T., and A. C. Spradling, 2007 Male and female *Drosophila* germline stem cells: two versions of immortality. *Science* 316: 402–404.
- Ganter, G. K., J. B. Desilets, J. A. Davis-Knowlton, A. E. Panaitiu, M. Sweezy *et al.*, 2012 *Drosophila* female precopulatory behavior is modulated by ecdysteroids. *J. Insect Physiol.* 58: 413–419.
- Garbuzov, A., and M. Tatar, 2010 Hormonal regulation of *Drosophila* microRNA let-7 and miR-125 that target innate immunity. *Fly* 4: 306–311.
- Garen, A., L. Kauvar, and J. A. Lepesant, 1977 Roles of ecdysone in *Drosophila* development. *Proc. Natl. Acad. Sci. USA* 74: 5099–5103.
- Giraldez, A. J., Y. Mishima, J. Rihel, R. J. Grocock, S. Van Dongen *et al.*, 2006 Zebrafish MiR-430 promotes deadenylation and clearance of maternal mRNAs. *Science* 312: 75–79.
- Hempel, L. U., and B. Oliver, 2007 Sex-specific DoublesexM expression in subsets of *Drosophila* somatic gonad cells. *BMC Dev. Biol.* 7: 113.
- Hildreth, P. E., 1965 Doublesex, recessive gene that transforms both males and females of *Drosophila* into intersexes. *Genetics* 51: 659–678.
- Jang, A. C.-C., Y.-C. Chang, J. Bai, and D. Montell, 2009 Border-cell migration requires integration of spatial and temporal signals by the BTB protein Abrupt. *Nat. Cell Biol.* 11: 569–579.
- Johnson, C. D., A. Esquela-Kerscher, G. Stefani, M. Byrom, K. Kelnar *et al.*, 2007 The let-7 microRNA represses cell proliferation pathways in human cells. *Cancer Res.* 67: 7713–7722.
- Kato, M., A. de Lencastre, Z. Pincus, and F. J. Slack, 2009 Dynamic expression of small non-coding RNAs, including novel microRNAs and piRNAs/21U-RNAs, during *Caenorhabditis elegans* development. *Genome Biol.* 10: R54.
- Kerman, B. E., A. M. Cheshire, and D. J. Andrew, 2006 From fate to function: the *Drosophila* trachea and salivary gland as models for tubulogenesis. *Differentiation* 74: 326–348.
- König, A., and H. R. Shcherbata, 2013 Visualization of adult stem cells within their niches using the *Drosophila* germline as a model system. *Methods Mol. Biol.* 1035: 25–33.
- König, A., A. S. Yatsenko, M. Weiss, and H. R. Shcherbata, 2011 Ecdysteroids affect *Drosophila* ovarian stem cell niche formation and early germline differentiation. *EMBO J.* 30: 1549–1562.
- Kucherenko, M. M., and H. R. Shcherbata, 2013 Steroids as external temporal codes act via microRNAs and cooperate with cytokines in differential neurogenesis. *Fly* 7: 173–183.
- Kucherenko, M. M., J. Barth, A. Fiala, and H. R. Shcherbata, 2012 Steroid-induced microRNA let-7 acts as a spatio-temporal code for neuronal cell fate in the developing *Drosophila* brain. *EMBO J.* 31: 4511–4523.
- Lazareva, A. A., G. Roman, W. Mattox, P. E. Hardin, and B. Dauwalder, 2007 A role for the adult fat body in *Drosophila* male courtship behavior. *PLoS Genet.* 3: e16.
- Leatherman, J. L., and S. Dinardo, 2010 Germline self-renewal requires cyst stem cells and stat regulates niche adhesion in *Drosophila* testes. *Nat. Cell Biol.* 12: 806–811.
- Lebo, M. S., L. E. Sanders, F. Sun, and M. N. Arbeitman, 2009 Somatic, germline and sex hierarchy regulated gene expression during *Drosophila* metamorphosis. *BMC Genomics* 10: 80.
- Lee, G., J. C. Hall, and J. H. Park, 2002 Doublesex gene expression in the central nervous system of *Drosophila melanogaster*. *J. Neurogenet.* 16: 229–248.
- Legube, G., S. K. McWeeney, M. J. Lercher, and A. Akhtar, 2006 X-chromosome-wide profiling of MSL-1 distribution and dosage compensation in *Drosophila*. *Genes Dev.* 20: 871–883.
- Li, W., M. Cressy, H. Qin, T. Fulga, D. Van Vactor *et al.*, 2013 MicroRNA-276a functions in ellipsoid body and mushroom body neurons for naive and conditioned olfactory avoidance in *Drosophila*. *J. Neurosci.* 33: 5821–5833.
- Liu, N., M. Landreh, K. Cao, M. Abe, G.-J. Hendriks *et al.*, 2012 The microRNA miR-34 modulates ageing and neurodegeneration in *Drosophila*. *Nature* 482: 519–523.
- Lo, U., D. Yang, and J. T. Hsieh, 2013 The role of microRNAs in prostate cancer progression. *Transl. Androl. Urol.* 2(3): 228–241.
- Luo, S. D., G. W. Shi, and B. S. Baker, 2011 Direct targets of the *D. melanogaster* DSXF protein and the evolution of sexual development. *Development* 138: 2761–2771.
- Luo, W., and A. Sehgal, 2012 Regulation of circadian behavioral output via a MicroRNA-JAK/STAT circuit. *Cell* 148: 765–779.
- Malone, C., J. Brennecke, B. Czech, A. Aravin, and G. J. Hannon, 2012 Preparation of small RNA libraries for high-throughput sequencing. *Cold Spring Harb Protoc* 2012: 1067–1077.
- Marrone, A. K., E. V. Edeleva, M. M. Kucherenko, N.-H. Hsiao, and H. R. Shcherbata, 2012 Dg-Dys-Syn1 signaling in *Drosophila* regulates the microRNA profile. *BMC Cell Biol.* 13: 26.
- Meiklejohn, C. D., E. L. Landeen, J. M. Cook, S. B. Kingan, and D. C. Presgraves, 2011 Sex chromosome-specific regulation in the *Drosophila* male germline but little evidence for chromosomal dosage compensation or meiotic inactivation. *PLoS Biol.* 9: e1001126.
- Mishima, T., T. Takizawa, S.-S. Luo, O. Ishibashi, Y. Kawahigashi *et al.*, 2008 MicroRNA (miRNA) cloning analysis reveals sex differences in miRNA expression profiles between adult mouse testis and ovary. *Reproduction* 136: 811–822.
- Morris, L. X., and A. C. Spradling, 2012 Steroid signaling within *Drosophila* ovarian epithelial cells sex-specifically modulates early germ cell development and meiotic entry. *PLoS ONE* 7: e46109.
- Neville, M. C., T. Nojima, E. Ashley, D. J. Parker, J. Walker *et al.*, 2014 Male-specific fruitless isoforms target neurodevelopmental genes to specify a sexually dimorphic nervous system. *Curr. Biol.* 24: 229–241.
- Parisi, M., R. Nuttall, P. Edwards, J. Minor, D. Naiman *et al.*, 2004 A survey of ovary-, testis-, and soma-biased gene expression in *Drosophila melanogaster* adults. *Genome Biol.* 5: R40.
- Parisi, M. J., V. Gupta, D. Sturgill, J. T. Warren, J.-M. Jallon *et al.*, 2010 Germline-dependent gene expression in distant non-gonadal somatic tissues of *Drosophila*. *BMC Genomics* 11: 346.
- Pasquinelli, A. E., B. J. Reinhart, F. Slack, M. Q. Martindale, M. I. Kuroda *et al.*, 2000 Conservation of the sequence and temporal expression of let-7 heterochronic regulatory RNA. *Nature* 408: 86–89.
- Rideout, E. J., A. J. Dornan, M. C. Neville, S. Eadie, and S. F. Goodwin, 2010 Control of sexual differentiation and behavior by the doublesex gene in *Drosophila melanogaster*. *Nat. Neurosci.* 13: 458–466.
- Ro, S., C. Park, K. M. Sanders, J. R. McCarrey, and W. Yan, 2007 Cloning and expression profiling of testis-expressed microRNAs. *Dev. Biol.* 311: 592–602.

- Robinett, C. C., A. G. Vaughan, J.-M. Knapp, and B. S. Baker, 2010 Sex and the single cell. II. There is a time and place for sex. *PLoS Biol.* 8: e1000365.
- Ruby, J. G., A. Stark, W. K. Johnston, M. Kellis, D. P. Bartel *et al.*, 2007 Evolution, biogenesis, expression, and target predictions of a substantially expanded set of *Drosophila* microRNAs. *Genome Res.* 17: 1850–1864.
- Ryazansky, S. S., V. A. Gvozdev, and E. Berezikov, 2011 Evidence for post-transcriptional regulation of clustered microRNAs in *Drosophila*. *BMC Genomics* 12: 371.
- Ryner, L. C., and B. S. Baker, 1991 Regulation of doublesex pre-mRNA processing occurs by 3'-splice site activation. *Genes Dev.* 5: 2071–2085.
- Salz, H. K., 2011 Sex determination in insects: a binary decision based on alternative splicing. *Curr. Opin. Genet. Dev.* 21: 395–400.
- Sanders, L. E., and M. N. Arbeitman, 2008 Doublesex establishes sexual dimorphism in the *Drosophila* central nervous system in an isoform-dependent manner by directing cell number. *Dev. Biol.* 320: 378–390.
- Sefton, L., J. R. Timmer, Y. Zhang, F. Béranger, and T. W. Cline, 2000 An extracellular activator of the *Drosophila* JAK/STAT pathway is a sex-determination signal element. *Nature* 405: 970–973.
- Sempere, L. F., E. B. Dubrovsky, V. A. Dubrovskaya, E. M. Berger, and V. Ambros, 2002 The expression of the let-7 small regulatory RNA is controlled by ecdysone during metamorphosis in *Drosophila melanogaster*. *Dev. Biol.* 244: 170–179.
- Sempere, L. F., N. S. Sokol, E. B. Dubrovsky, E. M. Berger, and V. Ambros, 2003 Temporal regulation of microRNA expression in *Drosophila melanogaster* mediated by hormonal signals and broad-Complex gene activity. *Dev. Biol.* 259: 9–18.
- Shcherbata, H. R., E. J. Ward, K. A. Fischer, J.-Y. Yu, S. H. Reynolds *et al.*, 2007 Stage-specific differences in the requirements for germline stem cell maintenance in the *Drosophila* ovary. *Cell Stem Cell* 1: 698–709.
- Shi, X.-B., L. Xue, J. Yang, A.-H. Ma, J. Zhao *et al.*, 2007 An androgen-regulated miRNA suppresses Bak1 expression and induces androgen-independent growth of prostate cancer cells. *Proc. Natl. Acad. Sci. USA* 104: 19983–19988.
- Smibert, P., and E. C. Lai, 2010 A view from *Drosophila*: multiple biological functions for individual microRNAs. *Semin. Cell Dev. Biol.* 21: 745–753.
- Sokol, N. S., P. Xu, Y.-N. Jan, and V. Ambros, 2008 *Drosophila* let-7 microRNA is required for remodeling of the neuromusculature during metamorphosis. *Genes Dev.* 22: 1591–1596.
- Soni, K., A. Choudhary, A. Patowary, A. R. Singh, S. Bhatia *et al.*, 2013 miR-34 is maternally inherited in *Drosophila melanogaster* and *Danio rerio*. *Nucleic Acids Res.* 41: 4470–4480.
- Sosnowski, B. A., J. M. Belote, and M. McKeown, 1989 Sex-specific alternative splicing of RNA from the transformer gene results from sequence-dependent splice site blockage. *Cell* 58: 449–459.
- Straub, T., C. Grimaud, G. D. Gilfillan, A. Mitterweger, and P. B. Becker, 2008 The chromosomal high-affinity binding sites for the *Drosophila* dosage compensation complex. *PLoS Genet.* 4: e1000302.
- Takamizawa, J., 2004 Reduced expression of the let-7 microRNAs in human lung cancers in association with shortened postoperative survival. *Cancer Res.* 64: 3753–3756.
- Tanaka, K., O. Barmina, L. E. Sanders, M. N. Arbeitman, and A. Kopp, 2011 Evolution of sex-specific traits through changes in HOX-dependent doublesex expression. *PLoS Biol.* 9: e1001131.
- Toledano, H., C. D'Alterio, B. Czech, E. Levine, and D. L. Jones, 2012 The let-7-imp axis regulates ageing of the *Drosophila* testis stem-cell niche. *Nature* 485: 605–610.
- Trang, P., P. P. Medina, J. F. Wiggins, L. Ruffino, K. Kelnar *et al.*, 2009 Regression of murine lung tumors by the let-7 microRNA. *Oncogene* 29: 1580–1587.
- Vibrantovski, M. D., H. F. Lopes, T. L. Karr, and M. Long, 2009 Stage-specific expression profiling of *Drosophila* spermatogenesis suggests that meiotic sex chromosome inactivation drives genomic relocation of testis-expressed genes. *PLoS Genet.* 5: e1000731.
- Vibrantovski M. D., Zhang Y. E., Kemkemmer C., Lopes H. F., Karr T. L., Long M., 2012 Re-analysis of the larval testis data on meiotic sex chromosome inactivation revealed evidence for tissue-specific gene expression related to the *Drosophila* X chromosome. *BMC Biol.* 10: 49–50.
- Weng, R., and S. M. Cohen, 2012 *Drosophila* miR-124 regulates neuroblast proliferation through its target anachronism. *Development* 139: 1427–1434.
- Whitworth, C., E. Jimenez, and M. Van Doren, 2012 Development of sexual dimorphism in the *Drosophila* testis. *Spermatogenesis* 2: 129–136.
- Williams, T. M., J. E. Selegue, T. Werner, N. Gompel, A. Kopp *et al.*, 2008 The regulation and evolution of a genetic switch controlling sexually dimorphic traits in *Drosophila*. *Cell* 134: 610–623.
- Wu, Y.-C., C.-H. Chen, A. Mercer, and N. S. Sokol, 2012 Let-7-complex microRNAs regulate the temporal identity of *Drosophila* mushroom body neurons via chinmo. *Dev. Cell* 23: 202–209.
- Xu, P., S. Y. Vernooy, M. Guo, and B. A. Hay, 2003 The *Drosophila* microRNA Mir-14 suppresses cell death and is required for normal fat metabolism. *Curr. Biol.* 13: 790–795.
- Zhu, S., S. Lin, C.-F. Kao, T. Awasaki, A.-S. Chiang *et al.*, 2006 Gradients of the *Drosophila* Chinmo BTB-zinc finger protein govern neuronal temporal identity. *Cell* 127: 409–422.

Communicating editor: B. Andrews

2.5 Soma influences GSC progeny differentiation via the cell adhesion-mediated steroid-let-7-Wingless signaling cascade that regulates chromatin dynamics

Annekatriin König, Halyna Shcherbata

All experiments were done by Annkatrin König.

Status of the manuscript: published (Biol Open. 2015 Feb 6;4(3):285-300)

RESEARCH ARTICLE

Soma influences GSC progeny differentiation via the cell adhesion-mediated steroid-*let-7*-Wingless signaling cascade that regulates chromatin dynamics

Annekatriin König and Halyna R. Shcherbata*

ABSTRACT

It is known that signaling from the germline stem cell niche is required to maintain germline stem cell identity in *Drosophila*. However, it is not clear whether the germline stem-cell daughters differentiate by default (because they are physically distant from the niche) or whether additional signaling is necessary to initiate the differentiation program. Previously, we showed that ecdysteroid signaling cell non-autonomously regulates early germline differentiation via its soma-specific co-activator and co-repressor, Taiman and Abrupt. Now, we demonstrate that this regulation is modulated by the miRNA *let-7*, which acts in a positive feedback loop to confer ecdysone signaling robustness via targeting its repressor, the transcription factor Abrupt. This feedback loop adjusts ecdysteroid signaling in response to some stressful alterations in the external and internal conditions, which include temperature stress and aging, but not nutritional deprivation. Upon *let-7* deficit, escort cells fail to properly differentiate: their shape, division, and cell adhesive characteristics are perturbed. These cells have confused cellular identity and form columnar-like rather than squamous epithelium and fail to send protrusions in between differentiating germline cysts, affecting soma-germline communication. Particularly, levels of the homophilic cell adhesion protein Cadherin, which recruits Wg signaling transducer β -catenin, are increased in mutant escort cells and, correspondingly, in the adjacent germline cells. Readjustment of heterotypic (soma-germline) cell adhesion modulates Wg signaling intensity in the germline, which in turn regulates histone modifications that promote expression of the genes necessary to trigger early germline differentiation. Thus, our data first show the intrinsic role for Wg signaling in the germline and support a model where the soma influences the tempo of germline differentiation in response to external conditions.

KEY WORDS: *Drosophila*, Oogenesis, Germline Stem cell, Ecdysone, miRNA *let-7*, Abrupt, Wingless signaling, Histone modifications, H2Bub1, Differential cell adhesion, Differentiation niche, Cell fate

INTRODUCTION

In a multicellular organism all cells are united to provide the best response to ever-changing internal and external cues, offering the

optimal conditions for organism welfare. This concerted action of different cell types is regulated at different levels, for example, hormones provide systemic signaling for the whole organism. However, cells can communicate more locally within organs or even talk to individual cells from other tissues using a lexicon of different signaling pathways, the majority of which are highly evolutionary conserved. In most cases, signaling molecules or ligands are distributed in the extracellular matrix and are diffused within few cell diameters (e.g. BMP, Hh, Wnt); sometimes, ligands are directly transmitted between the neighboring cells (e.g. Notch signaling). In addition, cells can converse via cell adhesion contacts that adjust tissue maintenance, form and function. All these communication modes are particularly important during embryonic development, but also play an essential role during adulthood for growth, homeostasis and tissue regeneration under certain physiological and pathological conditions. Although a great deal is known about the role of different signaling pathways for development and maintenance of different cells and tissues, it remains challenging to hierarchically connect different levels of cell communication to clearly understand how signals received by one cell type are transmitted to regulate the fate of another cell.

In all organisms, the mature egg production is known to be one of the most highly regulated events; therefore, this process can serve as a great paradigm to study the hierarchical signaling cascade that involves communication between the two cell types of extremely different origin: the germline and the soma. In general, the decision to produce a mature egg is based on the whole organism status and specific tissues, which greatly depend on age, health, nutrition, etc. Currently the knowledge at the molecular level of how germline differentiation is regulated in adults is limited; therefore, it is important to identify the extracellular ligands, membrane receptors and transcription factors involved in the signal transduction pathways that dynamically guide oocyte maturation to reach a consensus between changing internal states and external environments.

In mammals, oocytes undergo an extensive maturation process that is carefully controlled and recent progress highlighted that, besides paracrine signals, cell to cell interactions with surrounding somatic cells play important roles in oocyte differentiation (Murray et al., 2010; Li and Albertini, 2013). Somatic epithelial granulosa cells that surround the developing oocytes are required to control oocyte meiotic arrest and growth (Von Stetina and Orr-Weaver, 2011). Following puberty, the luteinizing hormone acts on granulosa cells, stimulates the activation of EGFR and subsequently MAPK kinase signaling, which then causes reversal of the inhibitory signals that are sent to the oocyte. In this manner, systemic signals are integrated in somatic granulosa cells to regulate oocyte differentiation. In

Max Planck Research Group of Gene Expression and Signaling, Max Planck Institute for Biophysical Chemistry, Am Fassberg 11, 37077, Göttingen, Germany.

*Corresponding author (halyna.shcherbata@mpibpc.mpg.de)

This is an Open Access article distributed under the terms of the Creative Commons Attribution License (<http://creativecommons.org/licenses/by/3.0>), which permits unrestricted use, distribution and reproduction in any medium provided that the original work is properly attributed.

Received 13 October 2014; Accepted 4 December 2014

addition, multiple components of the Wnt/Wingless (Wg) signaling pathway are expressed in the adult ovary. During adulthood, the monthly fluctuations in Wnt/ β -catenin signaling are balanced by sex hormones in the endometrium (soma) to manage estrogen-induced proliferation and progesterone-induced oocyte differentiation (germline). Abnormal Wnt/ β -catenin signaling strength in gonads causes reproduction defects and cancer (van der Horst et al., 2012). Wnt/Wg pathway is highly evolutionary conserved and is considered as one of the most important developmental pathways (Clevers and Nusse, 2012). A key Wnt/Wg signaling mediator is the nuclear transcription factor β -catenin, which also is a binding partner of the major component of adherens junctions, E-Cadherin. β -catenin levels not only affect the cell adhesiveness, but also the expression profile of multiple genes, as Wnt/Wg signaling cell autonomously regulates gene expression via interaction with chromatin modifying complexes (Liu et al., 2008; Parker et al., 2008; Saito-Diaz et al., 2013). Slight variations in β -catenin amounts and/or its cellular localization have a profound effect on cell status. While functional studies indicate that Wnt/Wg signaling has a role in several aspects of ovarian function including folliculogenesis and steroidogenesis (Boyer et al., 2010; Usongo et al., 2012), a number of questions regarding its functions in the germline remain open.

Drosophila ovary provides an excellent system to study at the molecular level how germline differentiation is adjusted in response to dynamic internal and external conditions. *Drosophila* oogenesis depends on the presence of adult germline stem cells (GSCs) that continuously divide. Mostly, stem cells divide asymmetrically when a mother cell gives rise to two daughter cells with different fates – another stem cell and a differentiating progeny (Gönczy, 2008). Alternatively, two daughters may be identical at birth and their fate is established later on, for instance through signaling from neighboring cells. *Drosophila* GSCs are an example of the latter, since the stem cell fate of the newborn germline cell depends on the signaling provided by the surrounding soma called the GSC niche (Losick et al., 2011). It is known that exit from the niche abolishes stemness, but it is not clear what combination of signals promotes germline differentiation. Physiologically, it seems likely that signaling that coordinates the GSC progeny differentiation and egg maturation efficiency with the whole organism needs and conditions exists. While a lot is known about GSC maintenance and division regulation upon different conditions, the questions what makes stem cell daughter to differentiate and whether the differentiation process *per se* can be regulated in response to physiological state of the whole organism have not been analyzed in depth.

Our previous data provide evidence that ecdysone signaling acts in the soma: (1) during pre-adult stages, to cell autonomously regulate the size of the GSC niche, and (2) during adulthood, to cell non-autonomously regulate the germline differentiation speed via the somatic cells of the differentiation niche (König et al., 2011). In this study we aimed to understand how information is exchanged between the soma and germline, specifically how changes in the somatic cells in the adult ovary are communicated to the germline and regulate germline differentiation. We found that ecdysteroids regulate cellular identity of escort cells (ECs), comprising the differentiation niche, which is juxtaposed to the GSC niche to coordinate the speed of the early GSC progeny differentiation. Depending on the ecdysone signaling strength, cell shape, proliferative ability and, most importantly, adhesive characteristics of ECs are modified, together resulting in squamous to cuboidal-like epithelium

transformation. The epithelial state depends on the function of the BTB transcription factor, Abrupt (Ab), subcellular localization of which is dose-dependent and is regulated by ecdysone signaling. This regulation in addition is fine-tuned by the steroid-induced miRNA *let-7*, which acts in a feedback loop to reinforce ecdysone signaling via Ab downregulation, since Ab also is a repressor of ecdysone signaling. Importantly, alterations in the EC adhesiveness influence the presentation of the cell adhesion proteins in the germline cells, because ovarian soma and the germline are connected via homophilic cell adhesion mediated by cadherins. As cadherin levels must match on the membranes of both cell types, somatic and germline, an increase or decrease of adhesion molecule amounts is immediately communicated to the other cell type via direct cell-cell contacts. Cadherins also have an ability to bind signaling molecules, for example DE-Cadherin (DE-Cad) binds Armadillo (Arm, *Drosophila* β -catenin), which in turn modulates the Wg signaling strength. Thus, ecdysone signaling in the soma influences Wg signaling in the germline via direct cell-cell contacts. The role for the Wg pathway in the *Drosophila* germline has not been reported previously, our data show that the Wg signaling intensity positively affects the early germline differentiation speed. Wg-mediated regulation of the GSC progeny differentiation occurs at the chromatin modification level that controls the initial steps of the GSC daughter decision to enter the differentiation program. Upon decreased Wg signaling, the GSC progeny is caught in the “pre-CB” state: it is not a stem cell anymore, since it cannot perceive signaling from the stem cell niche; however, it is not a differentiating CB yet, since its chromatin remains in the “stem-cell-like” state and is not properly modified to allow the expression of genes necessary for differentiation (e.g. *bam*). In particular, histone H2B monoubiquitination (H2Bub1) is affected upon ecdysone and Wg deficit, postponing *bam* expression and the pre-CB entrance into the differentiation program. In summary, we show that systemic steroid hormone signaling fine-tunes the tempo of GSC progeny differentiation in response to environmental fluctuations. It acts in the somatic differentiation niche to cell non-autonomously, via adjustment of cell adhesion complexes, manage the Wg signaling strength in the germline cells, which modulates their chromatin state, favoring differentiation.

MATERIALS AND METHODS

Fly strains and genetics

Flies were raised on standard cornmeal-yeast-agar-medium at 25°C and fattened on wet yeast paste one day before dissection unless otherwise stated. *w¹¹¹⁸* and *OregonR* were used for controls. The two knockout strains *let-7-C^{GK1}/CyO* and *let-7-C^{KO1}/CyO* lack the whole *let-7-C*, in addition *let-7-C^{GK1}/CyO* contains the transcriptional activator *Gal4* under the control of the *let-7-C* promoter (gift from Nicholas Sokol). Flies with a transgene rescuing the whole *let-7-C* (*let-7-C*; *let-7-C^{GK1}/let-7-C^{KO1}*) were referred to as “Rescue” (Sokol et al., 2008). The *let-7-C^{Allet-7}* construct restores expression of all *let-7-C* members except for *let-7*; *let-7-C^{GK1}/let-7-C^{KO1}*; *let-7-C^{Allet-7}* flies, therefore, were, abbreviated as *Allet-7* (Sokol et al., 2008). *FRT 40A let-7 miR-125/CyO* flies (Caygill and Johnston, 2008) were used for clonal analysis. The following additional fly stocks were used: *ab¹*, *ab^{k02807}*, *w¹¹¹⁸*; *ab^{1D}/CyO*, *y¹ w^{67c23}*; *bam^{EY04821}*, *y¹ w^{67c23}*; *bam^{EY03755}*, *w¹¹¹⁸*; *UASab.B*, *ecd^{1ts}*, *EcR^{Q50st}*, *FRT 101 arm²/FM7a*, *FRT 101 arm³/FM7a*, *usp⁴/FM7a*, *hsbam/TM6*, *hsEcR.B1* (BDSC); *UASat^{RNAi}*, *UASab^{RNAi}* (VDRC), *bamGFP* (gift from Dennis McKearin), *FRT 101 sgg^{D127}/FM7*, *UASp arm* (gift from Andreas Wodarz), *FRT 2A Bre1^{P1549}* (gift from Sarah Bray), *FRT 19A usp⁴/FM7* (*usp⁴* allele from BDSC, recombined in this study), *UAS Cad⁽¹⁰⁹⁰⁰⁴⁾* (DGRC). The *VALIUM20* lines in

which dsRNA expression system was constructed to work in both, the soma and germline: *UASarm^{RNAi}* (35004), *UASfz^{RNAi}* (34321), *UASsgg^{RNAi}* (38293), *UASpan^{RNAi}* (40848) and *UASBre1^{RNAi}* (35443), *UASRtf1^{RNAi}* (36586) (BDSC).

Perturbation of ecdysone signaling, the Wg pathway or H2B monoubiquitination

The *ecd¹¹⁸* temperature-sensitive mutation is known to reduce ecdysone levels at the non-permissive temperature. Fly stocks were kept at the permissive temperature (18°C) and 2- to 4 day old adults were shifted to the restrictive temperature (29°C) for 4 days in order to repress ecdysone synthesis. As control, *OregonR* flies were kept at 29°C for the same time. To disrupt ecdysone signaling specifically in the somatic cells of the germlarium, *UASab.B*, *UAS let-7* or *UASfz^{RNAi}* were expressed using the soma-specific drivers *bab1Gal4*, *ptcGal4* or *let-7-C^{GK1}* (contains *Gal4*). In addition, to disrupt ecdysone signaling during adulthood only, the *tubGal80^{ts}* system was used where the flies were raised at 18°C and switched to 29°C for 3–5 days. Interaction of ecdysone signaling pathway and Bam was analyzed by heat-shocking *hsEcR.B1/+*, *hsbam/+* and *hsEcR.B1/+*; *hsbam/+* flies for 1 hour, 2 days in a row in a 37°C water bath; not heat-shocked flies of the same genotypes were used as controls.

To alter the strength of Wg signaling in the germline, *UASarm^{RNAi}*, *UASfz^{RNAi}*, *UASarm* or *UASpan^{RNAi}* flies were crossed to the germline specific driver *nosGal4* (*NGT40/+*; *nanosGAL4/+*). To analyze the interaction between ecdysone signaling components and Cad or Arm, dominant-negative mutations of *EcR* and *usp* were used: *w¹¹¹⁸*; *hs-Gal4-EcR.LBD/+* or *w¹¹¹⁸*; *hs-Gal4-usp.LBD/+* flies were crossed to *shg^{E17B}/SM6b*, or *FRT 101 arm²/FM7A*. 1–3 day old adult progeny were heat-shocked in empty vials for 60 min per day, 4 days in a row. To analyze the interaction between ecdysone signaling components and Bre1, *EcR^{Q50st/+}*; *FRT 2A Bre1^{P1549/+}* flies were analyzed.

For perturbing H2B monoubiquitination in the germline, *Bre1^{RNAi}* or *Rtf1^{RNAi}* were crossed to germline specific driver *nosGal4* (*NGT40/+*; *nanosGAL4/+*).

Clonal analysis

Germline and somatic cell clones were induced as described previously (Shcherbata et al., 2004; Shcherbata et al., 2007) using the *hsFlp/FRT* system for mitotic recombination. *let-7* mutant clones in CpCs and ECs were obtained via crossing *FRT 40A let-7 miR-125/CyO*; *let-7-C^{Δlet-7}* to *FRT 40A Ubi-GFP/CyO*; *bab1Gal4:UASFlp/TM2* flies (gift from Acaimo González-Reyes). Alternatively, the MARCM system was used and *FRT 40A let-7 miR-125/CyO*; *let-7-C^{Δlet-7}* flies were crossed to *hsFlp*, *FRT 40A tubGal80^{ts}/CyO*; *tubGal4/TM6B*. To induce *usp⁴* mutant clones, *FRT 19A usp⁴/FM7* flies were crossed to *w*, *FRT 19A tubGal80*, *hsFLP*; *UASnucLacZ*, *UAS CD8GFP*; *tubPGal4/TM6B* flies (gift from Frank Hirth). Third instar larvae were heat-shocked for 2 hours, 2 days in a row in a 37°C water bath. To induce adult germline clones, *FRT 40A let-7 miR-125/CyO*; *let-7-C^{Δlet-7}* males were crossed to *hsFlp*; *FRT 40A GFP/CyO* females.

To obtain adult *Bre1* germline clones, *FRT 2A Bre1^{P1549}/TM3* flies were crossed to *hsFlp*; *FRT 2A GFP/TM3*. For inducing *arm²*, *arm³* and *sgg^{D127}* mutant clones *FRT 101 arm²/FM7a*, *FRT 101 arm³/FM7a* or *FRT 101 sgg^{D127}/FM7* flies were crossed to *FRT 101 GFP*; *hsFlp/CyO*. 2–4 day old adult F1 females were heat-shocked in empty vials for 60 min, 2 days in a row in a 37°C water bath.

The GSC loss per day is determined by division of the percentage of clonal germlaria with lost GSCs by the elapsed time after clonal induction (5 days). For *let-7* mutant clones, females were analyzed 7 and 14 days after heat-shock, for *Bre1^{P1549}*, *arm²*, *arm³* and *sgg^{D127}* mutant clones 5 days after heat-shock. Parental *FRT 40A*, parental *FRT 2A* and parental *FRT 101* flies were used as controls. Mutant clones were identified by the absence of GFP; or by the presence of GFP (MARCM).

Expression patterns of let-7 and Ab at different conditions

In situ hybridization was performed as described previously (Kucherenko et al., 2012). To analyze *let-7* levels at different conditions, germlaria of

OregonR flies were dissected and analyzed using RT-qPCR: young (1–3 days) and old (21 days) flies were compared; flies were kept on rich food or poor food (sugarfree) for 2 days; or were kept at 18°C or 29°C for 2 days. In order to measure the levels of Ab, *OregonR* and *ecd¹¹⁸* animals were kept at 18°C or 29°C for 4 days and germlaria were analyzed using RT-qPCR; *OregonR* animals were heat-shocked for 1 h at 37°C and immediately dissected for immunostaining.

RT-qPCR

Ovaries were dissected to perform quantitative reverse transcription (RT-qPCR). Eggs and follicles of later stages were removed and only ovary tips containing germlaria were used for analysis. RNA was extracted using Trizol according to the manufacturers instructions. For *let-7* RT-qPCR, reverse transcription and qPCR were performed following the manufacturers protocol using TaqMan® MicroRNA assay for *let-7* and for *S2* as endogenous control. For analysis of *RpL32* levels as endogenous control and *esg*, *Imp*, *upd*, *ab*, *arm*, *sgg*, *pan* and *fz* cDNA was generated using the cDNA Reverse Transcription kit (Applied Biosystems) according to the manufacturers instructions. qPCR was performed using the fast SYBR® Green Master Mix (Applied Biosystems). A Step One Plus 96 well system (Applied Biosystems) was used for all analysis, all reactions were run in triplicates with appropriate blanks. The reactions were incubated at 95°C for 20 sec (RpL32) or 10 min (TaqMan® MicroRNA) followed by 40 cycles of 95°C for 3 sec (RpL32) or 15 sec (TaqMan® MicroRNA) and 60°C for 30 sec (RpL32) or 60 sec (TaqMan® MicroRNA). Primers were used as follows: *RpL32* forward – 5'-AAGATGACCATCCGCCAGC-3', *RpL32* reverse – 5'-GTGCG-ATACCCCTGGGCTTGC-3', *esg* forward – 5'-CGCCCATGAGATCT-GAAATC-3', *esg* reverse – 5'-GGTCTTGTCACAATCCTTGC-3', *Imp* forward – 5'-GGTGGCCGTATCATTGG-3', *Imp* reverse – 5'-TCAC-GCGCTGCAATTCC-3', *upd* forward – 5'-TTCTGGCTCCTCTGCT-GCTTCT-3', *upd* reverse – 5'-TACCGCAGCCTAAACAGTAGC-3', *ab* forward – 5'-AGCACCCGATAGTCATCCTG-3', *ab* reverse – 5'-GGCCTTGAATAGGGATAGC-3', *arm* forward – 5'-CCACTGGGCTGCTGATCT-3', *arm* reverse – 5'-ATGCTTGGACCAGAAGAAGC-3', *sgg* forward – 5'-ATCAACTGGTGTCCCTGCT-3', *sgg* reverse – 5'-GCACTAGGCTGGGCTGTATT-3', *pan* forward – 5'-AGCGCAG-GAACTTCCATAA-3', *pan* reverse – 5'-TTGATGTGTGCTTTG-CTTCC-3', *fz* – 5'-GCTGCTTGTTACGGTGCT-3', *fz* reverse – 5'-CTGGGTGATGGTGGACAT-3'. The ΔC_T value was determined by subtracting the C_T value of the endogenous control from the experimental C_T value. $\Delta\Delta C_T$ was calculated by subtracting the ΔC_T of the control sample from the respective ΔC_T value. The relative RNA levels were calculated as $2^{-\Delta\Delta C_T}$.

Analysis of mitotic divisions in ECs

In order to determine whether ECs are mitotically active upon perturbed ecdysone signaling, PH3 antibody was used to detect ECs in M phase and EdU assay in S phase.

Immunofluorescence and antibodies

Ovaries were fixed in 5% formaldehyde (Polysciences, Inc.) for 10 min and the staining procedure was performed as described (König and Shcherbata, 2013). For H2Bub1 staining: following fixation, ovaries were washed three times for 15 min and ovarioles were separated using needles. After permeabilization (performed in PBS with 2% Triton X) ovaries were incubated in 2N HCl for 30 min at 37°C. The following primary antibodies were used: mouse monoclonal anti-Adducin (1:50), anti-LaminC (1:50), anti-Arm (1:50), anti-Engrailed; (1:50) (Developmental Studies Hybridoma Bank); rat monoclonal anti-DE-Cad (1:50, Developmental Studies Hybridoma Bank); mouse anti-MAP Kinase (1:500, Sigma); mouse anti-H2Bub1 (1:500, Millipore); rabbit anti-pMad (1:5000, D. Vasiliauskas, S. Morton, T. Jessell and E. Laufer); rabbit anti-Abrupt (1:1000 S. Crews); rabbit anti-Vasa (1:5000, R. Pflanz); rabbit anti-β-Gal and rabbit anti-PH3 (1:3000, Upstate Biotechnology); rabbit anti-H3K4me3 (1:1000, Abcam), rabbit anti-H4K20me3 (1:1000), anti-H3K36me2 (1:1000), anti-H3K9me2 (1:1000), anti-H4K20me1 (1:1000), H4 hyperacetylation (1:1000), anti-H3K27me3 (1:1000) (Upstate

Biotechnology) and guinea pig anti-Tj (1:3000, D. Godt). Secondary antibodies were used: anti-GFP-directly conjugated with AF488 (1:3000, Invitrogen), Alexa 488, 568, or 633 goat anti-mouse, anti-rabbit (1:500, Molecular Probes) and goat anti-rat Cy5 (1:250, Jackson ImmunoResearch). The Click-iT® EdU Cell Proliferation Assay (Invitrogen) was used according to the manufacturers instructions. Images were obtained with a confocal laser-scanning microscope (Leica SPE5) and processed with Adobe Photoshop.

Analysis and statistics

To determine the number of CpCs, LamC positive cells at the tip of the germarium were counted. Germline cells that were touching CpCs were counted as GSCs and pMad staining was used to prove stem cell identity. To determine the intensity of pMad levels, the gray value of pMad positive cells was measured using Zen Software. The gray value of the background was determined and subtracted from the GSC pMad levels for normalization. GSC maintenance was determined by comparing the percentage of germaria with clonal GSCs between two different time points after clonal induction. Cells that had a single spherical spectrosome but were not in contact with the niche: pre-CBs/pro-CBs/CBs were counted separately and GSCs and pre-CBs/pro-CBs/CBs were added together to calculate the number of spectrosome-containing GCs (SpGCs). In addition, the number of fusomes (indicating the number of differentiating cysts) until region 2b, where follicle cells start cyst encapsulation, was counted. To describe the differentiation efficiency in a given germarium the number of cysts was divided by the number of single spectrosome containing cells (ratio=cysts/SpSCs). In addition, germaria containing clonal mutant germline cysts were analyzed: based on the fusome morphology, the number of cells in a cyst and the location in the germarium, it was compared whether clonal germline cysts were of the same stage of differentiation as their non-clonal neighbors. MAP Kinase, Tj, Cad and Arm staining was used to analyze EC morphology. At least three independent biological replicates were done. The two tailed Student's t-test or two-way tables and χ^2 test were used to determine the statistical significance.

RESULTS

Ecdysone signaling deficiency delays GSC progeny at pre-CB stage by preventing histone modification (H2Bub1) that triggers differentiation

In *Drosophila*, the oogenesis depends on the presence of GSCs that reside in their stem cell niche, which is located at the apex of the ovariole in the structure called the germarium (Fig. 1A). The GSC niche consists of specialized somatic cells, namely terminal filaments, cap cells and escort cells (TFs, CpCs and ECs, Fig. 1A). These somatic cells make physical contacts with the GSCs via tight, adherens, and gap junctions, the basement membrane and extracellular matrix proteins that often regulate transcription to ensure the stem cell fate maintenance (Song et al., 2002; Gilboa et al., 2003; González-Reyes, 2003; Ward et al., 2006; Hayashi et al., 2009). TGF- β signaling is clearly one of the most important signaling pathways controlling the ovarian GSC population (Chen and McKearin, 2003; Song et al., 2004); it is activated in GSCs by the ligands Dpp and Gbb, which are sent from the niche. As a consequence of this activation, the differentiation factor Bag-of-marbles (Bam) is excluded from the GSCs. Bam is a master differentiation factor that is both necessary and sufficient to induce differentiation in the germline and thus is only expressed in differentiating germline cysts or cystoblasts (CBs) (McKearin and Ohlstein, 1995). In the germarium, there are at least three categories of germline cells (GCs) based on their differentiation state: the GSC maintains undifferentiated stem cell characteristics, the pre-CB lingers in a transient state between stemness and differentiation, and the differentiating CB commits to the egg production program. These

germline cell types are proportionally represented in the normal germarium: two to three GSCs, followed by one to three pre-CBs/CBs and four to five differentiating cysts typically are situated in the region 1–2A in the wild type germarium (Fig. 1A). Each germline cell type can be identified using different markers, among which are components of niche-derived TGF- β signaling. Stem cells express the phosphorylated TGF- β transcription factor Mad (pMad), which suppresses the differentiation factor *bam* expression, which is present in the differentiating cysts. Transient GSC progeny or pre-CBs express neither of these markers. In addition, all single cell germline types (GSCs, pre-CBs and CBs) have spherical fusomes (also called spectrosomes), while multicellular cysts are marked with elongated (2- and 4-cell cysts) and branched (8- and 10-cell cysts) fusomes (Lin et al., 1994; McKearin, 1997). Upon ecdysone signaling deficit, the differentiation index measured by the ratio between the numbers of fusome-containing (cysts) to spectrosome-containing germline cells (SpGCs) that do not express either stem cell or differentiation factors is significantly decreased (König et al., 2011). We named these supernumerary SpGCs as “limbo-GCs” due to their delayed in differentiation status (Fig. 1B).

The GSC ability to self-renew and differentiate is often regulated at the level of chromatin structure (Xi and Xie, 2005; Maines et al., 2007; Buszczak et al., 2009; Wang et al., 2011; Yan et al., 2014). Therefore, we analyzed several histone modifications that would be differentially displayed in GSCs vs differentiating cysts (supplementary material Fig. S1). Our analysis shows that the majority of histone modifications are present in both, the germline and soma. H3K20me3, H3K4me3, H3K36me2 and H3K27me3 are equally distributed among all somatic cell types in the germarium, while H3K9me2, H4K20me1 and H3K27me3 show differential expression in the CpCs, ECs and FCs. In the germline, 16-cell cysts have higher levels of H3K4me3, H3K36me2 and H4K20me1 than all other differentiating GCs. Among analyzed histone modifications, only monoubiquitination of the histone H2B (H2Bub1) was present in the differentiating germline, but not in stem cells (supplementary material Fig. S1; Fig. 1C). Previously, we have demonstrated that H2Bub1 modification is one of the events that precede entering the differentiation program (Karpiuk et al., 2012). H2Bub1 resolves the bivalency state of numerous genes, which are essential for stem cell progeny differentiation in multiple systems (Johnsen, 2012). Interestingly, the limbo-GCs in *ecd^{lts}* mutants are devoid of this histone modification and rather exhibit the stem cell-like chromatin state (Fig. 1C). To prove that this process is relevant to germline differentiation, we analyzed mutants for *Drosophila* E3 ubiquitin ligase dBre1 required for the histone H2B monoubiquitination (Bray et al., 2005; Mohan et al., 2010). dBre1 was shown to be important intrinsically for GSC maintenance and extrinsically for the germline differentiation (Xuan et al., 2013). Since the differentiating cells in the germarium showed H2Bub1, we considered that this histone modification could be also required intrinsically for efficient germline differentiation. Therefore, we induced *dBre1* loss-of-function clones and found that *dBre1* deficient GSCs that were not lost produced 1.8 times less progeny than control clonal GSCs (supplementary material Fig. S2B,C). Similar delay was observed when *dBre1* or *dRtf1*, the subunit of the Paf1 complex, which we found to be required for proper monoubiquitination of histone H2B in the germline (supplementary material Fig. S2D), were downregulated specifically in the germline (supplementary material Fig. S2E,F). Together, these findings suggest that histone H2B monoubiquitination via Bre1 or Rtf1 is important for



289

successful early germline differentiation. Additionally, we found a genetic interaction between ecdysone signaling and *dBre1* mutants, showing that these pathways are functionally related (Fig. 1D).

Interestingly, H2Bub1 spatial and quantitative expression pattern paralleled with Bam protein levels, implying a correlation between H2Bub1 histone modification and the differentiation factor *bam* expression (supplementary material Fig. S2A). Absence of Bam, similarly to steroid deficit, makes GSC progeny unable to differentiate, and *bam* mutant germline cells also lack all of the before-mentioned markers (McKearin and Ohlstein, 1995; Song et al., 2004). Despite this similarity in TGF- β component expression patterns, there is a critical difference between the limbo-GCs emerging due to *bam*- and ecdysone signaling deficit. While *bam* mutant germline cells have a differentiation block, ecdysone deficit merely causes a differentiation delay. To understand the rationale of this dissimilarity, we tested the H2Bub1 pattern in *bam* and *ecd* mutants and found that *ecd^{lts}* limbo-GCs do not contain H2Bub1, while *bam* limbo-GCs have this histone modification present, just like all other differentiating cells (Fig. 1C,E). These data show the clear distinction in the limbo-GC identity if caused by the TGF- β or steroid hormone signaling mutations. Ecdysone signaling mutant GSC progeny are kept at the pre-CB stage [(König et al., 2011); Fig. 1B], where chromatin is not yet properly modified to induce the differentiation program (e.g. *bam* expression). *bam* mutant GSC progeny successfully transit through the pre-CB stage (Fig. 1B), modifying chromatin into a ready to differentiate state; however, due to the lack of the major differentiation factor, Bam, these germline cells are not capable of proceeding to the differentiation program. This proposes that *bam* deficient germline cells are blocked in between the pre-CB and CB stage, which we named the “pro-CB” stage (Fig. 1B, GSC→pre-CB→pro-CB→CB). These data suggest that in the hierarchical sequence of events that take place during the transition from stemness to differentiation in the germline, ecdysone signaling operates upstream of Bam. If this is true, then the forced induction of *bam* expression should rescue the delayed differentiation phenotype of ecdysone signaling mutants. We simultaneously perturbed ecdysone signaling and promoted Bam through a combination of heat shock-inducible transgenes, *EcR^{hs}* and *bam^{hs}*. Forced *EcR* expression negatively regulates ecdysone signaling and causes germline differentiation delay (Schubiger and Truman, 2000; Schubiger et al., 2005; König et al., 2011) and forced *bam* expression leads to stem cell loss by differentiation (Ohlstein and McKearin, 1997) and enhances the germline differentiation index (Fig. 1F). We found that the germline differentiation delay caused by ecdysone signaling deficit was released, if Bam was provided. In *EcR^{hs}/bam^{hs}* germaria, the differentiation index was significantly increased in comparison to *EcR^{hs}* (Fig. 1F). This supports the idea that ecdysone-regulated entrance into the differentiation program operated at the level of chromatin modifications temporally precedes Bam-induced onset of germline differentiation.

Moreover, soma-specific ecdysone signaling perturbation also leads to the H2Bub1 absence in the limbo-GCs showing that ecdysone signaling influences early germline differentiation cell non-autonomously (Fig. 1G). Previously, we and others found that ecdysone signaling is predominantly active in the somatic cells of the germarium (Gancz et al., 2011; König et al., 2011; Morris and Spradling, 2012), here we wanted to decipher the mechanism of how steroids control germline differentiation through the surrounding soma.

EC function and morphology are impaired by ecdysone signaling perturbations

Ecdysone signaling is important for GSC niche formation during development, but also, for proper EC function during adult stages (Gancz et al., 2011; König et al., 2011; Morris and Spradling, 2012). We examined in a greater detail what happens with the somatic cells in the germaria, depleted of ecdysone signaling during adulthood. Somatic cells in the germarium are responsible not only for germarium architecture organization, mechanical support and physical protection of the germline cells, but they also actively participate in signaling that organizes a microenvironment for proper GSC maintenance and differentiation. For example, the stem cell niche cells (CpCs and, to a lesser extend, ECs) produce TGF- β ligands, required for female germline stemness (Xie and Spradling, 1998; Xie and Spradling, 2000; Eliazar et al., 2014). In contrast, somatic cells in the differentiation niche (ECs) are required to spatially restrict the stem cell niche activity and, as we propose here, to stimulate germline differentiation. Normally, ECs are terminally differentiated squamous epithelial cells that do not divide (Kirilly et al., 2011; Morris and Spradling, 2011); our analysis also revealed that less than 2% of control germaria contained an EC in S-phase marked by EdU (Fig. 2A). In contrast, ecdysone deficit stimulates ECs to proliferate; *ecd^{lts}* flies had 2.5 times more germaria containing ECs in S-phase of the cell cycle (Fig. 2A,B). The specificity of this systemic signaling in the germarial soma is achieved via cell-specific cofactors, Taiman (Tai) and Abrupt (Ab) (König et al., 2011). Tai is a co-activator of the ecdysone receptor complex that can be inhibited by the transcription factor Ab (Bai et al., 2000; Jang et al., 2009). Importantly, EC division phenotype is also seen when ecdysone signaling is perturbed in the soma only: Tai downregulation and Ab upregulation in the somatic cells similarly stimulated normally quiescent ECs to undergo divisions. Mutant ECs at different cell cycle stages were observed (Fig. 2C–E shows cells in S-, meta- and telophase, respectively). Moreover, these changes in EC characteristics were seen when ecdysone production and its signaling co-factors were altered during post-developmental stages (adult-implemented temperature shift for *ecd^{lts}* mutants and induction of temperature sensitive *Gal4/Gal80^{ts}* system for adult *tai* and *ab* misexpression). This suggests that the EC destiny as a terminally differentiated squamous epithelial cell is not permanently fixed. Instead, ECs can be transformed under certain conditions during adulthood to exhibit properties of active mitotic division. These cellular alterations could also affect the ability of the cell to properly send and receive signals necessary for early germline maintenance and differentiation.

To prove this assumption, firstly, we tested whether disruption of ecdysone signaling specifically in the stem cell niche cells would affect the TGF- β signaling strength. Both downregulation of ecdysone receptor co-activator *tai* and upregulation of its repressor *ab* in CpCs resulted in a decrease in TGF- β signaling, which could be directly measured via the intensity of antibody staining against pMad. The pMad levels were significantly decreased in GSCs that were located next to the stem cell niche, mutant for ecdysone signaling (Fig. 2F–H). This result demonstrates that upon ecdysone deficit, the GSC niche functions with a reduced efficiency.

Secondly, we tested whether disruption of ecdysone signaling specifically in the differentiation niche cells would affect the strength of the major epithelial pathway, epidermal growth factor

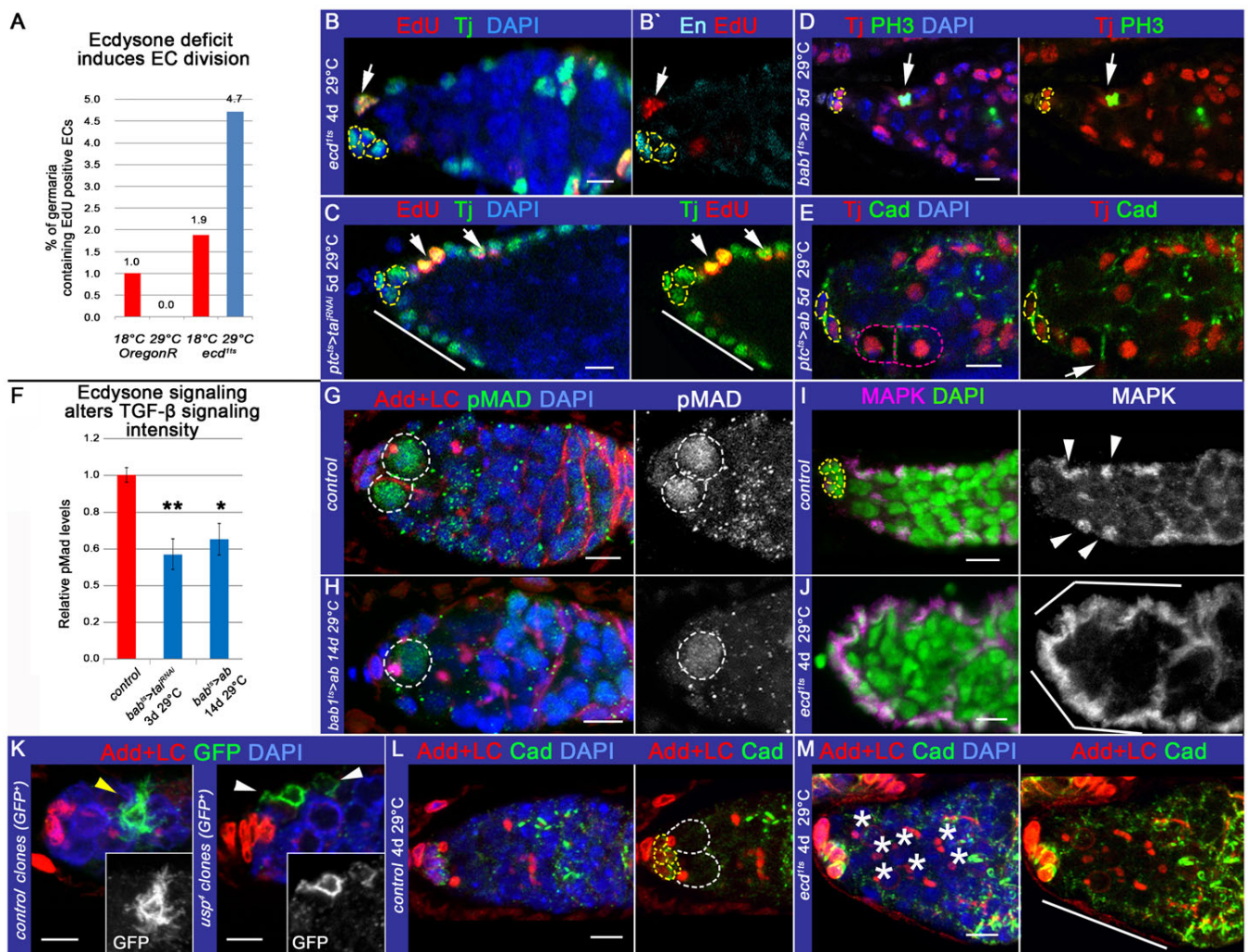


Fig. 2. EC function and morphology are impaired by cell-autonomous ecdysone signaling abolishment. (A,B) Perturbed ecdysone signaling induces ECs to divide. In control, less than 2% of germaria exhibit at least one EC in S-phase (*OregonR* 18°C: 1%, $n=99$; *ecd^{1ts}* 18°C: 1.9%, $n=106$), in *ecd^{1ts}* adult animals, 4.7% of germaria contain ECs in S-phase (*OregonR*, 4 days at 29°C: 0%, $n=69$; *ecd^{1ts}* 4 days at 29°C: 4.7%, $n=127$). (B–B') Note the appearance of the EC in S-phase marked by EdU staining. (C–E) Adult specific ecdysone signaling disruption in the soma by *ab* overexpression or *tai* downregulation using the soma-specific *Gal4* drivers (*ptcGal4* or *bab1Gal4*) together with the *Gal4/tubGal80^{ts}* system alters EC characteristics (*ptc^{ts}>tai^{RNAi}*: *ptcGal4/tai^{RNAi}*, *tubGal80^{ts}/+*, *bab1^{ts}>ab*: *tubGal80^{ts}/+*; *bab1Gal4/UASab*, and *ptc^{ts}>ab*: *ptcGal4/+*; *tubGal80^{ts}/UASab*, adults kept for 5 days at 29°C). ECs are clustered, resembling columnar epithelia (white line, C). Mutant ECs are also mitotically active; EdU staining shows the presence of ECs in S-phase of the cell cycle (C), and PH3 staining - in M-phase [metaphase (D) and telophase (E)]. (F–H) Upon soma-specific perturbation of ecdysone signaling, the relative pMad levels in the GSCs are decreased. pMad levels are measured by gray value (relative pMad levels, control: *tai^{RNAi}/+*: 1 ± 0.04 , $n=23$; *bab1^{ts}>tai^{RNAi}*: *tubGal80^{ts}/+*; *bab1Gal4/tai^{RNAi}*: 0.57 ± 0.08 , $n=10$, $p=1.48 \times 10^{-3}$; *bab1^{ts}>ab*: *tubGal80^{ts}/+*; *bab1Gal4/UASab*: 0.65 ± 0.08 , $n=12$, $p=7.04 \times 10^{-3}$). Control (G) and ecdysone signaling defective (H) germaria are shown to compare pMad levels in the GSCs (*OregonR* and *bab1^{ts}>ab*: *tubGal80^{ts}/+*; *bab1Gal4/UASab*, 14 days at 29°C). (I,J) In controls, Map Kinase (MAPK) stains nuclei and clearly defines cytoplasmic protrusions in ECs (arrowheads). In *ecd^{1ts}* adults, ECs do not form protrusions and show higher levels of MAPK (control: *OregonR*, 4 days at 29°C and *ecd^{1ts}*, 4 days at 29°C). (K) MARCM analysis illustrates cytoplasmic protrusions in ECs: clonal ECs are marked by GFP presence. Yellow arrowhead depicts control clonal EC (*w⁻/+*, *FRT 19A tubGal80*, *hsFlp/FRT 19A parental*; *UAS CD8GFP*, *tubGal4/+*); white arrowheads mark EC homozygous mutant for *usp*, the hetero-dimerization partner of EcR (*w⁻/+*, *FRT 19A tubGal80*, *hsFlp/FRT 19A usp⁴*; *UAS CD8GFP*, *tubGal4/+*). Note that protrusions of *usp* mutant ECs are less developed in comparison to control. (L,M) High levels of the cell adhesion protein DE-Cad are present on the CpC membranes in the control germarium (*OregonR*, 4 days at 29°C, L). In *ecd^{1ts}* (4 days at 29°C, M), higher DE-Cad levels are also detected at the EC membranes. Note that *ecd^{1ts}* germaria are filled with a large number of SpGCs delayed in differentiation (asterisks). Germaria are stained with EdU to mark S-phase (red, B,C), PH3 to mark mitotic division (green, D) and LaminC (LC red, G,H,K–M) to visualize TFs and CpCs and Adducin (Add red, G,H,K–M) to mark spectrosomes and fusomes. ECs are at the anterior of the germarium, and are positive for the somatic marker Traffic jam (Tj, green, B, C, red D, E) and negative for Engrailed (En, cyan, B'). EC protrusions are visualized using MAPK staining (magenta, I,J). Cadherin (Cad) marks cell adhesion complexes (green, E,L,M); pMad marks GSCs (green, G,H). ECs were marked with GFP⁺ clones (green, K). Nuclei are marked by DAPI (blue, B–H and K–M, green, I,J). CpCs are outlined in yellow, GSCs in white. Atypical epithelium is highlighted with white lines; mitotically active ECs are marked with white arrows (B–E), EC in telophase is outlined in pink (E). p-values were calculated using the two tailed Student's t-test and error bars represent S.E.M. * $p<0.05$, ** $p<0.005$, *** $p<0.0005$. Scale bars, 5 μ m.

receptor (EGFR), that acts in the somatic cells to maintain germline homeostasis. Importantly, compromised EGFR-activated mitogen-activated kinase (MAPK) signaling in ECs results in a similar increase in the SpGC number as is observed in ecdysone-deficient germaria (Liu et al., 2010). In ecdysone signaling mutant ECs, MAPK levels were dramatically elevated (Fig. 2I,J; supplementary material Fig. S3A–C), causing aberrant expression of its downstream targets (supplementary material Fig. S3D), which plausibly leads to sexual identity confusion of the somatic cells that compose the GSC and differentiation niches.

The abnormal signaling and behavior causes alterations in EC morphology. While in *controls*, ECs completely enfold germline cells with protrusions to protect differentiating cysts from niche signaling and guide them to the posterior end of the germarium, where the germline becomes encapsulated by the follicular epithelium, in *ecd^{lts}* mutants, these protrusions were not formed and the normally squamous ECs look more like cuboidal epithelial cells outlining the whole germarium (Fig. 2I,J; supplementary material Fig. S3). To visualize EC shape, we also induced MARCM single cell clones and found that in *controls*, the EC formed multiple delicate protrusions, while the EC, deficient for EcR co-receptor, *ultraspiracle* (*usp*) lacked these fine cellular structures (Fig. 2K). In addition, ecdysone signaling mutant ECs express higher amounts of cell adhesion molecules, e.g. DE-Cad and Arm (Fig. 2L,M; supplementary material Fig. S4), which is consistent with the alteration of their epithelial status. Collectively, these data show that ecdysone signaling deficit is sufficient to alter EC properties: they transform their cell cycle status from quiescent to active and take on a cuboidal rather than a squamous epithelial appearance.

Levels of Ab, a switch and a manager of epithelial gene expression must be fine-tuned in the germarial soma

Next, we wanted to understand what molecular mechanism induces transformation of epithelial somatic cells in the germarium and how this transformation can affect early germline differentiation. We turned our attention to the negative regulator of ecdysone signaling, the BTB-zinc finger transcription factor Ab, since it has been found to act even as a potent transdetermination factor that, when misexpressed, is capable of stimulating neuronal identity switch in the developing *Drosophila* brain or induce homeotic arista-leg transformation (Grieder et al., 2007; Kucherenko et al., 2012). In addition, multiple epithelial cell fate regulators have been shown to be direct targets of Ab global transcriptional regulation (Terkel et al., 2013). Similar to other BTB-containing proteins, Ab acts in a highly dosage-dependent manner; depending on the cellular concentration, it can form homo- and heterodimers, which allows for the establishment of both stable and transient interactions with multiple proteins (Hu et al., 1995; Stogios et al., 2005). This explains the ability of BTB-containing proteins to participate in multiple processes and proposes that management of their proper levels is of a particular significance (Kucherenko and Shcherbata, 2013). Previously, we showed that overexpression of Ab in the somatic cells of the germarium recapitulates all of the germline phenotypes associated with a deficit in ecdysone signaling (König et al., 2011). Now, we analyzed the effects of reduced Ab levels using different *ab* amorphic and hypomorphic allelic combinations. Surprisingly, Ab downregulation results in the same phenotypes as its upregulation: the SpGC number was increased, while the ratio between differentiating cysts and

SpGCs was decreased (Fig. 3A), confirming that fine-tuning of Ab levels is important for effective early germline differentiation.

An interesting question is therefore, how Ab levels are regulated in the germarial soma and via which molecular mechanisms its expression is coordinated with stress-responsive ecdysone signaling. Previously, it has been shown that Ab represses ecdysone signaling (Jang et al., 2009; König et al., 2011); interestingly, now we found that Ab expression levels itself depend on ecdysone signaling. In ecdysone-deficient flies, *ab* mRNA levels were more than three times higher than in *controls* (Fig. 3E). In addition, Ab protein cellular localization was altered: in *ecd^{lts}* mutant, almost all somatic cells in the germarium exhibited strong nuclear Ab pattern, while in *controls*, only sparse cytoplasmic staining was detected in rare somatic cells (Fig. 3B,C). This pattern changed upon stress; for example, in the wild type germaria analyzed after heat-shock, the majority of the somatic cells contained nuclear Ab, which was present in similar amounts to those found in ecdysone-depleted germaria (Fig. 3B–D). These data show that the BTB transcription factor Ab not only acts as a negative regulator of ecdysone signaling but that its levels are regulated by steroids and stress, which supports the existence of a feedback regulatory loop. Ab was confirmed as a *let-7* target *in vitro* and *in vivo* during pre-adult stages and we found that during metamorphosis, *let-7* miRNA acts as a mediator between Ab and ecdysone signaling in the nervous system (Burgler and Macdonald, 2005; Caygill and Johnston, 2008; Kucherenko et al., 2012). Therefore, we postulated that this regulation might also occur in adult gonads (Fig. 3F).

Steroid-dependent miRNA *let-7* targets Ab to adjust the ecdysone signaling strength and mediates stress response

It has been shown before that steroid-coupled regulation of *let-7* expression takes place during the developmental transition from larval-to-reproductive animals and in adult gonads (Sempere et al., 2002; Sempere et al., 2003; Garbuzov and Tatar, 2010; Chawla and Sokol, 2012; Kucherenko et al., 2012; Fagegaltier et al., 2014). To test whether *let-7* is expressed in the correct cell type to act as a transmitter of steroid-modulated response to stress to control oogenesis in adults, we firstly assayed *let-7* miRNA expression. We performed *in situ* hybridization using *let-7* LNA probe, which confirmed that, like ecdysone signaling components, the miRNA *let-7* is present in the germarial somatic cells (Fig. 4A).

Secondly, we analyzed whether *let-7* loss-of-function would phenocopy the germline phenotypes associated with the ecdysone-signaling deficit. We found that *let-7* deficient mutants, analogously to ecdysone signaling mutants, show retarded germline differentiation that can be restored via exogenous expression of a wild-type *let-7* construct and abnormal EC morphology (Fig. 4B–D). To prove that the *let-7* effect on GSC progeny differentiation is also cell non-autonomous, we induced *let-7* somatic clones and found that clonal ECs, similarly to ecdysone pathway mutants, have a columnar instead of squamous epithelium shape and this affects early germline differentiation (Fig. 4G). Consistent with the somatic *let-7* expression pattern, it does not have a cell autonomous role for GSC maintenance and differentiation (supplementary material Fig. S5A). Since *let-7* loss mimics the phenotypes associated with ecdysone signaling deficit, this implies that ecdysone signaling acts via the miRNA *let-7* to regulate the EC morphology that in turn controls the GSC progeny differentiation.

Thirdly, we analyzed whether Ab is the *bona fide* target of *let-7* in the ECs. We generated adult-induced *let-7* clones and analyzed the expression pattern and cellular localization of Ab protein

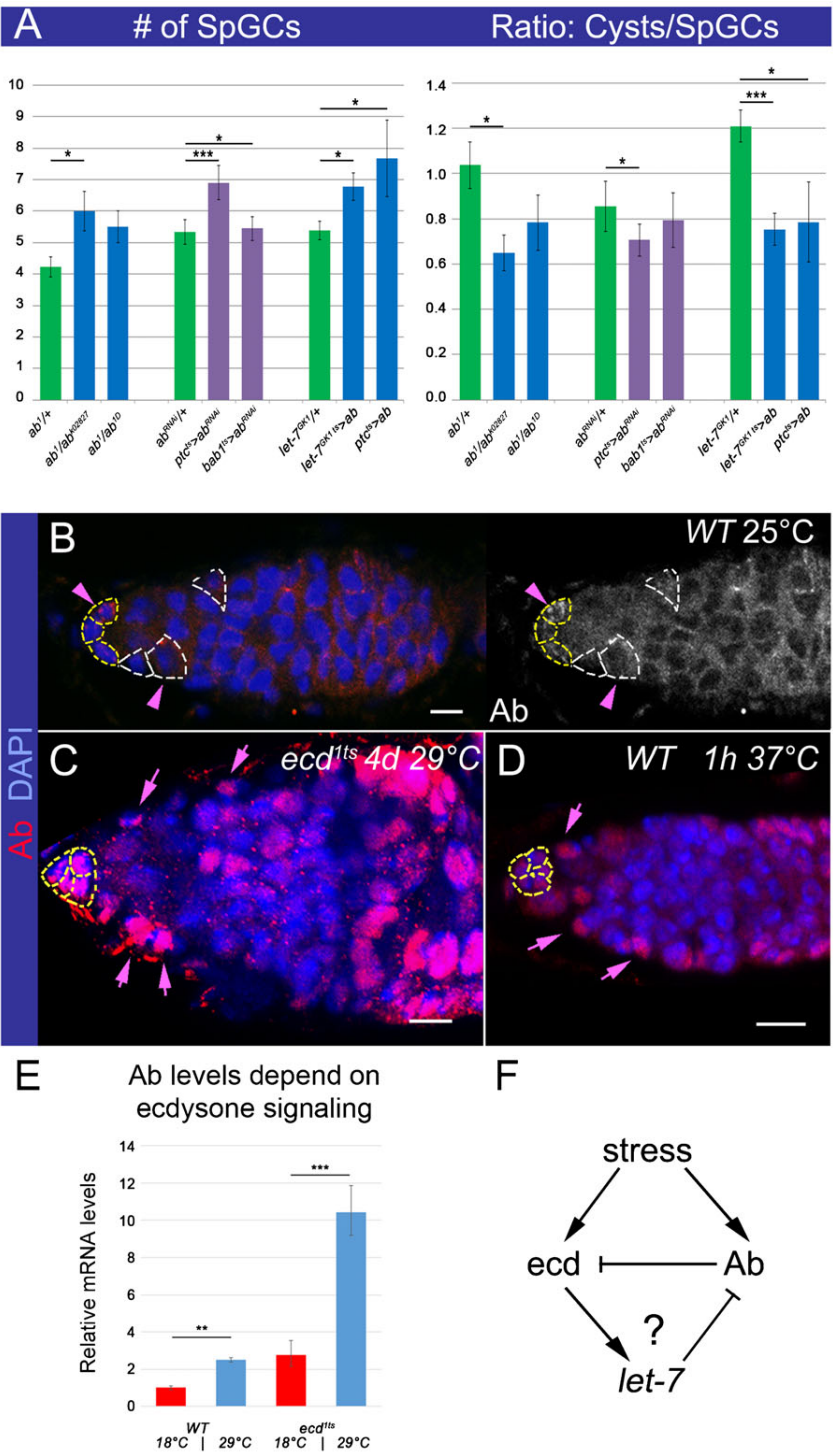


Fig. 3. Levels of the transcription factor Abrupt depend on ecdysone signaling and stress and are critical for its subcellular localization. (A) Decreased Ab levels result in the significantly increased number of SpGCs and lower Cysts/SpGCs ratio. Similar effects are observed upon soma-specific *ab* downregulation or overexpression (*ptc^{ts}>ab^{RNAi}*; *ptcGal4/ab^{RNAi}*; *tubGal80^{ts}/+*; *bab1^{ts}>ab^{RNAi}*; *tubGal80^{ts}/ab^{RNAi}*; *bab1Gal4/+*; *let-7^{GK1}ts>ab: let-7^{GK1}/+*; *tubGal80^{ts}/UASab* and *ptc^{ts}>ab: ptcGal4/+*; *tubGal80^{ts}/UASab*, 7 days at 29°C, see supplementary material Table S2). (B) In controls (*OregonR* at 25°C), Ab is only found in the cytoplasm of few somatic cells. ECs are marked with white and CpCs with yellow dashed lines. (C) Ecdysone-depleted or (D) temperature-stressed germaria show strong nuclear Ab staining in the somatic cells. Pink arrows depict strong nuclear and arrowheads cytoplasmic Ab staining in the somatic cells (*ecd^{1ts}*, 4 days at 29°C and *OregonR*, 1 h at 37°C). (E) The relative Ab mRNA levels are increased in *WT* flies kept at high temperature conditions (*OregonR*, 4 days at 18°C or 29°C). This tendency is even more pronounced in *ecd^{1ts}* flies (4 days at 18°C or 29°C, supplementary material Table S3). (F) Hypothetical scheme of the interplay between ecdysone signaling and Ab in response to stress. miRNA *let-7* ensures that the intensity of the steroid hormone ecdysone signaling in adult ovaries is adjusted via downregulation of *let-7* target Ab, which also is a negative regulator of ecdysone signaling. Germaria are stained with Ab (red, B–D), nuclei are marked with DAPI (blue, B–D). p-values were calculated using the two tailed Student’s t-test and error bars represent S.E.M. **p*<0.05, ***p*<0.005, ****p*<0.0005. Scale bars, 5 μm.

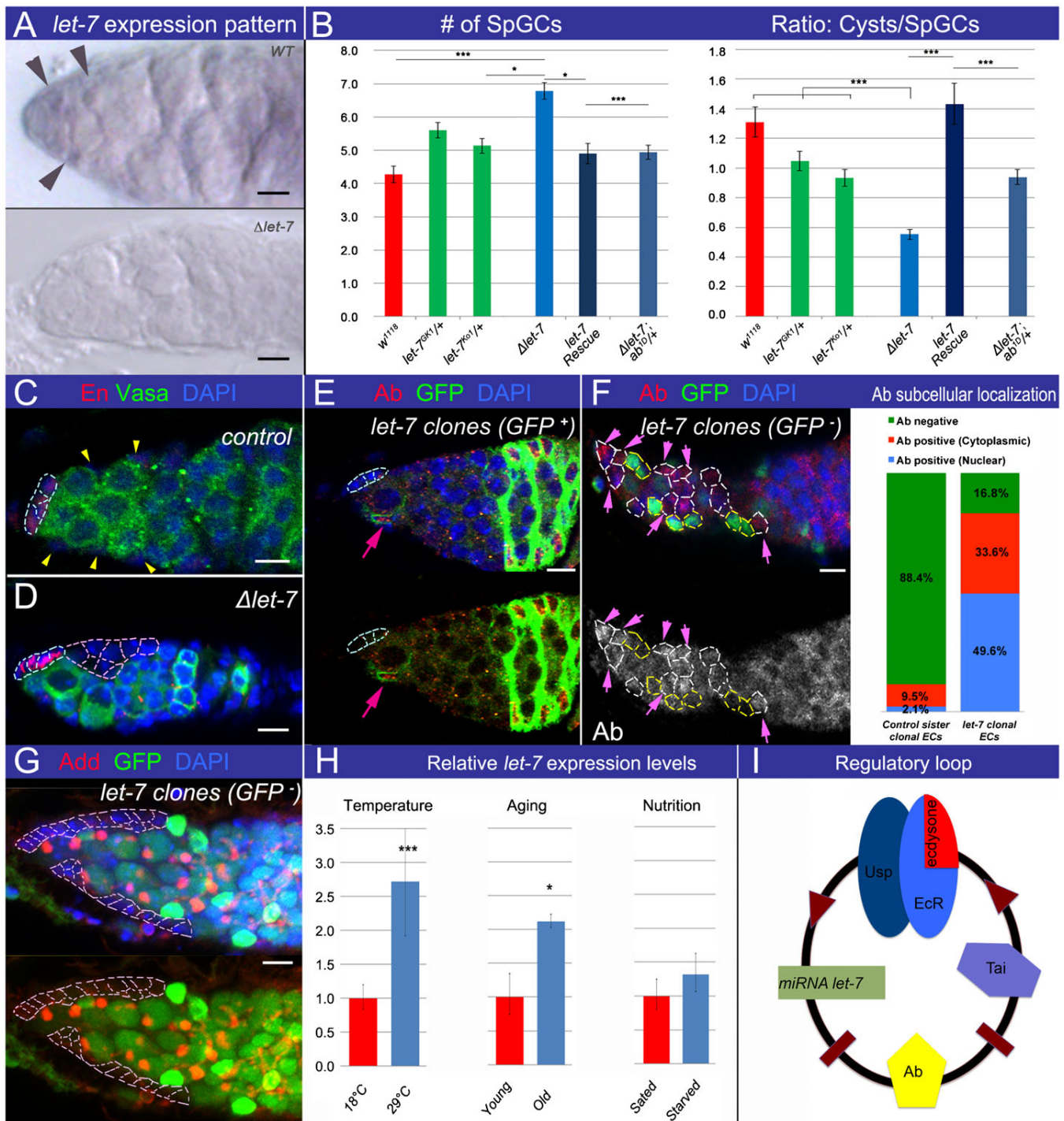


Fig. 4. See next page for legend.

using Ab specific antibody. *let-7* deficient ECs and follicle cells show high levels of nuclear Ab, indicating that Ab is a *let-7* target in these cells (Fig. 4E). Moreover, Ab overexpression explicitly in *let-7* expressing cells using *let-7* endogenous promoter recapitulates phenotypes associated with ecdysone signaling deficit and results in altered EC shape and delayed GSC progeny differentiation (supplementary material Fig. S4C,D), showing that these two studied components interact in the same

cell type. Also, reducing Ab levels by one copy in the *let-7* mutant background significantly rescued *let-7* phenotypes in the germlarium (Fig. 4B), confirming the specificity of this regulation in somatic ovarian cells.

Importantly, *let-7* presence in these cells is affecting Ab cellular localization. In control germlaria, this transcription factor is largely undetectable; only in ~10% of ECs a weak cytoplasmic staining was observed. However, of the *let-7* deficient cells,

Fig. 4. miRNA *let-7* targets Ab to modulate ecdysone signaling response.

(A) *let-7* LNA in situ hybridization shows that the mature miRNA is present in ECs of WT controls (arrowheads). (B) *let-7* deficiency ($\Delta let-7: let-7-C^{GK1}/let-7-C^{KO1}; let-7-C^{\Delta let-7}$) leads to delayed early germline differentiation, defined by an increased number of SpGCs and a decreased Cysts/SpGCs ratio. Restoring *let-7* expression (*let-7* Rescue: *let-7-C; let-7-C^{GK1}/let-7-C^{KO1}*) or reducing Ab levels in the *let-7* deficient background ($\Delta let-7; ab^{1D}/+; let-7, miR-125, ab^{1D}/let-7^{KO1}; let-7-C^{\Delta let-7}$) rescues this phenotype (supplementary material Table S2). (C,D) In control *OregonR*, single ECs (marked by absence of germline marker Vasa and CpC marker En, depicted with yellow arrowhead) reside along the germarial side. In $\Delta let-7$ mutants, ECs (marked by the absence of germline marker Vasa and CpC marker En, outlined in pink) clump together. (E) *let-7* MARCM clonal EC (marked by GFP presence, *hsFlp UAS CD8GFP; tubGal80 FRT 40A/let-7 miR-125 FRT 40A; tubGal4/let-7-C^{\Delta let-7}*) shows high Ab levels (nuclear). (F) The majority of control ECs (GFP-positive, green) are negative for Ab, a high percentage of *let-7* clonal ECs (GFP-negative, black, *hsFlp/+; FRT 40A GFP/FRT 40A let-7 miR-125; let-7-C^{\Delta let-7}/+*) display cytoplasmic or nuclear Ab. Bar graph shows the percentages of ECs that are Ab-negative or positive for cytoplasmic or nuclear Ab staining. About 50% of *let-7* ECs contain nuclear Ab in comparison to ~2% in controls ($n=96$ and 116 in *let-7* and control clonal ECs, respectively). (G) *let-7* clonal ECs (marked by the GFP absence, *hsFlp/+; FRT 40A GFP/FRT 40A let-7 miR-125; let-7-C^{\Delta let-7}/+*) form the columnar-like epithelium, outlining the anterior tip of the germarium. (H) Germaria, kept at 29°C or aged for 21 days have increased *let-7* levels. Different food conditions do not affect *let-7* levels (see supplementary material Table S4). (I) Scheme showing that in response to stress conditions, *let-7* is capable of generating a sharper threshold response to systemic signaling in the germarial soma via fine-tuning levels of the transcription factor Ab. ECs are located at the anterior of the germarium, and are negative for the CpC marker Engrailed (En, red, C,D) and the germline marker Vasa (green, C,D). Germaria are stained with Abrupt (Ab,E,F). Adducin (Add) marks spectrosomes and fusomes (red, G). GFP presence (E) or GFP absence (F,G) marks *let-7* mutant clones. Nuclei are marked with DAPI (blue, C–G). CpCs are outlined in cyan (C–E). Control ECs are marked with yellow arrowheads (C), *let-7* deficient EC epithelia are outlined in pink (D,G). *let-7* clonal ECs are outlined in white (F) and control sister ECs with yellow (F) dashed lines. Pink arrows indicate *let-7* deficient ECs with nuclear Ab (E,F). p-values were calculated using the two tailed Student's t-test and error bars represent S.E.M. * $p<0.05$, ** $p<0.005$, *** $p<0.0005$. Scale bars, 5 μ m.

~50% exhibit nuclear and ~30% cytoplasmic Ab staining (Fig. 4E,F). As mentioned before, Ab is a potent regulator of cell fate choices, in order to function as a transcription factor, Ab must localize to the nucleus. Our analyses prove that *let-7* miRNA is capable of targeting Ab in the germarial soma and reveal that in the *let-7* absence, Ab protein levels both increase and undergo altered cellular localization. Recall that nuclear Ab was also seen in ecdysone deficient and stressed wild type ovaries (Fig. 3B–D). Therefore, we propose that upon stress and ecdysone deficit, Ab acts as a regulator of gene expression to adjust function and form of epithelial cells of the germarium, which cell non-autonomously affects the germline differentiation speed. These data are an example of the interesting phenomenon, where transcription factor localization, hence activity, is regulated via miRNAs and steroids in response to stress.

Since Ab subcellular localization is altered due to stress and steroid deficit and ecdysone is considered as a stress hormone (Schwedes and Carney, 2012), we hypothesize that the ecdysone/*let-7*/Ab signaling cascade acts as a modulator of oogenesis in response to different external conditions, where *let-7* is capable of generating a sharper threshold response to systemic signaling in the germarial soma. To test this hypothesis, we analyzed *let-7* levels in the germaria at different stress conditions (heat-shock, aging, and starvation). Interestingly, *let-7* levels were significantly upregulated in the germaria in response to heat

stress and aging, but not to malnutrition, suggesting that miRNA *let-7* could be involved in a steroid-dependent adjustment of oogenesis progression in response to some conditions (Fig. 4H). Thus, depending on external conditions, ecdysteroid signaling regulates the early germline differentiation speed via miRNA *let-7* expression induction. Since this miRNA targets a negative ecdysteroid signaling regulator Ab, it suggests a model in which miRNA *let-7* intensifies the ecdysone signaling strength. Notably, stress (for example heat-shock) results in both, an increase in *let-7* expression and activation (nuclear localization) of its target, Ab (Fig. 3B,D and Fig. 4E,F). If there is more of *let-7*, Ab is downregulated and ecdysone signaling is “ON”; if there is more of Ab, ecdysone signaling (and subsequently *let-7*) is “OFF” (Fig. 4I). Thus, *let-7*-modulated adjustment of the ecdysone signaling strength in the germarial soma establishes a certain state of epithelium, defined by the activity of BTB transcription factor Ab. Therefore, we conclude that in the differentiation niche, steroid-induced miRNA *let-7* targets a key epidermal cell fate regulator Abrupt and reinforces ecdysone signaling via a positive feedback loop. We subsequently hoped to probe the mechanism underlying how steroid effects on soma influence germline differentiation.

Ecdysone signaling modulates differential cell adhesion between the soma and germline that modulates Wg signaling activity in the germline

We next wanted to understand what the nature of this cell non-autonomous signaling between the soma and germline is and when and under what conditions it actually functions. Since (1) Ab is a global regulator of epithelial cell state that is often defined by the specific cell adhesive characteristics and (2) abnormal amounts of cell adhesion proteins, including Cadherin and β -catenin (Fig. 1L,M; supplementary material Fig. S4A,B; Table S3), were detected in ecdysone signaling mutants, we hypothesized that the differential cell adhesion might be a language used for the germline and soma communication. Cadherins normally mediate homophilic adhesion between cells of the same type; however, occasionally cadherins can also be involved in heterotypic adhesion, such as between germline and somatic cells, which occurs across a range of species, including *Drosophila* (González-Reyes and St Johnston, 1998). As a signal transducer, cadherin operates via its binding partner β -catenin, which has a dual role as a mediator in the interplay of adherens junction proteins with the actin cytoskeleton and as a critical Wg signaling pathway component that has been shown to be involved in chromatin remodeling (Liu et al., 2008; Parker et al., 2008; Song et al., 2009; Mohan et al., 2010). A complex non-linear relation between β -catenin and cadherin levels, their subcellular distribution and Wg signaling has been shown in vitro and in vivo (Wodarz et al., 2006; Somorjai and Martinez-Arias, 2008), and proper balance between signaling vs adhesive functions is critical for normal development (Gottardi et al., 2001; Brembeck et al., 2006). Since it has been shown that in *Drosophila*, both Wg signaling and cell adhesion mediated by cadherins in the soma play a role in the earliest oogenesis stages (Forbes et al., 1996; Gottardi et al., 2001; Song and Xie, 2003; Brembeck et al., 2006; Sahai-Hernandez and Nystul, 2013) and our data demonstrate that levels of cadherin/ β -catenin complexes in the ovarian soma are changed in response to ecdysteroid levels, we tested whether ecdysone signaling via adjustment of cadherin and β -catenin levels can cell non-autonomously modulate the Wg signaling strength in the germline.

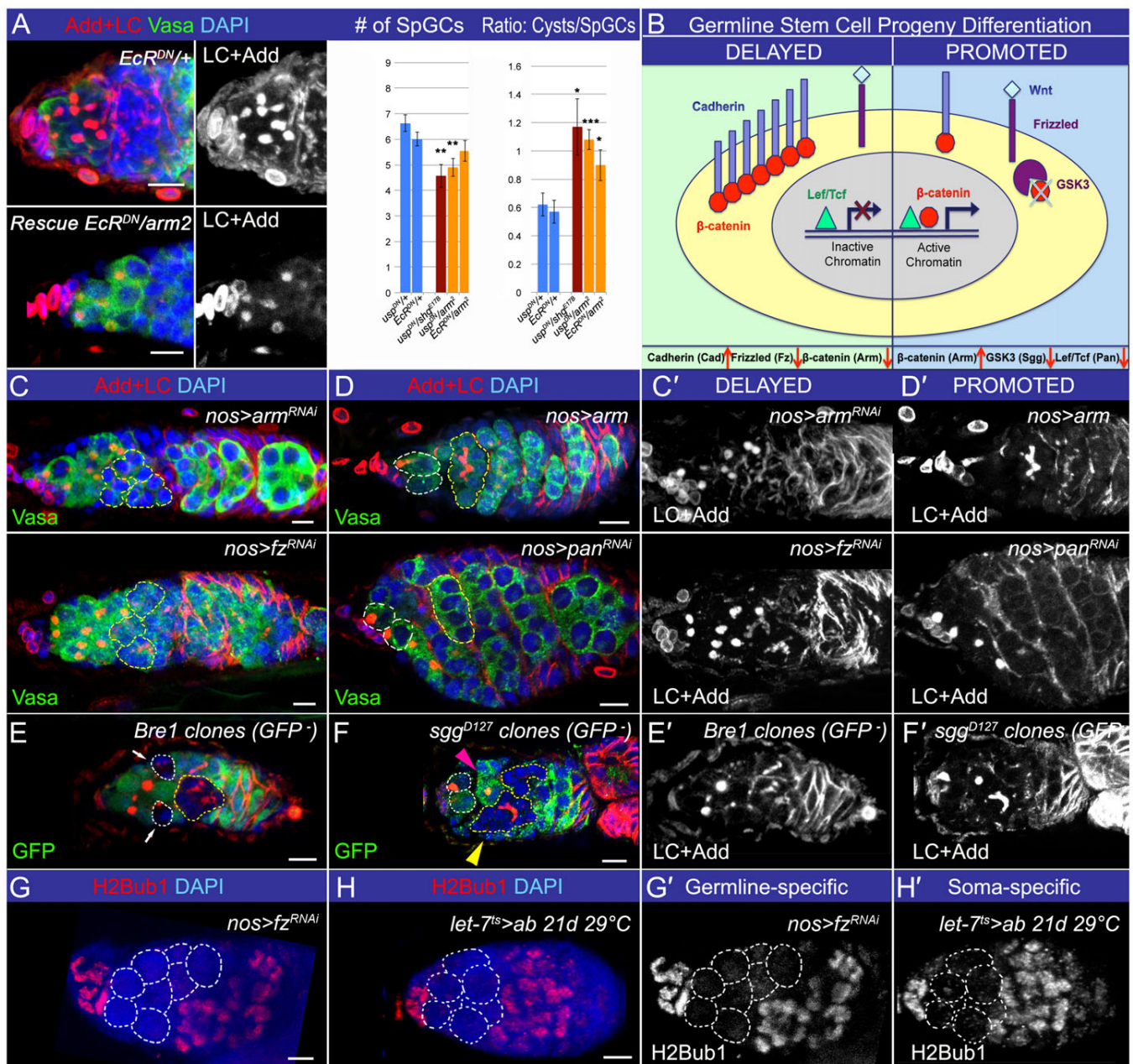


Fig. 5. Wg signaling cell autonomously influences the germline differentiation speed. (A) The defects caused by heat-shock induced overexpression of *usp^{DN}* or *EcR^{DN}* (increased number of SpGCs and decreased Cysts/SpGCs ratio) can be significantly alleviated by reducing the dose of *DE-Cad* or *arm* (*hs-Gal4-usp.LBD/+*, *hs-Gal4-EcR.LBD/+*, *hs-Gal4-usp.LBD/shg^{E187}*, *hs-Gal4-usp.LBD/arm²* and *hs-Gal4-EcR.LBD/arm²*, see supplementary material Table S2). (B) Scheme shows the presumable consequences of Wg signaling perturbation on the germline differentiation speed. (C,C') Downregulation of Wg signaling activity in the germline (*nos>fz^{RNAi}*: *NGT40/fz^{RNAi}*; *nanosGAL4/+* and *nos>arm^{RNAi}*: *NGT40/arm^{RNAi}*; *nanosGAL4/+*) increases the number of SpGCs delayed in differentiation, marked by the presence of the spectrosomes (dot-like Adducin (Add)-positive structures) (see supplementary material Tables S1, S5). (E,E') Similarly, germline *Bre1* mutant cysts (marked by the absence of GFP, *hsFlp*; *FRT 2A Bre1^{P1549}/FRT 2A GFP*) show delayed differentiation (marked by arrows). Additionally, 10% of germaria with *Bre1* mutant germline cysts contain dying cysts, which was not observed in control (see supplementary material Table S6). (D,D') In contrast, upregulation of Wg signaling activity in the germline (*nos>pan^{RNAi}*: *NGT40/pan^{RNAi}*; *nanosGAL4/+* and *nos>arm*: *NGT40/UASarm*; *nanosGAL4/+*) leads to premature germline differentiation, 8–16-cell cysts are observed already in region 1 of the germarium (see supplementary material Tables S1, S5). (F,F') The same is observed in *sgg* germline clones (*FRT 101 sgg^{D127}/FRT 101 GFP*; *hsFlp/+*, clones are marked by the absence of GFP). Note that *sgg* clonal germline cells containing a spherical spectrosome (pink arrowhead) and 16-cell cysts (yellow arrowhead) are found side by side (supplementary material Table S6). (G,G',H,H') Similar defects in H2Bub1 modification pattern are observed in supernumerary pre-CBs caused by either germline-specific Wg or soma-specific ecdysone signaling perturbations (Fig. 1G). Germaria are stained with LaminC (LC red, A,C–F) to visualize TFs and CpCs and Adducin (Add red, A, C–F) to mark spectrosomes and fusomes. Vasa marks germline (green, A,C,D). Absence of GFP (green, E,F) marks clonal mutant cells. Monoubiquitination of H2B is shown (red, G,H). Nuclei are marked with DAPI (blue, A,C–H). White dashed lines mark GSCs (D,F), differentiation delayed GCs (E) or GSCs and additional SpGCs (G,H). Yellow dashed lines depict differentiating cysts (C,D) or clonal mutant differentiating cysts (E,F). p-values were calculated using the two tailed Student's t-test and error bars represent S.E.M. **p*<0.05, ***p*<0.005, ****p*<0.0005. Scale bars, 5 μm.

Our data show that increased DE-Cad levels in ecdysone signaling-deficient ECs correlate with pre-CB differentiation delay (Fig. 2L–M; supplementary material Fig. S4). Importantly, we found that soma-specific reduction of DE-Cad or Arm levels in ecdysone mutant background rescues early germline differentiation phenotypes (Fig. 5A), while overexpression of DE-Cad in ECs phenocopies ecdysone signaling phenotype (supplementary material Fig. S4E); together demonstrating that ecdysone signaling and DE-Cad/Arm interact in the ECs. This observation suggests that readjustment of cadherin and β -catenin levels can mediate ecdysone-dependent cell adhesive characteristics that influence the germline differentiation progression.

One implication for this cell non-autonomous signaling is that in response to increase in DE-Cad in the soma, more DE-Cad would be recruited to adherens junctions in the germline. This would affect the cellular Arm distribution in the germline cells, tethering it to the cell membrane to be associated with DE-Cad (Fig. 5B). Normally, in the absence of Wg ligands, the cytoplasmic β -catenin pool is easily degraded by a complex containing APC, CKI, Axin, and GSK3/Shaggy(Sgg) (Kim et al., 2013). Upon Wg ligand binding to its receptors, such as Frizzled (Fz), a protein called Dishevelled (Dsh) is activated and leads to the Arm degrading complex inactivation. When the Arm degradation is inhibited, it allows its entrance to the nucleus, where Arm forms a complex with the Lef/TCF/Pangolin(Pan), activating the transcription of target genes (Chien et al., 2009). Without Arm, Lef/TCF/Pan together with their cofactors recruit histone deacetylases, triggering chromatin modifications that promote transcriptional silencing (Saito-Diaz et al., 2013). Upon Arm binding, multiple co-activators involved in chromatin remodeling are recruited, which stimulates transcription (Valenta et al., 2012). Since Arm pools involved in cell adhesion and Wg signaling exchange, we propose that differential cell adhesion between the germline and somatic cells affects the Wg signaling activity in the germline that regulates the GSC progeny chromatin state. If this hypothesis is right, we would expect that genetic manipulations that downregulate Wg signaling in the germline would delay, while Wg signaling overactivation would promote early germline differentiation (Fig. 5B).

To test this, we first examined whether Wg signaling is acting in the germline by specific Wg pathway components targeting in the germline, using recently created VALIUM20 *UAS RNAi* library and the germline specific *nanosGal4* driver. Downregulating Wg signaling (*UASFz^{RNAi}*, *UASarm^{RNAi}*) resulted in the appearance of huge ecdysoneless-like germaria, containing supernumerary limbo-GCs indicative of delayed differentiation (compare Fig. 5C and Fig. 1D, Fig. 2M, Fig. 4C). In contrast, increasing Wg pathway activity (*UASarm*, *UASsgg^{RNAi}*, *UASpan^{RNAi}*) accelerated germline differentiation. Precociously differentiating 8–16 cell cysts were seen already in region 1 (instead of 2B) of the germarium (Fig. 5D). Similar phenotypes were observed when germline clones lacking *arm* and *sgg* were analyzed; 6–13% of clonal germaria contained *arm* germline cysts delayed in differentiation, while 47% of clonal germaria contained *sgg* germline cysts precociously differentiating, as judged by the differentiation stage of non-clonal neighbors (Fig. 5F; supplementary material Table S6). These data show that Wg signaling acts in the germline to cell autonomously influence the early germline differentiation tempo. Similarly to Wg downregulation, germline-specific perturbations of H2Bub1

modification (*UASBrel^{RNAi}* and *UASRtf1^{RNAi}*) influenced the efficiency of germline differentiation (supplementary material Fig. S2; Table S1). Also, 20% of *dbel* clonal germaria contained cysts that were delayed in differentiation (Fig. 5E; supplementary material Table S6). Since Wg signaling has been shown to interact with chromatin remodelers (Liu et al., 2008; Parker et al., 2008; Song et al., 2009), we analyzed whether perturbed Wg signaling would affect the chromatin status of the germline cells. As expected, and in contrast to the cell non-autonomous function of steroid signaling, Wg signaling controls this process cell autonomously, since its germline-specific perturbation results in the H2Bub1-negative pre-CB accumulation (Fig. 5G,H). This supports the idea that intrinsic Wg signaling controls germline differentiation at the level of chromatin modification.

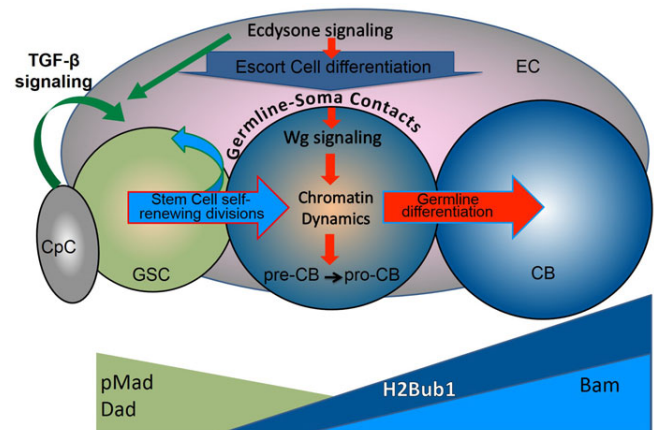


Fig. 6. Model showing ecdysone signaling function in early germline differentiation. The efficiency of early germline differentiation is managed by multiple proteins involved in different signaling pathways, which act in both the germline and soma. The GSC progeny differentiates in a sequential manner via specific transitional steps (GSC→pre-CB→pro-CB→CB) that are easily identified by the expression patterns of the specific markers. Importantly, these transitions between the germline differentiation stages in the germarium are controlled by signaling from the surrounding soma. As the stem cell niche (CpCs) controls the stemness of GSCs, the differentiation niche (ECs) coordinates the efficiency of GSC progeny differentiation with the status of the whole organism via systemic signaling. The GSC maintains its stem cell characteristics due to TGF- β signaling from the stem cell niche. Upon GSC division, its daughter is pushed away from the stem cell niche and, therefore, cannot receive sufficient TGF- β signaling to support the stem cell identity. However, being away from the niche is not enough to start the differentiation program. As the GSC progeny (pre-CB) is detached from the niche, its adhesive connection to the soma weakens; Cad levels are reduced. This releases Arm (β -catenin) from binding to Cad; instead, more Arm becomes available for Wg signaling, as Arm is not only involved in the cell adhesion in complex with Cad, but also, it is the transducer of Wg signaling. As the germline and soma are connected via homophilic cell adhesion, reduction of Cad levels results in strengthening of Wg signaling in the germline. Combination of decreased TGF- β and increased Wg signaling in the germline promotes chromatin modifications (e.g. H2Bub1) from the stem cell state into the differentiation-ready state, which endorses expression of the differentiation genes. The cell becomes the pro-CB, the key differentiation factor Bam begins to be expressed, initiating the differentiation processes in the germline. Importantly, the efficiency of these early germline differentiation events is modulated by systemic signaling. Particularly, ecdysone signaling cell autonomously alters somatic cell characteristics in the differentiation niche in response to stress, affecting adhesive contacts between the soma and germline, which, in turn, influences Wg signaling in the germline (CB). Thus, steroids cell non-autonomously affect the early steps of germline progression to coordinate the germline differentiation speed with the status of the whole organism.

Together these data demonstrate a communication flow, where the signal from the soma (ecdysone signaling-cell adhesion) induces in the germline a transition from stemness to differentiation, which requires a specific histone modification that promotes the expression of differentiation genes, enabling efficient GSC progeny differentiation (cell adhesion-Wg signaling-H2Bub1-Bam) (Fig. 6). Importantly, ecdysone and Wg signaling alterations or H2Bub1 histone modification do not cause a complete germline differentiation block, just a delay. This supports the idea that described here mechanism provides an additional layer of adult oogenesis regulation that is used to fine-tune the GSC progeny differentiation tempo in response to organism fitness fluctuations caused by internal and external environment changes.

DISCUSSION

In summary, our results show a cooperative function between hormonal steroid and Wg signaling in the fine-tuning of the early germline differentiation speed in response to variations in the organism physiology and environmental conditions. Ecdysone signaling robustness is conferred via the *let-7* miRNA feedback loop: *let-7* expression is ecdysone-dependent, while the *let-7* target Ab is a negative ecdysone signaling regulator. This allows upon *let-7* expression to enhance the steroid signaling strength, which then cell autonomously adjusts EC characteristics and cell non-autonomously influences the early germline differentiation speed. This regulation occurs via differential cell adhesion between the germline and soma that, in turn, modifies the Wg signaling strength in the germline (Fig. 6). The balance in Wg pathway activity is important for normal germline differentiation, since Wg overactivation stimulates premature germline differentiation, while Wg downregulation slows-down the process. These data for the first time reveal that Wg signaling has cell autonomous role in the *Drosophila* germline. It is important to stress that neither Wg signaling in the germline, nor ecdysone signaling in the soma are absolutely required for germline progeny differentiation, both pathways just add an additional layer of regulation, possibly interacting with other pathways, which would result in formation of a complex regulatory network that fine-tunes the efficiency of egg maturation in accordance with alterations in the external and internal environment of the organism.

Multiple studies propose that the GSC progeny differentiates by performing an orderly sequence of steps that are defined by expression of multiple factors (Fig. 6). The GSC maintains its stem cell identity due to signaling from the niche. Its daughter is pushed away from the niche, does not receive the sufficient amount of stem cell niche signaling and is transformed into the pre-CB. The pre-CB starts to modify its chromatin and becomes committed to differentiate, turning into the pro-CB. The pro-CB has all the conditions necessary for expression of differentiation genes. The key differentiation factor starts to be expressed and the cell is transformed into the CB. Thus, complex sequences of cellular transformation steps are required to produce the mature egg, many of which are already happening in the germarium and influenced by the surrounding soma that assembles the stem cell and the differentiation niches that can sense and transduce the extracellular signals to coordinate the tempo of germline differentiation.

Principally, our data demonstrate that oogenesis is a highly regulated process that depends on external and internal status of the female and that systemic signaling coordinates the oogenesis

speed depending on these conditions. Steroids act in the soma and cell non-autonomously and, via the direct cell adhesion-based soma-germline communication, govern germline differentiation. If conditions are unfavorable, insufficient steroid signaling can delay the GSC progeny in the pre-CB state, meaning that the cell is caught in the in-between stem cell and differentiating cell transition. This delayed cell does not receive the stem cell niche signaling anymore (because it is detached from the niche), but it also does not receive the signal to differentiate that, as we propose here, is generated in the differentiation niche (ECs) in response to ecdysone signaling. This signal is extremely dosage-dependent and, as we show here, multiple pathways can add to its implementation (supplementary material Fig. S6). Biologically, this makes sense, since this information controls the reproductive efficiency and thus, the success of organism survival. However, steroids are not the sole regulators of the process. It is known that oogenesis is an energy demanding process and strongly depends on the nutritional state. Kept on rich food, flies produce 60 times more eggs than those on poor food (Drummond-Barbosa and Spradling, 2001). Insulin signaling and other pathways were shown to mediate the response to food availability; GSCs and FSCs respond to the nutritional conditions by adjusting their proliferative rate (Biteau et al., 2010). Two systemic signaling pathways, insulin and ecdysone regulate the oogenesis efficiency, however act upon different cell types and germline progression stages. Interestingly, upon starvation, oogenesis is blocked at stage 8 and most of the dramatically decreased egg production rate seems to result from an increased degeneration of later egg chambers (Drummond-Barbosa and Spradling, 2001). Ecdysone is produced in older follicles that passed the stages 8–9 and is required to progress past this master checkpoint (Buszczak et al., 1999; Carney and Bender, 2000). Thus, there are two independent checkpoints that control the oogenesis progression: at stage 8, an insulin-dependent or “nutritional checkpoint” that influences the GSC division speed, and at stage 8–9 an ecdysone-dependent or “stress checkpoint” that influences the GSC progeny differentiation speed. Ecdysone control of germline development, therefore, presents a positive feedback mechanism with which germline development in the germarium is synchronized with the presence or absence of older follicles. Together, orchestrated regulation of oogenesis executed by insulin and ecdysone hormones reassures that the germline differentiation speed is perfectly attuned to external and internal cues.

The cell is what it is because it expresses a certain combination of genes that establish its form and function. Not surprisingly, control of the quantity and quality of gene expression is key for the cell morphology establishment and cellular signal transduction. We show that in the ovary, the differentiation niche, comprised of specifically shaped ECs exists and that the shape of these cells regulates the differentiation ability of the neighboring GSC progeny. The EC shape and function are dramatically impaired in ecdysone signaling mutants: the squamous ECs line the germarium and form long cytoplasmic protrusions that envelop the developing germline cells. However, if ecdysone signaling is perturbed, ECs form layers that resemble columnar epithelium. In addition, thin cytoplasmic protrusions are no longer present and the levels of cell adhesion proteins are elevated. Earlier experiments already demonstrated how critical EC protrusions are: if the protrusion formation is inhibited specifically in the ECs – for example via interfering with the cytoskeleton – the germline differentiation is affected and a larger number of SpGCs was detected (Decotto and Spradling, 2005;

Wang et al., 2008; Kirilly et al., 2011). A lack of EC protrusions therefore can cause a differentiation delay in the germline and we propose that EC malformation, and specifically the absence of protrusions, contributes to the differentiation delay observed in the germline. How exactly EC protrusions enable germline differentiation has previously been poorly understood; it was thought that they physically shield differentiating germline cells against diffusible signals from the anterior CpCs, forming another barrier to locally restrict TGF- β signaling. Now we show that the EC's ability to form protrusions depends on levels of cell adhesion proteins. Due to homophilic cell adhesion rules, alterations in cell adhesion protein quantities and qualities in the soma lead to the readjustment of these in the adjacent germline, as cadherin levels must perfectly match, this information is conveyed to the germline. Cell adhesion proteins are not only involved in establishment of cell connections, they also participate in intercellular signaling (Edeleva and Shcherbata, 2013), particularly, β -catenin is the binding partner of a homophilic cell adhesion receptor DE-Cad and the effector of the canonical Wg/Wnt signaling pathway (MacDonald et al., 2009). Since β -catenin pools involved in both processes are interchangeable, an increase or decrease in β -catenin involvement in cell adhesion would affect pools available for Wg signaling, subsequently readjusting the Wg pathway efficiency (Valenta et al., 2012). This pathway is one of the key developmental pathways that, via its interaction with the histone modification machinery, globally regulates gene expression (Saito-Diaz et al., 2013). Therefore, by simply changing one cell type's morphology, the transcriptional status of the juxtaposed cell could be affected. This kind of regulation is especially attractive for communication between cells of different types that are joining together to build a tissue or an organ and have to coordinate their signaling in order to function in unison. In particular, such heterotypic cell interaction modes are interesting in the regulation of stem cell maintenance and stem cell progeny differentiation via niches in response to systemic organismal demands.

Acknowledgements

We thank Laura Johnston, Nicholas Sokol, Frank Hirth, Stephen Crews, Dennis McKearin, Andreas Wodarz, Todd Nystul, Ken Cadigan, Sarah Bray for flies and reagents, Naomi Latorraca and Roman Shcherbaty for comments on the manuscript, Toni Bäuml for work on Wg experiments, the Herbert Jäckle Department, Steven Johnsen, Wolfgang Fischle, and the Shcherbata lab for discussions.

Competing interests

The authors declare no competing or financial interests.

Author contributions

HRS and AK: research plan; data acquisition, analysis, and interpretation; manuscript draft, figure design.

Funding

This work was supported by the Max Planck Society.

References

Bai, J., Uehara, Y. and Montell, D. J. (2000). Regulation of invasive cell behavior by taiman, a Drosophila protein related to AIB1, a steroid receptor coactivator amplified in breast cancer. *Cell* **103**, 1047–1058.

Biteau, B., Karpac, J., Supoyo, S., Degennaro, M., Lehmann, R. and Jasper, H. (2010). Lifespan extension by preserving proliferative homeostasis in Drosophila. *PLoS Genet.* **6**, e1001159.

Boyer, A., Goff, A. K. and Boerboom, D. (2010). WNT signaling in ovarian follicle biology and tumorigenesis. *Trends Endocrinol. Metab.* **21**, 25–32.

Bray, S., Musisi, H. and Bienz, M. (2005). Bre1 is required for Notch signaling and histone modification. *Dev. Cell* **8**, 279–286.

Brembeck, F. H., Rosário, M. and Birchmeier, W. (2006). Balancing cell adhesion and Wnt signaling, the key role of beta-catenin. *Curr. Opin. Genet. Dev.* **16**, 51–59.

Burgler, C. and Macdonald, P. M. (2005). Prediction and verification of microRNA targets by MovingTargets, a highly adaptable prediction method. *BMC Genomics* **6**, 88.

Buszczak, M., Freeman, M. R., Carlson, J. R., Bender, M., Cooley, L. and Segaves, W. A. (1999). Ecdysone response genes govern egg chamber development during mid-oogenesis in Drosophila. *Development* **126**, 4581–4589.

Buszczak, M., Paterno, S. and Spradling, A. C. (2009). Drosophila stem cells share a common requirement for the histone H2B ubiquitin protease scrawny. *Science* **323**, 248–251.

Carney, G. E. and Bender, M. (2000). The Drosophila ecdysone receptor (EcR) gene is required maternally for normal oogenesis. *Genetics* **154**, 1203–1211.

Caygill, E. E. and Johnston, L. A. (2008). Temporal regulation of metamorphic processes in Drosophila by the let-7 and miR-125 heterochronic microRNAs. *Curr. Biol.* **18**, 943–950.

Chau, J., Kulnane, L. S. and Salz, H. K. (2009). Sex-lethal facilitates the transition from germline stem cell to committed daughter cell in the Drosophila ovary. *Genetics* **182**, 121–132.

Chawla, G. and Sokol, N. S. (2012). Hormonal activation of let-7-C microRNAs via EcR is required for adult Drosophila melanogaster morphology and function. *Development* **139**, 1788–1797.

Chen, D. and McKearin, D. M. (2003). A discrete transcriptional silencer in the bam gene determines asymmetric division of the Drosophila germline stem cell. *Development* **130**, 1159–1170.

Chien, A. J., Moore, E. C., Lonsdorf, A. S., Kulikaukas, R. M., Rothberg, B. G., Berger, A. J., Major, M. B., Hwang, S. T., Rimm, D. L. and Moon, R. T. (2009). Activated Wnt/beta-catenin signaling in melanoma is associated with decreased proliferation in patient tumors and a murine melanoma model. *Proc. Natl. Acad. Sci. USA* **106**, 1193–1198.

Clevers, H. and Nusse, R. (2012). Wnt/ β -catenin signaling and disease. *Cell* **149**, 1192–1205.

Decotto, E. and Spradling, A. C. (2005). The Drosophila ovarian and testis stem cell niches: similar somatic stem cells and signals. *Dev. Cell* **9**, 501–510.

Drummond-Barbosa, D. and Spradling, A. C. (2001). Stem cells and their progeny respond to nutritional changes during Drosophila oogenesis. *Dev. Biol.* **231**, 265–278.

Edeleva, E. V. and Shcherbata, H. R. (2013). Stress-induced ECM alteration modulates cellular microRNAs that feedback to readjust the extracellular environment and cell behavior. *Front. Genet.* **4**, 305.

Eliazar, S., Palacios, V., Wang, Z., Kollipara, R. K., Kittler, R. and Buszczak, M. (2014). Lsd1 restricts the number of germline stem cells by regulating multiple targets in escort cells. *PLoS Genet.* **10**, e1004200.

Fagegaltier, D., König, A., Gordon, A., Lai, E. C., Gingeras, T. R., Hannon, G. J. and Shcherbata, H. R. (2014). A genome-wide survey of sexually dimorphic expression of Drosophila miRNAs identifies the steroid hormone-induced miRNA let-7 as a regulator of sexual identity. *Genetics* **198**, 647–668.

Forbes, A. J., Spradling, A. C., Ingham, P. W. and Lin, H. (1996). The role of segment polarity genes during early oogenesis in Drosophila. *Development* **122**, 3283–3294.

Gancz, D., Lengil, T. and Gilboa, L. (2011). Coordinated regulation of niche and stem cell precursors by hormonal signaling. *PLoS Biol.* **9**, e1001202.

Garbuzov, A. and Tatar, M. (2010). Hormonal regulation of Drosophila microRNA let-7 and miR-125 that target innate immunity. *Fly (Austin)* **4**, 306–311.

Gilboa, L., Forbes, A., Tazuke, S. I., Fuller, M. T. and Lehmann, R. (2003). Germ line stem cell differentiation in Drosophila requires gap junctions and proceeds via an intermediate state. *Development* **130**, 6625–6634.

Gönczy, P. (2008). Mechanisms of asymmetric cell division: flies and worms pave the way. *Nat. Rev. Mol. Cell Biol.* **9**, 355–366.

González-Reyes, A. (2003). Stem cells, niches and cadherins: a view from Drosophila. *J. Cell Sci.* **116**, 949–954.

González-Reyes, A. and St Johnston, D. (1998). The Drosophila AP axis is polarised by the cadherin-mediated positioning of the oocyte. *Development* **125**, 3635–3644.

Gottardi, C. J., Wong, E. and Gumbiner, B. M. (2001). E-cadherin suppresses cellular transformation by inhibiting beta-catenin signaling in an adhesion-independent manner. *J. Cell Biol.* **153**, 1049–1060.

Grieder, N. C., Charlafti, I., Kloter, U., Jäckle, H., Schäfer, U. and Gehring, W. J. (2007). Misexpression screen in Drosophila melanogaster aiming to reveal novel factors involved in formation of body parts. *Genetics* **175**, 1707–1718.

Hayashi, Y., Kobayashi, S. and Nakato, H. (2009). Drosophila glypicans regulate the germline stem cell niche. *J. Cell Biol.* **187**, 473–480.

Hu, S., Fambrough, D., Atashi, J. R., Goodman, C. S. and Crews, S. T. (1995). The Drosophila abrupt gene encodes a BTB-zinc finger regulatory protein that controls the specificity of neuromuscular connections. *Genes Dev.* **9**, 2936–2948.

Jang, A. C., Chang, Y. C., Bai, J. and Montell, D. (2009). Border-cell migration requires integration of spatial and temporal signals by the BTB protein Abrupt. *Nat. Cell Biol.* **11**, 569–579.

Johnsen, S. A. (2012). The enigmatic role of H2Bub1 in cancer. *FEBS Lett.* **586**, 1592–1601.

- Karpiuk, O., Najafova, Z., Kramer, F., Hennion, M., Galonska, C., König, A., Snaidero, N., Vogel, T., Shchebet, A., Begus-Nahrmann, Y. et al. (2012). The histone H2B monoubiquitination regulatory pathway is required for differentiation of multipotent stem cells. *Mol. Cell* **46**, 705–713.
- Kim, W., Kim, M. and Jho, E. H. (2013). Wnt/ β -catenin signalling: from plasma membrane to nucleus. *Biochem. J.* **450**, 9–21.
- Kirilly, D., Wang, S. and Xie, T. (2011). Self-maintained escort cells form a germline stem cell differentiation niche. *Development* **138**, 5087–5097.
- König, A. and Shcherbata, H. R. (2013). Visualization of adult stem cells within their niches using the *Drosophila* germline as a model system. *Methods Mol. Biol.* **1035**, 25–33.
- König, A., Yatsenko, A. S., Weiss, M. and Shcherbata, H. R. (2011). Ecdysteroids affect *Drosophila* ovarian stem cell niche formation and early germline differentiation. *EMBO J.* **30**, 1549–1562.
- Kucherenko, M. M. and Shcherbata, H. R. (2013). Steroids as external temporal codes act via microRNAs and cooperate with cytokines in differential neurogenesis. *Fly (Austin)* **7**, 173–183.
- Kucherenko, M. M., Barth, J., Fiala, A. and Shcherbata, H. R. (2012). Steroid-induced microRNA let-7 acts as a spatio-temporal code for neuronal cell fate in the developing *Drosophila* brain. *EMBO J.* **31**, 4511–4523.
- Li, R. and Albertini, D. F. (2013). The road to maturation: somatic cell interaction and self-organization of the mammalian oocyte. *Nat. Rev. Mol. Cell Biol.* **14**, 141–152.
- Lin, H., Yue, L. and Spradling, A. C. (1994). The *Drosophila* fusome, a germline-specific organelle, contains membrane skeletal proteins and functions in cyst formation. *Development* **120**, 947–956.
- Liu, Y. I., Chang, M. V., Li, H. E., Barolo, S., Chang, J. L., Blauwkamp, T. A. and Cadigan, K. M. (2008). The chromatin remodelers ISWI and ACF1 directly repress Wingless transcriptional targets. *Dev. Biol.* **323**, 41–52.
- Liu, M., Lim, T. M. and Cai, Y. (2010). The *Drosophila* female germline stem cell lineage acts to spatially restrict DPP function within the niche. *Sci. Signal.* **3**, ra57.
- López-Onieva, L., Fernández-Miñán, A. and González-Reyes, A. (2008). Jak/Stat signalling in niche support cells regulates dpp transcription to control germline stem cell maintenance in the *Drosophila* ovary. *Development* **135**, 533–540.
- Losick, V. P., Morris, L. X., Fox, D. T. and Spradling, A. (2011). *Drosophila* stem cell niches: a decade of discovery suggests a unified view of stem cell regulation. *Dev. Cell* **21**, 159–171.
- MacDonald, B. T., Tamai, K. and He, X. (2009). Wnt/ β -catenin signaling: components, mechanisms, and diseases. *Dev. Cell* **17**, 9–26.
- Maines, J. Z., Park, J. K., Williams, M. and McKearin, D. M. (2007). Stonewalling *Drosophila* stem cell differentiation by epigenetic controls. *Development* **134**, 1471–1479.
- McKearin, D. (1997). The *Drosophila* fusome, organelle biogenesis and germ cell differentiation: if you build it.... *BioEssays* **19**, 147–152.
- McKearin, D. and Ohlstein, B. (1995). A role for the *Drosophila* bag-of-marbles protein in the differentiation of cystoblasts from germline stem cells. *Development* **121**, 2937–2947.
- Mohan, M., Herz, H. M., Takahashi, Y. H., Lin, C., Lai, K. C., Zhang, Y., Washburn, M. P., Florens, L. and Shilatifard, A. (2010). Linking H3K79 trimethylation to Wnt signaling through a novel Dot1-containing complex (DotCom). *Genes Dev.* **24**, 574–589.
- Morris, L. X. and Spradling, A. C. (2011). Long-term live imaging provides new insight into stem cell regulation and germline-soma coordination in the *Drosophila* ovary. *Development* **138**, 2207–2215.
- Morris, L. X. and Spradling, A. C. (2012). Steroid signaling within *Drosophila* ovarian epithelial cells sex-specifically modulates early germ cell development and meiotic entry. *PLoS ONE* **7**, e46109.
- Murray, S. M., Yang, S. Y. and Van Doren, M. (2010). Germ cell sex determination: a collaboration between soma and germline. *Curr. Opin. Cell Biol.* **22**, 722–729.
- Ohlstein, B. and McKearin, D. (1997). Ectopic expression of the *Drosophila* Bam protein eliminates oogenic germline stem cells. *Development* **124**, 3651–3662.
- Parker, D. S., Ni, Y. Y., Chang, J. L., Li, J. and Cadigan, K. M. (2008). Wingless signaling induces widespread chromatin remodeling of target loci. *Mol. Cell Biol.* **28**, 1815–1828.
- Sahai-Hernandez, P. and Nystul, T. G. (2013). A dynamic population of stromal cells contributes to the follicle stem cell niche in the *Drosophila* ovary. *Development* **140**, 4490–4498.
- Saito-Diaz, K., Chen, T. W., Wang, X., Thorne, C. A., Wallace, H. A., Page-McCaw, A. and Lee, E. (2013). The way Wnt works: components and mechanism. *Growth Factors* **31**, 1–31.
- Schubiger, M. and Truman, J. W. (2000). The RXR ortholog USP suppresses early metamorphic processes in *Drosophila* in the absence of ecdysteroids. *Development* **127**, 1151–1159.
- Schubiger, M., Carré, C., Antoniewski, C. and Truman, J. W. (2005). Ligand-dependent de-repression via EcR/USP acts as a gate to coordinate the differentiation of sensory neurons in the *Drosophila* wing. *Development* **132**, 5239–5248.
- Schwedes, C. C. and Carney, G. E. (2012). Ecdysone signaling in adult *Drosophila melanogaster*. *J. Insect Physiol.* **58**, 293–302.
- Sempere, L. F., Dubrovsky, E. B., Dubrovskaya, V. A., Berger, E. M. and Ambros, V. (2002). The expression of the let-7 small regulatory RNA is controlled by ecdysone during metamorphosis in *Drosophila melanogaster*. *Dev. Biol.* **244**, 170–179.
- Sempere, L. F., Sokol, N. S., Dubrovsky, E. B., Berger, E. M. and Ambros, V. (2003). Temporal regulation of microRNA expression in *Drosophila melanogaster* mediated by hormonal signals and broad-Complex gene activity. *Dev. Biol.* **259**, 9–18.
- Shcherbata, H. R., Althausen, C., Findley, S. D. and Ruohola-Baker, H. (2004). The mitotic-to-endocycle switch in *Drosophila* follicle cells is executed by Notch-dependent regulation of G1/S, G2/M and M/G1 cell-cycle transitions. *Development* **131**, 3169–3181.
- Shcherbata, H. R., Ward, E. J., Fischer, K. A., Yu, J. Y., Reynolds, S. H., Chen, C. H., Xu, P., Hay, B. A. and Ruohola-Baker, H. (2007). Stage-specific differences in the requirements for germline stem cell maintenance in the *Drosophila* ovary. *Cell Stem Cell* **1**, 698–709.
- Sokol, N. S., Xu, P., Jan, Y. N. and Ambros, V. (2008). *Drosophila* let-7 microRNA is required for remodeling of the neuromusculature during metamorphosis. *Genes Dev.* **22**, 1591–1596.
- Somorjai, I. M. and Martinez-Arias, A. (2008). Wingless signalling alters the levels, subcellular distribution and dynamics of Armadillo and E-cadherin in third instar larval wing imaginal discs. *PLoS ONE* **3**, e2893.
- Song, X. and Xie, T. (2003). Wingless signaling regulates the maintenance of ovarian somatic stem cells in *Drosophila*. *Development* **130**, 3259–3268.
- Song, X., Zhu, C. H., Doan, C. and Xie, T. (2002). Germline stem cells anchored by adherens junctions in the *Drosophila* ovary niches. *Science* **296**, 1855–1857.
- Song, X., Wong, M. D., Kawase, E., Xi, R., Ding, B. C., McCarthy, J. J. and Xie, T. (2004). Bmp signals from niche cells directly repress transcription of a differentiation-promoting gene, bag of marbles, in germline stem cells in the *Drosophila* ovary. *Development* **131**, 1353–1364.
- Song, H., Spichiger-Hausermann, C. and Basler, K. (2009). The ISWI-containing NURF complex regulates the output of the canonical Wingless pathway. *EMBO Rep.* **10**, 1140–1146.
- Stogios, P. J., Downs, G. S., Jauhal, J. J., Nandra, S. K. and Privé, G. G. (2005). Sequence and structural analysis of BTB domain proteins. *Genome Biol.* **6**, R82.
- Toledano, H., D'Alterio, C., Czech, B., Levine, E. and Jones, D. L. (2012). The let-7-lmp axis regulates ageing of the *Drosophila* testis stem-cell niche. *Nature* **485**, 605–610.
- Turkel, N., Sahota, V. K., Bolden, J. E., Goulding, K. R., Doggett, K., Willoughby, L. F., Blanco, E., Martin-Blanco, E., Corominas, M., Ellul, J. et al. (2013). The BTB-zinc finger transcription factor abrupt acts as an epithelial oncogene in *Drosophila melanogaster* through maintaining a progenitor-like cell state. *PLoS Genet.* **9**, e1003627.
- Usongo, M., Rizk, A. and Farookhi, R. (2012). β -Catenin/Tcf signaling in murine oocytes identifies nonovulatory follicles. *Reproduction* **144**, 669–676.
- Valenta, T., Hausmann, G. and Basler, K. (2012). The many faces and functions of β -catenin. *EMBO J.* **31**, 2714–2736.
- van der Horst, P. H., Wang, Y., van der Zee, M., Burger, C. W. and Blok, L. J. (2012). Interaction between sex hormones and WNT/ β -catenin signal transduction in endometrial physiology and disease. *Mol. Cell. Endocrinol.* **358**, 176–184.
- Von Stetina, J. R. and Orr-Weaver, T. L. (2011). Developmental control of oocyte maturation and egg activation in metazoan models. *Cold Spring Harb. Perspect. Biol.* **3**, a005553.
- Wang, L., Li, Z. and Cai, Y. (2008). The JAK/STAT pathway positively regulates DPP signaling in the *Drosophila* germline stem cell niche. *J. Cell Biol.* **180**, 721–728.
- Wang, X., Pan, L., Wang, S., Zhou, J., McDowell, W., Park, J., Haug, J., Staehling, K., Tang, H. and Xie, T. (2011). Histone H3K9 trimethylase Eggless controls germline stem cell maintenance and differentiation. *PLoS Genet.* **7**, e1002426.
- Ward, E. J., Shcherbata, H. R., Reynolds, S. H., Fischer, K. A., Hatfield, S. D. and Ruohola-Baker, H. (2006). Stem cells signal to the niche through the Notch pathway in the *Drosophila* ovary. *Curr. Biol.* **16**, 2352–2358.
- Wodarz, A., Stewart, D. B., Nelson, W. J. and Nusse, R. (2006). Wingless signaling modulates cadherin-mediated cell adhesion in *Drosophila* imaginal disc cells. *J. Cell Sci.* **119**, 2425–2434.
- Xi, R. and Xie, T. (2005). Stem cell self-renewal controlled by chromatin remodeling factors. *Science* **310**, 1487–1489.
- Xie, T. and Spradling, A. C. (1998). decapentaplegic is essential for the maintenance and division of germline stem cells in the *Drosophila* ovary. *Cell* **94**, 251–260.
- Xie, T. and Spradling, A. C. (2000). A niche maintaining germ line stem cells in the *Drosophila* ovary. *Science* **290**, 328–330.
- Xuan, T., Xin, T., He, J., Tan, J., Gao, Y., Feng, S., He, L., Zhao, G. and Li, M. (2013). dBre1/dSet1-dependent pathway for histone H3K4 trimethylation has essential roles in controlling germline stem cell maintenance and germ cell differentiation in the *Drosophila* ovary. *Dev. Biol.* **379**, 167–181.
- Yan, D., Neumüller, R. A., Buckner, M., Ayers, K., Li, H., Hu, Y., Yang-Zhou, D., Pan, L., Wang, X., Kelley, C. et al. (2014). A regulatory network of *Drosophila* germline stem cell self-renewal. *Dev. Cell* **28**, 459–473.

3 Discussion

The present thesis describes how the steroid hormone ecdysone controls several processes in the germarium of *D. melanogaster*: reduced ecdysone signaling leads to the appearance of enlarged niches that facilitate a higher number of SSCs. In addition, ecdysone controls the differentiation of the GSC progeny cell non-autonomously via the surrounding ECs. Perturbing ecdysone signaling in the ECs leads to altered cell-adhesion between ECs and the germline; the squamous ECs adopt an epithelial-like fate and fail to envelope the differentiating germline cells with cytoplasmic protrusions. The Cad associated protein Arm is trapped at the adhesive complexes between germline and ECs, which alters the Arm pool in the germline cells. Canonical Wg signaling, in turn, depends on the availability of free cytoplasmic Arm and thus, the germline cells responsiveness to Wg signaling is altered, resulting in differentiation delayed germline cells.

3.1 Ecdysone signaling is non cell-autonomously acting on the germline

We showed that ecdysone signaling is predominantly active in the somatic cells of the germarium, in CpCs and ECs (König et al., 2011). Interestingly, germline cells show a dramatic differentiation delay if ecdysone signaling is disturbed. Consequently, the ECs must convert the ecdysone signaling into another signal to communicate with the germline cells. However, the range of TGF- β signaling, the main pathway for GSC maintenance in *D. melanogaster* ovaries, is not enlarged due to perturbed ecdysone signaling and, thus, it seems that ECs and GSCs communicate via alternative pathways. Not much is known about the communication between ECs and differentiating germline cells (see Section 1.2.4, page 12) and therefore, how the systemic hormonal ecdysone signal is transmitted to a signal that cell non-autonomously acts on the germline, is a key question.

3.1.1 EC function is compromised upon loss of ecdysone signaling

Interestingly, shape and function of the ECs are dramatically impaired in ecdysone signaling mutants: the squamous ECs line the germarium and form long cytoplasmic protrusions that envelop the developing germline cells. However, if the ecdysone signaling is perturbed, ECs form layers that resemble columnar epithelium. In addition, the thin cytoplasmic protrusions are no longer present and the

levels of cell adhesion proteins are elevated. Earlier experiments already demonstrated how critical EC protrusions are: if the formation of protrusions is inhibited specifically in the ECs – for example via interfering with the cytoskeleton – the germline differentiation is affected and a larger number of SSCs was detected (Decotto and Spradling, 2005; Kirilly et al., 2011; Wang et al., 2008a). A lack of EC protrusions therefore can cause a differentiation delay in the germline and we propose that the EC malformation and specifically the absence of protrusions contributes to the differentiation delay observed in the germline. How exactly EC protrusions enable germline differentiation is poorly understood; it is thought that they physically shield the differentiating germline cells against diffusible signals from the anterior CpCs, forming another barrier to locally restrict TGF- β signaling. Nevertheless, signaling processes most probably play a role in EC-germline communication, and so far, only few were identified.

Ecdysone signaling was suggested to act on the GSCs directly A recent report by Ables and Drummond-Barbosa, 2010 showed that ecdysone signaling regulates GSC self renewal and proliferation by functional interaction with the chromatin remodeling factors ISWI and NURF301. However, in contrast to our findings, Ables and Drummond-Barbosa, 2010 suggest that the ecdysone signaling is directly received by GSCs. While there are no conflicts regarding the results of experiments that overlap between our studies, the conclusions are different. Interestingly, Gancz et al., 2011 reported a non cell-autonomous effect of ecdysone signaling on primordial germ cells – the germ line stem cell precursors. Upon perturbing the ecdysone signaling in the soma, primordial germ cells are delayed in differentiation and similar to what we observed in adult GSCs, do not display Bam or pMad.

3.1.2 ECs form a differentiation niche for the germline progeny

The diverse signals and factors that are required for the maintenance of GSCs in their somatic niche were examined by many studies in the past decades (reviewed in Spradling et al., 2011). It was shown that the two daughters of a stem cell do not differ inherently, but instead their fate is determined by their environment; in order to be maintained as a stem cell, the germline cell has to be physically attached to the niche and receive the signaling from the CpCs. However, due to the limited size of the niche, stem cells compete for the available space and usually only one stem cell daughter can be maintained in the niche. The other one was thought to undergo differentiation simply because of the lack of niche contact and signaling. Only recently it was suggested that differentiation is not the default fate of cells that cannot be maintained as stem cells (Kirilly et al., 2011). Instead, it seems that the germline cells need specific microenvironments – consisting of signaling and cell contacts from the ECs – that enable differentiation to proceed.

The differentiation delayed germline cells in ecdysone signaling mutants lack the differentiation factor Bam TGF- β signaling is clearly the most important

signaling pathway controlling the stem cell population in the female GSC niche (Song et al., 2004; Xie and Spradling, 1998). Activation of the TGF- β pathway by the ligands Gbb and Dpp, that are secreted by CpCs and ECs, is crucial for GSC maintenance. But is the loss of TGF- β signaling in CBs sufficient to induce the differentiation program or is another "pro-differentiation" signal from the surrounding soma required? In wildtype germaria, expression of the differentiation factor *bam* is repressed by pMad and, hence, Bam becomes excluded from the GSCs and misexpression of *bam* is indeed sufficient to induce differentiation throughout the germline (McKearin and Ohlstein, 1995; McKearin and Spradling; Ohlstein and McKearin, 1997). Ecdysone-deficient germaria display a population of differentiation delayed pre-CBs that – not surprisingly – do not express *bam*. The pMad/Med complex that forms upon TGF- β activation is to date the only known repressor of *bam*; it was, therefore, rather unexpected that the pMad expression radius is unchanged in ecdysone deficient germaria. Is *bam* expression not allowed because of another yet unidentified factor? Or is an unknown activator missing that would promote *bam* expression? Apart from intrinsic and extrinsic signaling pathways that control stem cell fate, chromatin modifying factors have been shown to be indispensable for stem cell maintenance and differentiation (reviewed in Buszczak and Spradling, 2006). Chromatin modifications are, therefore, great candidates for a mechanistic link between ecdysone signaling and Bam-driven differentiation.

Histone H2B ubiquitination precedes germline differentiation Which epigenetic features define the stem cell state and how they change upon differentiation are key questions that need to be resolved in order to fully understand and to potentially manipulate stem cell maintenance and differentiation. Stem cells exhibit a certain set of chromatin modifications, governing their unique gene expression patterns (reviewed in Buszczak and Spradling, 2006). At the same time, the epigenetic state has to be flexible enough to allow for differentiation (reviewed in Buszczak and Spradling, 2006). A number of chromatin remodelers, like ISWI and NURF301 were shown to be required for GSC maintenance (Buszczak et al., 2009; Xi and Xie, 2005 and Section 1.6, page 30). The role of chromatin modifications in germline differentiation is, however, far less understood. Many developmental genes exhibit both "active" and "repressive" chromatin modifications at the same time. Interestingly, the monoubiquitination of histone H2B was shown to parallel resolving this bivalency during differentiation in human mesenchymal stem cells and the patterns of H2Bub1 and *bam* correlate (Karpiuk et al., 2012). We therefore suggest that the monoubiquitination of H2B precedes differentiation and *bam* expression. Furthermore, ecdysone deficient flies show non-differentiating germline cells that lack H2Bub1, indicating that this epigenetic mark is regulated in response to steroid hormone signaling. The exact mechanism by which H2Bub1 and possibly other chromatin remodelers regulate *bam* expression, and thus germline differentiation, is a key question that will be subject of further studies.

Adhesion complexes are affected by hormonal ecdysone signaling DE-Cad and Arm are normally found at high levels in the junctions between CpCs and between CpCs and GSCs where they are necessary to maintain GSCs (Song et al., 2002). More towards the posterior in CBs and ECs, Arm and DE-Cad levels are strongly reduced in wildtype germaria. Adhesive junctions are critical for germline-soma interaction: subtle differences in the adhesive strength determine which GSCs are maintained and which ones are outcompeted (Jin et al., 2008). The local levels of adhesion proteins are controlled by other signals like insulin or JAK/STAT signaling and, thus, are adjusted to the overall body status (Hsu and Drummond-Barbosa, 2009; Leatherman and Dinardo, 2010). The intensity of the adhesive connections, therefore, provide a mechanism by which soma and germline communicate and govern each other and serves as an interface for other signaling pathways.

Increased levels of cell adhesion proteins affect EC protrusions We now describe, that the ecdysone signaling also affects the levels or turnover of the cell adhesion proteins Arm and DE-Cad, that were found in abnormally high levels between ECs and the germline. In order to escort the constantly moving germline cells, ECs and germline cells have to attach and detach frequently, and especially the formation and movement of cytoplasmic EC protrusions have to be highly dynamic. During these rearrangements, the adhesive complexes between ECs and the germline have to assemble and disassemble repeatedly and we suggest, that ECs protrusions cannot form properly if this process is defective. The ecdysone signaling pathway regulates the expression of various genes; in addition to directly acting on the levels of DE-Cad and Arm it may also interfere with their turnover. Bai et al., 2000 observed elevated levels of DE-Cad in border cells in which ecdysone signaling was reduced. Artificial overexpression of *DE-Cad* however did not phenocopy the ecdysone signaling mutant phenotype, nor did it lead to visible accumulation of DE-Cad at the cell membrane, suggesting that the cell can compensate for high DE-Cad and degrade it (Bai et al., 2000). Thus, ecdysone signaling acts on the formation of adhesive complexes, which dampens EC ability to form cytoplasmic protrusions and ultimately affects germline differentiation (see Figure 3.1, page 117).

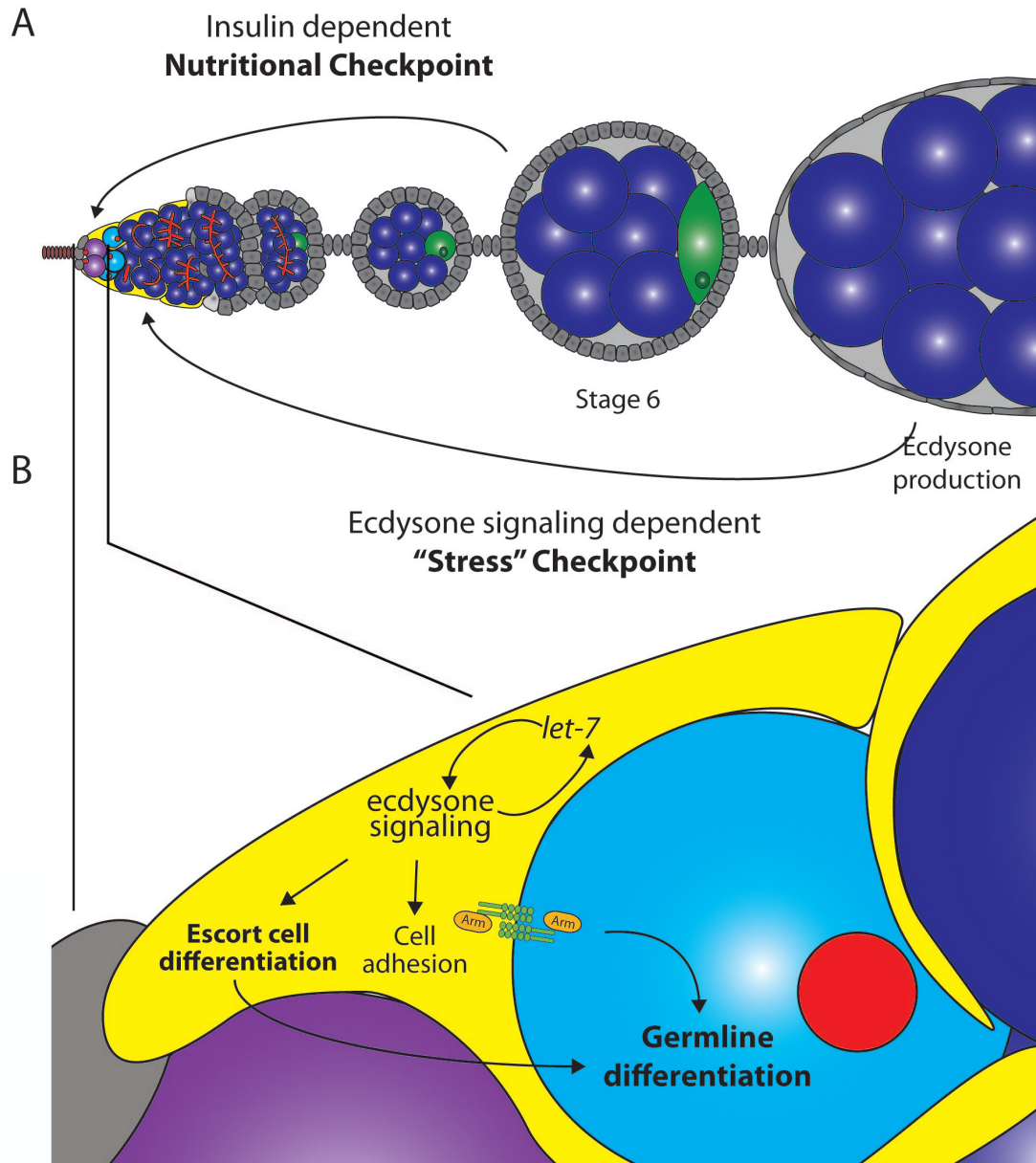


Figure 3.1: Ecdysone signaling acts on germline differentiation in a cell non-autonomous way

(A) GSC division and germline differentiation are controlled by systemic hormonal signaling: insulin signaling regulates GSC maintenance and division and integrates the overall nutritional status. Ecdysone signaling controls a stress and starvation dependent checkpoint at which egg chambers undergo apoptosis if applicable.

(B) Ecdysone signaling acts on the levels or turn-over of the cell adhesion molecules DE-Cad and Arm and thereby also influences EC shape and function. Altered Arm levels in the germline alter the cells responsiveness to canonical Wg signaling. Thus, via the ECs, ecdysone signaling cell non-autonomously regulates the differentiation of the germline cells. The miRNA *let-7* attenuates the cell specific response to ecdysone.

3.2 Wg signaling – a connection between ECs and GSCs

As was mentioned, ECs are thought to mainly function by mechanically supporting the differentiating germline and via physically shielding from "self renewal" signaling, coming from the niche. If this was the only function of ECs, one would expect that a lack of EC protrusions would lead to more germline cells receiving TGF- β signaling. However, our data show that the area in which TGF- β responsive cells can be found is not enlarged upon perturbed ecdysone signaling, and thus altered TGF- β signaling does not account for the observed germline differentiation delay. Another mechanism must contribute to the EC mediated ecdysone signaling mutant phenotype in the germline. The only so far characterized pathway that is used by germline and ECs is the EGFR signaling, that was shown to be activated in the ECs by germline-sent ligands. Activated EGFR-mitogen-activated protein kinase signaling leads to the downregulation of the Dpp stabilizing glypican Dally. EGFR signaling thus limits the diffusion of Dpp and, hence, TGF- β signaling (Liu et al., 2010; Schulz et al., 2002; Yarden and Shilo, 2007). Whereas the phenotypes caused by perturbing the EGFR in the soma are somewhat similar to the ones that are caused by loss of ecdysone signaling (germline differentiation delay, lack of cytoplasmic EC protrusions), an important difference is the spatially expanded area of TGF- β receiving cells in EGFR signaling mutants. As it was discussed previously, this is not the case if ecdysone signaling is perturbed and EGFR signaling is, therefore, most likely not the downstream effector of ecdysone signaling in the germarium that accounts for the observed phenotypes.

3.2.1 Arm levels in the germline are cell non-autonomously affected by DE-Cad levels in the soma

We had observed higher levels of DE-Cad and Arm between ECs and GSCs of ecdysone signaling mutants: since DE-Cad is a homophilic adhesion molecule, we hypothesize that high levels of DE-Cad lead to the recruitment of additional DE-Cad molecules to the membrane of the adjacent cell. Arm is bound to the cytoplasmic domain of DE-Cad and, as expected, we also observed higher Arm levels between ECs and GSCs. Arm is not only a structural component of cell adhesion complexes, but also the effector of the canonical Wnt signaling pathway. The Wnt signaling pathway is highly conserved and is required for cell fate decisions: proliferation, cell death and polarity in all metazoans (reviewed in MacDonald et al., 2009). In addition, a number of human diseases is associated with Wnt signaling components. If Wnt signaling is not active, Arm is recruited to a complex in the cytoplasm, that leads to its degradation. Upon binding of Wnt ligands to the receptor, the Arm degrading complex becomes inactive, Arm accumulates, translocates to the nucleus and acts on the transcription of target genes (reviewed in Chien et al., 2009).

3.2.2 Arm is at the intersection of Wnt signaling, cell adhesion and other pathways

Due to the limited amount of Arm molecules in the cell and the exclusiveness of Arm binding partners, the bifunctional Arm molecule serves as a link between Wnt signaling and cell adhesion. Binding of β -Catenin (the human Arm homolog) to Cad masks a PEST motif which is a hallmark for fast protein turnover on the Cad molecule, protecting it from proteasomal degradation (Huber and Weis, 2001). Vice versa, Arm is also stabilized by binding to Cad. A loss of Cad therefore leads to the release of Arm, whereas high levels of Cad can titrate free cytoplasmic Arm (Sanson et al., 1996). It was shown in several studies that artificial overexpression of *Cad* leads to the translocation of Arm to the membrane, which reduces the pool of Arm in the cytoplasm and inhibits Wnt target gene expression. Any changes in cell-cell adhesion processes also influence the pools of free cytoplasmic and nuclear Cad and, therefore, also the transcription of Wnt targets (reviewed in Somorjai and Martinez-Arias, 2008). Interestingly, it was shown that proteases that cleave Cad itself are targets of Wnt signaling, suggesting the existence of a positive feedback loop with which the β -Catenin signal is amplified (reviewed in Valenta et al., 2012). Wodarz et al., 2006 suggest the existence of a negative feedback loop in a tissue culture system: upon activation of the Wnt signaling pathway the level of Cad decreases first, but increases later, sequestering Arm and thereby attenuating Wg transcriptional response. Furthermore, a variety of signaling pathways including TGF- β and other growth factor pathways were shown to control Wnt controlled transcription via altering the availability of Arm (reviewed in Valenta et al., 2012). In summary, Arm/ β -Catenin is an important molecule intersecting with canonical Wnt signaling, cell adhesion and various other pathways.

Is the Wg signaling pathway in the germline affected by altered DE-Cad levels? The question is, whether the transcriptional activity of Arm can be influenced by changes in DE-Cad levels in the *D. melanogaster* germarium. Can the Wnt signaling pathway in the germline be influenced by higher somatic DE-Cad levels? Indeed, we show that downregulation of Wg signaling in the germline also leads to a germline differentiation delay while overactivation of Wg signaling has the opposite effect: differentiating cysts are found close to the niche. Wg signaling can, thus, cell autonomously influence germline differentiation. In addition, a function for Wnt signaling in adult stem cell lineages is very well documented: depending on the context, Wnt signaling can promote self renewal or control lineage commitment (reviewed in Holland et al., 2013). In *D. melanogaster*, for example, Wg signaling is required for the self renewal of midgut and hindgut stem cells (reviewed in Saito-Diaz et al., 2013). We therefore propose, that cell autonomous changes in the germline are caused by higher levels of DE-Cad, subsequent recruitment of Arm and downregulation of the Wg signaling pathway (see Figure 3.1, page 117).

3.3 Ecdysone signaling links germline differentiation to the overall body status

Kept on rich food, flies produce 60 times more eggs than on poor food (Drummond-Barbosa and Spradling, 2001). Thus, oogenesis is a highly energy demanding process that strongly depends on the flies nutritional situation.

3.3.1 Ecdysone signaling mediates effects of stress and starvation

Insulin signaling and other pathways were shown to mediate the response to food availability; GSCs and FSCs respond to the nutritional status: they adjust their proliferative rate and the progression of germ cells is slowed down upon food deprivation (reviewed in Jasper and Jones, 2010). However, the dramatically decreased egg production rate seems to also result from an increased degeneration of egg chambers at stage 8–9 (Drummond-Barbosa and Spradling, 2001). Ecdysone signaling is required to progress past this master checkpoint and we now show, that perturbation of ecdysone signaling also affects germline development in the germarium: if ecdysone signaling in the soma is altered, the interaction between germline and ECs is affected and the germline development is slowed down. Ecdysone is produced in older follicles that passed the stage 8–9 checkpoint (see Section 1.3.3, page 19): ecdysone control of germline development, therefore, presents a positive feedback mechanism, with which germline development in the germarium is synchronized with the presence or absence of older follicles.

Ecdysone function in the adult is complex and poorly defined Understanding the role of ecdysone signaling in oogenesis is complicated by several findings: first, the levels of ecdysone in the adult were measured by multiple research groups (Ishimoto et al., 2009; Schwartz et al.; Schwedes and Carney, 2012; Terashima and Bownes, 2006; Tu et al., 2002). However, the results obtained are contradictory and it is, for example, unclear whether ecdysone titers increase or decrease upon starvation. Second, even though ecdysone signaling is clearly indispensable for oogenesis (Buszczak et al., 1999; Carney and Bender, 2000), high ecdysone titers also negatively affect oogenesis. Terashima et al., 2005 reported that ecdysone injection – similar to starvation – induces apoptosis of nurse cells at stage 8 and 9 (Terashima and Bownes, 2006). Presumably, ecdysone function depends on whether its levels are below or above a certain threshold. Supporting this hypothesis, accumulating evidence suggests that – depending on ecdysone presence – the EcR can carry out both, transcription activating and repressing functions, which is further discussed in Section 3.3.2, page 122. Third, while ecdysone is a major regulator at the larval–pupal transition, its role in the adult fly is remarkably different: high ecdysone signaling activity was shown to promote stress resistance and ecdysone levels are changed if flies are exposed to unfavorable conditions like heat, food or sleep deprivation (Ishimoto and Kitamoto, 2010; Rauschenbach

et al., 2000; Simon et al., 2003; Terashima and Bownes, 2005; Terashima et al., 2005; Tricoire et al., 2009).

Ecdysone is a "stress hormone" in the adult fly In adults, ecdysone signaling controls various aspects of behavior, reproduction, body size, longevity and memory (see Section 1.3.3, page 19). Considering that the ecdysone titers, measured by several research groups in differently treated flies are remarkably different, it is reasonable to conclude that the ecdysone levels are highly dynamic and responsive to external conditions. In addition, we could show that the levels of *let-7*, the fine-tuner of ecdysone signaling, are increased upon food or temperature stress. In addition to the ecdysone dependent checkpoint at stage 8-9, we showed that ecdysone signaling also controls progression through the early stages of oogenesis (Buszczak et al., 1999; Carney and Bender, 2000; Terashima and Bownes, 2006; Terashima et al., 2005). Ecdysone functions independently from the GSC maintenance regulation by insulin signaling, suggesting that the hormones insulin and ecdysone control the speed of oogenesis in parallel (see Figure 3.1, page 117). We, therefore, suggest that ecdysone signaling is a master regulator or "stress hormone" that links vitellogenesis and the overall body status.

3.3.2 The tissue- and time-specific response to ecdysone signaling is controlled by a complex network of interacting partners

Given the diverse functions of ecdysone signaling in adults and larvae, it is understandable, that the time- and tissue-specific actions of ecdysone are mediated by a variety of different interacting partners. EcR/Usp cofactors include chromatin remodelers, histone modifier and transcriptional cofactors (see Section 1.3.2, page 18).

Ab is a potent transcription factor whose function depends of its concentration Ab inhibits the strength of the ecdysone signaling by interacting with the cofactor Tai and interestingly, is targeted by the miRNA *let-7* that is itself regulated by ecdysone signaling. Based on the analysis of penetrance and severity of *ab* mutant phenotypes, it was suggested that Ab controls dendrite branching and formation of other adult structures in a dosage dependent way (Hu et al., 1995; Li et al., 2004). Ab contains the BTB/POZ protein domain, that is highly conserved among metazoans and defines a protein-protein interaction interface (Zollman et al., 1994). Transcription factors containing BTB/POZ domains are involved in diverse cellular functions including regulation of transcription and cytoskeleton dynamics, ion channels and protein degradation (reviewed in Stogios et al., 2005). Ab belongs to the "tkk" subgroup that also contains Bab, Br, Pipsqueak, the GAGA factor and Batman. Whereas the sequence homology between members of the tkk subgroup and other BTB proteins is 24%, it is 49% on average within members of the tkk subgroup (Bonchuk et al., 2011). Recently it was shown, that

the BTB domains of the tkk subgroup members Batman, Mod(mdg4), Pipsqueak, Tramtrack and GAF are able to form multimers (Bonchuk et al., 2011). Interestingly, Bonchuk et al., 2011 performed cross-linking experiments that suggest that the Ab BTB domain is also able to form major multimers. Given the similarity between the members of the tkk subgroup, the reported interaction between BTB domains of different proteins and the ability of Ab to form dimers, it is very likely that the Ab BTB domain is able to mediate the formation of Ab multimers. This provides a possible explanation for the observed dosage dependent action of Ab. Importantly, Ab was shown to be a transdetermination factor, since overexpressing Ab in antennal imaginal discs leads to the transformation of arista into putative legs (Grieder et al., 2007). In addition, Ab is a global transcriptional regulator in the epithelium (Turkel et al., 2013). Altogether, Ab is a potent transcription factor that acts in a dosage dependent way to modulate the ecdysone signaling response, explaining the necessity for its precise regulation by the miRNA *let-7*. Apart from the various interacting factors, the EcR/Usp itself contributes to the complexity of ecdysone signaling in *D. melanogaster*: the unliganded EcR/Usp complex is not only transcriptionally inactive, but even repressive.

The unliganded EcR complex represses transcription Previously it was shown that in the absence of ecdysone, the basal expression of a test vector was lower in vectors containing ecdysone responsive elements compared to empty ones. In addition, loss of Usp or EcR function was shown to lead to precocious differentiation of sensory neurons and expression of Br-Z1 (an isoform of Br) even at developmental stages with low ecdysone titers. Based on these results, it was suggested that the EcR/Usp complex can repress the expression of target genes if unliganded (Cherbas et al., 1991; Dobens et al., 1991; Schubiger and Truman, 2000; Schubiger et al., 2005), a phenomenon that has also been described for the retinoid X and retinoic acid receptors (reviewed in Glass and Rosenfeld, 2000). We observed that overexpression of the *EcR* and lowering the levels of ecdysone in the adult led to similar phenotypes: an increased number of SSCs and a reduced cysts/single spectrosome ratio. We, therefore, speculated that the similarity of the phenotypes may arise because in both cases the activating function of the EcR was inhibited: either because of an artificially high level of EcR that was shown *in vitro* to form homodimers (Elke et al., 1997) or because of low ecdysone levels. In order to prove this hypothesis, we fed ecdysone to *EcR* overexpressing flies: as expected, this led to a partial rescue of the observed phenotypes. Our results, therefore, support the hypothesis that unliganded receptor complexes can have a repressive function. Indeed Gancz et al., 2011 also reported that the repressive function of EcR/Usp in early third instar larvae – when ecdysone levels are low – is required for the correct formation of the gonad. Later in mid and late third instar larvae, active ecdysone signaling is required for niche formation and triggers primordial germ cell differentiation (Gancz et al., 2011). Recently Johnston et al., 2011 showed that in salivary glands the unliganded EcR does not repress the transcription of target genes, but is localized to the cytoplasm. Rising ecdysone titers lead to the translocation of the EcR/Usp complex to the nucleus, activating

the transcription of target genes, for example *E75A*, a nuclear hormone receptor itself. As ecdysone titers increase at the larval–pupal transition, *E75A* replaces the EcR/Usp complex and represses the expression of target genes, including the *EcR* itself. The results provided by Johnston et al., 2011 present an additional mechanism by which tissue- and time-specific actions of the ecdysone regulated networks could be provided.

3.3.3 Maintaining the sexual identity requires intact ecdysone signaling

Steroid hormones are major regulators of mammalian sex determination and gametogenesis (reviewed in Arnold, 2012; Sim et al., 2008). Interestingly, we and others could show that ecdysone signaling regulates different aspects of gonadogenesis and adult gonad function in female *D. melanogaster* (Buszczak et al., 1999; Carney and Bender, 2000; Hackney et al., 2007; König et al., 2011; Morris and Spradling, 2012). Data for a differential expression of ecdysone signaling pathway genes between male and female gonads remain poor, but there is evidence for sex specific differences of ecdysone levels (reviewed in Schwedes and Carney, 2012). Morris and Spradling, 2012 recently reported that reducing ecdysone signaling in the male testis for eight days does not lead to visible effects on GSCs, developing cysts or primary spermatocyte clusters. In contrast, Garen et al., 1977 reported that ecdysone is essential for male fertility. Our own analysis reveal that ecdysone signaling mutant testes exhibit several severe phenotypes including a germline differentiation delay and formation of somatic epithelia (Fagegaltier et al.). Importantly, we have observed similar phenotypes in males lacking the miRNA *let-7* that is a downstream effector of ecdysone signaling.

A confused sexual identity can contribute to the observed germline differentiation delay The soma has an important function in controlling the germlines sexual identity, but the genetic sex of the germline also is important. Interestingly, germline differentiation defects and tumors can also be the consequence of non-matching sexual identities in germline and soma; this happens for example if XX:AA germline cells are transplanted into male soma. JAK/STAT signaling is used by the male soma to masculinize the associated germline cells (reviewed in Murray et al., 2010). Furthermore, mutants of the master differentiation factor *bam* display a confused sexual identity as well: ovaries express a set of normally testis specific markers (Chau et al., 2009; Staab et al., 1996; Wei et al., 1994). We, thus, analyzed ovaries and testes with respect to the expression pattern of sex specific transcripts. Interestingly, especially *let-7* deficient males strongly up-regulate transcripts of the opposite sex; however, the phenotypes observed upon ecdysone signaling loss in testes and ovaries seem to be equally strong (Fagegaltier et al.). The ecdysone signaling target *let-7* is expressed at higher levels in males, but whether ecdysone titers itself differ between sexes is not clear (reviewed in Schwedes et al., 2011). We, thus, speculate that downstream effectors of

ecdysone signaling affect the maintenance of the sexual identity and that the importance of these downstream effectors differs between sexes. The ecdysone/*let-7* cascade cooperates with the JAK/STAT pathway in neuronal cell fate determination (Kucherenko and Shcherbata, 2013) and it is tempting to speculate and will be subject of further analysis that the ecdysone/*let-7* cascade may affect the male sexual identity via JAK/STAT.

3.3.4 The ecdysone/*let-7*/Ab signaling cascade modulates oogenesis in response to different conditions

The BTB protein Ab is not only the negative regulator of ecdysone signaling, its levels itself are negatively regulated by steroids and stress. *ab* mRNA levels are increased in ecdysone-depleted ovaries; in addition, the cellular localization of Ab is variable, depending on ecdysone availability and external conditions. Given the severity of phenotypes induced by alterations of Ab on the one hand and the changes in localization that we observed upon stress on the other hand, it is understandable that changes in level and localization of this potent epithelial regulator have to be robustly buffered, which is provided by the miRNA *let-7*. *let-7* is induced by steroids in the *D. melanogaster* germarium and *let-7* itself promotes ecdysone signaling by reducing the levels of the ecdysone signaling inhibitor Ab. We, thus, showed that the ecdysone signaling/*let-7*/Ab cascade regulates oogenesis in response to stress. While the purpose of this regulation is to flexibly adjust gene expression in response to external stimuli, "overshooting" reactions have to be prevented. miRNAs can ensure biological robustness and provide a buffer against stochastic fluctuations or "overshooting" gene expression in a system (reviewed in Siciliano et al., 2013); which – considering the strong concentration dependent effects of Ab – is extremely important.

3.4 The *D. melanogaster* germarium provides a model to decipher the more complex mechanisms of steroid hormone/*let-7* action in vertebrates

The studies presented in this thesis describe how steroid hormones (1) influence the formation of the stem cell niche and (2) non cell-autonomously influence the germline and lead to the expansion of a cell population that is delayed in differentiation. Furthermore it is described how other factors act to fine-tune this regulation. Whether events, similar to the ones described in the *D. melanogaster* germarium, play a role during the development and adult function of human stem cell niches or contribute to the development of cancers should be subject of further analysis. However, in the light of several studies it seems likely that ecdysteroid action in the *D. melanogaster* germarium may provide insights into some aspects of steroid hormone signaling action in humans.

3.4.1 Steroid action in *D. melanogaster* and humans show some parallels

It was already shown that the steroids estrogen and progesterone, are critical for the regenerative capability of mammary stem cells. Interestingly, it seems that, like we could show for ecdysone regulating germline cells, this regulation may be indirect via surrounding cells (reviewed by Joshi et al., 2012; Lydon, 2010).

Tai and its homolog AIB1 share important characteristics AIB1, the human homolog of Tai, was shown to be elevated in breast cancer specimens. High AIB1 levels are associated with a poor prognosis and AIB1 acts as a coactivator of estrogen and progesterone receptor. In addition to its rather well studied role in breast cancer, it appears that AIB1 is also important for the development and progression of other tumors, like ovarian and prostate cancer (reviewed in Chang and Wu, 2012). Bai et al., 2000 showed that Tai is required for the migration of border cells in *D. melanogaster* egg chambers and because of the similarities that exist between migrating border cells and cancerous cells in the human ovary, Yoshida et al. analyzed the role of AIB1 in human ovarian cancer cells and, indeed, found that AIB1 regulates the migration of epithelial ovarian cancer cells. It is, therefore, interesting, whether AIB1 function in humans resembles more features of Tai action, such as indirectly influencing the germline via the surrounding niche cells.

Steroid hormone pathways in *D. melanogaster* are far less complex than in mammals Steroid hormones are of great importance for various aspects of human life, including development, organogenesis, reproduction, and malignant diseases. The diversity of human steroids, the immense number of factors involved in the signaling process, and the complexity of the hormone controlled networks complicate their analysis. The sophisticated genetic tools available in *D. melanogaster*, the presence of only one major steroid hormone, and the extensive knowledge about the GSC niche make *D. melanogaster* an invaluable model system for deciphering details about steroid hormone function.

3.4.2 Various aspects of *let-7* function are conserved in bilateria

The miRNA *let-7* was first described as a heterochronic gene in *C. elegans* and was later shown to serve similar functions in *D. melanogaster*. Its loss of function leads to the repeat of larval cell fates: hypodermal blast cells fail to differentiate and to form adult structures, but instead undergo an additional round of replication in *C. elegans* (Reinhart et al., 2000; Slack et al., 2000). In *D. melanogaster*, larval muscles persist, while adult body wall muscles are smaller and neuromuscular junctions are immature; in addition, cells in the wing disc do not exit the cell cycle (Caygill and Johnston, 2008; Sokol et al., 2008). In summary, *let-7* promotes

differentiation and its loss of function leads to immature adult structures and persisting larval tissues.

Germline differentiation delay as a heterochronic defect? The present thesis describes that *let-7* modulates the strength of ecdysone signaling in the germarium and its absence cell non-autonomously causes a developmental arrest of the germline cells. Considering that the production of eggs also has to be paused before the flies hatch, this differentiation arrest in the germarium upon *let-7* and/or ecdysone signaling deficiency could also be considered a heterochronic defect. However, *let-7* was also shown to play numerous other roles in the adult animal or human: it regulates cancer, stem cells or aging (reviewed in Boyerinas et al., 2010; Bussing et al., 2008; Mondol and Pasquinelli, 2012 and Toledano et al., 2012). Supporting this, the ecdysone signaling pathway that acts in a feedback loop with *let-7*, also is involved in numerous aspects of the adult life (reviewed in Schwedes and Carney, 2012).

The steroid regulation of *let-7* may represent a conserved mechanism Given the importance of *let-7* in cancer progression and development, it is critical to understand how its levels are regulated. In many organisms, including *C. elegans*, *D. melanogaster* and *D. rerio*, *let-7* is only found later in development. Mature and pre-*let-7* first appear at the same time in *D. melanogaster*, indicating that *let-7* expression is controlled at the transcriptional level. In other organisms, however, it had been shown that *let-7* expression can be regulated post-transcriptionally as well (reviewed in Roush and Slack, 2008). Despite earlier reports that were contradictory about this question, it seems to be clear now that the expression of pre-*let-7* is controlled at the transcriptional level by ecdysone (Bashirullah et al., 2003; Garbuzov and Tatar, 2010; Sempere et al., 2002, 2003). *C. elegans* does not have ecdysone, nevertheless *let-7* expression is precisely regulated in the temporal dimension and, like in *D. melanogaster*, *let-7* appears first at the last larval stages. Under good environmental conditions, *C. elegans* goes through four larval stages; but in response to unfavorable conditions, it enters an alternative "dauer" state. This non-feeding stage can last up to 6 months, but as soon as the conditions are improving, development is resumed. Initiation of the "dauer" state is controlled by the steroid hormone receptor DAF-12 (dauer formation 12). DAF-12 is bound by the steroid hormone dafachronic acid; in the presence of dafachronic acid development is promoted, while the absence of dafachronic acid induces "dauer" formation. DAF-12 is important for several other processes in development, reproduction and longevity and, thus, similar to ecdysone in *D. melanogaster*, it is a master hormonal regulator of *C. elegans* (reviewed in Galikova et al.; Tennessen and Thummel, 2011). Interestingly, in both, *D. melanogaster* and *C. elegans*, the steroid hormone production is regulated by TGF- β and insulin signaling and thus, several studies suggested that the EcR and DAF-12 pathways are functional orthologs (reviewed in Sokol, 2012). Furthermore, like in *D. melanogaster*, *let-7* expression is also regulated by steroid hormones in *C. elegans*: in the absence of DA, DAF-12 represses the expression of *let-7* family members while it activates

let-7 expression if dafachronic acid is present (Bethke et al., 2009; Hammell et al., 2009). Whether steroid hormone regulation of *let-7* is a common motif also in vertebrates is a very interesting question and should be subject of further studies. *let-7* was, indeed, found at certain developmental stages in the vertebrate clade, where animals develop without molts. How the levels of *let-7* family members in humans are regulated and whether they even follow a distinct developmental pattern was not described in detail (reviewed in Sokol, 2012). However, the results gained in *D. melanogaster* indicate, that steroid hormones are capable of regulating *let-7* and further analysis in model organisms and humans will help deciphering *let-7* regulation in more detail.

3.4.3 *let-7* acts as a tumor suppressor in humans

Several cancers, including breast, prostate, endometrium, testis, ovary, thyroid, and osteosarcoma are grouped as hormone-dependent cancers. Steroid hormones, like estrogen and progesterone, are critical for the development, progression and clinical prognosis of these cancer types and are thought to promote cell proliferation and, thereby, to increase the opportunity for random mutations to occur and accumulate (reviewed in Henderson and Feigelson, 2000). Since cancers of the reproductive system belong to the most common causes of cancer death in the Western world, improving methods for their treatment and cure are critical and require a better understanding of their development. There is evidence, that tumors can arise from a rather small subset of cells – the so-called cancer stem cells (reviewed in Elshamy and Duhe, 2013). Cancer stem cells share a number of characteristics with adult tissue stem cells: they are able to both, self-renew and to give rise to more or less differentiated progeny and, in addition, are located in tissues that often develop cancer. It is believed that cancer stem cells can arise from adult stem cells by escaping the niche-dependent and internal restrictions on their self renewal. Cancer stem cells can become independent from niche signals or recruit cells to form a niche. In addition, an enlarged niche is able to host a larger number of normal and/or cancer stem cells (reviewed in Clarke and Fuller, 2006). Therapeutic approaches therefore should specifically consider and target cancer stem cells, which makes it crucial to understand which factors and events contribute to the generation of self renewing cancer stem cells.

Detailed analysis of *let-7* function in *D. melanogaster* adult stem cells may precede research in mammals It was shown that miRNAs in general are required for the maintenance of embryonic stem cells and several miRNAs are differentially expressed in differentiated, cancer and adult stem cells (Croce, 2009; Qi et al., 2009; Shcherbata et al., 2006). Given the multiple roles that *let-7* carries out for cell-fate decisions during development, it is not surprising that *let-7* also plays a role in cancer biology. *let-7* suppresses pluripotency of embryonic stem cells and enhances differentiation. Several studies indicate that *let-7* acts as a tumor suppressor, especially in lung and breast cancer (reviewed in Nimmo and Slack, 2009). Analysis in vertebrates are, however, complicated by the number of *let-7*

family members that may serve redundant functions, with some of them being encoded by several loci. Consequently, not much is known about the developmental role of *let-7* in vertebrates. Studies in *D. melanogaster* often provide first hints that lead to important findings in vertebrates and help to decipher complex mechanisms: the present thesis describes how *let-7* acts on the differentiating progeny of adult stem cells in the *D. melanogaster* germarium, not directly, but in a cell non-autonomous way via surrounding ECs. Given the high conservation of *let-7* sequence, temporal expression and function in *C. elegans*, *D. melanogaster* and humans, it is very likely, that the *let-7* function that is described in the present thesis is also at least partially important in humans. Whether *let-7*/steroid signaling cascade may also cell non-autonomously act on the stem cell or progeny differentiating niche of adult and/or cancer stem cells in vertebrates, is – especially in the light of tumor development and progression – a critical question.

References

- E. T. Ables and D. Drummond-Barbosa. The steroid hormone ecdysone functions with intrinsic chromatin remodeling factors to control female germline stem cells in *Drosophila*. *Cell Stem Cell*, 7(5):581–92, 2010.
- A. P. Arnold. The end of gonad-centric sex determination in mammals. *Trends Genet*, 28(2):55–61, 2012.
- P. Badenhorst, H. Xiao, L. Cherbas, S. Y. Kwon, M. Voas, I. Rebay, P. Cherbas, and C. Wu. The *Drosophila* nucleosome remodeling factor NURF is required for Ecdysteroid signaling and metamorphosis. *Genes Dev*, 19(21):2540–5, 2005.
- J. Bai, Y. Uehara, and D. J. Montell. Regulation of invasive cell behavior by taiman, a *Drosophila* protein related to AIB1, a steroid receptor coactivator amplified in breast cancer. *Cell*, 103(7):1047–58, 2000.
- L. J. Barton, B. S. Pinto, L. L. Wallrath, and P. K. Geyer. The *Drosophila* nuclear lamina protein otefin is required for germline stem cell survival. *Dev Cell*, 25(6):645–54, 2013.
- A. Bashirullah, A. E. Pasquinelli, A. A. Kiger, N. Perrimon, G. Ruvkun, and C. S. Thummel. Coordinate regulation of small temporal RNAs at the onset of *Drosophila* metamorphosis. *Dev Biol*, 259(1):1–8, 2003.
- R. Beckstead, J. A. Ortiz, C. Sanchez, S. N. Prokopenko, P. Chambon, R. Losson, and H. J. Bellen. Bonus, a *Drosophila* homolog of TIF1 proteins, interacts with nuclear receptors and can inhibit betaFTZ-F1-dependent transcription. *Mol Cell*, 7(4):753–65, 2001.
- A. Bethke, N. Fielenbach, Z. Wang, D. J. Mangelsdorf, and A. Antebi. Nuclear hormone receptor regulation of microRNAs controls developmental progression. *Science*, 324(5923):95–8, 2009.
- C. Blanpain, G. Q. Daley, K. Hochedlinger, E. Passegue, J. Rossant, and S. Yamanaka. Stem cells assessed. *Nat Rev Mol Cell Biol*, 13(7):471–6, 2012.
- A. Bonchuk, S. Denisov, P. Georgiev, and O. Maksimenko. *Drosophila* BTB/POZ domains of "ttk group" can form multimers and selectively interact with each other. *J Mol Biol*, 412(3):423–36, 2011.
- M. Bownes. Ecdysteroids in adult males and females of *Drosophila melanogaster*. *Journal of Insect Physiology*, 30(10):823–830, 1984.

- B. Boyerinas, S. M. Park, A. Hau, A. E. Murmann, and M. E. Peter. The role of let-7 in cell differentiation and cancer. *Endocr Relat Cancer*, 17(1):F19–36, 2010.
- I. Bussing, F. J. Slack, and H. Grosshans. let-7 microRNAs in development, stem cells and cancer. *Trends Mol Med*, 14(9):400–9, 2008.
- M. Buszczak and A. C. Spradling. Searching chromatin for stem cell identity. *Cell*, 125(2):233–6, 2006.
- M. Buszczak, M. R. Freeman, J. R. Carlson, M. Bender, L. Cooley, and W. A. Segraves. Ecdysone response genes govern egg chamber development during mid-oogenesis in *Drosophila*. *Development*, 126(20):4581–9, 1999.
- M. Buszczak, S. Paterno, and A. C. Spradling. *Drosophila* stem cells share a common requirement for the histone H2B ubiquitin protease scrawny. *Science*, 323(5911):248–51, 2009.
- G. E. Carney and M. Bender. The *Drosophila* ecdysone receptor (EcR) gene is required maternally for normal oogenesis. *Genetics*, 154(3):1203–11, 2000.
- M. O. Casanueva and E. L. Ferguson. Germline stem cell number in the *Drosophila* ovary is regulated by redundant mechanisms that control Dpp signaling. *Development*, 131(9):1881–90, 2004.
- A. Casper and M. Van Doren. The control of sexual identity in the *Drosophila* germline. *Development*, 133(15):2783–91, 2006.
- A. L. Casper and M. Van Doren. The establishment of sexual identity in the *Drosophila* germline. *Development*, 136(22):3821–30, 2009.
- E. E. Caygill and L. A. Johnston. Temporal regulation of metamorphic processes in *Drosophila* by the let-7 and miR-125 heterochronic microRNAs. *Curr Biol*, 18(13):943–50, 2008.
- A. K. Chang and H. Wu. The role of AIB1 in breast cancer. *Oncol Lett*, 4(4):588–594, 2012.
- J. Chau, L. S. Kulnane, and H. K. Salz. Sex-lethal facilitates the transition from germline stem cell to committed daughter cell in the *Drosophila* ovary. *Genetics*, 182(1):121–32, 2009.
- J. Chau, L. S. Kulnane, and H. K. Salz. Sex-lethal enables germline stem cell differentiation by down-regulating Nanos protein levels during *Drosophila* oogenesis. *Proc Natl Acad Sci U S A*, 109(24):9465–70, 2012.
- G. Chawla and N. S. Sokol. Hormonal activation of let-7-C microRNAs via EcR is required for adult *Drosophila melanogaster* morphology and function. *Development*, 139(10):1788–97, 2012.

- D. Chen and D. McKearin. Dpp signaling silences bam transcription directly to establish asymmetric divisions of germline stem cells. *Curr Biol*, 13(20):1786–91, 2003.
- S. Chen, S. Wang, and T. Xie. Restricting self-renewal signals within the stem cell niche: multiple levels of control. *Curr Opin Genet Dev*, 21(6):684–9, 2011.
- L. Cherbas, K. Lee, and P. Cherbas. Identification of ecdysone response elements by analysis of the *Drosophila* Eip28/29 gene. *Genes Dev*, 5(1):120–31, 1991.
- A. J. Chien, W. H. Conrad, and R. T. Moon. A Wnt survival guide: from flies to human disease. *J Invest Dermatol*, 129(7):1614–27, 2009.
- J. L. Christensen, D. E. Wright, A. J. Wagers, and I. L. Weissman. Circulation and chemotaxis of fetal hematopoietic stem cells. *PLoS Biol*, 2(3):E75, 2004.
- M. F. Clarke and M. Fuller. Stem cells and cancer: two faces of eve. *Cell*, 124(6):1111–5, 2006.
- E. Clough, W. Moon, S. Wang, K. Smith, and T. Hazelrigg. Histone methylation is required for oogenesis in *Drosophila*. *Development*, 134(1):157–65, 2007.
- J. Colombani, L. Bianchini, S. Layalle, E. Pondeville, C. Dauphin-Villemant, C. Antoniewski, C. Carre, S. Noselli, and P. Leopold. Antagonistic actions of ecdysone and insulins determine final size in *Drosophila*. *Science*, 310(5748):667–70, 2005.
- D. N. Cox, A. Chao, J. Baker, L. Chang, D. Qiao, and H. Lin. A novel class of evolutionarily conserved genes defined by piwi are essential for stem cell self-renewal. *Genes Dev*, 12(23):3715–27, 1998.
- C. M. Croce. Causes and consequences of microRNA dysregulation in cancer. *Nat Rev Genet*, 10(10):704–14, 2009.
- G. Q. Daley. The promise and perils of stem cell therapeutics. *Cell Stem Cell*, 10(6):740–9, 2012.
- E. Decotto and A. C. Spradling. The *Drosophila* ovarian and testis stem cell niches: similar somatic stem cells and signals. *Dev Cell*, 9(4):501–10, 2005.
- L. Dobens, K. Rudolph, and E. M. Berger. Ecdysterone regulatory elements function as both transcriptional activators and repressors. *Mol Cell Biol*, 11(4):1846–53, 1991.
- U. Dressel, D. Thormeyer, B. Altincicek, A. Paululat, M. Eggert, S. Schneider, S. P. Tenbaum, R. Renkawitz, and A. Baniahmad. Alien, a highly conserved protein with characteristics of a corepressor for members of the nuclear hormone receptor superfamily. *Mol Cell Biol*, 19(5):3383–94, 1999.

- D. Drummond-Barbosa and A. C. Spradling. Stem cells and their progeny respond to nutritional changes during *Drosophila* oogenesis. *Dev Biol*, 231(1):265–78, 2001.
- S. Eliazer, N. A. Shalaby, and M. Buszczak. Loss of lysine-specific demethylase 1 nonautonomously causes stem cell tumors in the *Drosophila* ovary. *Proc Natl Acad Sci U S A*, 108(17):7064–9, 2011.
- C. Elke, M. Vogtli, P. Rauch, M. Spindler-Barth, and M. Lezzi. Expression of EcR and USP in *Escherichia coli*: purification and functional studies. *Arch Insect Biochem Physiol*, 35(2):59–69, 1997.
- W. M. Elshamy and R. J. Duhe. Overview: cellular plasticity, cancer stem cells and metastasis. *Cancer Lett*, 341(1):2–8, 2013.
- M. J. Evans and M. H. Kaufman. Establishment in culture of pluripotential cells from mouse embryos. *Nature*, 292(5819):154–6, 1981.
- D. Fagegaltier, A. König, A. Gordon, E. C. Lai, T. R. Gingeras, G. J. Hannon, and H. R. Shcherbata. *Sexually dimorphic expression and functions of Drosophila miRNAs*.
- A. J. Forbes, H. Lin, P. W. Ingham, and A. C. Spradling. hedgehog is required for the proliferation and specification of ovarian somatic cells prior to egg chamber formation in *Drosophila*. *Development*, 122(4):1125–35, 1996a.
- A. J. Forbes, A. C. Spradling, P. W. Ingham, and H. Lin. The role of segment polarity genes during early oogenesis in *Drosophila*. *Development*, 122(10):3283–94, 1996b.
- K. Forstemann, Y. Tomari, T. Du, V. V. Vagin, A. M. Denli, D. P. Bratu, C. Klattehoff, W. E. Theurkauf, and P. D. Zamore. Normal microRNA maturation and germ-line stem cell maintenance requires Loquacious, a double-stranded RNA-binding domain protein. *PLoS Biol*, 3(7):e236, 2005.
- V. A. Francis, A. Zorzano, and A. A. Teleman. dDOR is an EcR coactivator that forms a feed-forward loop connecting insulin and ecdysone signaling. *Curr Biol*, 20(20):1799–808, 2010.
- M. T. Fuller and A. C. Spradling. Male and female *Drosophila* germline stem cells: two versions of immortality. *Science*, 316(5823):402–4, 2007.
- M. Galikova, P. Klepsatel, G. Senti, and T. Flatt. Steroid hormone regulation of *C. elegans* and *Drosophila* aging and life history. *Exp Gerontol*, 46(2).
- D. Gancz, T. Lengil, and L. Gilboa. Coordinated regulation of niche and stem cell precursors by hormonal signaling. *PLoS Biol*, 9(11):e1001202, 2011.
- A. Garbuzov and M. Tatar. Hormonal regulation of *Drosophila* microRNA let-7 and miR-125 that target innate immunity. *Fly (Austin)*, 4(4):306–11, 2010.

- A. Garen, L. Kauvar, and J. A. Lepesant. Roles of ecdysone in *Drosophila* development. *Proc Natl Acad Sci U S A*, 74(11):5099–103, 1977.
- J. Gates, G. Lam, J. A. Ortiz, R. Losson, and C. S. Thummel. rigor mortis encodes a novel nuclear receptor interacting protein required for ecdysone signaling during *Drosophila* larval development. *Development*, 131(1):25–36, 2004.
- L. I. Gilbert and J. T. Warren. A molecular genetic approach to the biosynthesis of the insect steroid molting hormone. *Vitam Horm*, 73:31–57, 2005.
- L. I. Gilbert, R. Rybczynski, and J. T. Warren. Control and biochemical nature of the ecdysteroidogenic pathway. *Annu Rev Entomol*, 47:883–916, 2002.
- L. Gilboa, A. Forbes, S. I. Tazuke, M. T. Fuller, and R. Lehmann. Germ line stem cell differentiation in *Drosophila* requires gap junctions and proceeds via an intermediate state. *Development*, 130(26):6625–34, 2003.
- C. K. Glass and M. G. Rosenfeld. The coregulator exchange in transcriptional functions of nuclear receptors. *Genes Dev*, 14(2):121–41, 2000.
- N. C. Grieder, I. Charlafti, U. Kloter, H. Jackle, U. Schafer, and W. J. Gehring. Misexpression screen in *Drosophila melanogaster* aiming to reveal novel factors involved in formation of body parts. *Genetics*, 175(4):1707–18, 2007.
- H. Grosshans, T. Johnson, K. L. Reinert, M. Gerstein, and F. J. Slack. The temporal patterning microRNA let-7 regulates several transcription factors at the larval to adult transition in *C. elegans*. *Dev Cell*, 8(3):321–30, 2005.
- Z. Guo and Z. Wang. The glypican Dally is required in the niche for the maintenance of germline stem cells and short-range BMP signaling in the *Drosophila* ovary. *Development*, 136(21):3627–35, 2009.
- J. B. Gurdon. The developmental capacity of nuclei taken from intestinal epithelium cells of feeding tadpoles. *J Embryol Exp Morphol*, 10:622–40, 1962.
- J. F. Hackney, C. Pucci, E. Naes, and L. Dobens. Ras signaling modulates activity of the ecdysone receptor EcR during cell migration in the *Drosophila* ovary. *Dev Dyn*, 236(5):1213–26, 2007.
- H. H. Hagedorn. The role of ecdysteroids in reproduction. In *Comprehensive Insect Physiology, Biochemistry and Pharmacology*, volume 8, pages 205–262. Pergamon Press, Oxford, 1985.
- C. M. Hammell, X. Karp, and V. Ambros. A feedback circuit involving let-7-family miRNAs and DAF-12 integrates environmental signals and developmental timing in *Caenorhabditis elegans*. *Proc Natl Acad Sci U S A*, 106(44):18668–73, 2009.
- R. E. Harris, M. Pargett, C. Sutcliffe, D. Umulis, and H. L. Ashe. Brat promotes stem cell differentiation via control of a bistable switch that restricts BMP signaling. *Dev Cell*, 20(1):72–83, 2011.

- K. Hashiyama, Y. Hayashi, and S. Kobayashi. *Drosophila* Sex lethal gene initiates female development in germline progenitors. *Science*, 333(6044):885–8, 2011.
- S. D. Hatfield, H. R. Shcherbata, K. A. Fischer, K. Nakahara, R. W. Carthew, and H. Ruohola-Baker. Stem cell division is regulated by the microRNA pathway. *Nature*, 435(7044):974–8, 2005.
- Y. Hayashi, S. Kobayashi, and H. Nakato. *Drosophila* glypicans regulate the germline stem cell niche. *J Cell Biol*, 187(4):473–80, 2009.
- L. He and G. J. Hannon. MicroRNAs: small RNAs with a big role in gene regulation. *Nat Rev Genet*, 5(7):522–31, 2004.
- B. E. Henderson and H. S. Feigelson. Hormonal carcinogenesis. *Carcinogenesis*, 21(3):427–33, 2000.
- P. J. Ho, M. L. Yen, S. F. Yet, and B. L. Yen. Current applications of human pluripotent stem cells: possibilities and challenges. *Cell Transplant*, 21(5):801–14, 2012.
- J. D. Holland, A. Klaus, A. N. Garratt, and W. Birchmeier. Wnt signaling in stem and cancer stem cells. *Curr Opin Cell Biol*, 25(2):254–64, 2013.
- H. J. Hsu and D. Drummond-Barbosa. Insulin levels control female germline stem cell maintenance via the niche in *Drosophila*. *Proc Natl Acad Sci U S A*, 106(4):1117–21, 2009.
- H. J. Hsu, L. LaFever, and D. Drummond-Barbosa. Diet controls normal and tumorous germline stem cells via insulin-dependent and -independent mechanisms in *Drosophila*. *Dev Biol*, 313(2):700–12, 2008.
- S. Hu, D. Fambrough, J. R. Atashi, C. S. Goodman, and S. T. Crews. The *Drosophila* abrupt gene encodes a BTB-zinc finger regulatory protein that controls the specificity of neuromuscular connections. *Genes Dev*, 9(23):2936–48, 1995.
- A. H. Huber and W. I. Weis. The structure of the beta-catenin/E-cadherin complex and the molecular basis of diverse ligand recognition by beta-catenin. *Cell*, 105(3):391–402, 2001.
- R. J. Ihry, A. L. Sapiro, and A. Bashirullah. Translational control by the DEAD Box RNA helicase belle regulates ecdysone-triggered transcriptional cascades. *PLoS Genet*, 8(11):e1003085, 2012.
- N. Iovino, A. Pane, and U. Gaul. miR-184 has multiple roles in *Drosophila* female germline development. *Dev Cell*, 17(1):123–33, 2009.
- H. Ishimoto and T. Kitamoto. The steroid molting hormone Ecdysone regulates sleep in adult *Drosophila melanogaster*. *Genetics*, 185(1):269–81, 2010.

- H. Ishimoto, T. Sakai, and T. Kitamoto. Ecdysone signaling regulates the formation of long-term courtship memory in adult *Drosophila melanogaster*. *Proc Natl Acad Sci U S A*, 106(15):6381–6, 2009.
- A. C. Jang, Y. C. Chang, J. Bai, and D. Montell. Border-cell migration requires integration of spatial and temporal signals by the BTB protein Abrupt. *Nat Cell Biol*, 11(5):569–79, 2009.
- H. Jasper and D. L. Jones. Metabolic regulation of stem cell behavior and implications for aging. *Cell Metab*, 12(6):561–5, 2010.
- X. Jiang, L. Xia, D. Chen, Y. Yang, H. Huang, L. Yang, Q. Zhao, L. Shen, and J. Wang. Otefin, a nuclear membrane protein, determines the fate of germline stem cells in *Drosophila* via interaction with Smad complexes. *Dev Cell*, 14(4):494–506, 2008.
- Z. Jin and T. Xie. Dcr-1 maintains *Drosophila* ovarian stem cells. *Curr Biol*, 17(6):539–44, 2007.
- Z. Jin, D. Kirilly, C. Weng, E. Kawase, X. Song, S. Smith, J. Schwartz, and T. Xie. Differentiation-defective stem cells outcompete normal stem cells for niche occupancy in the *Drosophila* ovary. *Cell Stem Cell*, 2(1):39–49, 2008.
- D. M. Johnston, Y. Sedkov, S. Petruk, K. M. Riley, M. Fujioka, J. B. Jaynes, and A. Mazo. Ecdysone- and NO-mediated gene regulation by competing EcR/Usp and E75A nuclear receptors during *Drosophila* development. *Mol Cell*, 44(1):51–61, 2011.
- D. L. Jones and A. J. Wagers. No place like home: anatomy and function of the stem cell niche. *Nat Rev Mol Cell Biol*, 9(1):11–21, 2008.
- P. A. Joshi, M. A. Di Grappa, and R. Khokha. Active allies: hormones, stem cells and the niche in adult mammopoiesis. *Trends Endocrinol Metab*, 23(6):299–309, 2012.
- T. Kai and A. Spradling. An empty *Drosophila* stem cell niche reactivates the proliferation of ectopic cells. *Proc Natl Acad Sci U S A*, 100(8):4633–8, 2003a.
- T. Kai and A. Spradling. An empty *Drosophila* stem cell niche reactivates the proliferation of ectopic cells. *Proc Natl Acad Sci U S A*, 100(8):4633–8, 2003b.
- T. Kai and A. Spradling. Differentiating germ cells can revert into functional stem cells in *Drosophila melanogaster* ovaries. *Nature*, 428(6982):564–9, 2004.
- O. Karpiuk, Z. Najafova, F. Kramer, M. Hennion, C. Galonska, A. König, N. Snaidero, T. Vogel, A. Shchebet, Y. Begus-Nahrman, M. Kassem, M. Simons, H. Shcherbata, T. Beissbarth, and S. A. Johnsen. The histone H2B monoubiquitination regulatory pathway is required for differentiation of multipotent stem cells. *Mol Cell*, 46(5):705–13, 2012.

- D. Kimelman and W. Xu. beta-catenin destruction complex: insights and questions from a structural perspective. *Oncogene*, 25(57):7482–91, 2006.
- F. J. King and H. Lin. Somatic signaling mediated by fs(1)Yb is essential for germline stem cell maintenance during *Drosophila* oogenesis. *Development*, 126(9):1833–44, 1999.
- F. J. King, A. Szakmary, D. N. Cox, and H. Lin. Yb modulates the divisions of both germline and somatic stem cells through piwi- and hh-mediated mechanisms in the *Drosophila* ovary. *Mol Cell*, 7(3):497–508, 2001.
- R.C. King. Aberrant fusomes in the ovarian cytotocytes of the fs(1)231 mutant of *Drosophila melanogaster* Meigen. *Int. J. Insect Morph. Embryol.*, 8(5).
- K. King-Jones and C. S. Thummel. Nuclear receptors—a perspective from *Drosophila*. *Nat Rev Genet*, 6(4):311–23, 2005.
- D. Kirilly, S. Wang, and T. Xie. Self-maintained escort cells form a germline stem cell differentiation niche. *Development*, 138(23):5087–97, 2011.
- C. M. Koch, M. Honemann-Capito, D. Egger-Adam, and A. Wodarz. Windei, the *Drosophila* homolog of mAM/MCAF1, is an essential cofactor of the H3K9 methyl transferase dSETDB1/Eggless in germ line development. *PLoS Genet*, 5(9):e1000644, 2009.
- A. König, A. S. Yatsenko, M. Weiss, and H. R. Shcherbata. Ecdysteroids affect *Drosophila* ovarian stem cell niche formation and early germline differentiation. *EMBO J*, 30(8):1549–62, 2011.
- T. Kozlova and C. S. Thummel. Steroid regulation of postembryonic development and reproduction in *Drosophila*. *Trends Endocrinol Metab*, 11(7):276–80, 2000.
- M. M. Kucherenko and H. R. Shcherbata. Steroids as external temporal codes act via miRNAs and cooperate with cytokines in differential neurogenesis. *Fly (Austin)*, 7(3), 2013.
- M. M. Kucherenko, J. Barth, A. Fiala, and H. R. Shcherbata. Steroid-induced microRNA let-7 acts as a spatio-temporal code for neuronal cell fate in the developing *Drosophila* brain. *EMBO J*, 31(24):4511–23, 2012.
- J. Ladewig, P. Koch, and O. Brustle. Leveling Waddington: the emergence of direct programming and the loss of cell fate hierarchies. *Nat Rev Mol Cell Biol*, 14(4):225–36, 2013.
- L. LaFever and D. Drummond-Barbosa. Direct control of germline stem cell division and cyst growth by neural insulin in *Drosophila*. *Science*, 309(5737):1071–3, 2005.
- J. L. Leatherman and S. Dinardo. Germline self-renewal requires cyst stem cells and stat regulates niche adhesion in *Drosophila* testes. *Nat Cell Biol*, 12(8):806–11, 2010.

- R. C. Lee, R. L. Feinbaum, and V. Ambros. The *C. elegans* heterochronic gene *lin-4* encodes small RNAs with antisense complementarity to *lin-14*. *Cell*, 75(5):843–54, 1993.
- W. Li, F. Wang, L. Menut, and F. B. Gao. BTB/POZ-zinc finger protein abrupt suppresses dendritic branching in a neuronal subtype-specific and dosage-dependent manner. *Neuron*, 43(6):823–34, 2004.
- Y. Li, N. T. Minor, J. K. Park, D. M. McKearin, and J. Z. Maines. Bam and Bgcn antagonize Nanos-dependent germ-line stem cell maintenance. *Proc Natl Acad Sci U S A*, 106(23):9304–9, 2009.
- Y. Li, J. Z. Maines, O. Y. Tastan, D. M. McKearin, and M. Buszczak. Mei-P26 regulates the maintenance of ovarian germline stem cells by promoting BMP signaling. *Development*, 139(9):1547–56, 2012.
- H. Lin, L. Yue, and A. C. Spradling. The *Drosophila* fusome, a germline-specific organelle, contains membrane skeletal proteins and functions in cyst formation. *Development*, 120(4):947–56, 1994.
- G Litwack. Steroids. 1994.
- M. Liu, T. M. Lim, and Y. Cai. The *Drosophila* female germline stem cell lineage acts to spatially restrict DPP function within the niche. *Sci Signal*, 3(132):ra57, 2010.
- L. Lopez-Onieva, A. Fernandez-Minan, and A. Gonzalez-Reyes. Jak/Stat signalling in niche support cells regulates dpp transcription to control germline stem cell maintenance in the *Drosophila* ovary. *Development*, 135(3):533–40, 2008.
- J. P. Lydon. Stem cells: Cues from steroid hormones. *Nature*, 465(7299):695–6, 2010.
- B. T. MacDonald, K. Tamai, and X. He. Wnt/beta-catenin signaling: components, mechanisms, and diseases. *Dev Cell*, 17(1):9–26, 2009.
- J. Margolis and A. Spradling. Identification and behavior of epithelial stem cells in the *Drosophila* ovary. *Development*, 121(11):3797–807, 1995.
- V. Marthiens, I. Kazanis, L. Moss, K. Long, and C. Ffrench-Constant. Adhesion molecules in the stem cell niche—more than just staying in shape? *J Cell Sci*, 123(10):1613–22, 2010.
- G. R. Martin. Isolation of a pluripotent cell line from early mouse embryos cultured in medium conditioned by teratocarcinoma stem cells. *Proc Natl Acad Sci U S A*, 78(12):7634–8, 1981.
- E. L. Matunis, R. R. Stine, and M. de Cuevas. Recent advances in *Drosophila* male germline stem cell biology. *Spermatogenesis*, 2(3):137–144, 2012.

- D. McKearin and B. Ohlstein. A role for the *Drosophila* bag-of-marbles protein in the differentiation of cystoblasts from germline stem cells. *Development*, 121(9):2937–47, 1995.
- D. M. McKearin and A. C. Spradling. bag-of-marbles: a *Drosophila* gene required to initiate both male and female gametogenesis. *Genes Dev*, 4(12).
- P. M. Meneely and R. K. Herman. Lethals, steriles and deficiencies in a region of the X chromosome of *Caenorhabditis elegans*. *Genetics*, 92(1):99–115, 1979.
- H. K. Mikkola and S. H. Orkin. The journey of developing hematopoietic stem cells. *Development*, 133(19):3733–44, 2006.
- V. Mondol and A. E. Pasquinelli. Let’s make it happen: the role of let-7 microRNA in development. *Curr Top Dev Biol*, 99:1–30, 2012.
- L. X. Morris and A. C. Spradling. Long-term live imaging provides new insight into stem cell regulation and germline-soma coordination in the *Drosophila* ovary. *Development*, 138(11):2207–15, 2011.
- L. X. Morris and A. C. Spradling. Steroid signaling within *Drosophila* ovarian epithelial cells sex-specifically modulates early germ cell development and meiotic entry. *PLoS One*, 7(10):e46109, 2012.
- S. J. Morrison and A. C. Spradling. Stem cells and niches: mechanisms that promote stem cell maintenance throughout life. *Cell*, 132(4):598–611, 2008.
- S. M. Murray, S. Y. Yang, and M. Van Doren. Germ cell sex determination: a collaboration between soma and germline. *Curr Opin Cell Biol*, 22(6):722–9, 2010.
- R. A. Neumuller, J. Betschinger, A. Fischer, N. Bushati, I. Poernbacher, K. Mechtler, S. M. Cohen, and J. A. Knoblich. Mei-P26 regulates microRNAs and cell growth in the *Drosophila* ovarian stem cell lineage. *Nature*, 454(7201):241–5, 2008.
- R. A. Nimmo and F. J. Slack. An elegant miRror: microRNAs in stem cells, developmental timing and cancer. *Chromosoma*, 118(4):405–18, 2009.
- T. Nystul and A. Spradling. An epithelial niche in the *Drosophila* ovary undergoes long-range stem cell replacement. *Cell Stem Cell*, 1(3):277–85, 2007.
- B. Ohlstein and D. McKearin. Ectopic expression of the *Drosophila* Bam protein eliminates oogenic germline stem cells. *Development*, 124(18):3651–62, 1997.
- B. Oliver, N. Perrimon, and A. P. Mahowald. The ovo locus is required for sex-specific germ line maintenance in *Drosophila*. *Genes Dev*, 1(9):913–23, 1987.
- A. E. Oro, M. McKeown, and R. M. Evans. Relationship between the product of the *Drosophila* ultraspiracle locus and the vertebrate retinoid X receptor. *Nature*, 347(6290):298–301, 1990.

- S. L. Page, K. S. McKim, B. Deneen, T. L. Van Hook, and R. S. Hawley. Genetic studies of mei-P26 reveal a link between the processes that control germ cell proliferation in both sexes and those that control meiotic exchange in *Drosophila*. *Genetics*, 155(4):1757–72, 2000.
- L. Pan, S. Chen, C. Weng, G. Call, D. Zhu, H. Tang, N. Zhang, and T. Xie. Stem cell aging is controlled both intrinsically and extrinsically in the *Drosophila* ovary. *Cell Stem Cell*, 1(4):458–69, 2007.
- J. K. Park, X. Liu, T. J. Strauss, D. M. McKearin, and Q. Liu. The miRNA pathway intrinsically controls self-renewal of *Drosophila* germline stem cells. *Curr Biol*, 17(6):533–8, 2007.
- A. E. Pasquinelli, B. J. Reinhart, F. Slack, M. Q. Martindale, M. I. Kuroda, B. Maller, D. C. Hayward, E. E. Ball, B. Degan, P. Muller, J. Spring, A. Srinivasan, M. Fishman, J. Finnerty, J. Corbo, M. Levine, P. Leahy, E. Davidson, and G. Ruvkun. Conservation of the sequence and temporal expression of let-7 heterochronic regulatory RNA. *Nature*, 408(6808):86–9, 2000.
- J. W. Pek, A. K. Lim, and T. Kai. *Drosophila* maelstrom ensures proper germline stem cell lineage differentiation by repressing microRNA-7. *Dev Cell*, 17(3):417–24, 2009.
- J. Qi, J. Y. Yu, H. R. Shcherbata, J. Mathieu, A. J. Wang, S. Seal, W. Zhou, B. M. Stadler, D. Bourgin, L. Wang, A. Nelson, C. Ware, C. Raymond, L. P. Lim, J. Magnus, I. Ivanovska, R. Diaz, A. Ball, M. A. Cleary, and H. Ruohola-Baker. microRNAs regulate human embryonic stem cell division. *Cell Cycle*, 8(22):3729–41, 2009.
- I. Y. Rauschenbach, M. Z. Sukhanova, A. Hirashima, E. Sutsugu, and E. Kuano. Role of the ecdysteroid system in the regulation of *Drosophila* reproduction under environmental stress. *Dokl Biol Sci*, 375:641–3, 2000.
- B. J. Reinhart, F. J. Slack, M. Basson, A. E. Pasquinelli, J. C. Bettinger, A. E. Rougvie, H. R. Horvitz, and G. Ruvkun. The 21-nucleotide let-7 RNA regulates developmental timing in *Caenorhabditis elegans*. *Nature*, 403(6772):901–6, 2000.
- L. Ringrose and R. Paro. Epigenetic regulation of cellular memory by the Polycomb and Trithorax group proteins. *Annu Rev Genet*, 38:413–43, 2004.
- P. Rojas-Rios, I. Guerrero, and A. Gonzalez-Reyes. Cytoneme-mediated delivery of hedgehog regulates the expression of bone morphogenetic proteins to maintain germline stem cells in *Drosophila*. *PLoS Biol*, 10(4):e1001298, 2012.
- S. Roush and F. J. Slack. The let-7 family of microRNAs. *Trends Cell Biol*, 18(10):505–16, 2008.

- P. Sahai-Hernandez and T. G. Nystul. A dynamic population of stromal cells contributes to the follicle stem cell niche in the *Drosophila* ovary. *Development*, 140(22):4490–8, 2013.
- K. Saito, H. Ishizu, M. Komai, H. Kotani, Y. Kawamura, K. M. Nishida, H. Siomi, and M. C. Siomi. Roles for the Yb body components Armitage and Yb in primary piRNA biogenesis in *Drosophila*. *Genes Dev*, 24(22):2493–8, 2010.
- K. Saito-Diaz, T. W. Chen, X. Wang, C. A. Thorne, H. A. Wallace, A. Page-McCaw, and E. Lee. The way Wnt works: components and mechanism. *Growth Factors*, 31(1):1–31, 2013.
- H. K. Salz. Sex determination in insects: a binary decision based on alternative splicing. *Curr Opin Genet Dev*, 21(4):395–400, 2011.
- H. K. Salz and J. W. Erickson. Sex determination in *Drosophila*: The view from the top. *Fly (Austin)*, 4(1):60–70, 2010.
- T. Samji. PIWI, piRNAs, and germline stem cells: what’s the link? *Yale J Biol Med*, 82(3):121–4, 2009.
- B. Sanson, P. White, and J. P. Vincent. Uncoupling cadherin-based adhesion from wingless signalling in *Drosophila*. *Nature*, 383(6601):627–30, 1996.
- S. Sawatsubashi, T. Murata, J. Lim, R. Fujiki, S. Ito, E. Suzuki, M. Tanabe, Y. Zhao, S. Kimura, S. Fujiyama, T. Ueda, D. Umetsu, T. Ito, K. Takeyama, and S. Kato. A histone chaperone, DEK, transcriptionally coactivates a nuclear receptor. *Genes Dev*, 24(2):159–70, 2010.
- R. Schofield. The relationship between the spleen colony-forming cell and the haemopoietic stem cell. *Blood cells*, 4:7–25, 1978.
- M. Schubiger and J. W. Truman. The RXR ortholog USP suppresses early metamorphic processes in *Drosophila* in the absence of ecdysteroids. *Development*, 127(6):1151–9, 2000.
- M. Schubiger, C. Carre, C. Antoniewski, and J. W. Truman. Ligand-dependent de-repression via EcR/USP acts as a gate to coordinate the differentiation of sensory neurons in the *Drosophila* wing. *Development*, 132(23):5239–48, 2005.
- B. R. Schulman, A. Esquela-Kerscher, and F. J. Slack. Reciprocal expression of lin-41 and the microRNAs let-7 and mir-125 during mouse embryogenesis. *Dev Dyn*, 234(4):1046–54, 2005.
- C. Schulz, C. G. Wood, D. L. Jones, S. I. Tazuke, and M. T. Fuller. Signaling from germ cells mediated by the rhomboid homolog stet organizes encapsulation by somatic support cells. *Development*, 129(19):4523–34, 2002.
- M.B. Schwartz, T.J. Kelly, R.B. Imberski, and E.C. Rubenstein.

- C. Schwedes, S. Tulsiani, and G. E. Carney. Ecdysone receptor expression and activity in adult *Drosophila melanogaster*. *J Insect Physiol*, 57(7):899–907, 2011.
- C. C. Schwedes and G. E. Carney. Ecdysone signaling in adult *Drosophila melanogaster*. *J Insect Physiol*, 58(3):293–302, 2012.
- Y. Sedkov, E. Cho, S. Petruk, L. Cherbas, S. T. Smith, R. S. Jones, P. Cherbas, E. Canaani, J. B. Jaynes, and A. Mazo. Methylation at lysine 4 of histone H3 in ecdysone-dependent development of *Drosophila*. *Nature*, 426(6962):78–83, 2003.
- L. F. Sempere, E. B. Dubrovsky, V. A. Dubrovskaya, E. M. Berger, and V. Ambros. The expression of the *let-7* small regulatory RNA is controlled by ecdysone during metamorphosis in *Drosophila melanogaster*. *Dev Biol*, 244(1):170–9, 2002.
- L. F. Sempere, N. S. Sokol, E. B. Dubrovsky, E. M. Berger, and V. Ambros. Temporal regulation of microRNA expression in *Drosophila melanogaster* mediated by hormonal signals and broad-Complex gene activity. *Dev Biol*, 259(1):9–18, 2003.
- L. F. Sempere, S. Freemantle, I. Pitha-Rowe, E. Moss, E. Dmitrovsky, and V. Ambros. Expression profiling of mammalian microRNAs uncovers a subset of brain-expressed microRNAs with possible roles in murine and human neuronal differentiation. *Genome Biol*, 5(3):R13, 2004.
- K. A. Senti and J. Brennecke. The piRNA pathway: a fly’s perspective on the guardian of the genome. *Trends Genet*, 26(12):499–509, 2010.
- H. R. Shcherbata, C. Althausen, S. D. Findley, and H. Ruohola-Baker. The mitotic-to-endocycle switch in *Drosophila* follicle cells is executed by Notch-dependent regulation of G1/S, G2/M and M/G1 cell-cycle transitions. *Development*, 131(13):3169–81, 2004.
- H. R. Shcherbata, S. Hatfield, E. J. Ward, S. Reynolds, K. A. Fischer, and H. Ruohola-Baker. The MicroRNA pathway plays a regulatory role in stem cell division. *Cell Cycle*, 5(2):172–5, 2006.
- H. R. Shcherbata, E. J. Ward, K. A. Fischer, J. Y. Yu, S. H. Reynolds, C. H. Chen, P. Xu, B. A. Hay, and H. Ruohola-Baker. Stage-specific differences in the requirements for germline stem cell maintenance in the *Drosophila* ovary. *Cell Stem Cell*, 1(6):698–709, 2007.
- R. Shen and T. Xie. NANOS: a germline stem cell’s Guardian Angel. *J Mol Cell Biol*, 2(2):76–7, 2010.
- R. Shen, C. Weng, J. Yu, and T. Xie. eIF4A controls germline stem cell self-renewal by directly inhibiting BAM function in the *Drosophila* ovary. *Proc Natl Acad Sci U S A*, 106(28):11623–8, 2009.

- V. Siciliano, I. Garzilli, C. Fracassi, S. Criscuolo, S. Ventre, and D. di Bernardo. MiRNAs confer phenotypic robustness to gene networks by suppressing biological noise. *Nat Commun*, 4:2364, 2013.
- H. Sim, A. Argentaro, and V. R. Harley. Boys, girls and shuttling of SRY and SOX9. *Trends Endocrinol Metab*, 19(6):213–22, 2008.
- A. F. Simon, C. Shih, A. Mack, and S. Benzer. Steroid control of longevity in *Drosophila melanogaster*. *Science*, 299(5611):1407–10, 2003.
- F. J. Slack, M. Basson, Z. Liu, V. Ambros, H. R. Horvitz, and G. Ruvkun. The lin-41 RBCC gene acts in the *C. elegans* heterochronic pathway between the let-7 regulatory RNA and the LIN-29 transcription factor. *Mol Cell*, 5(4):659–69, 2000.
- A. G. Smith, J. K. Heath, D. D. Donaldson, G. G. Wong, J. Moreau, M. Stahl, and D. Rogers. Inhibition of pluripotential embryonic stem cell differentiation by purified polypeptides. *Nature*, 336(6200):688–90, 1988.
- N. S. Sokol. Small temporal RNAs in animal development. *Curr Opin Genet Dev*, 22(4):368–73, 2012.
- N. S. Sokol, P. Xu, Y. N. Jan, and V. Ambros. *Drosophila* let-7 microRNA is required for remodeling of the neuromusculature during metamorphosis. *Genes Dev*, 22(12):1591–6, 2008.
- M. Soller, M. Bownes, and E. Kubli. Control of oocyte maturation in sexually mature *Drosophila* females. *Dev Biol*, 208(2):337–51, 1999.
- I. M. Somorjai and A. Martinez-Arias. Wingless signalling alters the levels, sub-cellular distribution and dynamics of Armadillo and E-cadherin in third instar larval wing imaginal discs. *PLoS One*, 3(8):e2893, 2008.
- X. Song and T. Xie. Wingless signaling regulates the maintenance of ovarian somatic stem cells in *Drosophila*. *Development*, 130(14):3259–68, 2003.
- X. Song, C. H. Zhu, C. Doan, and T. Xie. Germline stem cells anchored by adherens junctions in the *Drosophila* ovary niches. *Science*, 296(5574):1855–7, 2002.
- X. Song, M. D. Wong, E. Kawase, R. Xi, B. C. Ding, J. J. McCarthy, and T. Xie. Bmp signals from niche cells directly repress transcription of a differentiation-promoting gene, bag of marbles, in germline stem cells in the *Drosophila* ovary. *Development*, 131(6):1353–64, 2004.
- A. Spradling, M. T. Fuller, R. E. Braun, and S. Yoshida. Germline stem cells. *Cold Spring Harb Perspect Biol*, 3(11):a002642, 2011.
- S. Staab, A. Heller, and M. Steinmann-Zwicky. Somatic sex-determining signals act on XX germ cells in *Drosophila* embryos. *Development*, 122(12):4065–71, 1996.

- P. J. Stogios, G. S. Downs, J. J. Jauhal, S. K. Nandra, and G. G. Prive. Sequence and structural analysis of BTB domain proteins. *Genome Biol*, 6(10):R82, 2005.
- K. Sugimura, D. Satoh, P. Estes, S. Crews, and T. Uemura. Development of morphological diversity of dendrites in *Drosophila* by the BTB-zinc finger protein abrupt. *Neuron*, 43(6):809–22, 2004.
- S. Swarup and E. M. Verheyen. Wnt/Wingless signaling in *Drosophila*. *Cold Spring Harb Perspect Biol*, 4(6), 2012.
- K. Takahashi and S. Yamanaka. Induction of pluripotent stem cells from mouse embryonic and adult fibroblast cultures by defined factors. *Cell*, 126(4):663–76, 2006.
- K. Takahashi, K. Tanabe, M. Ohnuki, M. Narita, T. Ichisaka, K. Tomoda, and S. Yamanaka. Induction of pluripotent stem cells from adult human fibroblasts by defined factors. *Cell*, 131(5):861–72, 2007.
- W. S. Talbot, E. A. Swyryd, and D. S. Hogness. *Drosophila* tissues with different metamorphic responses to ecdysone express different ecdysone receptor isoforms. *Cell*, 73(7):1323–37, 1993.
- J. M. Tennessen and C. S. Thummel. Coordinating growth and maturation - insights from *Drosophila*. *Curr Biol*, 21(18):R750–7, 2011.
- J. Terashima and M. Bownes. A microarray analysis of genes involved in relating egg production to nutritional intake in *Drosophila melanogaster*. *Cell Death Differ*, 12(5):429–40, 2005.
- J. Terashima and M. Bownes. E75A and E75B have opposite effects on the apoptosis/development choice of the *Drosophila* egg chamber. *Cell Death Differ*, 13(3):454–64, 2006.
- J. Terashima, K. Takaki, S. Sakurai, and M. Bownes. Nutritional status affects 20-hydroxyecdysone concentration and progression of oogenesis in *Drosophila melanogaster*. *J Endocrinol*, 187(1):69–79, 2005.
- H. E. Thomas, H. G. Stunnenberg, and A. F. Stewart. Heterodimerization of the *Drosophila* ecdysone receptor with retinoid X receptor and ultraspiracle. *Nature*, 362(6419):471–5, 1993.
- J. A. Thomson, J. Itskovitz-Eldor, S. S. Shapiro, M. A. Waknitz, J. J. Swiergiel, V. S. Marshall, and J. M. Jones. Embryonic stem cell lines derived from human blastocysts. *Science*, 282(5391):1145–7, 1998.
- C. S. Thummel. Flies on steroids—*Drosophila* metamorphosis and the mechanisms of steroid hormone action. *Trends Genet*, 12(8):306–10, 1996.
- H. Toledano, C. D’Alterio, B. Czech, E. Levine, and D. L. Jones. The let-7-imp axis regulates ageing of the *Drosophila* testis stem-cell niche. *Nature*, 485(7400):605–10, 2012.

- H. Tricoire, V. Battisti, S. Trannoy, C. Lasbleiz, A. M. Pret, and V. Monnier. The steroid hormone receptor EcR finely modulates *Drosophila* lifespan during adulthood in a sex-specific manner. *Mech Ageing Dev*, 130(8):547–52, 2009.
- C. C. Tsai, H. Y. Kao, T. P. Yao, M. McKeown, and R. M. Evans. SMRTER, a *Drosophila* nuclear receptor coregulator, reveals that EcR-mediated repression is critical for development. *Mol Cell*, 4(2):175–86, 1999.
- M. P. Tu, C. M. Yin, and M. Tatar. Impaired ovarian ecdysone synthesis of *Drosophila melanogaster* insulin receptor mutants. *Aging Cell*, 1(2):158–60, 2002.
- N. Turkel, V. K. Sahota, J. E. Bolden, K. R. Goulding, K. Doggett, L. F. Willoughby, E. Blanco, E. Martin-Blanco, M. Corominas, J. Ellul, T. Aigaki, H. E. Richardson, and A. M. Brumby. The BTB-zinc finger transcription factor abrupt acts as an epithelial oncogene in *Drosophila melanogaster* through maintaining a progenitor-like cell state. *PLoS Genet*, 9(7):e1003627, 2013.
- T. Valenta, G. Hausmann, and K. Basler. The many faces and functions of beta-catenin. *EMBO J*, 31(12):2714–36, 2012.
- J. A. van der Knaap, E. Kozhevnikova, K. Langenberg, Y. M. Moshkin, and C. P. Verrijzer. Biosynthetic enzyme GMP synthetase cooperates with ubiquitin-specific protease 7 in transcriptional regulation of ecdysteroid target genes. *Mol Cell Biol*, 30(3):736–44, 2010.
- V. Volarevic, B. Ljubic, P. Stojkovic, A. Lukic, N. Arsenijevic, and M. Stojkovic. Human stem cell research and regenerative medicine—present and future. *Br Med Bull*, 99:155–68, 2011.
- J. Voog and D. L. Jones. Stem cells and the niche: a dynamic duo. *Cell Stem Cell*, 6(2):103–15, 2010.
- C. H. Waddington and H. Kacser. *The Strategy of the Genes: A Discussion of Some Aspects of Theoretical Biology*. 1957.
- M. R. Walker, K. K. Patel, and T. S. Stappenbeck. The stem cell niche. *J Pathol*, 217(2):169–80, 2009.
- L. Wang, Z. Li, and Y. Cai. The JAK/STAT pathway positively regulates DPP signaling in the *Drosophila* germline stem cell niche. *J Cell Biol*, 180(4):721–8, 2008a.
- X. Wang, R. E. Harris, L. J. Bayston, and H. L. Ashe. Type IV collagens regulate BMP signalling in *Drosophila*. *Nature*, 455(7209):72–7, 2008b.
- Z. Wang and H. Lin. Nanos maintains germline stem cell self-renewal by preventing differentiation. *Science*, 303(5666):2016–9, 2004.

- E. J. Ward, H. R. Shcherbata, S. H. Reynolds, K. A. Fischer, S. D. Hatfield, and H. Ruohola-Baker. Stem cells signal to the niche through the Notch pathway in the *Drosophila* ovary. *Curr Biol*, 16(23):2352–8, 2006.
- M. Wawersik, A. Milutinovich, A. L. Casper, E. Matunis, B. Williams, and M. Van Doren. Somatic control of germline sexual development is mediated by the JAK/STAT pathway. *Nature*, 436(7050):563–7, 2005.
- G. Wei, B. Oliver, D. Pauli, and A. P. Mahowald. Evidence for sex transformation of germline cells in ovarian tumor mutants of *Drosophila*. *Dev Biol*, 161(1):318–20, 1994.
- M. Weiss. Germline stem cell - niche interactions in *drosophila melanogaster*. Master’s thesis, Medical Faculty University of Rostock and Max Planck Institute for Biophysical Chemistry Göttingen, 2009.
- B. Wightman, I. Ha, and G. Ruvkun. Posttranscriptional regulation of the heterochronic gene *lin-14* by *lin-4* mediates temporal pattern formation in *C. elegans*. *Cell*, 75(5):855–62, 1993.
- I. Wilmut, A. E. Schnieke, J. McWhir, A. J. Kind, and K. H. Campbell. Viable offspring derived from fetal and adult mammalian cells. *Nature*, 385(6619):810–3, 1997.
- A. Wodarz, D. B. Stewart, W. J. Nelson, and R. Nusse. Wingless signaling modulates cadherin-mediated cell adhesion in *Drosophila* imaginal disc cells. *J Cell Sci*, 119(12):2425–34, 2006.
- D. E. Wright, C. Y. Wang, and C. F. Kao. Flickin’ the ubiquitin switch: the role of H2B ubiquitylation in development. *Epigenetics*, 6(10):1165–75, 2011.
- R. Xi. Anchoring stem cells in the niche by cell adhesion molecules. *Cell Adh Migr*, 3(4):396–401, 2009.
- R. Xi and T. Xie. Stem cell self-renewal controlled by chromatin remodeling factors. *Science*, 310(5753):1487–9, 2005.
- L. Xia, S. Jia, S. Huang, H. Wang, Y. Zhu, Y. Mu, L. Kan, W. Zheng, D. Wu, X. Li, Q. Sun, A. Meng, and D. Chen. The Fused/Smurf complex controls the fate of *Drosophila* germline stem cells by generating a gradient BMP response. *Cell*, 143(6):978–90, 2010.
- T. Xie and A. C. Spradling. *decapentaplegic* is essential for the maintenance and division of germline stem cells in the *Drosophila* ovary. *Cell*, 94(2):251–60, 1998.
- T. Xie and A. C. Spradling. A niche maintaining germ line stem cells in the *Drosophila* ovary. *Science*, 290(5490):328–30, 2000.

- T. Xuan, T. Xin, J. He, J. Tan, Y. Gao, S. Feng, L. He, G. Zhao, and M. Li. dBre1/dSet1-dependent pathway for histone H3K4 trimethylation has essential roles in controlling germline stem cell maintenance and germ cell differentiation in the *Drosophila* ovary. *Dev Biol*, 379(2):167–81, 2013.
- S. Yamanaka. A fresh look at iPS cells. *Cell*, 137(1):13–7, 2009.
- S. Yamanaka and H. M. Blau. Nuclear reprogramming to a pluripotent state by three approaches. *Nature*, 465(7299):704–12, 2010.
- J. S. Yang and E. C. Lai. Alternative miRNA biogenesis pathways and the interpretation of core miRNA pathway mutants. *Mol Cell*, 43(6):892–903, 2011.
- L. Yang, D. Chen, R. Duan, L. Xia, J. Wang, A. Qurashi, and P. Jin. Argonaute 1 regulates the fate of germline stem cells in *Drosophila*. *Development*, 134(23):4265–72, 2007.
- T. P. Yao, B. M. Forman, Z. Jiang, L. Cherbas, J. D. Chen, M. McKeown, P. Cherbas, and R. M. Evans. Functional ecdysone receptor is the product of EcR and Ultraspiracle genes. *Nature*, 366(6454):476–9, 1993.
- Y. Yarden and B. Z. Shilo. SnapShot: EGFR signaling pathway. *Cell*, 131(5):1018, 2007.
- J. Yoon, K. S. Lee, J. S. Park, K. Yu, S. G. Paik, and Y. K. Kang. dSETDB1 and SU(VAR)3-9 sequentially function during germline-stem cell differentiation in *Drosophila melanogaster*. *PLoS One*, 3(5):e2234, 2008.
- H. Yoshida, J. Liu, S. Samuel, W. Cheng, D. Rosen, and H. Naora. Steroid receptor coactivator-3, a homolog of Taiman that controls cell migration in the *Drosophila* ovary, regulates migration of human ovarian cancer cells. *Mol Cell Endocrinol*, 245(1).
- J. Y. Yu, S. H. Reynolds, S. D. Hatfield, H. R. Shcherbata, K. A. Fischer, E. J. Ward, D. Long, Y. Ding, and H. Ruohola-Baker. Dicer-1-dependent Dacapo suppression acts downstream of Insulin receptor in regulating cell division of *Drosophila* germline stem cells. *Development*, 136(9):1497–507, 2009.
- A. G. Zapata, D. Alfaro, and J. Garcia-Ceca. Biology of stem cells: the role of microenvironments. *Adv Exp Med Biol*, 741:135–51, 2012.
- C. H. Zhu and T. Xie. Clonal expansion of ovarian germline stem cells during niche formation in *Drosophila*. *Development*, 130(12):2579–88, 2003.
- S. Zollman, D. Godt, G. G. Prive, J. L. Couderc, and F. A. Laski. The BTB domain, found primarily in zinc finger proteins, defines an evolutionarily conserved family that includes several developmentally regulated genes in *Drosophila*. *Proc Natl Acad Sci U S A*, 91(22):10717–21, 1994.

Appendix

**Ecdysteroids affect *Drosophila* ovarian stem cell
niche formation and early germline differentiation:
Supplementary Material**

Supplementary Figure Legends

Supplementary Figure 1. PH3 staining reveals, that the high number of SSCs that is caused by EcR overexpression is not due to fusome breakdown.

(A) Cells in developing germline cysts that are connected via a fusome are dividing simultaneously as shown here by PH3 mitotic marker. (B) The SSCs that are observed upon exogenous *hsEcR.A* expression do not have their division synchronized. Red, Adducin+LaminC; blue, DAPI; and green PH3.

Supplementary Figure 2. Tai expression in escort cells.

(A-B) To confirm the specificity of Tai antibody staining in escort cells we generated *tai* loss of function somatic clones (*hs Flp; tai^{61G1} FRT40A/UbiGFP FRT40A*) and observed that Tai staining is diminished in *tai* mutant cells. Compare levels of antibody staining in *tai* mutant escort cell (white arrows) and sister clones (green arrows).

Red, Taiman; blue, DAPI; and green, GFP.

Supplementary Figure 3.

Tai is not required for progressive oocyte development and GSC maintenance.

(A) *tai^{61G1}* loss of function clones in the germarium do not affect the steady production of egg chambers, showing that loss of Tai does not affect GSC division or oocyte differentiation.

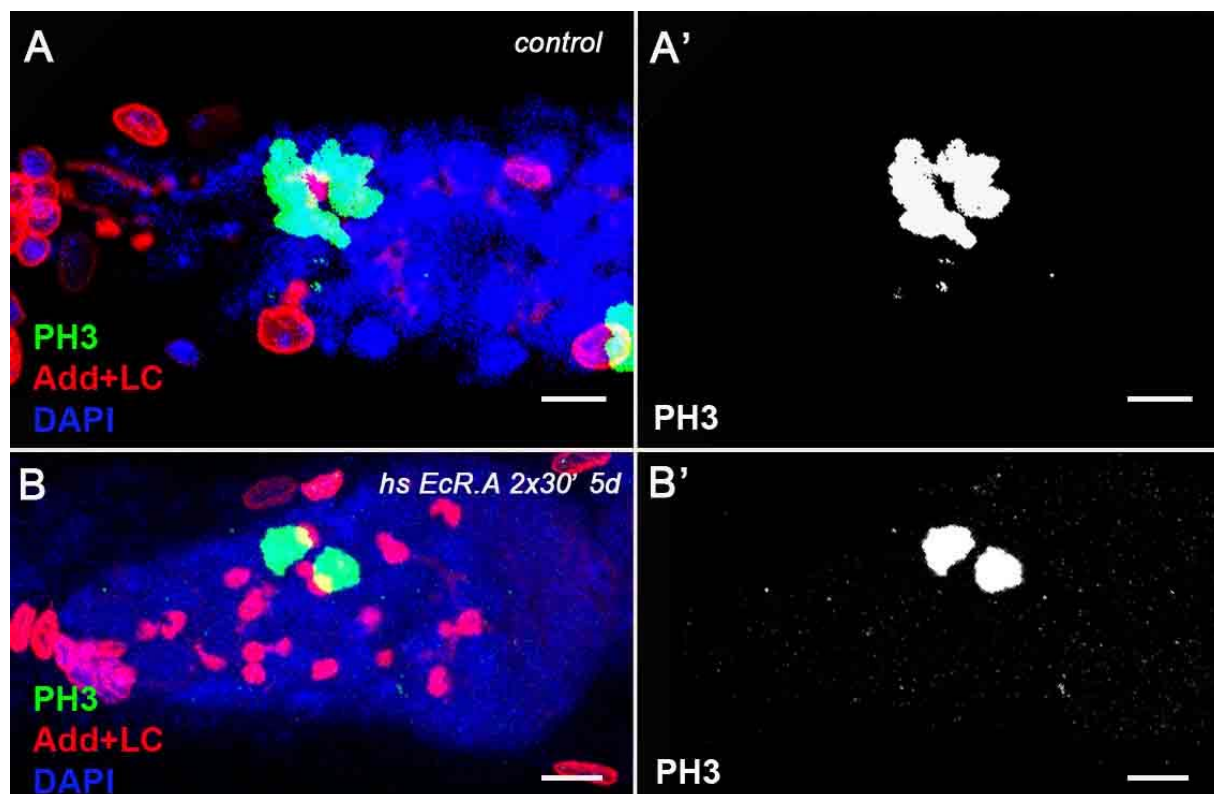
(B) *tai^{61G1}* or *tai^{k15101}* mutations do not affect the maintenance of GSC compared to parental GSC clones.

Red, Adducin+LaminC; blue, DAPI; and green, GFP.

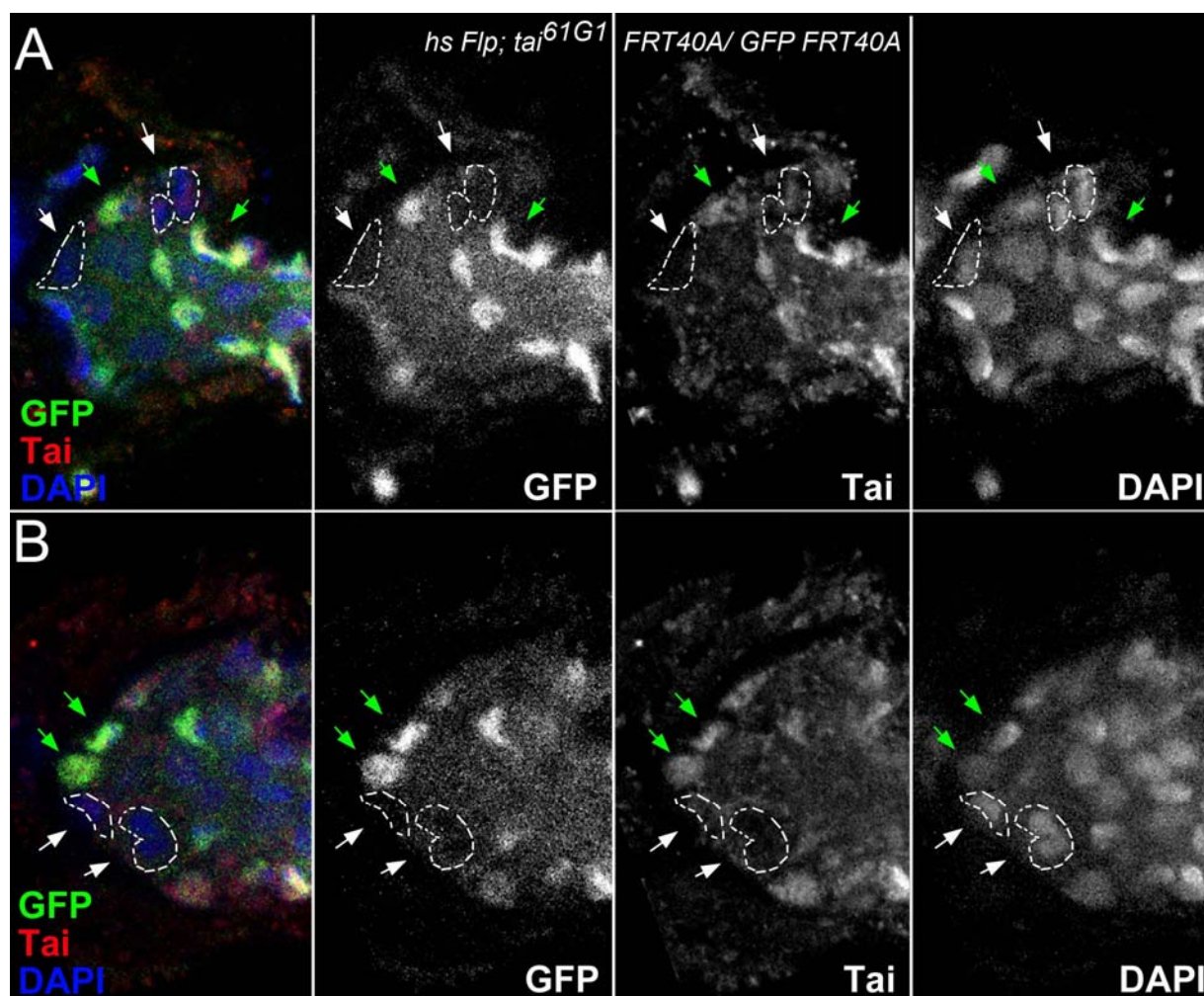
Supplementary Figure 4. *ptcGal4* and *bab1Gal4*, the drivers used in this study drive *UAS lacZ* expression in the somatic cells of the germarium

Whereas *bab1Gal4* (*UAS lacZ/+; bab1Gal4/+*) drives expression in CpCs (pink arrowheads), ECs and FCs (A), *ptcGal4* (*UAS lacZ/ptcGal4*) is only active in ECs and FCs, but not in the CpCs (pink arrowheads, B).

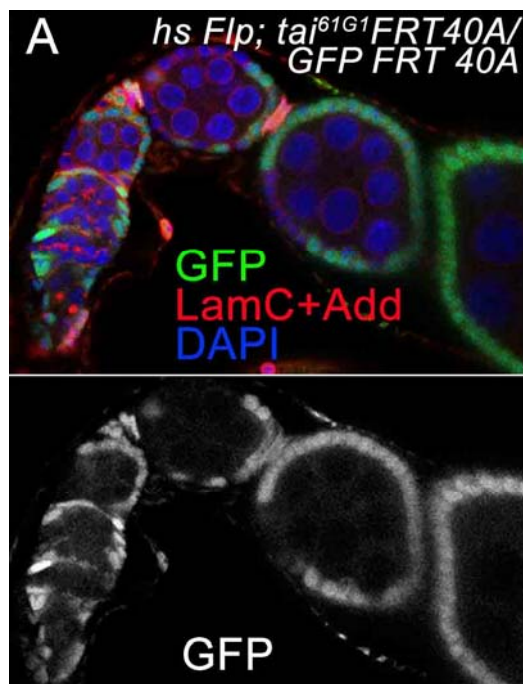
(A, B) are projections of optical sections assembled through the germarial tissue. Red, Adducin+LaminC; blue, DAPI; and green, β -Galactosidase.



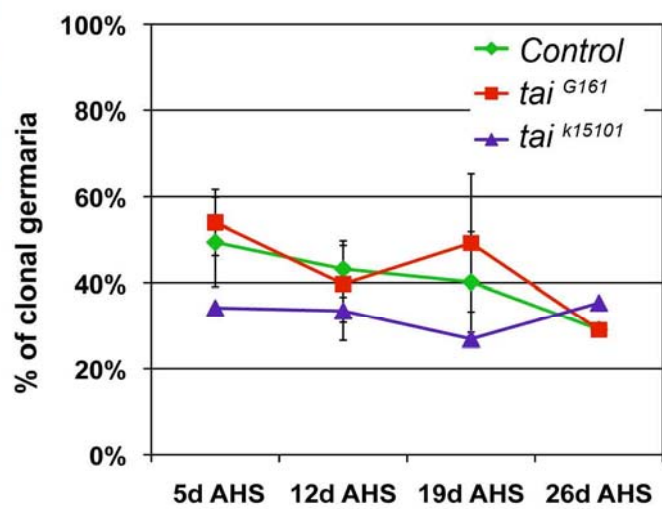
Supplementary Figure 1



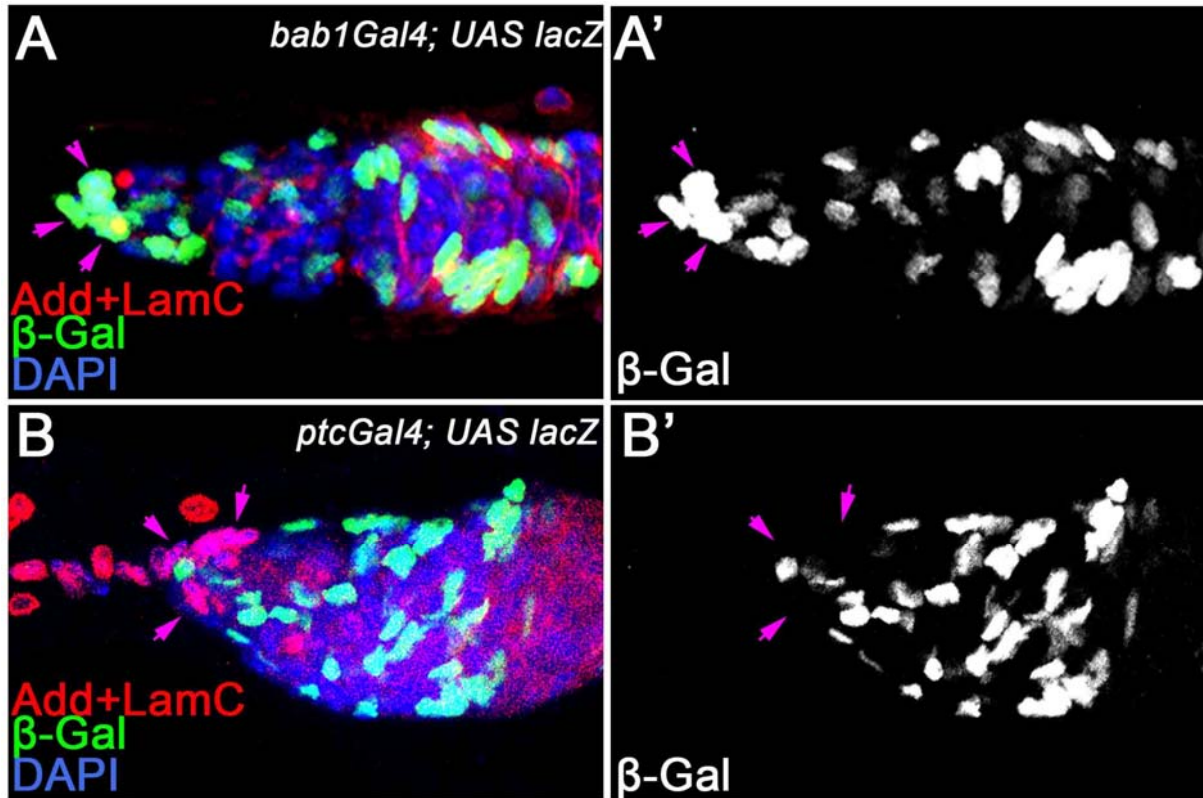
Supplementary Figure 2



B **GSC maintenance is not affected in *tai* mutants**



Supplementary Figure 3



Supplementary Figure 4

Supplementary Table S1. Loss of function of ecdysone receptor co-activator *tai* increases number of niche and germline stem cells

Allele	<i>x tai^{G161}</i>			<i>x tai^{k15101}</i>		
	# of CpCs AVE±SEM	# of GSCs AVE±SEM	# of germaria analyzed	# of CpCs AVE±SEM	# of GSCs AVE±SEM	# of germaria analyzed
	p (compared to <i>tai^{G161}/w¹¹¹⁸</i>)			p (compared to <i>tai^{k15101}/w¹¹¹⁸</i>)		
<i>Control, w¹¹¹⁸</i>	6.56±0.24	2.44±0.13	25	5.63±0.22	2.11±0.08	27
<i>tai^{G161}</i>	lethal			7.10±0.28 p=2.08x10 ⁻⁴	3.45±0.20 p=1.52x10 ⁻⁷	31
<i>tai⁰¹³¹⁵</i>	10.50±0.61 p=6.20x10 ⁻¹¹	4.00±0.25 p=6.30x10 ⁻¹¹	11	6.33±0.53 p=0.16	3.22±0.32 p=2.55x10 ⁻⁶	9
<i>tai^{EY11718}</i>	7.40±0.51 p=0.16	3.67±0.26 p=4.49x10 ⁻³	5	N/A		
<i>tai^{KG02309}</i>	9.40±0.70 p=0.02	3.40±0.54 p=2.34x10 ⁻⁵	10	N/A		
<i>tai^{BG02711}</i>	10.56±0.60 p=1.11x10 ⁻⁹	5.11±0.39 p=1.60x10 ⁻⁸	10	N/A		
<i>EcR^{Q50st}</i>	8.40±0.78 p=5.08x10 ⁻³	3.70±0.21 p=1.30x10 ⁻⁵	10	7.86±0.93 p=1.31x10 ⁻³	3.71±0.61 p=3.88x10 ⁻⁵	7
<i>usp⁴</i>	9.00±0.85 p=9.68x10 ⁻⁴	3.67±0.27 p=3.30x10 ⁻⁵	12	8.07±0.38 p=6.70x10 ⁻⁷	2.79±0.19 p=0.10	14
<i>usp^{EP1193}</i>	8.13±0.31 p=4.50x10 ⁻³	3.50±0.51 p=1.05x10 ⁻³	8	5.92±0.36 p=0.48	2.25±0.13 p=0.36	12

p-value was calculated using the two tailed Students t-test.

Supplementary Table S2. Reduction of ecdysone signaling via *ecd1^{ts}* mutation or dominant negative EcR forms increases the number of single spectrosome cells and delays cyst differentiation

Genotype	Number of CpCs Ave ± SEM	Number of GSCs Ave ± SEM	Number of SSCs Ave ± SEM	Number of Cysts Ave ± SEM	Ratio Cyst/SSC Ave ± SEM	# of analyzed germaria
<i>w¹¹¹⁸</i> 5d at 29°C	5.78±0.25	2.18±0.12	3.91±0.31	4.82±0.38	1.30±0.12	11
<i>ecd^{4210 ts}</i> 1d at 29°C	5.71±0.30 (p=0.89)	2.19±0.19 (p=0.98)	9.81±1.12 (p=2.38x10 ⁻⁴)***	4.63±0.87 (p=0.86)	0.63±0.13 (p=1.76x10 ⁻³)**	16
<i>ecd^{4210 ts}</i> 3-5d at 29°C	5.77±0.17 (p=0.98)	1.80±0.19 (p=0.26)	7.47±0.36 (p=1.58x10 ⁻⁶)***	5.80±0.46 (p=0.23)	0.84±0.08 (p=4.16x10 ⁻³)**	30
<i>ecd^{4210 ts}</i> 7d at 29°C	6.00±0.22 (p=0.59)	1.62±0.20 (p=0.04)*	7.23±0.99 (p=0.01)*	3.85±0.47 (p=0.15)	0.66±0.10 (p=6.61x10 ⁻⁴)***	15
<i>hs-Gal4- usp.LBD</i> hs 30' 1-3d	6.20±0.30 (p=0.47)	3.20±0.37 (p=4.73x10 ⁻³)**	7.20±0.74 (p=2.34x10 ⁻⁴)***	5.40±0.51 (p=0.39)	0.78±0.10 (p=0.02)*	5
<i>hs-Gal4- EcR.LBD</i> hs 30' 1-3d	6.29±0.18 (p=0.23)	2.75±0.31 (p=0.08)	7.13±0.72 (p=3.00x10 ⁻⁴)***	4.86±0.38 (p=0.95)	0.67±0.05 (p=1.30x10 ⁻³)**	8

p-value was calculated using the two tailed Students t-test. *p<0.05, **p<0.005. ***p<0.0005

Supplementary Table S3. Adult EcR overexpression causes germline differentiation delay in the germarium that can be recovered by supplying 20E

Genotype	Condition	exp	Number of CpCs Ave \pm SEM	Number of GSCs Ave \pm SEM	Number of SSCs Ave \pm SEM	Number of Cysts Ave \pm SEM	Ratio Cyst/SSC Ave \pm SEM	# of analyzed germaria
<i>w¹¹¹⁸</i>	control 25°C	I	6.33 \pm 0.20	2.88 \pm 0.23	4.5 \pm 0.38	4.63 \pm 0.46	1.09 \pm 0.16	8
	20E 25°C	I	5.78 \pm 0.19 ^a (p=0.27)	2.26 \pm 0.24 ^a (p=0.14)	3.84 \pm 0.32 ^a (p=0.24)	4.16 \pm 0.24 ^a (p=0.34)	1.34 \pm 0.23 ^a (p=0.51)	19
<i>hsEcR.A/+</i>	control 25°C	I	6.00 \pm 0.22 ^a (p=0.53)	2.67 \pm 0.19 ^a (p=0.50)	4.80 \pm 0.31 ^a (p=0.84)	5.31 \pm 0.27 ^a (p=0.20)	1.13 \pm 0.16 ^a (p=0.91)	15
		II	5.58 \pm 0.26	2.42 \pm 0.15	4.50 \pm 0.38	5.76 \pm 0.28	1.35 \pm 0.11	12
		III	5.67 \pm 0.24	2.22 \pm 0.22	4.00 \pm 0.33	5.44 \pm 0.44	1.44 \pm 0.16	9
	20E 25°C	I	6.40 \pm 0.31 ^a (p=0.91)	2.50 \pm 0.17 ^a (p=0.19)	4.50 \pm 0.65 ^a (p=1.00)	5.40 \pm 0.40 ^a (p=0.22)	1.57 \pm 0.33 ^a (p=0.25)	10
		II	6.43 \pm 0.36	2.20 \pm 0.13	3.80 \pm 0.42	6.40 \pm 0.27	1.89 \pm 0.22	10
		III	5.67 \pm 0.27	2.44 \pm 0.18	5.44 \pm 0.73	5.33 \pm 0.33	1.27 \pm 0.29	9
<i>w¹¹¹⁸</i>	control heat shock	I	5.90 \pm 0.28 ^a (p=0.44)	2.50 \pm 0.27 ^a (p=0.32)	4.50 \pm 0.56 ^a (p=1.00)	5.80 \pm 0.36 ^a (p=0.06)	1.49 \pm 0.22 ^a (p=0.18)	10
		III	6.13 \pm 0.26	2.30 \pm 0.15	4.90 \pm 0.55	5.80 \pm 0.44	1.32 \pm 0.19	10
<i>hsEcR.A/+</i> +	heat shock	I	5.70 \pm 0.21 ^b (p=0.57) ^c (p=0.36)	2.90 \pm 0.28 ^b (p=0.31) ^c (p=0.48)	11.0 \pm 0.75 ^b (p=1.68 \times 10 ⁻⁶)*** ^c (p=5.24 \times 10 ⁻⁹)***	2.30 \pm 0.67 ^b (p=2.14 \times 10 ⁻⁴)*** ^c (p=1.94 \times 10 ⁻⁴)***	0.19 \pm 0.05 ^b (p=1.95 \times 10 ⁻⁵)*** ^c (p=1.49 \times 10 ⁻⁴)***	10
		II	6.09 \pm 0.28 ^c (p=0.20)	2.82 \pm 0.18 ^c (p=0.10)	13.8 \pm 1.40 ^c (p=1.79 \times 10 ⁻⁶)***	2.6 \pm 0.29 ^c (p=4.33 \times 10 ⁻⁷)***	0.17 \pm 0.03 ^c (p=1.99 \times 10 ⁻⁹)***	11
		III	5.91 \pm 0.23 ^c (p=0.48)	3.15 \pm 0.19 ^c (p=4.93 \times 10 ⁻³)**	13.46 \pm 1.26 ^c (p=5.72 \times 10 ⁻⁶)***	5.69 \pm 0.54 ^c (p=0.74)	0.50 \pm 0.10 ^c (p=3.39 \times 10 ⁻⁵)***	13
	20E heat shock	I	5.9 \pm 0.35 ^d (p=0.63)	3.6 \pm 0.22 ^d (p=0.06)	10.2 \pm 0.87 ^d (p=0.50)	4.70 \pm 0.50 ^d (p=0.01)*	0.50 \pm 0.08 ^d (p=4.53 \times 10 ⁻³)**	10
		II	6.00 \pm 0.21 ^d (p=0.80)	3.00 \pm 0.15 ^d (p=0.44)	12.5 \pm 0.67 ^d (p=0.44)	3.86 \pm 0.35 ^d (p=0.02)*	0.33 \pm 0.04 ^d (p=0.01)*	14
		III	5.92 \pm 0.22 ^d (p=0.98)	2.46 \pm 0.14 ^d (p=7.96 \times 10 ⁻³)*	9.62 \pm 0.74 ^d (p=1.45 \times 10 ⁻²)*	7.15 \pm 0.30 ^d (p=2.52 \times 10 ⁻²)*	0.79 \pm 0.07 ^d (p=2.00 \times 10 ⁻²)*	13

Adult *hsEcR.A/+* or *w¹¹¹⁸* flies were treated as indicated. Heat shocks were performed twice per day for 30 min each. 1 μ M Ecdysone (20E) was diluted in 5% Ethanol. For control 5% Ethanol was used.

p-value was calculated using the two tailed Students t-test. *p<0.05. **p<0.005. ***p<0.0005

a Compared to *w¹¹¹⁸* flies that were kept without heat shocks on 5% Ethanol for control.

b Compared to *w¹¹¹⁸* flies that were heat shocked for control.

c Compared to *hsEcR.A/+* flies of the respective experiment that were kept without heat shocks on 5% Ethanol for control.

d Compared to *hsEcR.A/+* flies of the respective experiment where overexpression of EcR.A was induced via daily heat shocks on 5% Ethanol.

Supplementary Table S4. Ecdysone receptor co-activator *tai* is not required for germline stem cell maintenance

Genotype	Experiment	% of germaria with clonal GSCs				Average GSC loss per day \pm SD, %	GSCs half-life, days
		Time-point I (5d after hs)	Time-point II (12d after hs)	Time-point III (19d after hs)	Time-point IV (26d after hs)		
Control, parental <i>hsFLP; FRT40A /FRT40A GFP</i>	Exp I	56.8% n=44	35.7% n=28	28.3% n=32	ND	1.74 \pm 2.82%	\geq 3 weeks
	Exp II	42.1% n=38	46.8% n=47	51.6% n=31	ND		
	Exp III	ND	47.3% n=55	40.9% n=66	29.1% n=86		
<i>tai</i>^{61G1} <i>hsFLP; FRT40A tai</i> ^{61G1} <i>/FRT40A GFP</i>	Exp I	48.7% n=37	30.8% n=26	46.2% n=13	ND	1.83 \pm 2.08%	\geq 3 weeks
	Exp II	59.5% n=37	48.7% n=39	66.7% n=15	ND		
	Exp III	ND	39.8% n=103	35.1% n=57	29.0% n=100		
<i>tai</i>^{k15101} <i>hsFLP; FRT40A tai</i> ^{k15101} <i>/FRT40A GFP</i>	Exp I	34.2% n=38	38.5% n=39	ND	ND	-1.07 \pm 1.68%	\geq 3 weeks
	Exp III	ND	28.6% n=77	26.9% n=67	35.4% n=48		

n=number of germaria analyzed

GSC loss per day=(% of clonal GSC at time-point 1 -% of clonal GSC at time-point 2)x100%/ % of clonal GSC at time-point 1/elapsed time

GSCs half-life=elapsed time x log[2]/log[% of clonal germaria at time-point1/% of clonal germaria at time-point2]

Supplementary Table S5. Ecdysone signaling alteration in soma causes germline differentiation delay

Genotype	days on 29°C	Number of CpCs Ave ± SEM	Number of GSCs Ave ± SEM	Number of SSCs Ave ± SEM	Number of Cysts Ave ± SEM	Ratio Cyst/SSC Ave ± SEM	# of analyzed germaria
Control*	*	6.19±0.19	2.15±0.15	4.00±0.31	4.82±0.27	1.40±0.12	33
<i>tubGal80^{ts}/+; UAS EcR RNAi⁹⁷/bab1Gal4</i>	7d	6.16±0.29 (p=0.94)	2.42±0.26 (p=0.34)	4.79±0.36 (p=0.11)	3.89±0.25 (p=0.03)*	0.88±0.09 (p=5.18x10 ⁻³)**	19
<i>tubGal80^{ts}/+; UAS EcR RNAi⁹⁷/bab1Gal4</i>	21d	6.93±0.32 (p=0.09)	2.21±0.21 (p=0.82)	8.57±0.83 (p=7.84x10 ⁻³)**	4.57±0.37 (p=0.60)	0.62±0.09 (p=3.41x10 ⁻⁴)***	14
<i>tubGal80^{ts}/+; UAS EcR RNAi¹⁰⁴/bab1Gal4</i>	7d	6.36±0.27 (p=0.67)	2.75±0.30 (p=0.06)	5.00±0.55 (p=0.11)	3.92±0.34 (p=0.07)	0.92±0.17 (p=0.04)*	12
<i>tubGal80^{ts}/+; UAS EcR RNAi¹⁰⁴/bab1Gal4</i>	15d	5.86±0.44 (p=0.52)	2.07±0.16 (p=0.76)	11.0±3.90 (p=0.01)*	3.55±0.57 (p=0.04)*	0.55±0.11 (p=3.34x10 ⁻⁴)***	14
<i>ptcGal4/+; UAS EcR RNAi⁹⁷/tubGal80^{ts}</i>	14d	6.47±0.36 (p=0.54)	2.80±0.34 (p=0.05)	6.00±0.59 (p=2.30x10 ⁻³)*	NC	NC	14
<i>ptcGal4/+; UAS EcR RNAi⁹⁷/tubGal80^{ts}</i>	21d	6.38±0.26 (p=0.671)	2.63±0.18 (p=0.150)	6.25±0.59 (p=1.86x10 ⁻³)*	NC	NC	8

Control*: *tubGal80^{ts}; UAS GFP/TM6*, *tubGal80^{ts}; UAS GFP/bab1Gal4*, *tubGal80^{ts}; UAS EcR RNAi⁹⁷/TM6*, *tubGal80^{ts}; bab1Gal4/CyO*; analyzed at different time points

The expression of *EcR RNAi* during larval development is lethal. Therefore we used the *tubGal80^{ts}* system. Flies were raised at 18°C where *tubGal80^{ts}* suppresses the expression of Gal4. Transferring the adult flies to 29°C caused Gal4 and therefore *UAS EcR RNAi* expression in the soma. NC: Counting of cysts not possible due to strong morphological abnormalities. p-value was calculated using two tailed Students t-test. *p<0.05, **p<0.005. ***p<0.0005

Supplementary Table S6. Overexpression of *EcR* during niche development in larval somatic ovarian cells causes an increase in the number of CpCs

Genotype		Number of CpCs Ave \pm SEM	Number of SSCs Ave \pm SEM	# of analyzed germaria
<i>ptcGal4</i> X	control <i>UAS lacZ</i>	5.70 \pm 0.34	4.20 \pm 0.25	10
	<i>UAS EcR.A</i>	7.47 \pm 0.32 ^a ($p=1.63 \times 10^{-3}$)**	4.47 \pm 0.47 ^a ($p=0.68$)	17
	<i>UAS EcR.B1</i>	6.14 \pm 0.32 ^a ($p=0.41$)	4.00 \pm 0.35 ^a ($p=0.72$)	22
<i>bab1Gal4</i> X	control <i>UAS lacZ</i>	5.91 \pm 0.29	4.91 \pm 0.37	11
	<i>UAS EcR.A</i>	9.31 \pm 0.42 ^a ($p=3.72 \times 10^{-5}$)*** ^b ($p=7.08 \times 10^{-3}$)*	7.38 \pm 0.49 ^a ($p=7.34^{-3}$)** ^b ($p=3.91^{-4}$)***	32
	<i>UAS EcR.B1</i>	9.29 \pm 0.53 ^a ($p=5.73 \times 10^{-5}$)*** ^b ($p=7.10 \times 10^{-6}$)***	5.94 \pm 0.37 ^a ($p=0.07$) ^b ($p=5.99 \times 10^{-4}$)**	17
<i>W¹¹¹⁸</i> X	control <i>UAS EcR.A</i>	6.36 \pm 0.24	5.73 \pm 0.57	11
	control <i>UAS EcR.B1</i>	6.83 \pm 0.50	5.00 \pm 1.00	12

UAS EcR.A/bab1Gal4 and *UAS EcR.B1/bab1Gal4* express exogenous *EcR* in the CpCs. *ptcGal4/+*; *UAS EcR.A/+* and *ptcGal4/+*; *UAS EcR.B1/+* express exogenous *EcR* in the other somatic ovarian cells, but not in CpCs (for expression patterns see Supplementary Figure S4). The stem cell marker pMad was used to confirm GSC identity if CpC number was increased. a *ptcGal4/+*; *UAS EcR/+* and *UAS EcR/bab1Gal4* were compared to *ptcGal4/+*; *UAS lacZ/+* or *bab1Gal4/UAS lacZ* respectively. b *UAS EcR.A* or *B1* driven by *bab1Gal4* were compared to the *UAS EcR.A* or *B1* driven by *ptcGal4*. The p-value was calculated using two tailed Student's t-test. * $p < 0.05$, ** $p < 0.005$, *** $p < 0.0005$.

The Histone H2B Monoubiquitination Regulatory Pathway is Required for Differentiation of Multipotent Stem Cells: Supplementary Material

Supplemental Information

The Histone H2B Monoubiquitination Regulatory Pathway Is Required for Differentiation of Multipotent Stem Cells

Oleksandra Karpiuk, Zeynab Najafova, Frank Kramer, Magali Hennion,
Christina Galonska, Annekatrin König, Nicolas Snaidero, Tanja Vogel,
Andrei Shchebet, Yvonne Begus-Nahrman, Moustapha Kassem, Mikael Simons, Halyna
Shcherbata, Tim Beissbarth, and Steven A. Johnsen

SUPPLEMENTAL INVENTORY

1) Supplemental figures:

- Figure S1 related to Figure 1. H2A and RNF40 levels during hMSC differentiation.
- Figure S2 related to Figure 2. RNF40 depletion decreases H2Bub1 levels and affects marker gene expression in differentiating hMSC.
- Figure S3 related to Figure 3. CDK9 and WAC depletion impair hMSC differentiation and decrease H2Bub1 levels.
- Figure S4 related to Figure 4. H3K4me3 after depletion of RNF40 or RNF20.

2) Supplemental Experimental Procedures:

- Cell culture, differentiation and knockdowns;
- Chromatin Immunoprecipitation (ChIP) and qRT-PCR;
- Immunofluorescence staining of *Drosophila* ovaries;
- Immunofluorescence staining of oligodendrocytes;
- Monolayer-embedding in Epon for electron microscopy;
- Pathway analysis;
- Oil Red O staining;
- Quantification of Oil Red O and alkaline phosphatase staining;
- List of siRNAs used in the study;
- List of antibodies used for ChIP, immunofluorescence and Western blot;
- List of qRT-PCR primers used in the study;
- List of ChIP primers used in the study.

3) Supplemental References

Figure S1 related to Figure 1

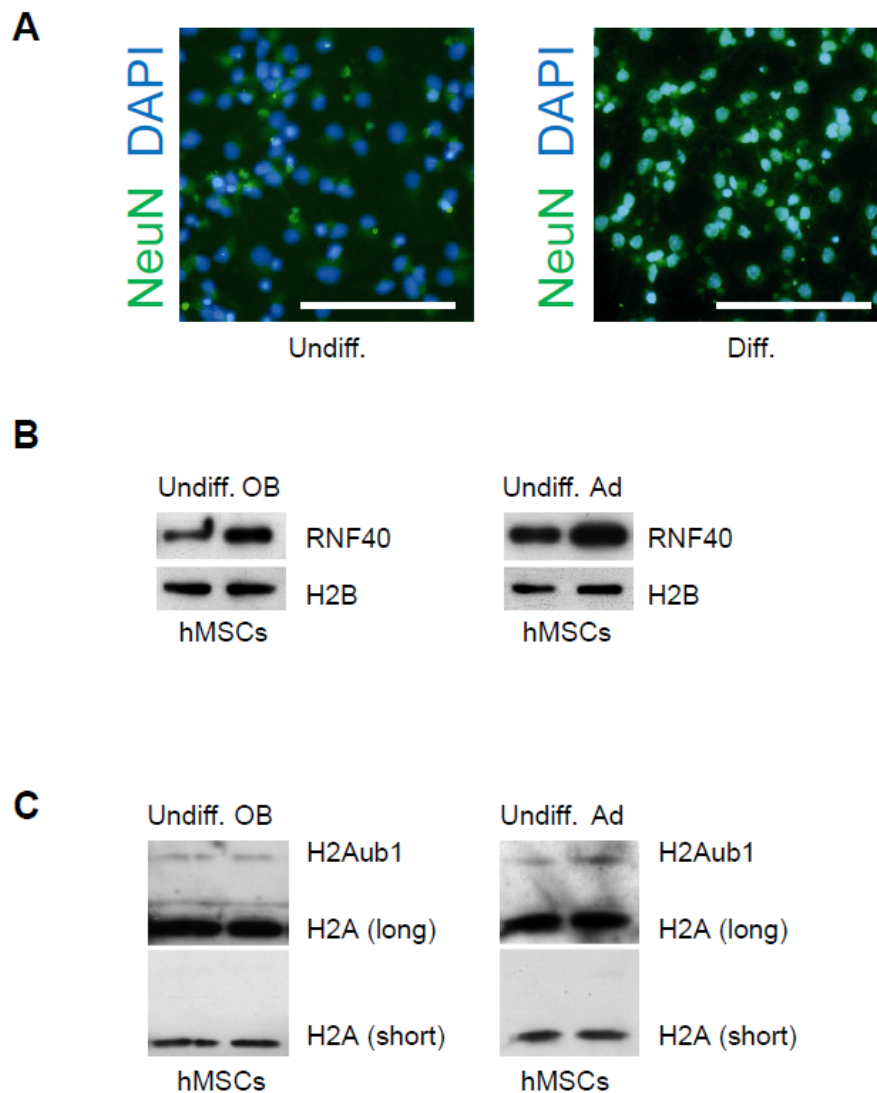


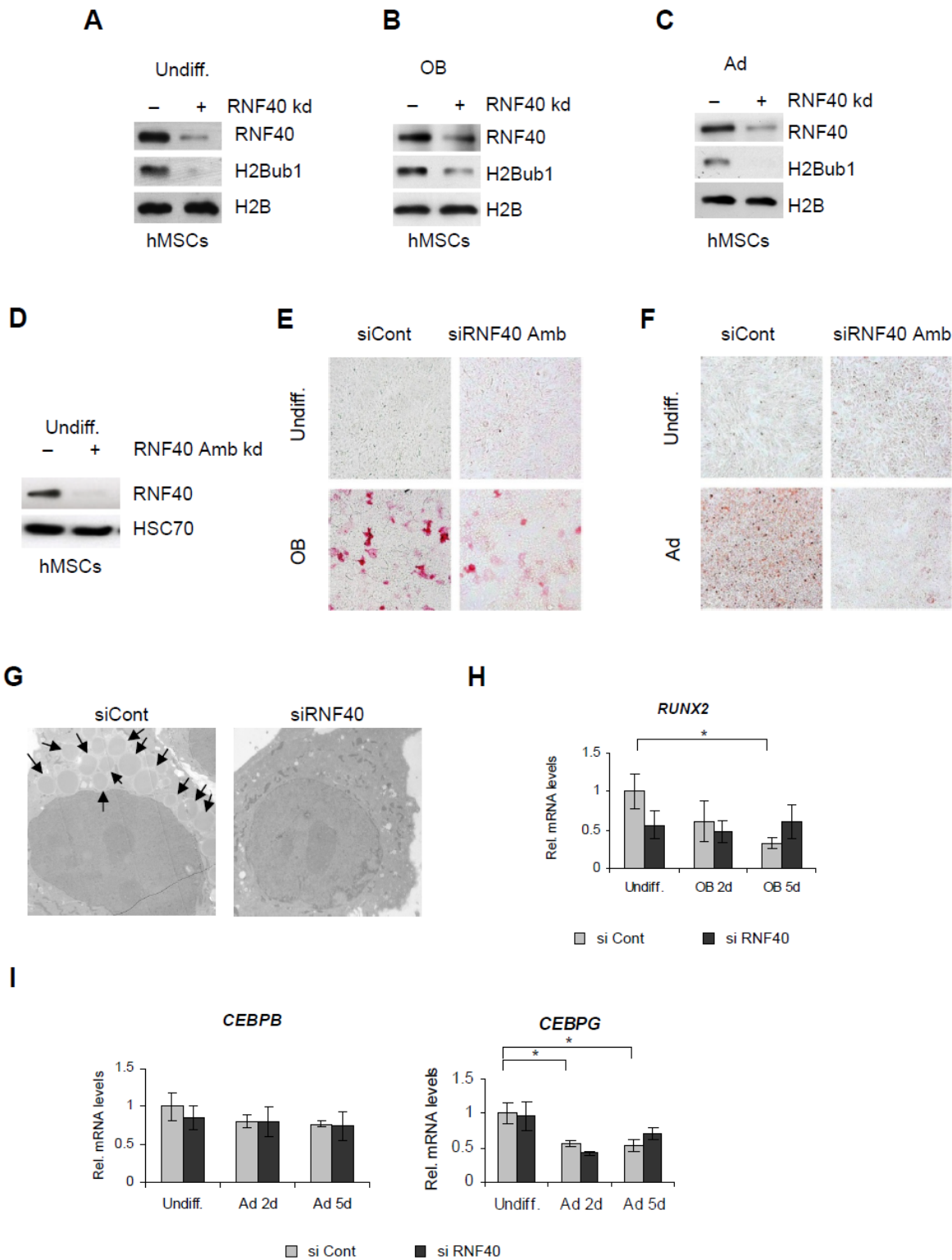
Figure S1

(A) Mouse neurospheres were differentiated as described in Supplemental Materials and Methods. Immunofluorescence staining against NeuN (green) was used to verify the differentiation. Nuclei were stained with DAPI.

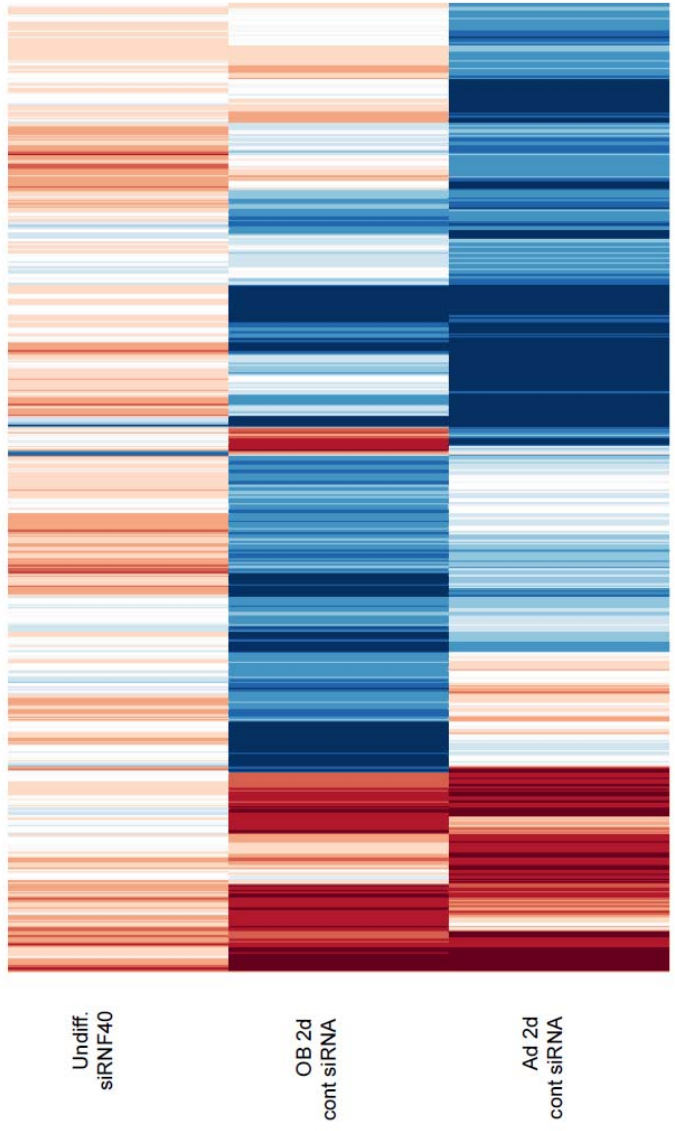
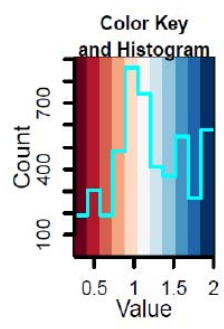
(B) hMSCs were differentiated to osteoblasts (OB) or adipocytes (Ad) for 2 d as described in Supplemental Materials and Methods. Protein extracts were analyzed by Western blot using antibodies against RNF40 and H2B (loading control).

(C) hMSC were differentiated as in S1B. Western blot against H2A was performed on protein extracts. H2Aub1 was visualized as a higher migrating band. Low exposure of H2A is shown as a loading control.

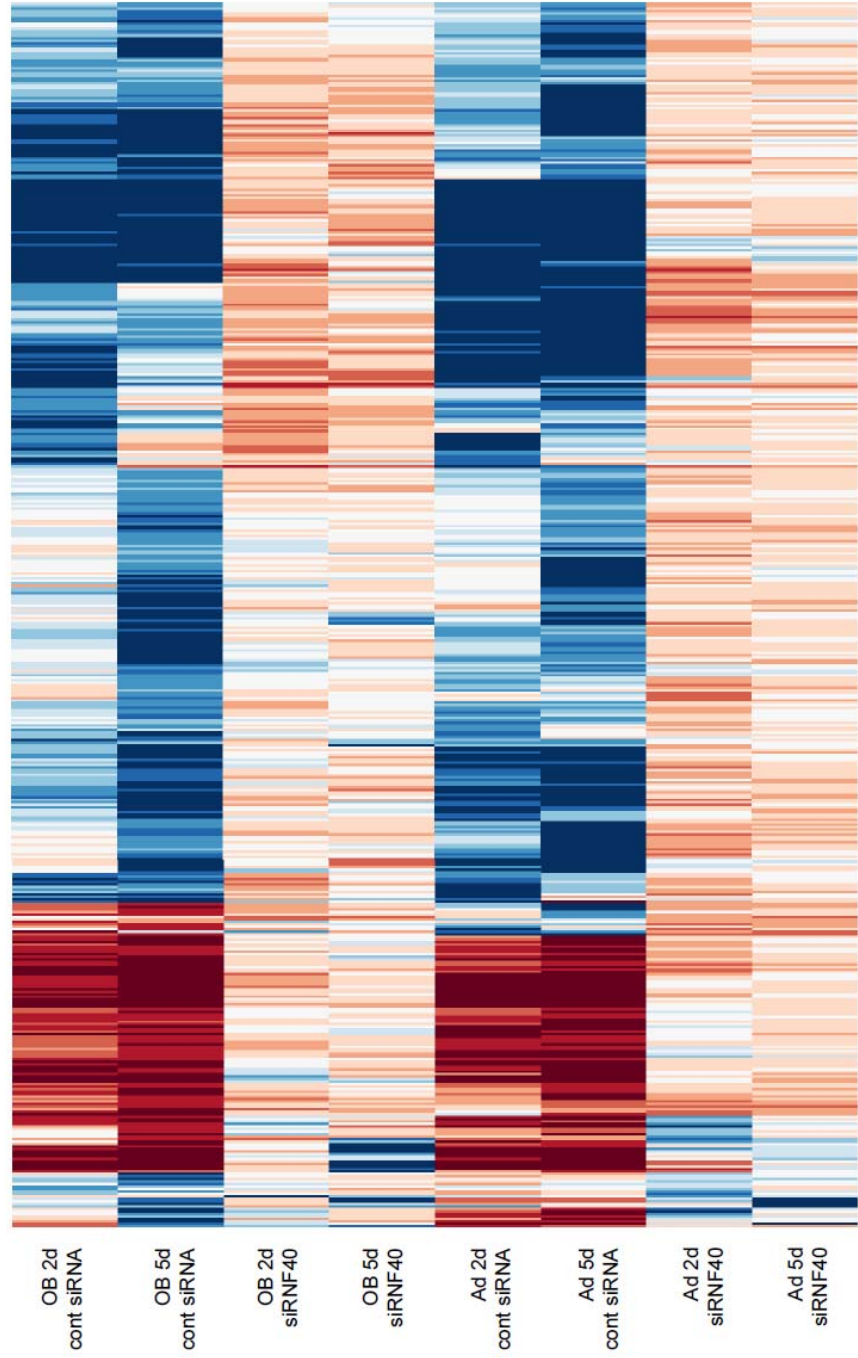
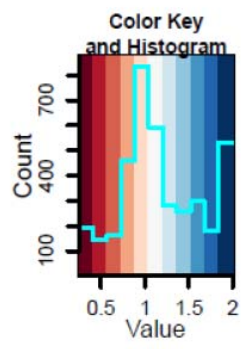
Figure S2 related to Figure 2



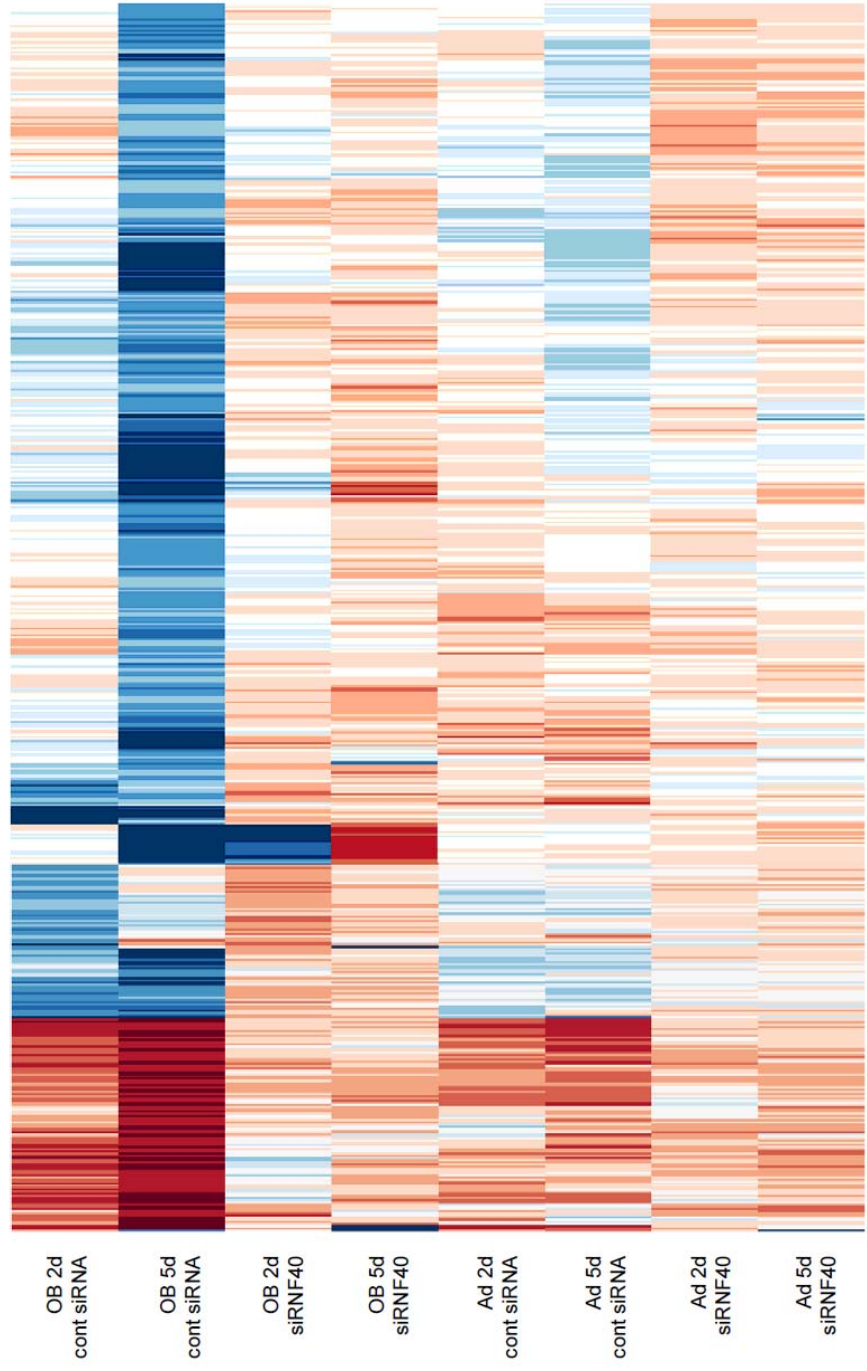
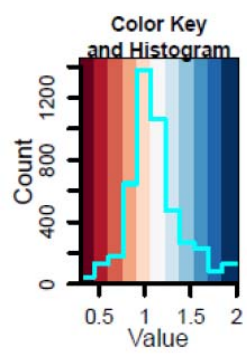
J



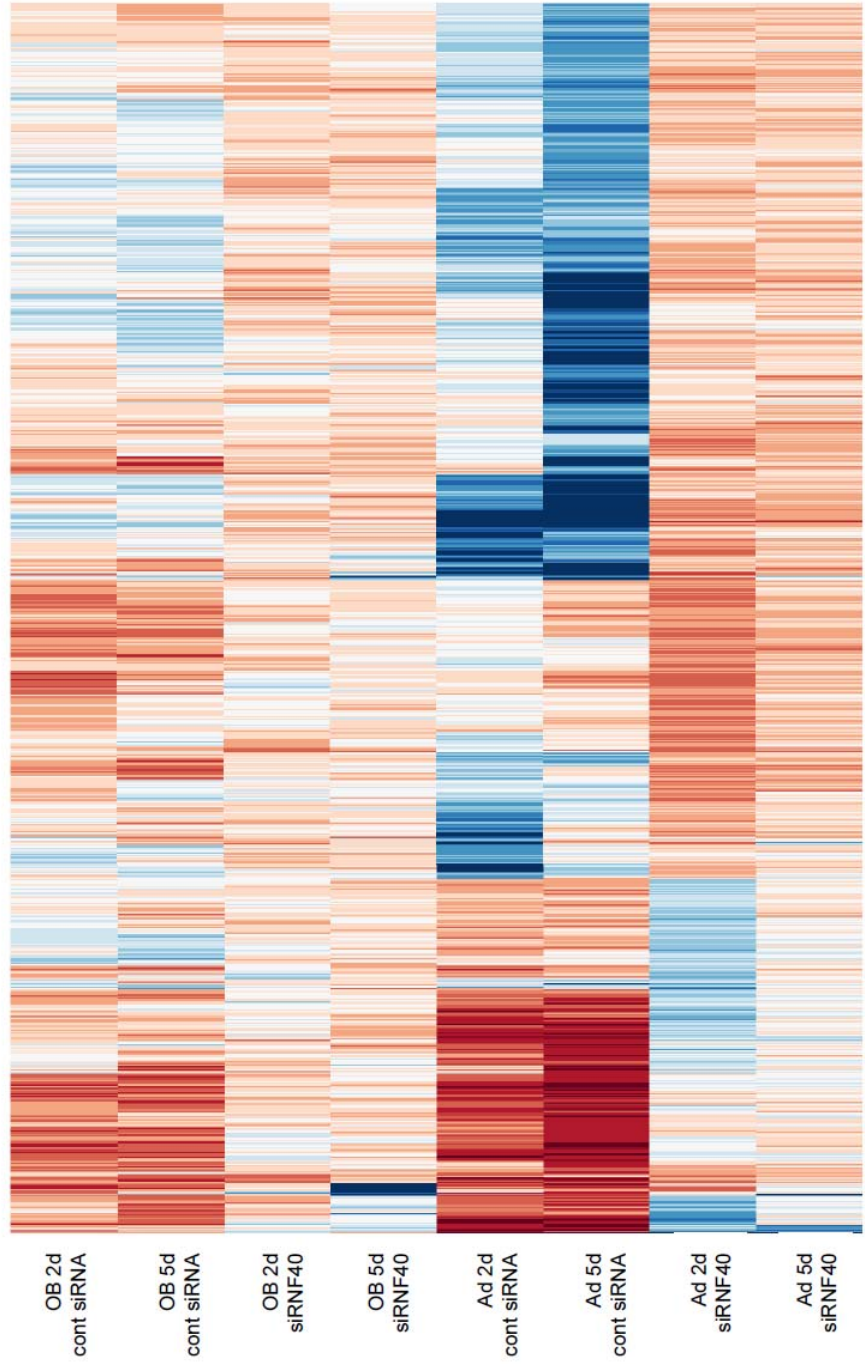
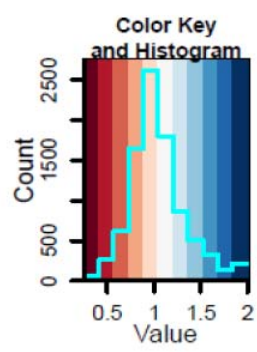
K



L



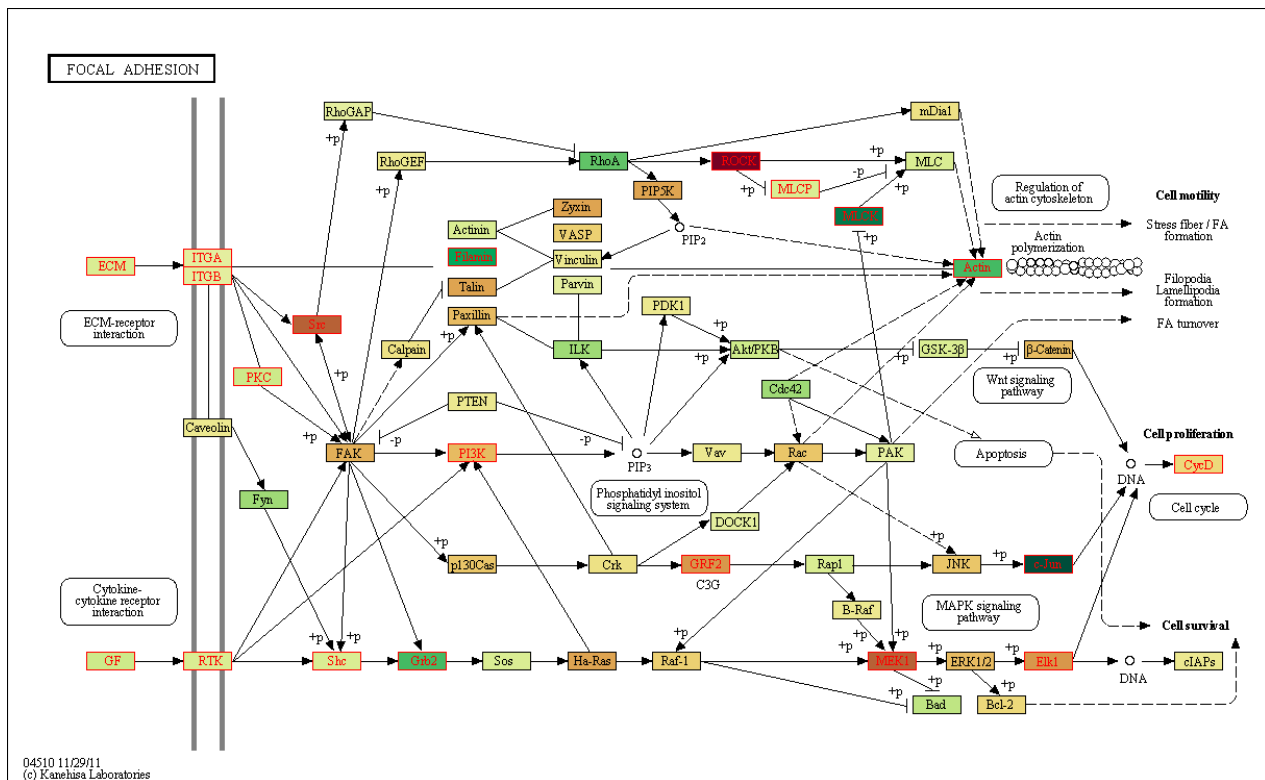
M



Undiff. vs. 5 day osteoblast differentiation

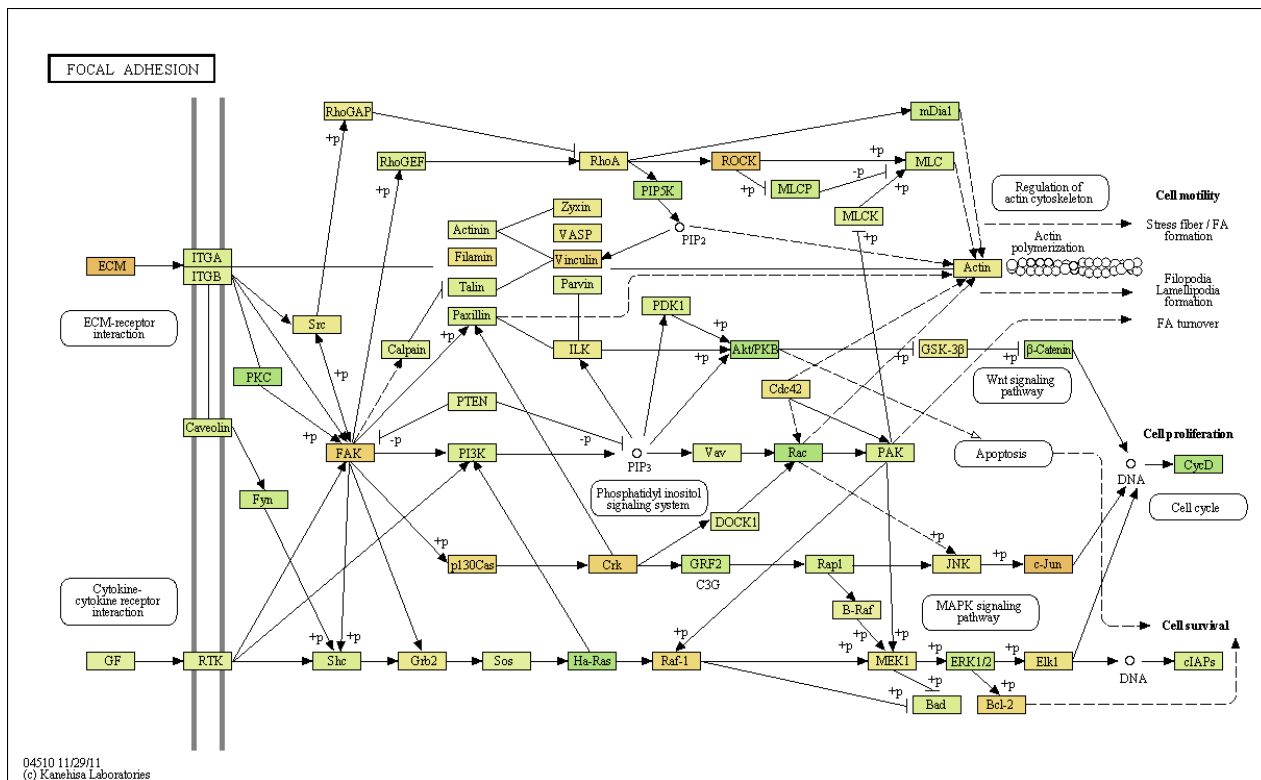
N

Focal adhesion (hsa04510); P = 1.49E-07



siCont vs. siRNF40 5 day osteoblast differentiation

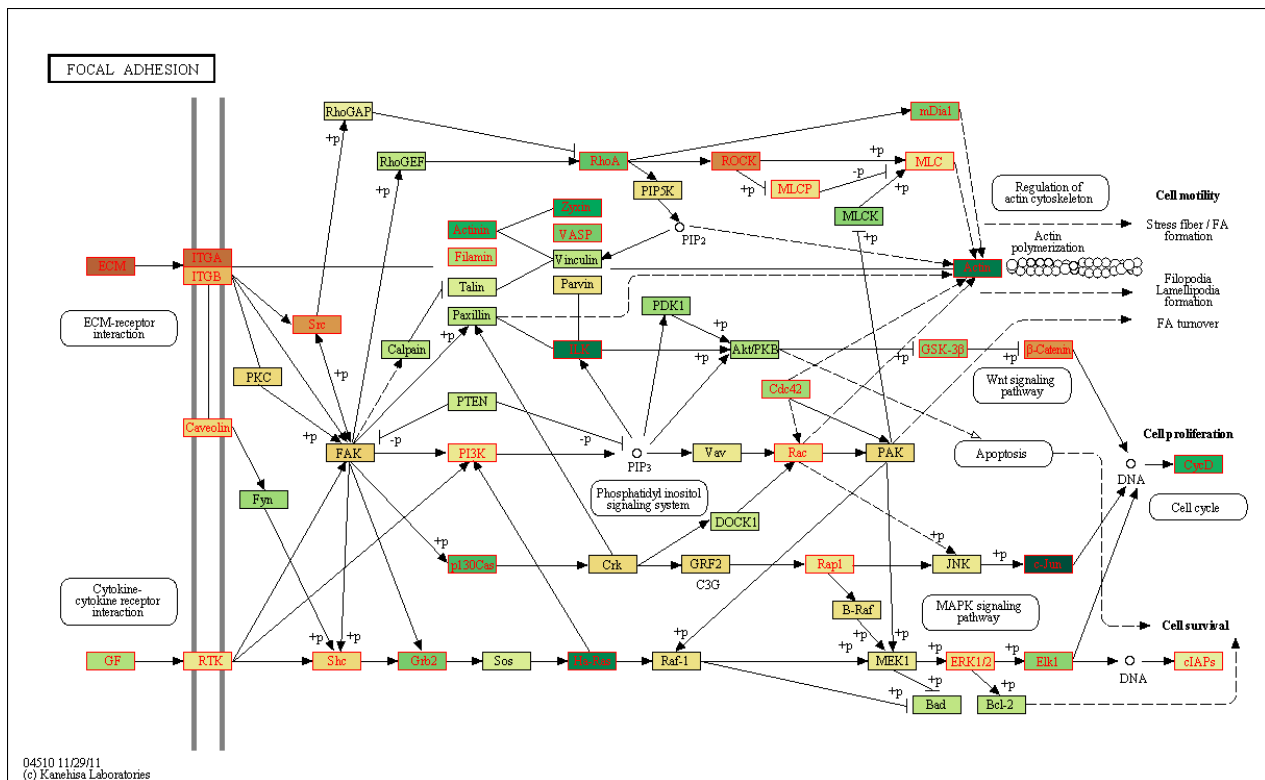
Focal adhesion (hsa04510); P = 8.47E-04



Undiff. vs. 5 day adipocyte differentiation

P

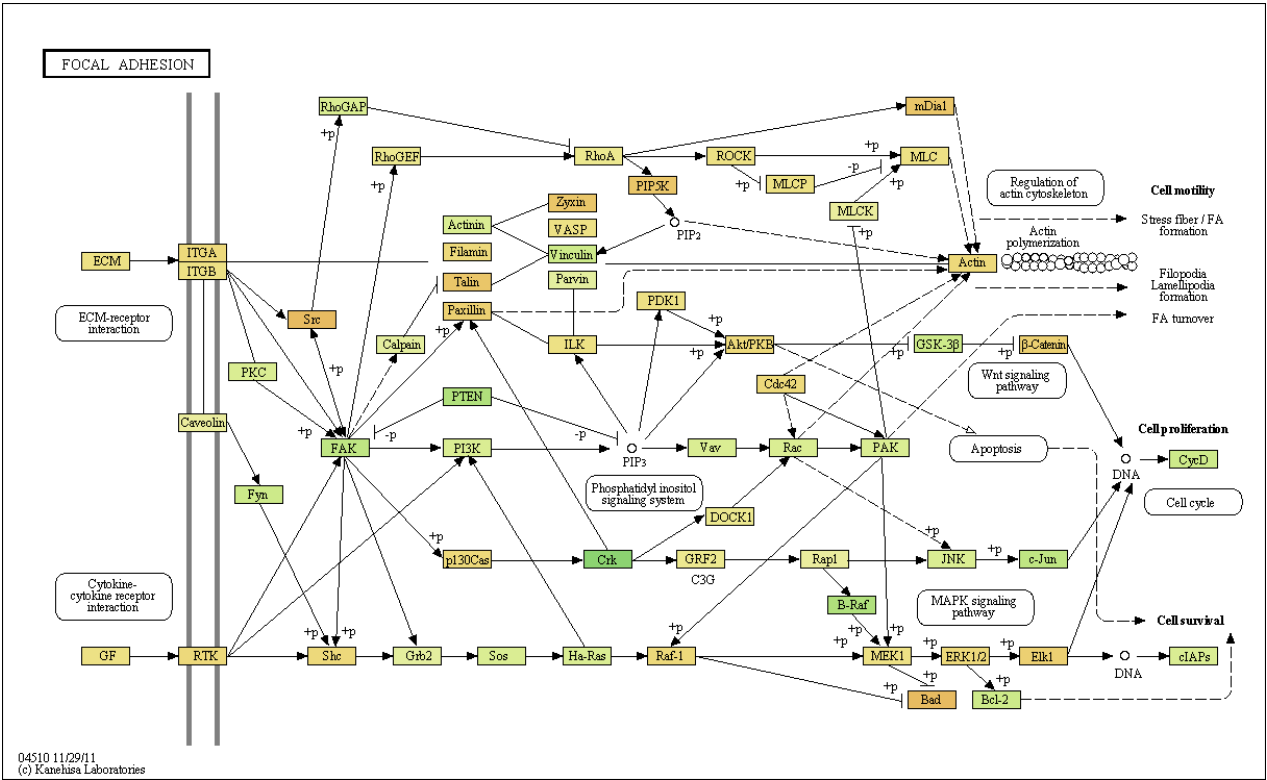
Focal adhesion (hsa04510); P = 2.70E-11



siCont vs. siRNF40 5 day adipocyte differentiation

Q

Focal adhesion (hsa04510); P = 6.66E-04



R

The diagram illustrates the cell cycle signaling pathways, showing the progression from G1 to S phase and the regulation of DNA biosynthesis. Key components include:

- Growth factor withdrawal:** Growth factor withdrawal leads to GSK3 β activation, which inhibits the MAPK signaling pathway. The MAPK signaling pathway is also inhibited by R-point (START).
- DNA damage checkpoint:** DNA damage activates p53, which leads to p21 and p27,57. p53 also leads to GADD45 and 14-3-3 σ . p53 inhibits pRb, which in turn inhibits CycE and CycA. p53 also leads to p21, which inhibits pRb and CycE. p53 also leads to p27,57, which inhibits CycE and CycA. p53 also leads to GADD45, which inhibits CycE and CycA. p53 also leads to 14-3-3 σ , which inhibits CycE and CycA.
- Ubiquitin-mediated proteolysis:** Ubiquitin-mediated proteolysis leads to APC/C, which targets CycB and CycE for degradation. APC/C also targets Cdh1, which inhibits CycB and CycE. APC/C also targets Cdc14, which inhibits CycB and CycE.
- Other components:** The diagram includes various other proteins and their interactions, such as p107, E2F4,5, DP-1,2, Mdm1, Mdm2, p16, p18, p19, p21, p27,57, p300, ARF, Mdm2, Rb, GADD45, 14-3-3 σ , Chk1,2, Mcl1, Mad1, Mcl2, BubR1, Cdc25A, Cdc25B, Cdc25C, Cdc25D, Cdc25E, Cdc25F, Cdc25G, Cdc25H, Cdc25I, Cdc25J, Cdc25K, Cdc25L, Cdc25M, Cdc25N, Cdc25O, Cdc25P, Cdc25Q, Cdc25R, Cdc25S, Cdc25T, Cdc25U, Cdc25V, Cdc25W, Cdc25X, Cdc25Y, Cdc25Z, Cdc25AA, Cdc25AB, Cdc25AC, Cdc25AD, Cdc25AE, Cdc25AF, Cdc25AG, Cdc25AH, Cdc25AI, Cdc25AJ, Cdc25AK, Cdc25AL, Cdc25AM, Cdc25AN, Cdc25AO, Cdc25AP, Cdc25AQ, Cdc25AR, Cdc25AS, Cdc25AT, Cdc25AU, Cdc25AV, Cdc25AW, Cdc25AX, Cdc25AY, Cdc25AZ, Cdc25BA, Cdc25BB, Cdc25BC, Cdc25BD, Cdc25BE, Cdc25BF, Cdc25BG, Cdc25BH, Cdc25BI, Cdc25BJ, Cdc25BK, Cdc25BL, Cdc25BM, Cdc25BN, Cdc25BO, Cdc25BP, Cdc25BQ, Cdc25BR, Cdc25BS, Cdc25BT, Cdc25BU, Cdc25BV, Cdc25BW, Cdc25BX, Cdc25BY, Cdc25BZ, Cdc25CA, Cdc25CB, Cdc25CC, Cdc25CD, Cdc25CE, Cdc25CF, Cdc25CG, Cdc25CH, Cdc25CI, Cdc25CJ, Cdc25CK, Cdc25CL, Cdc25CM, Cdc25CN, Cdc25CO, Cdc25CP, Cdc25CQ, Cdc25CR, Cdc25CS, Cdc25CT, Cdc25CU, Cdc25CV, Cdc25CW, Cdc25CX, Cdc25CY, Cdc25CZ, Cdc25DA, Cdc25DB, Cdc25DC, Cdc25DD, Cdc25DE, Cdc25DF, Cdc25DG, Cdc25DH, Cdc25DI, Cdc25DJ, Cdc25DK, Cdc25DL, Cdc25DM, Cdc25DN, Cdc25DO, Cdc25DP, Cdc25DQ, Cdc25DR, Cdc25DS, Cdc25DT, Cdc25DU, Cdc25DV, Cdc25DW, Cdc25DX, Cdc25DY, Cdc25DZ, Cdc25EA, Cdc25EB, Cdc25EC, Cdc25ED, Cdc25EE, Cdc25EF, Cdc25EG, Cdc25EH, Cdc25EI, Cdc25EJ, Cdc25EK, Cdc25EL, Cdc25EM, Cdc25EN, Cdc25EO, Cdc25EP, Cdc25EQ, Cdc25ER, Cdc25ES, Cdc25ET, Cdc25EU, Cdc25EV, Cdc25EW, Cdc25EX, Cdc25EY, Cdc25EZ, Cdc25FA, Cdc25FB, Cdc25FC, Cdc25FD, Cdc25FE, Cdc25FF, Cdc25FG, Cdc25FH, Cdc25FI, Cdc25FJ, Cdc25FK, Cdc25FL, Cdc25FM, Cdc25FN, Cdc25FO, Cdc25FP, Cdc25FQ, Cdc25FR, Cdc25FS, Cdc25FT, Cdc25FU, Cdc25FV, Cdc25FW, Cdc25FX, Cdc25FY, Cdc25FZ, Cdc25GA, Cdc25GB, Cdc25GC, Cdc25GD, Cdc25GE, Cdc25GF, Cdc25GG, Cdc25GH, Cdc25GI, Cdc25GJ, Cdc25GK, Cdc25GL, Cdc25GM, Cdc25GN, Cdc25GO, Cdc25GP, Cdc25GQ, Cdc25GR, Cdc25GS, Cdc25GT, Cdc25GU, Cdc25GV, Cdc25GW, Cdc25GX, Cdc25GY, Cdc25GZ, Cdc25HA, Cdc25HB, Cdc25HC, Cdc25HD, Cdc25HE, Cdc25HF, Cdc25HG, Cdc25HH, Cdc25HI, Cdc25HJ, Cdc25HK, Cdc25HL, Cdc25HM, Cdc25HN, Cdc25HO, Cdc25HP, Cdc25HQ, Cdc25HR, Cdc25HS, Cdc25HT, Cdc25HU, Cdc25HV, Cdc25HW, Cdc25HX, Cdc25HY, Cdc25HZ, Cdc25IA, Cdc25IB, Cdc25IC, Cdc25ID, Cdc25IE, Cdc25IF, Cdc25IG, Cdc25IH, Cdc25II, Cdc25IJ, Cdc25IK, Cdc25IL, Cdc25IM, Cdc25IN, Cdc25IO, Cdc25IP, Cdc25IQ, Cdc25IR, Cdc25IS, Cdc25IT, Cdc25IU, Cdc25IV, Cdc25IW, Cdc25IX, Cdc25IY, Cdc25IZ, Cdc25JA, Cdc25JB, Cdc25JC, Cdc25JD, Cdc25JE, Cdc25JF, Cdc25JG, Cdc25JH, Cdc25JI, Cdc25JJ, Cdc25JK, Cdc25JL, Cdc25JM, Cdc25JN, Cdc25JO, Cdc25JP, Cdc25JQ, Cdc25JR, Cdc25JS, Cdc25JT, Cdc25JU, Cdc25JV, Cdc25JW, Cdc25JX, Cdc25JY, Cdc25JZ, Cdc25KA, Cdc25KB, Cdc25KC, Cdc25KD, Cdc25KE, Cdc25KF, Cdc25KG, Cdc25KH, Cdc25KI, Cdc25KJ, Cdc25KK, Cdc25KL, Cdc25KM, Cdc25KN, Cdc25KO, Cdc25KP, Cdc25KQ, Cdc25KR, Cdc25KS, Cdc25KT, Cdc25KU, Cdc25KV, Cdc25KW, Cdc25KX, Cdc25KY, Cdc25KZ, Cdc25LA, Cdc25LB, Cdc25LC, Cdc25LD, Cdc25LE, Cdc25LF, Cdc25LG, Cdc25LH, Cdc25LI, Cdc25LJ, Cdc25LK, Cdc25LL, Cdc25LM, Cdc25LN, Cdc25LO, Cdc25LP, Cdc25LQ, Cdc25LR, Cdc25LS, Cdc25LT, Cdc25LU, Cdc25LV, Cdc25LW, Cdc25LX, Cdc25LY, Cdc25LZ, Cdc25MA, Cdc25MB, Cdc25MC, Cdc25MD, Cdc25ME, Cdc25MF, Cdc25MG, Cdc25MH, Cdc25MI, Cdc25MJ, Cdc25MK, Cdc25ML, Cdc25MM, Cdc25MN, Cdc25MO, Cdc25MP, Cdc25MQ, Cdc25MR, Cdc25MS, Cdc25MT, Cdc25MU, Cdc25MV, Cdc25MW, Cdc25MX, Cdc25MY, Cdc25MZ, Cdc25NA, Cdc25NB, Cdc25NC, Cdc25ND, Cdc25NE, Cdc25NF, Cdc25NG, Cdc25NH, Cdc25NI, Cdc25NJ, Cdc25NK, Cdc25NL, Cdc25NM, Cdc25NN, Cdc25NO, Cdc25NP, Cdc25NQ, Cdc25NR, Cdc25NS, Cdc25NT, Cdc25NU, Cdc25NV, Cdc25NW, Cdc25NX, Cdc25NY, Cdc25NZ, Cdc25OA, Cdc25OB, Cdc25OC, Cdc25OD, Cdc25OE, Cdc25OF, Cdc25OG, Cdc25OH, Cdc25OI, Cdc25OJ, Cdc25OK, Cdc25OL, Cdc25OM, Cdc25ON, Cdc25OO, Cdc25OP, Cdc25OQ, Cdc25OR, Cdc25OS, Cdc25OT, Cdc25OU, Cdc25OV, Cdc25OW, Cdc25OX, Cdc25OY, Cdc25OZ, Cdc25PA, Cdc25PB, Cdc25PC, Cdc25PD, Cdc25PE, Cdc25PF, Cdc25PG, Cdc25PH, Cdc25PI, Cdc25PJ, Cdc25PK, Cdc25PL, Cdc25PM, Cdc25PN, Cdc25PO, Cdc25PP, Cdc25PQ, Cdc25PR, Cdc25PS, Cdc25PT, Cdc25PU, Cdc25PV, Cdc25PW, Cdc25PX, Cdc25PY, Cdc25PZ, Cdc25QA, Cdc25QB, Cdc25QC, Cdc25QD, Cdc25QE, Cdc25QF, Cdc25QG, Cdc25QH, Cdc25QI, Cdc25QJ, Cdc25QK, Cdc25QL, Cdc25QM, Cdc25QN, Cdc25QO, Cdc25QP, Cdc25QQ, Cdc25QR, Cdc25QS, Cdc25QT, Cdc25QU, Cdc25QV, Cdc25QW, Cdc25QX, Cdc25QY, Cdc25QZ, Cdc25RA, Cdc25RB, Cdc25RC, Cdc25RD, Cdc25RE, Cdc25RF, Cdc25RG, Cdc25RH, Cdc25RI, Cdc25RJ, Cdc25RK, Cdc25RL, Cdc25RM, Cdc25RN, Cdc25RO, Cdc25RP, Cdc25RQ, Cdc25RR, Cdc25RS, Cdc25RT, Cdc25RU, Cdc25RV, Cdc25RW, Cdc25RX, Cdc25RY, Cdc25RZ, Cdc25SA, Cdc25SB, Cdc25SC, Cdc25SD, Cdc25SE, Cdc25SF, Cdc25SG, Cdc25SH, Cdc25SI, Cdc25SJ, Cdc25SK, Cdc25SL, Cdc25SM, Cdc25SN, Cdc25SO, Cdc25SP, Cdc25SQ, Cdc25SR, Cdc25SS, Cdc25ST, Cdc25SU, Cdc25SV, Cdc25SW, Cdc25SX, Cdc25SY, Cdc25SZ, Cdc25TA, Cdc25TB, Cdc25TC, Cdc25TD, Cdc25TE, Cdc25TF, Cdc25TG, Cdc25TH, Cdc25TI, Cdc25TJ, Cdc25TK, Cdc25TL, Cdc25TM, Cdc25TN, Cdc25TO, Cdc25TP, Cdc25TQ, Cdc25TR, Cdc25TS, Cdc25TT, Cdc25TU, Cdc25TV, Cdc25TW, Cdc25TX, Cdc25TY, Cdc25TZ, Cdc25UA, Cdc25UB, Cdc25UC, Cdc25UD, Cdc25UE, Cdc25UF, Cdc25UG, Cdc25UH, Cdc25UI, Cdc25UJ, Cdc25UK, Cdc25UL, Cdc25UM, Cdc25UN, Cdc25UO, Cdc25UP, Cdc25UQ, Cdc25UR, Cdc25US, Cdc25UT, Cdc25UU, Cdc25UV, Cdc25UW, Cdc25UX, Cdc25UY, C

T

The diagram illustrates the complex regulatory network of the cell cycle, showing the progression from G1 to S phase and the effects of DNA damage checkpoints. Key components include:

- Growth factor signaling:** Growth factor withdrawal leads to GSK3p, which inhibits p107, E2F4.5, and DP-1.2. Growth factor stimulation leads to p107, E2F4.5, and DP-1.2, which inhibit p130 and p135. p130 and p135 inhibit p18, p19, p27.57, p21, and p21. p18, p19, p27.57, p21, and p21 inhibit p16, p15, p18, p19, p27.57, p21, and p21.
- MAPK signaling pathway:** Growth factor stimulation leads to MAPK signaling pathway, which activates p38, p39, p40, p41, p42, p43, p44, p45, p46, p47, p48, p49, p50, p51, p52, p53, p54, p55, p56, p57, p58, p59, p60, p61, p62, p63, p64, p65, p66, p67, p68, p69, p70, p71, p72, p73, p74, p75, p76, p77, p78, p79, p80, p81, p82, p83, p84, p85, p86, p87, p88, p89, p90, p91, p92, p93, p94, p95, p96, p97, p98, p99, p100, p101, p102, p103, p104, p105, p106, p107, p108, p109, p110, p111, p112, p113, p114, p115, p116, p117, p118, p119, p120, p121, p122, p123, p124, p125, p126, p127, p128, p129, p130, p131, p132, p133, p134, p135, p136, p137, p138, p139, p140, p141, p142, p143, p144, p145, p146, p147, p148, p149, p150, p151, p152, p153, p154, p155, p156, p157, p158, p159, p160, p161, p162, p163, p164, p165, p166, p167, p168, p169, p170, p171, p172, p173, p174, p175, p176, p177, p178, p179, p180, p181, p182, p183, p184, p185, p186, p187, p188, p189, p190, p191, p192, p193, p194, p195, p196, p197, p198, p199, p200, p201, p202, p203, p204, p205, p206, p207, p208, p209, p210, p211, p212, p213, p214, p215, p216, p217, p218, p219, p220, p221, p222, p223, p224, p225, p226, p227, p228, p229, p230, p231, p232, p233, p234, p235, p236, p237, p238, p239, p240, p241, p242, p243, p244, p245, p246, p247, p248, p249, p250, p251, p252, p253, p254, p255, p256, p257, p258, p259, p260, p261, p262, p263, p264, p265, p266, p267, p268, p269, p270, p271, p272, p273, p274, p275, p276, p277, p278, p279, p280, p281, p282, p283, p284, p285, p286, p287, p288, p289, p290, p291, p292, p293, p294, p295, p296, p297, p298, p299, p300, p301, p302, p303, p304, p305, p306, p307, p308, p309, p310, p311, p312, p313, p314, p315, p316, p317, p318, p319, p320, p321, p322, p323, p324, p325, p326, p327, p328, p329, p330, p331, p332, p333, p334, p335, p336, p337, p338, p339, p340, p341, p342, p343, p344, p345, p346, p347, p348, p349, p350, p351, p352, p353, p354, p355, p356, p357, p358, p359, p360, p361, p362, p363, p364, p365, p366, p367, p368, p369, p370, p371, p372, p373, p374, p375, p376, p377, p378, p379, p380, p381, p382, p383, p384, p385, p386, p387, p388, p389, p390, p391, p392, p393, p394, p395, p396, p397, p398, p399, p400, p401, p402, p403, p404, p405, p406, p407, p408, p409, p410, p411, p412, p413, p414, p415, p416, p417, p418, p419, p420, p421, p422, p423, p424, p425, p426, p427, p428, p429, p430, p431, p432, p433, p434, p435, p436, p437, p438, p439, p440, p441, p442, p443, p444, p445, p446, p447, p448, p449, p450, p451, p452, p453, p454, p455, p456, p457, p458, p459, p460, p461, p462, p463, p464, p465, p466, p467, p468, p469, p470, p471, p472, p473, p474, p475, p476, p477, p478, p479, p480, p481, p482, p483, p484, p485, p486, p487, p488, p489, p490, p491, p492, p493, p494, p495, p496, p497, p498, p499, p500, p501, p502, p503, p504, p505, p506, p507, p508, p509, p510, p511, p512, p513, p514, p515, p516, p517, p518, p519, p520, p521, p522, p523, p524, p525, p526, p527, p528, p529, p530, p531, p532, p533, p534, p535, p536, p537, p538, p539, p540, p541, p542, p543, p544, p545, p546, p547, p548, p549, p550, p551, p552, p553, p554, p555, p556, p557, p558, p559, p560, p561, p562, p563, p564, p565, p566, p567, p568, p569, p570, p571, p572, p573, p574, p575, p576, p577, p578, p579, p580, p581, p582, p583, p584, p585, p586, p587, p588, p589, p590, p591, p592, p593, p594, p595, p596, p597, p598, p599, p600, p601, p602, p603, p604, p605, p606, p607, p608, p609, p610, p611, p612, p613, p614, p615, p616, p617, p618, p619, p620, p621, p622, p623, p624, p625, p626, p627, p628, p629, p630, p631, p632, p633, p634, p635, p636, p637, p638, p639, p640, p641, p642, p643, p644, p645, p646, p647, p648, p649, p650, p651, p652, p653, p654, p655, p656, p657, p658, p659, p660, p661, p662, p663, p664, p665, p666, p667, p668, p669, p670, p671, p672, p673, p674, p675, p676, p677, p678, p679, p680, p681, p682, p683, p684, p685, p686, p687, p688, p689, p690, p691, p692, p693, p694, p695, p696, p697, p698, p699, p700, p701, p702, p703, p704, p705, p706, p707, p708, p709, p710, p711, p712, p713, p714, p715, p716, p717, p718, p719, p720, p721, p722, p723, p724, p725, p726, p727, p728, p729, p730, p731, p732, p733, p734, p735, p736, p737, p738, p739, p740, p741, p742, p743, p744, p745, p746, p747, p748, p749, p750, p751, p752, p753, p754, p755, p756, p757, p758, p759, p760, p761, p762, p763, p764, p765, p766, p767, p768, p769, p770, p771, p772, p773, p774, p775, p776, p777, p778, p779, p780, p781, p782, p783, p784, p785, p786, p787, p788, p789, p790, p791, p792, p793, p794, p795, p796, p797, p798, p799, p

U

CELL CYCLE

G1

Growth factor withdrawal → GSK3β → MAPK signaling pathway

Growth factor → p107, E2F4,5, DP-1,2 → c-Myc → Mxi1 → p16, p15, p18, p19 → Ink4a, Ink4b, Ink4c, Ink4d → p27,57, p21 → Kip1,2, Cip1 → CycD, CDK4,6 → CycE, CDK2 → CycA, CDK2 → CycH, CDK7 → CycA, CDK1 → CycB, CDK1 → Plk1 → APC/C, Cdh1 → Cdc14 → MEN → Bub2

S

DNA damage checkpoint: ARF → Mdm2 → p53 → p300 → DNA-PK → ATM/ATR → p53 → GADD45 → PCNA → Cdc25A → CycE, CDK2 → CycA, CDK2 → CycH, CDK7 → CycA, CDK1 → CycB, CDK1 → Plk1 → APC/C, Cdh1 → Cdc14 → MEN → Bub2

G2

Ubiquitin-mediated proteolysis: APC/C, Cdh1 → Cdc14 → MEN → Bub2

M

ORC (Origin Recognition Complex): Orc1, Orc2, Orc3, Orc4, Orc5, Orc6

MCM (Mini-Chromosome Maintenance) complex: Mcm2, Mcm3, Mcm4, Mcm5, Mcm6, Mcm7

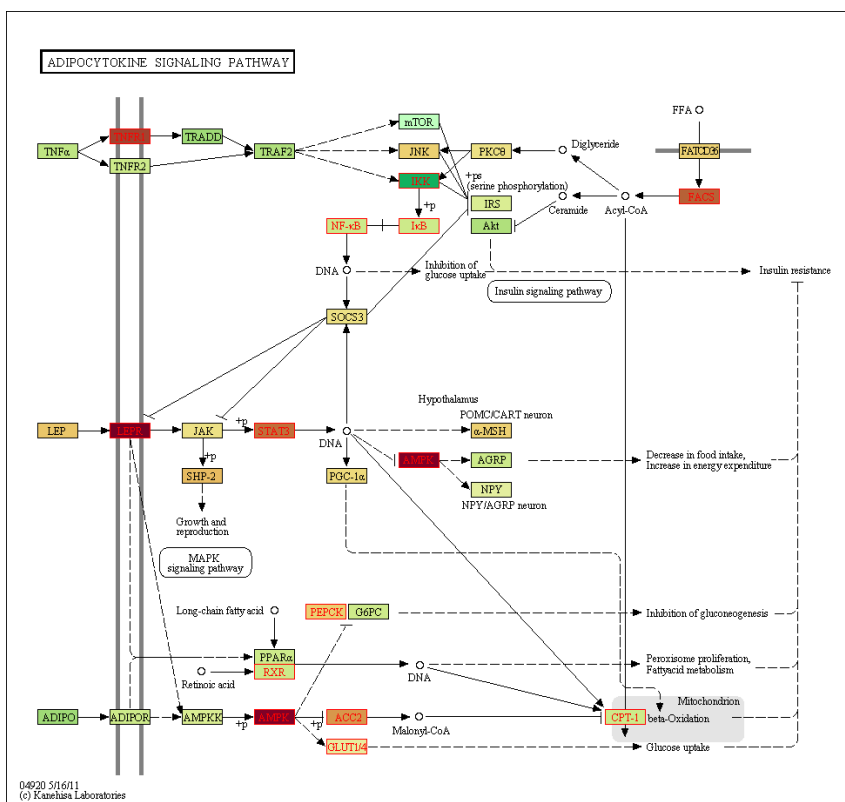
S-phase proteins, CycE → DNA → DNA biosynthesis

DNA → DNA biosynthesis

Undiff. vs. 5 day adipocyte differentiation

v

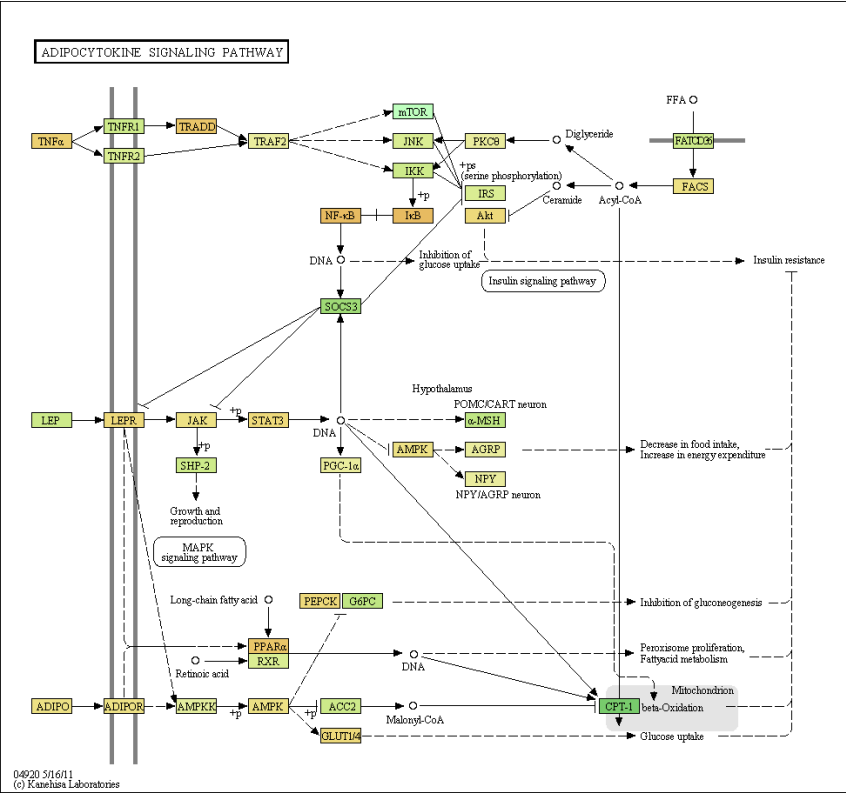
Adipocytokine signaling pathway (hsa04920); P = 4.97E-7



siCont. vs. siRNF40 5 day adipocyte differentiation

W

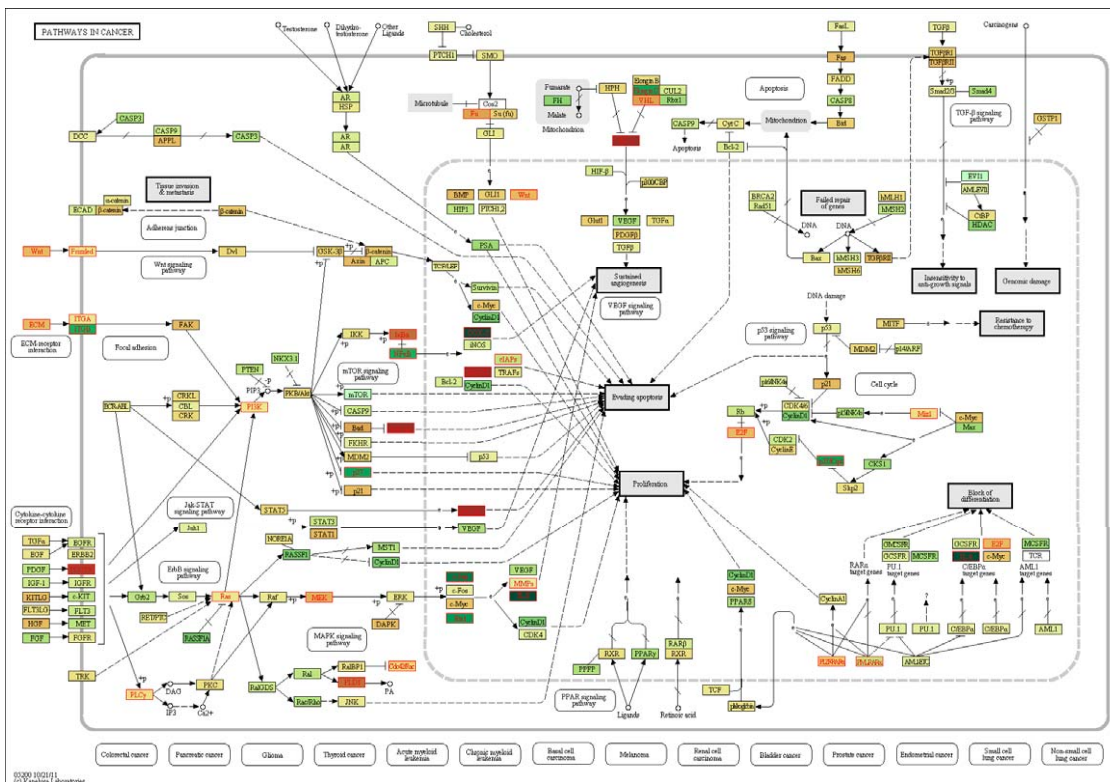
Adipocytokine signaling pathway (hsa04920); P = 2.84E-2



Undiff. vs. 2 day osteoblast differentiation

X

Pathways in cancer (hsa05200); P = 1.46E-10



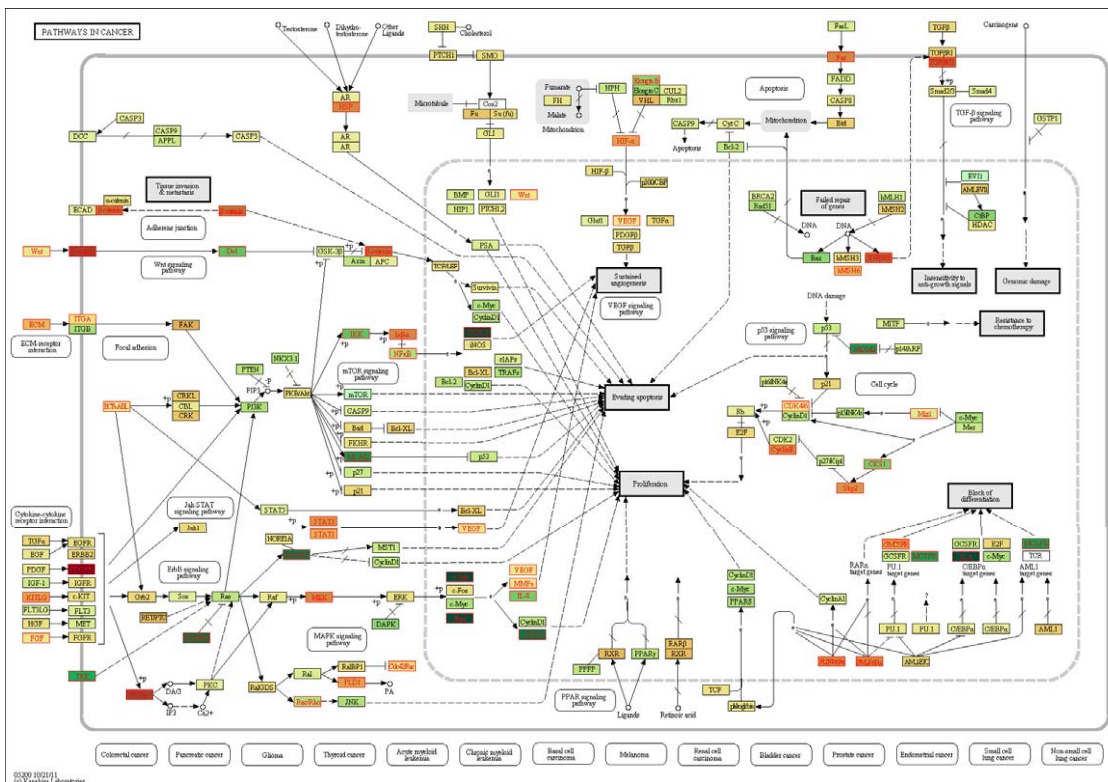
Y

Y



Pathways in cancer (hsa05200); P = 7.81E-11

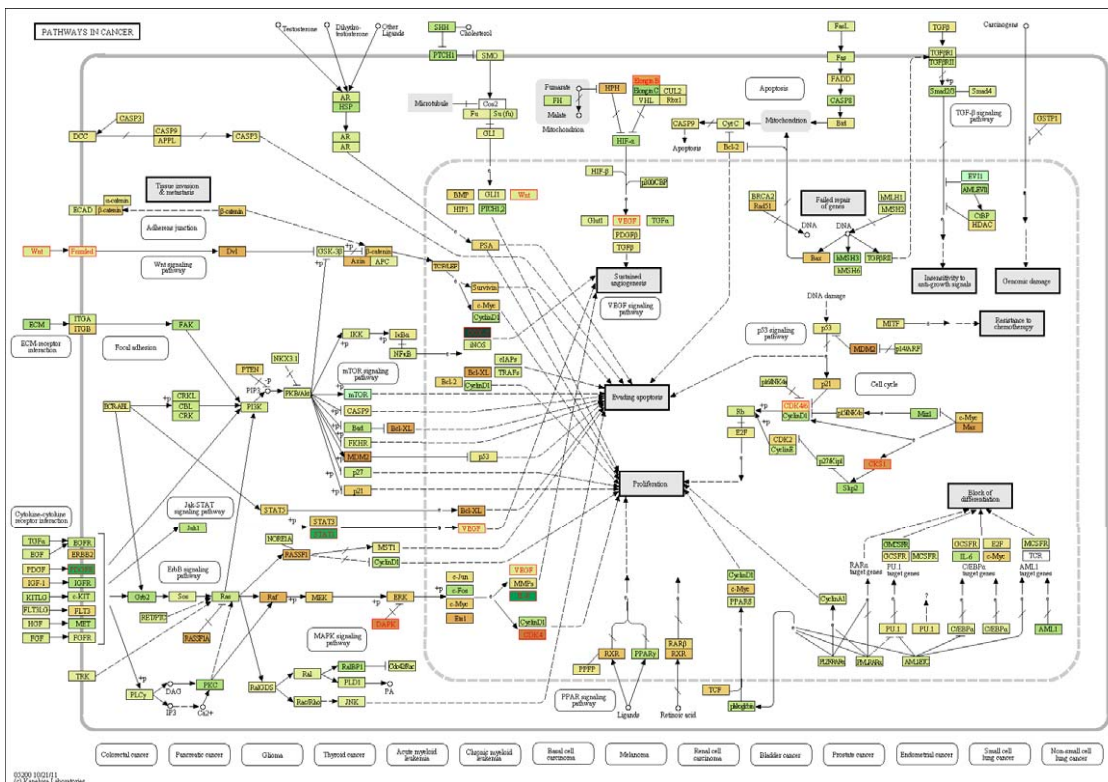
Z

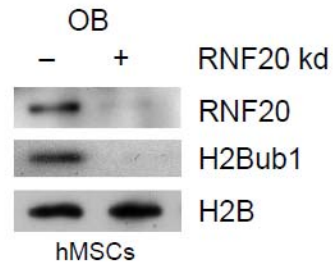
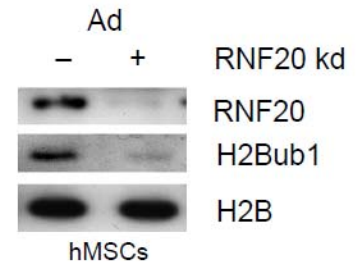
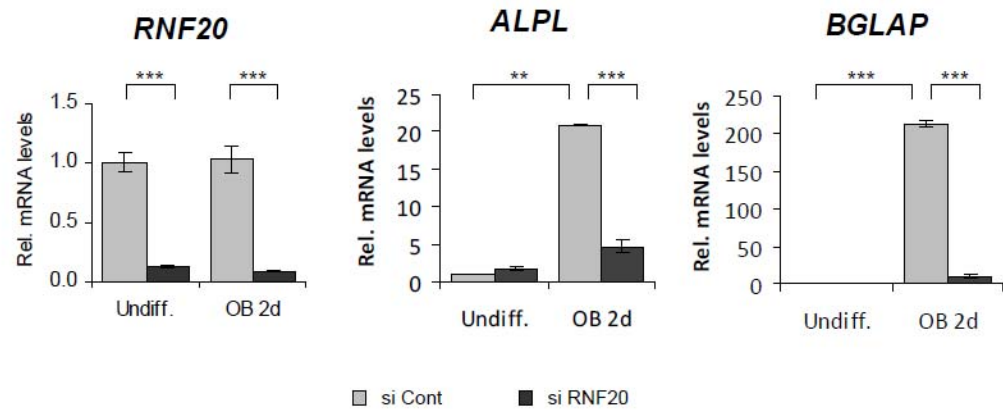
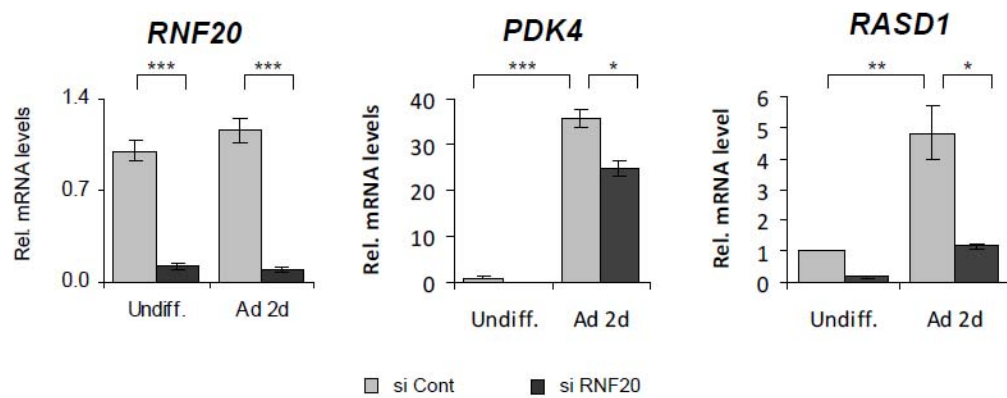


Cont. vs. siRNF40 2 day adipocyte differentiation

AA

Pathways in cancer (hsa05200); P = 5.46E-04



AB**AC****AD****AE**

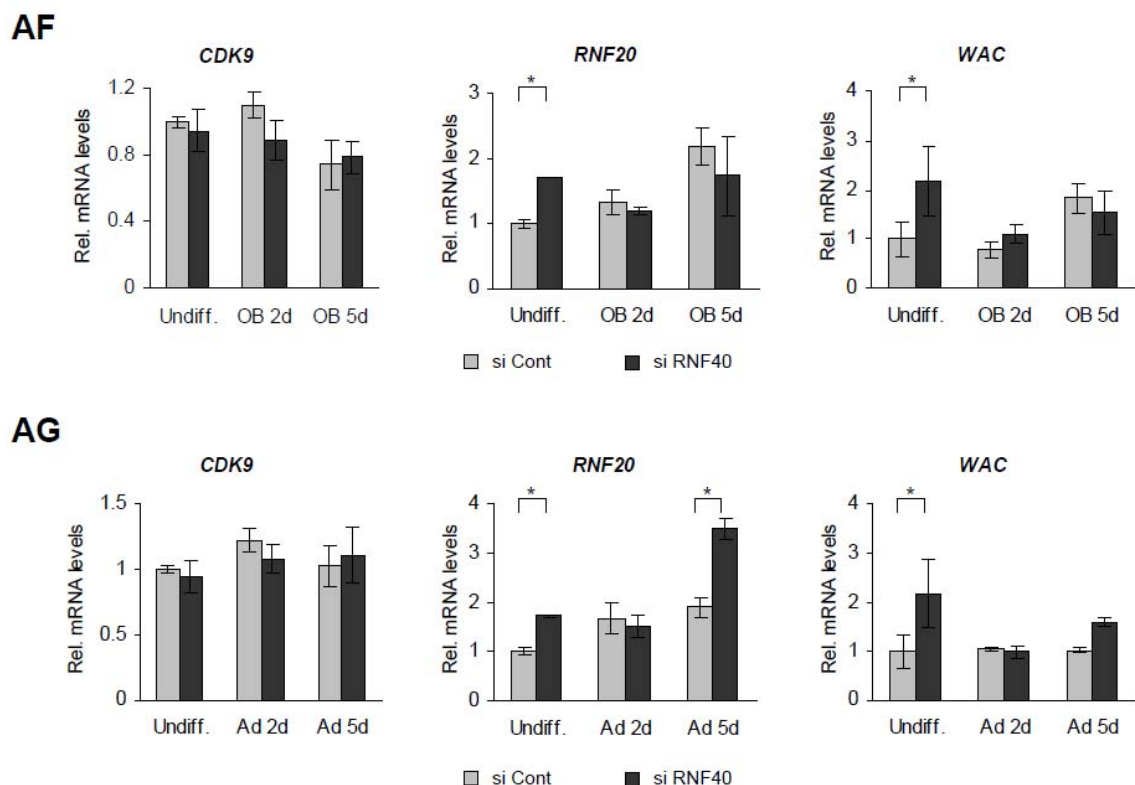


Figure S2

(A-C) hMSCs were transfected with control or RNF40 siRNAs (SmartPool) for 24 h and induced to differentiate into osteoblasts (B), adipocytes (C) or left undifferentiated (A) for 5 d. Protein extracts were analyzed by western blot using antibodies against RNF40, monoubiquitinated H2B (H2Bub1) and H2B as a loading control.

(D) RNF40 knockdown (siRNA from Ambion, see List of siRNAs) was performed in undifferentiated hMSCs for 2 d. Proteins were analyzed by Western blot for RNF40 and Hsc70 (loading control).

(E-F) hMSCs were transfected with control or RNF40 siRNAs (Ambion) for 24 h, induced to differentiate into osteoblasts (E) or adipocytes (F) for 5 d and then stained for alkaline phosphatase activity (E) or the presence of lipid drops (F) as described in Materials and Methods.

(G) Electron microscopy of differentiated adipocytes treated with control siRNA (left) and RNF40 siRNA (right). Arrows indicate lipid droplets.

(H-I) RNF40 knockdown was performed in hMSCs followed by osteoblast (H) or adipocyte (I) differentiation for 2 and 5 d. Expression of osteoblast (RUNX2; S2H) or adipocyte (CEBPB and CEBPG; S2I) marker genes was examined by qRT-PCR. Statistical analysis: * $p < 0.05$; ** $p < 0.01$; *** $p < 0.001$. Mean \pm SD, $n = 3$.

(J) Transcriptome-wide gene expression microarray analysis of hMSC induced to differentiate into the osteoblast or adipocyte lineages for 2 d after RNF40 knockdown versus undifferentiated hMSC under the same siRNA treatment. Color code indicates downregulated genes in red and up-regulated genes in blue. Mean values, $n = 3$.

(K) hMSCs were transfected with control or RNF40 siRNAs (SmartPool) for 24 h and induced to differentiate into osteoblasts or adipocytes for 2 and 5 d. Heat map was composed of the genes that were similarly regulated in both osteoblast and adipocyte differentiations. Color code indicates downregulated genes in red and upregulated genes in blue. Mean values, $n = 3$.

(L-M) Microarray analysis was performed as in (K). Genes that were specifically regulated in osteoblasts (L) or adipocytes (M) were used for the heat-maps. Color code indicates downregulated genes in red and up-regulated genes in blue. Mean values, $n = 3$.

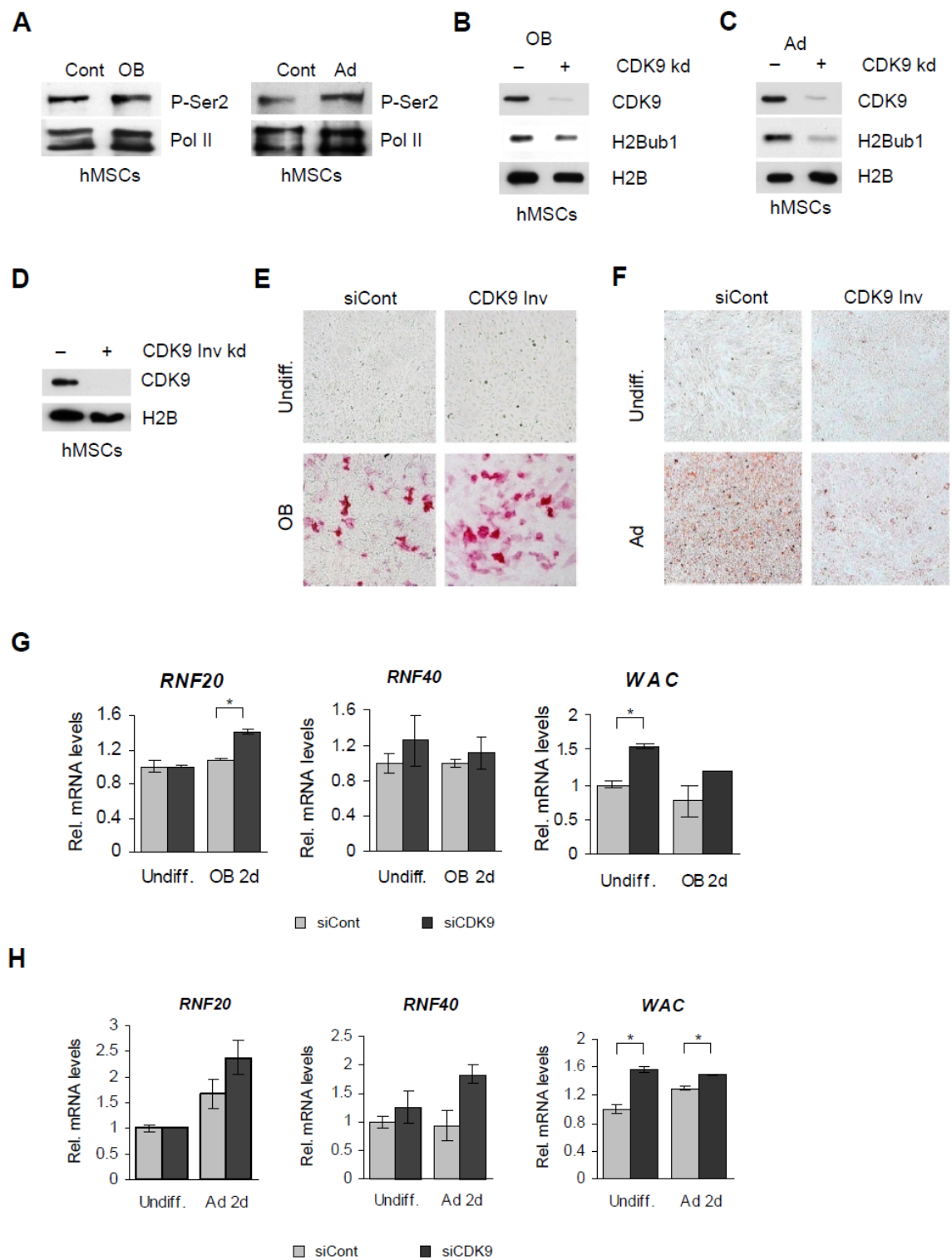
(N-AA) Pathway analysis was performed as indicated in Supplemental Materials and Methods using various comparisons from the hMSC differentiation microarray data with control or RNF40 siRNAs. Downregulated genes are shown in green squares, up-regulated in red squares. Red color for the text indicates significantly regulated genes. Mean values, $n = 3$.

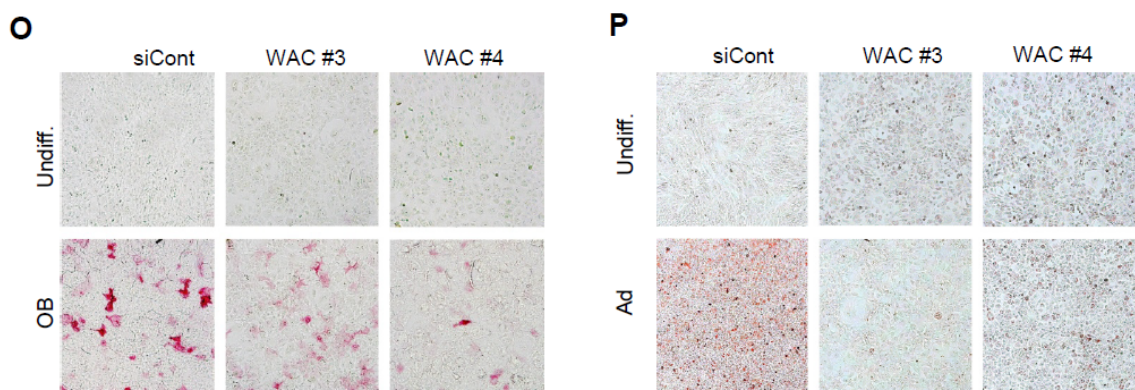
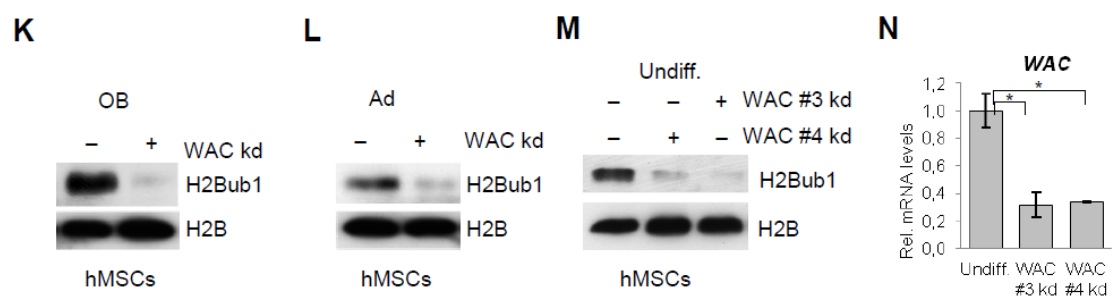
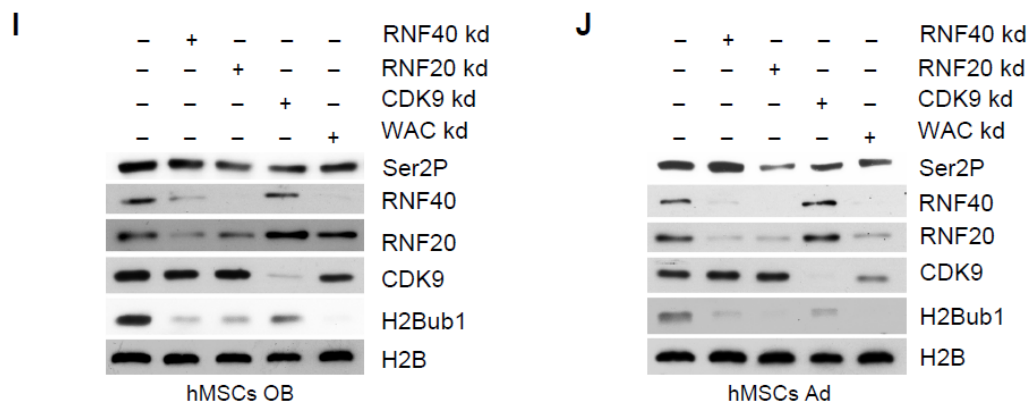
(AB-AC) hMSCs were transfected with control or RNF20 siRNAs (SmartPool) for 24 h and differentiated to either osteoblasts (OB) or adipocytes (Ad) for 2 d. Protein lysates were analyzed by Western blot for RNF20, monoubiquitinated H2B (H2Bub1) and H2B as a loading control.

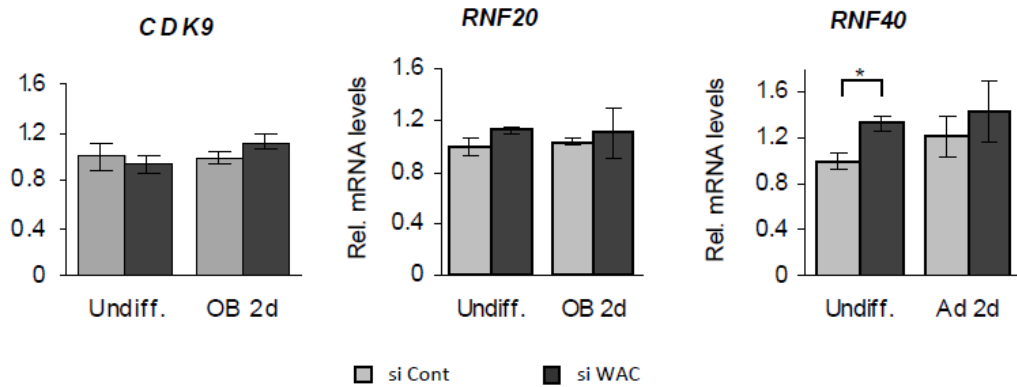
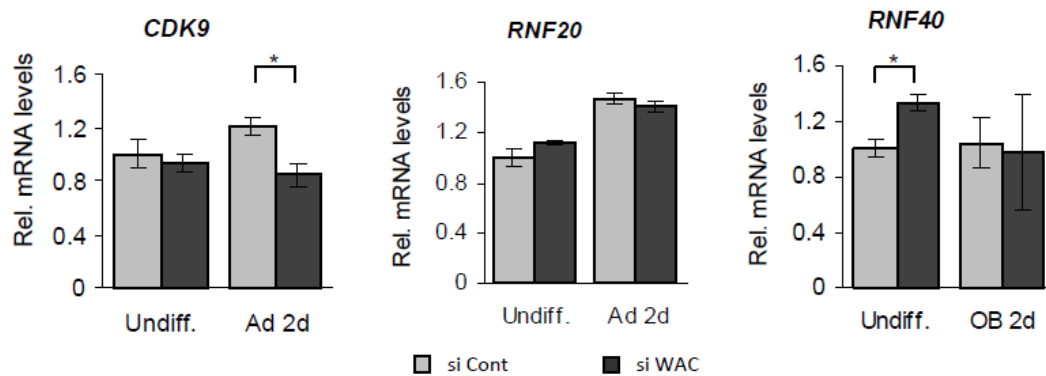
(AD-AE) Knockdowns and differentiation were performed as in (AB). The efficiency of knockdown and the changes in osteoblast (AD) and adipocyte (AE) gene expression were determined by qRT-PCR. Statistical analysis: * $p < 0.05$; ** $p < 0.01$; *** $p < 0.001$. Mean \pm SD, $n = 3$.

(AF-AG) hMSCs were transfected with control or RNF40 siRNAs (SmartPool) for 24 h and induced to differentiate into osteoblasts (AF) or adipocytes (AG) for 2 or 5 d. qRT-PCR was used to monitor osteoblast (AF) and adipocyte (AG)-specific gene expression. Statistical analysis: * $p < 0.05$; ** $p < 0.01$; *** $p < 0.001$. Mean \pm SD, $n = 3$.

Figure S3 related to Figure 3





Q**R****Figure S3**

(A) hMSCs were differentiated for 2 d to osteoblasts (OB) or adipocytes (Ad). Protein extracts were analyzed by Western blot for Ser2 phosphorylation of CTD (P-Ser2) and total polymerase II (loading control).

(B-C) hMSCs were transfected with control or CDK9 siRNAs (Ambion) for 24 h and differentiated to either osteoblasts (OB) or adipocytes (Ad) for 2 d. Protein lysates were analyzed by Western blot with antibodies to CDK9, monoubiquitinated H2B (H2Bub1) and H2B as a loading control.

(D) CDK9 knockdown was performed using an independent siRNA (Invitrogen, Inv) in undifferentiated hMSCs for 2 d. Proteins were analyzed by Western blot for CDK9 and H2B (loading control).

(E-F) hMSCs were transfected with control or CDK9 siRNAs (Invitrogen) for 24 h and induced to differentiate into osteoblasts (E) or adipocytes (F) for 5 d and stained for alkaline phosphatase activity (E) or presence of lipid drops (F) as described in Materials and Methods.

(G-H) Knockdowns with control or CDK9 siRNAs (Ambion) were performed in hMSCs for 24 h. After that cells were induced to differentiate into osteoblasts (G) or adipocytes (H) for 2 d. qRT-PCR was used to monitor osteoblast (G) and adipocyte (H)-specific gene expression. Statistical analysis: * $p < 0.05$; ** $p < 0.01$; *** $p < 0.001$. Mean \pm SD, $n = 3$.

(I-J) hMSC were transfected with siRNAs to RNF40 (SmartPool), RNF20 (SmartPool), CDK9 (Ambion), WAC (SmartPool) and control siRNAs for 24 h and differentiate to osteoblasts (I) or adipocytes (J) for 2 d. Protein lysates were checked for the levels of Ser2 phosphorylation of CTD (P-Ser2), RNF40, RNF20, CDK9, monoubiquitinated H2B (H2Bub1) and H2B (loading control) by Western blot.

(K-L) WAC knockdown (SmartPool) was performed in hMSCs for 24 h. After that cells were differentiated in either osteoblasts (K) or adipocytes (L). Protein extracts were analysed by Western blot for monoubiquitinated H2B (H2Bub1) and H2B as a loading control.

(M) Undifferentiated hMSCs were transfected with control siRNA and siRNAs for WAC (#3 and #4, Dharmacon) for 48 h. Protein extracts were examined for levels of monoubiquitinated H2B (H2Bub1) and H2B (loading control) by Western blot.

(N) Knockdowns were performed as in (M). Knockdown efficiency was verified by WAC expression using qRT-PCR. Statistical analysis: * $p < 0.05$; ** $p < 0.01$; *** $p < 0.001$. Mean \pm SD, $n = 3$.

(O-P) hMSCs were transfected with control siRNA and siRNAs for WAC (#3 and #4, Dharmacon) for 24 h and then differentiated to osteoblast (O) or adipocytes (P) for 5 d. Cells were stained for alkaline phosphatase activity (O) or presence of lipid drops (P).

(Q-R) WAC knockdown (SmartPool) was performed in hMSCs for 24 h, followed by differentiation to osteoblasts (Q) or adipocytes (R). qRT-PCR was used to monitor expression of the osteoblast (Q) or adipocyte (R)-specific genes. Statistical analysis: * $p < 0.05$; ** $p < 0.01$; *** $p < 0.001$. Mean \pm SD, $n = 3$.

Figure S4 related to Figure 4

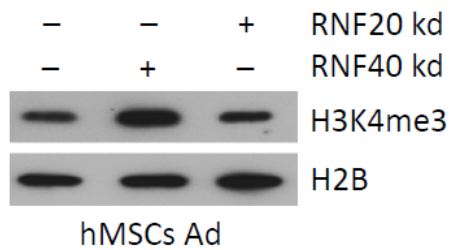


Figure S4

hMSC were transfected with control, RNF40 (SmartPool) or RNF20 (SmartPool) siRNAs for 24h and differentiated to adipocytes for 2d. Protein lysates were analyzed by Western blot using antibodies to H3K4me3 and H2B (loading control).

2) SUPPLEMENTAL EXPERIMENTAL PROCEDURES

Cell culture, differentiation and knockdowns

hMSC-Tert cells (Simonsen et al., 2002) were cultured in low glucose, phenol red free MEM (Invitrogen, Carlsbad, CA), supplemented with 10% bovine growth serum (BGS; HyClone, USA) and 1X penicillin/streptomycin (Invitrogen). For osteoblast differentiation growth medium was supplemented with 10 mM β -glycerophosphate, 0.2 mM ascorbate, 10^{-8} M calcitriol, and 10^{-7} M dexamethasone. For adipocyte differentiation normal growth

medium containing 15% BGS was supplemented with 2×10^{-6} M insulin, 0.45 mM isobutylmethyl-xanthine, 10^{-5} M troglitazone, and 10^{-7} M dexamethasone. hFOB1.17 cells (Harris et al., 1995) were provided by Tom Spelsberg (Mayo Clinic, Rochester, Minnesota) and cultured at the permissive temperature (33°C) in high glucose, phenol red free DMEM/F12 (Invitrogen) supplemented with 10% BGS (Hyclone) and 1X penicillin/streptomycin (Invitrogen). Osteoblast differentiation was induced by shifting to the restrictive temperature (39°C) and growing for 7 d. Neurospheres were prepared from E17.5 mouse brains according to standard procedures. Spheres were maintained in proliferation medium (NB with B27 and N2 supplement, 20 ng/ml FGF2, 20 ng/ml EGF). Spheres were differentiated by culturing in NB with B27 and N2 supplement containing 2% horse serum for 5 d. Primary mouse oligodendrocyte cultures were prepared as described previously (Trajkovic et al., 2006). For differentiation the progenitors of oligodendrocytes were cultured for 5 d in MEM containing B27 supplement, 1% horse serum, L-thyroxine, tri-iodothyroxine, glucose, glutamine, penicillin, streptomycin, gentamycin, pyruvate, and bicarbonate (Sato-B27) on poly-L-lysine-coated dishes or glass-coverslips.

Knockdowns were performed using Lipofectamine RNAiMAX (Invitrogen) according to the manufacturer's instructions. siRNAs utilized are listed in Table S1.

Cell culture for microarray studies. Total RNA for microarray experiments was isolated from control or RNF40 siRNA transfected cells prior to differentiation or after differentiation for 2 or 5 d into osteoblasts or adipocytes.

Chromatin immunoprecipitation (ChIP) and qPT-PCR

ChIP was performed using a modified protocol based on (Gomes et al., 2006; Nelson et al., 2006). Adherent cells were crosslinked for 10 min in PBS containing 1% formaldehyde. Crosslinking was quenched by adding glycine to a final concentration of 156 mM for 5 min.

Fixed cells were washed twice with PBS and scraped in a buffer containing 150 mM NaCl, 5 mM EDTA, 50 mM Tris (pH 8), 0.5% (v/v) NP-40, 1% (v/v) Triton X-100, 20 mM NaF and inhibitor cocktail (1 mM N-ethylmaleimide, 10 mM β -glycerophosphate, 1 ng/ μ l Aprotinin, 1 ng/ μ l Leupeptin, 1 mM Pefabloc, 10 μ M iodoacetamide and 1 mM nickel chloride). The nuclei were pelleted and washed with the same buffer before lysing in 300 μ l of Lysis Buffer (150 mM NaCl, 1% (v/v) NP-40, 0.5% w/v sodium deoxycholate, 0.1% SDS, 50 mM Tris-HCl (pH 8), 20 mM EDTA, 20 mM sodium fluoride and inhibitor cocktail). Pre-clearing was performed with 100 μ l of Sepharose 4B (GE Healthcare, Uppsala, Sweden) in Lysis Buffer (50% slurry) for 1 hour at 4°C. After that chromatin was diluted with Lysis Buffer, aliquoted in 50 μ l aliquots and stored at -80 °C. After thawing, each 50 μ l aliquot was brought to the final volume of 1 ml with Lysis Buffer and 2 μ g of corresponding antibodies (Supplemental Table 4) were added. Samples were incubated with the antibodies overnight at 4°C before adding 30 μ l of Protein-G Sepharose slurry (GE Healthcare) and incubating for another 2 hours at 4°C. After centrifugation (2000g, 2 min, 4°C) beads were washed three times with Lysis Buffer, three times with Wash Buffer (100 mM Tris (pH 8.5), 500 mM LiCl, 1% (v/v) NP-40, 1% w/v sodium deoxycholate, 20 mM EDTA, 20 mM NaF and inhibitor cocktail), three additional times with Lysis Buffer and twice with TE-buffer. Reverse crosslinking was performed by adding 100 μ l of 10% (w/v) Chelex 100 slurry (Bio-Rad) and incubating at 95 °C for 10 min. After that 2 μ l of Proteinase K (20 μ g/ μ l, Invitrogen) were added to each sample, followed by the incubation at 55°C for 30 minutes and inactivation by heating to 95 °C for 10 min. Samples were centrifuged at 12,000 X g for 1 min at 4°C and the supernatant containing DNA was utilized for quantitative real-time PCR. The background binding was determined by performing a ChIP with a non-specific IgG antibody. To prepare inputs 5 μ l (10% relative to ChIPs) of chromatin extracts were precipitated by adding 100% EtOH and 1 μ l of Pink Precipitant (5 mg/ml, Bioline, Luckenwalde, Germany) and incubating overnight at -20°C. The pellets were washed twice with 70% EtOH and processed as described above for ChIP samples. ChIP samples were normalized to input DNA samples, and displayed as “% of input”.

RNA isolation, reverse transcription and quantitative RT-PCR was performed as described previously (Prenzel et al., 2011). All qRT-PCR samples were normalized to an internal reference gene (*HNRNPK*) and displayed relative to the control non-differentiated sample.

Statistical analysis was done with ANOVA test.

Primers utilized for gene expression and ChIP analyses are indicated in corresponding lists in Supplemental Materials and Methods.

Immunofluorescence staining of *Drosophila* ovaries

Drosophila melanogaster OregonR stocks were raised on standard cornmeal-yeast-agar-medium at 25°C. Ovaries were fixed in 5% formaldehyde (Polysciences, Inc.) for 10 min and the staining procedure was essentially performed as described (Konig et al., 2011; Shcherbata et al., 2004). Additionally, after fixation ovaries were permeabilized (3 washes in PBT (PBS with 0.2% Triton X-100), followed by 30 min incubation in 2% Triton X-100 in PBS) and incubated in HCl to allow for access of the anti-H2Bub1 antibody to the chromatin. Samples were washed 3 times in PBT, then incubated in 2N HCl at 37°C for 30 min). The following antibodies were used: mouse monoclonal H2Bub1 (1:500, Millipore); rabbit polyclonal pMad (1:1000, D. Vasiliauskas, S. Morton, T. Jessell and E. Laufer), Alexa 488, 568 goat anti-mouse, anti-rabbit (1:500, Molecular Probes).

Immunofluorescence staining of oligodendrocytes

Oligodendrocyte precursors or mature oligodendrocytes were fixed with 4% formaldehyde, 0.2% glutaraldehyde in PBS for 15 minutes. After that cells were washed 3 times with PBS, permeabilized for 1 min with 0.1% Triton X-100, again washed 3x with PBS followed by 30 min blocking with blocking solution (2% BSA, 2% Fetal Calf Serum Gold, 20 µl/ml fish gelatine in PBS). Then samples were incubated for 1h with MBP antibody (1:200, DakoCytomation, Carpinteria, CA, USA) in 10% blocking solution at room temperature, washed 3x with PBS and incubated with Alexa 488 goat anti-rabbit (1:200, Invitrogen) and Phalloidin rodamin (1:200, Invitrogen) in 10% blocking solution followed by 3x PBS wash and mounting in mounting media (0.4 g/ml Mowiol, Merck; 1 g/ml glycerol; 24 mg/ml Anti-fading reagent, DABCO in 0.1M Tris-HCl).

Monolayer-embedding in Epon for electron microscopy

For electron microscopy hMSCs were differentiated to adipocytes for 5 d. Cells were washed in 0.1 M phosphate buffer and fixed for 1h in 1% OsO₄ in 0.1 M PB at 4°C. After that cells were washed (10 min each time) 3 times with DI water, twice with 50% EtOH and once with 70% EtOH. Contrasting was done with 1.5 % uranylacetate and 1.5 % tungstophosphoric acid in 70 % EtOH for 90 min. Then cells were washed twice in 90% EtOH (for 10 min) and 5 times in 99.9% EtOH (for 5 min). After that EtOH was replaced with Epon in EtOH (3 washes, 30 min each): 1st wash – 1:2 Epon to EtOH, 2nd wash – 1:1 Epon to EtOH, 3rd wash – 2:1 Epon to EtOH. Finally cells were incubated in 100% Epon for 1h and then enclosed in

BEEM-capsules. After 24 h of Epon polymerization at 60°C BEEM-capsules were disassembled from the plates and prepared for ultrathin sectioning. Sections were prepared and imaged with a Leo 912AB electron microscope equipped with

a CCD camera 2048 3 2048 (Proscan, Scheuring, Germany) as described (Aggarwal et al., 2011).

Pathway analysis

Pathway analysis was performed to assess biological functions influenced by cell differentiations and knockdowns. All non-metabolic pathways of the KEGG database (www.genome.jp/kegg/) were tested for enrichment using a one-sided wilcoxon rank-sum test on the ranked p-values of differential gene expression analyses. Results were adjusted for multiple testing using Benjamini-Hochbergs method. All analyses were performed using the free statistical software R (version 2.14.1).

Oil Red O staining

Oil Red O staining was performed to visualize lipid drops accumulation. Oil Red O working solution was prepared by mixing 3 parts of Oil Red O stock solution (3mg/ml Oil Red O in 99% isopropanol) and 2 parts of DI water followed by 10 min incubation at RT and filtering. Cells were fixed with 10% formaldehyde in PBS for 30 min, washed 3 times in DI water and incubated with 60% isopropanol for 5 min. After that cells were incubated with Oil Red O working solution for 5 min and rinsed in DI water.

Quantification of Oil Red O and alkaline phosphatase staining

Pictures of the stained plates were taken under microscope using 10x magnification. Each picture showed approximately 500-1000 cells. The staining was quantified using the Threshold_Color plugin (<http://www.dentistry.bham.ac.uk/landinig/software/software.html>) of ImageJ software (<http://rsb.info.nih.gov/ij/>). For Oil Red O staining, the threshold was defined in RGB color space for each experiment (typically : R:150-255 ; G:0-140 ; B:0-140) and the positive area of each picture was measured. For alkaline phosphatase staining, the threshold was defined in CIE Lab color space for each experiment (typically : L*:5-255 ; a*:125-255 ; b*:0-255) and the positive area of each picture was measured.

List of siRNAs used in this study.

Target Gene	siRNA target sequence	Source	Cat.No.
siGENOME Non-targeting siRNA pool # 1	-	Dharmacon	D-001206-13
RNF20 si Genome (#1)	CCAAUGAAAUCAAGUCUAA	Dharmacon	D-007027-01
RNF20 si Genome (#2)	UAAGGAAACUCCAGAAUUAU	Dharmacon	D-007027-02
RNF20 si Genome (#3)	GCAAAUGUCCCAAGUGUAA	Dharmacon	D-007027-03
RNF20 si Genome (#4)	AGAAGAAGCUACAUGAUUU	Dharmacon	D-007027-04
RNF40	UGAGGACAUGCAGGAACAGAA	Ambion	s18960
RNF40 siGENOME (# 1)	GAGAUGCGCCACCUGAUUAUU	Dharmacon	D-006913-01
RNF40 siGENOME (# 2)	GAUGCCAACUUUAAGCUAAUU	Dharmacon	D-006913-02
RNF40 siGENOME (# 3)	GAUCAAGGCCAACCAGAUUUU	Dharmacon	D-006913-03
RNF40 siGENOME (# 4)	CAACGAGUCUCUGCAAGUGUU	Dharmacon	D-006913-04
CDK9	UGAGAUUUUGUCGAACCAAAtt	Ambion	S2834
CDK9	GUCAACUUGAUUGAGAUUUGU CGAA	Invitrogen Val. Stealth	
WAC siGENOME (# 1)	CAACAUAACGUCUCUGAUU	Dharmacon	D-013325-01
WAC siGENOME (# 2)	UAAGCACACCUCAAACUAA	Dharmacon	D-013325-02
WAC siGENOME (# 3)	GAGACAAACCCGUAUCACA	Dharmacon	D-013325-03
WAC siGENOME (# 4)	CGAUCCACGUGUUCAUUA	Dharmacon	D-013325-04

List of antibodies used for ChIP and Western blot analysis.

Target protein	ChIP	WB	IF	Clone	Cat. No.	Source
CDK9		1:1000		C-20	sc-484	Santa Cruz
H2B		1:3000			07-371	Millipore
H2Bub1		1:100		7B4		(Prenzel et al., 2011)
H2Bub1			1:500	56	05-1312	Millipore
H2Bub1	2 μ l			D11	5546	Cell Signaling
H3K4me3	2 μ g	1:1000			MAB-003-050	Diagenode
H3K27me3	2 μ g				pAb-069-050	Diagenode
GFAP			1:400		MAB360	Chemicon International
IgG	2 μ g				ab46540-1	Abcam
MBP			1:200		A0623	Dako
NeuN			1:500		NUN	Aves Labs
pMAD			1:1000			D. Vasiliauskas, et al.
P-Ser2 RNAPII		1:10		3E10		(Chapman et al., 2007)
RNF40		1:1000		KA7-27	R9029	Sigma
Goat anti-mouse IgG-HRP		1:5000			sc-2005	Santa Cruz
Goat anti-rabbit IgG-HRP		1:5000			sc-2004	Santa Cruz
Goat Anti-Rat IgG + IgM-HRP		1:10000			112-035-068	Jackson ImmunoResearch
Goat anti-mouse Alexa 488			1:500			Molecular Probes
Goat anti-rabbit Alexa 568			1:500			Molecular Probes
Fluorescein-Labeled goat anti-Chicken			1:500		F-1005	Aves Labs
Goat anti-Mouse 568			1:500			Invitrogen

Goat anti-rabbit 488			1:200		A-11070	Invitrogen
Phalloidin rodamin			1:200		R415	Invitrogen

List of qRT-PCR primers used in this study.

Name	Sequence	Source
ALPL F	TGGGCCAAGGACGCTGGGAA	This study.
ALPL R	AAGGCCTCAGGGGGCATCTCG	This study.
BGLAP F	GCCCTCACACTCCTCGCCCT	This study.
BGLAP R	CGGGTAGGGGACTGGGGCTC	This study.
CDK9 F	AGAGGGTTTCCATGGGGTAG	This study.
CDK9 R	TCAGCCCGAGAATAGGATTG	This study.
G6PD F	CGACGAAGCGCAGACAGCGTCA	This study.
G6PD R	CAGCCACATAGGAGTTGCGGGC	This study.
HNRNPK F	ATCCGCCCCTGAACGCCCAT	This study.
HNRNPK R	ACATACCGCTCGGGGCCACT	This study.
LPL F	TCAGCCGGCTCATCAGTCGGT	This study.
LPL R	AGAGTCAGCACGAGCAGGGCT	This study.
PDK4 F	TTCACTCCGCGGCACCCTCA	This study.
PDK4 R	TCGGAGCAGAGCCTGGTTCCG	This study.
PPARG F	ACCTCCGGGGCCCTGGCAAAA	This study.
PPARG R	TGCTCTGCTCCTGCAGGGGG	This study.
RASD1 F	CAAGACGGCCATCGTGTGCGG	This study.
RASD1 R	GCTGCACCTCCTCGAAGGAGTCG	This study.
RNF20 F	TGGCCAAGCAGGAAGAAG	This study.
RNF20 R	ACGCTCTGACATGAGCTTGA	This study.
RNF40 F	AGTACAAGGCGCGGTTGA	(Prenzel et al., 2011)
RNF40 R	GAAGCAGAAAACGTGGAAGC	(Prenzel et al., 2011)
RPLP F	GATTGGCTACCCAAGTGTG	(Fritah et al., 2005)
RPLP R	CAGGGGCAGCAGCCACAAA	(Fritah et al., 2005)
WAC F	AGTGGGTTTGCCAGTGGAATGGAAGA	This study.
WAC R	ACAGTGCTTGGGGTAGCAGTTGGA	This study.

List of ChIP primers used in this study

Name	Sequence	Source
HIST1H2AC F	AAAAGCGGCCATGTTTTACA	(Pirngruber et al., 2009)
HIST1H2AC R	AAAAATCACCAAAACCAGCG	(Pirngruber et al., 2009)
GAPDH +1061F	CCGGGAGAAGCTGAGTCATG	(Shema et al., 2008)
GAPDH +1111R	TTTGCGGTGGAAATGTCCTT	(Shema et al., 2008)
PDK4-BV+468F	GCGTCGAGGCTCCAGGGCT	This study.
PDK4-BV+570R	GCCCAAGCTGGGTCTAGGGTT	This study.
PDK4 +3831F	CTCGGATGCTGATGAACCAGCACAGTAAG	This study.
PDK4 +3963R	AGTACTATCACTGAGAATGTGACCCGCTGAT	This study.
PPARG-BV+655F	AGCCGCTCCGGGGGAAGTT	This study.
PPARG-BV+850R	ACAGGGCCTGGCCAGCTACAA	This study.
PPARG +91888F	GGCCCACCAACTTTGGGATCAGC	This study.
PPARG +91922R	GAGTGGGAGTGGTCTTCCATTACGGAG	This study.
RASD1-BV +768R	GATCTGCTGCCTGAGCCGCTG	This study.
RASD1-BV +666F	CGGCCACCCTCACCTTCTCCT	This study.
TFF1 +6KB F	CAGGCTTCTCCCTTGATGAAT	(Pirngruber and Johnsen, 2010)
TFF1 +6KB R	ACACCCACCTTCCACAACAC	(Pirngruber and Johnsen, 2010)

3) SUPPLEMENTAL REFERENCES

- Chapman,R.D., Heidemann,M., Albert,T.K., Mailhammer,R., Flatley,A., Meisterernst,M., Kremmer,E., and Eick,D. (2007). Transcribing RNA polymerase II is phosphorylated at CTD residue serine-7. *Science* 318, 1780-1782.
- Fritah,A., Saucier,C., Mester,J., Redeuilh,G., and Sabbah,M. (2005). p21WAF1/CIP1 selectively controls the transcriptional activity of estrogen receptor alpha. *Mol. Cell Biol.* 25, 2419-2430.
- Gomes,N.P., Bjerke,G., Llorente,B., Szostek,S.A., Emerson,B.M., and Espinosa,J.M. (2006). Gene-specific requirement for P-TEFb activity and RNA polymerase II phosphorylation within the p53 transcriptional program. *Genes Dev.* 20, 601-612.
- Konig,A., Yatsenko,A.S., Weiss,M., and Shcherbata,H.R. (2011). Ecdysteroids affect *Drosophila* ovarian stem cell niche formation and early germline differentiation. *EMBO J.* 30, 1549-1562.
- Nelson,J.D., Denisenko,O., and Bomsztyk,K. (2006). Protocol for the fast chromatin immunoprecipitation (ChIP) method. *Nat. Protoc.* 1, 179-185.
- Pirngruber,J. and Johnsen,S.A. (2010). Induced G1 cell-cycle arrest controls replication-dependent histone mRNA 3' end processing through p21, NPAT and CDK9. *Oncogene* 29, 2853-2863.
- Pirngruber,J., Shchebet,A., Schreiber,L., Shema,E., Minsky,N., Chapman,R.D., Eick,D., Aylon,Y., Oren,M., and Johnsen,S.A. (2009). CDK9 directs H2B monoubiquitination and controls replication-dependent histone mRNA 3' end processing. *EMBO Rep.* 10, 894-900.
- Prenzel,T., Begus-Nahrmann,Y., Kramer,F., Hennion,M., Hsu,C., Gorsler,T., Hintermair,C., Eick,D., Kremmer,E., Simons,M., Beissbarth,T., and Johnsen,S.A. (2011). Estrogen-Dependent Gene Transcription in Human Breast Cancer Cells Relies upon Proteasome-Dependent Monoubiquitination of Histone H2B. *Cancer Res.* 71, 5739-5753.
- Shcherbata,H.R., Althausen,C., Findley,S.D., and Ruohola-Baker,H. (2004). The mitotic-to-endocycle switch in *Drosophila* follicle cells is executed by Notch-dependent regulation of G1/S, G2/M and M/G1 cell-cycle transitions. *Development* 131, 3169-3181.
- Shema,E., Tirosh,I., Aylon,Y., Huang,J., Ye,C., Moskovits,N., Raver-Shapira,N., Minsky,N., Pirngruber,J., Tarcic,G., Hublarova,P., Moyal,L., Gana-Weisz,M., Shiloh,Y., Yarden,Y., Johnsen,S.A., Borivoj,V., Berger,S.L., and Oren,M. (2008). The histone H2B-specific ubiquitin ligase RNF20/hBRE1 acts as a putative tumor suppressor through selective regulation of gene expression. *Genes Dev.* 22, 2664-2.
- Trajkovic,K., Dhaunchak,A.S., Goncalves,J.T., Wenzel,D., Schneider,A., Bunt,G., Nave,K.A., and Simons,M. (2006). Neuron to glia signaling triggers myelin membrane exocytosis from endosomal storage sites. *J. Cell Biol.* 172, 937-948.

A Genome-Wide Survey of Sexually Dimorphic Expression of *Drosophila* miRNAs Identifies the Steroid Hormone-Induced miRNA let-7 as a Regulator of Sexual Identity: Supplementary Material

GENETICS

Supporting Information

<http://www.genetics.org/lookup/suppl/doi:10.1534/genetics.114.169268/-/DC1>

A Genome-Wide Survey of Sexually Dimorphic Expression of *Drosophila* miRNAs Identifies the Steroid Hormone-Induced miRNA let-7 as a Regulator of Sexual Identity

Delphine Fagegaltier, Annekatrin König, Assaf Gordon, Eric C. Lai, Thomas R. Gingeras,
Gregory J. Hannon and Halyna R. Shcherbata

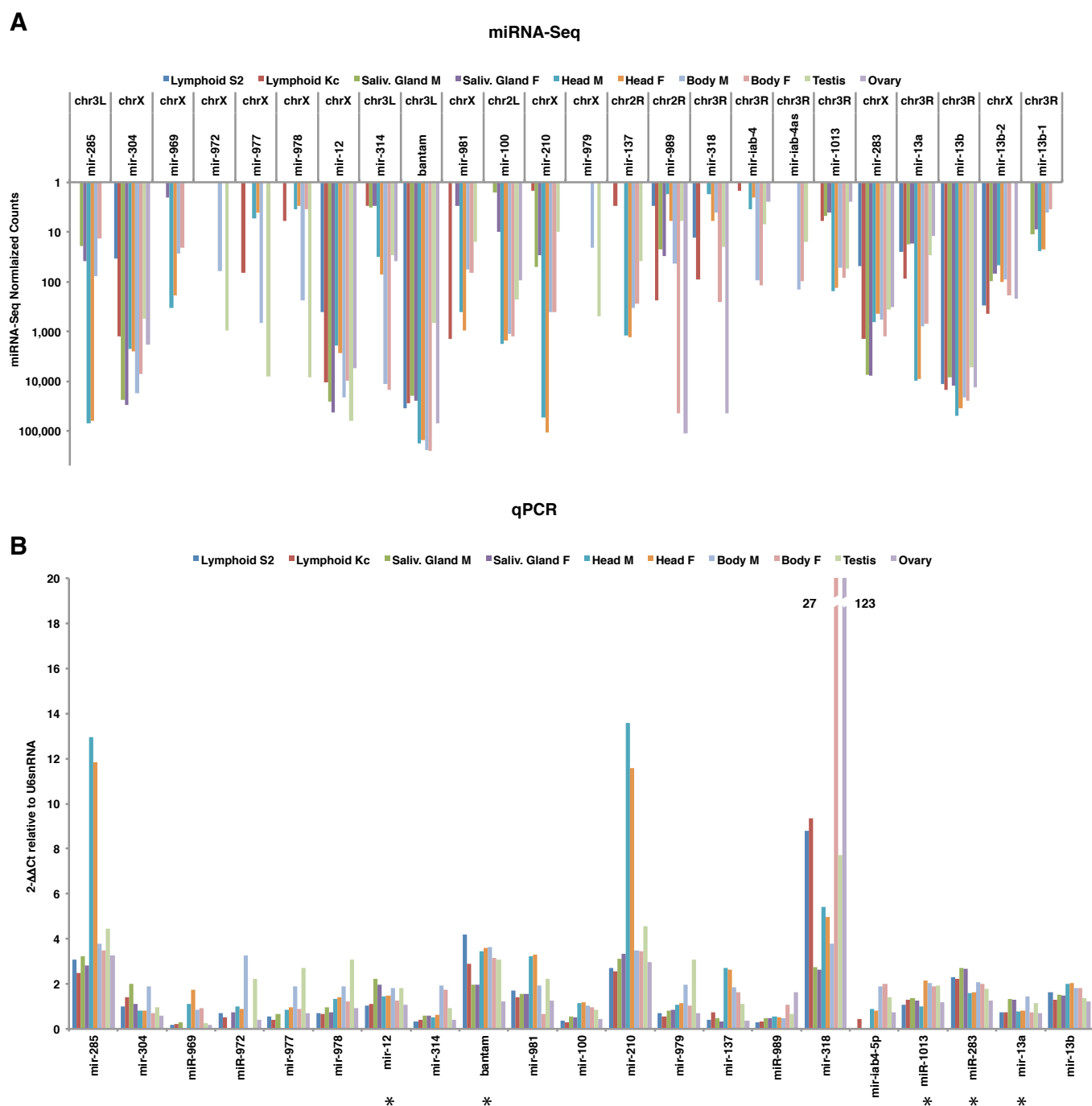


FIGURE S1: qPCR validation of the expression levels of 22 miRNAs across all samples. The trends of miRNA expression levels and relative abundance across all samples by miRNA-Seq (A) and qPCR (B) are similar for 16 miRNAs. Five additional miRNAs showing differences between miRNA-Seq and qPCR trends in one or more tissues (miR-12, bantam, miR-1013, miR-283, and miR-13a) are denoted with an asterisk. The genome presents several copies of mature miR-13b undistinguishable by qPCR: miR-13b and miR-13b-1 on chr3R, and miR-13b-2 on chrX. MiRNA normalized reads are reported in (A). qPCR assays were performed with at least two independent biological replicates and gave similar trends in (B). M: male ; F: female.

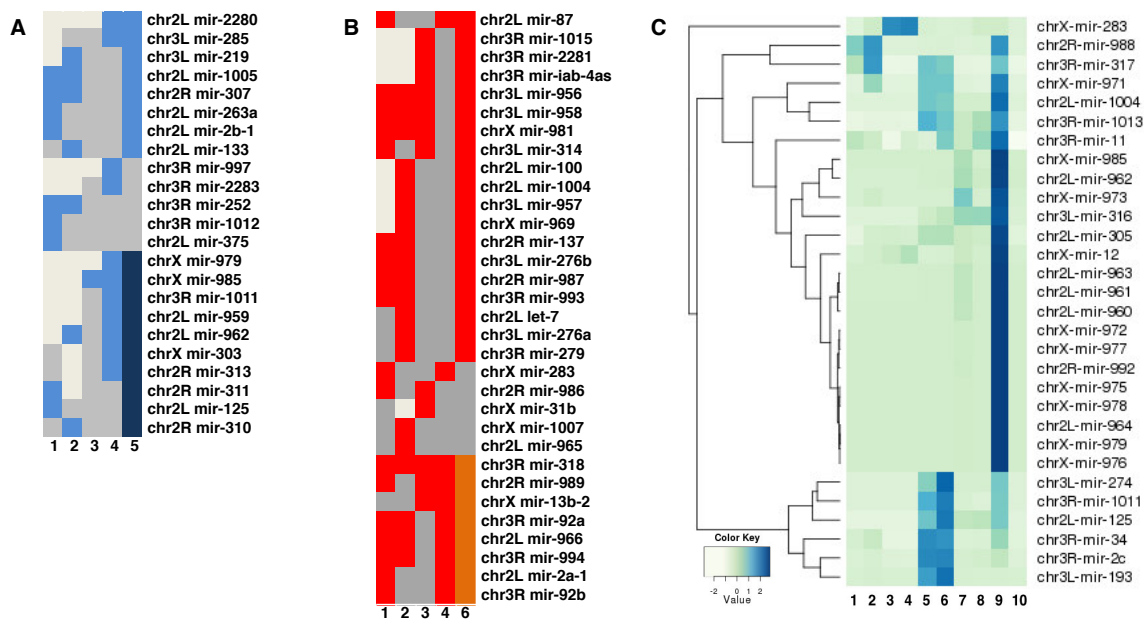


Figure S2: Male-enriched, female-enriched and X-linked testis-enriched miRNAs. (A) 23 miRNAs enriched in male somatic tissues in pairwise comparisons of S2 vs. Kc cells (1), male vs. female salivary glands (2), heads (3), and decapitated body (4). Colors indicate male-enriched miRNAs (light blue), miRNAs present at similar levels in both sexes (grey), poorly expressed miRNAs (white) and whether these miRNAs are more abundant in the male body (light blue) or testis (dark blue) in (5). (B) 32 female-enriched miRNAs in somatic tissues. Colors indicate female-enriched miRNAs (red), miRNAs present at similar levels in both sexes (grey), poorly expressed miRNAs (white) in somatic tissues [tissues (1) to (4) as in (A)], and whether these miRNAs are more abundant in the female body (red) or ovary (orange) in (6). (C) Relative abundance across all sexed tissues of the 30 miRNAs enriched exclusively in testis compared to the male body and not enriched in ovaries in females. 11 of the 30 testis-enriched miRNAs reside on the X chromosome. These miRNAs are highly and almost exclusively expressed in testis. S2 cells (1), Kc cells (2), male (3) and female (4) salivary glands, heads [male (5), female (6)], body [male (7), female (8)], testis (9), ovary (10).

TABLE S1: PCR primers used in this study

2S rRNA depletion:

5'-AGTCTTACAACCCTCAACCATATGTAGTCCAAGCAGCACT-3'

qPCR (miScript assay):

bantam-fwd	5'-GAGATCATTTTGAAGCTGATT-3'	
miR-12-fwd	5'-GAGTATTACATCAGGTAAGT-3'	
mir-13b-1-2-fwd	5'-TATCACAGCCATTTTGACGAGT-3'	
mir-13a-fwd	5'-TATCACAGCCATTTTGATGAGT-3'	
mir-283-fwd	5'-TAAATATCAGCTGGTAATTCT-3'	
mir-304-fwd	5'-AATCTCAATTTGTAAATGTGAG-3'	
mir-210-fwd	5'-TTGTGCGTGTGACAGCGGCTA-3'	
mir-iab-4-5p-fwd	5'-ACGTATACTGAATGTATCCTGA-3'	
mir-iab-4-3p-fwd	5'-GTATACCTTCAGTATACGTAAC-3'	
mir-318-fwd	5'-TCACTGGGCTTTGTTTATCTCA-3'	
mir-985-fwd	5'-CAAATGTTCCAATGGTCGGGCA-3'	
mir-979-fwd	5'-TTCCTTCCCGAACTCAGGCTAA-3'	
mir-981-fwd	5'-TTCGTTGTGCGACGAAACCTGCA-3'	
mir-977-fwd	5'-TGAGATATTCACGTTGTCTAA-3'	
mir-285-fwd	5'-TAGCACCATTTCGAAATCAGTGC-3'	
mir-969-fwd	5'-GAGTTCCACTAAGCAAGTTTT-3'	
mir-972-fwd	5'-TGTACAATACGAATATTTAGGC-3'	
mir-978-fwd	5'-TGTCCAGTGCCGTAAATTGCAG-3'	
mir-314-fwd	5'-TATTCGAGCCAATAAGTTCGG-3'	
mir-100-fwd	5'-AACCCGTAAATCCGAACCTTGTG-3'	
mir-137-Fwd	5'-TATTGCTTGAGAATACACGTAG-3'	
mir-989-fwd	5'-ATGTGATGTGACGTAGTGGAAC-3'	
mir-1013-fwd	5'-AATAAAAGTATGCCGAACCTCG-3'	
mir-Spike-fwd	5'-CTCAGGATGGCGGAGCGGTGT-3'	external reference
U6snRNA-fwd	5'-ATTGGAACGATACAGAGAAGATTAG-3'	reference
Dspt-4-fwd	5'-TTGACGCGATACCCAAGGAT-3'	reference
Dspt4-rev	5'-CTAGTGTGATCATAGACATTGTCCTTGTT-3'	

qPCR on sex-specific transcripts:

RpL32-fwd	5'-AAGATGACCATCCGCCAGC-3'	endogenous control
RpL32-rev	5'-GTCGATACCCCTGGGCTTGC-3'	
Esg-fwd	5'-CGCCCATGAGATCTGAAATC-3'	
Esg rev	5'-GGTCTTGTCAATCCTTGC-3'	(Chau et al. 2009)
DsxM fwd	5'-TCCTTGGGAGCTGATGCCAC-3'	
DsxM rev	5'-GGCTACAGTGCGATTTATT-3'	
Yp1-fwd	5'-TGAGCGTCTGGAGAACATGAA-3'	
Yp1-rev	5'-GCGACAGGTGGTAGACTTGCT-3'	
tra1-fwd	5'-GGAACCCAGCATCGAGATTC-3'	
tra1-rev	5'-ATCGCCCATGGTATTCTCTTTC-3'	
Sxl-fwd	5'-ACAACGACAGCAGCAGGCCA-3'	
Sxl-rev	5'-TTGTAACACGACGCGACGAT-3'	(Hashiyama et al. 2011)

TABLE S2: Late embryo-derived Lymphoid S2 (male) and Kc (female) cells biased miRNAs

S2 biased

chrom	miRNA	S2 reads	Kc reads	M/M+F	F/M+F	Sum reads	% miRNA
chr3R	dme-mir-252	13294	205	0.98479	0.01521	13499	1.1771
chr2R	dme-mir-307	932	33	0.96584	0.03416	965	0.0841
chr2L	dme-mir-263a	66	4	0.93623	0.06377	70	0.0061
chrX	dme-mir-980	1534	453	0.77219	0.22781	1987	0.1732
chr3L	dme-mir-282	13543	4622	0.74557	0.25443	18165	1.5839
chr2R	dme-mir-311	8	3	0.72746	0.27254	11	0.001
chr3R	dme-mir-1012	164	63	0.72266	0.27734	227	0.0198
chr2L	dme-mir-2b-1	498	207	0.70658	0.29342	705	0.0615
chr2L	dme-mir-125	10	4	0.68986	0.31014	14	0.0013
chr2R	dme-mir-286	43	21	0.67209	0.32791	64	0.0056

Kc biased

chrom	miRNA	S2	Kc reads	M/M+F	F/M+F	Sum reads	% miRNA
chrX	dme-mir-971	0	52	0	1	52	0.0046
chrX	dme-mir-973	0	12	0	1	12	0.001
chrX	dme-mir-982	0	16	0	1	16	0.0014
chrX	dme-mir-981	1	1427	0.00070	0.99930	1428	0.1245
chr3R	dme-mir-1000	1	1299	0.00077	0.99923	1300	0.1134
chr3R	dme-mir-92a	13	2215	0.00584	0.99416	2228	0.1943
chr3R	dme-mir-1010	1	106	0.00931	0.99069	107	0.0094
chr2R	dme-mir-989	3	237	0.01251	0.98749	240	0.0209
chrX	dme-mir-977	1	66	0.01494	0.98506	67	0.0058
chr3L	dme-mir-276b	5	187	0.02600	0.97400	192	0.0168
chrX	dme-mir-304	34	1260	0.02627	0.97373	1294	0.1129
chr2L	dme-mir-932	5	177	0.02750	0.97250	182	0.0159
chr2R	dme-mir-278	47	1647	0.02775	0.97225	1694	0.1477
chr3R	dme-mir-92b	20	670	0.02899	0.97101	690	0.0602
chr3L	dme-mir-193	3	96	0.03033	0.96967	99	0.0086
chrX	dme-mir-283	48	1394	0.03330	0.96670	1442	0.1257
chr3L	dme-mir-958	1	28	0.03393	0.96607	29	0.0026
chr3R	dme-mir-10	1	27	0.03575	0.96425	28	0.0024
chrX	dme-mir-12	415	10569	0.03778	0.96222	10984	0.9578
chr2R	dme-mir-986	3	43	0.06457	0.93543	46	0.0041
chr2L	dme-mir-124	8	94	0.07812	0.92188	102	0.0089
chr4	dme-mir-954	11	91	0.10741	0.89259	102	0.0089
chr3R	dme-mir-994	5	40	0.10998	0.89002	45	0.004
chr2R	dme-mir-8	4003	27812	0.12582	0.87418	31815	2.7742
chr3R	dme-mir-318	13	90	0.12632	0.87368	103	0.009
chr2L	dme-mir-9b	2463	11885	0.17166	0.82834	14348	1.2511
chr2L	dme-mir-2a-2	2015	9699	0.17202	0.82798	11714	1.0214
chrX	dme-mir-984	25	102	0.19700	0.80300	127	0.0111
chr2L	dme-mir-966	15	58	0.20424	0.79576	73	0.0064
chr2L	dme-mir-2b-2	431	1648	0.20727	0.79273	2079	0.1813
chr2L	dme-mir-2a	7839	29779	0.20838	0.79162	37618	3.2803
chr2R	dme-mir-31a	5	18	0.21756	0.78244	23	0.002

chr2L	dme-mir-1	23	82	0.21817	0.78183	105	0.0092
chr3R	dme-mir-13a	25	85	0.22641	0.77359	110	0.0096
chr3L	dme-mir-276	4524	15417	0.22687	0.77313	19941	1.7389
chr2L	dme-mir-305	3321	10310	0.24364	0.75636	13631	1.1886
chr2R	dme-mir-312	3	9	0.25018	0.74982	12	0.001
chr2L	dme-mir-9c	1896	5648	0.25132	0.74868	7544	0.6578
chr2R	dme-mir-1008	94	262	0.26386	0.73614	356	0.0311
chr2L	dme-mir-275	461	1247	0.26994	0.73006	1708	0.1489
chr3L	dme-mir-190	171	462	0.27033	0.72967	633	0.0552
chr2L	dme-mir-79	2043	5420	0.27374	0.72626	7463	0.6508
chr3L	dme-mir-9a	49	124	0.28262	0.71738	173	0.0151
chr2L	dme-mir-1006	58	145	0.28521	0.71479	203	0.0177
chr2L	dme-mir-306	2500	6128	0.28977	0.71023	8628	0.7523
chr3R	dme-mir-317	9157	21083	0.30281	0.69719	30240	2.6369
chr3R	dme-mir-999	247	560	0.30590	0.69410	807	0.0704
chr2R	dme-mir-1009	4	9	0.30790	0.69210	13	0.0011
chrX	dme-mir-983	6	13	0.30790	0.69210	19	0.0017
chr2L	dme-mir-2a-1	173	388	0.30831	0.69169	561	0.0489
chr3R	dme-mir-2c	9	19	0.31600	0.68400	28	0.0025
chr3L	dme-mir-33	1927	4040	0.32294	0.67706	5967	0.5203
chr2L	dme-mir-2b	9981	20837	0.32387	0.67613	30818	2.6874
chr2R	dme-mir-184	54062	109778	0.32997	0.67003	163840	14.2868

At least 10 normalized reads in the summed normalized reads were required. S2: Male (M); Kc: Female (F).

A ratio (F/M+F) >=0.66 is female biased. A ratio (M/M+F) >=0.66 is male biased.

TABLE S3: Male and female biased miRNAs in L3 larval salivary glands

Male biased

chrom	miRNA	Male S. Gland reads	Female S. Gland reads	M/M+F	F/M+F	Sum Reads	% miRNA
chr2L	dme-mir-275	21773	2588	0.89376	0.10624	24361	2.63097
chr2R	dme-mir-1009	8	2	0.80000	0.20000	10	0.00108
chr2R	dme-mir-278	1275	526	0.70797	0.29203	1801	0.19453
chr2L	dme-mir-133	10	4	0.70588	0.29412	14	0.00147
chr2L	dme-mir-1005	26	11	0.69945	0.30055	37	0.00395
chr3R	dme-mir-252	1330	644	0.67369	0.32631	1974	0.21315

Female biased

chrom	miRNA	Male S. Gland reads	Female S. Gland reads	M/M+F	F/M+F	Sum Reads	% miRNA
chr2L	dme-mir-100	2	10	0.13793	0.86207	12	0.00125
chr3L	dme-mir-282	6635	31936	0.17202	0.82798	38571	4.1657
chr2L	dme-let-7	48	219	0.17978	0.82022	267	0.02884
chr3R	dme-mir-279	514	1492	0.25608	0.74392	2006	0.21661
chr2L	dme-mir-965	210	567	0.26989	0.73011	777	0.08387
chr2R	dme-mir-987	14	36	0.28571	0.71429	50	0.00544
chr2L	dme-mir-305-as	3	7	0.31373	0.68627	10	0.0011
chr3R	dme-mir-92a	3	7	0.31373	0.68627	10	0.0011
chr3L	dme-mir-957	3	7	0.31373	0.68627	10	0.0011
chr2R	dme-mir-307-as	8	17	0.32000	0.68000	25	0.0027
chr3L	dme-mir-276a	1853	3728	0.33200	0.66800	5581	0.60273
chr3L	dme-mir-285	19	38	0.33566	0.66434	57	0.00618

At least 10 normalized reads in the summed normalized reads were required. M: male ; F: female.

A ratio (F/M+F) >=0.66 is female biased in salivary glands (S. glands). A ratio(M/M+F) >=0.66 is male biased.

TABLE S4: Male and female biased miRNAs in adult heads

Male biased

chrom	miRNA	Male Head reads	Female Head reads	M/M+F	F/M+F	Sum Reads	% miRNA
chrX	dme-mir-974	9	2	0.81405	0.18595	11	0.000247
chr3L	dme-mir-190	2189	634	0.77540	0.22460	2823	0.06472
chr2L	dme-mir-305-as	21	8	0.72426	0.27574	29	0.000665
chr3L	dme-mir-276	119752	58112	0.67328	0.32672	177864	4.077941
chr2R	dme-mir-1008	208	104	0.66707	0.33293	312	0.007162

Female biased

chrom	miRNA	Male Head reads	Female Head reads	M/M+F	F/M+F	Sum Reads	% miRNA
chr3L	dme-mir-958	5	29	0.15336	0.84664	34	0.000785
chrX	dme-mir-31b	12	44	0.21788	0.78212	56	0.00129
chr2L	dme-mir-964	12	41	0.23015	0.76985	53	0.001221
chr3L	dme-mir-956	7	20	0.25938	0.74062	27	0.000619
chrX	dme-mir-980	611	1464	0.29450	0.70550	2075	0.047577
chrX	dme-mir-981	404	968	0.29472	0.70528	1372	0.031468
chr3L	dme-mir-274	24301	55708	0.30373	0.69627	80009	1.834398
chr3L	dme-mir-314	32	72	0.30448	0.69552	104	0.002373
chr2L	dme-mir-961	9	20	0.30448	0.69552	29	0.000659
chr2L	dme-mir-963	9	20	0.30448	0.69552	29	0.000659
chr3R	dme-mir-284	907	2009	0.31105	0.68895	2916	0.066857
chr2R	dme-mir-286	7	15	0.31831	0.68169	22	0.000504
chr2L	dme-mir-275	1170	2503	0.31849	0.68151	3673	0.084205
chrX	dme-mir-13b-2	47	101	0.31885	0.68115	148	0.0034
chr2R	dme-mir-986	475	1006	0.32052	0.67948	1481	0.033945
chrX	dme-mir-210	54115	106957	0.33597	0.66403	161072	3.692947
chr3R	dme-mir-11	10872	21450	0.33637	0.66363	32322	0.741065
chr2L	dme-mir-960	53	103	0.33776	0.66224	156	0.003566
chr2L	dme-mir-133	8468	16473	0.33953	0.66047	24941	0.571834

At least 10 normalized reads in the summed normalized reads were required.

A ratio (F/M+F) ≥ 0.66 is female biased in the head. A ratio (M/M+F) ≥ 0.66 is male biased. F: female; M: Male.

TABLE S5: Male vs. female biased miRNAs in the adult body

Male body biased

chrom	miRNA	Male Body reads	Female Body reads	M/M+F	F/M+F	Sum Reads	% miRNA
chrX	dme-mir-972	61	0	1	0	61	0.001355886
chrX	dme-mir-975	33	0	1	0	33	0.000733512
chrX	dme-mir-977	680	0	1	0	680	0.015114796
chrX	dme-mir-979	21	0	1	0	21	0.00046678
chr3R	dme-mir-997	184	0	1	0	184	0.004089886
chrX	dme-mir-978	241	3	0.98597	0.01403	244	0.00543307
chrX	dme-mir-974	236	3	0.98568	0.01432	239	0.005321932
chrX	dme-mir-976	380	7	0.98227	0.01773	387	0.008598921
chr2L	dme-mir-959	478	10	0.97894	0.02106	488	0.010853439
chrX	dme-mir-303	142	3	0.97642	0.02358	145	0.003232534
chrX	dme-mir-985	214	7	0.96895	0.03105	221	0.004909133
chrX	dme-mir-983	724	24	0.96791	0.03209	748	0.016626275
chrX	dme-mir-984	551	24	0.95826	0.04174	575	0.012780893
chrX	dme-mir-973	76	3	0.95683	0.04317	79	0.00176551
chr2L	dme-mir-963	368	21	0.94706	0.05294	389	0.008637026
chr2R	dme-mir-991	120	7	0.94595	0.05405	127	0.002819735
chr2L	dme-mir-960	1717	117	0.93642	0.06358	1834	0.040755964
chr2R	dme-mir-992	45	3	0.92920	0.07080	48	0.001076453
chr2L	dme-mir-964	437	34	0.92725	0.07275	471	0.010475569
chrX	dme-mir-982	118	10	0.91982	0.08018	128	0.002851489
chr2L	dme-mir-961	177	17	0.91170	0.08830	194	0.004315337
chr3L	dme-mir-285	76	14	0.84713	0.15287	90	0.001994137
chr2R	dme-mir-1009	38	10	0.78698	0.21302	48	0.001073277
chr3L	dme-mir-193	12	3	0.77778	0.22222	15	0.000342941
chr2L	dme-mir-962	401	134	0.74993	0.25007	535	0.011885434
chrX	dme-mir-304	17186	7227	0.70396	0.29604	24413	0.542652738
chrX	dme-mir-12	21306	9603	0.68930	0.31070	30909	0.687043433
chr2R	dme-mir-313	59	27	0.68264	0.31736	86	0.001921103

Female body biased

chrom	miRNA	Male Body reads	Female Body reads	M/M+F	F/M+F	Sum Reads	% miRNA
chr2R	dme-mir-989	44	45010	0.00098	0.99902	45054	1.001449337
chr3R	dme-mir-318	4	261	0.01512	0.98488	265	0.005880792
chr3R	dme-mir-994	4	261	0.01512	0.98488	265	0.005880792
chr3R	dme-mir-92b	42	233	0.15265	0.84735	275	0.006115771
chr2L	dme-mir-966	5	21	0.19553	0.80447	26	0.000568392
chr2L	dme-mir-2a-1	21	75	0.21778	0.78222	96	0.002143378
chr3L	dme-mir-190	162	579	0.21850	0.78150	741	0.016480193
chr3L	dme-mir-276	47955	128270	0.27212	0.72788	176225	3.917056396
chr2L	dme-mir-275	1122	2616	0.30016	0.69984	3738	0.083086855
chr3R	dme-mir-92a	254	579	0.30477	0.69523	833	0.018525136
chrX	dme-mir-283	577	1245	0.31676	0.68324	1822	0.040489204
chrX	dme-mir-13b-2	92	189	0.32790	0.67210	281	0.006236436

chr2L	dme-mir-87	908	1834	0.33111	0.66889	2742	0.060954495
-------	------------	-----	------	---------	---------	-------------	-------------

At least 10 normalized reads in the summed normalized reads were required.

A ratio $(F/M+F) \geq 0.66$ is female biased. A ratio $(M/M+F) \geq 0.66$ is male biased. F: female; M: male.

TABLE S6: Testis and Ovary biased miRNAs

Testis biased

chrom	miRNA	Testes reads	Ovary reads	T/Ov+T	Ov/T+Ov	Sum Reads	% miRNA
chr2L	dme-mir-1004	144	0	1	0	144	0.01472903
chr2R	dme-mir-137	38	0	1	0	38	0.003886827
chrX	dme-mir-210	10	0	1	0	10	0.001022849
chr3L	dme-mir-263b	13	0	1	0	13	0.001329704
chr3L	dme-mir-315	12	0	1	0	12	0.001227419
chr2L	dme-mir-375	1491	0	1	0	1491	0.152506835
chrX	dme-mir-971	33	0	1	0	33	0.003375403
chrX	dme-mir-972	961	0	1	0	961	0.098295821
chrX	dme-mir-973	51	0	1	0	51	0.005216532
chrX	dme-mir-974	82	0	1	0	82	0.008387364
chrX	dme-mir-975	2134	0	1	0	2134	0.218276047
chrX	dme-mir-976	7525	0	1	0	7525	0.76969412
chrX	dme-mir-977	8100	0	1	0	8100	0.828507956
chrX	dme-mir-978	8457	0	1	0	8457	0.865023677
chrX	dme-mir-979	497	0	1	0	497	0.050835612
chrX	dme-mir-981	16	0	1	0	16	0.001636559
chr2R	dme-mir-992	395	0	1	0	395	0.040402548
chr3R	dme-mir-997	59	0	1	0	59	0.006034811
chr3R	dme-mir-iab-4as	16	0	1	0	16	0.001636559
chr2L	dme-mir-959	17252	10	0.99943	0.00057	17262	1.765620246
chr2L	dme-mir-964	10115	12	0.99879	0.00121	10127	1.035862826
chr3L	dme-mir-274	7928	12	0.99846	0.00154	7940	0.812165678
chr2L	dme-mir-963	926	2	0.99737	0.00263	928	0.094965994
chr2L	dme-mir-960	5436	27	0.99508	0.00492	5463	0.558772501
chrX	dme-mir-985	321	2	0.99244	0.00756	323	0.033083609
chr3L	dme-mir-9a	6846	98	0.98591	0.01409	6944	0.710248489
chr2L	dme-mir-124	151	2	0.98406	0.01594	153	0.015695171
chr3R	dme-mir-277	9542	213	0.97819	0.02181	9755	0.997765528
chr2L	dme-mir-961	477	12	0.97501	0.02499	489	0.050040643
chr3R	dme-mir-1013	54	2	0.95667	0.04333	56	0.005773532
chr3R	dme-mir-252	990	51	0.95068	0.04932	1041	0.106515149
chr2L	dme-mir-133	38	2	0.93953	0.06047	40	0.004136973
chr2R	dme-mir-991	127	10	0.92848	0.07152	137	0.01399077
chr2R	dme-mir-988	6587	523	0.92640	0.07360	7110	0.727282088
chr2R	dme-mir-310	3356	289	0.92082	0.07918	3645	0.372785458
chrX	dme-mir-12	62228	5576	0.91776	0.08224	67804	6.935319591
chr2L	dme-mir-932	45	5	0.90196	0.09804	50	0.005103114
chr3R	dme-mir-1010	168	20	0.89569	0.10431	188	0.019185036
chr2R	dme-mir-278	2426	286	0.89450	0.10550	2712	0.277410324
chr3R	dme-mir-2c	19	2	0.88596	0.11404	21	0.00219356
chrX	dme-mir-983	6732	1010	0.86954	0.13046	7742	0.791892449
chr2R	dme-mir-311	3582	582	0.86022	0.13978	4164	0.425919368
chr2L	dme-mir-962	471	81	0.85372	0.14628	552	0.05643102
chr2L	dme-mir-125	3331	614	0.84439	0.15561	3945	0.403497747

chr3L	dme-mir-316	4417	814	0.84433	0.15567	5231	0.535091153
chr2L	dme-let-7	11559	2179	0.84139	0.15861	13738	1.405191589
chr2R	dme-mir-1008	11	2	0.81811	0.18189	13	0.00137528
chr3R	dme-mir-999	673	179	0.79034	0.20966	852	0.087098415
chr3R	dme-mir-317	4489	1294	0.77628	0.22372	5783	0.591484276
chr2L	dme-mir-305	18583	6588	0.73826	0.26174	25171	2.574654122
chr3L	dme-mir-956	54	22	0.71043	0.28957	76	0.0077747
chr2L	dme-mir-100	226	93	0.70861	0.29139	319	0.032621941
chr3R	dme-mir-13a	29	12	0.70341	0.29659	41	0.004216993
chrX	dme-mir-31b	875	416	0.67790	0.32210	1291	0.132024129

Ovary biased

chrom	miRNA	Testes reads	Ovary reads	T/Ov+T	Ov/T+Ov	Sum Reads	% miRNA
chr2R	dme-mir-989	6	111853	0.00005	0.99995	111859	11.44153945
chr3R	dme-mir-318	20	44135	0.00045	0.99955	44155	4.516429825
chr3R	dme-mir-994	19	18298	0.00104	0.99896	18317	1.873535481
chr2L	dme-mir-2b-1	2	460	0.00433	0.99567	462	0.04723201
chrX	dme-mir-13b-2	1	218	0.00457	0.99543	219	0.022365275
chr3R	dme-mir-996	348	36033	0.00957	0.99043	36381	3.72124572
chr3L	dme-bantam	687	69609	0.00977	0.99023	70296	7.190174187
chr2R	dme-mir-184	540	38992	0.01366	0.98634	39532	4.043561038
chr2R	dme-mir-1009	5	220	0.02221	0.97779	225	0.023024561
chr2L	dme-mir-965	9	355	0.02475	0.97525	364	0.037191728
chr2L	dme-mir-79	219	8506	0.02510	0.97490	8725	0.892408047
chr2L	dme-mir-263a	245	8899	0.02679	0.97321	9144	0.935340954
chr3L	dme-mir-33	166	5092	0.03157	0.96843	5258	0.537783186
chr2L	dme-mir-2b-2	40	1091	0.03538	0.96462	1131	0.115656495
chr2R	dme-mir-308	30	790	0.03659	0.96341	820	0.083865693
chr2L	dme-mir-275	605	15923	0.03660	0.96340	16528	1.690582725
chr3L	dme-mir-276	123	3194	0.03708	0.96292	3317	0.33927167
chr2R	dme-mir-281-2	21	430	0.04652	0.95348	451	0.046173672
chr3R	dme-mir-995	228	4654	0.04670	0.95330	4882	0.499348725
chr2L	dme-mir-1	241	3788	0.05981	0.94019	4029	0.41212676
chr2R	dme-mir-307	42	599	0.06551	0.93449	641	0.065581727
chr3R	dme-mir-998	84	986	0.07854	0.92146	1070	0.109400756
chr2L	dme-mir-87	12	139	0.07926	0.92074	151	0.015485739
chr2L	dme-mir-2a-1	13	149	0.08016	0.91984	162	0.016588608
chr2L	dme-mir-1005	3	34	0.08056	0.91944	37	0.003808898
chr2R	dme-mir-281-1	143	1277	0.10073	0.89927	1420	0.145202936
chr2L	dme-mir-966	6	51	0.10461	0.89539	57	0.005866775
chr2L	dme-mir-2a-2	112	829	0.11902	0.88098	941	0.096255393
chr3R	dme-mir-929	4	29	0.11995	0.88005	33	0.003410891
chr2R	dme-mir-313	370	1538	0.19389	0.80611	1908	0.195187234
chrX	dme-mir-1007	6	24	0.19701	0.80299	30	0.003115169
chr3R	dme-mir-284	16	56	0.22146	0.77854	72	0.007389916
chr2R	dme-mir-7	863	2981	0.22450	0.77550	3844	0.393199821
chr3L	dme-mir-190	13	44	0.22799	0.77201	57	0.005832331
chr2L	dme-mir-2b	6058	20095	0.23163	0.76837	26153	2.675091471

chr2L	dme-mir-2a	14216	47031	0.23211	0.76789	61247	6.264639548
chrX	dme-mir-304	556	1817	0.23430	0.76570	2373	0.24272887
chr2L	dme-mir-9c	2050	5715	0.26399	0.73601	7765	0.794275219
chr2L	dme-mir-306	951	2472	0.27779	0.72221	3423	0.350170536
chr3R	dme-mir-13b	5212	13392	0.28015	0.71985	18604	1.902908343
chr2R	dme-mir-986	309	736	0.29566	0.70434	1045	0.106899978
chr3R	dme-mir-1012	46	98	0.31984	0.68016	144	0.014710945
chr2R	dme-mir-312	1704	3546	0.32457	0.67543	5250	0.537005167
chr2L	dme-mir-9b	6727	13372	0.33469	0.66531	20099	2.055868849

At least 10 normalized reads in the summed normalized reads in male and female gonads are required.

A ratio (Testis/Ovary+Testis) ≥ 0.66 is Testis biased. A ratio(Ovary/Ovary +Testis) ≥ 0.66 is Ovary biased

T: Testis; Ov: Ovaries

TABLE S7: miRNAs with testis vs. male body biases

Male Body (male somatic tissues) biased miRNAs

chrom	miRNA	Male Body reads	Testis reads	BM/BM+T	Testis/BM+T	Sum reads	% miRNA
chr3R	dme-mir-1014	248	0	1	0	248	0.007666282
chr3L	dme-mir-285	76	0	1	0	76	0.002349344
chr2R	dme-mir-5	14	0	1	0	14	0.000432774
chrX	dme-mir-927	41	0	1	0	41	0.001267409
chr3L	dme-mir-957	839	0	1	0	839	0.025935526
chrX	dme-mir-969	27	0	1	0	27	0.000834636
chr2L	dme-mir-1	496888	844	0.99831	0.00169	497732	15.38608851
chr3R	dme-mir-993	1448	4	0.99759	0.00241	1452	0.044869387
chr3R	dme-mir-1000	875	4	0.99602	0.00398	879	0.027156567
chr3L	dme-mir-958	7379	32	0.99575	0.00425	7411	0.229076539
chr3R	dme-mir-929	1810	14	0.99232	0.00768	1824	0.056384267
chr3L	dme-mir-314	11627	102	0.99135	0.00865	11729	0.362556399
chr3L	dme-mir-276	47955	431	0.99110	0.00890	48386	1.495713233
chr3L	dme-bantam	244113	2405	0.99025	0.00975	246518	7.620454209
chr2L	dme-mir-2b-1	623	7	0.98889	0.01111	630	0.019474829
chr2R	dme-mir-987	803	11	0.98709	0.01291	814	0.025147259
chr2R	dme-mir-281-2	5100	74	0.98579	0.01421	5174	0.159925441
chr3L	dme-mir-276b	530	11	0.98057	0.01943	541	0.016708167
chr2L	dme-mir-965	1129	32	0.97286	0.02714	1161	0.035873872
chr2R	dme-mir-281-1	17602	501	0.97235	0.02765	18103	0.559592219
chr3R	dme-mir-10	19132	599	0.96967	0.03033	19731	0.609917652
chrX	dme-mir-13b-2	92	4	0.96335	0.03665	96	0.002952137
chr3L	dme-mir-263b	1144	46	0.96175	0.03825	1190	0.036770333
chr3R	dme-mir-996	29997	1218	0.96098	0.03902	31215	0.964931435
chr3L	dme-mir-219	84	4	0.96000	0.04000	88	0.002704837
chr3L	dme-mir-956	4342	189	0.95829	0.04171	4531	0.140064211
chr2L	dme-mir-87	908	42	0.95579	0.04421	950	0.029366807
chr2R	dme-mir-308	1864	105	0.94667	0.05333	1969	0.060866571
chr3L	dme-mir-33	9633	581	0.94312	0.05688	10214	0.315739544
chr2L	dme-mir-79	12143	767	0.94063	0.05937	12910	0.399063995
chr3R	dme-mir-1001	106	7	0.93805	0.06195	113	0.003493104
chr2R	dme-mir-307	2063	147	0.93348	0.06652	2210	0.068316467
chr2L	dme-mir-263a	11829	858	0.93241	0.06759	12687	0.392170527
chrX	dme-mir-210	409	35	0.92117	0.07883	444	0.013725119
chr2L	dme-mir-1005	122	11	0.92075	0.07925	133	0.004095897
chr3L	dme-mir-276a	90583	7868	0.92008	0.07992	98451	3.043359558
chr3R	dme-mir-284	523	56	0.90328	0.09672	579	0.017898297
chr3R	dme-mir-1015	62	7	0.89855	0.10145	69	0.002132958
chrX	dme-mir-304	17186	1946	0.89829	0.10171	19132	0.591416607
chr2R	dme-mir-184	15336	1890	0.89028	0.10972	17226	0.53249752
chr2L	dme-mir-133	1065	133	0.88898	0.11102	1198	0.037033091
chr2L	dme-mir-1006	415	53	0.88770	0.11230	468	0.014451561
chr3R	dme-mir-13a	797	102	0.88703	0.11297	899	0.027774818
chr3R	dme-mir-1017	25	4	0.87719	0.12281	29	0.000881004

chr2R	dme-mir-31a	24842	3969	0.86224	0.13776	28811	0.890618047
chrX	dme-mir-980	2995	539	0.84748	0.15252	3534	0.109244532
chr2L	dme-mir-124	2863	529	0.84417	0.15583	3392	0.104839511
chr2L	dme-mir-2b-2	615	140	0.81457	0.18543	755	0.023338886
chr3R	dme-mir-iab-4	94	25	0.79325	0.20675	119	0.003663123
chr3R	dme-mir-998	1074	294	0.78509	0.21491	1368	0.042288209
chr3L	dme-mir-190	162	46	0.78072	0.21928	208	0.00641433
chr2R	dme-mir-1008	106	39	0.73356	0.26644	145	0.004466847
chr3R	dme-mir-279	14571	5439	0.72819	0.27181	20010	0.618557825
chr2L	dme-mir-2a-2	1047	392	0.72759	0.27241	1439	0.044482994
chr3R	dme-mir-iab-4as	144	56	0.72000	0.28000	200	0.006182487
chr2R	dme-mir-137	341	133	0.71941	0.28059	474	0.014652494
chr3L	dme-mir-955	59	25	0.70659	0.29341	84	0.002581188
chr3R	dme-mir-277	76053	33397	0.69487	0.30513	109450	3.383366128
chr2R	dme-mir-8	447346	198170	0.69301	0.30699	645516	19.95447212
chrX	dme-mir-1007	47	21	0.69118	0.30882	68	0.002102046
chr2R	dme-mir-1009	38	18	0.68468	0.31532	56	0.00171564
chr2R	dme-mir-989	44	21	0.67692	0.32308	65	0.002009308

Testis enriched miRNAs

chrom	miRNA	Male Body reads	Testis reads	BM/BM+T	Testis/BM+T	Sum Reads	% miRNA
chrX	dme-mir-975	33	7469	0.00440	0.99560	7502	0.231905256
chr2R	dme-mir-310	55	11746	0.00466	0.99534	11801	0.36479791
chr2R	dme-mir-311	68	12537	0.00539	0.99461	12605	0.389651525
chr2L	dme-mir-959	478	60382	0.00785	0.99215	60860	1.881332152
chrX	dme-mir-978	241	29600	0.00808	0.99192	29841	0.922443182
chrX	dme-mir-979	21	1740	0.01193	0.98807	1761	0.054421381
chr2L	dme-mir-964	437	35403	0.01219	0.98781	35840	1.107887009
chrX	dme-mir-976	380	26338	0.01422	0.98578	26718	0.825903573
chr2R	dme-mir-312	95	5964	0.01568	0.98432	6059	0.187298577
chr3R	dme-mir-92b	42	2615	0.01581	0.98419	2657	0.082118942
chrX	dme-mir-972	61	3364	0.01781	0.98219	3425	0.105859709
chrX	dme-mir-977	680	28350	0.02342	0.97658	29030	0.897388622
chrX	dme-mir-983	724	23562	0.02981	0.97019	24286	0.750739922
chr2R	dme-mir-992	45	1383	0.03152	0.96848	1428	0.044127532
chrX	dme-mir-971	4	116	0.03347	0.96653	120	0.003694039
chr2R	dme-mir-988	876	23055	0.03661	0.96339	23931	0.739750538
chr2R	dme-mir-313	59	1295	0.04357	0.95643	1354	0.041855466
chr3R	dme-mir-92a	254	4984	0.04849	0.95151	5238	0.161919445
chr3R	dme-mir-318	4	70	0.05405	0.94595	74	0.002287522
chr3R	dme-mir-994	4	67	0.05674	0.94326	71	0.002179328
chr2R	dme-mir-3	2	28	0.06667	0.93333	30	0.000927374
chrX	dme-mir-984	551	7704	0.06675	0.93325	8255	0.255166864
chr2L	dme-mir-1004	44	504	0.08029	0.91971	548	0.016940025
chr2L	dme-mir-960	1717	19026	0.08277	0.91723	20743	0.641217054
chr3R	dme-mir-1011	1	11	0.08696	0.91304	12	0.000355493
chrX	dme-mir-12	21306	217798	0.08911	0.91089	239104	7.391291592
chr2L	dme-mir-961	177	1670	0.09586	0.90414	1847	0.057079847

chr2L	dme-mir-963	368	3241	0.10197	0.89803	3609	0.111563048
chr3L	dme-mir-274	3593	27748	0.11464	0.88536	31341	0.968827221
chr3R	dme-mir-317	2370	15712	0.13107	0.86893	18082	0.558943528
chr2L	dme-mir-9b	4263	23545	0.15330	0.84670	27808	0.859598032
chrX	dme-mir-985	214	1124	0.16000	0.84000	1338	0.041345405
chr2L	dme-mir-305	13965	65041	0.17676	0.82324	79006	2.442253734
chr4	dme-mir-954	50	217	0.18727	0.81273	267	0.008253625
chr3R	dme-mir-34	9383	40124	0.18953	0.81047	49507	1.530382746
chr2L	dme-mir-966	5	21	0.19231	0.80769	26	0.000803724
chr2L	dme-mir-962	401	1649	0.19566	0.80434	2050	0.063355069
chr2R	dme-mir-991	120	445	0.21258	0.78742	565	0.017450079
chr3R	dme-mir-1013	52	189	0.21577	0.78423	241	0.007449901
chrX	dme-mir-982	118	420	0.21933	0.78067	538	0.016630899
chr2L	dme-mir-306	1152	3329	0.25711	0.74289	4481	0.13850323
chr3L	dme-mir-316	5546	15460	0.26403	0.73597	21006	0.649331456
chrX	dme-mir-303	142	396	0.26419	0.73581	538	0.016615442
chr3R	dme-mir-2c	27	67	0.28877	0.71123	94	0.002890314
chrX	dme-mir-973	76	179	0.29862	0.70138	255	0.007867218
chr3R	dme-mir-11	14438	32372	0.30844	0.69156	46810	1.446996236
chr2L	dme-mir-125	5238	11659	0.31000	0.69000	16897	0.522312177
chrX	dme-mir-283	577	1257	0.31470	0.68530	1834	0.056677973
chr2L	dme-mir-2a-1	21	46	0.31579	0.68421	67	0.002055678
chr3L	dme-mir-193	12	25	0.32877	0.67123	37	0.001128304

At least 10 normalized reads in the summed normalized reads were required. A ratio (BodyM/BodyM+Testis) ≥ 0.66 is male body biased. A ratio (Testis/Body M+Testis) ≥ 0.66 is testis biased. BM: Body Male; T: testis

TABLE S8: Adult Female Body vs. Ovary biased miRNAs

Female Body (female somatic tissues) biased:

chrom	miRNA	Female Body reads	Ovary reads	BF/BF+Ov	BF/BF+Ov	Sum Reads	% miRNA
chr3R	dme-mir-1000	206	0	1	0	206	0.016796842
chr3R	dme-mir-1001	29	0	1	0	29	0.002364604
chr2L	dme-mir-1004	13	0	1	0	13	0.001059995
chr3R	dme-mir-1014	66	0	1	0	66	0.005381513
chr3R	dme-mir-1015	15	0	1	0	15	0.001223071
chr2R	dme-mir-137	80	0	1	0	80	0.006523046
chrX	dme-mir-210	121	0	1	0	121	0.009866106
chr3L	dme-mir-219	21	0	1	0	21	0.001712299
chr3L	dme-mir-263b	263	0	1	0	263	0.021444512
chr3L	dme-mir-276b	112	0	1	0	112	0.009132264
chr2L	dme-mir-375	811	0	1	0	811	0.066127374
chr3L	dme-mir-957	307	0	1	0	307	0.025032187
chr3L	dme-mir-958	2103	0	1	0	2103	0.171474559
chrX	dme-mir-981	19	0	1	0	19	0.001549223
chr2R	dme-mir-987	308	0	1	0	308	0.025113725
chr3R	dme-mir-993	314	0	1	0	314	0.025602954
chr3R	dme-mir-iab-4as	28	0	1	0	28	0.002283066
chr2L	dme-mir-124	470	2	0.99590	0.00410	472	0.038480513
chr2L	dme-mir-133	300	2	0.99360	0.00640	302	0.024619041
chr3L	dme-mir-314	4449	31	0.99310	0.00690	4480	0.365284793
chr3L	dme-mir-274	1179	10	0.99187	0.00813	1189	0.096921485
chr3R	dme-mir-277	19989	168	0.99166	0.00834	20157	1.643577423
chr3L	dme-mir-9a	8813	77	0.99130	0.00870	8890	0.724899812
chr3L	dme-mir-956	1393	17	0.98766	0.01234	1410	0.115001112
chr3R	dme-mir-10	6256	79	0.98749	0.01251	6335	0.51656459
chr2L	dme-mir-1	199357	2994	0.98520	0.01480	202351	16.4993386
chr3R	dme-mir-929	819	23	0.97246	0.02754	842	0.068671122
chr3R	dme-mir-252	1420	41	0.97221	0.02779	1461	0.119094084
chr3R	dme-mir-13a	202	10	0.95434	0.04566	212	0.017258791
chr2R	dme-mir-1008	36	2	0.94904	0.05096	38	0.003092991
chr2L	dme-mir-932	70	4	0.94766	0.05234	74	0.006022905
chr3R	dme-mir-iab-4	35	2	0.94766	0.05234	37	0.003011453
chr3L	dme-mir-276	37412	2525	0.93678	0.06322	39937	3.256354306
chr3L	dme-mir-955	26	2	0.93080	0.06920	28	0.00227761
chr2L	dme-mir-1006	101	8	0.92889	0.07111	109	0.008865826
chr3R	dme-mir-1013	24	2	0.92546	0.07454	26	0.002114534
chr3L	dme-mir-276a	31855	2710	0.92159	0.07841	34565	2.818378803
chr2R	dme-mir-278	2040	226	0.90020	0.09980	2266	0.184779232
chrX	dme-mir-980	908	106	0.89518	0.10482	1014	0.082705681
chr2R	dme-mir-31a	11038	1703	0.86633	0.13367	12741	1.038880662
chr3R	dme-mir-1010	92	15	0.85610	0.14390	107	0.008762464
chr3R	dme-mir-999	771	141	0.84529	0.15471	912	0.074372131
chr2R	dme-mir-281-1	5351	1009	0.84134	0.15866	6360	0.518587988
chr3R	dme-mir-2c	10	2	0.83801	0.16199	12	0.000973001

chr2R	dme-mir-281-2	1730	340	0.83566	0.16434	2070	0.168802027
chr2L	dme-mir-100	366	73	0.83285	0.16715	439	0.035832503
chr3L	dme-mir-190	169	35	0.82926	0.17074	204	0.016617099
chr2L	dme-mir-87	535	110	0.82922	0.17078	645	0.052607222
chr2L	dme-let-7	8023	1722	0.82326	0.17674	9745	0.794619587
chr2R	dme-mir-8	191101	44755	0.81024	0.18976	235856	19.23123099
chr2L	dme-mir-125	1718	485	0.77977	0.22023	2203	0.17964509
chr3R	dme-mir-279	4143	1208	0.77422	0.22578	5351	0.436324888
chr3L	dme-mir-316	1713	644	0.72686	0.27314	2357	0.192162262
chr3R	dme-mir-284	116	44	0.72292	0.27708	160	0.013083682

Ovary enriched miRNAs:

chrom	miRNA	Female Body reads	Ovary reads	BF/BF+Ov	Ov/BF+Ov	Sum Reads	% miRNA
chr3R	dme-mir-318	76	34886	0.00217	0.99783	34962	2.850769902
chrX	dme-mir-984	7	1378	0.00505	0.99495	1385	0.112954019
chr3R	dme-mir-994	76	14463	0.00523	0.99477	14539	1.185511752
chr2R	dme-mir-313	8	1216	0.00654	0.99346	1224	0.099795454
chrX	dme-mir-303	1	128	0.00778	0.99222	129	0.010484476
chrX	dme-mir-983	7	798	0.00869	0.99131	805	0.065667938
chr2R	dme-mir-312	40	2803	0.01407	0.98593	2843	0.231810914
chr2R	dme-mir-1009	3	174	0.01695	0.98305	177	0.014430438
chr2R	dme-mir-311	13	460	0.02748	0.97252	473	0.038573619
chrX	dme-mir-982	3	89	0.03264	0.96736	92	0.007495147
chr2R	dme-mir-310	9	228	0.03796	0.96204	237	0.019333034
chr2L	dme-mir-275	763	12586	0.05716	0.94284	13349	1.088479123
chr3R	dme-mir-92b	68	990	0.06429	0.93571	1058	0.086246167
chr3R	dme-mir-92a	169	1514	0.10044	0.89956	1683	0.137196605
chr3R	dme-mir-995	459	3679	0.11093	0.88907	4138	0.337377347
chr2L	dme-mir-966	6	41	0.12877	0.87123	47	0.003799254
chr2R	dme-mir-989	13128	88414	0.12929	0.87071	101542	8.279510048
chr2L	dme-mir-9b	1608	10570	0.13204	0.86796	12178	0.99298085
chr2L	dme-mir-2a-1	22	118	0.15723	0.84277	140	0.011408674
chr2L	dme-mir-306	499	1954	0.20340	0.79660	2453	0.200041589
chr2R	dme-mir-184	7879	30821	0.20359	0.79641	38700	3.155536026
chr4	dme-mir-954	11	43	0.20550	0.79450	54	0.004364565
chr3R	dme-mir-996	8051	28482	0.22038	0.77962	36533	2.978840048
chrX	dme-mir-13b-2	55	172	0.24224	0.75776	227	0.018512798
chr2L	dme-mir-79	2196	6723	0.24621	0.75379	8919	0.727260898
chr2L	dme-mir-2b-2	319	862	0.27007	0.72993	1181	0.096309284
chr2L	dme-mir-959	3	8	0.27953	0.72047	11	0.000875095
chr2R	dme-mir-7	928	2356	0.28254	0.71746	3284	0.267806437
chr3L	dme-mir-33	1974	4025	0.32907	0.67093	5999	0.48912155
chr3R	dme-mir-34	3245	6344	0.33839	0.66161	9589	0.781900759

At least 10 normalized reads in summed normalized reads were required. A ratio (BodyF/BodyF+Ovary) ≥ 0.66 is female body biased and a ratio (Ovary/Body M+Ovary) ≥ 0.66 is ovary biased. BF: Body Female; Ov: Ovary.

TABLE S9: Raw Counts miRNA-Seq

Chrom	miRNA	Late Embryo Lymphoid Cells		L3 Larvae Salivary Glands		Adult Head		Adult Body		Adult Gonads	
		S2 (M)	Kc (F)	S. Glands M	S. Glands F	Head M	Head F	Body M	Body F	Testis	Ovary
chr3L	dme-bantam	35460	18240	12348	24423	103920	152727	244113	72941	28463	687
chr2L	dme-let-7	5	5	30	219	20606	51163	28931	8023	891	11559
chr2L	dme-let-7-as	0	0	0	0	0	0	0	0	0	0
chr2L	dme-mir-1	23	55	679	1503	126814	175008	496888	199357	1549	241
chr3R	dme-mir-10	1	18	199	395	3730	4794	19132	6256	41	171
chr2L	dme-mir-100	0	0	1	10	1004	1527	1103	366	38	226
chr3R	dme-mir-1000	1	867	13	27	18668	25776	875	206	0	1
chr3R	dme-mir-1001	0	0	0	0	162	208	106	29	0	2
chr2L	dme-mir-1002	0	0	0	0	0	0	0	0	0	0
chr3R	dme-mir-1003	1487	902	34	30	107	228	124	34	16	63
chr2L	dme-mir-1004	0	0	0	1	157	253	44	13	0	144
chr2L	dme-mir-1004-as	0	0	0	0	1	0	0	0	0	0
chr2L	dme-mir-1005	1	0	16	11	101	332	122	44	14	3
chr2L	dme-mir-1006	58	97	71	107	315	519	415	101	4	15
chr2L	dme-mir-1006-as	0	0	0	0	0	0	0	0	0	0
chrX	dme-mir-1007	13	5	0	4	109	125	47	19	10	6
chr2R	dme-mir-1008	94	175	8	9	119	104	106	36	1	11
chr2R	dme-mir-1009	4	6	5	2	30	85	38	3	90	5
chr3R	dme-mir-1010	1	71	1	0	851	1677	319	92	8	168
chr3R	dme-mir-1011	0	0	0	0	8	19	1	0	0	3
chr3R	dme-mir-1012	164	42	230	346	374	623	215	79	40	46
chr3R	dme-mir-1013	1	4	3	4	90	131	52	24	1	54
chr3R	dme-mir-1014	0	0	0	0	0	0	248	66	0	0
chr3R	dme-mir-1015	0	0	0	0	0	1	62	15	0	2
chr2R	dme-mir-1016	5	4	3	4	35	76	18	8	0	6
chr3R	dme-mir-1017	0	0	0	0	183	278	25	6	0	1
chr3R	dme-mir-11	15690	9328	5007	12439	6209	21450	14438	5606	3338	9249
chrX	dme-mir-12	415	7053	16391	43021	1117	2682	21306	2801	2280	62228
chr2L	dme-mir-124	8	63	10	16	29849	48896	2863	470	1	151
chr2L	dme-mir-124-as	0	0	0	0	0	0	0	0	0	0
chr2L	dme-mir-125	10	3	23	63	7175	20670	5238	1718	251	3331
chrX	dme-mir-12-as	0	0	0	0	0	0	0	0	0	0
chr2L	dme-mir-133	5	3	6	4	4836	16473	1065	300	1	38
chr2R	dme-mir-137	0	2	0	1	701	1301	341	80	0	38
chr3R	dme-mir-13a	25	57	11	17	5608	9074	797	202	5	29
chr3R	dme-mir-13b	11557	9820	5207	12399	27953	34823	21017	7131	5476	5212
chr3R	dme-mir-13b-1	0	0	7	9	14	22	4	1	0	0
chrX	dme-mir-13b-2	299	300	62	70	27	101	92	55	89	1
chr2R	dme-mir-14	182756	130160	2602	2658	31243	68581	26146	5504	1571	6722
chr2R	dme-mir-14-as	0	0	0	0	2	1	0	0	0	0
chr2R	dme-mir-184	54062	73256	810	1085	51441	89330	15336	7879	15944	540
chr3L	dme-mir-190	171	308	130	168	1250	634	162	169	18	13
chr3L	dme-mir-193	3	64	0	4	1978	4491	12	1	1	7
chr2L	dme-mir-1-as	0	0	0	0	0	0	0	0	0	0
chrX	dme-mir-210	1	1	31	29	30904	106957	409	121	0	10
chr3L	dme-mir-219	0	0	1	0	259	437	84	21	0	1
chr2RHet	dme-mir-2279	8	9	2	5	7	16	12	3	0	3
chr2RHet	dme-mir-2279-as	0	1	0	1	0	0	0	0	0	0
chr2L	dme-mir-2280	0	0	0	0	0	0	1	0	0	0
chr3R	dme-mir-2281	0	0	0	0	0	1	4	1	0	0
chr3L	dme-mir-2282	1	3	0	0	0	0	0	0	0	0
chr3R	dme-mir-2283	0	0	0	0	3	3	4	0	0	1
chr3R	dme-mir-252	13294	137	831	644	14416	37717	4036	1420	21	990
chr2L	dme-mir-263a	66	3	27399	39275	17316	25950	11829	3892	3639	245
chr2L	dme-mir-263a-as	0	0	0	0	0	0	0	0	0	0
chr3L	dme-mir-263b	1	2	2	6	3141	6005	1144	263	0	13
chr3L	dme-mir-274	1	0	12	16	13878	55708	3593	1179	5	7928
chr2L	dme-mir-275	461	832	13608	2588	668	2503	1122	763	6511	605
chr2L	dme-mir-275-as	0	0	0	1	1	1	0	0	0	0
chr3L	dme-mir-276	4524	10288	1946	5840	68388	58112	47955	37412	1306	123
chr3L	dme-mir-276a	9143	7257	1158	3728	73713	163232	90583	31855	1402	2248
chr3L	dme-mir-276b	5	125	1	8	7324	16746	530	112	0	3
chr3R	dme-mir-277	3703	1688	807	1660	59156	104947	76053	19989	87	9542
chr2R	dme-mir-278	47	1099	797	526	2829	9122	4966	2040	117	2426
chr3R	dme-mir-279	16526	10095	321	1492	8345	13021	14571	4143	625	1554
chr3R	dme-mir-279-as	0	0	0	0	0	0	0	0	0	0
chr2R	dme-mir-281-1	179	132	55	118	260	557	17602	5351	522	143
chr2R	dme-mir-281-2	34	23	53	84	277	439	5100	1730	176	21
chr3L	dme-mir-282	13543	3084	4147	31936	6842	6760	23325	12554	3427	11072
chr3L	dme-mir-282-as	0	0	0	0	0	0	0	0	0	0
chrX	dme-mir-283	48	930	4683	7791	370	448	577	363	133	359
chr3R	dme-mir-284	0	5	2	1	518	2009	523	116	23	16
chr3L	dme-mir-285	0	0	12	38	40821	63213	76	4	0	0
chr2R	dme-mir-286	43	14	23	31	4	15	5	1	0	0
chr2L	dme-mir-287	0	0	0	0	0	0	0	1	0	0
chr3L	dme-mir-289	0	0	0	0	0	0	0	1	0	0
chr2L	dme-mir-2a	7839	19872	7976	9677	40963	62518	42678	21855	19231	14216
chr2L	dme-mir-2a-1	173	259	16	27	34	64	21	22	61	13
chr2L	dme-mir-2a-2	2015	6472	112	164	1780	4486	1047	363	339	112
chr2L	dme-mir-2b	9981	13905	6378	7854	43346	58488	18220	8986	8217	6058
chr2L	dme-mir-2b-1	498	138	461	465	1684	1927	623	328	188	2
chr2L	dme-mir-2b-2	431	1100	189	177	714	1184	615	319	446	40
chr3R	dme-mir-2c	9	13	3	0	163	287	27	10	1	19
chr2R	dme-mir-3	15	8	1	1	3	5	2	1	3	8
chrX	dme-mir-303	7	8	0	0	1	3	142	1	66	113
chrX	dme-mir-304	34	841	15014	30430	1286	2492	17186	2108	743	556
chrX	dme-mir-304-as	0	0	0	0	0	0	0	0	0	0
chr2L	dme-mir-305	3321	6880	7165	9763	11336	20428	13965	3692	2694	18583
chr2L	dme-mir-305-as	0	3	2	7	12	8	0	1	1	0
chr2L	dme-mir-306	2500	4089	1067	1144	752	2067	1152	499	1011	951
chr2R	dme-mir-307	932	22	1	0	5587	15933	2063	482	245	42
chr2R	dme-mir-307-as	1	0	5	17	0	3	6	1	0	0

chr2R	dme-mir-308	1483	1685	2781	5046	1048	1674	1864	684	323	30
chr2R	dme-mir-309	4	3	1	0	0	1	0	0	0	0
chr2R	dme-mir-310	8	4	1	0	2	2	55	9	118	3356
chr2R	dme-mir-311	8	2	0	0	1	2	68	13	238	3582
chr2R	dme-mir-312	3	6	0	0	8	9	95	40	1450	1704
chr2R	dme-mir-313	2	2	0	0	4	4	59	8	629	370
chr3L	dme-mir-314	0	2	2	3	18	72	11627	4449	16	29
chr3L	dme-mir-314-as	0	0	0	0	0	0	0	1	0	0
chr3L	dme-mir-315	0	0	0	0	1204	2424	24	7	0	12
chr3L	dme-mir-316	0	0	8	14	1119	3236	5546	1713	333	4417
chr3L	dme-mir-316-as	0	0	0	0	0	0	1	0	0	0
chr3R	dme-mir-317	9157	14069	718	1536	8974	14533	2370	561	529	4489
chr3R	dme-mir-317-as	0	0	0	0	0	0	0	1	0	0
chr3R	dme-mir-318	13	60	0	1	1	6	4	76	18047	20
chr2R	dme-mir-31a	5	12	521	763	11606	22138	24842	11038	881	1134
chrX	dme-mir-31b	3	3	0	0	7	44	2068	447	170	875
chr3L	dme-mir-33	1927	2696	1239	2256	1864	3555	9633	1974	2082	166
chr3R	dme-mir-34	13980	15190	1643	2983	45375	77345	9383	3245	3282	11464
chr2L	dme-mir-375	1	0	18745	34030	57	182	4698	811	0	1491
chr2R	dme-mir-4	6	2	1	6	3	5	2	0	0	0
chr2R	dme-mir-5	14	9	18	26	7	22	14	4	4	0
chr2R	dme-mir-6-1	7	1	0	0	0	0	0	0	0	0
chr2R	dme-mir-6-2	1	1	0	0	0	0	0	0	0	0
chr2R	dme-mir-6-3	2	1	0	0	0	0	0	0	0	0
chr2R	dme-mir-6-3-as	0	0	0	0	0	0	0	0	0	0
chr2R	dme-mir-7	332	243	176	270	13849	20729	3010	928	1219	863
chr2L	dme-mir-79	2043	3617	1604	3518	7700	13318	12143	2196	3478	219
chr2R	dme-mir-8	4003	18559	84972	180692	184826	244757	447346	191101	23152	56620
chr2L	dme-mir-87	0	2	2	4	2344	4107	908	535	57	12
chrX	dme-mir-927	0	1	0	0	662	994	41	9	0	0
chr3R	dme-mir-929	1	2	20	39	12012	13343	1810	819	12	4
chr3R	dme-mir-929-as	0	0	0	0	0	0	2	0	0	0
chr3R	dme-mir-92a	13	1478	2	7	1421	2484	254	169	783	1424
chr3R	dme-mir-92a-as	0	0	0	0	0	0	0	0	0	0
chr3R	dme-mir-92b	20	447	31	64	54	68	42	68	512	747
chr2L	dme-mir-932	5	118	4	2	3614	8766	276	70	2	45
chr4	dme-mir-954	11	61	1	1	59	124	50	11	22	62
chr3L	dme-mir-955	0	0	0	0	54	84	59	26	1	7
chr3L	dme-mir-956	0	1	0	1	4	20	4342	1393	9	54
chr3L	dme-mir-957	0	0	2	7	6154	12255	839	307	0	0
chr3L	dme-mir-958	1	19	0	1	3	29	7379	2103	0	9
chr2L	dme-mir-959	0	0	0	0	7	18	478	3	4	17252
chr2L	dme-mir-960	0	1	0	2	30	103	1717	34	11	5436
chr2L	dme-mir-961	0	0	0	0	5	20	177	5	5	477
chr2L	dme-mir-962	0	0	1	0	28	55	401	39	33	471
chr2L	dme-mir-963	0	1	0	0	5	20	368	6	1	926
chr2L	dme-mir-964	0	0	0	0	7	41	437	10	5	10115
chr2L	dme-mir-965	559	608	131	567	361	613	1129	201	145	9
chr2L	dme-mir-966	15	39	1	4	8	12	5	6	21	6
chr2L	dme-mir-967	10	7	0	1	4	2	3	0	0	0
chr2L	dme-mir-967-as	0	0	0	0	0	0	0	1	0	0
chr2L	dme-mir-968	0	0	0	0	2	3	0	0	0	0
chrX	dme-mir-969	0	0	0	2	194	192	27	6	0	0
chrX	dme-mir-970	1140	1185	177	198	1442	3119	656	205	59	100
chrX	dme-mir-971	0	35	0	1	40	70	4	0	0	33
chrX	dme-mir-972	0	0	0	0	0	1	61	0	0	961
chrX	dme-mir-973	0	8	0	0	0	0	76	1	0	51
chrX	dme-mir-974	0	2	0	0	5	2	236	1	0	82
chrX	dme-mir-975	0	3	0	0	0	0	33	0	0	2134
chrX	dme-mir-976	0	1	0	0	0	2	380	2	0	7525
chrX	dme-mir-977	1	44	0	0	3	4	680	0	0	8100
chrX	dme-mir-978	1	4	0	0	2	3	241	1	0	8457
chrX	dme-mir-979	0	0	0	0	0	0	21	0	0	497
chrX	dme-mir-980	1534	302	3	3	349	1464	2995	908	55	154
chrX	dme-mir-981	1	952	0	3	231	968	56	19	0	16
chrX	dme-mir-981-as	1	4	0	0	1	1	0	0	0	0
chrX	dme-mir-982	0	11	0	0	1	3	118	3	46	120
chrX	dme-mir-983	6	9	0	0	9	16	724	7	413	6732
chrX	dme-mir-983-1	0	0	0	0	0	0	1	0	2	1
chrX	dme-mir-984	25	68	0	0	10	11	551	7	713	2201
chrX	dme-mir-985	0	0	0	0	1	0	214	2	1	321
chr2R	dme-mir-986	3	29	211	226	271	1006	1880	510	301	309
chr2R	dme-mir-987	0	3	9	36	14710	16043	803	308	0	3
chr2R	dme-mir-988	13800	15082	558	539	620	1460	876	280	214	6587
chr2R	dme-mir-988-as	1	0	0	0	0	0	0	0	0	0
chr2R	dme-mir-989	3	158	14	30	1	6	44	13128	45737	6
chr2R	dme-mir-990	0	0	0	0	382	430	8	2	0	0
chr2R	dme-mir-991	0	0	0	0	0	1	120	2	4	127
chr2R	dme-mir-992	2	4	0	0	0	1	45	1	0	395
chr3R	dme-mir-993	0	1	0	2	982	1433	1448	314	0	1
chr3R	dme-mir-994	5	27	0	2	2	3	4	76	7482	19
chr3R	dme-mir-995	3761	3754	1631	3220	2255	3287	909	459	1903	228
chr3R	dme-mir-995-as	0	0	0	0	0	0	1	0	0	0
chr3R	dme-mir-996	23117	10275	2982	6077	10447	27396	29997	8051	14734	348
chr3R	dme-mir-997	0	0	0	0	0	0	184	0	0	59
chr3R	dme-mir-998	3118	3965	2123	5021	4751	5610	1074	459	403	84
chr3R	dme-mir-999	247	374	27	35	7193	10562	1464	771	73	673
chr3L	dme-mir-9a	49	83	1540	2193	12061	32808	28787	8813	40	6846
chr2L	dme-mir-9b	2463	7931	1257	1648	1557	3726	4263	1608	5468	6727
chr2L	dme-mir-9c	1896	3769	737	920	2615	5475	5508	2430	2337	2050
chr3R	dme-mir-9ab-4	0	1	0	0	2	2	94	35	1	7
chr3R	dme-mir-9ab-4as	0	0	0	0	0	1	144	28	0	16

S. Glands: Salivary Glands; M: Male; F: Female

TABLE S10: Normalized read counts in libraries

Chrom	miRNA	S2	Kc	S. Glands M	S. Glands F	Head M	Head F	Body M	Body F	Testis	Ovary	SUM
chr3L	dme-bantam	35460	27334	19757	24423	181971	152727	244113	250083	2405	55022	993293
chr2L	dme-let-7	5	7	48	219	36082	51163	28931	27507	40457	1722	186142
chr2L	dme-let-7-as	0	0	0	0	0	0	0	0	0	0	0
chr2L	dme-mir-1	23	82	1086	1503	222060	175008	496888	683509	844	2994	1583998
chr2L	dme-mir-1-as	0	0	0	0	0	0	0	0	0	0	0
chr3R	dme-mir-10	1	27	318	395	6531	4794	19132	21449	599	79	53326
chr2L	dme-mir-100	0	0	2	10	1758	1527	1103	1255	791	73	6519
chr3R	dme-mir-1000	1	1299	21	27	32689	25776	875	706	4	0	61398
chr3R	dme-mir-1001	0	0	0	0	284	208	106	99	7	0	704
chr2L	dme-mir-1002	0	0	0	0	0	0	0	0	0	0	0
chr3R	dme-mir-1003	1487	1352	54	30	187	228	124	117	221	31	3830
chr2L	dme-mir-1004	0	0	0	1	275	253	44	45	504	0	1121
chr2L	dme-mir-1004-as	0	0	0	0	2	0	0	0	0	0	2
chr2L	dme-mir-1005	1	0	26	11	177	332	122	151	11	27	857
chr2L	dme-mir-1006	58	145	114	107	552	519	415	346	53	8	2316
chrX	dme-mir-1007	13	7	0	4	191	125	47	65	21	19	493
chr2R	dme-mir-1008	94	262	13	9	208	104	106	123	39	2	960
chr2R	dme-mir-1009	4	9	8	2	53	85	38	10	18	174	400
chr3R	dme-mir-1010	1	106	2	0	1490	1677	319	315	588	15	4514
chr3R	dme-mir-1011	0	0	0	0	14	19	1	0	11	0	45
chr3R	dme-mir-1012	164	63	368	346	655	623	215	271	161	77	2943
chr3R	dme-mir-1013	1	6	5	4	158	131	52	82	189	2	630
chr3R	dme-mir-1014	0	0	0	0	0	0	248	226	0	0	474
chr3R	dme-mir-1015	0	0	0	0	0	1	62	51	7	0	121
chr2R	dme-mir-1016	5	6	5	4	61	76	18	27	21	0	224
chr3R	dme-mir-1017	0	0	0	0	320	278	25	21	4	0	648
chr3R	dme-mir-11	15690	13979	8011	12439	10872	21450	14438	19221	32372	6453	154924
chrX	dme-mir-12	415	10569	26226	43021	1956	2682	21306	9603	217798	4407	337984
chr2L	dme-mir-124	8	94	16	16	52268	48896	2863	1611	529	2	106303
chr2L	dme-mir-125	10	4	37	63	12564	20670	5238	5890	11659	485	56620
chr2L	dme-mir-133	5	4	10	4	8468	16473	1065	1029	133	2	27193
chr2R	dme-mir-137	0	3	0	1	1228	1301	341	274	133	0	3281
chr3R	dme-mir-13a	25	85	18	17	9820	9074	797	693	102	10	20640
chr3R	dme-mir-13b	11557	14716	8331	12399	48948	34823	21017	24449	18242	10586	205067
chr3R	dme-mir-13b-1	0	0	11	9	25	22	4	3	0	0	74
chrX	dme-mir-13b-2	299	450	99	70	47	101	92	189	4	172	1522
chr2R	dme-mir-14	182756	195051	4163	2658	54709	68581	26146	18871	23527	3037	579498
chr2R	dme-mir-184	54062	109778	1296	1085	90077	89330	15336	27014	1890	30821	420688
chr3L	dme-mir-190	171	462	208	168	2189	634	162	579	46	35	4653
chr3L	dme-mir-193	3	96	0	4	3464	4491	12	3	25	2	8099
chrX	dme-mir-210	1	1	50	29	54115	106957	409	415	35	0	162012
chr3L	dme-mir-219	0	0	2	0	454	437	84	72	4	0	1052
chr2RHet	dme-mir-2279	8	13	3	5	12	16	12	10	11	0	91
chr2RHet	dme-mir-2279-as	0	1	0	1	0	0	0	0	0	0	2
chr2L	dme-mir-2280	0	0	0	0	0	0	1	0	0	0	1
chr3R	dme-mir-2281	0	0	0	0	0	1	4	3	0	0	8
chr3L	dme-mir-2282	1	4	0	0	0	0	0	0	0	0	5
chr3R	dme-mir-2283	0	0	0	0	5	3	4	0	4	0	16
chr3R	dme-mir-252	13294	205	1330	644	25243	37717	4036	4869	3465	41	90843
chr2L	dme-mir-263a	66	4	43838	39275	30321	25950	11829	13344	858	7035	172520
chr3L	dme-mir-263b	1	3	3	6	5500	6005	1144	902	46	0	13610
chr3L	dme-mir-274	1	0	19	16	24301	55708	3593	4042	27748	10	115438
chr2L	dme-mir-275	461	1247	21773	2588	1170	2503	1122	2616	2118	12586	48183
chr2L	dme-mir-275-as	0	0	0	1	2	1	0	0	0	0	4
chr3L	dme-mir-276	4524	15417	3114	5840	119752	58112	47955	128270	431	2525	385939
chr3L	dme-mir-276a	9143	10875	1853	3728	129076	163232	90583	109217	7868	2710	528285
chr3L	dme-mir-276b	5	187	2	8	12825	16746	530	384	11	0	30697
chr3R	dme-mir-277	3703	2530	1291	1660	103586	104947	76053	68534	33397	168	395869
chr2R	dme-mir-278	47	1647	1275	526	4954	9122	4966	6994	8491	226	38248

chr3R	dme-mir-279	16526	15128	514	1492	14613	13021	14571	14205	5439	1208	96716
chr2R	dme-mir-281-1	179	198	88	118	455	557	17602	18346	501	1009	39053
chr2R	dme-mir-281-2	34	34	85	84	485	439	5100	5931	74	340	12606
chr3L	dme-mir-282	13543	4622	6635	31936	11981	6760	23325	43042	38752	6625	187220
chrX	dme-mir-283	48	1394	7493	7791	648	448	577	1245	1257	257	21157
chr3R	dme-mir-284	0	7	3	1	907	2009	523	398	56	44	3949
chr3L	dme-mir-285	0	0	19	38	71480	63213	76	14	0	0	134840
chr2R	dme-mir-286	43	21	37	31	7	15	5	3	0	0	162
chr2L	dme-mir-287	0	0	0	0	0	0	0	3	0	0	3
chr3L	dme-mir-289	0	0	0	0	0	0	0	3	0	0	3
chr2L	dme-mir-2a	7839	29779	12762	9677	71729	62518	42678	74931	49756	37175	398844
chr2L	dme-mir-2a-1	173	388	26	27	60	64	21	75	46	118	997
chr2L	dme-mir-2a-2	2015	9699	179	164	3117	4486	1047	1245	392	655	22999
chr2L	dme-mir-2b	9981	20837	10205	7854	75902	58488	18220	30809	21203	15884	269383
chr2L	dme-mir-2b-1	498	207	738	465	2949	1927	623	1125	7	363	8901
chr2L	dme-mir-2b-2	431	1648	302	177	1250	1184	615	1094	140	862	7704
chr3R	dme-mir-2c	9	19	5	0	285	287	27	34	67	2	735
chr2R	dme-mir-3	15	12	2	1	5	5	2	3	28	6	79
chrX	dme-mir-303	7	12	0	0	2	3	142	3	396	128	692
chrX	dme-mir-304	34	1260	24022	30430	2252	2492	17186	7227	1946	1436	88286
chr2L	dme-mir-305	3321	10310	11464	9763	19850	20428	13965	12658	65041	5208	172008
chr2L	dme-mir-305-as	0	4	3	7	21	8	0	3	0	2	49
chr2L	dme-mir-306	2500	6128	1707	1144	1317	2067	1152	1711	3329	1954	23008
chr2R	dme-mir-307	932	33	2	0	9783	15933	2063	1653	147	474	31019
chr2R	dme-mir-307-as	1	0	8	17	0	3	6	3	0	0	38
chr2R	dme-mir-308	1483	2525	4450	5046	1835	1674	1864	2345	105	624	21951
chr2R	dme-mir-309	4	4	2	0	0	1	0	0	0	0	11
chr2R	dme-mir-310	8	6	2	0	4	2	55	31	11746	228	12081
chr2R	dme-mir-311	8	3	0	0	2	2	68	45	12537	460	13124
chr2R	dme-mir-312	3	9	0	0	14	9	95	137	5964	2803	9034
chr2R	dme-mir-313	2	3	0	0	7	4	59	27	1295	1216	2613
chr3L	dme-mir-314	0	3	3	3	32	72	11627	15254	102	31	27126
chr3L	dme-mir-315	0	0	0	0	2108	2424	24	24	42	0	4622
chr3L	dme-mir-316	0	0	13	14	1959	3236	5546	5873	15460	644	32745
chr3R	dme-mir-317	9157	21083	1149	1536	15714	14533	2370	1923	15712	1023	84200
chr3R	dme-mir-318	13	90	0	1	2	6	4	261	70	34886	35333
chr2R	dme-mir-31a	5	18	834	763	20323	22138	24842	37845	3969	1703	112439
chrX	dme-mir-31b	3	4	0	0	12	44	2068	1533	3063	329	7055
chr3L	dme-mir-33	1927	4040	1982	2256	3264	3555	9633	6768	581	4025	38031
chr3R	dme-mir-34	13980	22763	2629	2983	79455	77345	9383	11126	40124	6344	266132
chr2L	dme-mir-375	1	0	29992	34030	100	182	4698	2781	5219	0	77002
chr2R	dme-mir-4	6	3	2	6	5	5	2	0	0	0	29
chr2R	dme-mir-5	14	13	29	26	12	22	14	14	0	8	152
chr2R	dme-mir-6	10	4	0	0	0	0	0	0	0	0	14
chr2R	dme-mir-7	332	364	282	270	24251	20729	3010	3182	3021	2356	57796
chr2L	dme-mir-79	2043	5420	2566	3518	13483	13318	12143	7529	767	6723	67511
chr2R	dme-mir-8	4003	27812	135955	180692	323642	244757	447346	655203	198170	44755	2262335
chr2L	dme-mir-87	0	3	3	4	4105	4107	908	1834	42	110	11116
chrX	dme-mir-927	0	1	0	0	1159	994	41	31	0	0	2227
chr3R	dme-mir-929	1	3	32	39	21034	13343	1810	2808	14	23	39107
chr3R	dme-mir-92a	13	2215	3	7	2488	2484	254	579	4984	1514	14541
chr3R	dme-mir-92b	20	670	50	64	95	68	42	233	2615	990	4845
chr2L	dme-mir-932	5	177	6	2	6328	8766	276	240	158	4	15962
chr4	dme-mir-954	11	91	2	1	103	124	50	38	217	43	680
chr3L	dme-mir-955	0	0	0	0	95	84	59	89	25	2	353
chr3L	dme-mir-956	0	1	0	1	7	20	4342	4776	189	17	9354
chr3L	dme-mir-957	0	0	3	7	10776	12255	839	1053	0	0	24933
chr3L	dme-mir-958	1	28	0	1	5	29	7379	7210	32	0	14686
chr2L	dme-mir-959	0	0	0	0	12	18	478	10	60382	8	60908
chr2L	dme-mir-960	0	1	0	2	53	103	1717	117	19026	21	21040
chr2L	dme-mir-961	0	0	0	0	9	20	177	17	1670	10	1902
chr2L	dme-mir-962	0	0	2	0	49	55	401	134	1649	64	2353

chr2L	dme-mir-963	0	1	0	0	9	20	368	21	3241	2	3662
chr2L	dme-mir-964	0	0	0	0	12	41	437	34	35403	10	35937
chr2L	dme-mir-965	559	911	210	567	632	613	1129	689	32	280	5622
chr2L	dme-mir-966	15	58	2	4	14	12	5	21	21	41	192
chr2L	dme-mir-967	10	10	0	1	7	2	3	0	0	0	33
chr2L	dme-mir-968	0	0	0	0	4	3	0	0	0	0	7
chrX	dme-mir-969	0	0	0	2	340	192	27	21	0	0	581
chrX	dme-mir-970	1140	1776	283	198	2525	3119	656	703	350	114	10864
chrX	dme-mir-971	0	52	0	1	70	70	4	0	116	0	313
chrX	dme-mir-972	0	0	0	0	0	1	61	0	3364	0	3426
chrX	dme-mir-973	0	12	0	0	0	0	76	3	179	0	270
chrX	dme-mir-974	0	3	0	0	9	2	236	3	287	0	540
chrX	dme-mir-975	0	4	0	0	0	0	33	0	7469	0	7507
chrX	dme-mir-976	0	1	0	0	0	2	380	7	26338	0	26728
chrX	dme-mir-977	1	66	0	0	5	4	680	0	28350	0	29106
chrX	dme-mir-978	1	6	0	0	4	3	241	3	29600	0	29857
chrX	dme-mir-979	0	0	0	0	0	0	21	0	1740	0	1761
chrX	dme-mir-980	1534	453	5	3	611	1464	2995	3113	539	106	10823
chrX	dme-mir-981	1	1427	0	3	404	968	56	65	56	0	2980
chrX	dme-mir-982	0	16	0	0	2	3	118	10	420	89	658
chrX	dme-mir-983	6	13	0	0	16	16	724	24	23562	798	25160
chrX	dme-mir-983-1	0	0	0	0	0	0	1	0	4	4	8
chrX	dme-mir-984	25	102	0	0	18	11	551	24	7704	1378	9812
chrX	dme-mir-985	0	0	0	0	2	0	214	7	1124	2	1348
chr2R	dme-mir-986	3	43	338	226	475	1006	1880	1749	1082	582	7383
chr2R	dme-mir-987	0	4	14	36	25758	16043	803	1056	11	0	43726
chr2R	dme-mir-988	13800	22601	893	539	1086	1460	876	960	23055	414	65683
chr2R	dme-mir-989	3	237	22	30	2	6	44	45010	21	88414	133789
chr2R	dme-mir-990	0	0	0	0	669	430	8	7	0	0	1114
chr2R	dme-mir-991	0	0	0	0	0	1	120	7	445	8	580
chr2R	dme-mir-992	2	6	0	0	0	1	45	3	1383	0	1440
chr3R	dme-mir-993	0	1	0	2	1720	1433	1448	1077	4	0	5684
chr3R	dme-mir-994	5	40	0	2	4	3	4	261	67	14463	14848
chr3R	dme-mir-995	3761	5626	2610	3220	3949	3287	909	1574	798	3679	29411
chr3R	dme-mir-996	23117	15398	4771	6077	18293	27396	29997	27603	1218	28482	182353
chr3R	dme-mir-997	0	0	0	0	0	0	184	0	207	0	391
chr3R	dme-mir-998	3118	5942	3397	5021	8319	5610	1074	1574	294	779	35128
chr3R	dme-mir-999	247	560	43	35	12595	10562	1464	2643	2356	141	30647
chr3L	dme-mir-9a	49	124	2464	2193	21120	32808	28787	30216	23961	77	141799
chr2L	dme-mir-9b	2463	11885	2011	1648	2726	3726	4263	5513	23545	10570	68350
chr2L	dme-mir-9c	1896	5648	1179	920	4579	5475	5508	8331	7175	4518	45229
chr3R	dme-mir-iab-4	0	1	0	0	4	2	94	120	25	2	247
chr3R	dme-mir-iab-4as	0	0	0	0	0	1	144	96	56	0	297
SUM_Norm_Reads_in_libr		476512	670269	419331	506593	2221284	2140318	1943944	2554945	1290996	481225	

TABLE S11: Abundance of miRNAs in *msl3* mutant salivary glands

	Genotype	Exp.	Average Ct ^a	Corrected amount ^b	Fold Difference (FD) ^c	log2 (FD)	Average log2(FD)	SD ^d	p value ^e
Dspt4	msl3-/msl3+	1	23.5091	95.762	1.000	0.000	0.000	0.000	
		2	23.7935	200.048	1.000	0.000			
	msl3-/msl3-	1	23.2659	106.222					
		2	23.2766	250.610					
mir-283	msl3-/msl3+	1	24.9728	89.769	0.514	-0.961	-0.901	0.086	0.00045
		2	24.7449	185.152	0.559	-0.840			
	msl3-/msl3-	1	26.4340	57.172					
		2	26.1674	129.580					
mir-304	msl3-/msl3+	1	29.9743	100.663	0.338	-1.564	-1.631	0.095	0.00070
		2	30.2644	203.835	0.308	-1.698			
	msl3-/msl3-	1	32.2164	37.754					
		2	32.3252	78.686					
mir-12	msl3-/msl3+	1	21.5294	88.515	0.406	-1.300	-1.284	0.022	0.00006
		2	21.8149	182.599	0.415	-1.269			
	msl3-/msl3-	1	23.8153	39.885					
		2	24.1442	94.941					
mir-979	msl3-/msl3+	1	36.2751	149.915	0.833	-0.263	-0.749	0.687	0.24047
		2	35.4645	209.309	0.425	-1.235			
	msl3-/msl3-	1	36.5484	138.570					
		2	37.5508	111.399					
mir-210	msl3-/msl3+	1	28.5830	100.340	1.425	0.511	0.384	0.180	0.07654
		2	29.1231	202.647	1.195	0.257			
	msl3-/msl3-	1	27.8037	158.625					
		2	28.3154	303.278					
U6	msl3-/msl3+	1	17.1883	100.088	0.611	-0.710	-0.627	0.117	0.01472
		2	17.7507	184.333	0.686	-0.544			
	msl3-/msl3-	1	18.0034	67.880					
		2	18.2684	158.374					

a. Dilution series were prepared in the control sample to construct standard curves for the Dspt4 autosomal gene reference and for each miRNA. C_T values measured in replicates for the target miRNA and Dspt4 reference in mutant and heterozygous mutant control samples respectively are averaged in individual experiments (Exp.1 and 2) and the corrected amount of target miRNA and Dspt4 reference inferred from the standard curve in b.

c. The amounts of miRNA are normalized in the mutant sample and in the heterozygous mutant control sample by dividing the calculated amount of miRNA by the amount of the Dspt4 reference. The fold difference (FD) or relative expression level of a miRNA corresponds to the

ratio of the normalized abundance of the miRNA in the mutant relative to the heterozygous mutant control sample, that is the ratio $[\text{miRNA/Dspt4}] \text{ Mutant} / [\text{miRNA/Dspt4}] \text{ Control}$; the average of the base 2 logarithm of the fold difference is plotted in Figure 2B,C.

d. SD is the standard deviation of the difference.

e. p-values are established in a two tailed Students t-test comparing the means of the normalized amounts of target miRNA in the mutant and in the heterozygous mutant control samples.

* $p < 0.05$, ** $p < 0.005$. *** $p < 0.0005$

TABLE S12: Abundance of miRNAs in *msl3* mutant L3 larvae

	Genotype	Exp.	Average Ct ^a	Corrected amount ^b	Fold Difference (FD) ^c	log2 (FD)	Average log2(FD)	SD ^d	p value ^e
Dspt4	msl3-/msl3+	1	25.9974	34.628	1.000	0.000			
		2	25.6265	92.801	1.000	0.000			
	msl3-/msl3-	1	24.8854	54.398					
		2	24.7720	132.066					
mir-283	msl3-/msl3+	1	26.9201	49.324	0.756	-0.403	-0.253	0.213	0.18885
		2	27.2713	98.504	0.932	-0.102			
	msl3-/msl3-	1	26.3534	58.590					
		2	26.1358	130.596					
mir-304	msl3-/msl3+	1	31.2445	57.627	0.356	-1.488	-1.475	0.019	0.03552
		2	31.5988	109.348	0.363	-1.462			
	msl3-/msl3-	1	32.5782	32.271					
		2	33.0699	56.492					
mir-12	msl3-/msl3+	1	22.7659	57.656	0.455	-1.136	-1.040	0.136	0.00881
		2	22.9153	134.505	0.520	-0.943			
	msl3-/msl3-	1	23.7208	41.214					
		2	23.9739	99.544					
mir-979	msl3-/msl3+	1	31.1498	1044.716	0.760	-0.396	-0.259	0.193	0.38647
		2	31.4659	927.357	0.918	-0.123			
	msl3-/msl3-	1	30.6831	1247.539					
		2	30.7420	1211.981					
mir-210	msl3-/msl3+	1	27.5383	185.744	1.197	0.259	0.065	0.275	0.38641
		2	27.5514	461.878	0.914	-0.129			
	msl3-/msl3-	1	26.4166	349.245					
		2	26.9873	600.996					
U6	msl3-/msl3+	1	17.1512	101.819	0.694	-0.526	-0.444	0.117	0.14280
		2	17.5728	194.135	0.778	-0.362			
	msl3-/msl3-	1	16.9733	111.054					
		2	17.2156	215.036					

a-e as in Table S11.

TABLE S13: Abundance of miRNAs in *msl3* mutant salivary glands

	Genotype	Exp.	Average Ct ^a	Corrected amount ^b	Fold Difference (FD) ^c	log2 (FD)	Average log2(FD)	SD ^d	p value ^e
Dspt4	msl3-/msl3+	1	24.216	100.872	1.000	0.000	0.000	0.000	
		2	24.262	99.102	1.000	0.000			
	msl3-/msl3-	1	23.663	124.744					
		2	24.150	103.457					
mir-314	msl3-/msl3+	1	31.225	100.048	2.258	1.175	1.149	0.037	0.0667
		2	30.498	152.880	2.178	1.123			
	msl3-/msl3-	1	29.463	279.422					
		2	29.089	347.564					
mir-981	msl3-/msl3+	1	32.920	117.805	0.958	-0.061	0.197	0.366	0.2414
		2	33.704	84.927	1.372	0.456			
	msl3-/msl3-	1	32.513	139.636					
		2	32.844	121.608					
mir-13b	msl3-/msl3+	1	23.450	122.437	0.411	-1.282	-0.884	0.564	0.0703
		2	24.218	81.676	0.714	-0.485			
	msl3-/msl3-	1	24.733	62.257					
		2	24.774	60.919					
mir-100	msl3-/msl3+	1	29.324	99.987	1.185	0.245	0.545	0.425	0.0596
		2	29.977	75.275	1.796	0.845			
	msl3-/msl3-	1	28.447	146.492					
		2	28.532	141.148					
mir-1013	msl3-/msl3+	1	31.660	84.010	1.176	0.234	-0.137	0.524	0.3233
		2	31.010	119.016	0.704	-0.507			
	msl3-/msl3-	1	30.962	122.159					
		2	31.585	87.439					
U6	msl3-/msl3+	1	18.097	100.004	0.726	-0.462	-0.418	0.061	0.0046
		2	18.127	98.736	0.771	-0.375			
	msl3-/msl3-	1	18.352	89.811					
		2	18.643	79.476					

a-e as in Table S11.

TABLE S14: Abundance of miRNAs in *msl3* mutant L3 larvae

	Genotype	Exp.	Average Ct ^a	Corrected amount ^b	Fold Difference (FD) ^c	log2 (FD)	Average log2(FD)	SD ^d	p value ^e
Dspt4	msl3-/msl3+	1	26.1455	48.078	1.000	0.000			
		2	26.1633	47.750	1.000	0.000			
	msl3-/msl3-	1	24.995	74.796					
		2	25.335	65.635					
mir-314	msl3-/msl3+	1	21.1699	35123.558	0.350	-1.514	-1.441	0.104	0.0003
		2	21.2272	33969.861	0.388	-1.367			
	msl3-/msl3-	1	22.213	19128.386					
		2	22.307	18104.321					
mir-981	msl3-/msl3+	1	29.5758	476.005	0.655	-0.609	-0.290	0.452	0.1481
		2	30.2449	359.989	1.021	0.030			
	msl3-/msl3-	1	29.529	485.377					
		2	29.433	505.205					
mir-13b	msl3-/msl3+	1	21.4858	344.693	0.540	-0.889	-0.905	0.022	0.0079
		2	21.5918	325.964	0.528	-0.921			
	msl3-/msl3-	1	21.817	289.481					
		2	22.199	236.640					
mir-100	msl3-/msl3+	1	26.8667	291.331	0.208	-2.262	-2.062	0.284	0.0032
		2	27.1654	255.822	0.275	-1.861			
	msl3-/msl3-	1	29.455	94.471					
		2	29.398	96.819					
mir-1013	msl3-/msl3+	1	29.240	142.324	0.573	-0.803	-0.610	0.273	0.0861
		2	28.286	126.568	0.749	-0.417			
	msl3-/msl3-	1	29.365	126.899					
		2	29.391	130.301					
U6	msl3-/msl3+	1	17.259	307.518	0.601	-0.734	-1.024	0.410	0.0125
		2	17.538	512.989	0.402	-1.314			
	msl3-/msl3-	1	17.532	287.625					
		2	17.469	283.612					

a-e as in Table S11.

TABLE S15: Abundance of miRNAs in *mle* mutant salivary glands

	Genotype	Exp.	Average Ct ^a	Corrected amount ^b	Fold Difference (FD) ^c	log2 (FD)	Average log2(FD)	SD ^d	p value ^e
Dspt4	mle-/mle+	1	24.693	102.093	1.000	0.000			
		2	24.533	100.668	1.000	0.000			
	mle-/mle-	1	23.901	170.434					
		2	23.827	158.044					
mir-283	mle-/mle+	1	25.142	100.816	0.740	-0.435	-0.430	0.008	0.0040
		2	24.812	102.914	0.745	-0.425			
	mle-/mle-	1	24.788	124.474					
		2	24.510	120.380					
mir-304	mle-/mle+	1	30.746	96.522	0.636	-0.652	-0.739	0.123	0.0031
		2	31.004	99.139	0.564	-0.826			
	mle-/mle-	1	30.568	102.559					
		2	31.168	87.778					
mir-12	mle-/mle+	1	21.652	101.133	0.532	-0.910	-0.946	0.051	0.0003
		2	21.533	100.745	0.506	-0.983			
	mle-/mle-	1	21.869	89.833					
		2	21.882	80.045					
mir-979	mle-/mle+	1	36.290	101.068	0.730	-0.454	-0.635	0.257	0.0203
		2	35.292	102.616	0.568	-0.817			
	mle-/mle-	1	36.064	123.209					
		2	35.753	91.460					
mir-210	mle-/mle+	1	29.642	107.507	0.782	-0.355	-0.182	0.244	0.2301
		2	29.573	109.561	0.994	-0.009			
	mle-/mle-	1	29.288	140.360					
		2	29.094	170.943					
U6	mle-/mle+	1	18.185	99.069	0.883	-0.180	0.098	0.393	0.3556
		2	18.095	99.106	1.298	0.376			
	mle-/mle-	1	17.555	146.012					
		2	17.022	201.962					

a-e as in Table S11.

TABLE S16: Abundance of miRNAs in *mle* mutant L3 larvae

	Genotype	Exp.	Average Ct ^a	Corrected amount ^b	Fold Difference (FD) ^c	log2 (FD)	Average log2(FD)	SD ^d	p value ^e
Dspt4	mle-/mle+	1	25.034	81.970	1.000	0.000			
		2	24.991	76.150	1.000	0.000			
	mle-/mle-	1	25.047	81.265					
		2	24.697	90.724					
mir-283	mle-/mle+	1	26.352	48.723	0.807	-0.309	-0.165	0.204	0.2143
		2	26.170	46.630	0.986	-0.021			
	mle-/mle-	1	26.717	38.996					
		2	25.887	54.769					
mir-304	mle-/mle+	1	33.859	16.253	1.264	0.338	0.117	0.313	0.2913
		2	33.412	15.797	0.930	-0.104			
	mle-/mle-	1	33.445	20.368					
		2	33.277	17.510					
mir-12	mle-/mle+	1	24.132	19.072	0.892	-0.165	-0.164	0.002	0.0126
		2	24.135	18.169	0.894	-0.162			
	mle-/mle-	1	24.311	16.868					
		2	24.037	19.341					
mir-979	mle-/mle+	1	32.007	1533.669	1.972	0.980	0.550	0.607	0.3187
		2	31.470	404.038	1.088	0.121			
	mle-/mle-	1	30.972	2998.693					
		2	30.760	523.538					
mir-210	mle-/mle+	1	26.990	1098.538	1.579	0.659	0.484	0.247	0.3002
		2	26.722	2357.685	1.239	0.309			
	mle-/mle-	1	26.467	1719.262					
		2	26.347	3479.985					
U6	mle-/mle+	1	16.909	227.810	1.506	0.591	0.559	0.046	0.3274
		2	16.978	208.576	1.440	0.526			
	mle-/mle-	1	16.296	340.231					
		2	16.160	357.836					

a-e as in Table S11.

Table S17: Levels of let-7 miRNA in adult females and males

Tissue		$C_T \text{let-7} \pm \text{StDev}$	$C_T \text{2SrRNA} \pm \text{StDev}$	$\Delta C_T (\Delta C_T \text{let-7} - \Delta C_T \text{2SrRNA})^a$	$\Delta\Delta C_T (\Delta C_T - \Delta C_T^{\text{control}})^b$	Average $\Delta\Delta C_T \pm \text{StDev}$	Fold Difference ^c
Female carcasses	Exp 1	25.33±0.30	6.14±0.24	19.19±0.39	0.00±0.39	0.00±0.28	1.00 (0.82 - 1.22)
	Exp 2	26.35±0.30	8.29±0.36	18.06±0.47	0.00±0.47		
Germlaria	Exp 1	22.18±0.18	6.29±0.09	15.90±0.20	3.29±0.20	-2.24±0.11	4.72 (4.38 - 5.09) p=7.76×10 ⁻⁶ **
	Exp 2	22.35±0.05	7.72±0.11	14.63±0.12	3.43±0.12		
Male carcasses	Exp 1	22.71±0.11	7.10±0.03	15.61±0.12	3.58±0.12	-1.92±0.09	3.79 (3.57 - 4.02) p=1.55×10 ⁻⁶ ***
	Exp 2	23.68±0.08	7.80±0.12	15.88±0.14	2.18±0.14		
Testes	Exp 1	21.14±0.26	6.56±0.03	14.58±0.26	4.61±0.26	-2.89±0.12	7.43 (6.84 - 8.07) p=7.73×10 ⁻⁸ ***
	Exp 2	22.40±0.05	8.41±0.09	13.99±0.10	4.07±0.10		

a: ΔC_T was determined by subtracting the average *2SrRNA* C_T value from the average Experimental C_T value. The standard deviation of the difference is calculated from the standard deviation of the Experimental and *2SrRNA* values using the formula $s = \sqrt{(s_1^2 + s_2^2)}$ where s = standard deviation

b: $\Delta\Delta C_T$ is calculated by subtracting the ΔC_T control value (ΔC_T of female carcasses). The standard deviation is the same as for ΔC_T

c: the fold difference between the Experimental Sample and the control is calculated by: $2^{\pm\Delta\Delta C_T}$ with $\Delta\Delta C_T$ -s and $\Delta\Delta C_T$ -s where s is the standard deviation of $\Delta\Delta C_T$ value. The fold difference of the experimental values was compared to the respective control. P-value was calculated using the two tailed Students t-test. *p<0.05.

p<0.005. *p<0.0005

Table S18: Levels of sex specific mRNAs in $\Delta let-7$ females and males

Genotype		C_T <i>SxIF</i> \pm StDev	C_T <i>RpL32</i> \pm StDev	ΔC_T (ΔC_T <i>SxIF</i> - ΔC_T <i>RpL32</i>) ^a	$\Delta\Delta C_T$ (ΔC_T - ΔC_T ^{control}) ^b	Fold Difference ^c
Females	Control: <i>let-7-C</i> Rescue	16.15 \pm 0.22	11.32 \pm 0.12	4.83 \pm 0.25	0.00 \pm 0.25	1.00 (0.840-1.190)
	$\Delta let-7$	15.95 \pm 0.03	11.16 \pm 0.09	4.78 \pm 0.25	-0.05 \pm 0.09	1.033 (0.969-1.102) p=0.70
Males	Control: <i>let-7-C</i> Rescue	21.48 \pm 0.12	12.28 \pm 0.16	9.21 \pm 0.20	0.00 \pm 0.20	1.00 (0.872-1.147)
	$\Delta let-7$	18.89 \pm 0.09	12.20 \pm 0.22	6.69 \pm 0.23	-2.51 \pm 0.23	5.704 (4.853-6.705) 1.73x10 ⁻⁴ ***
Genotype		C_T <i>tra1</i> \pm StDev	C_T <i>RpL32</i> \pm StDev	ΔC_T (ΔC_T <i>tra1</i> - ΔC_T <i>RpL32</i>) ^a	$\Delta\Delta C_T$ (ΔC_T - ΔC_T ^{control}) ^b	Fold Difference ^c
Females	Control: <i>let-7-C</i> Rescue	21.30 \pm 0.13	11.32 \pm 0.12	9.98 \pm 0.17	0.00 \pm 0.17	1.00 (0.886-1.129)
	$\Delta let-7$	20.72 \pm 0.14	11.16 \pm 0.09	9.56 \pm 0.16	-0.42 \pm 0.16	1.334 (1.190-1.495) p=0.06
Males	Control: <i>let-7-C</i> Rescue	29.84 \pm 0.03	12.28 \pm 0.16	17.57 \pm 0.16	0.00 \pm 0.16	1.00 (0.896-1.116)
	$\Delta let-7$	29.66 \pm 0.09	12.20 \pm 0.22	17.46 \pm 0.23	-0.11 \pm 0.23	1.079 (0.917-1.270) p=0.40
Genotype		C_T <i>DsxM</i> \pm StDev	C_T <i>RpL32</i> \pm StDev	ΔC_T (ΔC_T <i>DsxM</i> - ΔC_T <i>RpL32</i>) ^a	$\Delta\Delta C_T$ (ΔC_T - ΔC_T ^{control}) ^b	Fold Difference ^c
Females	Control: <i>let-7-C</i> Rescue	25.23 \pm 0.09	11.32 \pm 0.12	13.90 \pm 0.15	0.00 \pm 0.15	1.00 (0.900-1.111)
	$\Delta let-7$	25.69 \pm 0.05	11.16 \pm 0.09	14.52 \pm 0.10	0.62 \pm 0.10	0.649 (0.605-0.697) p=1.83x10 ⁻³ **
Males	Control: <i>let-7-C</i> Rescue	17.89 \pm 0.33	12.28 \pm 0.16	5.61 \pm 0.37	0.00 \pm 0.37	1.00 (0.950-1.052)
	$\Delta let-7$	17.94 \pm 0.03	12.20 \pm 0.22	5.74 \pm 0.22	0.30 \pm 0.17	0.914 (0.786-1.062) 0.75

Genotype		C_T <i>Yp1</i> ± StDev	C_T <i>RpL32</i> ± StDev	ΔC_T (ΔC_T <i>Yp1</i> - ΔC_T <i>RpL32</i>) ^a	$\Delta\Delta C_T$ (ΔC_T - ΔC_T control) ^b	Fold Difference ^c
Females	Control: <i>let-7-C</i> Rescue	10.33±0.07	11.32±0.12	-1.00±0.14	0.00±0.14	1.00 (0.908-1.101)
	Δ <i>let-7</i>	12.93±0.10	11.16±0.09	1.77±0.13	2.76±0.13	0.147 (0.134-0.162) p=3.29x10 ⁻⁶ ***
Males	Control: <i>let-7-C</i> Rescue	25.99±0.05	12.28±0.16	13.71±0.16	0.00±0.16	1.00 (0.894-1.119)
	Δ <i>let-7</i>	25.01±0.13	12.20±0.22	12.81±0.25	-0.90±0.25	1.867 (1.568-2.223) p=9.85x10 ⁻⁴ **

a: ΔC_T was determined by subtracting the average *RpL32* C_T value from the average Experimental C_T value. The standard deviation of the difference is calculated from the standard deviation of the Experimental and *RpL32* values using the formula $s = \sqrt{(s_1^2 + s_2^2)}$ where s = standard deviation

b: $\Delta\Delta C_T$ is calculated by subtracting the ΔC_T control. The standard deviation is the same as for ΔC_T

c: the fold difference between the Experimental Sample and the control is calculated by: $2^{-\Delta\Delta C_T}$ with $\Delta\Delta C_T + s$ and $\Delta\Delta C_T - s$ where s is the standard deviation of $\Delta\Delta C_T$ value. The fold difference of the experimental values was compared to the respective control. P-value was calculated using the two tailed Students t-test. *p<0.05, **p<0.005. ***p<0.0005

Table S19: *let-7* expression depends on ecdysone signaling in adult ovaries and testes

	Genotype, conditions	$C_T \text{ let-7} \pm \text{StDev}^a$	$C_T \text{ RpL32} \pm \text{StDev}$	$\Delta C_T (\Delta C_T \text{ let-7} - \Delta C_T \text{ RpL32})^a$	$\Delta \Delta C_T (\Delta C_T - \Delta C_T^{\text{control}})^b$	Fold Difference ^c	Relative change of <i>let-7</i> levels ^d
Females	<i>OregonR</i> , 4d at 18°C	25.88±0.16	14.13±0.21	11.74±0.06	0.00±0.06	1.00 (0.96-1.04)	1.00 (0.88-1.13)
	<i>OregonR</i> , 4d at 29°C	25.00±0.04	14.39±0.17	10.58±0.18	-1.16±0.18	2.24 (1.98-2.54) p=2.01x10 ^{-5***}	
	<i>ecd1^{ts 4210}</i> , 4d at 18°C	24.07±0.04	13.42±0.28	10.65±0.05	0.00±0.05	1.00 (0.97-1.03)	0.38 (0.37-0.38) p=2.44x10 ^{-4***}
	<i>ecd1^{ts 4210}</i> , 4d at 29°C	24.80±0.15	13.96±0.45	10.92±0.001	0.27±0.001	0.84 (0.84-0.84) p=0.14	
	Genotype, conditions	$C_T \text{ let-7} \pm \text{StDev}$	$C_T \text{ 2SrRNA} \pm \text{StDev}$	$\Delta C_T (\Delta C_T \text{ let-7} - \Delta C_T \text{ 2SrRNA})^a$	$\Delta \Delta C_T (\Delta C_T - \Delta C_T^{\text{control}})^b$	Fold Difference ^c	Relative change of <i>let-7</i> levels ^d
Males	<i>OregonR</i> , 4d at 18°C	22.90±0.03	8.41±0.11	14.49±0.13	0.00±0.13	1.00 (0.91-1.09)	1.00 (0.92-1.08)
	<i>OregonR</i> , 4d at 29°C	22.55±0.03	8.35±0.12	14.20±0.12	-0.29±0.12	1.23 (1.14-1.33) p=0.02*	
	<i>ecd1^{ts 4210}</i> , 4d at 18°C	22.13±0.55	8.33±0.09	13.80±0.15	0.00±0.15	1.00 (0.90-1.11)	0.24 (0.23-0.25) p=1.77x10 ^{-4***}
	<i>ecd1^{ts 4210}</i> , 4d at 29°C	23.49±0.02	7.87±0.11	15.64±0.08	1.85±0.08	0.29 (0.28-0.31) p=3.59x10 ^{-4***}	

a: ΔC_T values were determined by subtracting the average *RpL32* or *2SrRNA* C_T value from the average Experimental C_T value. The standard deviation of the difference is calculated from the standard deviation of the Experimental and *RpL32* or *2SrRNA* values using the formula $s = \sqrt{(s_1^2 + s_2^2)}$ where s = standard deviation

b: $\Delta \Delta C_T$ is calculated by subtracting the ΔC_T control value (ΔC_T of the respective genotype at 18°C). The standard deviation is the same as for ΔC_T

c: the fold difference between the Experimental Sample and the control is calculated by: $2^{-\Delta \Delta C_T}$ with $\Delta \Delta C_T + s$ and $\Delta \Delta C_T - s$ where s is the standard deviation of $\Delta \Delta C_T$ value. The fold difference of the experimental values was compared to the respective control. P-value between ΔC_T values of the experiments was calculated using the two tailed Students t-test

d: The relative changes of *let-7* levels were calculated by dividing the fold difference ranges of *ecd1^{ts}* and *OrR*. Students T-test was used to compare the relative changes
*p<0.05, **p<0.005

Table S20: Levels of sex specific mRNAs are misregulated upon ecdysone deficit

Genotype, conditions			C_T <i>DsxM</i> ± StDev	C_T <i>Rpl32</i> ± StDev	ΔC_T (ΔC_T <i>DsxM</i> - ΔC_T <i>Rpl32</i>) ^a	$\Delta\Delta C_T$ (ΔC_T - ΔC_T control) ^b	Fold Difference ^c
Females	Control: <i>OrR</i>	18°C	26.20±0.07	15.40±0.20	10.80±0.21	0.00±0.21	1.00 (0.866-1.155)
	<i>OrR</i>	29°C	26.34±0.01	13.95±0.03	12.39±0.03	1.58±0.03	0.334 (0.326-0.341) p=3.73x10 ^{-3**}
	Control: <i>ecd1^{ts}</i>	18°C	26.41±0.07	13.69±0.07	12.72±0.10	0.00±0.10	1.00 (0.935-1.070)
	<i>ecd1^{ts}</i>	29°C	25.88±0.12	14.36±0.07	11.52±0.14	-1.20±0.14	2.299 (2.081-2.539) 2.59x10 ^{-4***}
Males	Control: <i>OrR</i>	18°C	17.84±0.04	15.67±0.15	2.17±0.16	0.00±0.16	1.00 (0.896-1.116)
	<i>OrR</i>	29°C	18.17±0.06	15.45±0.29	2.72±0.30	0.55±0.30	0.681 (0.553-0.838) p=0.06
	Control: <i>ecd1^{ts}</i>	18°C	18.40±0.02	15.77±0.20	2.63±0.20	0.00±0.20	1.00 (0.868-1.152)
	<i>ecd1^{ts}</i>	29°C	18.04±0.05	14.60±0.14	3.45±0.25	0.81±0.15	0.569 (0.511-0.633) p=7.97x10 ^{-3*}

Genotype, conditions			C_T <i>Esg</i> ± StDev	C_T <i>Rpl32</i> ± StDev	ΔC_T (ΔC_T <i>Esg</i> - ΔC_T <i>Rpl32</i>) ^a	$\Delta\Delta C_T$ (ΔC_T - ΔC_T control) ^b	Fold Difference ^c
Females	Control: <i>OrR</i>	18°C	29.30±0.09	15.40±0.20	13.90±0.22	0.00±0.22	1.00 (0.862-1.161)
	<i>OrR</i>	29°C	27.90±0.08	13.95±0.03	13.94±0.09	0.04±0.09	0.970 (0.912-1.032) p=0.81
	Control: <i>ecd1^{ts}</i>	18°C	24.39±0.28	13.69±0.07	10.70±0.28	0.00±0.28	1.00 (0.821-1.218)
	<i>ecd1^{ts}</i>	29°C	24.69±0.22	14.36±0.07	10.33±0.24	-0.37±0.24	1.293 (1.097-1.523) p=0.07
Males	Control: <i>OrR</i>	18°C	26.86±0.05	15.67±0.15	11.19±0.16	0.00±0.16	1.00 (0.894-1.119)
	<i>OrR</i>	29°C	27.48±0.00 ₃	15.45±0.29	12.03±0.29	0.84±0.29	0.559 (0.456-0.685) p=0.55
	Control: <i>ecd1^{ts}</i>	18°C	25.89±0.02	15.77±0.20	10.12±0.20	0.00±0.20	1.00 (0.868-1.152)
	<i>ecd1^{ts}</i>	29°C	25.34±0.13	14.60±0.14	10.75±0.20	0.63±0.20	0.648 (0.566-0.742) p=8.77x10 ^{-3*}

Genotype, conditions			C_T <i>SxIF1</i> ± StDev	C_T <i>Rpl32</i> ± StDev	ΔC_T (ΔC_T <i>SxIF1</i> - ΔC_T <i>Rpl32</i>) ^a	$\Delta\Delta C_T$ (ΔC_T - ΔC_T control) ^b	Fold Difference ^c
Females	Control: <i>OrR</i>	18°C	17.81±0.08	15.40±0.20	2.41±0.21	0.00±0.21	1.00 (0.864-1.158)
	<i>OrR</i>	29°C	15.96±0.16	13.95±0.03	2.00±0.16	-0.41±0.16	1.330 (1.189-1.487) p=5.00x10 ^{-2*}
	Control: <i>ecd1^{ts}</i>	18°C	16.02±0.04	13.69±0.07	2.33±0.08	0.00±0.08	1.00 (0.947-1.056)
	<i>ecd1^{ts}</i>	29°C	16.18±0.16	14.36±0.07	1.82±0.17	-0.51±0.17	1.424 (1.262-1.607) p=1.64x10 ^{-3**}
Males	Control: <i>OrR</i>	18°C	21.05±0.12	15.67±0.15	5.38±0.20	0.00±	1.00 (0.873-1.146)
	<i>OrR</i>	29°C	21.44±0.07	15.45±0.29	5.99±0.30	0.61±	0.653 (0.530-0.805) p=0.15
	Control: <i>ecd1^{ts}</i>	18°C	22.24±0.12	15.77±0.20	6.47±0.24	0.00±	1.00 (0.848-1.179)
	<i>ecd1^{ts}</i>	29°C	19.38±0.07	14.60±0.14	4.78±0.16	-1.69±	3.222 (2.883-3.600) p=9.13x10 ^{-3**}

Genotype, conditions			C_T <i>tra1</i> ± StDev	C_T <i>Rpl32</i> ± StDev	ΔC_T (ΔC_T <i>tra1</i> - ΔC_T <i>Rpl32</i>) ^a	$\Delta\Delta C_T$ (ΔC_T - ΔC_T control) ^b	Fold Difference ^c
Females	Control: <i>OrR</i>	18°C	21.04±0.05	15.40±0.20	5.64±0.20	0.00±0.20	1.00 (0.868-1.152)
	<i>OrR</i>	29°C	19.87±0.11	13.95±0.03	5.92±0.11	0.28±0.11	0.826 (0.765-0.891) p=0.14
	Control: <i>ecd1^{ts}</i>	18°C	20.01±0.08	13.69±0.07	6.32±0.11	0.00±0.11	1.00 (0.927-1.079)
	<i>ecd1^{ts}</i>	29°C	20.69±0.11	14.36±0.07	6.33±0.13	0.008±0.13	0.994 (0.909-1.088) p=0.93
Males	Control: <i>OrR</i>	18°C	28.84±0.09	15.67±0.15	13.18±0.18	0.00±0.18	1.00 (0.885-1.129)
	<i>OrR</i>	29°C	28.67±0.05	15.45±0.29	13.22±0.30	0.05±0.30	0.969 (0.789-1.190) p=0.73
	Control: <i>ecd1^{ts}</i>	18°C	28.69±0.12	15.77±0.20	12.92±0.23	0.00±0.23	1.00 (0.850-1.176)
	<i>ecd1^{ts}</i>	29°C	23.68±0.06	14.60±0.14	9.08±0.16	-3.84±0.16	14.277 (12.801-15.924) p=1.76x10 ^{-5***}

Genotype, conditions			C_T <i>Yp1</i> ± StDev	C_T <i>RpL32</i> ± StDev	ΔC_T (ΔC_T <i>Yp1</i> - ΔC_T <i>RpL32</i>) ^a	$\Delta\Delta C_T$ (ΔC_T - ΔC_T control) ^b	Fold Difference ^c
Females	Control: <i>OrR</i>	18°C	12.33±0.14	15.40±0.20	-3.07±0.24	0.00±0.24	1.00 (0.846-1.182)
	<i>OrR</i>	29°C	11.21±0.23	13.95±0.03	-2.74±0.23	0.33±0.23	0.794 (0.678-0.930) p=0.12
	Control: <i>ecd1^{ts}</i>	18°C	10.86±0.31	13.69±0.07	-2.82±0.32	0.00±0.32	1.00 (0.800-1.249)
	<i>ecd1^{ts}</i>	29°C	11.24±0.20	14.36±0.07	-3.12±0.21	-0.30±0.21	1.231 (1.061-1.428) p=0.15
Males	Control: <i>OrR</i>	18°C	26.15±0.11	15.67±0.15	10.48±0.19	0.00±0.19	1.00 (0.876-1.142)
	<i>OrR</i>	29°C	25.57±0.03	15.45±0.29	10.12±0.29	-0.36±0.29	1.285 (1.048-1.576) p=0.14
	Control: <i>ecd1^{ts}</i>	18°C	24.63±0.08	15.77±0.20	8.86±0.22	0.00±0.22	1.00 (0.86-1.163)
	<i>ecd1^{ts}</i>	29°C	16.76±0.06	14.60±0.14	2.16±0.16	-6.702±0.16	104.080 (93.395-115.987) p=3.22x10 ⁻⁶ ***

a: ΔC_T was determined by subtracting the average *RpL32* C_T value from the average Experimental C_T value. Since the same set of samples was used for all PCRs, the same *RpL32* C_T values are used as internal control. The standard deviation of the difference is calculated from the standard deviation of the Experimental and *RpL32* values using the formula $s = \sqrt{(s_1^2 + s_2^2)}$ where s = standard deviation.

b: $\Delta\Delta C_T$ is calculated by subtracting the ΔC_T control value (ΔC_T of the sample of the respective sex and genotype at 18°C). The standard deviation is the same as for ΔC_T .

c: the fold difference between the Experimental Sample and the control is calculated by: $2^{-\Delta\Delta C_T}$ with $\Delta\Delta C_T + s$ and $\Delta\Delta C_T - s$ where s is the standard deviation of $\Delta\Delta C_T$ value. The fold difference of the experimental values was compared to the respective control. P-value was calculated using the two tailed Students t-test. *p<0.05, **p<0.005. ***p<0.0005.

Table S21. Ecdysteroid deficit leads to differentiation defects in the CySC lineage cells in adult testes

Genotype, conditions	Clustering of somatic cyst cells				Appearance of epithelium-like clusters			
	< 5 cells	≥ 5 cells	> 10 cells	P value	None	Apical	Lateral	P value
Control: <i>ecd</i> ^{1ts} , 5 days, 18°	40%	60%	0%		100%	0%	0%	
<i>ecd</i> ^{1ts} , 5 days, 29°	7%	57%	36%	0.0368*	43%	43%	14%	0.0137*
Control: <i>ecd</i> ^{1ts} , 11 days, 18°	50%	50%	0%		83%	17%	0%	
<i>ecd</i> ^{1ts} , 11 days, 29°	17%	8%	75%	0.0113*	0%	50%	50%	0.0001***

To calculate the significance two-way tables and chi-squared test with 2 degrees of freedom were used. The frequencies of the testes with the somatic cell clustering phenotype (<5, ≥ 5 or >10 somatic cell in the cluster) and the frequencies of the testes with epithelial sheets (none, apical or lateral) acquired by induction of ecdysone deficit for 5d or 11d at the restrictive temperature (29°) were compared to the frequencies of the same phenotypes in flies with the same genotype but kept for the same periods of time (5d or 11d) at the permissive temperature (18°). N=10-20 testes for each genotype. *p<0.05, **p<0.005. ***p<0.0005.

TABLE S22: Ranked abundance of miRNAs in each sexed library (Complete list)

Chrom	Late embryo Lymphoid Cells				L3 Larvae Salivary Glands				Adult Head				Adult Body				Adult Gonads			
	miRNA	S2 M (%)	miRNA	Kc F (%)	miRNA	S. Gland M (%)	miRNA	S. Gland F (%)	miRNA	Head M (%)	miRNA	Head F (%)	miRNA	Body M (%)	miRNA	Body F (%)	miRNA	Testis (%)	miRNA	Ovary (%)
chr2R	mir-14	38.35286	mir-14	29.10042	mir-8	32.42188	mir-8	35.66808	mir-8	14.57004	mir-8	11.43554	mir-1	25.56082	mir-1	26.75240	mir-12	16.87054	mir-989	18.37262
chr2R	mir-184	11.34536	mir-184	16.37821	mir-263a	10.45437	mir-12	8.49222	mir-1	9.99692	mir-1	8.17673	mir-8	23.01229	mir-8	25.64550	mir-8	15.35016	bantam	11.43364
chr3L	bantam	7.44158	mir-2a	4.44288	mir-375	7.15235	mir-263a	7.75277	bantam	8.19215	mir-276a	7.62653	bantam	12.55761	bantam	9.78819	mir-305	5.03802	mir-8	9.30021
chr3R	mir-996	4.85129	mir-8	4.14932	mir-12	6.25415	mir-375	6.71742	mir-276a	5.81087	bantam	7.13572	mir-276a	4.65975	mir-276	5.02046	mir-959	4.67717	mir-2a	7.72512
chr3R	mir-279	3.46812	bantam	4.07801	mir-304	5.72874	mir-282	6.30407	mir-276	5.39112	mir-210	4.99725	mir-277	3.91230	mir-276a	4.27473	mir-2a	3.85408	mir-318	7.24950
chr3R	mir-11	3.29268	mir-34	3.39610	mir-275	5.19227	mir-304	6.00679	mir-277	4.66334	mir-277	4.90334	mir-276	2.46689	mir-2a	2.93279	let-7	3.13374	mir-184	6.40474
chr3R	mir-34	2.93382	mir-988	3.37195	bantam	4.71150	bantam	4.82103	mir-184	4.05515	mir-184	4.17368	mir-2a	2.19543	mir-277	2.68239	mir-34	3.10799	mir-996	5.91867
chr2R	mir-988	2.89604	mir-317	3.14547	mir-2a	3.04332	mir-11	2.45542	mir-34	3.57697	mir-34	3.61372	mir-996	1.54310	mir-989	1.76169	mir-282	3.00171	mir-2b	3.30079
chr3L	mir-282	2.84211	mir-2b	3.10880	mir-305	2.73388	mir-13b	2.44753	mir-2b	3.41702	mir-14	3.20424	let-7	1.48826	mir-282	1.68466	mir-964	2.74226	mir-994	3.00554
chr3R	mir-252	2.78986	mir-276	2.30014	mir-2b	2.43359	mir-305	1.92719	mir-2a	3.22916	mir-285	2.95344	mir-9a	1.48086	mir-31a	1.48123	mir-277	2.58692	mir-275	2.61547
chr3R	mir-13b	2.42533	mir-996	2.29723	mir-13b	1.98678	mir-2a	1.91021	mir-285	3.21797	mir-2a	2.92097	mir-14	1.34500	mir-2b	1.20586	mir-11	2.50748	mir-13b	2.19972
chr2L	mir-2b	2.09460	mir-279	2.25699	mir-11	1.91047	mir-2b	1.55036	mir-14	2.46292	mir-2b	2.73268	mir-31a	1.27792	mir-9a	1.18265	mir-978	2.29276	mir-9b	2.19650
chr3R	mir-317	1.92167	mir-13b	2.19551	mir-283	1.78685	mir-283	1.53792	mir-210	2.43620	mir-276	2.71511	mir-282	1.19988	mir-996	1.08039	mir-977	2.19598	mir-263a	1.46179
chr3L	mir-276a	1.91873	mir-11	2.08551	mir-282	1.58233	mir-996	1.19958	mir-124	2.35303	mir-274	2.60279	mir-12	1.09602	let-7	1.07663	mir-274	2.14935	mir-79	1.39712
chr2L	mir-2a	1.64508	mir-9b	1.77317	mir-996	1.13781	mir-276	1.15280	mir-13b	2.20357	let-7	2.39044	mir-13b	1.08115	mir-184	1.05731	mir-976	2.04009	mir-282	1.37663
chr3L	mir-276	0.94940	mir-276a	1.62248	mir-308	1.06112	mir-308	0.99607	let-7	1.62439	mir-124	2.28452	mir-10	0.98418	mir-13b	0.95693	mir-9a	1.85601	mir-11	1.34088
chr2R	mir-8	0.84006	mir-12	1.57688	mir-14	0.99282	mir-998	0.99113	mir-200a	1.47162	mir-252	1.76221	mir-2b	0.93727	mir-10	0.83951	mir-983	1.82510	mir-34	1.31839
chr3R	mir-995	0.78928	mir-305	1.53819	mir-998	0.81005	mir-276a	0.73590	mir-133a	1.36504	mir-13b	1.62700	mir-281	0.90548	mir-11	0.75229	mir-9b	1.82375	mir-305	1.08218
chr3R	mir-277	0.77711	mir-2a-2	1.44698	mir-276	0.74252	mir-79	0.69444	mir-987	1.15961	mir-9a	1.53286	mir-304	0.88408	mir-14	0.73860	mir-14	1.82239	mir-9c	0.93878
chr2L	mir-305	0.69694	mir-306	0.91420	mir-34	0.62690	mir-995	0.63562	mir-252	1.13643	mir-996	1.28000	mir-184	0.78891	mir-281-1	0.71807	mir-988	1.78579	mir-12	0.91588
chr3R	mir-998	0.65434	mir-998	0.88647	mir-995	0.62232	mir-34	0.58884	mir-274	1.09402	mir-263a	1.21244	mir-279	0.74956	mir-31a	0.59703	mir-2b	1.64237	mir-33	0.83634
chr2L	mir-306	0.52465	mir-9c	0.84265	mir-79	0.61202	mir-14	0.52468	mir-7	1.09173	mir-1000	1.20431	mir-11	0.74272	mir-279	0.55596	mir-960	1.47375	mir-995	0.76444
chr2L	mir-9b	0.51688	mir-995	0.83930	mir-9a	0.58760	mir-275	0.51086	mir-9a	0.95078	mir-31a	1.03433	mir-305	0.71838	mir-263a	0.52228	mir-13b	1.41302	mir-14	0.63107
chr2L	mir-79	0.42874	mir-79	0.80867	mir-9b	0.47962	mir-33	0.44533	mir-929	0.94692	mir-11	1.00219	mir-79	0.62466	mir-305	0.49544	mir-317	1.21701	mir-1	0.62224
chr2L	mir-2a-2	0.42286	mir-282	0.68950	mir-33	0.47275	mir-9a	0.43289	mir-31a	0.91492	mir-7	0.96850	mir-263a	0.60851	mir-34	0.43546	mir-316	1.19749	mir-312	0.58247
chr3L	mir-33	0.40440	mir-33	0.60276	mir-276a	0.44185	mir-277	0.32768	mir-305	0.89363	mir-125	0.96574	mir-31a	0.59811	mir-12	0.37588	mir-311	0.97111	mir-276a	0.56319
chr2L	mir-9c	0.39789	mir-277	0.37739	mir-306	0.40712	mir-9b	0.32531	mir-996	0.82355	mir-305	0.95444	mir-33	0.49554	mir-9c	0.32609	mir-310	0.90984	mir-276	0.52462
chrX	mir-980	0.32192	mir-308	0.37672	mir-252	0.31708	mir-317	0.30320	mir-317	0.70743	mir-276b	0.78241	mir-34	0.48268	mir-79	0.29469	mir-125	0.90306	mir-7	0.48967
chr3R	mir-1003	0.31206	mir-92a	0.33044	mir-184	0.30906	mir-1	0.29669	mir-279	0.65784	mir-133	0.76965	mir-958	0.37959	mir-304	0.28288	mir-278	0.65771	mir-306	0.40612
chr2R	mir-308	0.31122	mir-970	0.26494	mir-277	0.30792	mir-279	0.29452	mir-79	0.60700	mir-987	0.74956	mir-316	0.28530	mir-958	0.28221	mir-276a	0.60945	let-7	0.35792
chrX	mir-970	0.23924	mir-2b-2	0.24593	mir-278	0.30410	mir-306	0.22582	mir-276b	0.57736	mir-307	0.74442	mir-9c	0.28334	mir-278	0.27375	mir-984	0.59671	mir-31a	0.35390
chr2R	mir-307	0.19559	mir-278	0.24571	mir-9c	0.28121	mir-184	0.21418	mir-999	0.56703	mir-317	0.67901	mir-125	0.26945	mir-33	0.26490	mir-975	0.57855	mir-92a	0.31453
chr2L	mir-965	0.11731	mir-981	0.21284	mir-317	0.27396	mir-9c	0.18161	mir-125	0.56561	mir-929	0.62341	mir-281-2	0.26235	mir-281-2	0.23215	mir-9c	0.55577	mir-304	0.29846
chr2L	mir-2b-1	0.10451	mir-283	0.20792	mir-1	0.25908	mir-31a	0.15061	mir-282	0.53936	mir-79	0.62224	mir-278	0.25546	mir-125	0.23054	mir-312	0.46197	mir-984	0.28641
chr2L	mir-275	0.09674	mir-1003	0.20166	mir-988	0.21291	mir-252	0.12712	mir-11	0.48946	mir-279	0.60837	mir-375	0.24167	mir-316	0.22987	mir-279	0.42130	mir-313	0.25267
chr2L	mir-2b-2	0.09045	mir-1000	0.19384	mir-31a	0.19879	mir-965	0.11192	mir-957	0.48513	mir-957	0.57258	mir-956	0.22336	mir-9b	0.21578	mir-375	0.40402	mir-279	0.25106
chrX	mir-12	0.08709	mir-304	0.18803	mir-2b-1	0.17590	mir-988	0.10640	mir-278	0.44209	mir-999	0.49348	mir-9b	0.21930	mir-252	0.19055	mir-92a	0.38606	mir-317	0.21250
chr2R	mir-7	0.06967	mir-275	0.18601	mir-279	0.12248	mir-278	0.10383	mir-307	0.44043	mir-278	0.42620	mir-252	0.20762	mir-956	0.18693	mir-31a	0.30744	mir-281-1	0.20969
chrX	mir-13b-2	0.06275	mir-965	0.13593	mir-1012	0.08776	mir-2b-1	0.09179	mir-133	0.38123	mir-13a	0.42396	mir-274	0.15821	mir-252	0.26840	mir-92b	0.20567		
chr3R	mir-999	0.05184	mir-92b	0.09994	mir-986	0.08051	mir-1	0.07797	mir-998	0.37453	mir-932	0.40957	mir-7	0.15484	mir-7	0.12453	mir-972	0.26054	mir-2b-2	0.17916
chr2R	mir-281-1	0.03756	mir-999	0.08362	mir-10	0.07593	mir-1012	0.06830	mir-10	0.29404	mir-282	0.31584	mir-980	0.15407	mir-980	0.12185	mir-306	0.25782	mir-983	0.16590
chr2L	mir-2a-1	0.03631	mir-190	0.06886	mir-2b-2	0.07211	mir-7	0.05330	mir-932	0.28490	mir-263b	0.28057	mir-124	0.14728	mir-929	0.10990	mir-963	0.25105	mir-998	0.16189
chr3L	mir-190	0.03589	mir-980	0.06752	mir-970	0.06754	mir-986	0.04461	mir-263b	0.24761	mir-998	0.26211	mir-317	0.12192	mir-375	0.10883	mir-31b	0.23722	mir-2a-2	0.13618
chr3R	mir-1012	0.03442	mir-13b-2	0.06707	mir-7	0.04323	mir-278	0.04230	mir-278	0.22301	mir-9c	0.25580	mir-31b	0.10638	mir-999	0.10346	mir-7	0.23397	mir-316	0.13377
chr2R	mir-1008	0.01973	mir-2a-1	0.05791	mir-965	0.04998	mir-970	0.03908	mir-9c	0.20614	mir-10	0.22399	mir-307	0.10612	mir-275	0.10239	mir-92b	0.20252	mir-308	0.12975
chr2L	mir-263a	0.01385	mir-7	0.05433	mir-190	0.04960	mir-2b-2	0.03494	mir-87	0.18478	mir-193	0.20983	mir-986	0.09671	mir-308	0.09178	bantam	0.18625	mir-986	0.12091
chr2L	mir-1006	0.01217	mir-1008	0.03913	mir-2a-2	0.04273	mir-190	0.03316	mir-995	0.17776	mir-2a-2	0.20960	mir-308	0.09589	mir-317	0.07528	mir-999	0.18246	mir-125	0.10083
chr3L	mir-9a	0.01028	mir-989	0.03532	mir-1006	0.02709	mir-2a-2	0.02327	mir-193	0.15593	mir-87	0.19189	mir-929	0.09311	mir-87	0.07179	mir-275	0.16402	mir-307	0.09842
chrX	mir-283	0.01007	mir-2b-1	0.03085	mir-13b-2	0.02369	mir-31	0.02329	mir-33	0.14694	mir-9b	0.17409	mir-960	0.08833	mir-986	0.06844	mir-304	0.15074	mir-311	0.09560
chr2R	mir-278	0.00986	mir-252	0.03063	mir-281-1	0.02099	mir-1006	0.02112	mir-2a-2	0.14032	mir-33	0.16610	mir-999	0.07531	mir-306	0.06696	mir-184	0.14640	mir-988	0.08596
chr2R	mir-286	0.00902	mir-281-1	0.02951	mir-281-2	0.02022	mir-281-2	0.01658	mir-281-2	0.13275	mir-995	0.15358	mir-993	0.07449	mir-307	0.06468	mir-979	0.13474	mir-2b-1	0.07552
chr2R	mir-281-2	0.00714	mir-276b	0.02795	mir-1003	0.01297	mir-13b-2	0.01382	mir-9b	0.12274	mir-316	0.15119								

chr2R	mir-989	0.00063 mir-284	0.00112 mir-100	0.00038 mir-314	0.00059 mir-1003	0.00843 mir-375	0.00850 mir-974	0.01214 mir-1008	0.00483 mir-2b-2	0.01084 mir-964	0.00201
chr2R	mir-313	0.00042 mir-1013	0.00089 mir-1010	0.00038 mir-980	0.00059 mir-1005	0.00796 mir-1013	0.00612 mir-1012	0.01106 mir-iab-4	0.00470 mir-133	0.01030 mir-1006	0.00161
chr2R	mir-992	0.00042 mir-1016	0.00089 mir-219	0.00038 mir-981	0.00059 mir-1013	0.00709 mir-1007	0.00584 mir-985	0.01101 mir-1003	0.00456 mir-137	0.01030 mir-5	0.00161
chr3R	mir-10	0.00021 mir-310	0.00089 mir-276b	0.00038 mir-1009	0.00039 mir-954	0.00465 mir-954	0.00579 mir-997	0.00947 mir-960	0.00456 mir-971	0.00895 mir-959	0.00161
chr3R	mir-1000	0.00021 mir-978	0.00089 mir-3	0.00038 mir-932	0.00039 mir-375	0.00449 mir-1008	0.00486 mir-961	0.00911 mir-1001	0.00389 mir-308	0.00813 mir-991	0.00161
chr2L	mir-1005	0.00021 mir-992	0.00089 mir-307	0.00038 mir-960	0.00039 mir-92b	0.00426 mir-960	0.00481 mir-190	0.00833 mir-iab-4as	0.00376 mir-13a	0.00786 mir-3	0.00121
chr3R	mir-1010	0.00021 mir-125	0.00067 mir-309	0.00038 mir-969	0.00039 mir-955	0.00426 mir-13b-2	0.00472 mir-iab-4as	0.00741 mir-955	0.00349 mir-314	0.00786 mir-932	0.00080
chr3R	mir-1013	0.00021 mir-133	0.00067 mir-310	0.00038 mir-993	0.00039 mir-971	0.00315 mir-1009	0.00397 mir-303	0.00730 mir-1013	0.00322 mir-281-2	0.00569 mir-983-1	0.00080
chrX	mir-210	0.00021 mir-2282	0.00067 mir-4	0.00038 mir-994	0.00039 mir-1016	0.00276 mir-955	0.00392 mir-1003	0.00638 mir-2a-1	0.00295 mir-318	0.00542 mir-1008	0.00040
chr3L	mir-2282	0.00021 mir-263a	0.00067 mir-954	0.00038 mir-1004	0.00020 mir-2a-1	0.00268 mir-1016	0.00355 mir-1005	0.00628 mir-219	0.00282 mir-2c	0.00515 mir-1013	0.00040
chr3L	mir-263b	0.00021 mir-305-as	0.00067 mir-962	0.00038 mir-137	0.00020 mir-1009	0.00236 mir-314	0.00336 mir-991	0.00617 mir-1007	0.00255 mir-994	0.00515 mir-124	0.00040
chr3L	mir-274	0.00021 mir-309	0.00067 mir-966	0.00038 mir-2279-as	0.00020 mir-960	0.00236 mir-971	0.00327 mir-982	0.00607 mir-981	0.00255 mir-284	0.00434 mir-133	0.00040
chr2R	mir-307-as	0.00021 mir-31b	0.00067 let-7-as	0.00000 mir-275-as	0.00020 mir-962	0.00221 mir-92b	0.00318 mir-1001	0.00545 mir-1015	0.00201 mir-981	0.00434 mir-193	0.00040
chr2L	mir-375	0.00021 mir-6	0.00067 mir-1-as	0.00000 mir-284	0.00020 mir-13b-2	0.00213 mir-2a-1	0.00299 mir-1008	0.00545 mir-1004	0.00174 mir-iab-4as	0.00434 mir-2c	0.00040
chr3R	mir-929	0.00021 mir-975	0.00067 mir-1001	0.00000 mir-3	0.00020 mir-314	0.00142 mir-962	0.00257 mir-312	0.00489 mir-311	0.00174 mir-1006	0.00407 mir-305-as	0.00040
chr3L	mir-958	0.00021 mir-987	0.00067 mir-1002	0.00000 mir-318	0.00020 mir-13b-1	0.00110 mir-31b	0.00206 mir-iab-4	0.00484 mir-954	0.00148 mir-190	0.00352 mir-955	0.00040
chrX	mir-977	0.00021 mir-137	0.00045 mir-1004	0.00000 mir-954	0.00020 mir-305-as	0.00095 mir-964	0.00192 mir-13b-2	0.00473 mir-2c	0.00134 mir-263b	0.00352 mir-963	0.00040
chrX	mir-978	0.00021 mir-263b	0.00045 mir-1004-as	0.00000 mir-956	0.00020 mir-984	0.00079 mir-958	0.00135 mir-219	0.00432 mir-964	0.00134 mir-2a-1	0.00352 mir-985	0.00040
chrX	mir-981	0.00021 mir-311	0.00045 mir-1007	0.00000 mir-958	0.00020 mir-983	0.00071 mir-13b-1	0.00103 mir-285	0.00391 mir-310	0.00121 mir-315	0.00325 mir-iab-4	0.00040
chr2L	let-7-as	0.00000 mir-313	0.00045 mir-1011	0.00000 mir-967	0.00020 mir-1011	0.00063 mir-5	0.00103 mir-973	0.00391 mir-927	0.00121 mir-87	0.00325 let-7-as	0.00000
chr2L	mir-1-as	0.00000 mir-314	0.00045 mir-1014	0.00000 mir-971	0.00020 mir-312	0.00063 mir-956	0.00093 mir-311	0.00350 mir-1016	0.00107 mir-1008	0.00298 mir-1-as	0.00000
chr2L	mir-100	0.00000 mir-4	0.00045 mir-1015	0.00000 let-7-as	0.00000 mir-966	0.00063 mir-961	0.00093 mir-1015	0.00319 mir-313	0.00107 mir-210	0.00271 mir-1000	0.00000
chr3R	mir-1001	0.00000 mir-87	0.00045 mir-1017	0.00000 mir-1-as	0.00000 mir-927	0.00055 mir-963	0.00093 mir-972	0.00314 mir-315	0.00094 mir-958	0.00244 mir-1001	0.00000
chr2L	mir-1002	0.00000 mir-929	0.00045 mir-137	0.00000 mir-1001	0.00000 mir-31b	0.00055 mir-1011	0.00089 mir-313	0.00304 mir-983	0.00094 mir-965	0.00244 mir-1002	0.00000
chr2L	mir-1004	0.00000 mir-974	0.00045 mir-193	0.00000 mir-1002	0.00000 mir-5	0.00055 mir-959	0.00084 mir-955	0.00304 mir-984	0.00094 mir-3	0.00217 mir-1004	0.00000
chr2L	mir-1004-as	0.00000 mir-210	0.00025 mir-2279-as	0.00000 mir-1004-as	0.00000 mir-959	0.00055 mir-2279	0.00075 mir-981	0.00288 mir-1017	0.00081 mir-193	0.00190 mir-1004-as	0.00000
chr3R	mir-1011	0.00000 mir-2279-as	0.00025 mir-2280	0.00000 mir-964	0.00000 mir-1010	0.00000 mir-964	0.00075 mir-310	0.00283 mir-963	0.00081 mir-955	0.00190 mir-1011	0.00000
chr3R	mir-1014	0.00000 mir-927	0.00022 mir-2281	0.00000 mir-1011	0.00000 mir-961	0.00039 mir-286	0.00070 mir-1013	0.00267 mir-966	0.00081 mir-iab-4	0.00190 mir-1014	0.00000
chr3R	mir-1015	0.00000 mir-956	0.00022 mir-2282	0.00000 mir-1014	0.00000 mir-963	0.00039 mir-966	0.00056 mir-954	0.00257 mir-969	0.00081 mir-1007	0.00163 mir-1015	0.00000
chr3R	mir-1017	0.00000 mir-960	0.00022 mir-2283	0.00000 mir-1015	0.00000 mir-974	0.00039 mir-984	0.00051 mir-1007	0.00242 mir-961	0.00067 mir-1016	0.00163 mir-1016	0.00000
chr2R	mir-137	0.00000 mir-963	0.00022 mir-275-as	0.00000 mir-1017	0.00000 mir-286	0.00032 mir-312	0.00042 mir-992	0.00231 mir-285	0.00054 mir-966	0.00163 mir-1017	0.00000
chr3R	mir-13b-1	0.00000 mir-976	0.00022 mir-287	0.00000 mir-219	0.00000 mir-313	0.00032 mir-305-as	0.00037 mir-1004	0.00226 mir-5	0.00054 mir-989	0.00163 mir-137	0.00000
chr3L	mir-219	0.00000 mir-993	0.00022 mir-289	0.00000 mir-2280	0.00000 mir-956	0.00032 mir-318	0.00028 mir-989	0.00226 mir-1009	0.00040 mir-1009	0.00136 mir-13b-1	0.00000
chr2Hhet	mir-2279-as	0.00000 mir-iab-4	0.00022 mir-303	0.00000 mir-967	0.00000 mir-967	0.00032 mir-989	0.00028 mir-92b	0.00216 mir-2279	0.00040 mir-929	0.00108 mir-210	0.00000
chr2L	mir-2280	0.00000 let-7-as	0.00000 mir-311	0.00000 mir-2282	0.00000 mir-2283	0.00024 mir-3	0.00023 mir-927	0.00211 mir-959	0.00040 mir-1005	0.00081 mir-219	0.00000
chr3R	mir-2281	0.00000 mir-1-as	0.00000 mir-312	0.00000 mir-2283	0.00000 mir-3	0.00024 mir-4	0.00023 mir-1009	0.00195 mir-982	0.00040 mir-1011	0.00081 mir-2279	0.00000
chr3R	mir-2283	0.00000 mir-100	0.00000 mir-313	0.00000 mir-287	0.00000 mir-4	0.00024 mir-313	0.00019 mir-975	0.00170 mir-976	0.00027 mir-2279	0.00081 mir-2279-as	0.00000
chr2L	mir-275-as	0.00000 mir-1001	0.00000 mir-315	0.00000 mir-289	0.00000 mir-958	0.00024 mir-977	0.00019 mir-2c	0.00139 mir-985	0.00027 mir-276b	0.00081 mir-2280	0.00000
chr3R	mir-284	0.00000 mir-1002	0.00000 mir-318	0.00000 mir-2c	0.00000 mir-977	0.00024 mir-2283	0.00014 mir-969	0.00139 mir-990	0.00027 mir-987	0.00081 mir-2281	0.00000
chr3L	mir-285	0.00000 mir-1004	0.00000 mir-31b	0.00000 mir-303	0.00000 mir-310	0.00000 mir-303	0.00014 mir-1017	0.00129 mir-991	0.00027 mir-1001	0.00054 mir-2282	0.00000
chr2L	mir-287	0.00000 mir-1004-as	0.00000 mir-6	0.00000 mir-307	0.00000 mir-968	0.00016 mir-307-as	0.00014 mir-315	0.00123 mir-13b-1	0.00013 mir-1015	0.00054 mir-2283	0.00000
chr3L	mir-289	0.00000 mir-1005	0.00000 mir-927	0.00000 mir-309	0.00000 mir-978	0.00016 mir-968	0.00014 mir-2a-1	0.00108 mir-193	0.00013 mir-2b-1	0.00054 mir-263b	0.00000
chr2L	mir-305-as	0.00000 mir-1011	0.00000 mir-955	0.00000 mir-310	0.00000 mir-994	0.00016 mir-978	0.00014 mir-979	0.00108 mir-2281	0.00013 mir-1000	0.00027 mir-275-as	0.00000
chr3L	mir-314	0.00000 mir-1014	0.00000 mir-956	0.00000 mir-311	0.00000 mir-iab-4	0.00016 mir-982	0.00014 mir-1016	0.00093 mir-286	0.00013 mir-1017	0.00027 mir-276b	0.00000
chr3L	mir-315	0.00000 mir-1015	0.00000 mir-958	0.00000 mir-312	0.00000 mir-1004-as	0.00008 mir-994	0.00014 mir-5	0.00072 mir-287	0.00013 mir-13b-2	0.00027 mir-285	0.00000
chr3L	mir-316	0.00000 mir-1017	0.00000 mir-959	0.00000 mir-313	0.00000 mir-275-as	0.00008 mir-310	0.00009 mir-193	0.00062 mir-289	0.00013 mir-219	0.00027 mir-286	0.00000
chr2L	mir-87	0.00000 mir-13b-1	0.00000 mir-960	0.00000 mir-315	0.00000 mir-303	0.00008 mir-311	0.00009 mir-2279	0.00062 mir-3	0.00013 mir-2283	0.00027 mir-287	0.00000
chrX	mir-927	0.00000 mir-219	0.00000 mir-961	0.00000 mir-31b	0.00000 mir-311	0.00008 mir-967	0.00009 mir-990	0.00041 mir-303	0.00013 mir-983-1	0.00027 mir-289	0.00000
chr3L	mir-955	0.00000 mir-2280	0.00000 mir-963	0.00000 mir-6	0.00000 mir-318	0.00008 mir-974	0.00009 mir-307-as	0.00031 mir-305-as	0.00013 mir-993	0.00027 mir-307-as	0.00000
chr3L	mir-956	0.00000 mir-2281	0.00000 mir-964	0.00000 mir-927	0.00000 mir-982	0.00008 mir-976	0.00009 mir-286	0.00026 mir-307-as	0.00013 let-7-as	0.00000 mir-309	0.00000
chr3L	mir-957	0.00000 mir-2283	0.00000 mir-967	0.00000 mir-955	0.00000 mir-985	0.00008 mir-966	0.00009 mir-966	0.00026 mir-973	0.00013 mir-1-as	0.00000 mir-315	0.00000
chr2L	mir-959	0.00000 mir-274	0.00000 mir-968	0.00000 mir-959	0.00000 mir-989	0.00008 mir-1015	0.00005 mir-13b-1	0.00021 mir-974	0.00013 mir-1002	0.00000 mir-375	0.00000
chr2L	mir-960	0.00000 mir-275-as	0.00000 mir-969	0.00000 mir-961	0.00000 let-7-as	0.00000 mir-2281	0.00005 mir-2281	0.00021 mir-978	0.00013 mir-1004-as	0.00000 mir-4	0.00000
chr2L	mir-961	0.00000 mir-285	0.00000 mir-971	0.00000 mir-962	0.00000 mir-1-as	0.00000 mir-275-as	0.00005 mir-2283	0.00021 mir-992	0.00013 mir-1014	0.00000 mir-6	0.00000
chr2L	mir-962	0.00000 mir-287	0.00000 mir-972	0.00000 mir-963	0.00000 mir-1002	0.00000 mir-309	0.00005 mir-318	0.00021 let-7-as	0.00000 mir-13b-1	0.00000 mir-927	0.00000
chr2L	mir-963	0.00000 mir-289	0.00000 mir-973	0.00000 mir-964	0.00000 mir-1014	0.00000 mir-972	0.00005 mir-971	0.00021 mir-1-as	0.00000 mir-2279-as	0.00000 mir-957	0.00000
chr2L	mir-964	0.00000 mir-307-as	0.00000 mir-974	0.00000 mir-968	0.00000 mir-1015	0.00000 mir-991	0.00005 mir-994	0.00021 mir-1002	0.00000 mir-2280	0.00000 mir-958	0.00000
chr2L	mir-968	0.00000 mir-315	0.00000 mir-975	0.00000 mir-972	0.00000 mir-2279-as	0.00000 mir-992	0.00005 mir-967	0.00015 mir-1004-as	0.00000 mir-2281	0.00000 mir-967	0.00000
chrX	mir-969	0.00000 mir-316	0.00000 mir-976	0.00000 mir-973	0.00000 mir-2280	0.00000 mir-iab-4as	0.00005 mir-3	0.00010 mir-1011	0.00000 mir-2282	0.00000 mir-968	0.00000
chrX	mir-971	0.00000 mir-375	0.00000 mir-977	0.00000 mir-974	0.00000 mir-2281	0.00000 let-7-as	0.00000 mir-4	0.00010 mir-2279-as	0.00000 mir-275-as	0.00000 mir-969	0.00000
chrX	mir-972	0.00000 mir-955	0.00000 mir-978	0.00000 mir-975	0.00000 mir-2282	0.00000 mir-1-as	0.00000 mir-1011	0.00005 mir-2280	0.00000 mir-285	0.00000 mir-971	0.00000
chrX	mir-973	0.00000 mir-957	0.00000 mir-979	0.00000 mir-976	0.00000 mir-287	0.00000 mir-1002	0.00000 mir-2280	0.00005 mir-2282	0.00000 mir-286	0.00000 mir-972	0.00000
chrX	mir-974	0.00000 mir-959	0.00000 mir-981	0.00000 mir-977	0.00000 mir-289	0.00000 mir-1004-as	0.00000 mir-983-1	0.00005 mir-2283	0.00000 mir-287	0.00000 mir-973	0.00000
chrX	mir-975	0.00000 mir-961	0.00000 mir-982	0.00000 mir-978	0.00000 mir-307-as	0.00000 mir-1014	0.00000 let-7-as	0.00000 mir-275-as	0.00000 mir-289	0.00000 mir-974	0.00000
chrX	mir-976	0.00000 mir-962	0.00000 mir-983	0.00000 mir-979	0.00000 mir-309	0.00000 mir-2279-as	0.00000 mir-1-as	0.00000 mir-309	0.00000 mir-30		

Soma influences GSC progeny differentiation via the cell adhesion-mediated steroid-let-7-Wingless signaling cascade that regulates chromatin dynamics: Supplementary Material

Supplementary Material
Annekatrin König and Halyna R. Shcherbata doi: 10.1242/
bio.201410553

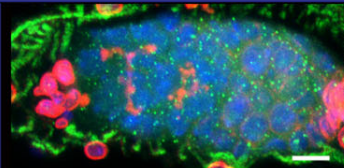
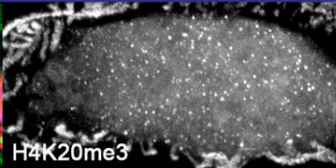
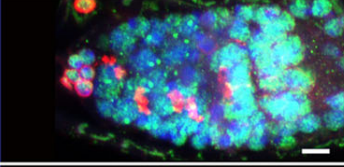
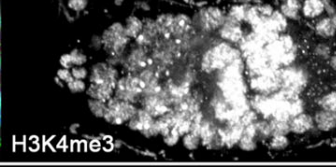
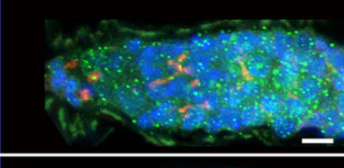
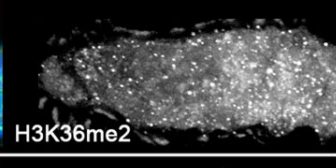
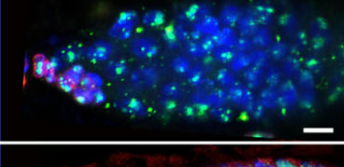
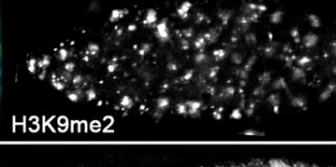
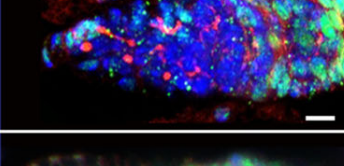
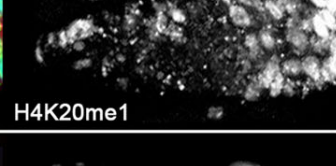
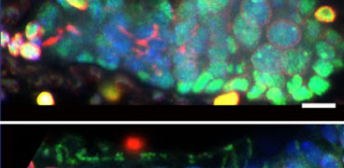
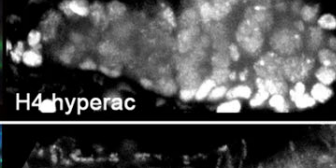
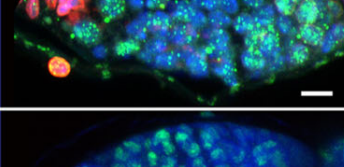
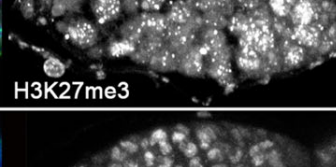


		Soma			Germline			
DAPI Add/LC		CpC	EC	FC	GSC	CB	4/8 cell cyst	16/cell cyst
H4K20me3			+	+	+	+	+	+
H3K4me3			+	+	+	+	+	++
H3K36me2			+	+	+	+	+	++
H3K9me2			++	++	+	+	+	+
H4K20me1			++	+	++	+	+	++
H4 hyperac			++	+	++	+	+	+
H3K27me3			+	+	+	++	++	+++
H2Bub1			++	+	+	-	++	++

Fig. S1. Histones are differentially modified in somatic and germline cells in the germarium. Wildtype (*OregonR*) germaria are stained with several histone modification antibodies (green); in addition, germaria are stained with LaminC (LC red) to visualize TFs and CpCs and Adducin (Add red) to mark spectrosomes and fusomes. Nuclei are marked with DAPI (blue). In particular, H4K20me3, H3K9me3, H3K9me2, H3K27me3 and H4K20me1 are associated with transcriptional repression, while H3K4me3, H4 hyperacetylation, H2Bub1 are known as active marks and often associated with ongoing transcription. Note that some histone modifications show differential pattern in certain somatic cells and differentially staged GCs; importantly, H2Bub1 is present in the differentiating cysts, but not in the GSCs. Scale bars, 5 μm.

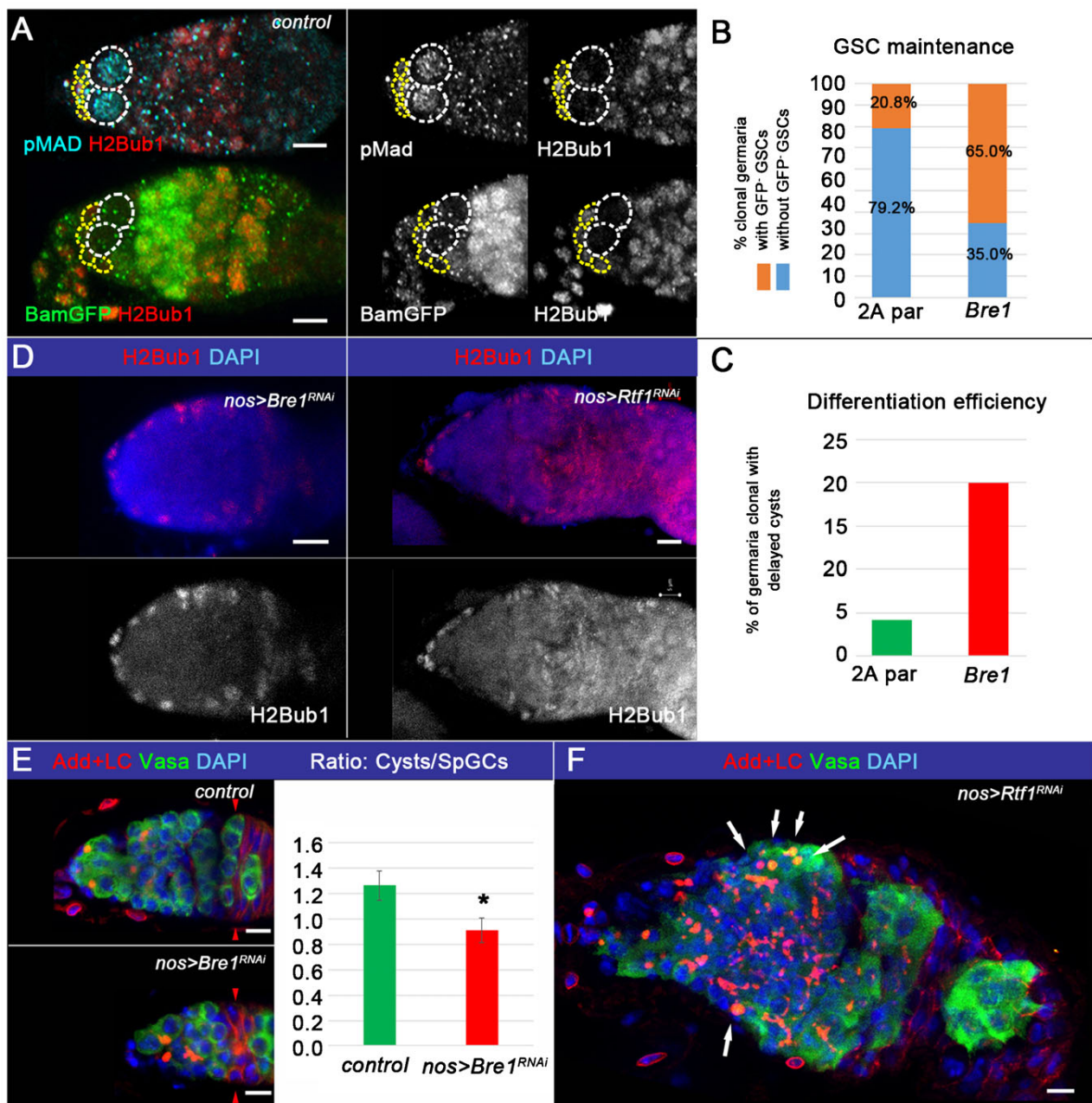


Fig. S2. H2Bub1-deficient germline cysts are delayed in differentiation. (A) In the control (*OregonR*) germlarium, GSCs exhibit pMad staining. The differentiation marker Bam (detected by the *bamGFP* transgene) is expressed in cysts. H2Bub1 is found in cysts that are also positive for Bam, but not in GSCs. (B,C) *Bre1* mutant (*hsFlp; FRT 2A Bre1^{P1549}/FRT 2A GFP*) and control (*hsFlp; FRT 2A parental/FRT 2A GFP*) germline clones are analyzed 5 days after adult clone induction. Germlaria containing *Bre1* germline clones frequently lack *Bre1* clonal GSCs; bar graph shows that 79.2% ($n=24$) of control germlaria contain one or more black GSCs, while *Bre1* clonal GSCs are partially lost and only 35.0% ($n=20$) of all clonal germlaria contained one or more black GSCs (B; see supplementary material Table S6). (C) *Bre1* clonal cysts are delayed in differentiation. 4.16% ($n=24$) of control and 20% ($n=20$) of *Bre1* germline clonal cysts show the differentiation delay. (D) Analysis of H2Bub1 modification upon downregulation of Rtf1 or *Bre1* using RNAi shows that *Bre1* and Rtf1 are specifically required for monoubiquitination of H2B in the germline, since their downregulation (*nos>Bre1^{RNAi}; NGT40/Bre1^{RNAi}; nanosGAL4/+* and *nos>Rtf1^{RNAi}; NGT40/Rtf1^{RNAi}; nanosGAL4/+*) results in the absence of this modification. (E,F) Germline-specific downregulation of *Bre1* affects differentiation (*control: NGT40/+; nanosGAL4/+* and *nos>Bre1^{RNAi}; NGT40/Bre1^{RNAi}; nanosGAL4/+*); (E) reducing *Bre1* levels in the germline leads to the appearance of small germlaria (red arrowheads mark beginning of region 2b) and the decrease in the differentiation index (Cysts/SpGCs, supplementary material Table S1). (F) Expression of *Rtf1^{RNAi}* in the germline (*NGT40/+; nanosGAL4/Rtf1^{RNAi}*) leads to severe perturbations of germlaria architecture and defects in germline differentiation; SpGCs are found at arbitrary positions (arrows) far from the stem cell niche. pMad marks GSCs (cyan, A), bamGFP (green, A) differentiating cysts. Monoubiquitination of H2B is shown (red, A,D), germline cells are Vasa-positive (green, E,F). Germlaria are stained with LaminC (LC red, E,F) to visualize TFs and CpCs and Adducin (Add red, E,F) to mark spectrosomes and fusomes. Nuclei are marked with DAPI (blue, D–F). GSCs are outlined in white, CpCs in yellow (A). H2Bub1-positive CpCs are marked with white arrows (D), H2Bub1-positive ECs with yellow arrows (D). Region 2b is indicated by red arrowheads (E) and SpGCs are depicted with white arrows (F). p-values were calculated using the two tailed Student's t-test and error bars represent S.E.M., * $p<0.05$. Scale bars, 5 μ m.

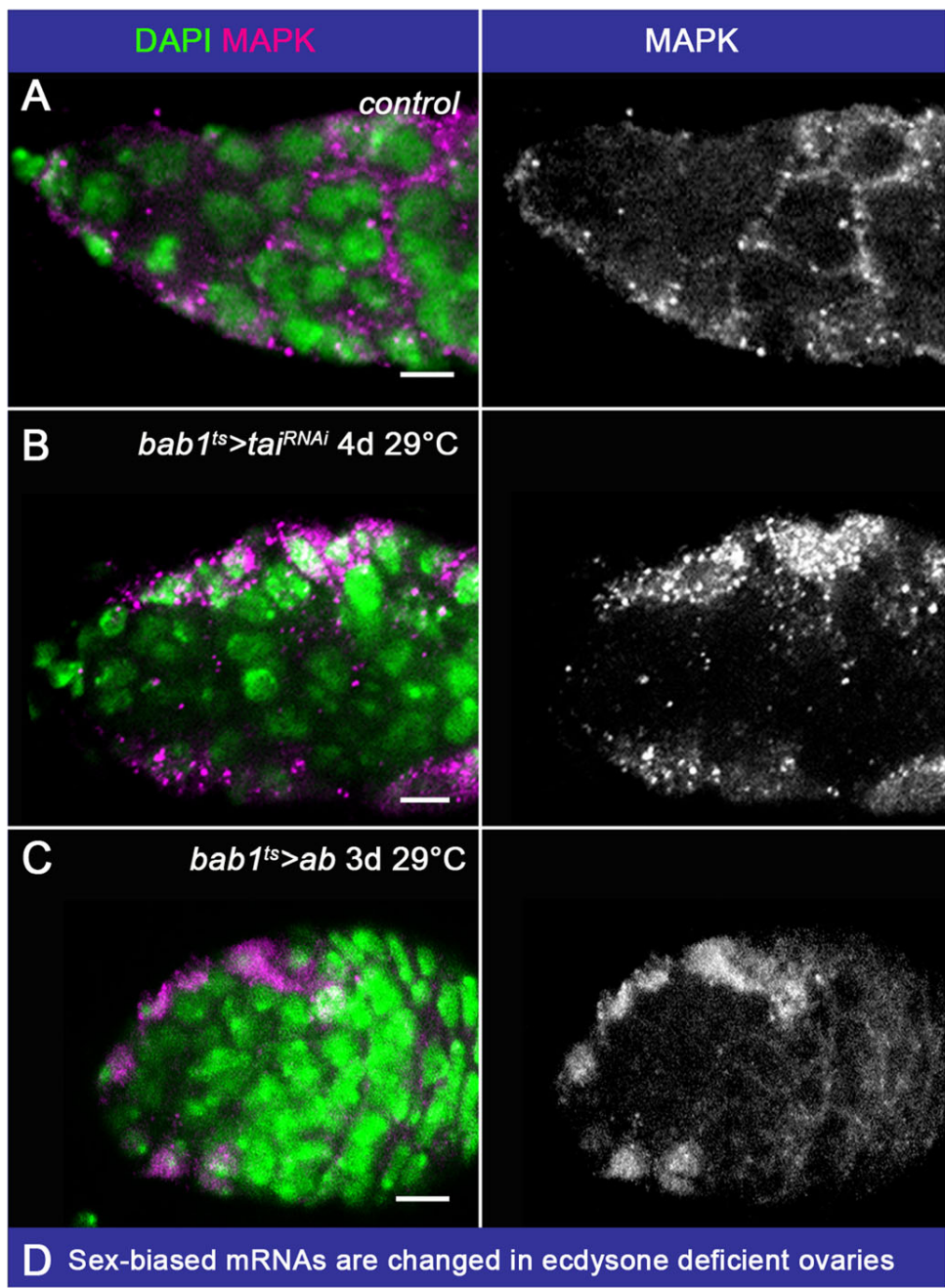
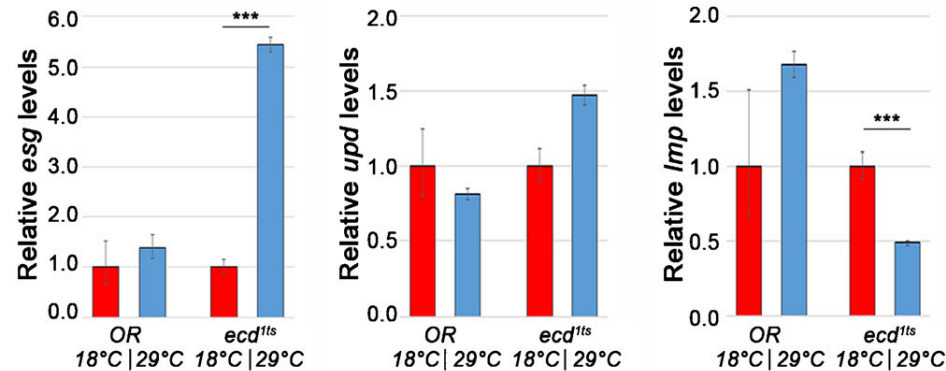


Fig. S3. EC cellular identity is affected upon soma-specific perturbation of ecdysone signaling. (A) ECs form long cytoplasmic protrusions with which they envelope the differentiating germline (control: *tubGal80^{ts}/+; bab1Gal4/+*). (B,C) Somatic alteration of ecdysone signaling during adulthood dampens the ability of ECs to form protrusions. The *Gal4/Gal80^{ts}* system was used to express *tai^{RNAi}* or *ab* using *bab1Gal4* somatic driver in adults (*bab1^{ts}>tai^{RNAi}; tubGal80^{ts}/tai^{RNAi}; bab1Gal4/+*, 4 days at 29°C and *bab1^{ts}>ab; tubGal80^{ts}/+; bab1Gal4/UASab*, 3 days at 29°C). MAP Kinase (MAPK) staining shows cytoplasmic protrusions in ECs (magenta). Note that MAPK levels are increased in ecdysone signaling-deficient ECs (D). Ecdysone signaling affects the maintenance of cellular sexual identity in adult *D. melanogaster* gonads (Fagegaltier et al., 2014) and multiple EGFR-MAPK downstream targets are sexually biased. mRNA levels of direct and indirect EGFR-MAPK signaling pathway downstream targets, *escargot* (*esg*), *unpaired* (*upd*) and *IGF-II mRNA-binding protein* (*Imp*) (López-Onieva et al., 2008; Chau et al., 2009; Toledano et al., 2012) are deregulated. In *ecd^{ts}* germaria, the expression levels of the male-specific mRNA *esg* increase ~5 fold and the mRNA levels of JAK/STAT ligand *upd* ~1.5 fold, while the levels of *Imp* decrease ~2 fold (supplementary material Table S3). These data show that upon defective ecdysone signaling, EGFR signaling is impaired, resulting in confused sexual identity in the somatic cells of the germarium. MAPK staining marks ECs and EC protrusions (magenta, A–C), DAPI marks nuclei (green, A–C). ****p*<0.0005. Scale bars, 5 μm.



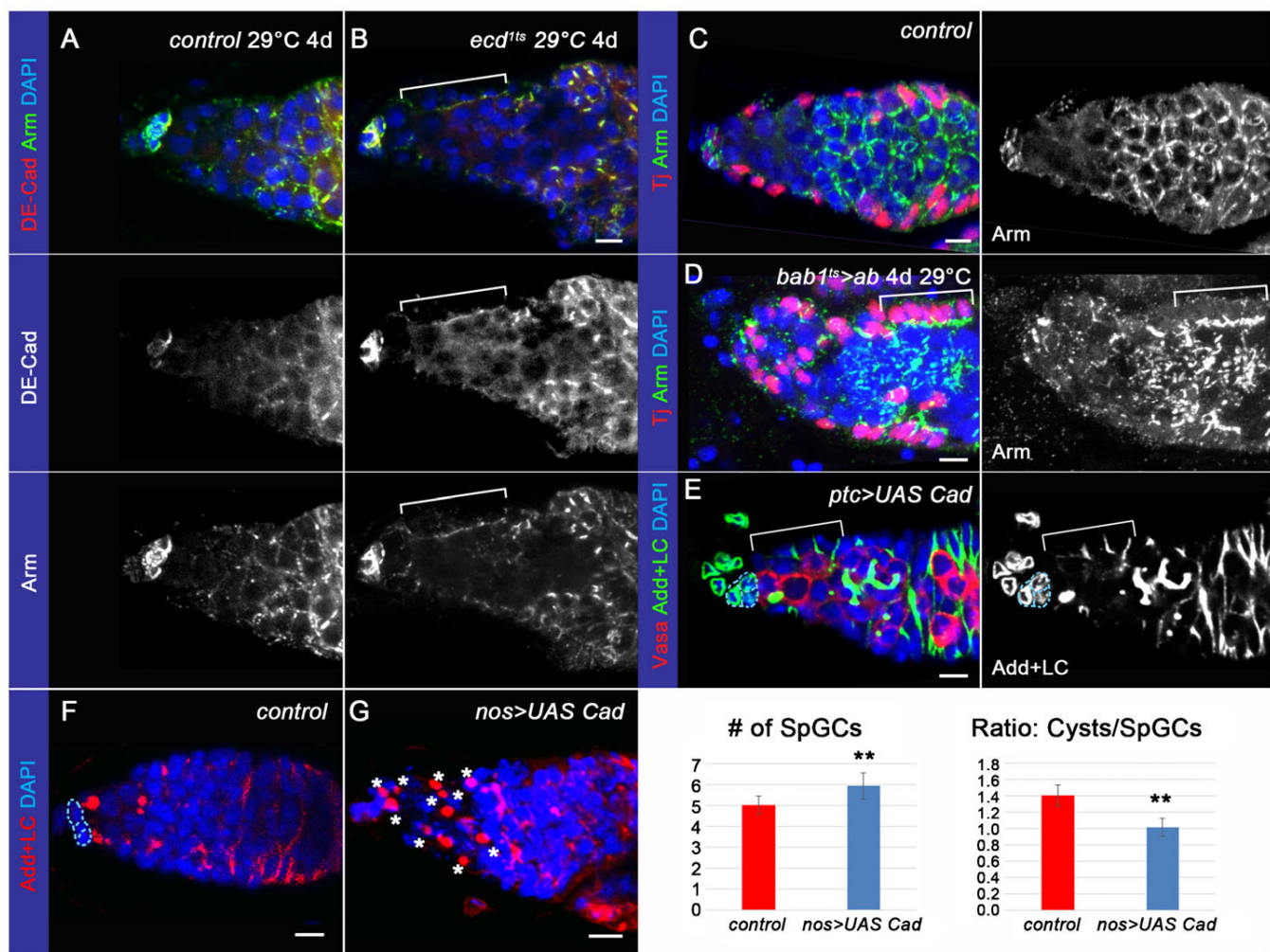


Fig. S4. Soma-specific disruption of ecdysone signaling causes altered cell adhesion between ECs and the germline. (A,B) High levels of the cell adhesion proteins DE-Cad and Arm are detected at the membrane of CpCs (*control: OregonR*). In *ecd^{1ts}* adult flies kept at the restrictive temperature (29°C) for four days, high levels of Arm and DE-Cad are also found on the EC membrane (marked with brackets). (C,D) Downregulation of ecdysone signaling in the soma by overexpressing its negative regulator Ab with the soma-specific driver (*control: tubGal80^{ts}/+*; *bab1Gal4/+* and *bab1^{ts}>ab: tubGal80^{ts}/+*; *bab1Gal4/UASab*, 4 days at 29°C) results in the increased Arm levels in the ECs, atypical ECs form epithelial layers (bracket). (E) Similarly, overexpression of DE-Cad with the somatic driver (*ptc/UAS Cad*) leads to formation of EC epithelial layers (bracket). (F,G) Germline-specific overexpression of Cad (*control: NGT40/+*; *nanosGAL4/+* and *nos>Cad: NGT40/UAS Cad;nanosGAL4/+*) leads to a higher number of SpGCs (asterisks) and an increased Cysts/SpGCs ratio (supplementary material Table S1). Cell adhesion complexes are marked by DE-Cad (red, A,B) and Arm (green, A–D). ECs are positive for Tj (red, C,D) and negative for the germline marker Vasa (red, E). Germaria are stained with LaminC (LC red, F,G, green, E) to visualize TFs and CpCs and Adducin (Add red, F–G, green, E) to mark spectrosomes and fusomes. Nuclei are marked with DAPI (blue, A–E). p-values were calculated using the two tailed Student’s t-test and error bars represent S.E.M., **p<0.005. Scale bars, 5 μ m.

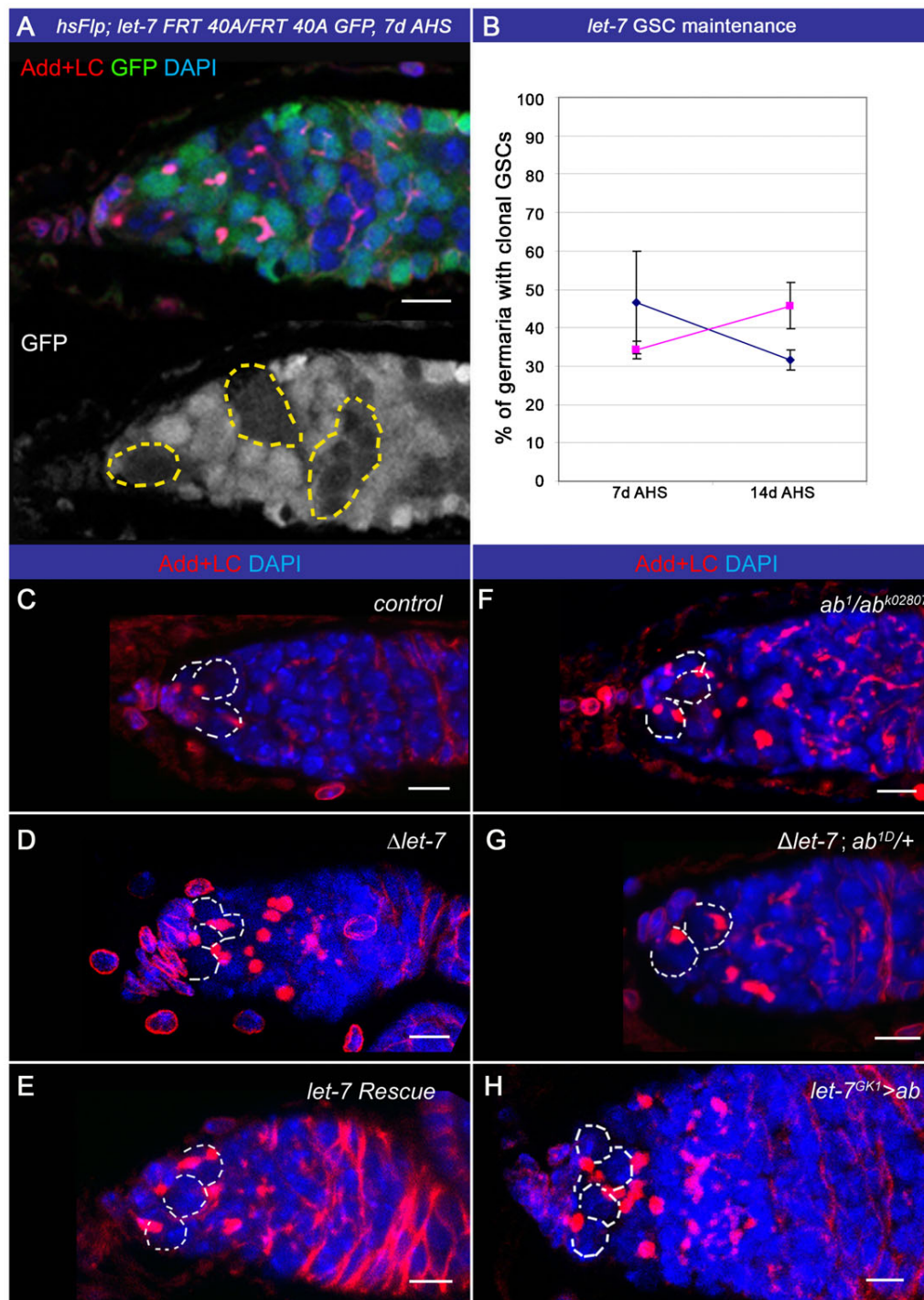


Fig. S5. *let-7* is not required for GSC maintenance, but together with Ab cell non-autonomously influences germline differentiation. (A,B) The *hsFlp/FRT* system for mitotic recombination was used to induce *let-7* mutant germline cells (*hsFlp/+; FRT 40A let-7 miR-125/FRT 40A GFP; let-7-C Δlet-7/+*), clonal cells are marked by the absence of GFP. Parental *FRT 40A* was used as control (*hsFlp/+; FRT 40A/FRT 40A GFP*). *let-7* mutation does not affect the maintenance of GSCs. The percentage of the germaria containing at least one *Δlet-7* clonal GSC did not significantly change with the time ($34.14 \pm 2.24\%$, $n=84$ and $45.69 \pm 6.10\%$, $n=43$ at 7 and 14 days after heat shock, respectively) in comparison to controls ($46.67 \pm 13.33\%$, $n=81$ and $31.71 \pm 2.57\%$, $n=62$ at 7 and 14 days after heat shock, respectively). (C) Wildtype (*OregonR*) germaria contain on average 4 SpGCs (supplementary material Table S2), (D,E) *let-7* mutants (*let-7-C^{GK1}/let-7-C^{KO1}*; *let-7-C^{Δlet-7}/+*) contain a higher number of SpGCs; introducing a *let-7* rescue construct (*let-7-C/+*; *let-7-C^{GK1}/let-7-C^{KO1}*) reverts the phenotype (supplementary material Table S2). (F) Reducing Ab levels by combining hypomorphic and amorphic alleles leads to an increased number of SpGCs (*ab¹/ab^{k02807}*, supplementary material Table S2). (G) The *let-7* mutant phenotype can be partially rescued by reducing *ab* levels [*let-7, miR-125, ab^{1D}/let-7^{KO1}*; *let-7-C^{Δlet-7}/+*, compare to panel D, supplementary material Table S2]. (H) Downregulation of Ab using the somatic *let-7^{GK1} Gal4* driver causes an increased number of SpGCs (*let-7^{GK1}/+; UASab/+*, supplementary material Table S2). Spectrosomes are marked with Adducin (Add, red, A,C–H), CpCs with LaminC (LC, red, A,C–H), nuclei with DAPI (blue, A,C–H), clones with GFP (green, A). Clonal germline cells are outlined in yellow, GSCs are outlined in white. Scale bars, 5 μm.

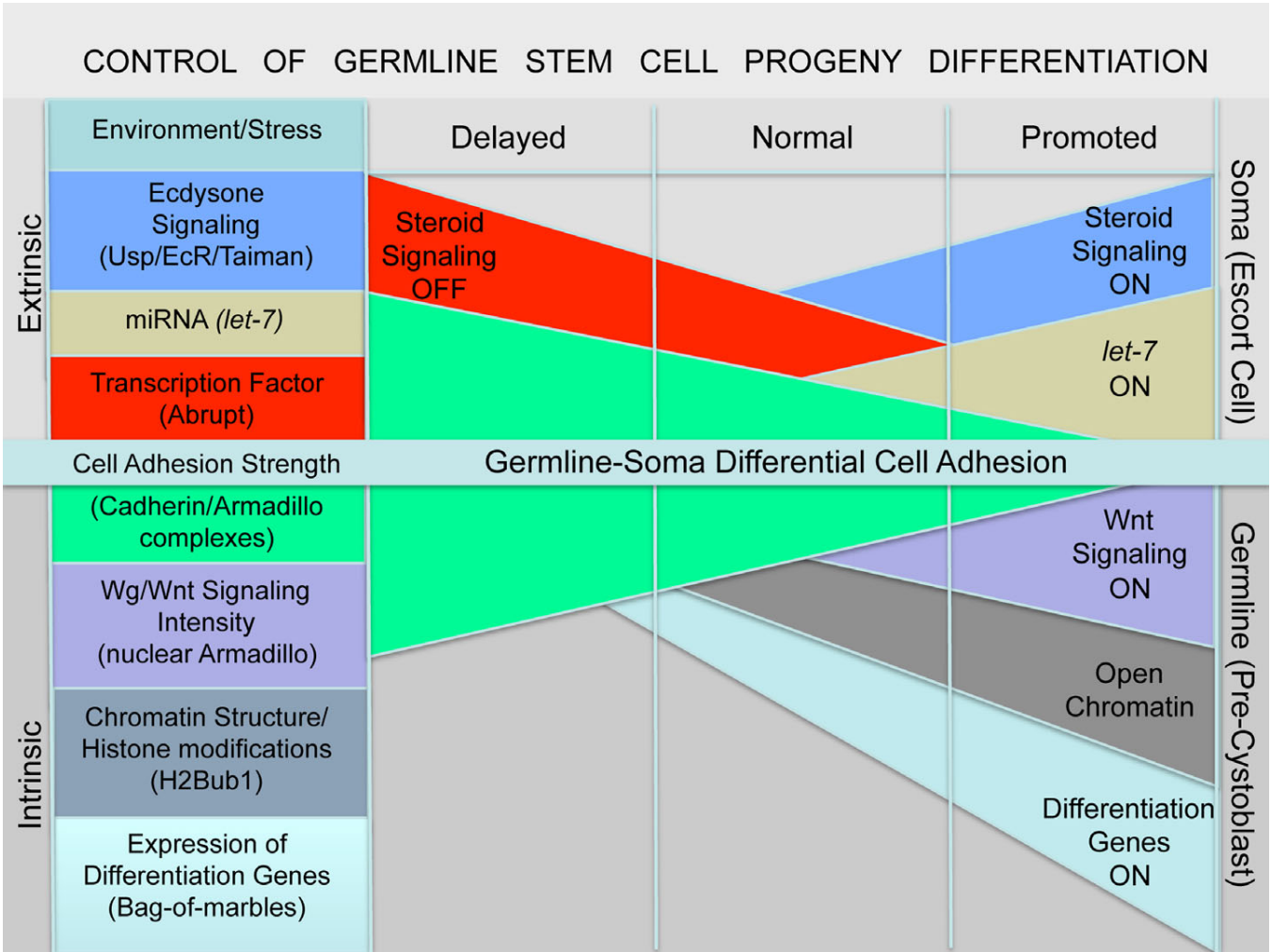


Fig. S6. Scheme of extrinsic and intrinsic signaling controlling early germline differentiation. Control of germline differentiation is highly dependent on precise levels of multiple proteins involved in different signaling pathways that act in the soma and the germline. Ecdysone signaling, miRNA *let-7* and Ab act in the ECs to regulate the adhesion strength between the soma and germline. This, via amounts of Cad/Arm complexes modulates Wg signaling activity in the germline. The Wg pathway establishes specific chromatin status permissive for the differentiation factor Bam expression, leading to GSC progeny differentiation.

Supplementary Table S1. Histone modification (H2Bub1) and ecdysone and Wg signaling defects influence germline differentiation

Genotype, conditions	Spectrosome-containing GCs Ave \pm S.E.M.	Fusome-containing cysts Ave \pm S.E.M.	Ratio fusome-containing cysts / spectrosome-containing GCs Ave \pm S.E.M.	# of analyzed germaria
<i>hsEcR.B1/+</i> , no hs	3.82 \pm 0.48	4.45 \pm 0.21	1.17 \pm 0.05	11
<i>hsEcR.B1/+</i> , 2 x 1h hs at 37°C	7.30 \pm 0.68 ^a ($p=4.63 \times 10^{-4}$)***	1.60 \pm 0.31 ^a ($p=2.18 \times 10^{-7}$)***	^b 0.22 \pm 0.04 ^a ($p=2.98 \times 10^{-11}$)***	10
<i>hsbam/+</i> , no hs	4.73 \pm 0.33	4.82 \pm 0.38	1.02 \pm 0.08	11
<i>hsbam/+</i> , 2 x 1h hs at 37°C	0.64 \pm 0.20 ^a ($p=1.41 \times 10^{-9}$)***	6.55 \pm 0.31 ^a ($p=2.1 \times 10^{-3}$)**	^b 10.29 \pm 0.49 ^a ($p=4.13 \times 10^{-14}$)***	11
<i>hsEcR.B1/+</i> ; <i>hsbam/+</i> , no hs	4.82 \pm 0.44	4.18 \pm 0.26	^b 0.87 \pm 0.05	11
<i>hsEcR.B1/+</i> ; <i>hsbam/+</i> , 2 x 1h hs at 37°C	0.80 \pm 0.25 ^a ($p=3.05 \times 10^{-7}$)*** ^c ($p=4.96 \times 10^{-8}$)*** ^d ($p=0.61$)	4.50 \pm 0.31 ^a ($p=0.44$) ^c ($p=2.82 \times 10^{-6}$)*** ^d ($p=1.73 \times 10^{-4}$)***	^b 5.63 \pm 0.38 ^a ($p=7.94 \times 10^{-11}$)*** ^c ($p=4.12 \times 10^{-11}$)*** ^d ($p=5.51 \times 10^{-7}$)***	10
<i>control: nos/+</i> (<i>NGT40/+</i> ; <i>nanosGAL4/+</i>), exp 1	4.90 \pm 0.25	6.11 \pm 0.21	1.26 \pm 0.12	15
<i>nos>Bre1^{RNAi}</i> (<i>NGT40/+</i> ; <i>nanosGAL4/Bre^{RNAi}</i>)	4.80 \pm 0.30 ^e ($p=8.01 \times 10^{-1}$)	4.37 \pm 0.27 ^e ($p=1.78 \times 10^{-5}$)***	0.91 \pm 0.09 ^e ($p=0.02$)*	15
<i>Bre1^{P1549/+}</i>	5.13 \pm 0.31	5.27 \pm 0.15	1.06 \pm 0.05	15
<i>EcR^{Q50st/+}</i>	5.40 \pm 0.49	4.33 \pm 0.25	0.89 \pm 0.09	15
<i>Bre1^{P1549}/EcR^{Q50st}</i>	8.67 \pm 0.91 ^f ($p=1.02 \times 10^{-3}$)** ^g ($p=3.80 \times 10^{-3}$)**	3.87 \pm 0.31 ^f ($p=3.35 \times 10^{-4}$)*** ^g ($p=0.25$)	0.52 \pm 0.07 ^f ($p=1.54 \times 10^{-6}$)*** ^g ($p=3.71 \times 10^{-3}$)**	12
<i>nos>fz^{RNAi}</i> (<i>NGT40/fz^{RNAi}</i> ; <i>nanosGAL4/+</i>)	5.59 \pm 0.41 ^e ($p=0.12$)	5.76 \pm 0.32 ^e ($p=0.037$)	1.15 \pm 0.13 ^e ($p=0.59$)	17
<i>nos>sgg^{RNAi}</i> (<i>NGT40/sgg^{RNAi}</i> ; <i>nanosGAL4/+</i>)	4.77 \pm 0.47 ^e ($p=0.72$)	7.38 \pm 0.42 ^e ($p=7.43 \times 10^{-3}$)*	1.67 \pm 0.13 ^e ($p=0.02$)*	13
<i>nos>arm</i> (<i>NGT40/UASarm</i> ; <i>nanosGAL4/+</i>)	4.93 \pm 0.21 ^e ($p=0.96$)	10.25 \pm 0.29 ^e ($p=3.37 \times 10^{-13}$)***	2.17 \pm 0.10 ^e ($p=2.98 \times 10^{-7}$)***	28
<i>nos>arm^{RNAi}</i> (<i>NGT40/arm^{RNAi}</i> ; <i>nanosGAL4/+</i>)	6.38 \pm 0.46 ^e ($p=0.01$)*	ⁱ n. d.	ⁱ n. d.	8

Supplementary Table S1. continued

<i>nos>Cad^{RNAi}</i> (<i>NGT40/+;</i> <i>nanosGAL4/Cad^{RNAi}</i>)	4.00±0.58 ^e (p=0.09)	6.89±0.82 ^e (p=0.25)	1.85±0.24 ^e (p=0.02)*	9
<i>nos>pan^{RNAi}</i> (<i>NGT40/pan^{RNAi};</i> <i>nanosGAL4/+</i>)	5.75±0.36 ^e (p=0.07)	7.00±0.35 ^e (p=0.04)*	1.34±0.10 ^e (p=0.61)	16
<i>control: nos/+</i> (<i>NGT40/+;</i> <i>nanosGAL4/+</i>), exp 2	5.00±0.43	5.85±0.36	1.40±0.13	13
<i>nos>Cad</i> (<i>NGT40/UASp Cad;</i> <i>nanosGAL4/+</i>)	5.93±0.64 ^h (p=2.85x10 ⁻³)**	5.73±0.40 ^h (p=0.73)	1.01±0.11 ^h (p=1.16x10 ⁻³)**	15

p-values were calculated using the two tailed Student's t-test. *p<0.05,

p<0.005, *p<0.0005;

a: compared to the respective genotype without hs;

b: since individual germaria displayed 0 single spectrosome cells, the ratio was calculated by dividing the average number of cysts by the average number of single spectrosome cells;

c: compared to *hsEcR.B1/+*; 2 x 1h hs at 37°C;

d: compared to *hsbam/+*; 2 x 1h hs at 37°C;

e: compared to *control: nos/+*, exp 1;

f: compared to *Brel^{P1549}/+*;

g: compared to *EcR^{Q50st}/+*;

h: compared to *control: nos/+*, exp 2;

i: was not determined (n. d.) due to strong phenotypic abnormalities, making it impossible to determine proper regions in the mutant germaria.

Supplementary Table S2. The speed of germline stem cell progeny differentiation depends on the levels of *let-7*, its target *Abrupt*, and the cell adhesion proteins, *DE-Cad* and *Arm*

Genotype	Spectrosome containing GCs Ave ± S.E.M.	Ratio fusome- containing cysts / spectrosome- containing GCs Ave ± S.E.M.	# of analyzed germaria
<i>control:</i> <i>ab¹/+</i>	4.23±0.32	1.04±0.10	13
<i>ab¹/ab^{k02807}</i>	6.00±0.63 ^a (<i>p</i> =1.21 x 10 ⁻²)*	0.65±0.08 ^a (<i>p</i> =1.58 x 10 ⁻²)*	8
<i>ab¹/ab^{1D}</i>	5.50±0.52 ^a (<i>p</i> =5.91 x 10 ⁻²)	0.78±0.12 ^a (<i>p</i> =1.35 x 10 ⁻¹)	16
<i>control: ab^{RNAi}/+,</i> 7d at 29°C	5.33±0.40	0.85±0.11	12
<i>ptc^{ts}>ab^{RNAi}</i> (<i>ptcGal4/ab^{RNAi}</i> ; <i>tubGal80^{ts}/+</i>), 7d at 29°C	6.90±0.55 ^b (<i>p</i> =2.36 x 10 ⁻⁴)*	0.71±0.07 ^b (<i>p</i> =2.09 x 10 ⁻²)*	10
<i>bab1^{ts}>ab^{RNAi}</i> (<i>tubGal80^{ts}/ab^{RNAi}</i> ; <i>bab1Gal4/+</i>), 7d at 29°C	5.44±0.38 ^b (<i>p</i> =2.46 x 10 ⁻²)*	0.79±0.12 ^b (<i>p</i> =1.43 x 10 ⁻¹)	9
<i>let-7-C^{GK1}/+, exp 1,</i> 7d at 29°C	5.38±0.30	1.21±0.07	16
<i>let-7-C^{GK1}ts>ab</i> (<i>let-7-C^{GK1}/+;</i> <i>tubGal80^{ts}/UASab</i>), 7d at 29°C	6.78±0.43 ^c (<i>p</i> =1.40 x 10 ⁻²)*	0.75±0.07 ^c (<i>p</i> =7.83 x 10 ⁻⁵)*	18
<i>ptc^{ts}>ab</i> (<i>ptcGal4/+</i> ; <i>tubGal80^{ts}/UASab</i>), 7d at 29°C	7.67±1.21 ^c (<i>p</i> =2.87 x 10 ⁻²)*	0.79±0.18 ^c (<i>p</i> =1.61 x 10 ⁻²)*	9
<i>control:</i> <i>w¹¹¹⁸-</i>	4.28±0.25	1.31±0.10	29
<i>let-7-C^{GK1}/+,</i> exp 2	5.61±0.23 ^d (<i>p</i> =2.49 x 10 ⁻⁴)*	1.05±0.07 ^d (<i>p</i> =3.64 x 10 ⁻²)*	28
<i>let-7^{K01}/+</i>	5.14±0.22 ^d (<i>p</i> =1.57 x 10 ⁻²)*	0.93±0.06 ^d (<i>p</i> =4.59 x 10 ⁻³)*	22
Δ <i>let-7</i> (<i>let-7-C^{GK1}/let-7-C^{K01}</i> ; <i>let-</i> <i>7-C^{Δlet-7}/+</i>), exp 2	6.79±0.25 ^d (<i>p</i> =2.78 x 10 ⁻⁵)* ^e (<i>p</i> =1.46 x 10 ⁻¹) ^f (<i>p</i> =2.50 x 10 ⁻²)*	0.55±0.03 ^d (<i>p</i> =6.01 x 10 ⁻¹³)* ^e (<i>p</i> =2.03 x 10 ⁻¹⁰)* ^f (<i>p</i> =8.20 x 10 ⁻⁸)*	52

Supplementary Table S2. continued

<i>let-7 Rescue</i> (<i>let-7-C</i> /+; <i>let-7-C^{GK1}/let-7-C^{KO1}</i>)	4.90±0.31 ^d (p=0.11) ^e (p=0.06) ^f (p=0.53) ^g (p=1.19 x 10 ⁻²)*	1.43±0.14 ^d (p=0.47) ^e (p=9.09 x 10 ⁻³)* ^f (p=1.38 x 10 ⁻³)** ^g (p=1.10 x 10 ⁻¹² ***)	20
Δ <i>let-7</i> (<i>let-7, miR-125/let-7^{KO1}</i> ; <i>let-7-C^{Δlet-7}/+</i>), exp 3	6.58±0.37	0.67±0.04	26
Δ <i>let-7, ab</i> reduced (<i>let-7, miR-125, ab^{1D}</i> / <i>let-7^{KO1}; let-7-C^{Δlet-7}/+</i>)	4.94±0.22 ^h (p=2.24 x 10 ⁻⁴ ***)	0.94±0.05 ^h (p=8.77 x 10 ⁻⁵ ***)	31
<i>w¹¹¹⁸</i> ; <i>hs-Gal4- usp.LBD</i> /+, 4 x 1h hs at 37°C	6.62±0.33	0.62±0.08	13
<i>w¹¹¹⁸</i> ; <i>hs-Gal4- EcR.LBD</i> /+, 4 x 1h hs at 37°C	6.00±0.27	0.57±0.08	16
<i>shg^{E17B}</i> /+, 4 x 1h hs at 37°C	4.92±0.58	1.14±0.11	13
<i>w¹¹¹⁸</i> ; <i>hs-Gal4-usp.LBD</i> / <i>shg^{E17B}</i> , 4 x 1h hs at 37°C	4.57±0.45 ⁱ (p=2.17 x 10 ⁻³)** ^k (p=0.47)	1.17±0.20 ⁱ (p=8.52 x 10 ⁻³)* ^k (p=0.83)	8
<i>arm²</i> /+, 4 x 1h hs at 37°C	4.31±0.31	1.38±0.15	13
<i>w¹¹¹⁸</i> ; <i>hs-Gal4-usp.LBD/arm²</i> , 4 x 1h hs at 37°C	4.90±0.35 ⁱ (p=2.26 x 10 ⁻³)** ^l (p=0.25)	1.08±0.07 ⁱ (p=1.34 x 10 ⁻⁴ ***) ^l (p=4.60 x 10 ⁻²)*	20
<i>w¹¹¹⁸</i> ; <i>hs-Gal4-EcR.LBD/arm²</i> , 4 x 1h hs at 37°C	5.54±0.40 ^m (p=0.33) ^l (p=2.29 x 10 ⁻²)*	0.90±0.11 ^m (p=2.81 x 10 ⁻²)* ^l (p=2.43 x 10 ⁻²)*	13

p-values were calculated using the two tailed Student's t-test. *p<0.05, **p<0.005, ***p<0.0005

Compared to:

a: *ab¹/+*;

b: control: *ab^{RNAi}/+*;

c: *let-7-C^{GK1}Gal4*/+, exp 1;

d: *w¹¹¹⁸*;

e: *let-7-C^{GK1}Gal4*/+, exp 2;

f: *let-7^{KO1}/+*;

g: Δ *let-7* (*let-7-C^{GK1}Gal4/let-7-C^{KO1}*; *let-7C Δ let-7*/+), exp 2;

h: Δ *let-7* (*let-7, miR-125/let-7-C^{KO1}*; *let-7C Δ let-7*/+), exp 3;

i: *w¹¹¹⁸*; *hs-Gal4-usp.LBD*/+; 4 x 1h hs at 37°C, exp 1;

k: *shg^{E17B}*/+;

l: *arm²/+*; 4 x 1h hs at 37°C;

m: *w¹¹¹⁸*; *hs-Gal4-EcR.LBD*/+; 4 x 1h hs at 37°C.

Supplementary Table S3. mRNA levels measured by RT-qPCR in *control* and adult-induced *ecdysoneless* mutant

Genotype, conditions	$C_T^{ab} \pm \text{StDev}$	$C_T^{RpL32} \pm \text{StDev}$	ΔC_T ($\Delta C_T^{ab} - \Delta C_T^{RpL32}$) ^a	$\Delta \Delta C_T \pm \text{StDev}$ ($\Delta C_T^{ab} - \Delta C_T^{\text{control}}$) ^b	Fold Difference ^c
<i>OregonR</i> germaria 4d at 18°C (control)	31.20±0.13	15.62±0.05	15.57±0.14	0.00±0.14	1.00 (0.91-1.09)
<i>OregonR</i> germaria 4d at 29°C	29.87±0.01	15.62±0.07	14.25±0.07	-1.33±0.07	2.51 (2.39-2.63) ^d (p=4.45×10 ⁻³) ^{**}
<i>ecd^{lts}</i> germaria 4d at 18°C	29.63±0.30	15.52±0.19	14.11±0.36	-1.46±0.36	2.76 (2.16-3.53)
<i>ecd^{lts}</i> germaria 4d at 29°C	28.03±0.17	15.84±0.08	12.19±0.18	-3.38±0.18	10.44 (9.19-11.86) ^d (p=1.57×10 ⁻⁴) [*] ^e (p=6.55×10 ⁻⁴) ^{***}
Genotype, conditions	$C_T^{arm} \pm \text{StDev}$	$C_T^{RpL32} \pm \text{StDev}$	ΔC_T ($\Delta C_T^{arm} - \Delta C_T^{RpL32}$) ^a	$\Delta \Delta C_T \pm \text{StDev}$ ($\Delta C_T^{arm} - \Delta C_T^{\text{control}}$) ^b	Fold Difference ^c
<i>OregonR</i> germaria 4d at 29°C	18.78±0.08	13.55±0.36	5.23±0.37	0.00±0.37	1.00 (0.77-1.29)
<i>ecd^{lts}</i> germaria 4d at 29°C	19.05±0.02	14.78±0.09	4.27±0.10	-0.96±0.10	1.95 (1.82-2.08) ^d (p=4.23×10 ⁻⁵)
Genotype, conditions	$C_T^{esg} \pm \text{StDev}$	$C_T^{RpL32} \pm \text{StDev}$	ΔC_T ($\Delta C_T^{esg} - \Delta C_T^{RpL32}$) ^a	$\Delta \Delta C_T \pm \text{StDev}$ ($\Delta C_T^{esg} - \Delta C_T^{\text{control}}$) ^b	Fold Difference ^c
<i>OregonR</i> germaria 4d at 18°C	32.83±0.50	10.15±0.32	22.67±0.59	0.00±0.59	1.00 (0.66-1.51)
<i>OregonR</i> germaria 4d at 29°C	32.48±0.24	10.28±0.07	22.20±0.25	-0.47±0.25	1.39 (1.17-1.64) ^d (p=0.23)
<i>ecd^{lts}</i> germaria 4d at 18°C	31.26±0.15	10.53±0.13	20.72±0.20	0.00±0.20	1.00 (0.87-1.14)
<i>ecd^{lts}</i> germaria 4d at 29°C	27.44±0.03	9.16±0.03	18.28±0.04	-2.44±0.04	5.43 (5.28-5.59) ^d (p=9.24×10 ⁻⁶) ^{***}

Supplementary Table S3. continued

Genotype, conditions	C_T <i>upd</i> ± StDev	C_T <i>RpL32</i> ± StDev	ΔC_T (ΔC_T <i>upd</i> - ΔC_T <i>RpL32</i>) ^a	$\Delta\Delta C_T \pm \text{StDev}$ ($\Delta C_T - \Delta C_T^{\text{control}}$) ^b	Fold Difference ^c
<i>OregonR</i> germaria 4d at 18°C	23.46±0.01	10.15±0.32 ^f	13.31±0.32	0.00±0.32	1.00 (0.80-1.24)
<i>OregonR</i> germaria 4d at 29°C	23.88±0.01	10.28±0.07 ^f	13.60±0.07	0.30±0.07	0.81 (0.78-0.86) ^d (p=0.42)
<i>ecd^{lts}</i> germaria 4d at 18°C	24.31±0.08	10.53±0.13 ^f	13.78±0.16	0.00±0.16	1.00 (0.90-1.11)
<i>ecd^{lts}</i> germaria 4d at 29°C	22.37±0.06	9.16±0.03 ^f	13.22±0.06	-0.56±0.06	1.48 (1.41-1.54) ^d (p=0.22)
Genotype, conditions	C_T <i>Imp</i> ± StDev	C_T <i>RpL32</i> ± StDev	ΔC_T (ΔC_T <i>Imp</i> - ΔC_T <i>RpL32</i>) ^a	$\Delta\Delta C_T \pm \text{StDev}$ ($\Delta C_T - \Delta C_T^{\text{control}}$) ^b	Fold Difference ^c
<i>OregonR</i> germaria 4d at 18°C	17.95±0.50	10.15±0.32 ^f	7.80±0.59	0.00±0.59	1.00 (0.67-1.50)
<i>OregonR</i> germaria 4d at 29°C	17.33±0.01	10.28±0.07 ^f	7.06±0.07	-0.74±0.07	1.68 (1.60-1.76) ^d (p=0.14)
<i>ecd^{lts}</i> germaria 4d at 18°C	22.48±0.01	10.53±0.13 ^f	11.95±0.13	0.00±0.13	1.00 (0.91-1.10)
<i>ecd^{lts}</i> germaria 4d at 29°C	22.14±0.03	9.16±0.03 ^f	12.99±0.04	1.04±0.04	0.49 (0.47-0.50) ^d (p=1.69×10 ⁻⁵)

a: ΔC_T was determined by subtracting the average *RpL32* C_T value from the average experimental C_T value. The standard deviation of the difference is calculated from the standard deviation of the control and experimental values using the formula $s = \sqrt{(s_1^2 + s_2^2)}$, where s = standard deviation.

b: $\Delta\Delta C_T$ is calculated by subtracting the ΔC_T calibrator value (ΔC_T of the respective *OregonR*). The standard deviation is the same as for ΔC_T .

c: The range of *arm*, *ab*, *esg*, *Upd* or *Imp* is calculated by: $2^{-\Delta\Delta C_T}$ with $\Delta\Delta C_T + s$ and $\Delta\Delta C_T - s$, where s is the standard deviation of $\Delta\Delta C_T$ value.

d, e: ΔC_T values of technical replicates are compared to *OregonR* germaria, 4d at 18°C (d) or *ecd^{lts}* germaria, 4d at 18°C (e).

f: *esg*, *upd* and *Imp* levels were measured in the same sample, thus, the same endogenous *RpL32* control was used. p-values were calculated using the two tailed Student's t-test. *p<0.05, **p<0.005, ***p<0.0005

Supplementary Table S4. *let-7* levels vary upon different environmental conditions

Genotype, conditions, age		$C_T^{let-7} \pm StDev$	$C_T^{S2} \pm StDev$	ΔC_T ($\Delta C_T^{let-7} - \Delta C_T^{S2}$) ^a	$\Delta \Delta C_T \pm StDev$ ($\Delta C_T - \Delta C_T^{control}$) ^b	Ave $\Delta \Delta C_T \pm StDev$	Fold Difference ^c
control: <i>OregonR</i> , Rich food, 2 days	Exp1	25.33±0.30	6.14±0.24	19.19±0.39	0.00±0.39	0.00±0.32	1.00 (0.80-1.25)
	Exp2	26.35±0.29	8.29±0.37	18.06±0.47	0.00±0.47		
	Exp3	28.80±0.34	6.61±0.09	22.19±0.35	0.00±0.35		
	Exp4	27.15±0.39 x10 ⁻⁴	6.89±0.09	20.26±0.09	0.00±0.19		
<i>OregonR</i> , Poor food, 2 days	Exp1	27.06±0.41	7.40±0.29	20.20±0.50	1.01±0.50	-0.40±0.30	1.32 (1.07-1.63)
	Exp2	26.32±0.28	7.96±0.05	18.36±0.29	0.30±0.29		
	Exp3	26.60±0.08	6.28±0.30	20.32±0.31	-1.87±0.31		
	Exp4	25.89±0.09	6.68±0.08	19.22±0.12	-1.04±0.12		
<i>OregonR</i> , 21 days	Exp1	24.32±0.06	6.31±3.46 x10 ⁻³	18.00±0.06	-1.19±0.06	-1.09±0.07	2.12 (2.02-2.22) (p=0.01) [*]
	Exp2	24.96±0.06	7.89±0.04	17.08±0.08	-0.98±0.08		
Genotype, conditions, age		$C_T^{let-7} \pm StDev$	$C_T^{RpL32} \pm StDev$	ΔC_T ($\Delta C_T^{let-7} - \Delta C_T^{RpL32}$) ^a	$\Delta \Delta C_T \pm StDev$ ($\Delta C_T - \Delta C_T^{control}$) ^d	Fold Difference ^c	
control: <i>OregonR</i> , 18°C, 4d		24.33±0.07	16.45±0.25	7.88±0.26	0.00±0.26	1.00 (0.84-1.20)	
<i>OregonR</i> , 29°C, 4d		23.64±0.08	17.21±0.50	6.44±0.50	-1.44±0.50	2.72 (1.92-3.85) (p=5.22x10 ⁻⁴) ^{***}	

p-values were calculated using the two tailed Student's t-test. *p<0.05, **p<0.005, ***p<0.0005;

a: ΔC_T was determined by subtracting the average control C_T value from the average *let-7* C_T value. The standard deviation of the difference is calculated from the standard deviation of the *let-7* and control values using the formula $s = \sqrt{(s_1^2 + s_2^2)}$, where s = standard deviation.

b: $\Delta \Delta C_T$ is calculated by subtracting the ΔC_T calibrator value (ΔC_T of the control: flies 2 days kept on rich food). The standard deviation is the same as for ΔC_T .

c: the range of *let-7* is calculated by: $2^{-\Delta \Delta C_T}$ with $\Delta \Delta C_T + s$ and $\Delta \Delta C_T - s$, where s is the standard deviation of $\Delta \Delta C_T$ value.

d: $\Delta \Delta C_T$ is calculated by subtracting the ΔC_T calibrator value (ΔC_T of the control: flies kept on 18°C). The standard deviation is the same as for ΔC_T . The fold difference of the experimental values was compared to the respective control.

Supplementary Table S5. The efficiency of downregulation of Wg signaling components in the germline by used RNAi mutants

Genotype	$C_T^{sgg} \pm \text{StDev}$	$C_T^{RpL32} \pm \text{StDev}$	ΔC_T ($\Delta C_T^{sgg} - \Delta C_T^{RpL32}$) ^a	$\Delta \Delta C_T \pm \text{StDev}$ ($\Delta C_T - \Delta C_T^{\text{control}}$) ^b	Fold Difference ^c
<i>control: w¹¹¹⁸</i>	19.35±0.08	15.89±0.04	3.45±0.09	0.00±0.09	1.00 (0.94-1.06)
<i>nos>sgg^{RNAi}</i> (<i>NGT40/sgg^{RNAi}</i> ; <i>nanosGAL4/+</i>)	19.95±0.05	15.31±0.08	4.64±0.10	1.19±0.10	0.44 (0.41-0.47)
Genotype	$C_T^{pan} \pm \text{StDev}$	$C_T^{RpL32} \pm \text{StDev}$	ΔC_T ($\Delta C_T^{pan} - \Delta C_T^{RpL32}$) ^a	$\Delta \Delta C_T \pm \text{StDev}$ ($\Delta C_T - \Delta C_T^{\text{control}}$) ^b	Fold Difference ^c
<i>control: w¹¹¹⁸</i>	19.85±0.13	15.89±0.04 ^d	3.96±0.14	0.00±0.14	1.00 (0.91-1.1)
<i>nos>pan^{RNAi}</i> (<i>NGT40/pan^{RNAi}</i> ; <i>nanosGAL4/+</i>)	23.74±0.01	14.75±0.00	8.99±0.01	5.04±0.01	0.03 (0.03-0.31)
Genotype	$C_T^{fz} \pm \text{StDev}$	$C_T^{RpL32} \pm \text{StDev}$	ΔC_T ($\Delta C_T^{fz} - \Delta C_T^{RpL32}$) ^a	$\Delta \Delta C_T \pm \text{StDev}$ ($\Delta C_T - \Delta C_T^{\text{control}}$) ^b	Fold Difference ^c
<i>control: w¹¹¹⁸</i>	22.33±0.04	15.89±0.04 ^d	6.44±0.06	0.00±0.06	1.00 (0.96-1.04)
<i>nos>fz^{RNAi}</i> (<i>NGT40/fz^{RNAi}</i> ; <i>nanosGAL4/+</i>)	24.49±0.09	15.09±0.01	9.40±0.09	2.96±0.09	0.13 (0.12-0.14)

a: ΔC_T was determined by subtracting the average *RpL32* C_T value from the average experimental C_T value. The standard deviation of the difference is calculated from the standard deviation of the control and experimental values using the formula $s = \sqrt{(s_1^2 + s_2^2)}$, where s = standard deviation.

b: $\Delta \Delta C_T$ is calculated by subtracting the ΔC_T calibrator value (ΔC_T of the respective *w¹¹¹⁸*). The standard deviation is the same as for ΔC_T .

c: The range of *sgg*, *pan* and *fz* is calculated by: $2^{-\Delta \Delta C_T}$ with $\Delta \Delta C_T + s$ and $\Delta \Delta C_T - s$, where s is the standard deviation of $\Delta \Delta C_T$ value.

d: *sgg*, *pan* and *fz* mRNA levels were measured in the same sample, thus, the same endogenous *RpL32* control was used.

Supplementary Table S6. Germline-specific clones of Bre1 and Wg signaling components result in differentiation defects

Genotype	Germaria containing GFP ⁺ clonal germline cells				
	GSC maintenance		GSC progeny differentiation status		
	with clonal GSCs	without clonal GSCs	with clonal cysts delayed in differentiation	with clonal cysts prematurely differentiated	n
<i>control</i> (<i>hsFlp; FRT 2A parental/ FRT 2A GFP</i>)	79.17%	20.83%	4.16%	0.00%	24
<i>Bre1</i> (<i>hsFlp; FRT 2A Bre1^{P1549}/ FRT 2A GFP</i>)	35.00%	65%	20.00%	0.00%	20
<i>control</i> (<i>FRT 101 parental/ FRT 101 GFP; hsFlp/+</i>)	71.43%	28.57%	0.00%	0.00%	28
<i>arm²</i> (<i>FRT 101 arm²/ FRT 101 GFP; hsFlp/+</i>)	72.23%	27.77%	5.55%	0.00%	18
<i>arm³</i> (<i>FRT 101 arm³/ FRT 101 GFP; hsFlp/+</i>)	29.17%	70.83%	12.5%	0.00%	24
<i>sgg</i> (<i>FRT 101 sgg^{D127}/ FRT 101 GFP; hsFlp/+</i>)	50.00%	50.00%	3.12%	46.87%	32

Differentiation status of clonal mutant cysts (GFP⁺) was characterized based on fusome morphology and number of cells in the cyst; cysts were defined as delayed in differentiation if the neighboring non-clonal cysts were of a later differentiation stage; cysts were defined as prematurely differentiated if the neighboring non-clonal cysts were of an earlier differentiation stage. In order to analyze the significance between the frequencies of the differentiation stages of clonal germline cells of different genotypes two-way tables and χ^2 test were used. The obtained χ^2 equals to 68.49, which is greater than the critical value of 18.30, suggesting that there is significant evidence to reject the null hypothesis. This signifies that there indeed is a relationship between the row and the column variables.

Acknowledgments

I would like to express my special appreciation and thanks to my supervisor PD Dr. Halyna Shcherbata for giving me the exciting opportunity to join her group and work on this project. Your constant support and advice were priceless.

The helpful questions, discussion and ideas provided by my thesis committee members Prof. Dr. Andreas Wodarz and Prof. Dr. Jörg Großhans were of great value for developing the project.

Furthermore, I would like to thank Prof. Dr. Steven Johnsen and Dr. Delphine Fagegaltier for fruitful collaborations.

In addition, I would like to thank all present and former members of the Gene expression and signaling group and the members of the Jäckle Department for the great working atmosphere and the valuable discussions. I also wish to acknowledge the following people who helped during lab rotations, internships and bachelor work: Eva Maj, Lena Musiol, Olena Zaitseva, Isabel Grafl, Naomi Latorraca, Kate Bredbenner, Alexander König and Alexander Santel.

I also would like to thank the Göttingen Graduate School for Neurosciences, Biophysics and Molecular Biosciences (GGNB) for their support throughout the course of my studies.

Special thanks go to my wonderful family, especially my parents and my husband for their continuous support, encouragement and patience throughout the last years. Thank you so much!

EDUCATION PhD student in the Max Planck Research Group of Oct 2009 until present
Gene Expression and Signaling

Diploma of Biology, Friedrich-Schiller University (Grade A) Oct 2003 - Sep 2009

PUBLICATIONS

- König A, Yatsenko AS, Weiss M, Shcherbata HR. Ecdysteroids affect *Drosophila* ovarian stem cell niche formation and early germline differentiation. *EMBO J.* 2011 Apr 20;30(8):1549-62. doi: 10.1038/emboj.2011.73. Epub 2011 Mar 18
- Karpiuk O, Najafova Z, Kramer F, Hennion M, Galonska C, **König A**, Snaidero N, Vogel T, Shchebet A, Begus-Nahrman Y, Kassem M, Simons M, Shcherbata H, Beissbarth T, Johnsen SA. The histone H2B monoubiquitination regulatory pathway is required for differentiation of multipotent stem cells. *Mol Cell.* 2012 Jun 8;46(5):705-13. doi: 10.1016/j.molcel.2012.05.022
- König A, Shcherbata HR. Visualization of adult stem cells within their niches using the *Drosophila* germline as a model system. *Methods Mol Biol.* 2013;1035:25-33. doi: 10.1007/978-1-62703-508-8 3
- Fagegaltier D, **König A**, Gordon A, Lai EC, Gingeras TR, Hannon GJ, Shcherbata HR. Sexually dimorphic expression and functions of *Drosophila* miRNAs. Manuscript is revised by "Genetics".
- König A, Shcherbata HR. Stress-related soma-germline communication is conveyed via cell adhesion-mediated steroid-Wingless signaling cascade. Manuscript in preparation.

CONFERENCE PRESENTATIONS

- EMBO/EMBL Symposium: The non-coding genome. Heidelberg, Germany, 2010 (poster presentation)
- Steroid hormone ecdysone signaling is required cell non-autonomously for germline differentiation. Annual *Drosophila* Research Conference, San-Diego, USA 2010 (short talk)
- Steroid hormone ecdysone signaling and miRNAs work together to control early germline differentiation and niche formation. European *Drosophila* Research Conference, Lisbon, Portugal, 2011 (short talk)
- Steroid hormone ecdysone signaling is required cell non-autonomously for germline differentiation. Regional *Drosophila* Meeting, Marburg, Germany, 2011 (short talk)
- Ecdysteroids and miRNA cooperate in regulating the *Drosophila* germline stem cell niche. EMBO/EMBL Symposium: Germline - Immortality through totipotency, Heidelberg 2012 (poster presentation)

COMPETENCES AND SKILLS

Language: German (native speaker), English (fluent), Spanish/French (basic)
Teaching: broad experience with supervision of method courses, summer students, lab rotation students and bachelor student
Laboratory skills: *Drosophila* genetics, Immunohistochemistry, Microscopy analysis (fluorescence and confocal), Molecular biology, mammalian tissue culture, western blot analysis